2020

NOVEL SMALL MOLECULE ANTIFUNGALS FOR INVASIVE FUNGAL INFECTIONS

Emily Dennis
University of Kentucky, emy.dennis2015@gmail.com
Author ORCID Identifier:
https://orcid.org/0000-0001-7928-9705
Digital Object Identifier: https://doi.org/10.13023/etd.2020.506

STUDENT AGREEMENT:

I represent that my thesis or dissertation and abstract are my original work. Proper attribution has been given to all outside sources. I understand that I am solely responsible for obtaining any needed copyright permissions. I have obtained needed written permission statement(s) from the owner(s) of each third-party copyrighted matter to be included in my work, allowing electronic distribution (if such use is not permitted by the fair use doctrine) which will be submitted to UKnowledge as Additional File.

I hereby grant to The University of Kentucky and its agents the irrevocable, non-exclusive, and royalty-free license to archive and make accessible my work in whole or in part in all forms of media, now or hereafter known. I agree that the document mentioned above may be made available immediately for worldwide access unless an embargo applies.

I retain all other ownership rights to the copyright of my work. I also retain the right to use in future works (such as articles or books) all or part of my work. I understand that I am free to register the copyright to my work.

REVIEW, APPROVAL AND ACCEPTANCE

The document mentioned above has been reviewed and accepted by the student's advisor, on behalf of the advisory committee, and by the Director of Graduate Studies (DGS), on behalf of the program; we verify that this is the final, approved version of the student's thesis including all changes required by the advisory committee. The undersigned agree to abide by the statements above.

Emily Dennis, Student

Dr. Sylvie Garneau-Tsodikova, Major Professor

Dr. David Feola, Director of Graduate Studies

NOVEL SMALL MOLECULE ANTIFUNGALS FOR INVASIVE FUNGAL INFECTIONS

DISSERTATION

A dissertation submitted in partial fulfillment of the requirements for the degree of Doctor of Philosophy in the College of Pharmacy at the University of Kentucky

By
Emily K. Dennis

Lexington, Kentucky

Director: Dr. Sylvie Garneau-Tsodikova, Professor of Pharmaceutical Sciences

Lexington, Kentucky

2020

https://orcid.org/0000-0001-7928-9705

ABSTRACT OF DISSERTATION

NOVEL SMALL MOLECULE ANTIFUNGALS FOR INVASIVE FUNGAL INFECTIONS

Human fungal pathogens cause a range of diseases from benign skin conditions (*i.e.*, ringworm) to thrush, mucosal membrane infections, and life-threatening systemic infections including bloodstream infections (*i.e.*, aspergillosis and candidiasis) and Cryptococcal meningitis. These systemic infections occur most often in immunocompromised individuals and have high mortality rates. Current antifungal agents used in the clinic belong to three main classes: the polyenes (*e.g.*, amphotericin B (AmB)), the echinocandins (*e.g.*, caspofungin (CFG)), and the azoles (*e.g.*, fluconazole (FLC)). In addition, the antimetabolite pyrimidine analogue flucytosine is used in combination with AmB. The three main classes class of antifungals each target different aspects of cell wall synthesis or cell membrane function and each class has different strengths and weaknesses depending on the strains of fungi that they are effective against, their route of administration, and their potential side effects. Problems associated with current antifungals include toxicity to patients, only effective against a limited spectrum of fungal strains, and the development of resistance of fungal strains to treatment. Discovering new antifungal therapies is a promising strategy to decrease mortality rates. Herein, three classes of molecules are evaluated for their potential as novel antifungals and reveal that (i) the antihistamines, terfenadine (TERF) and ebastine (EBA) improve the efficacy of azole antifungals when used in combination against a range of *Candida* strains, (ii) square-planar gold(I)-phosphine complexes exhibit broad-spectrum antifungal activity, and (iii) fluorinated aryl- and heteroaryl-substituted monohydrazones display broad-spectrum activity against fungi with little toxicity to mammalian cells, and (iv) other classes of molecules in recent literature that have shown antifungal activity. This work serves to identify promising scaffolds for novel classes of antifungals with the ultimate goal of bringing newer and more effective antifungals to be used clinically for systemic fungal infections.

KEYWORDS: drug synergy, biofilm, drug resistance, *Candida*, gold complexes, monohydrazone

Emily K. Dennis

September 29, 2020

Date

NOVEL SMALL MOLECULE ANTIFUNGALS FOR INVASIVE FUNGAL INFECTIONS

By

Emily K. Dennis

Sylvie Garneau-Tsodikova
Director of Dissertation

David J. Feola
Director of Graduate Studies

September 29, 2020
Date

DEDICATION

"The education of young people in science is at least as important, maybe more so, than the research itself."

-Glenn T. Seaborg

ACKNOWLEDGEMENTS

First and foremost, I would like to thank my advisor, Professor Sylvie Garneau-Tsodikova for her mentorship. Sylvie not only helped me become a better scientist at the bench, but also has been wonderful in meeting me where I am and providing helpful nudges to keep me on track. From asking me to sing the ABC's to get me to project my voice to encouraging me to do SciCats, I thank you for helping me to be a better writer, presenter, and educator as well as a scientist.

I would like to thank my committee members Professors Kyung Bo Kim, Jürgen Rohr, H. Peter Spielmann, Oleg V. Tsodikov, and Steven G. Van Lanen for providing thoughtful suggestions and useful feedback on my research projects. I also am very thankful for the letters of recommendation that were written on my behalf.

I also want to thank Professor David S. Watt for his collaboration on both the antifungal review featured in Chapter 1, the monohydrazone project presented in Chapter 4, and for writing a letter of recommendation. Similarly, thank you to Professor Samuel G. Awuah and his team for synthesizing the gold complexes studied in Chapter 3.

Thank you to the past and present members of the Garneau-Tsodikova and Tsodikov groups for being great colleagues and friends. Thanks to Dr. Sanjib K. Shrestha, Dr. Selina Y.L. Holbrook, and Dr. Huy X. Ngo for sharing their collective wisdom and training me on the various fungal and cell culture techniques. Dr. Nishad Thamban Chandrika and

Katelyn R. Brubaker, without your synthesized molecules the monohydrazone project of Chapter 4 would not be possible. I would also like to thank Nishad for his help with NMR and chemistry mechanism practice as well as his simple and necessary reminders to take projects one step at a time. I would like to thank Kaitlind C. Howard for working with me to write the antifungal review in Chapter 1. Both Kaitlind and Sylvie dedicated many weekends to working on the review which could have been spent otherwise. I am very happy with how the review paper turned out and I appreciate all their precious time spent working on it. To my two research mentees, Sarah C. Foree and Hannah A. Hilliard, you were a pleasure to work with and Sarah was a welcome help with the MIC assays in Chapter 4. A giant thanks to my friend and colleague, the now Dr. Taylor A. Lundy! It was great being able to go through all the big graduate school landmarks together with you (or a month or two behind you). And thank you for being my person to celebrate the highs with and a shoulder to cry on during the low moments. Another great friend and colleague along this journey has been Dr. Ankita Punetha, who has such a bright smile and great attitude. And finally, Dr. Marina Y. Fosso, Dr. Keith D. Green, and Dr. Caixia Hou, you all have been wonderful colleagues and are always so reliable for being great sources of knowledge and role models.

All this research would not be possible without funding. I need to thank the University of Kentucky College of Pharmacy for funding through start-up funds to S.G.-T as well as the 2019-2020 Pharmaceutical Sciences Excellence in Graduate Achievement Fellowship to myself. I have been very fortunate to be able to present my research both in the college and to travel to two conferences in 2019. Travel to conferences was possible with thanks to the

Peter G. Glavinos, Jr., Ph.D. Travel Award, departmental travel funds, and a travel award from the University of Kentucky Graduate Student Congress which I received.

The Department of Pharmaceutical Sciences in the College of Pharmacy has been a wonderful place to work! Thank you to Catina Rossoll for all her hard work keeping everyone else on track and to Dr. Joe Chappell and the AAPS student chapter for affording graduate student trips to places like Eli Lily and other career development events. In addition, within the University of Kentucky, I thank the staff at the counseling center for providing helpful resources to students.

Outside of lab, it has been a joy to do Science Cultivates Academically Talented Students (SciCats) with the 3rd grade classes of Tiffany Brown, Kristi Boaz, and Valerie Byrd at Ashland Elementary and the 4th and 5th graders in Bari Douglas's class at Maxwell Elementary School. In addition, Ryan Wheeler, Jasmine Woods, and Taylor Lundy who made planning activities fun and full of laughs.

Additionally, it has been a joy to be able foster my four cute and not-so-small pups from Camp Jean Dog Rescue in Lawrenceburg, KY. Thanks Ollie, Layla, Zoe, and Chance for being my walking buddies and filling my spare time the past year with lots of smiles.

I am very grateful for my family close friends who have continually supported me every step of the way. Words are hard to find for how thankful I am for all of you. I love you all.

TABLE OF CONTENTS

LIST OF TABLES

LIST OF FIGURES

LIST OF ABBREVIATIONS

5FC	5-Flucytosine
5FU	5-Fluorouracil
A549	Human adenocarcinoma
AB	Antibiotic
AFG	Anidulafungin
ALB	Albaconazole
AmA	Amphotericin A
AmB	Amphotericin B
AMP	Ampicillin
ATCC	American Type Culture Collection
BEAS-2B	Human bronchial epithelial
BUT	Butenafine
CD101	Rezafungin
CFG	Caspofungin
CFU	Colony forming unit
CIP	Ciprofloxacin
CLT	Clotrimazole
CYP	Cytochrome P450
DMEM	Dulbecco's Modified Eagle Medium
EBA	Ebastine
ECO	Econazole

EFI	Eficonazole
ESI	Electrospray ionization
FBS	Fetal bovine serum
FEX	Fexofenadine
FICI	Fractional inhibitory concentration index
FLC	Fluconazole
GPI	Glycosylphosphatidylinositol
HaCaT	Human skin keratinocyte
HEK-293	Human embryonic kidney
HeLa	Human cervical cancer
HepG2	Human liver cancer
hERG	Human ether-à-go-go-related gene or protein
HRMS	High resolution mass spectrometry
ICP-OES	Inductively coupled plasma optical emission spectroscopy
ISA	Isavuconazonium
ITC	Itraconazole
KANA	Kanamycin A
KANB	Kanamycin B
KTC	Ketoconazole
J774A.1	Murine macrophage
LUL	Luliconazole
MCZ	Miconazole
MEC	Minimum effective concentration

MFG	Micafungin
MH	Mueller-Hinton
MHC	Minimum hemolytic concentration
MIC	Minimum inhibitory concentration
NAF	Naftifine
NAT	Natamycin
NEA	Neamine
NEB	Nebramine
NEO	Neomycin B
NYT	Nystatin B
PBS	Phosphate buffered saline
POS	Posaconazole
RBC	Red blood cell
ROS	Reactive oxygen species
RP-HPLC	Reverse-phase high-performance liquid chromatography
SAR	Structure-activity relationship
SER	Sertaconazole
SMIC	Sessile minimal inhibitory concentration
SUL	Sulconazole
TER	Terconazole
TERF	Terfenadine
TET	Tetracycline
THT	Tetrahydrothiophene

TIO	Tioconazole
TLC	Thin layer chromatography
TOB	Tobramycin
TRB	Terbinafine
TRI	Trimethoprim
VAN	Vancomycin
VERO	African green monkey kidney cell
VNI	(*R*)-*N*-(1-(2,4-Dichlorophenyl)-2-(1*H*-imidazol-1-yl)ethyl)-4-(5-phenyl-1,3,4-oxadiazol-2-yl)benzamide
VRC	Voriconazole
VT-1161	Otesaconazole
VT-1129	Quilseconazole
XTT	[2,3-bis(2-methoxy-4-nitro-5-sulfophenyl)-2*H*-tetrazolium-5-carboxanilide]
YEPD	Yeast extract peptone dextrose

PREFACE

The following dissertation contains 6 chapters covering the most important projects of my Ph.D. studies aimed at the *in vitro* biological evaluation of novel small molecule antifungals. The first 4 chapters are adapted from my previous publications. Chapter 1 provides a comprehensive overview of currently available antifungal agents and scaffolds in preclinical studies published in recent years (Howard, K.C.,† **Dennis, E.K.,**† Watt, D.S., & Garneau-Tsodikova, S. (2020). A comprehensive overview of the medicinal chemistry of antifungal drugs: Perspectives and promise. *Chem. Soc. Rev*. 49:2426-2480). Chapter 2 discusses the synergistic activity of two antihistamines in combination with azole antifungals (**Dennis, E.K.** & Garneau-Tsodikova, S. (2019). Synergistic combinations of azoles and antihistamines against *Candida* species *in vitro*. *Med. Mycol.* 57(7):874-884.) Chapter 3 reports 6 gold(I)-phosphine complexes and their broad-spectrum activity against fungal strains (**Dennis, E.K.**, Kim, J.H., Parkin, S., Awuah, S.G., & Garneau-Tsodikova, S. (2020). Distorted gold(I)-phosphine complexes as antifungal agents. *J. Med. Chem*. (special issue on Women in Medicinal Chemistry), 63(5):2455-2469). Chapter 4 looks at the promise of fluorinated aryl- and heteroaryl-substituted hydrazones (Chandrika, N.T., **Dennis, E.K.**, Brubaker, K.R., Kwiatkowski, S., Watt, D.S., & Garneau-Tsodikova, S. Fluorinated aryl- and heteroaryl-substituted hydrazones: Broad spectrum antifungal agents. (Submitted for publication in August 2020). Chapter 5 describes works in progress related to the projects that are unfinished at this time. Finally, Chapter 6 provides the conclusions and future directions for the projects discussed here.

Chapter 1

A comprehensive overview of antifungal drug development: Perspectives and promise

1.1. ABSTRACT

The emergence of new fungal pathogens makes the development of new antifungal drugs a medical imperative that in recent years motivates the talents of numerous investigators across the world. Understanding not only the structural families of these drugs but also their biological targets provides a rational means for evaluating the merits and selectivity of new agents for fungal pathogens and normal cells. An equally important aspect of modern, antifungal drug development takes a balanced look at the problems of drug potency and drug resistance. The future development of new antifungal agents will rest with those who employ synthetic and semisynthetic methodology as well as natural product isolation to tackle these problems and with those who possess a clear understanding of fungal cell architecture and drug resistance mechanisms. This review endeavors to provide an introduction to a growing and increasingly important literature, including coverage of the new developments in medicinal chemistry since 2015 and also endeavors to spark the curiosity of investigators who might enter this fascinatingly complex fungal landscape.

1.2. INTRODUCTION

Spurred on by the specter of widespread, drug-resistant, fungal infections that might derail modern medical advances and threaten human health, scientists seek to understand fungal

pathogens at a molecular level and design new agents to control their promulgation in human populations. New research techniques and ever more complex drugs than their antifungal progenitors provide hope that medicinal chemistry will prove equal to the challenges presented by these infections. Are we entering a "Golden Age" of antifungal drug discovery? Certainly, a steady, annual increase in the number of scientific publications (Fig. 1.1) appears to herald such a period of discovery. Perhaps even more telling is the appearance of front-page articles in the popular press such as the *New York Times* that alert the general population as to the threat that these fungal infections represent and underscore the importance of research in this arena.[1-3] The first antifungal drug, amphotericin B (AmB), entered the pharmaceutical market only sixty years ago.[4] The discovery of subsequent antifungal drugs for human use continued at a slow, but not insignificant, pace. Although many interesting reviews summarize the therapeutic use of antifungal agents since 2010 (Fig. 1.2),[5-6] only a few provide a comprehensive overview of the discovery and development of new agents for molecular, fungal targets and provide guidance as to the direction that future drug discovery may take.[7-11] This overview of human, fungal pathogens, antifungal agents used in the clinic or in clinical trials, and mechanisms of resistance against current antifungal agents will focus on summarizing the voluminous literature related to the discovery and development of new antifungals and will ambitiously predict the future for drug discovery in this important arena.

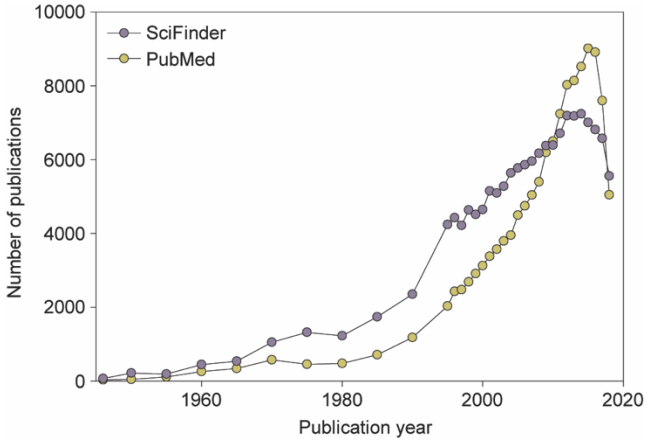

Fig. 1.1. Graph showing the number of publications related to antifungal research found in PubMed (yellow circles) or in SciFinder (purple circles) from 1945-2018.

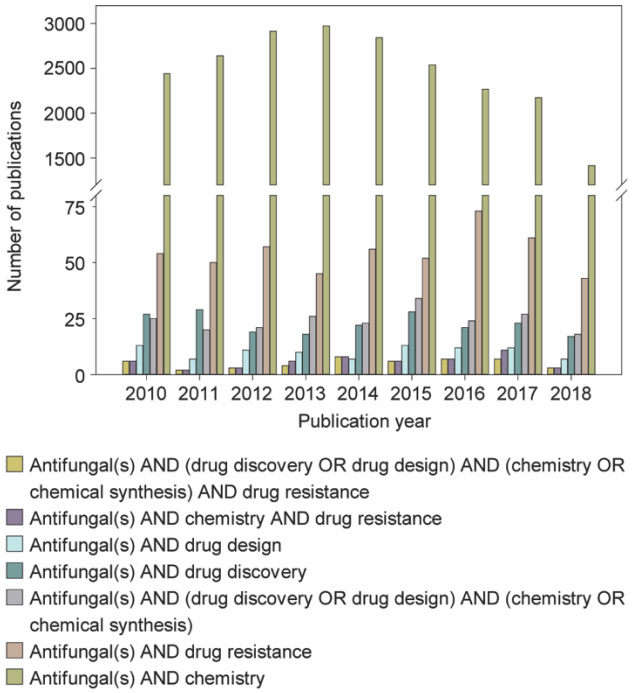

Fig. 1.2. Graph showing the number of reviews found in PubMed published from 2010-2018 when searching for the combinations of terms shown in the legend above.

1.2.1. Fungal pathogens and their associated ailments

The most common types of fungal infections are cutaneous, ringworm infections of the skin and nails. Most people, who are unfamiliar with the sinister, systemic fungal infections, associate fungal infections only with those affecting the skin because these

infections produce an effect visible even to the untrained eye. The name ringworm is itself misleading as these infections are not caused by worms but by pathogenic fungi called dermatophytes that live on the skin. The cutaneous fungal infections known as ringworm typically occur in otherwise healthy individuals, and although they are contagious, these infections are treatable and not life-threatening. On the other hand, systemic fungal infections, including infections that appear in immunocompromised individuals, are life-threatening, as evidenced by current mortality rates exceeding 50%.[12]

For healthy individuals, fungi are ubiquitous and a generally benign part of our environment. Conditions that either destroy immune cells, such as acquired immune deficiency syndrome, or require treatments that weaken the immune response, such as organ transplantations or cancer chemotherapies, temporarily compromise the ability of the immune system to surmount systemic fungal infections. For these immunocompromised patients, fungal infections represent anything but a benign presence. As medical advances lead to a larger population of immunocompromised individuals than those in the past, clinical practitioners will require an ever increasing number of new, selective antifungal drugs to treat patients affected by systemic, fungal diseases.[13]

Fungi are arbitrarily divided into four categories according to cellular, structural features: yeasts, filamentous fungi, dimorphic fungi, and dermatophytes. Without digressing into a detailed discussion of taxonomical variations in these four categories, we will briefly summarize the well-known strains and the pernicious strains in each category that affect human health since these are the strains that attracted the interest of medicinal chemists

interested in drug development. We refer the reader to detailed, well-written discussions of molecular and morphological differences among these organisms.[14-16]

Yeasts immediately bring to mind thoughts of bread and beer that use the non-pathogenic and much-valued Baker's yeast, *Saccharomyces cerevisiae*. Cutaneous candidiasis is a common cause of diaper rash in newborns and *Candida* spp. also affect mucosal membranes in the form of oral thrush in newborns and vaginal infections in women. However, several other closely related *Candida* spp. are also responsible for an estimated 400,000-700,000 cases of systemic human infections. *Candida albicans* is the causal agent in approximately 70% of the cases,[13] but other *Candida* spp., including *Candida glabrata* and *Candida auris*, represent strains of increasing importance as will become clear in our subsequent discussion of antifungal drug resistance. These systemic infections, if left untreated, may result in damage to the heart, liver, and kidneys. The spore-forming yeast, *Cryptococcus* spp., specifically *Cryptococcus neoformans* and *Cryptococcus gattii*, represent important species of pathogenic fungi in the yeast group that lead primarily to infections in the lungs and the central nervous system.

Infections caused by pathogenic, filamentous fungi or molds, commonly described as aspergillosis, develop after the inhalation of *Aspergillus* spp. spores. Aspergillosis occurs primarily in the lungs of individuals who are already compromised by unrelated, underlying lung problems, such as asthma or chronic obstructive pulmonary disorder. Invasive aspergillosis represents a severe form of this infection that spreads from the lungs to the brain, heart, and kidneys. Invasive pulmonary aspergillosis typically occurs in

patients whose immune systems are weakened as a result of cancer chemotherapy, bone marrow transplantation or a disease of the immune system, and if left untreated, this form of aspergillosis may be fatal.

The pathogenic, dimorphic fungi have a complex lifecycle that involves a stage in which the dimorphic fungi resemble yeast and another stage where they resemble molds. These chameleon-like, dimorphic fungi cause an extensive list of infections that include those described as mucormycosis, blastomycosis, histoplasmosis, fungal keratitis, and valley fever resulting from *Mucor* spp., *Blastomyces* spp., *Histoplasma* spp., *Fusarium* spp., and *Coccidioides* spp., respectively.[12-13]

Finally, as noted earlier in our discussion, the pathogenic dermatophytes affect the superficial skin, hair, and nails. These cutaneous infections, commonly referred to as ringworm, athlete's foot or jock itch (so-called "tinea" infections), involve some forty types of fungi in the *Trichophyton*, *Microsporum*, or *Epidermophyton* genera and tend to involve irritation or reddening of the skin as a consequence of dilation of capillary blood vessels. Although rarely life-threatening or painful and barely noticeable in some cases, dermatophytoses produce "chronic progressive eruptions that last months or years, causing considerable discomfort and disfiguration".[17]

In summary, this brief tour through the four categories of pathogenic fungi provides the rationale for testing new antifungal agents against the following fungal strains: *Candida albicans*, non-*albicans Candida* (*e.g.*, *C. auris*, *C. dubliniensis*, *C. famata*, *C. glabrata*, *C.*

guilliermondii, *C. inconspicua*, *C. kefyr*, *C. krusei, C. lambica, C. lipolytica*, *C. lusitaniae*, *C. mycoderma*, *C. parapsilosis*, *C. pulcherrima*, *C. pseudotropicalis*, *C. rugosa*, *C. sake*, *C. tropicalis*, and *C. utilis*), *Aspergillus* spp. (*e.g.*, *A. brasiliensis*, *A. candidus*, *A. clavatus*, *A. fumigatus*, *A. ochraceus*, *A. niger*, and *A. terreus*), as well as *Cryptococcus* spp. (*C. neoformans*, *C. gatti*, and *C. humicolus*). Other fungal strains less commonly tested include the yeasts *S. cerevisiae* and *Rhodotorula* spp. (*e.g.*, *R. bogoriensis* and *R. pilimanae*); the molds *Fusarium* spp. (*e.g.*, *F. graminearum*, *F. oxysporum*, *F. sambucinumi* and *F. solani*) and *Rhizopus* spp. (*e.g.*, *R. oryzae*); the dimorphic *Histoplasma* spp. (e.g. *H. capsulatum*), *Mucor* spp. (*e.g.*, *M. hiemalis*), and *Sporothrix* spp. (*e.g. S. schenkii*); the dermatophytes *Microsporum* spp. (*e.g.*, *M. canis*), *Trichophyton* spp. (*e.g.*, *T. mentagrophytes* and *T. rubrum*), and *Trichosporon* spp. (*e.g.*, *T. cutaneum*); those that are primarily plant pathogens (*e.g.*, *Colletotrichum coccodes* and *Botrytis cinereal*) and the non-pathogenic mold and model organism for genetics, *Neurospora crassa*.

The key to developing successful antifungal agents rests with their specificity for arresting (*i.e.*, fungistatic) or killing (*i.e.*, fungicidal) pathogenic fungal cells in preference to normal cells. What features discriminate between these two eukaryotic cell types and thereby offer unique targets for drug therapy? Most importantly, fungal cells, but not normal cells, possess a cell wall, called the pellicle, constructed principally of an aminopolysaccharide, chitin. This chitin layer in yeast cells possesses an overlaying matrix of β-1,3-glucans and then β-1,6-glucans, and this chitin layer in filamentous cells possesses an overlaying matrix of β-1,3-glucans and then α-1,3-glucans (Fig. 1.3). Final variable layers of galactosaminoglycans and proteins in yeast cells or galactosaminoglycans,

galactomannans and proteins in filamentous cells complete the architectural picture. Fungal cells also have cell membranes underlying the cell walls that contain a sterol called ergosterol rather than cholesterol that appears in the membranes of normal cells. In summary, fungal cells (*e.g.*, the yeasts *Candida* spp. and *Cryptococcus* spp., and the filamentous *Aspergillus* spp.), possess cell walls that display structural variations and cell membranes that differ from those of normal eukaryotic cells. The chitin "basement layer" of the cell wall provides a strong, shell-like framework that resists internal osmotic pressure from the cytoplasm. The glucan-based, outer layer of the cell wall in fungi provides chemical diversity and distinguishes one fungal species from another. For example, *Cryptococcus* have a thick capsule outside their cell wall made from the capsular polysaccharide, glucuronoxylomannan; *Histoplasma* and *Blastomyces* have a layer of α-1,3-glucan; and, most interestingly, *Aspergillus conidium* has a layer of melanin.[14] The variance between fungal and normal cells as well as the variance among different fungal cells provide the basis on which to identify druggable targets for new antifungal agents.

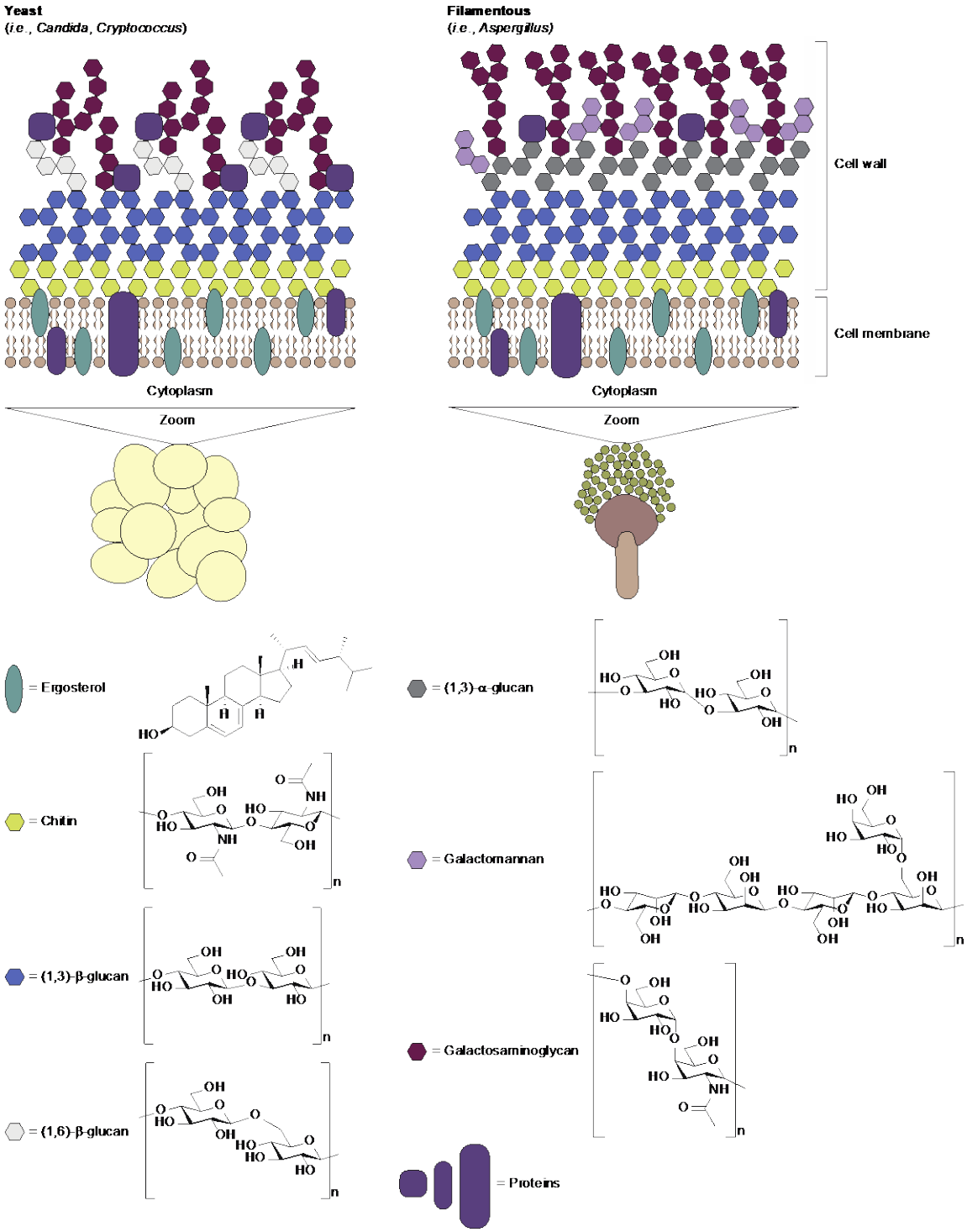

Fig. 1.3. Contrasting structures of fungal cell walls and membranes for yeast and filamentous fungi. Proteins and ergosterol are found in the cell membrane. Chitin and (1,3)-β-glucans are layered on top of the membrane to reinforce it and build the foundation for the cell wall. The rest of the cell wall is composed of proteins and various polysaccharides including (1,6)-β-glucans, (1,3)-α-glucans, galactomannans, and galactosaminoglycans.

1.2.2. Classes of antifungal agents and their mechanisms of action

Understanding the structural differences between pathogenic fungi and normal cells provides a rational basis on which to discuss the five classes of antifungal agents approved for human consumption: (i) the azoles (Fig. 1.4), (ii) the polyenes (Fig. 1.5), (iii) the echinocandins (Fig. 1.6), (iv) the allylamines (Fig. 7A), and (v) the antimetabolites (Fig. 1.7B). It also provides the basis on which to discuss directions that new therapeutic advances might take. The prior discussion of fungal cell architecture (Fig. 1.3) represented the affiliations among the glycans, chitin and the fungal cell membranes as flexible, even disorganized, arrangements in "layers". In fact, the evolution of these species derives from specific needs and affiliations among these polymeric species. Probing the structures and precise affiliations at molecular levels will provide the basis for designing drugs capable of dismantling these affiliations and achieving the desired fungistatic or fungicidal activities.

The azoles are a principal class of small-molecules used to treat fungal infections by targeting the lanosterol 14α-demethylase enzyme crucial for ergosterol biosynthesis. All antifungal azoles consist of an imidazole or triazole attached to a quaternary carbon (Fig. 1.4). The original azoles that emerged from the mid 1970s to the 1990s were imidazole-based and included the now, well-known representatives such as miconazole (MCZ; marketed in 1974), clotrimazole (CLT; 1975), econazole (ECO; 1982); ketoconazole (KTC; 1981), tioconazole (TIO; 1983), and sulconazole (SUL; 1989). More recently, additional imidazole-containing antifungals gained approval (*e.g.*, serconazole (SER; 2003) and luliconazole (LUL; 2013)). Starting as early as 1981 but emerging

predominantly in the 1990s, additional, important azoles, such as terconazole (TER; 1981), fluconazole (FLC; 1990), itraconazole (ITC; 1992), voriconazole (VRC; 2002), posaconazole (POS; 2006), efinaconazole (EFI; 2014), and the prodrug of isavuconazole called isavuconazonium (ISA; 2015), entered the armamentarium of medical practitioners. These new azoles possessed a triazole ring in place of the imidazole ring. The nitrogen-containing, aromatic ring in triazole-based azoles offered greater specificity against the fungal cytochrome P450 (CYP) enzyme than the early imidazole-based counterparts. In addition to the triazoles that are already on the market, two additional azoles are in clinical trials: albaconazole (ALB) and PC945.[18-19]

Most recently, tetrazoles gained popularity as potential antifungals because of their activity against a broad spectrum of fungal species and their good oral bioavailability.[20-21] In a similar fashion to the triazoles that showed better specificity for fungal CYP enzymes than the imidazoles, the tetrazoles showed the best improvement in this respect. Otesaconazole (VT-1161), which is currently in phase III clinical trials, inhibits the fungal cytochrome P450 (CYP) enzyme, has undetectable levels of binding to human CYP enzymes, and exhibits similar potency to VRC in minimal inhibitory concentration (MIC) assays.[20, 22] In addition to VT-1161, two other tetrazoles, quilseconazole (VT-1129) and VT-1598, are in preclinical development for treatment of *Cryptococcus* and *Coccidioides* infections, respectively.[21, 23-25] Today, imidazole-based antifungals are typically used as topical agents with the exception of KTC that still finds some systemic applications, whereas triazoles are generally used for systemic infections with the exception of EFI and TER that are used for topical infections. Of particular note are VT-1161 and ALB that, if successful in clinical

trials, will be only the second and third orally formulated treatments for onychomycosis, a fungal infection of the fingernails and most commonly, the toenails. The azoles possess two important benefits: oral activity and a broad spectrum of activities against various fungal strains. Their continued, wide-spread use drives both new analog development and concerns about the emergence of resistant strains that might accommodate 14α-methylated sterols in place of ergosterol in fungal membranes.

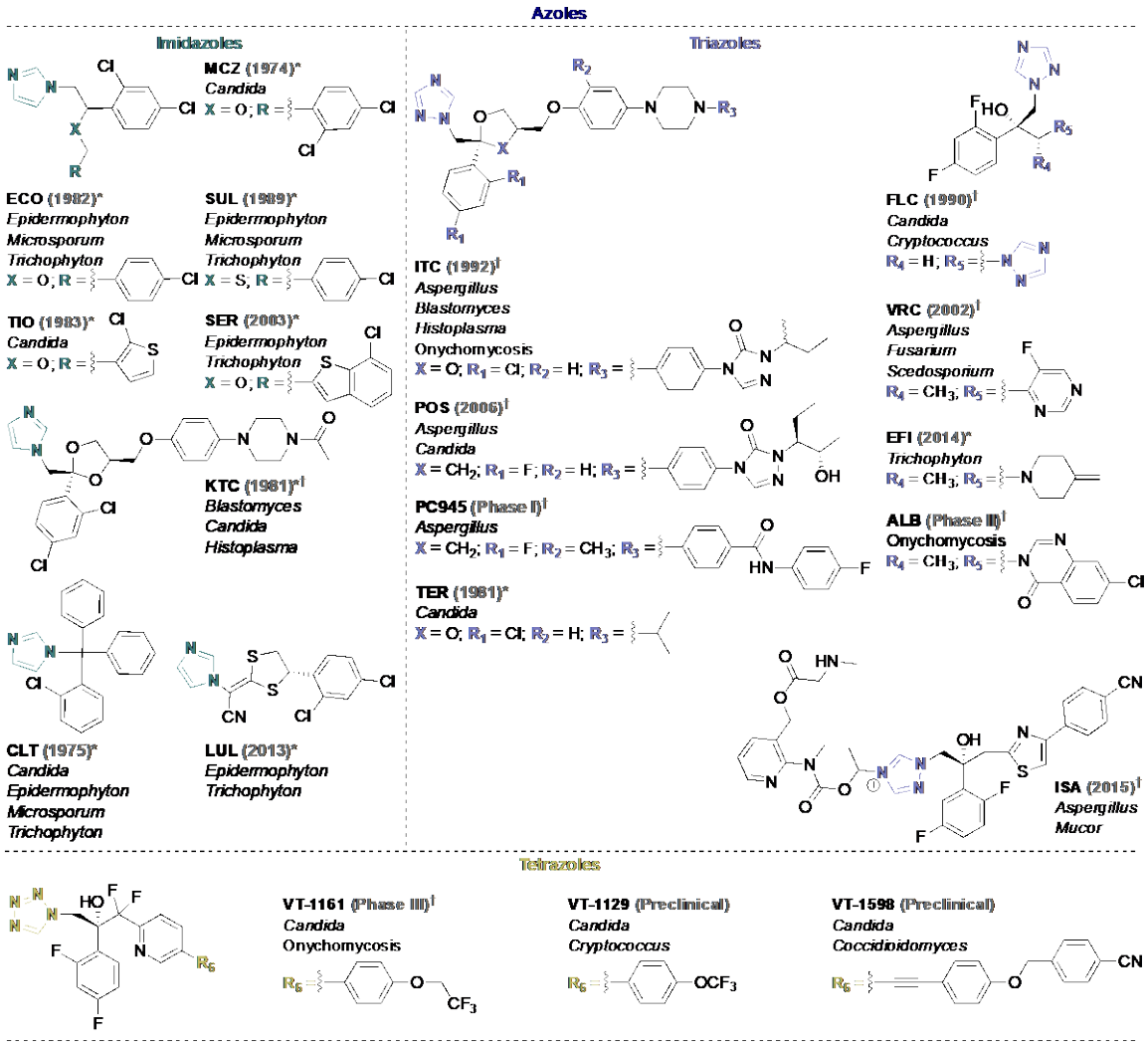

Fig. 1.4. Structures of approved imidazole-based and triazole-based antifungals along with the year of their introduction on the market and the fungal genera they target. Also depicted are tetrazole-based antifungal in preclinical and clinical development. *Imidazoles:* clotrimazole (CLT), econazole (ECO), ketoconazole (KTC), luliconazole (LUL), miconazole (MCZ), sertaconazole (SER), sulconazole (SUL), and tioconazole

(TIO). *Triazoles:* albaconazole (ALB), efinaconazole (EFI), fluconazole (FLC), isavuconazonium (ISA), itraconazole (ITC), PC945, posaconazole (POS), terconazole (TER), and voriconazole (VRC). *Tetrazoles:* otesaconazole (VT-1161), quilseconazole (VT-1129), and VT-1598. * = topical use; † = systemic use.

A second-line of defense against pathogenic fungi are the polyene class of antifungals (Fig. 1.5). Unlike the azoles that are synthesized in a laboratory setting, the polyenes are naturally occurring macrolides that are produced by Gram-positive bacteria, *Streptomyces* spp. presumably as a defense mechanism. Antifungal polyenes consist of a 25- or 37-carbon, unsaturated macrolactone ring attached to a mycosamine saccharide. The unsaturated macrolide ring disrupts the cell membrane by binding to and sequestering ergosterol in the fungal cell membrane.[26] The most potent polyenes, such as amphotericin B (AmB), contain seven units of unsaturation in the ring (*i.e.*, heptaenes). As the fungal ergosterol is structurally and functionally similar to the mammalian cholesterol, the polyenes display unfortunate, high levels of toxicity in addition to their desired, potent antifungal activity. Heptaenes such as AmB also display higher levels of toxicity than that of the related hexaenes such as nystatin (NYT) and natamycin (NAT).[27-28]

Despite requiring intravenous injection for drug delivery, AmB is the most commonly used polyene and the "gold standard" of antifungal agents for systemic infections. It is not surprising that different liposomal formulations of AmB were developed to improve the safety and efficacy of this important antifungal agent.[29] Both NYT and NAT are also used topically for skin and eye infections, respectively.[4] For some fungal infections, such as those caused by *Cryptococcus* spp. and dimorphic fungi, AmB remains as the final line-of-defense because other antifungals, such as echinocandins, are inactive against these fungi. In these cases, AmB often finds use in combination with other classes of antifungals

including the antimetabolites.[30] In addition, sertraline, a selective, serotonin-reuptake inhibitor, possesses unexpected activity against *Cryptococcus* spp. and a combination of sertraline and AmB is currently in phase III clinical trials.[31-32]

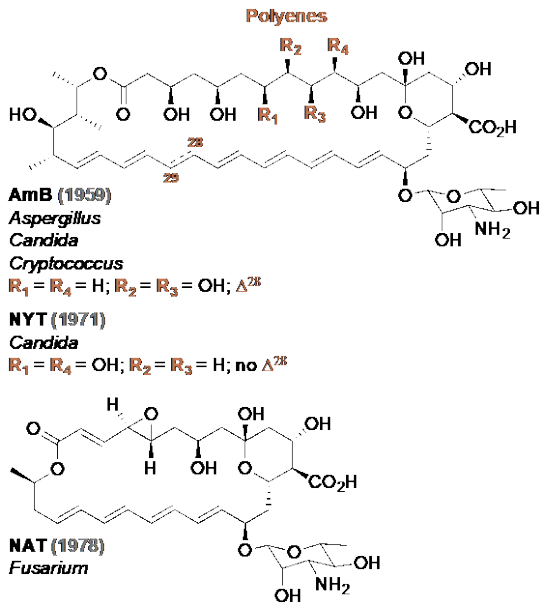

Fig. 1.5. Structures of polyene antifungal agents along with the year of their introduction on the market and the fungal genera they target. *Polyenes:* amphotericin B (AmB), natamycin (NAT), and nystatin (NYT).

A third class of antifungals comprise the semisynthetic natural products in the echinocandin family (Fig. 1.6). These antifungal agents possess hexapeptide cores bearing hydrophobic, lipid side-chains. Unlike the azoles that are man-made and the polyenes that are natural products, the echinocandins represent semisynthetic agents in which natural products undergo laboratory-based modifications to achieve a desired, therapeutic result. Specifically, the lipid moiety attached to the echinocandin hexapeptide framework is the site most frequently modified in efforts to develop new variants of the echinocandins. The mechanism of action of the echinocandins involves the inhibition of a β-1,3-glucan

synthase necessary for cell wall integrity. The absence of cell walls in normal cells makes the echinocandins particularly attractive agents for treating fungal pathogens.

The echinocandins that are in current clinical use consist of a hexapeptide core with variable lipid side-chains. Representative members of this family include caspofungin (CAS), micafungin (MFG), and anidulafungin (AFG). In addition, rezafungin (CD101) is currently in phase III clinical trials. The echinocandins produced by filamentous fungi presumably evolved as a defense mechanism to kill other fungi competing for nutrients. Their specificity for cell walls in fungi required a level of complexity that emerged from evolutionary pressures without regard to issues such as membrane absorption. Not surprisingly, the echinocandins have poor oral bioavailability and like AmB, require intravenous injection. In contrast to the polyenes, the echinocandins have a different and somewhat better toxicity profile than AmB and find application within a narrow spectrum of fungal infections including candidiasis and aspergillosis.[33]

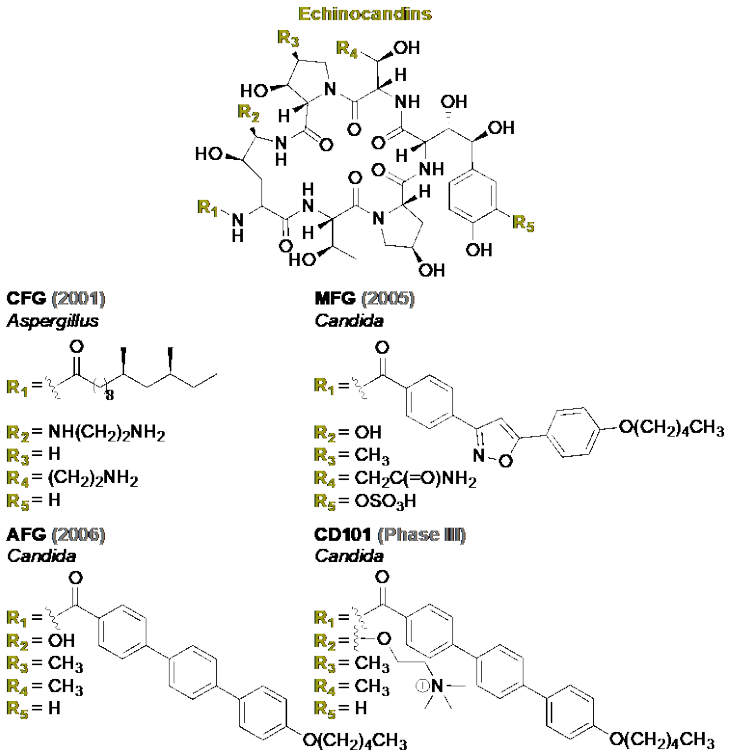

Fig. 1.6. Structures of echinocandin antifungal agents along with their year of introduction on the market and the fungal genera that they target. *Echinocandins:* anidulafungin (AFG), rezafungin (CD101), caspofungin (CFG), and micafungin (MFG).

Returning to the theme of wholly, man-made, antifungal agents, two additional classes of antifungal agents in this category warrant discussion: the allylamines (Fig. 1.7A) and the antimetabolites (Fig. 1.7B). The allylamines target another critical, biosynthetic enzyme, squalene epoxidase, the first enzyme in the biosynthesis pathway leading from squalene to lanosterol and hence to ergosterol and cholesterol. Representative examples of the allylamines include terbinafine (TRB), naftifine (NAF), and butenafine (BUT). These agents are typically formulated as powders or creams for the treatment of cutaneous ringworm infections. In addition to its powder-based formulation, TRB is also the only approved, oral drug for the treatment of onychomycosis (*i.e.*, fungal infections of the fingernails or toenails). At first glance, it might seem unusual to use TRB for an application requiring drug absorption since TRB would concomitantly interfere with cholesterol

biosynthesis in normal cells as well as ergosterol biosynthesis in fungal cells. Presumably, dietary foodstuffs make up for any potential inhibition of cholesterol biosynthesis in humans.

5-Flucytosine (5FC) is a pyrimidine antimetabolite that unfortunately also possesses a high level of toxicity and triggers the development of fungal resistance. As a consequence, 5FC is primarily used sparingly for severe cases of candidiasis and in combination with AmB.[30] Toxicity and resistance may be linked: the deamination of 5FC to 5-fluorouracil (5FU), capture of 5FU as a nucleotide FUMP, and subsequent inhibition of thymidylate synthase affects this key enzyme that links the RNA and DNA worlds.

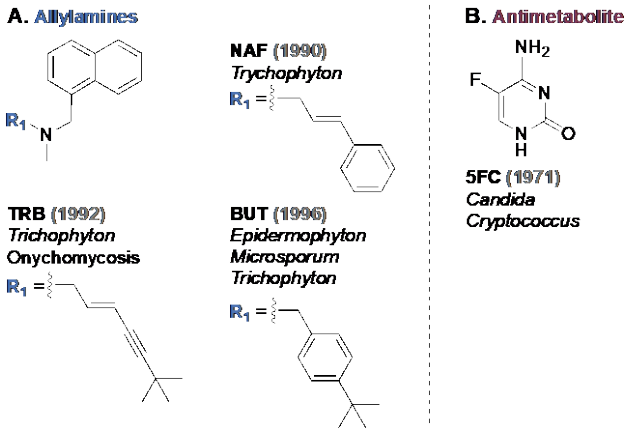

Fig. 1.7. Structures of **A.** allylamine and **B.** antimetabolite antifungal agents along with the year of their introduction on the market and the fungal genera that they target. *Allylamines:* butenafine (BUT), naftifine (NAF), and terbinafine (TRB). *Antimetabolite:* 5-flucytosine (5FC).

The limited armamentarium of antifungal agents and the increasing number of drug-resistant fungal pathogens mandates the continued development of new classes of antifungal agents. In the echinocandin-like class, ibrexafungerp (SCY-078) (NCT03734991) (Fig. 1.8), that is currently in phase III clinical trials, resembles the

echinocandins in that it is a glucan synthase inhibitor but, unlike the echinocandins, is orally available.[34-35] Preclinical studies showed that SCY-078 is active against *Candida* spp. and *Aspergillus* spp. with fungicidal activity at concentrations above MIC values. SCY-078 also shows synergistic effects in combination therapy with AmB.[36-38] While SCY-078 has the same cellular target as the echinocandins, resistance studies showed variance in the binding sites for these two types of molecules and suggested that SCY-078 may be an attractive, treatment option for multidrug-resistant infections.[39-40]

F901318 (NCT03583164) is a first-in-class "orotomide" antifungal agent that targets the dihydroorotate dehydrogenase enzyme in pyrimidine nucleotide biosynthesis.[41] The orotomides are narrow-spectrum antifungal agents that display oral activity against *Aspergillus* spp. and some dimorphic fungi including *Scedosporium* spp.[42] with MIC values that are better than those of azoles and AmB.[43-44] Another new drug in phase II clinical trials is an inhibitor of the biosynthesis of glycosylphosphatidylinositol (GPI), a lipid-rich anchor attached to membrane-associated proteins.[45] APX001 (formerly E1210, NCT03604707) has broad-spectrum activity against *Candida* spp., *Cryptococcus* spp., *Coccidioides* spp., *Aspergillus* spp., *Fusarium* spp., and *Scedosporium* spp.,[46-53] and although it shows potency comparable to that seen in current antifungals, it has a high clearance rate. APX001 is actually a prodrug that leads to the active metabolite named APX001A that lacks the methylphosphate group on the 2-aminopyridyl ring in APX001.[46, 54-55] In addition, given the wide-spread use of GPI anchors in normal cells, it is unclear what selectivity this drug has for fungal pathogens *versus* normal cells.

A third new drug in phase II studies, ME1111 (NCT02022215), is a topical treatment for onychomycosis. ME111 inhibits the succinate dehydrogenase complex that appears as complex II in the electron-transport chain and effects the succinate-to-fumarate conversion in the citric acid cycle and thereby disrupts oxidative phosphorylation.[56] MIC values for ME1111 are comparable to current antifungal nail lacquers,[57] but its small molecular mass relative to other agents, affords it considerable improvement in its ability to penetrate nails.[58-59]

A fourth potential antifungal agent completing phase II studies is a natural product isolated from *Acremonium persicinum*, found among Malaysian leaf litter.[60] This fungal genus is formerly known as *Cephalosporium* and different strains produce antibiotics in the cephalosporin family.[61] Like the echinocandins, VL-2397 (formerly ASP2397, NCT03327727) is a cyclic hexapeptide that resembles the fungal siderophore, ferrichrome, but preferentially chelates aluminum ions instead of ferric ions.[60] VL-2937 is narrow spectrum antifungal agent with activity against *Aspergillus* spp.[62]

AR-12 (formerly OSU-03012, NCT00978523) represents another new class of antifungal agents. Although it is currently in phase I clinical trials as an antineoplastic agent, it also displays a broad spectrum of antifungal activity including some synergistic interactions with FLC.[63-64] AR-12 has antineoplastic activity that derives from its mechanism of action as a protein-kinase inhibitor, but in fungi, its activity resides in the inhibition of acetyl-CoA synthetase.[65-66] In addition to the new antifungal agents described above, synthetic lactoferricin, derived antimicrobial peptide, hLF1-11 (NCT00509834), is undergoing

clinical trials to treat candidemia,[67] and two other trials are underway to evaluate vaccines for vulvovaginal candidiasis (NCT01926028 and NCT01067131).[68]

Several antifungal agents entered clinical trials but were unsuccessful due to a lack of efficacy in patients. For example, nikkomycin Z (NCT00614666) was a chitin-synthase inhibitor with a nucleoside-peptide scaffold that was under development to treat *Coccidioides* infections (Fig. 1.8).[69] Similar to AR-12, a histone deacetylase inhibitor, MGCD290 (NCT01497223), originally developed as an antineoplastic agent, failed as an agent to be used in combination with FLC for vulvovaginal candidiasis.[70] Finally, a human recombinant monoclonal antibody, called mycograb (NCT00847678), targeted heat shock protein 90 passed phase I trials for cryptococcal meningitis, but failed to complete phase II trials.[71]

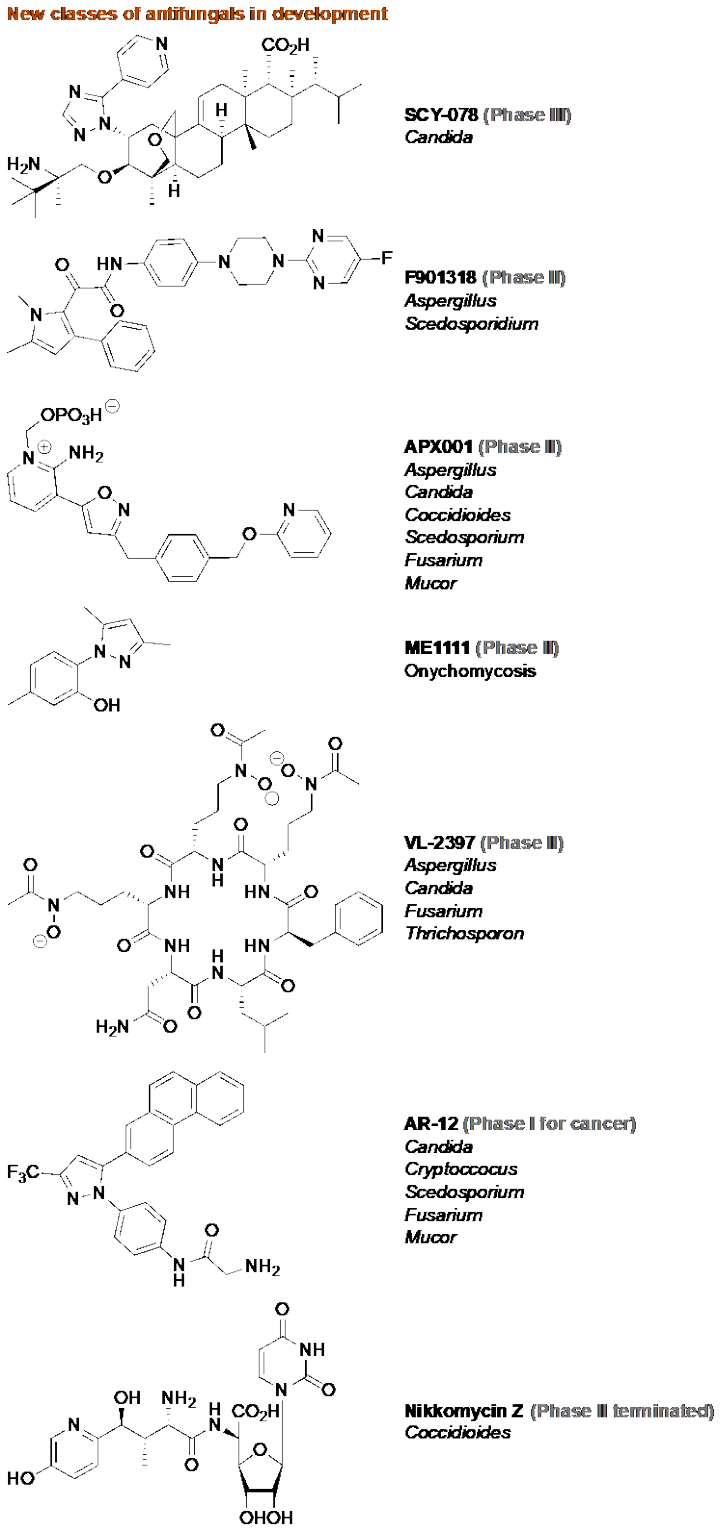

Fig. 1.8. Structures of new classes of antifungal agents in development: inhibitors of glucan synthase (SCY-078) in Phase III; a pyrimidine biosynthesis (F901318) in Phase II, GPI biosynthesis (APX001), citric acid cycle (ME1111), and a siderophore-like molecule (VL-2397). The kinase inhibitor (AR-12) is in phase I trials for cancer and has potential to enter clinical trials as an antifungal. In addition, the chitin synthase inhibitor, nikkomycin Z, started phase II development, but trials were terminated.

1.2.3. Modes of resistance to various classes of antifungal agents

Fungal resistance to drug treatment occurs not only with 5-flucytosine (5FC), as described earlier in this review, but also with other antifungal drug classes. While it is common for some fungi to be intrinsically resistant to a class of antifungal agents, it is quite rare for a pathogen to be pan-resistant to all antifungal agents. As an exception to this generalization, *C. auris* is a pathogen that has made headlines[1-3] recently because of its easy transmissibility and because it is frequently resistant to all three main classes of antifungals. Fungi employ four main strategies to resist drug therapy: (i) overexpression of targeted proteins (observed in azoles); (ii) mutations induced in targeted proteins (observed in azoles and echinocandins); (iii) upregulation of biosynthesis of efflux pumps and/or augmented insertion of efflux pumps in cell membranes (observed in azoles); and (iv) decreased access to target as in the sequestration of ergosterol (observed in polyenes).

Most reports of antifungal drug resistance involve infections by fungal pathogens that show decreased susceptibility to the azoles, probably because of their widespread use and not because of some intrinsic property of the azoles. For *Candida* spp., approximately 7% of all systemic infections display decreased susceptibility to the azoles.[72] Resistance to the azoles is due to three mechanisms that fungal cells use alone or in combination to defeat the fungicidal activity of these drugs: [1] overexpression of ERG11 (*i.e.*, resistance strategy "i") (Fig. 1.9A), [2] mutations in ERG11 (*i.e.*, resistance strategy "ii") (Fig. 1.9B, Table 1.1), and [3] expression of efflux pumps (*i.e.*, resistance strategy "iii") (Fig. 1.9C). The *ERG11* gene encodes the putative enzymatic target of the azoles, lanosterol 14α-

demethylase, and various studies reported increased transcriptional levels of ERG11 mRNA in azole-resistant *Candida* strains that in turn leads to elevated levels of the targeted enzyme. This robust expression of lanosterol 14α-demethylase overcompensates for any loss of activity due to azole inhibition (Fig. 1.9A).[73-74]

The second effective strategy that fungi use to acquire resistance to azoles involves principally the appearance of lanosterol 14α-demethylase mutations in *C. albicans* clinical isolates (Table 1.1) and the appearance of a few mutations in non-*albicans Candida* (see last row of Table 1.1). Furthermore, the widespread use of azoles in agriculture led, perhaps as expected, to reports of resistance to *Aspergillus* spp., and susceptibility monitoring of molds in different environments suggests this is also a concern (Table 1.2).[75-82] Mutations conferring resistance to the azoles are numerous but appear to localize near the heme-binding group in lanosterol 14α-demethylase (Fig. 1.9B).[83-84] Of the mutations observed, only eight mutations have been confirmed by *in vitro* methods to have a role in azole resistance (*i.e.,* A61V, Y132H, K143R, F145L, S405F, V456I, G464S, and R467K), and these single-site, mutations decrease susceptibility to azoles by 4- to 64-fold.[85] Of these eight mutations, two (*e.g.*, K143R and V456I) play a particularly important role in the induction of resistance. In pan-azole strains, the strains invariably have both mutations as well as augmented expression of efflux pumps[86-90] such as Cdr1, Cdr2, and Mdr1 in yeasts that are ATP-binding cassette transporters and appear to be strongly correlated with azole cross-resistance (*i.e.*, resistant to VRC and ITC in addition to FLC) (Fig. 1.9C).[83, 91]

Table 1.1. Mutations found in ERG11 of *C. albicans* clinical isolates.

Mutation(s)	Hot spot[§]	R/S	Ref.	Mutation(s)	Hot spot[§]	R/S	Ref.
Q21R		R	86	F449V	III	R	86
Y79C		R	87	G450E	III	R	86-87, 92-93
K99T		R	87	V452A	III	R	94
F105L	I	R/S	92	**V456I**	III		95
A107T	I	R	94	**G464S** [c]	III	R	86, 90, 94, 96-99
A114S	I	R	100-102	G465S	III	R	103
A114V	I	R	74	**R467K**	III	R	96, 104-105
D116E	I	R/S	74, 83, 93-94, 96-98, 100, 103, 106-111	**I471T**	III	R	100, 112
D117E	I	R	74	Q474H	III	R	83
F126L	I	R	93	Q474K	III		100
K128T	I	R/S	92-93, 96-98, 100, 106-107, 113	L480F	III	R	111
G129A	I	R	96	V488I	III	R	87, 90, 92
V130I	I	R	87	P503L		R	87
Y132F [a, b, c]	I	R	86-87, 90, 113-118	V509M		R	94
Y132H	I	R	93, 96, 100, 112	T525I		R	119
N136Y	I	R	95	F72L, E266D	II	S	120
K143E	I	R	87, 93	F105L, E266D	II	R/S	92
K143R [a, c]	I	R	86-87, 94, 106, 115-117, 119, 121-122	F105L, G464S	III	R	92
F145L	I	R	83, 87, 94	F105L, G450E	III	R	92
F145R	I	R	86	A114S, Y257H	I	R/S	86, 88, 103, 110
K147R	I	S	92	D116E, K128T	I	R/S	94, 98, 102-103, 110
D153E	I	R	108	D116E, **Y132H**	I	R	111
V159I	I	R/S	95, 107	D116E, E165K	I	R	74
E165Y	I	S	120	D116E, Y205E	I	S	109
I166S [e]	I	R	88	D116E, G346A	I	R	111
E174A		R	74	D116E, E266D	I, II	R/S	89, 98
T199I		R	87	D116E, **S405F**	I, III	R	111
G206D		R	105	D116E, V437I	I, III	R/S	89, 109
Y221H		R	95	D116E, G450E	I, III	R	113
T229A		R	93	D116E, V488I	I, III	R	103, 110
I253V		R	87	T123I, **Y132H**	I	R	74, 111
Y257H		R	100	F126L, **Y132F**	I	R	86
I261V		R	89	F126L, K143R	I	R	113
R265G		R	87	K128T, S145L	I	R	94
E266Q	II	R	96	K128T, V452A	I, III	R	94
E266D	II	R/S	74, 83, 87, 93, 97-98, 106-108, 110-111	K128T, Q474K	I, III	R	102
L276S	II	R	95	**Y132F**, K143R	I	R	86
D278E	II	R	98	**Y132F**, F145L	I	R	86
H283D	II	R	87	**Y132F**, S154F [c]	I	R	88, 123
H283R	II	R	90	**Y132H**, S405F	I, III	R	94
K287R	II	R	92	**Y132H**, G448E	I, III	R/S	94, 103, 110
A294V		R	97	**Y132H**, G450E	I, III	R	94, 110-111, 119
G303D		R	87	K143R, E226D	I	R	86
L305P		R	87	F145L, E226D	I	R	86
G307S		R	87, 98	D153E, F145I	I	R	105
V332L		R/S	103	D153F, E266D	II	S	120
K342R		R	87, 110	Y205E, V437I	III	S	109
F380S		R	87	E208K, T525I		R	119
S405F	III	R	90, 93-94, 96, 113	D225H, E266D	II	R	110
S405L	III	R	86	Y257H, G464S	II, III	R	94
P406L	III	R/S	83	M258L, **G464S**	III	R	86
A434V	III	R/S	111	E266D, V332L	II	R	103
V437I	III	R/S	83, 87, 89, 93-94, 96, 98, 105-106, 108, 110, 113, 119	E266D, K342R	II	R	110
D446E	III	R	86	E266D, V437I	II, III	R/S	89, 98
D446N	III	R	86	E266D, **G464S**	II, III	R	86, 92
G448E	III	R	86, 92	E266D, L480F	II, III	R	111
G448R	III	R/S	106	E266D, V488E	II, III	R	92
G448V	III	R	97	E266D, V488I	II, III	R/S	86, 88-89, 98, 105, 110

Table 1.1. Mutations found in ERG11 of *C. albicans* clinical isolates (Continued)

F449L	III	R	[93]	D278N, **G464S**	II, III	R	[86]
F449S	III	S	[94, 113]	K287R, **G464S**	II, III	R	[92]
G307S, G450E	III	R	[86]	F145L, E266D, V488I	I, III	R/S	[94, 98]
V332L, V437I	III	S	[103]	Y205E, E226D, V437I	III	S	[109]
V371I, D446N	III	R/S	[113]	Y205E, A255V, V437I		S	[109]
V371I, **G464S**	III	R	[113]	Y257H, G307S, G464S	II, III	R	[94]
F449S, T229A	III	R	[113]	E266D, L280Y, L281M	II	S	[108]
G450E, D153E	I, III	S	[90]	G307S, L403F, G448R	III	R	[86]
G450E, I483V	III	R	[86]	G307S, V437I, Y447S	III	R	[86]
G450E, G464S	III	R	[94]	**A61V**, Y257H, G307S, G464S	II, III	R	[94]
G450E, V488E	III	R	[92]	A114S, Y205E, Y257H, V437I	I, III	R	[109]
F72L, Y132H, G450E	I, III	R	[119]	A114V, D153E, E266D, G450E	I, II, III	R	[86]
A114V, E226D, H283R	I	R	[86]	A114V, **Y132F**, E266D, V437I	I, II, III	R	[86]
D116E, K128T, A149V	I	R	[120]	D116E, K128T, Y205E, V437I	I, III	R	[109]
D116E, K128T, E266D	I, II	S	[108]	D116E, K128T, **Y132H**, G465S	I, III	R/S	[103, 110-111]
D116E, K128T, **Y132H**	I	R	[102]	D116E, D153E, F72S, F416S	I, III	R	[105]
D116E, K128T, F499Y	I	R	[102]	D116E, I261V, E266D, V437I	I, II, III	R	[89]
D116E, K128T, Q474K	I, III	R	[102]	D116E, E266D, **G464S**, G465S	I, II, III	R	[108]
D116E, E226D, V437I	I, III	R/S	[89, 110]	D116E, L280F, L281M, S284I	I, II	R	[108]
D116E, E226D, V488I	I, III	R/S	[98, 110]	**Y132F**, E266D, I471M, I483V	I, II, III		[86]
D116E, **Y132H**, S405F	I, III	R	[120]	**Y132H**, Y205E, V437I, G472R	I, III	R	[109]
D116E, **Y132H**, G448R	I	R	[103]	**Y132H**, Y205E, V437I, G448E	I	R	[109]
D116E, G307S, G450E	I, III	R	[113]	**Y132H**, G448E, **G464S**, T482A	I, III	R	[105]
T123I, Y123H, L376F	I	R	[111]	E266D, L281Y, I282D, T285H	II	S	[108]
K128T, Y132F, F145L	I	R	[94]	E266D, G307S, G450E, V488I	II, III	S	[124]
K128T, **G464S**, R467I	I, III	R	[94]	E266D, V488I, N349S, G227D	II, III	R	[105]
Y132F, S154F, F145L[c]	I	R	[88]	A61E, E266D, G307S, G450E, V488I	II, III	R	[124]
Y132F, T229A, F449L	I, III	R	[86]	D116E, K128T, K143R, Y205E, V437I	I, III	R	[109]
Y132F, V437I, F449L	I, III	R	[86]	D116E, **Y132F**, K143Q, Y205E, Y257H	I	R	[109]
Y132H, S279F, **G464S**	I, II, III	R	[120]	D116E, **Y132F**, K143Q, Y205E, V437I	I, III	R	[109]
Y132H, Y257H, E266D	I, II	R	[94]	**Y132H**, Y205E, N435V, G448E, D502E	I, III	R	[109]
Y132H, H283R, **G464S**	I, II, III	R	[94]	**Y132H**, G448E, F103L, F198L, F422L	I, III	R	[105]
Y132H, **G464S**, R467K	I, III	R	[120]	K143R, E226D, S412T, R469K, V488I	I, III	R	[108]
K143R, E266D, V488I	I, III	R	[98, 108]	**Y132H**, Y205E, Y257H, E260V, V437I, G448E	I, III	R	[109]

[a] = *C. auris*, [b] = *C. parapsilosis*, [c] = *C. tropicalis*, [d] = *C. neoformans*, [e] = *C. glabrata*

Bold = verified to contribute to resistance by either heterologous gene expression in *S. cerevisiae*, functional expression of *C. albicans* PCR-amplified ERG11, or decreased affinity of ERG11 for azole.

R = resistant, S = sensitive.

[§]Hot spots I, II, and III refer to clusters of residues where mutations commonly occur. I = residues 105-166, II = 266-287, III = 405-488.

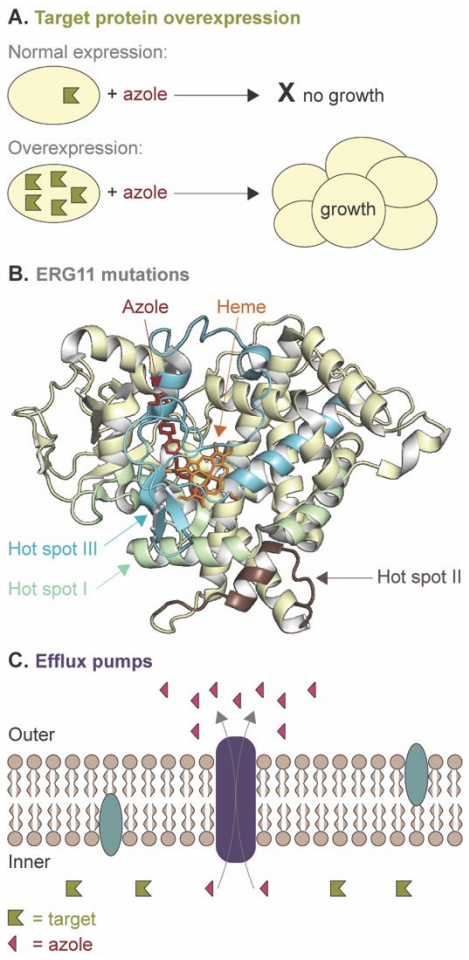

Fig. 1.9. Mechanisms of resistance to azole antifungals include **A.** target protein overexpression, **B.** target protein mutations, and **C.** efflux pumps.

The polyenes are the chronologically oldest class of antifungal drugs but still find frequent use in treating fungal infections. AmB is used clinically for systemic infections, especially in severe cases of candidemia and aspergillosis and in cases where fungal strains display decreased susceptibility to other antifungals, such as the azoles. Investigators report only a few instances of fungal resistance to AmB and other polyenes presumably because the toxicity of polyenes limits patient exposure levels. A few reports describe fungal strains that show reduced susceptibility to AmB at clinically relevant doses (>2 mg/mL).[125-128] With only a few resistant clinical isolates, it is not surprising that there are equally few

reports focused on the specific mechanisms of resistance in clinical isolates. However, studies reveal two resistance mechanisms: (1) decreased amounts of ergosterol in fungal cell membranes (*i.e.*, resistance strategy "iv") (Fig. 1.10A); and (2) increased filamentation (*i.e.*, resistance strategy "iv") (Fig. 1.10B). Typically, polyenes bind to ergosterol in the fungal cell membrane, disrupt the membrane, and induce metal-ion leakage. Fungi capable of surviving with reduced levels of ergosterol thereby decrease their susceptibility to polyenes (Fig. 1.10A)[125-126, 129] and acquire a form of resistance that confers increased survivability. Some evidence suggests that resistant fungi replace ergosterol with another, related sterol, zymosterol (Fig. 1.10A), from the lanosterol-to-ergosterol biosynthetic pathway, and this replacement leads to the retention of membrane integrity (Fig. 1.10A).[125] This process possibly occurs naturally and involves the inhibition of ergosterol biosynthesis by the azoles that in turn drives fungal cells to scavenge for other, structurally related sterols.

Another resistance mechanism against polyenes prevents access of the drug to the ergosterol target by increasing filamentation (Fig. 1.10B). These structures, hyphae, are important for gathering nutrients and also have roles in virulence.[130] Interestingly, in experiments designed to promote the development of resistance with *C. albicans*, increased filamentation also correlated with a decrease in virulence, a finding consistent with the observation that relatively few fungal strains develop resistance to the polyenes.[127, 131]

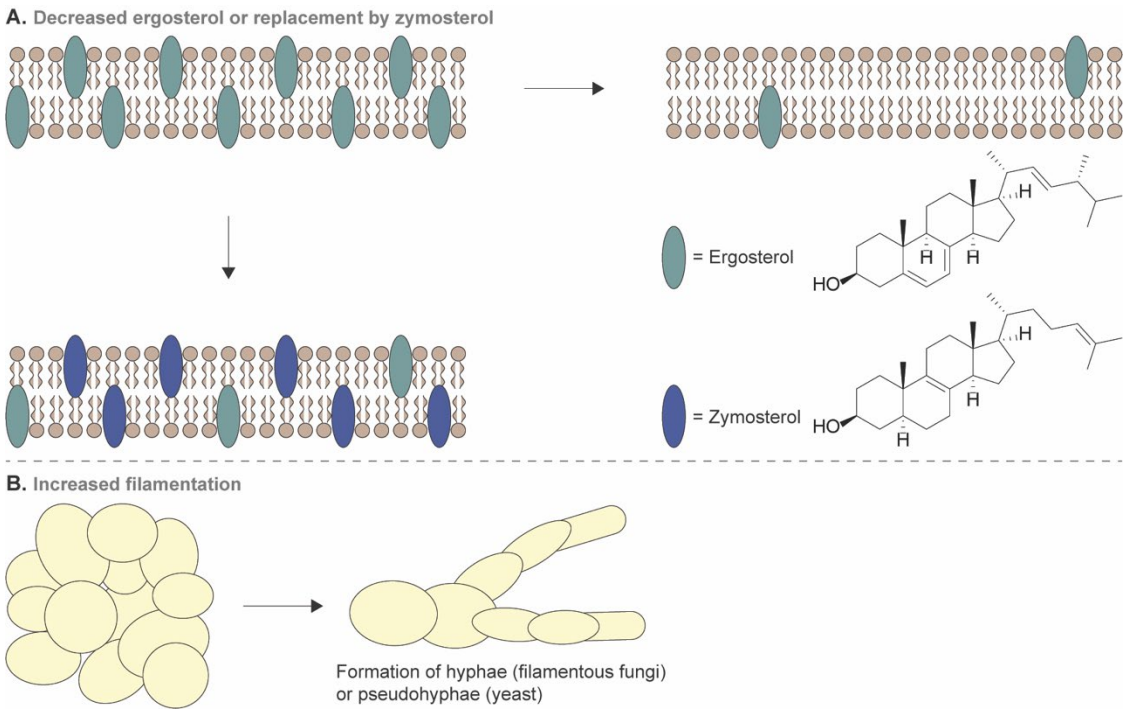

Fig. 1.10. Mechanisms of resistance to polyenes. **A.** Decreased ergosterol levels or ergosterol replacement by zymosterol. **B.** Cartoon illustrating increased filamentation.

The echinocandins are chronologically the newest class of antifungals and have a narrow-spectrum of applications. While resistance to echinocandins is still considered rare, several reports, primarily using *C. glabrata*, show decreased susceptibility to CAS and other echinocandins.[132-138] The target of the echinocandins, β-1,3-glucan synthase, appears in the fungal plasma membrane and possesses Fks1, a catalytic subunit regulated by the GTP-binding protein, Rho (Fig. 1.11A). In addition to Fks1, fungi also possess highly homologous Fks2 and Fks3 proteins that may have resulted from gene duplication events. Although Fks2 and Fks3 have lower expression levels than Fks1, they may play some role in the regulation of Fks1.[139] Resistance to echinocandins ties to mutations in the Fks1 and Fks2 proteins (*i.e.*, resistance strategy "iii") (Fig. 1.11). Of the strains that show reduced susceptibility to echinocandins, most possess mutations in Fks1. These mutations commonly occur in three hot spot regions of the Fks1 protein: hot spot region I involves

residues FLTLSLRDPI, region III involves WRNIFTRL, and region II involves residues PAIDWIRR (Fig. 1.11B, Table 1.2).[140-141] These hot spot regions are highly conserved sequences among the *Candida* species and are the focus for Fks mutations. However, residue numbering for these hot spots varies among reports; therefore, we summarize this information in Table 1.2 in Fig. 1.12 and we normalize the numbering systems to emphasize the specificity of mutations in these hot spots. All of these hot spot regions occur on the extracellular surface of the protein that is the binding site for echinocandins.[141] These mutations not only decrease fungal susceptibility to CAS, but also to other echinocandins.[132, 142] Studies of resistance development *in vitro* corroborate the locations and effects of these mutations.[143] Although less common, other echinocandin-resistant strains contain mutations in the Fks2 regulatory subunit.[144-145] Finally, a few reports describe examples of strains resistant to echinocandins with no mutations in the glucan synthase genes. In these strains, the resistance results from decreased expression levels of the *fks* genes, and an increase in chitin production compensates for the loss of β-1,3-glucan.[139, 146-148]

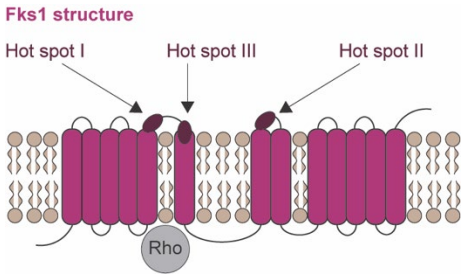

Fig. 1.11. Mechanism of resistance to echinocandins. Mutations in the target protein, Fks1, are located in three hot spot regions.

Table 1.2. Mutations found in Fks1 and Fks2 of *C. glabrata* clinical isolates unless otherwise noted by a superscript letter beside the mutations.

Fks1 Mutations	Hot spot[§]	R/S	Ref.	Fks2 Mutations	Hot spot[§]	R/S	Ref.
F625C	I	S	149	F641Y[a]	I	R	150
F625Y	I	S	151-152	F641V	I	R	150
F625S	I	R	152-155	L644W	I	S	156
S629P[a]	I	R	136, 149, 152-153, 155, 157	**S645P**	I	R	156, 158
L630I	I	S	152-153	**E655K**	I	R	159
R631G	I	R/S	136, 152, 154	F658S	I	R	160
R631S	I	R	153	F658Y	I	R	160
S631Y[e]	I	R	161	F658del	I	R	160
D632E	I	R/S	152, 154	F659S	I	R/S	153, 155, 162-163
D632Y	I	R/S	152-153, 159	F659V	I	R	153
I634V	I	R/S	149, 152, 154, 160	F659Y	I	R	151, 153, 155
S638P[e]	I	R	161	F659del	I	R	153, 162
S638Y[e]	I	R	161	S662F	I	R/S	160, 164
F641S[a,f]	I	R	152, 156, 158	S662P	I	R	160
F641Y[a]	I	R/S	152, 156	L662W	I	R	153
S645S[a]	I	R	152	S663F	I	R/S	136, 149, 153, 157
S645P[a,b,f]	I	R	151-152, 155-159, 163	S663P	I	R	136, 149, 151, 153, 155, 157
F645Y[a]	I	R	152	S663Y	I	R	153
R647G[a]	I	R/S	165	L664R	I	R/S	153
D648Y[a]	I	S	152	R665G	I	S	136
P649L[a]	I	S	165	D666Y	I	R/S	153
P649H[a]	I	S	152	P667H	I	R	136, 160
F658del	I	R	152, 154	P667T	I	R/S	155
F659L	I	R/S	159	P1371S	II	R/S	153
F659S	I	R/S	152, 159	R1377K	II	R	164
F659V	I	R	152, 154	**Multiple mutations**			
F659Y	I	R/S	152	F625S, F659Y	I	R	155
S662P	I	R	160	F629P, R631S	I	R	152
L662W	I	R/S	152	F629P, S663P	I	R	155
S663Y	I	R	152	R664G, D665V	I	R	160
S663F	I	S	152	S629P, D665V	I	R/S	160
S663P	I	R	152, 154, 159	L635V, T655A[b]	I	S	157
R664G	I	R/S	160	R647G, P649L[a]	I	R	165
R665G	I	R/S	152, 154	**W695L**, Y696N	III	R	166
R665S	I	R/S	152, 154	F659S, S663A	I	R	163
D665V	I	R	160	F659S, S663A, D666E	I	R	163
D665Y	I	S	160				
P667F	I	R/S	152				
P667T	I	R	154				
H675Q[d]		R/S	157				
W695L	III	R	166				
L701M[d]	III	R/S	152-153				
I1379V	II	S	152, 154				
R1344S[c]	II	R	151, 159				

[a] = C. albicans, [b] = C. dubliensis, [c] = C. kefyr, [d] = C. krusei, [e] = C. lusitanea, [f] = C. tropicalis.
Bold = verified to contribute to resistance by either heterologous gene expression in *S. cerevisiae* or *C. glabrata*, site-directed mutagenesis, or inhibition of purified protein.
R = resistant, S = sensitive.
[§]Regions of the Fks proteins where mutations are commonly found are divided into three regions: residues 625-667 (I), 695-701 (III), and 1371-1379 (II).

FKS1, hot spot 1

Strain	F	L	T	L	S	L	R	D	P	I
CG	625C/Y/S	-	-	-	629P	630I	631G/S	632E/Y	-	634V
CA	-	-	-	-	629P	-	-	-	-	-
CL	-	-	-	-	631Y	-	-	-	-	-
CT	641S	-	-	-	-	-	-	-	-	-
CA	641S/Y	-	-	-	645F/P/Y	-	647G	648Y	649 L/H	-
CD	-	-	-	-	645P	-	-	-	-	-
CG	-	-	-	-	645P	-	-	-	-	-
CG	658del	-	-	-	662P	-	664G	665V/Y	-	-
CG	659L/S/V/Y	-	-	662W	663F/P/Y	-	665G/S	-	667F/T	-

FKS2, hot spot 1

Strain	F	L	T	L	S	L	R	D	P	I
CA	641Y	-	-	-	-	-	-	-	-	-
CG	641V	-	-	644W	645P	-	-	-	-	-
CG	658S/Y/del	-	-	-	662F/P	-	-	-	-	-
CG	659S/V/Y/del	-	-	662W	663F/P/Y	664R	665G	666Y	667H/T	-

FKS1, hot spot 3

Strain	W	R	N	I	F	T	R	L
CG	695L	-	-	-	-	-	-	-
CK	-	-	-	-	-	-	-	701M

FKS1, hot spot 2

Strain	P	A	I	D	W	I	R	R
CG	-	-	-	-	-	1379V	-	-
CG	-	-	-	-	-	-	1344S	-
C kefyr	-	-	-	-	-	-	1344S	-

FKS2, hot spot 2

Strain	P	A	I	D	W	I	R	R
CG	1371S	-	-	-	-	-	-	1377K

Fig. 1.12. Summary of Table 1.2 showing the different numbering based on the different fungal strains. *Note*: CA = *C. albicans*, CD = *C. dubliniensis*, CG = *C. glabrata*, CK = *C. krusei*, CL = *C. lusitaniae*, CT = *C. tropicalis*.

1.2.4. Fungal biofilms

Within the human body, fungi survive only if successful in scavenging for nutrients, avoiding the host immune system, and resisting antifungal drug treatment. Many fungal pathogens produce biofilms as a barrier to evade antifungal drugs and as a mechanism to avoid detection by the immune system. Fungi that manufacture biofilms include *Candida*,[167] *Aspergillus*,[168] *Cryptococcus*,[169] *Fusarium*,[170] *Coccidioides*,[171] *Trichosporon*,[172] *Malassezia*,[173] *Blastoschizomyces*,[174] and *Zygomycetes* (*Mucor* and *Rhizopus*).[175] Biofilm production commonly occurs on biological surfaces such as mucosal membranes and, most diabolically, also occurs on medical devices such as catheters. The first step in biofilm formation requires the attachment of fungal cells to surfaces (Fig. 1.13).

During the initiation of this process, the fungal cells divide and produce hyphal filaments to increase their surface area as a means of scavenging for nutrients. As the biofilm matures, the fungi produce an extracellular matrix that is the identifying characteristic of a biofilm. This extracellular matrix possesses many of the same elements that appear in fungal cell walls including glucan and mannan polymers. This matrix acts as a "glue" that surrounds fungal cells within the biofilm's perimeter, sequesters antifungal drugs, and prevents them from penetrating into the fungal cells. In addition, fungal cells also express efflux pumps that expel any drug that might avoid capture in the biofilm. As a result, fungal cells with biofilms show as much as a 10,000-fold decrease in their susceptibility to antifungal drugs relative to the susceptibility of planktonic (free-floating) fungal cells.[172] Given the magnitude of the protection from drugs that biofilms provide, it is not surprising that fungal cells within biofilms are better able to survive than those without it. Once the biofilm reaches maturity, it opens to release fungal cells that disperse and form new biofilms elsewhere. The importance of this *in vivo* process for the survival of fungal cells underscores the importance of developing *in vitro* biofilm models to study biofilm growth patterns during infection[176] and to understand the role of biofilms in the re-occurrence of fungal infections.

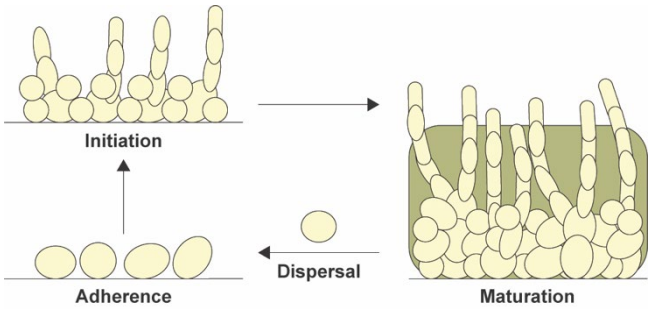

Fig. 1.13. Fungal cells that successfully adhere to medical devices or biological surfaces initiate biofilm development (shown as a green rectangle) by replicating and forming hyphae. Mature biofilms develop an extracellular matrix of various glucans to form a protective barrier to drugs.

1.3. DISCOVERY AND DEVELOPMENT OF NEW COMPOUNDS WITH ANTIFUNGAL ACTIVITY

The development of new mutants of known fungi and the appearance of new species of fungi unresponsive to current drug therapies provide the momentum for studies of fungal resistance. Given the rapidity with which an unknown organism, such as *C. auris*, leaps from obscurity to the popular press, it is not surprising that none of the compounds described in the following sections of this review, are yet tested against *C. auris*. This pathogen must be included in future, antifungal drug discovery. Studies designed to combat resistance utilize four strategies: (i) design and synthesis of new derivatives of current antifungal agents, (ii) design and synthesis of new synthetic scaffolds as antifungal agents, (iii) repositioning of drugs or their derivatives used for other medicinal purposes as antifungal agents, and (iv) isolation and/or derivatization of newly discovered natural products possessing antifungal activity. In the sub-sections below, we will discuss these categories and present the leading, representative compounds developed under each of these strategies.

We will only briefly summarize the synthetic routes and the data from the subsequent biochemical, computational, and biological assays. In this review, we will arbitrarily define antifungal activity as follows: excellent (≤2 μg/mL), good (3.9-8 μg/mL), and poor (≥15.6 μg/mL). We will not endeavor to show all molecules synthesized for each scaffold; but instead, we will depict a select group of the most active representatives. We acknowledge and understand the many contributions of scientists who synthesized molecules not

appearing in this review, and we trust that they understand the space limitations that dictate this course of action.

1.3.1. Design and synthesis of derivatives of current antifungal agents

Extensive derivatization of compounds from the five classes of FDA-approved antifungal agents, namely the azoles, polyenes, echinocandins, allylamines, and antimetabolites (Figs. 1.4-1.7), continues unabated. This section of this review briefly defines prior efforts and describes the challenges that these studies must overcome. These efforts, coupled with a renewed interest in the identification of new pharmacophores, underscore the "promise and perspective" phrase in the title of this review.

1.3.1.1. Azole derivatives - imidazoles

Although azoles find widespread use in clinical settings because of their broad-spectrum antifungal activity and oral bioavailability, further efforts to modify this important pharmacophore focus on reducing cytotoxicity and drug-drug interactions as well as identifying new candidates to help in the fight against fungal resistance. Among the imidazole-based antifungals, MCZ and ECO served as a starting point for the preparation of four new types of antifungal agents (Fig. 1.14).[177-180] In two cases (*i.e.*, **1**-**4** and **10**-**12**), either the 4-chlorobenzyloxy group of ECO or the 2,4-dichlorobenzyloxy group of MCZ was replaced by different substituents in the 1-(2,4-dichlorophenethyl)-1*H*-imidazole core. In two other cases, either the 4-chlorobenzyloxy group and the 2,4-dichlorophenyl group in ECO underwent modification (*i.e.*, **5**-**9**) or the imidazole, the 4-chlorobenzyloxy group and the 2,4-dichlorophenyl group in MCZ underwent modification (*i.e.*, **13**). The following

discussion will consider the four cases in turn and will summarize the synthetic approach and highlight the reported activities.

In the first case, replacement of either the 4-chlorobenzyloxy of ECO or the 2,4-dichlorobenzyloxy of MCZ led to analogs with benzyloxy or phenethyloxy substituents in the 1-(2,4-dichlorophenethyl)-1*H*-imidazole core. A three-step synthesis that illustrated the approach taken to these pharmacophores involved a Corey-Chaykovsky epoxidation of aldehydes[181-182] using dimethylsulfonium methylide followed by epoxide opening and coupling with alkyl halides (**1-4**; Fig. 1.14).[177] The imidazoles **1-4** displayed excellent activity (MIC values of 0.06-1 μg/mL (comparable to those of ITC that served as a standard) against twenty-nine *C. albicans* and seven non-*albicans Candida* strains (*C. glabrata*, *C. krusei*, *C. lipolytica*, *C. parapsilosis*, *C. pseudotropicalis*, *C. tropicalis*, and *C. utilis*). However, these analogs were inactive against four filamentous fungal strains (*M. hiemalis*, *A. fumigatus*, *T. cutaneum*, and *R. oryzae*). MIC data were provided without comparable MIC values for MCZ and ECO from which these compounds were derived, and consequently, the potential benefits of these new derivatives **1-4** relative to those of the parent antifungals ECO and MCZ remained unclear.

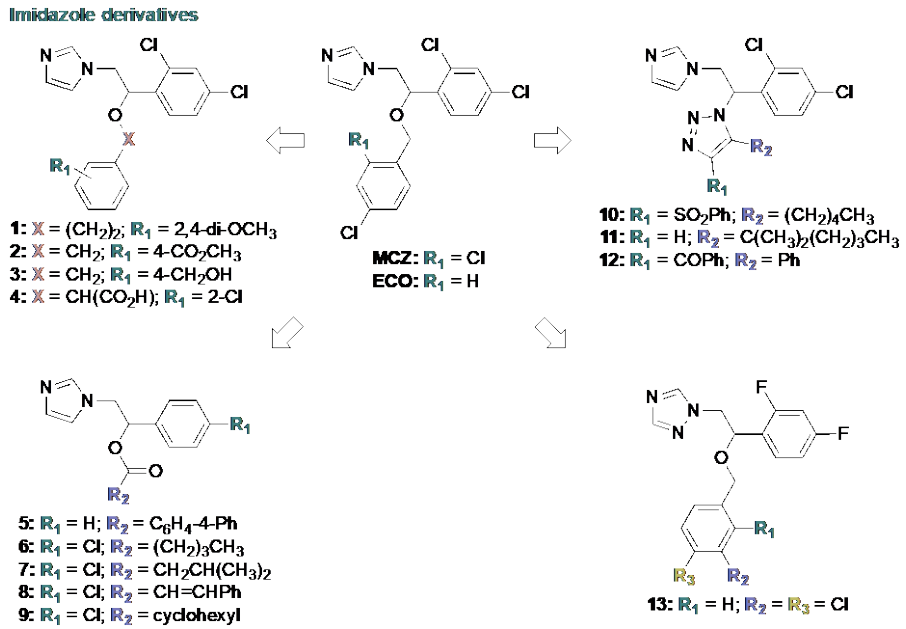

Fig. 1.14. Representative, new scaffolds tested as potential antifungals that are derived from current imidazoles MCZ and ECO.

In the second case, both the 4-chlorobenzyloxy group and the 2,4-dichlorophenyl group in ECO underwent modification. Replacement of the 4-chlorobenzyloxy of ECO with aliphatic or aromatic esters and replacement of the 2,4-dichlorophenyl of ECO by either a 4-chlorophenyl or a phenyl group afforded a total of thirty new ECO derivatives including representative examples **5-9** (Fig. 1.14).[178] When tested against *C. albicans* and *C. parapsilosis*, thirteen of these compounds displayed excellent activity with MIC values of 0.125-2 μg/mL that were comparable to that of FLC (Fig. 1.4) (MIC = 0.25 μg/mL). When examined against a FLC-resistant *C. glabrata* clinical isolate, five of these compounds **5-9** displayed excellent activity (MIC values 0.25-2 μg/mL) (Fig. 1.14). Compounds **5-7** and **9** also inhibited *C. albicans* biofilm formation at a concentration of 8 μg/mL, but required concentrations in the 512-1024 μg/mL range to eradicate the biofilm. Computational modeling of the relative binding affinity of compounds **5**, **6**, and **9** in the *C. albicans* CYP51

active site was consistent with the observed levels of antifungal activity. Although comparison of MIC values was not made with the parent ECO, these imidazole-containing molecules possessed promise as antifungals.

In a third case, replacement of either the 4-chlorobenzyloxy group of ECO or the 2,4-dichlorobenzyloxy group of MCZ by a series of 1,2,3-triazoles made use of 1,3-dipolar cycloadditions to furnish **10-12** (Fig. 1.14).[179] When tested against *A. fumigatus*, *C. albicans*, *C. tropicalis*, *C. utilis*, *M. hiemalis*. *R. oryzae*, and *T. cutaneum*, the triazole-imidazole **10** displayed excellent activity against these fungal strains with MIC values of 0.06-2 μg/mL that was comparable to that of ITC (Fig. 1.4) (MIC = 0.03-1 μg/mL). Triazole-imidazole **11** also showed excellent activity against four of these strains (MIC values of 0.03-2 μg/mL), but triazole-imidazole **12** only showed activity against two *Candida* spp. strains (MIC values of 0.03-0.06 μg/mL). In yeast sensitivity assays, *C. utilis* was generally resistant to **10-12**, while *C. albicans* and *C. tropicalis* were susceptible to these agents. Although the MCZ analogs showed promise because of their low MIC values, further comparisons with MCZ as well as determinations of cytotoxicity in mammalian cells, mechanism of action studies, and potential for resistance development will be needed to establish the promise of these compounds as antifungal agents.

In a final case, the imidazole, the 2,4-dichlorobenzyloxy group and the 2,4-dichlorophenyl group in MCZ underwent modification to afford the difluoro analogs such as **13** (Fig. 1.14).[180] Among the reported twenty-four compounds that were synthesized, only compound **13** displayed excellent to good antifungal activity against five fungal strains (*A.*

flavus, *Beer yeast*, *C. mycoderma*, *C. albicans*, and *C. utilis*) with MIC values of 0.5-8 μg/mL that were better than those of the standards: FLC (MIC = 1-256 μg/mL) and MCZ (MIC = 4-256 μg/mL). Computational modeling of **13** in the CYP51 active site provided a preliminary explanation of the observed antifungal activity as a lanosterol 14α-demethylase inhibitor. Testing against a broad panel or resistant fungal clinical isolates, cytotoxicity studies, as well as confirmation of the mode of action of compound **13** will be needed to ascertain the value of this scaffold as an antifungal agent.

1.3.1.2. Azole derivatives - triazoles

Fluconazole (FLC) (Fig. 1.15) served as a departure point for numerous studies leading to promising, new antifungal agents. In most cases, investigators modified only one of the two 1-(1*H*-1,2,4-triazol-1-yl)methylene subunits in FLC. Two synthetic strategies involving replacement of one of the 1-(1*H*-1,2,4-triazol-1-yl)methylene subunits led to racemic mixtures: (1) nucleophilic addition of Grignard reagents to a 2-(1*H*-1,2,4-triazol-1-yl)-acetophenone derivative (*i.e.*, "ketone strategy"); and (2) nucleophilic addition of primary or secondary amines, azides, or thiols to the unsubstituted terminus of an epoxide group in modified 1-((2-(phenyl)oxiran-2-yl)methyl)-1*H*-1,2,4-triazole (*i.e.*, "epoxide strategy") (Fig. 1.15). Both strategies are, in fact, linked in the sense that the epoxides are derived from the acetophenones using a sulfur ylid addition.

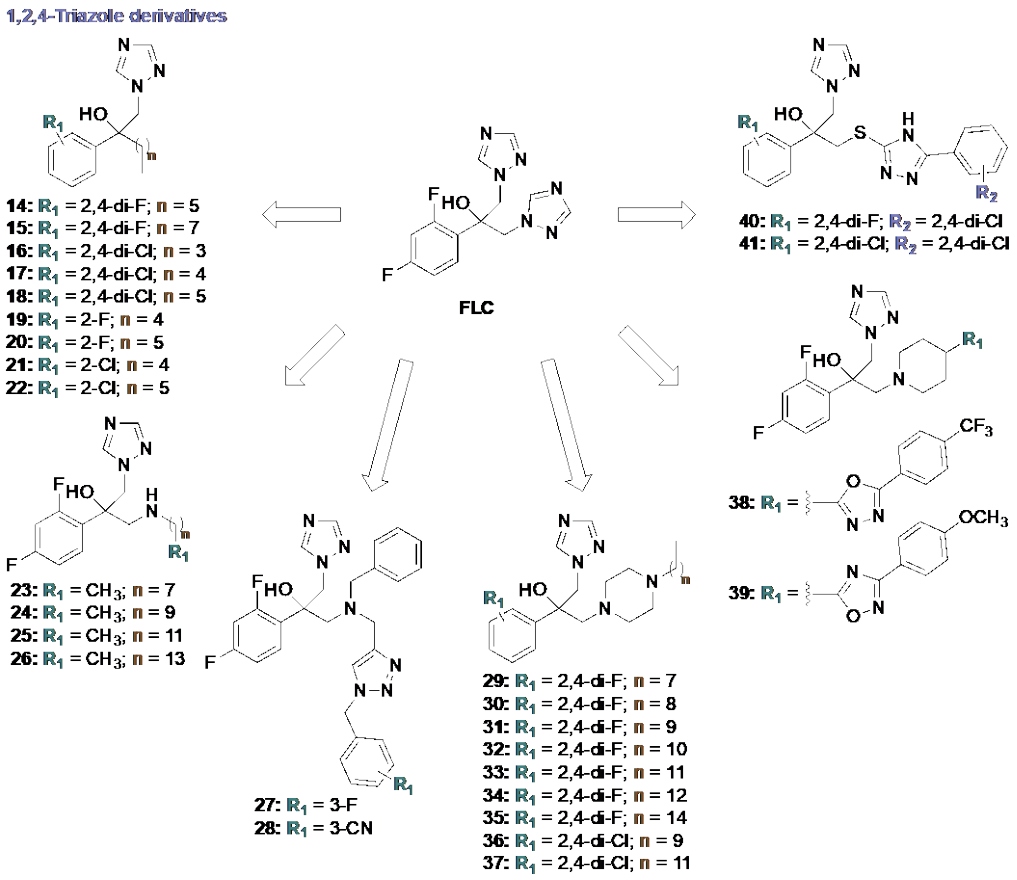

Fig. 1.15. Representative examples of six new scaffolds derived from FLC and tested as potential antifungals.

In a comprehensive study, one of 1-(1*H*-1,2,4-triazol-1-yl)methylene subunits in FLC was replaced by hydrophobic, alkyl chains to render the molecule more amphiphilic than FLC, and in addition, the 2,4-difluorophenyl of FLC was modified as either a monofluoro-, monochloro-, difluoro-, or dichlorophenyl group in relatively few synthetic steps to afford twenty-seven FLC derivatives **14-22** (Fig. 1.15).[183] When tested against seven strains of *C. albicans*, three strains of non-*albicans Candida* (*C. glabrata*, *C. krusei*, and *C. parapsilosis*), and three strains of *Aspergillus* spp. (*A. flavus*, *A. terreus*, and *A. nidulans*), nine of these monotriazoles **14-22**, displayed excellent activity against at least eight of the thirteen strains tested (MIC values of <0.03-1.95 μg/mL that were comparable to that of FLC (MIC = 1.95 μg/mL) and also displayed activity against three ITC- and FLC-resistant

C. albicans strains. These FLC derivatives displayed chain-length dependent, hemolysis activity (<50% at 10× MIC). In cytotoxicity experiments using the normal human bronchial epithelial cell line (BEAS-2B), eight of these FLC derivatives had no toxicity at concentrations of >31.3 μg/mL. Monotriazoles **14** and **18** showed fungistatic activity at 1× MIC and fungicidal activity at 4× MIC against *C. albicans*. The mechanism of action of these monotriazoles was investigated using a membrane-permeabilization assay and an analysis of the sterol composition of the fungal cell lysates with and without monotriazole treatment. Consistent with FLC, the monotriazole **18** inhibited the lanosterol 14α-demethylase enzyme of the ergosterol biosynthetic pathway. These FLC derivatives showed great promise as antifungal agents because of their low MIC values, minimal toxicity, and no adverse hemolysis outcomes.

In another thorough study, the 1-(1*H*-1,2,4-triazol-1-yl)methylene subunit of FLC was similarly replaced by a series of *N*-(alkylamino)-, *N*-(arylamino)-, and *N*-(cycloalkylamino)methylene substituents or by a series of *N,N*-(dialkylamino)methylene substituents using the epoxide strategy described earlier to afford twelve FLC derivatives **23-26** (Fig. 1.15).[184] When tested against the same thirteen strains as those in the study focused on the FLC derivatives **14-22**,[183] eight of the twelve compounds displayed excellent activity against at least one of the thirteen strains. Compounds **23-26** displayed excellent activity against anywhere from three to six of the thirteen strains tested, including three ITC- and FLC-resistant *C. albicans* strains with MIC values of 0.03-1.95 μg/mL comparable to that of FLC (MIC = 1.95 μg/mL). The compounds **23-26** also exhibited excellent activity against clinical isolates of *C. glabrata*, *C. parapsilosis*, and *C.*

neoformans with MIC values of 0.03-1.95 μg/mL comparable to that of FLC (MIC = 0.975-1.95 μg/mL). In cytotoxicity experiments using the human embryonic kidney (HEK-293), BEAS-2B, and human adenocarcinoma (A549) mammalian cell lines, compounds **23** and **24** were less toxic than **25** and **26** at concentrations up to 31 μg/mL. Compounds **23** and **24** displayed fungistatic activity at 4× MIC against *C. albicans* and *C. parapsilosis*. In a mechanism of action study using a membrane-permeabilization assay, compound **25** with a C_{12} alkyl chain caused membrane disruption in *C. albicans*, while compound **26** with a C_{14} alkyl chain did not. Determination of sterol composition showed that **25** and **26** inhibit ergosterol biosynthesis, once again a finding that was consistent with the known mechanism of action of the parent compound FLC. With low MIC values, minimal toxicity, and no adverse hemolysis outcomes, these FLC derivatives warranted further investigation.

The epoxide strategy was also utilized in a third study that was limited in scope to the determination of MIC_{80} values for seventeen FLC derivatives in which the 1-(1*H*-1,2,4-triazol-1-yl)methylene subunit in FLC was replaced by a tertiary amine bearing a second, more distant 1-(1*H*-1,2,4-triazol-1-yl)methylene subunit than the one in FLC.[185] Unfortunately, none of the seventeen, tertiary amines synthesized in the course of this study affected any of the eight fungal strains (two *C. albicans*, *C. glabrata, C. parapsilosis*, *C. neoformans*, *A. fumigatus*, *T. rubrum*, *M. gypseum*). Only two compounds, **27**-**28** (Fig. 1.15), had similar MIC_{80} values to FLC against two *C. albicans* and one *C. neoformans*, and displayed better activity than FLC against one *M. gypseum* found in skin and nail infections. These data clearly underscored the notion that the structure and the relative proximity of the two 1-(1*H*-1,2,4-triazol-1-yl)methylene subunits in FLC was crucial for

antifungal activity and analogs along the lines of those in tertiary amines **27-28** did not warrant further investigation.

The epoxide strategy again appeared in a fourth study involving the addition of *N*-alkylpiperazines that led to nine new FLC analogs **29-37**, two of which contained a 2,4-dichlorophenyl in place of the 2,4-difluorophenyl of FLC (Fig. 1.15).[184] Two of these nine compounds (*i.e.*, those with *N*-methyl and *N*-n-pentyl chains on the *N*-alkylpiperazines) did not display strong activity against the thirteen fungal strains (seven *C. albicans*, three non-*albicans Candida*, and three *Aspergillus*). The remaining nine derivatives **29-37** (Fig. 1.15) displayed excellent activity against the three *Aspergillus* spp. tested (*A. flavus*, *A. nidulans*, and *A. terreus*) with MIC values of 0.975-1.95 μg/mL. These values were much better than that that of FLC (MIC = 62.5 μg/mL). Eight of these nine compounds had excellent activity against *C. parapsilosis* (excluding **35**) as well as *C. krusei* and one *C. albicans* (excluding **29**) with MIC values of 0.015-1.95 μg/mL that were comparable or better than that of FLC (MIC = 1.95 μg/mL against *C. parapsilosis*, ≥31.3 μg/mL against *C. krusei*, and 62.5 μg/mL against *C. albicans*). In general, most compounds had good activity (3.9-7.8 μg/mL) against *C. glabrata* and six other *C. albicans* strains for which the parent FLC was inactive (≥15.6 μg/mL). Compounds **31**, **33**, **36**, and **37** were also able to eliminate pre-formed *C. albicans* biofilms. Two of these compounds, **31** and **33**, demonstrated fungicidal activity at 4× MIC against *C. albicans* and *C. glabrata*. Compounds with alkyl chains greater than C_{10} exhibited higher hemolytic activity compared to compounds with alkyl chains with eight or fewer carbons. Compound **31** displayed the lowest hemolytic effect, similar to that of the standard VRC (Fig. 1.4). Chain

length dependence appeared in cytotoxicity studies using HEK-293, A549, and BEAS-2B mammalian cell lines, and compounds **31** and **36** with a C_{10} alkyl chain were generally safe up to 7.8 μg/mL whereas compounds **33** and **37** with a C_{12} alkyl chain were toxic at the same concentrations. Membrane-permeabilization assays of **31** and **37** in *C. albicans* showed that the mechanism of action was not membrane disruption but once again, inhibition of ergosterol biosynthesis. Molecular docking into the CYP51 active site of *C. albicans* with compound **31** was consistent with this proposed mechanism of action. On balance, the development of these FLC derivatives as antifungal agents warranted additional investigation.

In a fifth study along similar lines, the epoxide strategy furnished new FLC analogs **38-39** (Fig. 1.15) in which 4-arylpiperidines replaced one of the 1-(1*H*-1,2,4-triazol-1-yl)methylene subunits in FLC.[186] The aryl substituents (*i.e.*, R_1 in Fig. 1.15) on the piperidine ring included 1,2,4- and 1,3,4-oxadiazoles substituted with various aromatic groups. Among the twenty-five FLC derivatives, several of these compounds were safe at concentrations of 160 μg/mL in the nematode, *Caenorhabditis elegans*, but none of these analogs completely killed (only MIC_{80} values provided) any of the seven fungal strains tested, including *C. albicans*, *C. parapsilosis*, *C. neoformans*, *C. glabrata*, *A. fumigatus*, *T. rubrum*, and *M. gypseum*. Overall the compounds showed MIC_{80} values similar to or slightly better than that of the standard FLC. When tested against three strains of FLC-resistant *C. albicans*, analogs **38** and **39** were not particularly active (mean MIC_{80} 8-16 μg/mL). Mechanism of action studies involved molecular docking studies consistent with **38** and **39** binding to the CYP51 active site, but they also showed mild activity against

hyphal formation in *C. albicans*. In the absence of complete fungal growth inhibition, additional studies in this series would not appear to be promising.

In a sixth study, the nucleophilic ring-opening of an epoxide by thiols served to generate eighteen new FLC analogs in which one of the 1-(1*H*-1,2,4-triazol-1-yl)methylene subunits in FLC was replaced by 5-aryl 4*H*-1,2,4-triazole-3-thiomethylene subunit and in some instances the 2,4-difluorophenyl group was also replaced by a 2,4-dichlorophenyl group (**40**-**41**; Fig. 1.15).[187] Among these new analogs, six displayed excellent activity with MIC values in the 0.03-1 μg/mL range against two *C. albicans* strains. These outcomes represented a 2- to 16-fold improvement over the values for the control FLC. Two of these, **40** and **41**, were also found to be active (MIC values of 0.25 μg/mL) against an FLC-resistant (MIC of FLC = 64 μg/mL) *C. glabrata* strain. None of the eighteen compounds synthesize were active against *A. fumigatus* and *C. neoformans*. The preliminary nature and limited scope of biological testing in this work precluded a complete understanding of the potential value of these compounds.

In a final study, albaconazole (ALB) instead of FLC was used as the departure point for the development of still other, antifungal agents.[188] Replacing the quinazolinone ring in ALB, which is currently in clinical development, with a 5,6-dihydro-4*H*-thieno[2,3-*c*]pyrrol-4-one ring or a 4,5-dihydro-6*H*-thieno[2,3-*c*]pyrrol-6-one ring led to the analogs **42**-**62** (Fig. 1.16). Two different synthetic strategies involving eight or nine steps and relying heavily on Suzuki couplings, were used to produce thirty ALB analogs **42**-**62** with varied orientation of the substituted thiophene indicated by **a** or **b** in Fig. 1.16. These

derivatives were potent against all *Candida* strains, including *C. albicans*, *C. parapsilosis*, and *C. glabrata* with MIC values of 0.0078-1 μg/mL comparable to that of ALB (MIC = 0.0078-0.0625 μg/mL). They also displayed excellent activity against *C. neoformans* (MIC values of 0.0078-0.25 μg/mL). Only derivatives with the thiophene in series **a** displayed good activity against *A. fumigatus* (MIC values mostly of 4-8 μg/mL compared to that of 0.25 μg/mL for ALB). These compounds warrant additional study focused on the level of cytotoxicity, the potential development of resistance, and the mechanism of action.

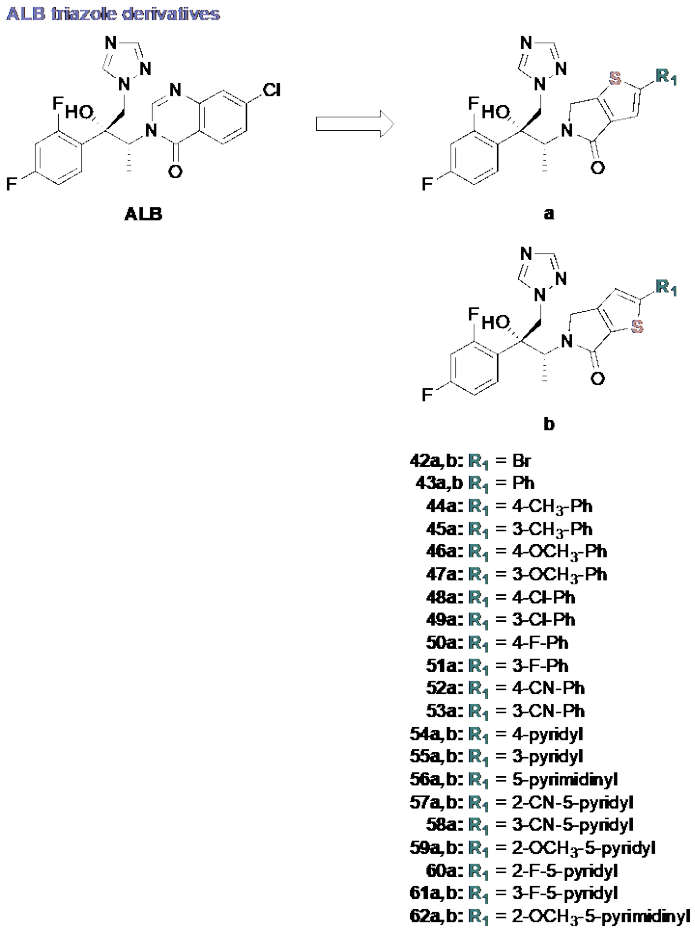

Fig. 1.16. Representative examples of compounds possessing a new scaffold derived from ALB and tested as potential antifungals.

In summary, the success of FLC in clinical practice naturally attracted interest in identifying new analogs that shared its broad spectrum of activities and possessed activity against FLC-resistant strains. Investigators sought to retain the facile, synthetic accessibility of this pharmacophore with the goal of increased potency against strains not affected by FLC, reduced cytotoxicity against normal mammalian cells, and reduced tendency to develop resistance. Reports for a number of these new analogs including **14-22**, **22-26**, **29-37**, and possibly **40-41** are sufficiently interesting to warrant additional effort to define the parameters that would comprise an improvement over FLC. Many of the new analogs shared a common feature in their mechanism of action that disrupted ergosterol biosynthesis. All of the new analogs shared an additional common feature in the possession of one (Fig. 1.15) or two stereogenic centers (Fig. 1.16). No reports, however, of stereoselective syntheses or resolution of enantiomers appeared in the literature surrounding these compounds. It would be interesting to determine, particularly since many of these analogs bind a specific enzyme in the ergosterol biosynthetic pathway, if one enantiomer in the FLC series (Fig. 1.15) or one diastereomer in the ALB series (Fig. 1.16) possessed differential antifungal activities.

1.3.1.3. Polyene derivatives

Polyenes such as amphotericin (AmB) and nystatin (NYT) are currently used as the second-line of defense against intractable fungal infections, and structural modifications invariably focus on the goal of decreasing their inherent toxicity and increasing both their therapeutic efficiency and water solubility. Structural modifications of AmB and NYT were non-trivial adventures given the complexity of these natural products. Several interesting reports

described three general types of modifications to AmB: (i) hydration of the Δ^{30}- and Δ^{32}-double bonds to furnish the C-31 and C-33 hydroxylated products, (ii) acylation of the primary amine on mycosamine, and/or (iii) coupling of the C-16 carboxylic acid to specialized, primary amines to afford carboxamides (Fig. 1.17A). Modifications of NYT followed a similar, specialized pathway involving (i) oxidation of NYT to introduce the Δ^{28}-double bond and/or (ii) acetal formation between the C-4 hydroxyl of mycosamine and the anomeric center of *N*-acetylglucosamine (Fig. 1.17B).

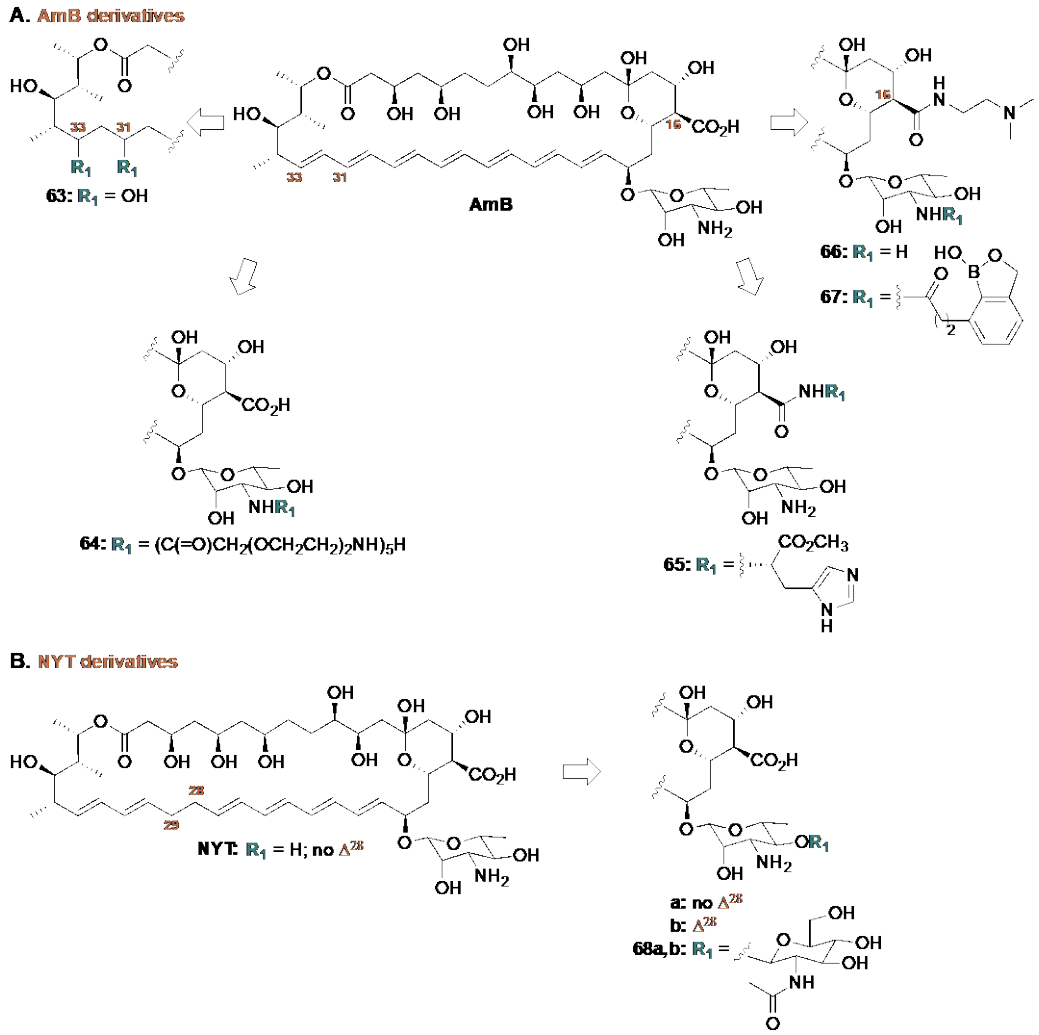

Fig. 1.17. Representative examples of compounds from five new scaffolds tested as potential antifungals, which are derivatives of **A.** AmB or **B.** NYT.

In a study designed to establish the importance of the unsaturated heptaene substructure in AmB, the Fe^{III}-catalyzed hydration of AmB led to the C-31,33 diol **63** (Fig. 1.17A).[189] Although AmB analog **63** displayed lower cytotoxicity than that of AmB in green monkey kidney cells, it unfortunately showed reduced antifungal activity when tested against *C. albicans* and *C. parapsilosis* (MIC values of 4-8 μg/mL compared to 0.25-0.5 μg/mL for the parent AmB). In addition, AmB analog **63** showed a decreased therapeutic index, defined as the ratio between half-maximal cytotoxic concentration and MIC value. This

outcome suggested that *in vivo* hydration of AmB leading to **63** would be harmful to patients.

In another study, acylation of the primary amine on the mycosamine moiety with various carboxylic acids led to nine, new AmB derivatives, including the carboxamide in analog **64** (Fig. 1.17A).[190] Five of these compounds displayed MIC values of 2-4 μg/mL, similar to that of the parent AmB (MIC = 1 μg/mL). One of these derivatives, namely the carboxamide **64**, showed increased water solubility and reduced toxicity in HEK-293 mammalian cells and mice compared to AmB. Preliminary safety studies were performed but an in-depth study will be necessary to assess the safety of AmB analogs of this type.

Eight additional AmB analogs were generated coupling the C-16 carboxylic acid to various amines to generate carboxamides including L-histidine methyl ester moiety to provide, for example, the analog **65** (Fig. 1.17A).[191] When tested against two strains of *C. albicans* and one *C. krusei*, analog **65** displayed excellent antifungal activity with MIC values of 0.28-7.5 μM comparable to that of AmB (MIC = 0.20 to >10 μM). This compound was neither hemolytic nor cytotoxic. Analog **65** showed an increase in safety when tested in adult male BALB/c mice compared to AmB. This compound warrants further investigation as a potential antifungal agent due to its excellent antifungal activity, selectivity, and safety profiles.

Finally, dual modifications of the C-16 carboxylic acid and the primary amino group in mycosamine led to eleven AmB derivatives including the carboxamide **66** and the

carboxamide **67** bearing an unusual β-hydroxy benzoxaborole moiety (Fig. 1.17A).[192] The latter analog **67** displayed the best antifungal activity, and four of these analogs displayed excellent antifungal activity against at least one of the following strains, *C. albicans*, *Cryptococcus humicolus*, *A. niger*, and *F. oxysporum* with MIC values of 0.5-2 μg/mL comparable to that of AmB (MIC = 0.25-2 μg/mL). Although compound **66** displayed excellent antifungal activity, it had high hemolytic toxicity. Compound **67**, however, showed the best antifungal activity and low cytotoxicity in human colon carcinoma HCT116 cells and showed sufficient promise as an antifungal agent to warrant further testing.

In lead optimization studies, wild-type *Pseudonocardia autotrophica* provided the NYT derivative **68a** with a unique disaccharide and a mutant of *P. autotrophica* lacking an enoyl reductase (ER) led to analog **68b** possessing the Δ^{28}-double bond (Fig. 1.17B).[27, 193] The analog **68a** with a tetraene core resembled NYT, and the analog **68b** with an heptaene core resembled AmB. In comparison to NYT, analog **68a** showed increased water solubility and lower hemolytic toxicity; however, its antifungal activity was slightly poorer than that of NYT when tested against *C. albicans* (MIC values of 16 μg/mL compared to that of NYT (MIC = 4 μg/mL) and AmB (MIC = 0.5-1 μg/mL)). Compound **68b** displayed comparable antifungal activity to AmB when tested against four *C. albicans* strains, one *C. humicolus*, and one *S. cerevisiae* (MIC = 1-4 μg/mL). In general, these biochemically driven NYT derivatives show promise as antifungal agents with low toxicity in rats and mice along with improved efficacy and pharmacological profile and herald future developments in which selective chemical and, in particular, biochemical modifications of these polyenes will

afford still other analogs useful in the second-line of defense against the continued appearance of resistant strains.

1.3.1.4. Echinocandin derivatives

In contrast to the azoles and polyenes, the echinocandins were the subject of relatively few modifications in the last decade, but the unique target of these echinocandins made them interesting scaffolds for continued exploration. Anidulafungin (AFG) inhibited a glucan synthase that played a crucial role in the formation of (1→3)-β-D-glucans in the fungal cell wall. Because this enzyme was not found in humans, synthesizing new, semisynthetic analogs of AFG represented an attractive target for antifungal drug development. A recent study reported the evaluation of six AFG analogs, in which the reactive, hemiaminal moiety within the hydroxylated ornithine subunit of AFG, underwent acetalization reactions with alcohols or amines (Fig. 1.18).[194] Among these, CD101, in which choline replaced the hydroxyl group in the hemiaminal moiety, showed excellent antifungal activity against seven *Candida* strains (*C. albicans*, *C. glabrata*, *C. guilliermondii*, *C. krusei*, *C. lusitaniae*, *C. parapsilosis*, and *C. tropicalis*) with MIC values of ≤0.015-2 μg/mL comparable to that of AFG (MIC ≤0.015-2 μg/mL). CD101 also displayed excellent minimum effective concentration (MEC) values of ≤0.015-0.03 μg/mL against seven *Aspergillus* strains (*A. candidus*, *A. clavatus*, *A. flavus*, two *A. fumigatus*, *A. niger*, and *A. ochraceus*) similar to that of AFG (MIC ≤0.015-0.03 μg/mL). In pharmacokinetic studies in dogs and mice, CD101 had an improved safety profile compared to AFG and showed promise for development as an antifungal agent.

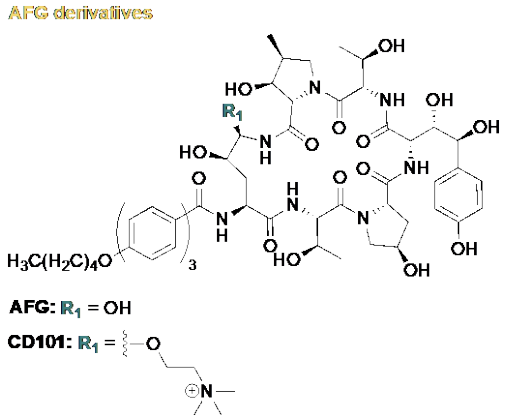

Fig. 1.18. A representative example of a potential semisynthetic antifungal, CD101, derived from AFG.

1.3.1.5. Allylamine derivatives

Just as in the case of the echinocandins, relatively few studies focused on the development of new allylamine analogs in the last decade. A recent study employed a five-step synthesis to incorporate phloroglucinol into seventeen allylamine analogs of naftifine (NAF) (Fig. 1.19).[195] Only analog **69** displayed good activity against *Trichophyton rubrum* and *Trichophyton mentagrophytes* (MIC values of 3.05-5.13 μg/mL), but this activity was not as good as that of the parent NAF (MIC = 1.036-1.072 μg/mL). Molecular docking studies indicated that **69** could potentially bind to squalene epoxidase, a target of NAF. The limited antifungal activity of most of these phloroglucinol-containing NAF derivatives suggested that additional effort on this series of analogs was unwarranted.

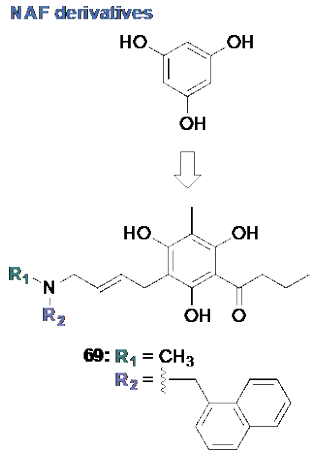

Fig. 1.19. A representative phloroglucinol-containing NAF analog as a potential antifungal agent.

1.3.1.6. Antimetabolite derivatives

Antimetabolites play a prominent role in recent efforts to develop new antifungal agents (Fig. 1.20). Modifications of 5-flucytosine (5FC), 5-fluorouracil (5FU), and pyrimidine scaffolds focused principally on structural changes that would reduce their cytotoxicity and the propensity of antimetabolites to develop fungal resistance. In general, investigators explored two types of modifications of 5FC: (i) incorporation of two 5FC subunits linked through a benzene moiety, and (ii) incorporation of 5FC and other antifungal agents, such as FLC, into a composite structure (Fig. 1.20A). Other modifications to antimetabolites included the linkage of 5FU to substituted benzimidazoles (Fig. 1.20B) and substitutions of pyrimidines and purines with various amino, cyano, aryl, and heterocyclic groups (Fig. 1.20C).

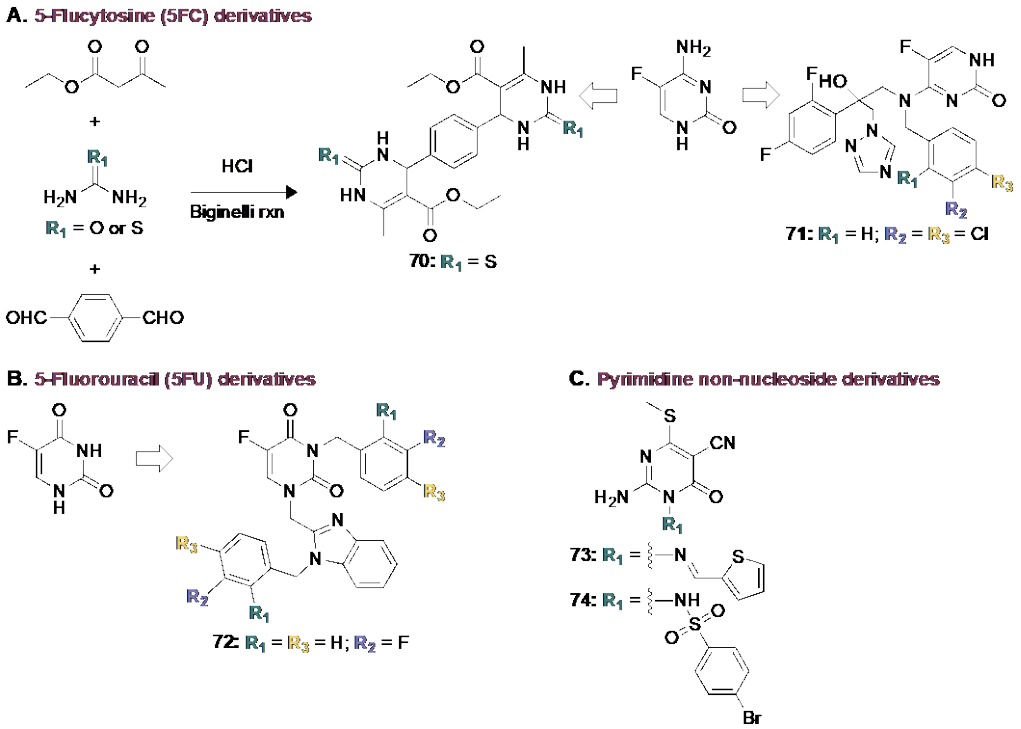

Fig. 1.20. Representative examples of potential antifungals derived from **A.** 5FC, **B.** 5FU, and **C.** pyrimidines.

Synthesis of analogs that incorporated two 5FC subunits with a phenyl group "spacer" made use of the Biginelli reaction, an acid-catalyzed, three-component reaction among an aldehyde, a β-ketoester and an urea/thiourea leading to dihydropyrimidones (Fig. 1.20A). Although limited in scope, this study led to a bis(thiopyrimidinone) **70** (Fig. 1.20A)[196] with antifungal activity (MIC values of 1-2 μg/mL against four out of eight *C. albicans* strains that were tested) that was comparable to that of AmB (MIC = 1-2 μg/mL). It was interesting that the corresponding bis(pyrimidinone) that lacked the thiocarbonyl groups displayed no antifungal activity. In combination studies with FLC or AmB against the same eight *C. albicans* strains, analog **70** displayed synergistic activity in twelve instances and additive in four instances. Although these 5FC-like derivatives showed some promise as antifungal agents in combination with AmB or FLC, the lack of comparison of MIC data with 5FC

from which these compounds were derived, the absence of cytotoxicity experiments, and experiments designed to evaluate fungal resistance limit our assessment of the potential benefits of these analogs.

Additional analogs derived from the incorporation of 5FC into FLC in which the 4-aminopyrimidinone replaced one of the 1-(1*H*-1,2,4-triazol-1-yl)methylene subunits in FLC and in which the C-4 amino group in the 4-aminopyrimidinone underwent alkylation with alkyl, benzyl, and halogenated benzyl substituents.[197] These synthetic efforts led to nineteen FLC-5FC hybrids in a straightforward five-step synthesis leading to analogs such as **71** (Fig. 1.20A). Unfortunately, these compounds displayed little activity with the exception of compound **71**, that showed good antifungal activity against *A. fumigatus*, *C. albicans*, *C. tropicalis*, and *C. parapsilosis* with MIC values of 0.008-0.03 mM (4.2-15.7 μg/mL) comparable to that of the parent FLC (MIC = 0.003-1.65 mM (1.83-50.3 μg/mL)) and 5FC (MIC = 0.03-1.98 mM (3.87-25.6 μg/mL)). Preliminary investigations into the mechanism of action utilized membrane-permeabilization experiments and molecular docking of compound **71** in the *C. albicans* CYP51 active site. Overall, the limited antifungal activity of this series suggested that FLC-5FC hybrids offer little promise as potential antifungal agents.

The incorporation of 5FU into substituted benzimidazoles appeared in a preliminary study that involved the *N*-alkylation of 5FU by alkyl groups and/or benzimidazoles decorated with substituted aryl moieties to furnish hybrids such as **72** (Fig. 1.20B).[198] Twenty-two 5FU hybrids emerged in one to three synthetic steps, but unfortunately, these compounds

were inactive with the exception of **72** that showed excellent antifungal activity when tested against *S. cerevisiae* (MIC value of 1 μg/mL). This activity of **72** was better than that of the standard FLC (MIC = 16 μg/mL); however, compound **72** displayed poor antifungal activity when tested against *C. albicans*, *C. mycoderma*, and *A. flavus*. Molecular docking studies against DNA topoisomerase IA suggested some basis for the antifungal activity observed with analog **72**. Based on their limited antifungal activity, the development of 5FU hybrids as antifungal agents appeared to have limited prospects for success.

Modification of pyrimidinone scaffolds appeared in a modest study using only zones-of-inhibition to establish preliminary readouts of antifungal activity.[199] In one such study, the synthesis of ten pyrimidines substituted with various groups (*e.g.*, amino, cyano, thiophenyl, furanyl, pyridinyl, and arylsulfonamidoyl) using one to two simple synthetic steps furnished analogs such as **73-74** (Fig. 1.20C). None of the compounds displayed activity against *A. flavus*. Only two compounds, **73** and **74**, were active against *C. albicans* (zone of inhibition 9-15 mm, comparable to that of the AmB standard (19 mm)). More detailed investigation of these compounds will be necessary to determine their potential value as antifungal agents.

In summary, with only a few exceptions, the development of new antimetabolite derivatives as antifungal agents was unsuccessful. Only the synthesis and evaluation of dimeric analogs of 5FC led to promising antifungal activity. Other modifications, such as the hybridization of 5FC to FLC, the binding of 5FU to benzimidazoles, and modifications

of pyrimidines with various groups, led to analogs with little promise as potential antifungal agents.

1.3.2. Design and preparation of novel synthetic scaffolds as antifungal agents

1.3.2.1. Imidazole, aminothiazole, and their benzimidazole/benzothiazole derivatives

In addition to making derivatives of FDA-approved imidazole-containing antifungal agents, investigators explored new compounds containing an imidazole group as a common pharmacophore. In one such study, a series of twenty-eight compounds were synthesized in two to four synthetic steps in which D-histidine provided the key imidazole ring. Acylation of the α-amino group of the histidine with biphenyl groups and esterification of the α-carboxylate group furnished the analogs **75-77** (Fig. 1.21A).[200] Among these compounds, eighteen displayed excellent antifungal activity against two strains of *C. albicans* and one strain of *C. tropicalis* (MIC values of 0.03125-2 μg/mL comparable to that of ITC (MIC = 0.0625-0.5 μg/mL)). Additionally, seven compounds showed excellent activity against *C. neoformans* (MIC = 0.5-2 μg/mL), an outcome that was in line with the MIC of ITC (1 μg/mL). Analogs **75-77** were the most active, but unfortunately, all compounds, including **75-77**, were inactive when tested against *A. fumigatus*. A detailed study of structure-activity relationships (SARs) revealed that compounds with (*S*) or L-stereochemistry at the quaternary center were less active than their (*R*) or D-counterparts. Compounds **75a** and **75b** displayed the best antifungal activity and showed limited inhibition of five major human cytochrome P450 isoforms (CYP1A2, CYP2C9, CYP2C19, CYP2D6, and CYP3A4-M). Molecular docking of **75a** in the active site of lanosterol 14α-demethylase (CYP51A1) along with investigation of sterol composition of the fungal cell

suggested that **75a** inhibited this specific enzyme. Further testing against a broad panel of fungi, testing against drug-resistant fungal clinical isolates, and cytotoxicity studies will ultimately determine the potential value of these imidazole analogs as antifungal agents.

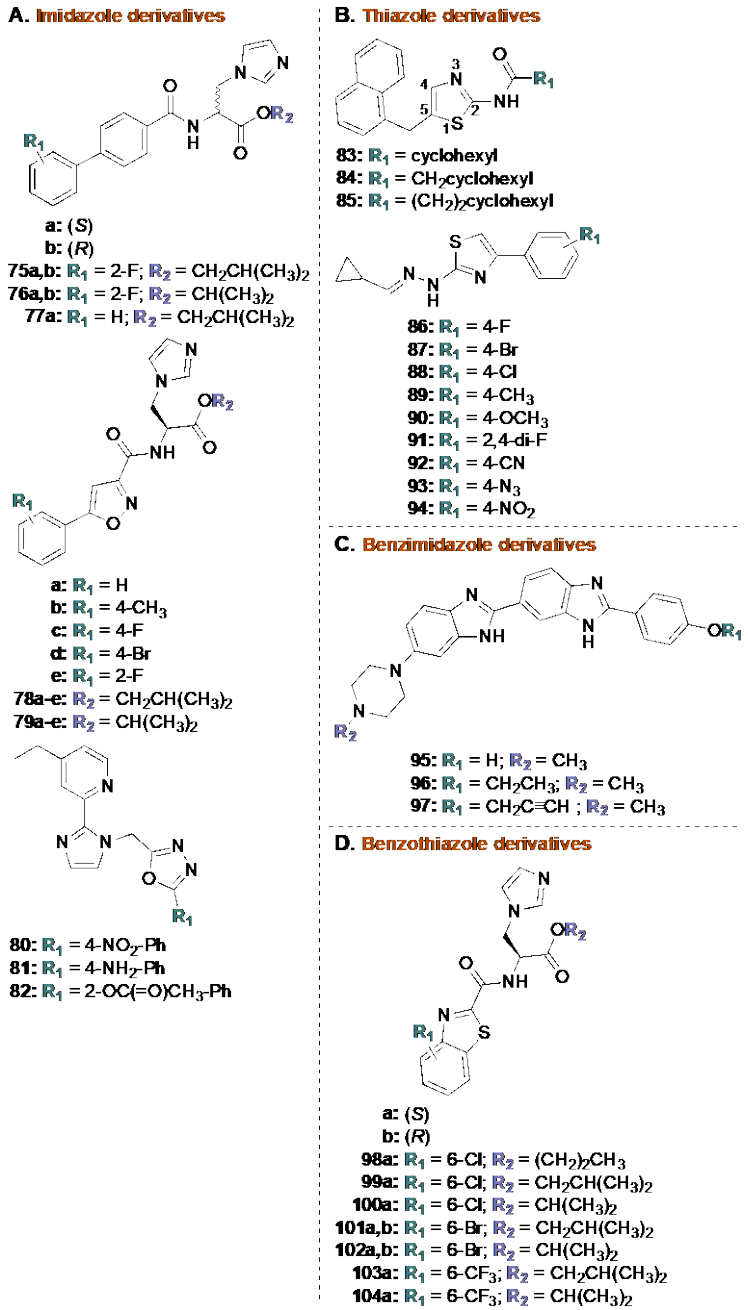

Fig. 1.21. Representative examples of compounds from seven new scaffolds tested as potential antifungals that contain **A.** imidazole, **B.** thiazole, **C.** benzimidazole, or **D.** benzothiazole in their structures.

Another study employed various four- to six-step syntheses to generate twenty-seven imidazole derivatives, represented by imidazoles **78-79** (Fig. 1.21A).[200] In this series, investigators again used D-histidine as the framework on which to make modifications. Coupling of the α-amino group in the unnatural histidine to carboxylate groups in various heterocycles (*e.g.*, thiophene, thiazole, isoxazole, pyrimidine, pyridine, furan, and oxazole) led to carboxamides such as the isoxazole-containing compounds **78-79** that displayed the best overall antifungal activity. These analogs displayed antifungal activity better than or equal to that of FLC and comparable to that of ITC when tested against two *C. albicans* (MIC values of 0.03125-2 μg/mL), *C. tropicalis* (MIC values of 0.03125-0.25 μg/mL), and *C. neoformans* (0.25-2 μg/mL). In general, analogs **78-79** showed good to poor activity against *A. fumigatus*, and analogs **78e** and **79e** showed excellent antifungal activity when tested against two strains of FLC-resistant *C. albicans* while exhibiting low inhibition of human cytochrome P450 isoforms, good metabolic profiles in human plasma stability experiments, and inhibition of CYP51 in sterol composition experiments. With low MIC values, a defined mechanism of action, and a good stability in human blood plasma, these compounds show good potential as antifungals and warrant additional exploration.

Yet another study led to ten compounds that contained an internal imidazole ring modified at the 2-position with 4-ethyl pyridine and at the 1-position with an oxadiazole decorated with aromatic substituents. The synthesis of these compounds in three simple steps led to representative imidazoles **80-82** (Fig. 1.21A).[201] When tested against four strains of *C. albicans* and three strains of *C. tropicalis*, imidazoles **80-82** in general exhibited poor

antifungal activity (MIC values of >1000 μg/mL) with the exception of three compounds that displayed MIC values of 2-125 μg/mL. These imidazoles inhibited ergosterol biosynthesis based on molecular docking in the active site of the cytochrome P450 lanosterol 14α-demethylase of *C. albicans*. Because of their poor activity, these compounds are unlikely to undergo further development.

Heterocycles other than imidazole served as attractive platforms for the development of new antifungal agents. SAR studies utilizing the 2-aminothiazole scaffold led to analogs modified at C-5 with benzyl, naphthyl, and cycloalkyl groups and acylated at the C-2 amino group with an array of carboxylic acids to acquire nineteen different carboxamides including **83**-**85** (Fig. 1.21B).[202] Introduction of methyl groups at C-3 and C-4 led to other analogs with decreased activity. Compound **83**, which was active against *Histoplasma* yeast, served as the leading scaffold from previous work[203] and was used to generate sixty-eight additional aminothiazole derivatives. When tested against *Histoplasma capsulatum*, twenty-nine of the compounds showed activity, and three **83**-**85**, displayed MIC values of 0.6-1.3 μM. The compounds were not active against *C. neoformans*. In cytotoxicity experiments using human hepatocyte (HepG2) cells compounds **83**-**85** were found to have low toxicity. A comparison with standard antifungal agents was not provided, and the absence of this information makes it difficult to evaluate the potential value of these compounds as antifungal agents.

A separate publication also reported the two-step synthesis and evaluation of ten, related hydrazine-substituted thiazole derivatives.[204] In this study, the 2-hydrazinothiazole core

contained an *N*-cyclopropylmethylene group and a variety of substituted phenyl groups at C-4 as in the representative examples **86-94** (Fig. 1.21B). When tested against three strains of *C. albicans* and fifteen strains of non-*albicans Candida*, hydrazinothiazoles **86-94**, with a few exceptions, displayed excellent antifungal activity against fourteen of the strains (three *C. albicans*, two *C. parapsilosis*, two *C. krusei*, *C. tropicalis*, *C. inconspicua*, *C. famata*, *C. guilliermondii*, *C. lusitaniae*, *C. sake*, and *C. dubliniensis*) with MIC values of 0.015-1.95 μg/mL that were comparable to that of NYT (MIC = 0.015-0.48 μg/mL). The compounds were inactive against *C. kefyr*, *C. pulcherrima*, *C. glabrata*, and *C. lambica*. Hydrazinothiazoles **88**, **90**, and **93** displayed good safety profiles in cytotoxicity experiments with mouse L929 fibroblast and African green monkey kidney VERO cells. Molecular docking studies suggested aspartic proteinase as a possible target. It is interesting that modifying the C-4 position in the presence of a C-2 hydrazino moiety provided potent antifungals in contrast to what was observed in the study discussed in the paragraph above. With their excellent antifungal activity and safety profile, these compounds warrant additional investigation.

Because of the somewhat promising results seen with imidazoles and thiazoles, the bicyclic benzimidazoles and benzothiazoles also attracted attention as scaffolds on which to develop antifungal agents. A series of eighteen, substituted benzimidazoles were synthesized in nine synthetic steps in which the C-2 position contained aryl substituents and the C-6 position contained *N*-alkylpiperazines, as in the representative benzimidazoles **95-97** (Fig. 1.21C).[205] Benzimidazoles **95-97** displayed excellent to good activity against at least one of eleven fungal strains that included six strains of *C. albicans*, three non-

albicans Candida (*C. glabrata*, *C. krusei*, and *C. parapsilosis*), and two *Aspergillus* spp. (*A. nidulans* and *A. terreus*) with MIC values of 0.975-7.8 μg/mL that were better than MIC values for FLC (MIC = 1.95-15.6 μg/mL). Fungistatic activity at 1× MIC and fungicidal activity at 2× MIC against *C. albicans* were observed with benzimidazoles **95** and **96**. Benzimidazole **95** was found to be safe at concentrations of ≥31.2 μg/mL in cytotoxicity experiments using A549 and BEAS-2B mammalian cell lines. Experimental results suggested a possible mechanism of action for these derivatives involving the induction of reactive oxygen species as the trigger for fungal inhibition in *C. albicans*. These benzimidazole derivatives show promise as antifungal agents and warrant further development.

Another study reported a series of twenty-five benzothiazole derivatives containing D-histidine in which the α-amino group underwent acylation by 1*H*-benzo[*d*]imidazole-2-carboxylic acid and the α-carboxylate underwent esterification in three or four steps to give representative carboxylic esters (*e.g.*, methyl, ethyl, propyl, isopropyl, and isobutyl), such as benzothiazoles **98-104** (Fig. 1.21D).[206] Ten benzothiazoles displayed excellent antifungal activity when tested against two strains of *C. albicans*, one strain of *C. neoformans*, and one strain of *C. tropicalis* (MIC values of 0.125-2 μg/mL comparable to that of ITC (MIC = 0.125-1 μg/mL)). All compounds were inactive against *A. fumigatus* and compounds **101a-103a** displayed little activity against two FLC-resistant strains of *C. albicans* (MIC = 8-32 μg/mL). Increased antifungal activity was observed with the addition of an electron-withdrawing group at C-6 and with the addition of bulky alkyl esters. Sterol composition studies and molecular docking into the CYP51 active site revealed that **101a**

inhibits lanosterol 14α-demethylase in *C. albicans*. More studies including, in-depth mechanism of action, cytotoxicity, resistance, and testing against a broader panel of fungal species will be necessary to evaluate the potential of these compounds. In summary, the preparations of imidazole, thiazole, benzimidazole, and benzothiazole derivatives was successful in providing leading antifungal agents that warrant further investigation.

1.3.2.2. Triazole derivatives

As discussed in the preceding "azole derivatives - triazoles" section leading to FDA-approved 1,2,4-triazole antifungal agents, the generation of amphiphilic molecules constitutes a strategy used to create effective antifungal agents. Amphiphiles will also be further discussed in the context of aminoglycosides and quinones in later sections of this review. In this section, we will take up a third category of amphiphiles based on the 1,2,3-triazole pharmacophore.

A recent study described modification of the C-1 position in a 1,2,3-triazole with either a hydrophobic, linear alkyl chain or with an ω-hydroxyalkyl chain as in triazole **105** (Fig. 1.22).[197] Four such 1,2,3-triazole derivatives were prepared in two-steps that involved the synthesis of appropriate alkyl azides and 1,3-cycloaddition reactions with *cis*-2-alkenoic acids. The addition of a terminal hydroxyl moiety abolished antifungal activity, and only the 1,2,3-triazoles with linear C_8 and C_{10} alkyl chains displayed inhibition of *C. albicans* cell growth. Out of the four compounds synthesized, 1,2,3-triazole **105** with a C_{10} alkyl chain showed the best activity with 90% inhibition of *C. albicans* growth as well as inhibition of hyphal growth and germ tube germination in *C. albicans*. Even though the

compound was somewhat active, the concentration needed to inhibit 90% growth was very high (*i.e.*, 60 μM (14.4 μg/mL)), a concentration that was comparable to the activity shown by the *cis*-2-dodecenoic acid from which **105** was derived. The high concentration needed to inhibit fungal growth dampen any enthusiasm for continued work in this series.

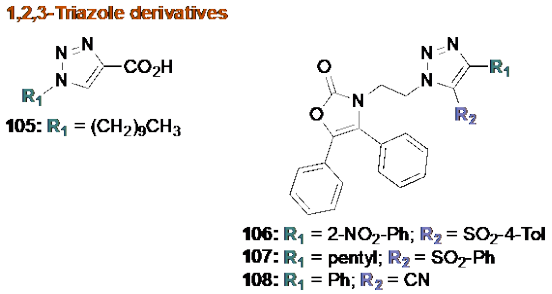

Fig. 1.22. Representative examples of compounds from two new scaffolds tested as potential antifungals, which contain 1,2,3-triazole in their structure.

Another series of eleven 1,2,3-triazole derivatives were synthesized in five steps using a similar 1,3-cycloaddition to the one described in the preceding paragraph.[207] All compounds contained a 4,5-diphenyloxazol-2-one at C-1 of the triazole and various moieties (*e.g.*, alkyl, aryl, acetyl, cyano, and heterocyclic groups) at C-4 and C-5 as illustrated by 1,2,3-triazoles **106-108** (Fig. 1.22). Three 1,2,3-triazoles **106-108** showed excellent activity against at least one of the following strains: *C. glabrata*, *M. hiemalis*, and *T. cutaneum* (MIC values of 0.125-2 μg/mL, that was better than that of ITC (MIC = 1-8 μg/mL)). In general, little to no activity was observed against *C. albicans*, *C. tropicalis*, *C. utilis*, *C. krusei*, *C. parapsilosis*, *A. fumigatus*, and *R. oryzae*. Other studies revealed that most of the *Candida* strains were resistant to almost all of the compounds tested; therefore, these compounds possessed very limited promise as potential antifungal agents.

1.3.2.3. Tetrazole derivatives

A number of tetrazoles are now in preclinical and clinical development as antifungal agents. Although promising, the synthesis of tetrazoles typically involves the reaction of an aryl nitrile with hydrazoic acid. The toxicity of hydrazoic acid and the risk of tetrazole explosions deterred interest in these pharmacophores until a recent protocol was developed for the preparation of 5-aryltetrazoles using a reaction of aryl nitriles with an arylamine, amine hydrochlorides, and sodium azide.[208] However, prior to development of this methodology, twelve 5-aryltetrazole derivatives were synthesized *via N*-alkylation or Michael-type additions using nitriles, sodium azide and ammonium chloride in *N,N*-dimethylformamide to generate the starting 5-aryltetrazoles. Position 2 of the 5-aryltetrazoles was modified to contain benzoxazole, benzothiazole, or phenylsulfonyl moieties (**109-112**; Fig. 1.23).[209] Excellent antifungal activity was observed with seven of the derivatives, **109-112**, when tested against one strain of *C. albicans* (>98% growth inhibition at 0.0313 μg/mL, that was better than that of AmB (MIC = 0.5 μg/mL)). All compounds were inactive against *Colletotrichum coccodes*, *F. sambucinum*, *F. oxysporum*, and *A. niger* strains. In combination experiments using FLC, **110b** and **111b** showed antagonism in *C. albicans*. These two compounds were also found to be safe at concentrations of 16 μg/mL in cytotoxicity studies using the moth, *Galleria mellonella*. Preliminary mechanism of action studies tested compound **110b** against *C. albicans* in the presence of sorbitol and indicated that compound **110b** modified the cell wall architecture of *C. albicans*. Testing against a broader panel or resistant fungal clinical isolates in addition to resistance studies of compound **110b** would be beneficial to establish the value of this scaffold as an antifungal.

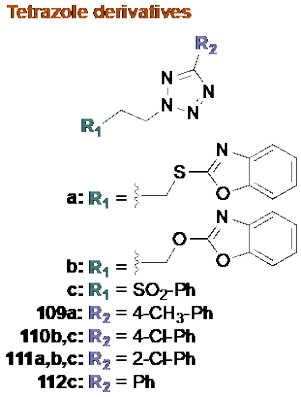

Fig. 1.23. Representative examples of compounds from a new scaffold tested as potential antifungals, which contain tetrazole in their structure.

1.3.2.4. Hydrazone derivatives

Acylhydrazones derived from the addition of acyl hydrazides to aryl aldehydes provided scaffolds that were explored in an attempt to combat azole-resistant *Candida* spp. A series of fifty-one acylhydrazone derivatives were synthesized in two to three convergent steps, but unfortunately, only MIC_{80} values instead of MIC values for complete *C. albicans* growth inhibition were determined.[210] Only four of the fifty-one compounds, all belonging to the *N′*-(2-hydroxybenzylidene)picolinohydrazide family, displayed some antifungal activity (MIC_{80} values of 1-8 μg/mL) when tested against azole-susceptible and azole-resistant *C. albicans* and *C. glabrata* (Fig. 1.24; **113-116**). Unfortunately, no standard antifungal agents were used as comparison points. In cytotoxicity studies using VERO and HepG2 cell lines, compounds **113** and **116** were non-toxic at up to levels that were 100× MIC. Acylhydrazone **115** was fungicidal against *C. albicans*, and **113** and **116** were fungistatic. Checkerboard assays (*i.e.*, simultaneous testing of two different agents at variable concentrations) revealed that none of the compounds exhibited synergy in combination with FLC. As some compounds exhibited reasonable MIC_{80} values and

toxicity to mammalian cells, it is unclear why MIC values for complete growth inhibition were not determined. Expanded studies of the *N*-(2-hydroxybenzylidene)picolinohydrazide family will establish their potential as new antifungal agents.

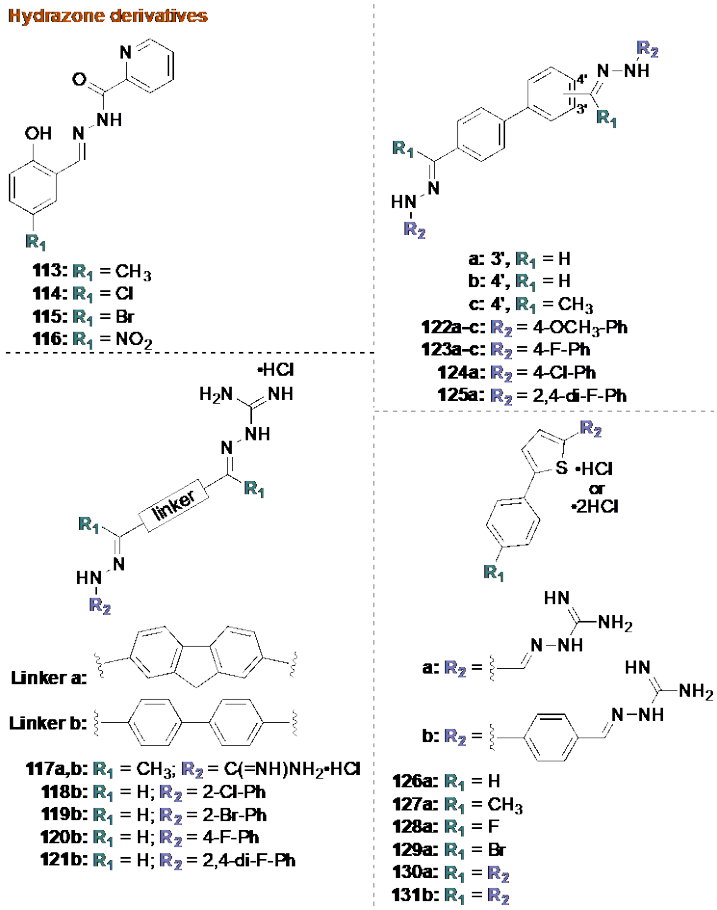

Fig. 1.24. Representative examples of compounds from four new scaffolds tested as potential antifungals, which contain hydrazone in their structure.

The positive results seen with monohydrazones prompted studies of bishydrazones in which the hydrazone moieties were attached through an hydrophobic linker (**117-121**; Fig. 1.24).[211] In an initial study, the synthesis of seventeen bishydrazones required one or two synthetic steps and incorporated either *N*-arylhydrazines or *N*-aminoguanidine into various linkers containing two aldehyde groups or two acetyl groups to obtain eight unsymmetrical

N-(amidino)-*N′*-aryl bishydrazones **117-121** (Fig. 1.24) and nine symmetrical bis(*N,N′*-amidinohydrazones). When tested against three azole-susceptible and four FLC-, ITC-, and VRC-resistant *C. albicans* strains, six compounds, namely the bishydrazones **117-121**, displayed excellent activity against at least one of the strains tested with MIC values of 1-2 μg/mL that was better than the MIC values for AmB (MIC = 2-3.9 μg/mL). Resistance studies revealed that, after thirteen passages, *C. albicans* did not develop resistance to **117b** or **118b**. Investigation into the mechanism of action of these two compounds showed an increase in intracellular reactive oxygen species (ROS) production in *C. albicans* at their 1× and 2× MIC values. In cytotoxicity experiments, compounds **120b** and **121b** showed low toxicity when tested against A549 and BEAS-2B mammalian cell lines along with only moderate interaction with the human *ether-à-go-go*-related gene (hERG) potassium channel. Additional testing against a broad panel of fungal species should precede their further development as antifungal agents.

Additionally, the synthesis of symmetrical bis(*N,N′*-arylhydrazones) linked by diaryl moieties used substituted arylhydrazines (*e.g.*, methoxy, nitro, halogen, cyano, and multiples of the aforementioned groups) and either [1,1'-biphenyl]-3,4'-dicarbaldehyde, [1,1'-biphenyl]-4,4'-dicarbaldehyde, or 4,4'-diacetyl-1,1-biphenyl and led to thirty bis(*N,N′*-arylhydrazones) **122-125** (Fig. 1.24).[212] Eight of the thirty derivatives, namely **122-125**, displayed excellent to good activity against at least one of the thirteen strains tested, including seven *C. albicans*, three non-*albicans Candida* (*C. glabrata*, *C. krusei*, and *C. parapsilosis*), and three *Aspergillus* spp. (*A. flavus*, *A. nidulans*, and *A. terreus*) with MIC values of 0.98-7.8 μg/mL comparable to that of CAS and VRC (MIC = 0.06 to >31.3).

Compound **123c** was able to eliminate pre-formed *C. albicans* biofilms, but at a concentration above the MIC value. In cytotoxicity experiments, compounds **122a,b** and **123a** were found to be safe at 31 μg/mL, while compounds **123c** and **125a** were safe at 15.5 μg/mL against the A459 mammalian cell line. When tested against the BEAS-2B mammalian cell line, **123a** was safe at 31 μg/mL, and compounds **122a,b**, **123c**, and **125a** were safe at 15.5 μg/mL. Compound **123c** also displayed low hemolytic activity, fungistatic activity, and no toxicity when tested in hERG binding studies. The positive outcomes seen in these bishydrazone derivatives warrant their further development as antifungal agents.

A two-step synthesis consisting of Suzuki cross-coupling followed by a condensation with *N*-aminoguanidine was used to generate a series of ten mono- and bishydrazone derivatives (**126-131**; Fig. 1.24).[213] These derivatives were linked *via* a thiophene or a furan group substituted at C-2 and 5 with iminoguanidines and various *para*-substituted phenyl groups (*e.g.*, methyl, methoxy, fluoro, bromo, cyano, and iminoguanidine). Among these compounds, nine displayed excellent activity (MIC values of 0.25-1.56 μg/mL) against at least one of the following strains *C. albicans*, *C. krusei*, *C. parapsilosis*, *A. fumigatus*, *F. oxysporum*, *M. canis*, and *T. mentagrophytes*, and these MIC values were only slightly poorer than the corresponding activity of the parent VRC (MIC = 0.06-0.5 μg/mL). Six of these displayed excellent to good activity (MIC = 0.25-7.8 μg/mL) against at least one of the VRC-resistant *C. albicans*, *C. parapsilosis*, or *F. oxysporum* strains. Compounds **127a**, **129a**, and **130a** were shown to be fungistatic. Compounds **127a** and **130a** were also able to disperse pre-formed biofilm of *C. albicans*. Mechanism of action studies through

molecular docking showed that these compounds bind the CYP51 active site. With low toxicity and minimal hemolysis, these hydrazone and bishydrazone derivatives show great promise as antifungal agents, but additional mechanistic studies remain to be done to fully understand the scope of these molecules as antifungal agents.

In general, hydrazone derivatives show great promise as antifungal agents. However, more mechanistic studies remain to be done to fully understand the scope of these molecules.

1.3.2.5. Aromatic and heterocyclic derivatives

Apart from the aforementioned studies, several reports described idiosyncratic aromatic and heterocyclic scaffolds as potential novel antifungal agents (**132**-**158**; Fig. 1.25). A two-step synthesis led to thirty-six compounds with an imidazolin-2-one core, including twenty substituted benzimidazolones and sixteen substituted imidazopyridines with an array of substituents (*e.g.*, acetyl, aryl, bromo, and nitro groups). These imidazolin-2-ones **132**-**135** (Fig. 1.25) displayed relatively poor outcomes using percent inhibition of spore germination and mycelial growth of *Botrytis cinerea*, which is primarily a plant pathogen.[214] Unfortunately, it took 50 μg/mL and 25 μg/mL for four of these imidazolin-2-ones to display >90% inhibition of spore germination and mycelial growth, respectively. All other compounds were inactive, and additional efforts to imidazolin-2-ones as antifungal agents does not appear to hold much promise.

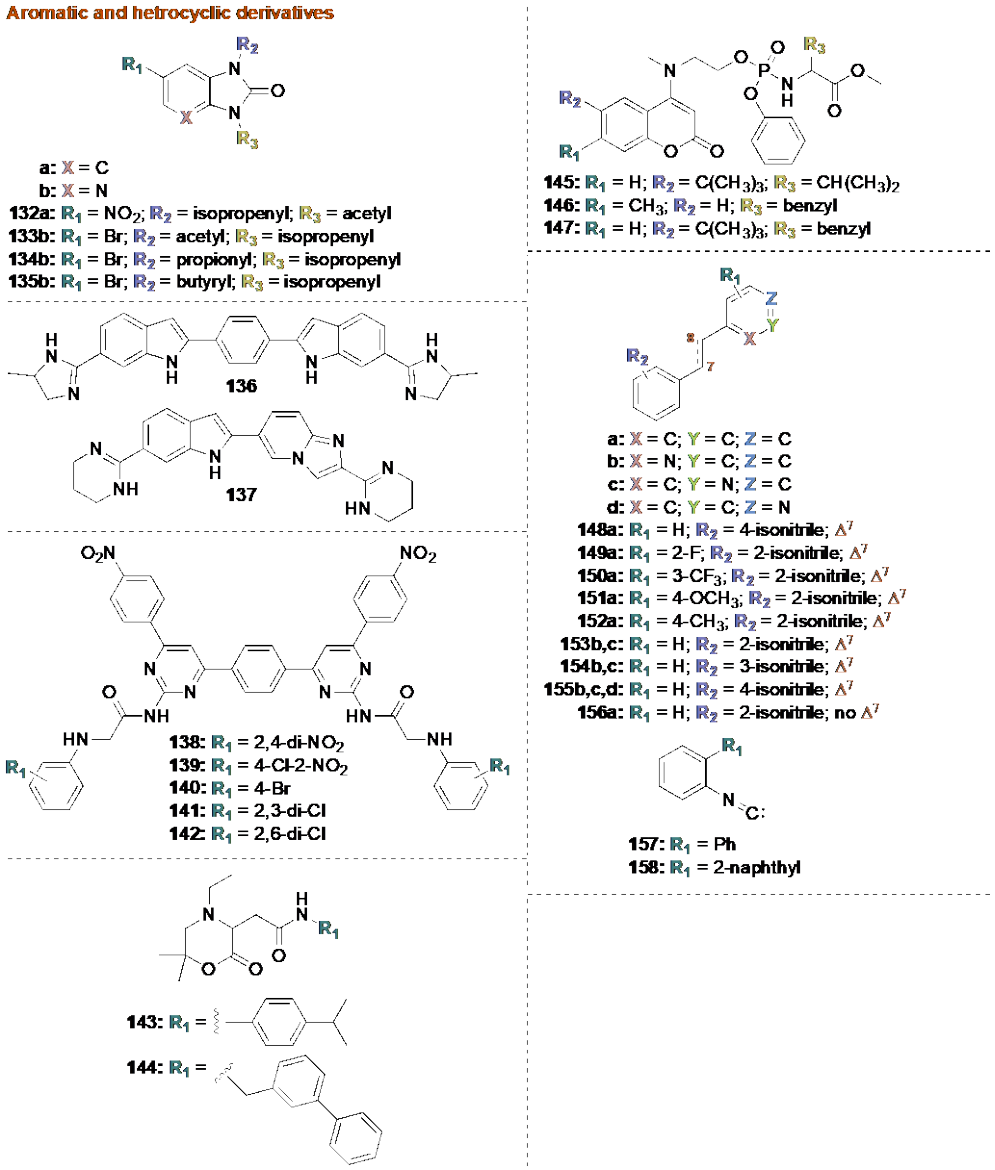

Fig. 1.25. Representative examples of compounds from six new scaffolds tested as potential antifungals, which contain an aromatic or heterocyclic group in their structure.

Because imidazoles and pyrimidines were structural components of several antifungal agents, efforts to employ 4,5-dihydro-1*H*-imidazoles and the 1,4,5,6-tetrahydropyrimidines, respectively, in a new generation of antifungal agents was a logical extension of these other studies. A report described an array of amidine derivatives, including symmetrical 4,5-dihydro-1*H*-imidazoles, such as **136** (Fig. 1.25), and

unsymmetrical 1,4,5,6-tetrahydropyrimidines, such as **137** (Fig. 1.25).[215] Among these compounds, eighteen showed excellent antifungal activity with MIC values of ≤0.03-2 μg/mL that were better than that of AmB (MIC = 0.13-32 μg/mL) against five fungal strains (*i.e.*, *C. albicans*, *C. krusei*, *C. glabrata*, *C. parapsilosis*, and *C. neoformans*). However, when tested against HeLa cells, only two compounds, **136-137**, displayed sufficiently low toxicity as well as excellent antifungal activity. Fungicidal activity at 4× MIC against *C. albicans* was observed for three other compounds in this series that were unfortunately toxic. Preliminary mechanism of action revealed that the compounds interacted with DNA and RNA and concomitantly inhibited cell wall biosynthesis in *C. albicans*, outcomes that possibly explain the observed toxicity toward mammalian cells. Further investigations will presumably focus on developing these compounds for cutaneous applications.

Another study that focused principally on antibacterial activity tested twenty bispyrimidines against two fungal strains (*C. albicans* and *A. niger*).[216] Five of these compounds **138-142** (Fig. 1.25) displayed better antifungal activity than FLC; however, because of inconsistencies between units used in the experimental procedures (reported to range between 1.562-50 μg/mL) and units in the MIC data presented in a table (reported in μmol/mL that would correspond to values >300 μg/mL), it is difficult to assess the potential value of these compounds as antifungal agents.

The synthesis of fifty-one acetamides bearing an α-(2-oxo-morpholin-3-yl) group required two to five steps and constituted a new scaffold for evaluation for antifungal activity, exemplified by acetamides **143-144** (Fig. 1.25).[217] This study focused on modifications of

the α-(2-oxo-morpholin-3-yl)acetamide at the nitrogen of the acetamide (*e.g.*, *N*-aryl, alkyl, heteroaryl, or mono- or bicyclic groups), at the C-4 nitrogen of the 2-oxo-morpholin-3-yl group (*e.g.*, *N*-alkyl, cycloalkyl, phenyl, acyl, and sulfonyl moieties), and at the C-6 position of the 2-oxo-morpholin-3-yl group (*e.g.*, alkyl and phenyl groups). Of the fifty-one compounds that were synthesized, twelve displayed minimum fungicidal activity (MFC) values of 6.25-12.5 μg/mL against one MCZ-tolerant *C. albicans* strain (MFC value for MCZ >100 μg/mL). Four of the twelve derivatives were selected for additional testing against *C. glabrata*, *A. fumigatus*, and *A. flavus*, and three displayed excellent antifungal activity against *A. fumigatus* (MIC values of ≤3.1-1.6 μg/mL). Compounds **143-144** were selected for further evaluation for their ADMET properties and *in vivo* efficacy in a *C. albicans* infection mouse model along with MOA investigation through a phenotype microarray assay. Because these compounds displayed only low antifungal activity, additional lead optimization studies will be required to improve the activity of analogs bearing this scaffold.

Coumarin-based phosphoramidate derivatives, such as **145-147**, were also investigated as potential antifungal agents (Fig. 1.25).[218] A six-step synthesis provided twenty analogs, but unfortunately, most compounds were inactive against *C. albicans*, *A. flavus*, *A. fumigatus*, and *C. neoformans* with the exception of three compounds **145-147** that displayed excellent activity against *A. flavus* (MIC values of 1-2 μg/mL, that was superior to that of FLC (MIC = 32 μg/mL). The general lack of antifungal activity in these coumarin-based phosphoramidates suggest that additional SAR effort should focus on compounds for the potential treatment of aspergillosis.

Several reports described the synthesis and evaluation of thirty-four *trans*-stilbenes bearing a substituted phenyl or pyridyl ring at one terminus and bearing a phenyl ring with the unusual isonitrile moiety at the other terminus (**148-158**; Fig. 1.25).[219-220] When tested against one strain of *C. albicans*, twenty-four compounds displayed excellent activity with MIC values of 0.5-8 μM (0.1-2 μg/mL) that were comparable of that to FLC (MIC = 0.5 μM). These stilbene-like compounds **148-158** displayed excellent activity with MIC values in the 0.5-2 μM range. An evaluation of six of the fifteen most active compounds against twenty-one clinical fungal isolates, including six *C. albicans*, two *C. krusei*, one *C. parapsilosis*, two *C. glabrata*, two *C. tropicalis*, two *C. gattii*, one *C. neoformans*, one *A. brasiliensis*, two *A. niger*, and two *A. fumigatus* strains, revealed that most of the compounds showed excellent antifungal activity against the *Candida* and *Cryptococcus* spp., but displayed little to no activity against *Aspergillus* spp. Additional testing of the cytotoxicity of thirteen of the most active compounds using human epithelial colorectal (HRT-18) cells concluded that these compounds were non-toxic at concentrations up to 256 μM. With their potent antifungal activity and excellent safety profiles, these stilbene-like isonitrile derivatives should be examined for their mechanism of action and evaluated in resistance, anti-biofilm, and animal studies.

1.3.2.6. Additional unrelated scaffolds

Fortuitous testing of scaffolds, often developed for other purposes other than antifungal drug development, provides potentially valuable information that may guide new antifungal drug development. In a study focused on identifying anticancer activity, the

four-step synthesis and evaluation of twenty quinolines bearing a C-3 (2*H*-tetrazol-2-yl)methyl) or a C-3 (1*H*-tetrazol-1-yl)methyl) group[221] for antifungal activity against *C. albicans* and *A. fumigatus* led to several compounds **159-162** (Fig. 1.26) that displayed excellent to good activity against *A. fumigatus* with MIC values of 2.5-5 μg/mL that were better than that of FLC (MIC = 30 μg/mL). All other compounds exhibited poor antifungal activity against both strains tested. The quinoline core also appeared in another study in which thirty-one compounds were made in three to four synthetic steps to generate compounds with either pyrrolidinyl or ω-hydroxyalkylamino groups attached to the C-3, 5, 6, or 8 positions of the quinoline ring (**163-166**; Fig. 1.26).[222] Once again, these compounds also displayed low antifungal activity against *C. albicans*. Compound **163**, however, displayed excellent activity against *A. flavus* with an MIC value of 2 μg/mL, that was better than that of AmB (MIC = 3.1 μg/mL). Compounds **164-166** also displayed good activity against the yeast, *Rhodotorula bogoriensis* with MIC values of 3.9-7.8 μg/mL, but these values are poorer than that of AmB (MIC = <0.2 μg/mL). In both of the preceding cases, a more detailed SAR study and evaluation of these quinolines would be required to determine if these compounds warrant progression as potential antifungal agents.

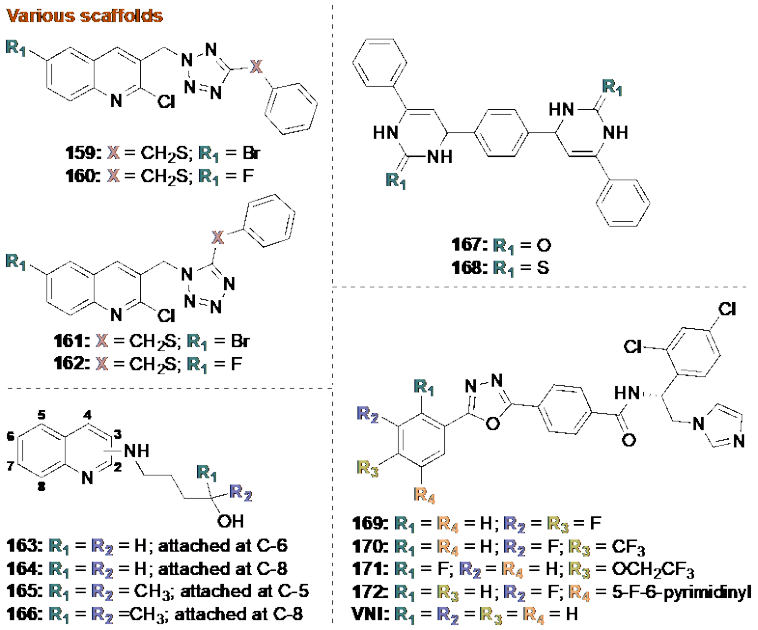

Fig. 1.26. Representative examples of compounds from four new scaffolds tested as potential antifungals, which contain different groups in their structure.

A two-step synthesis and evaluation of five tricyclic compounds containing one heterocyclic moiety and five pentacyclic compounds containing two heterocyclic moieties (*e.g.*, pyrazole, pyrazolecarbothioamide, dihydroisoxazole, dihydropyrimidinone, and dihydropyrimidinethione) interspersed with phenyl groups led to compounds **167-168** (Fig. 1.26).[223] Four out of the ten compounds displayed excellent activity against one azole-susceptible *C. albicans* strain with MIC values of 0.5-2 μg/mL that were better than that of FLC (MIC = 4 μg/mL). Two compounds, **167-168**, also displayed excellent to good activity against one azole-resistant *C. albicans* strain (MIC = 2-4 μg/mL) as well as synergy in both strains of *C. albicans* when tested in combination with FLC. Mechanism of action studies revealed that the compounds depressed ergosterol levels but did not overcome efflux pump resistance in *C. albicans*. At a minimum, additional SAR work on the leading compounds

167-168 and testing against a broad panel of fungal clinical isolates will determine if this pharmacophore warrants additional study.

An investigation of a CYP51 inhibitor, called (*R*)-*N*-(1-(2,4-dichlorophenyl)-2-(1*H*-imidazol-1-yl)ethyl)-4-(5-phenyl-1,3,4-oxadiazol-2-yl)benzamide (VNI), led to fifteen, pentacyclic compounds, including **169-172**, in a ten-step synthesis (Fig. 1.26).[224] This study examined the influence of substituents (*e.g.*, fluoro, chloro, trifluoromethyl, trifluoroethoxy, pyridinyl, fluoropyrimidinyl, and morpholino groups) in the terminal phenyl ring that had no substituents in the parent VNI on the activity of these compounds. When tested at 0.75 μM with 0.5 μM of CYP51 from a *C. albicans* strain, eight of the fifteen compounds, including **169-172**, displayed 83-94% inhibition of the enzyme. When tested against three strains of *A. fumigatus*, compounds **169-172** displayed excellent antifungal activity with MIC values of 0.06-0.78 μg/mL that was comparable to that of VNI (MIC = 0.08-0.48 μg/mL). Additional, interesting data in support of compounds **169-172** as potential antifungal agents included promising, half-life stability experiments in human, rat, and mouse microsomes and the co-crystallization of compound **171** with in the active site of CYP51B from *A. fumigatus* that confirmed the mechanism of action. These compounds warrant additional in-depth investigation.

1.3.2.7. Additional scaffolds developed as inactive antifungals

Reports describing work on unusual scaffolds that fail to produce significant differences in antifungal activity rarely reach the medicinal chemistry literature. These failures, nevertheless, provide important lessons that may point other investigators away from

unproductive, research avenues. Herein, we provide a brief review of eleven pharmacophores in which the synthesis and evaluation of a leading compound failed to generate useful antifungal agents (Fig. 1.27).[225-235] We will arbitrarily organize this discussion by grouping these compounds into two categories: (1) those that show highly limited improvement in activity (Fig. 1.27A); and (2) those that show no improvement in activity (Fig. 1.27B).

Twenty 3-amino-4-hydroxycoumarin derivatives were tested against *C. albicans*, *A. flavus*, *A. fumigatus*, and *C. neoformans* with both FLC and polyoxin B as standards. These analogs were inactive although in some instances they displayed a two- to four-fold improvement over the standards (**173-174**; Fig. 1.27A).[225] A series of twenty-five imidazole[2,1-*b*]-1,3,4-thiadiazole derivatives were tested against two *C. albicans*, two *C. neoformans*, and one *A. niger*, as well as some bacterial strains.[226] Three analogs (**175-177**; Fig. 1.27A) had excellent activity against the two *C. neoformans* strains with similar activity to AmB. Other analogs in the series, however, showed only good to poor activity against these same strains. All analogs were inactive against all other fungal and bacterial strains. In yet another study, the synthesis and evaluation of more than 100 1,3-thiazolidin-4-one against twenty-two FLC-sensitive *Candida* spp. strains identified only nine compounds, **178-186** (Fig. 1.27), that displayed activity that was on a par with the controls (*i.e.*, FLC, KTC, CLT, MCZ, TIO, and AmB).[227]

A. Highly limited improvement

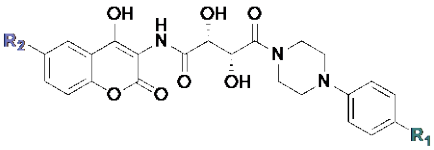

173: R_1 = Cl; R_2 = H
174: R_1 = OCH_3; R_2 = OH
MIC = 4 - 512 µg/mL
Aspergillus
Candida
Cryptococcus

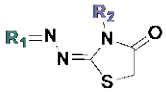

a: R_2 = H
b: R_2 = benzyl
178a,b: R_1 = 2-propanyl
179a,b: R_1 = 2-pentanyl
180a,b: R_1 = 3-pentanyl
181a,b: R_1 = 2-heptanyl
182a,b: R_1 = 2-methylcyclopentyl
183a,b: R_1 = 3-methylcyclopentyl
184a,b: R_1 = 2-methylcyclohexyl
185a,b: R_1 = 1-ethyl-2-thiophenyl
186a,b: R_1 = 1-ethyl-2-pyridinyl

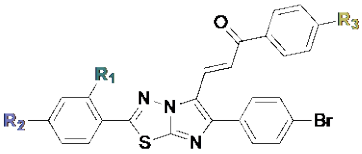

175: R_1 = Br; R_2 = R_3 = H
176: R_1 = Br; R_2 = H; R_3 = CH_3
177: R_1 = H; R_2 = OCH_3; R_3 = CH_3
MIC = 1.56 - >200 µg/mL
Aspergillus
Candida
Cryptococcus

B. No improvement or activity

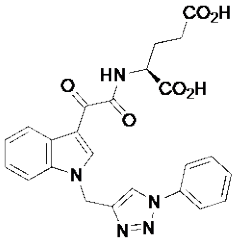

187: MIC = 312.5 µg/mL
Candida

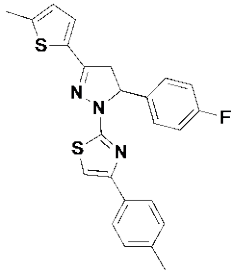

191: MIC = 125 - 1000 µg/mL
Aspergillus
Candida
Fusarium

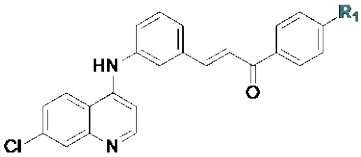

196: R_1 = Cl
197: R_1 = CH_3
MIC = 7.8 - >250 µg/mL
Candida
Cryptococcus

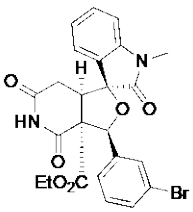

188: MIC = 50 µg/mL
Alternaria
Fusarium
Rhizoctonia
Valsa

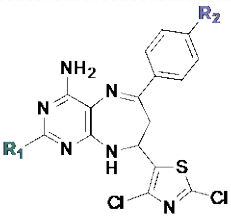

192: R_1 = NH_2; R_2 = H
193: R_1 = NH_2; R_2 = Cl
MIC = 7.8 - 62.5 µg/mL
Candida
Cryptococcus

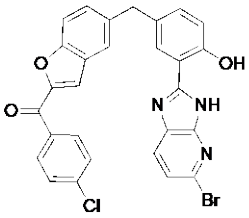

198

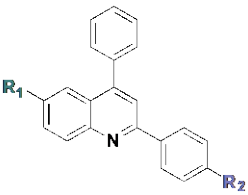

189: R_1 = Br; R_2 = F
190: R_1 = Br; R_2 = CH_3
MIC = 3.9 - >250 µg/mL
Candida
Cryptococcus

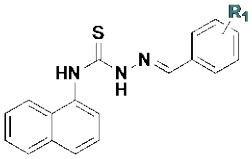

194: R_1 = 2,3-di-F
195: R_1 = 2,5-di-F
MIC = 125 - 250 µg/mL
Aspergillus
Candida
Fusarium

Fig. 1.27. Representative examples of compounds from eleven new scaffolds tested as potential antifungals against the fungal strains listed, which were found to **A.** show limited improvement or no activity when compared to standard antifungal agents, or **B.** to not be active at all.

The synthesis and evaluation of four indole-triazole-amino acid conjugates against only one *C. albicans* strain (Fig. 1.27B) using a disk-diffusion assay identified an analog **187** that achieved 84% inhibition at a very high concentration (*i.e.*, 600 μg/mL).[229] The evaluation of twenty-three spirooxindole analogs against not only human fungal pathogens but also phytopathogens (Fig. 1.27B) led to analogs, such as **188** that failed to show complete inhibition of fungal growth at 50 μg/mL against five dimorphic fungi, including two *Fusarium* spp.[230] Another report described the synthesis and evaluation of twenty-eight quinoline analogs, such as **189-190** (Fig. 1.27B) using only their MIC_{50} and MIC_{80} values against one strain of *C. albicans* and one strain of *C. neoformans*.[235] These analogs were inactive with the exception of two of them, **189-190**, that showed 50% inhibition of fungal growth against *C. neoformans* at high concentrations of 15.6 μg/mL. The synthesis and evaluation of twenty-two thiazolyl-pyrazoline scaffold, including the representative example **191** (Fig. 1.27B), against ten fungal strains (six *Candida* spp., three *Aspergillus* spp., and one *Fusarium* spp.) produced inactive analogs with MIC values in the range of 125-1000 μg/mL.[231] The synthesis and evaluation of fourteen 8,9-dihydro-7*H*-pyrimido[4,5-*b*] [1,4]diazepine analogs against one strain of *C. albicans* and one strain of *C. neoformans* (**192-193**; Fig. 1.27B) failed to produce a compound with antifungal activity.[232] Two analogs, **192-193**, showed 100% inhibition of *C. albicans* growth but only at the high concentrations of 15.6-31.3 μg/mL. The synthesis and evaluation of ten naphthalene-substituted thiosemicarbazone analogs (**194-195**; Fig. 1.27B) against ten fungal strains (*i.e.*, six *Candida* spp., three *Aspergillus* spp., and one *Fusarium* spp.) failed

to produce an analog with significant antifungal activity.[233] The synthesis and evaluation of thirty-seven chalcones (**196-197**; Fig. 1.27B) against *C. albicans* and *C. neoformans* identified two compounds that showed 80% inhibition at high concentrations (*i.e.*, 7.8-15.6 μg/mL).[234] Finally, the synthesis and evaluation of twenty-one benzimidazole analogs (**198**; Fig. 1.27B) against four fungal strains (*i.e.*, *A. niger*, *C. albicans*, *F. oxysporum*, and *Fusarium solani*) led only to completely inactive compounds.[228] Conclusions must be tempered by the limited number of compounds, the equally limited number of strains, and the limited information about important pharmaceutical properties (*e.g.*, cytotoxicity) for the compounds discussed in this section.

1.3.3. Repositioning of FDA-approved drugs or their derivatives used for other medicinal purposes as antifungal agents

The repurposing of existing drugs developed for non-fungal-related diseases as new antifungal agents is an attractive pursuit given the extraordinary costs associated with new drug development. In recent studies, investigators identified antibacterial agents, such as aminoglycoside-based amphiphiles as potential antifungal agents. In addition, other investigators found that the organoselenium drug, ebselen, used in clinical trials for chemotherapy-induced hearing loss (NCT01451853),[236] Ménière's disease (NCT02603081), and cerebral ischemia,[237] possessed potential antifungal activity. This section of the review endeavors to provide a summary of our current understanding of efforts along these lines.

1.3.3.1. Aminoglycoside amphiphiles

Recent years saw the expansion of amphiphilic aminoglycosides from their traditional role as antibacterial agents to a potentially new, important role as antifungal agents. Apart from efforts involving the testing of natural products in the aminoglycoside family, efforts are underway to develop semisynthetic analogs designed to improve activity, identify selectivity, and decrease cytotoxicity. Seven general approaches focus on developing aminoglycoside amphiphiles as antifungal agents: (i) modification of the C-1, 3, 2', and 6' amino groups in nebramine (NEB) with linear alkyl chains, imidazoles, or triazoles (Fig. 1.28); (ii) alkylation of the C-2, 3, 2', and 3' hydroxyl groups of trehalose with linear alkyl chains (Fig. 1.28); (iii) alkylation of the C-6" and 4" hydroxyl groups of kanamycin A (KANA) (Fig. 1.29); (iv) alkylation of the C-6" hydroxyl group of tobramycin (TOB) (Fig. 1.29); (v) modification of the C-6" hydroxyl group of kanamycin B (KANB) with a thioalkoxide group (Fig. 1.29); (vi) modification of the C-6" hydroxyl group of tobramycin (TOB) with C_{18} lipid chains with varied levels of unsaturation and configuration of the double bonds (Fig. 1.30); and (vii) linking of neomycin B (NEO) to mono- or bisbenzimidazoles (Fig. 1.31).

Alkylation of the hydroxyl groups in NEB-derived cationic amphiphiles led to alkoxy analogs with chains that varied in length from C_5-C_7. Modifications at the C-1, 3, 2', and 6' amino groups furnished either the corresponding imidazoles or 1,2,3-triazoles in three or four steps as in the imidazole **199** (Fig. 1.28).[238] Testing of eight NEB-based analogs against nine fungal strains (*i.e.*, three *C. albicans*, one *C. parapsilosis*, four *C. glabrata*, and one *S. cerevisiae*) indicated that three analogs with alkoxy groups and primary amines displayed better antifungal activity than analogs with alkoxy groups and imidazoles;

however, these alkoxy- and amine-substituted analogs also displayed high hemolytic activity. Two of the eight compounds displayed no antifungal activity, including one that contained alkoxy and 1,2,3-triazole groups and the other that contained imidazoles but no alkoxy groups. Alkoxy and imidazole-based analogs such as **199** showed chain-length dependence with respect to antifungal activity in which analogs with C_7 and C_6 alkoxy groups and imidazoles displayed selective and excellent antifungal activity against the four *C. glabrata* strains tested with MIC values of 0.5-1 μg/mL that were better than that of FLC (MIC = 8 to >64 μg/mL). The analogs with C_5 alkoxy groups and imidazoles only displayed good to poor activity (MIC values of 4-16 μg/mL). Compound **199** displayed good activity against *S. cerevisiae*, but was inactive against *C. albicans* and *C. parapsilosis* and displayed improved hemolytic activity up to 128 μg/mL relative to the standard AmB where *ca.* 80% hemolysis was seen at 4 μg/mL. Combination studies displayed synergistic activity between compound **199** and FLC in *C. albicans* and *C. glabrata*. Although these compounds do not display broad spectrum antifungal activity, their selectivity, low hemolytic activity, and synergy with FLC warranted continued investigation.

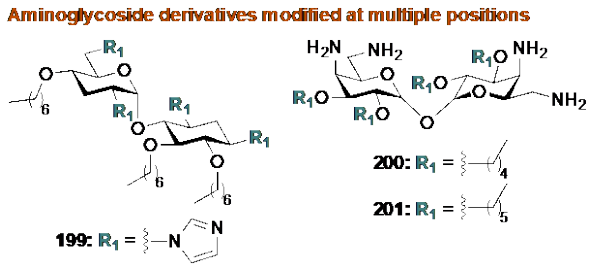

Fig. 1.28. Representative examples of compounds from two new scaffolds tested as potential antifungals, which are derivatives of nebramine (NEB) (**199**) or trehalose (**200-201**).

Alkylation of the C-2, 3, 2', and 3' hydroxyl groups in trehalose furnished six alkoxy analogs (*e.g.*, C_4-C_{10}) in eight synthetic steps including the analogs **200-201** (Fig. 1.28).[239] When tested against two FLC-susceptible *C. albicans*, one FLC-resistant *C. albicans*, and one *C. glabrata* strains, analogs **200-201** with C_5 and C_6 alkyl chains displayed excellent to good antifungal activity with MIC values of 1-4 μg/mL that were better than that of FLC (MIC = 0.25-64 μg/mL). As observed with NEB analog **199**, the antifungal activity of these derivatives depended on the length of the alkyl chains, and analogs with C_5 and C_6 alkyl chains exhibited better antifungal activity than those with either shorter or longer chains than five or six carbons (*i.e.*, C_4, C_8, and C_{10} analogs were completely inactive). The analog with a C_7 chain displayed good activity only against the FLC-resistant *C. albicans* and the *C. glabrata* strains. Unlike the NEB analog **199**, the trehalose analogs **200-201** were broad-spectrum antimicrobial agents that displayed activity against Gram-positive and Gram-negative bacterial species, but unfortunately, the trehalose **200-201** also displayed high hemolytic activity at 4 μg/mL in rat red blood cells. Membrane-permeabilization assays with the trehalose derivative **200** using fluorescent microscopy in *C. albicans* showed that the mechanism of action was, as expected, membrane disruption, an outcome consistent with their lack of selectivity and high hemolytic activity. Although the most active compounds displayed unacceptably high hemolytic activity, their broad-spectrum activity made these analogs attractive for potential development as topical antibacterial or antifungal agents.

Alkylation of KANA at its C-4" and 6" hydroxyl groups produced twenty-two analogs in a three-step sequence including the trisaccharide analogs **202-204** (Fig. 1.29).[240] Just as in

the cases discussed previously, these analogs displayed chain-length dependent antifungal activity, but in this particular case, the optimal chain length for these KANA analogs was eight carbons. These analogs **202-204** showed poor to no antifungal activity against *A. flavus* and *F. graminearum* with MIC values of 31.3 to >500 μg/mL that was less than that of VRC (MIC = 1-32 μg/mL), but combination studies against one strain of azole-resistant *C. albican*, using either **202** or **204** displayed synergy in combination with CLT, FLC, ITC, POS, or VRC. In cytotoxicity experiments, compounds **202-204** displayed little to no cytotoxicity using a human cervical cancer cell line (HeLa) at concentrations ranging from 1-1000 μg/mL. Because of these synergistic effects in combination with other azoles and their good safety profile, these compounds may find application in therapies to combat azole resistance.

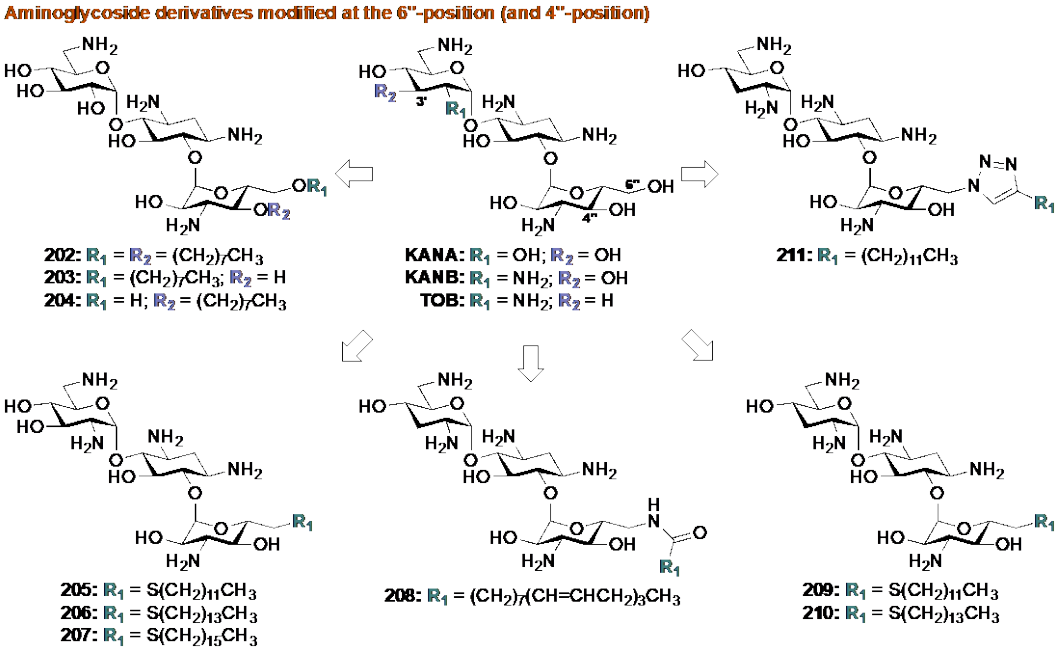

Fig. 1.29. Representative examples of compounds from five new scaffolds tested as potential antifungals, which are derivatives of KANA, KANB, or TOB.

A continued search for new, broad spectrum and potent amphiphilic Aminoglycosides led to the substitution of the C-6" hydroxyl group in KANB by thioalkoxy groups to give the analogs **205-207** (Fig. 1.29).[241] A three-step synthesis furnished seven KANB derivatives along these lines, and once again, activity proved to be chain-length dependent. Analogs **205-207** with C_{12} and C_{14} possessed the optimal alkyl chain lengths. Six derivatives displayed excellent to good activity when tested against one strain of *A. nidulans* with MIC values of ≤1.95-3.9 μg/mL that were better than that of FLC (MIC >62.5 μg/mL). When tested against two strains of azole-susceptible *C. albicans* and five strains of azole-resistant *C. albicans*, four out of the seven derivatives displayed good activity against at least one or all of the *C. albicans* strains tested with MIC = 3.9-7.8 μg/mL that was better than that of FLC (MIC = 15.6 to >125 μg/mL). Thioalkoxy analogs **205-206** displayed synergy in combination with POS against all seven *C. albicans* strains tested as well as fungicidal activity against azole-resistant *C. albicans*. These KANB derivatives displayed limited chain length-dependent hemolysis: 40% at 4× MIC for C_{12} and 15% at 1× MIC for C_{14} chain lengths. In cytotoxicity experiments using the A549 and BEAS-2B mammalian cell lines, four of these KANB derivatives were found to be safe at concentrations as high as 62.5 μg/mL. The mechanism of action was investigated using a membrane-permeabilization assay, and compounds **205-206** disrupted the fungal membrane of azole-resistant *C. albicans*. Consequently, the promising activity and properties seen in these KANB derivatives warrants their continued development as antifungal agents.

In another study, the alkylation of the C-6" hydroxyl group of TOB with C_{18} lipid chains varying in degrees of unsaturation and stereochemistry led in three steps to six analogs

such as the TOB carboxamide **208** (Fig. 1.29).[242] Testing against nineteen fungal strains (*i.e.*, three azole-susceptible, four azole-resistant, and two echinocandin-resistant *C. albicans*, one *C. parapsilosis*, one *C. tropicalis*, one *C. dubliniensis*, one *C. guilliermondii*, four *C. glabrata*, and two *C. neoformans*) indicated that all six TOB derivatives displayed activity (MIC values of 4-8 μg/mL) that was comparable or better than that of the standards, FLC (MIC = 0.25 to >64 μg/mL) and CAS (MIC = 0.25-64 μg/mL)). A high degree of *cis*-unsaturation, but not *trans*-unsaturation, in the C_{18} lipid chains correlated with the desired, low hemolytic activity and increased specificity for the fungal cell membrane. In cytotoxicity experiments using HEK-293, HepG2, and a mouse embryonic fibroblast (3T9MEF) cell line, compound **208** possessed the best safety profile at concentrations up to 216 μg/mL for the HepG2 cell line, and >256 μg/mL for the other cell lines. Mechanism of action studies revealed that compound **208** disrupted fungal cell membranes without disturbing comparable mammalian membranes. The increased antifungal activity, selectivity for fungal cells, and increased safety profile of compound **208** warrants its further development as an antifungal agent.

The conversion of the C-6" hydroxyl group of TOB to a thioalkoxy group furnished the analogs **209-210** (Fig. 1.29) that possessed broad-spectrum antifungal activity.[243] The most potent compounds, namely **209-210**, possessed C_{12} and C_{14} chain lengths, respectively, and were active against *C. neoformans*, *A. nidulans*, and *F. graminearum* with MIC values of 1.95-7.8 μg/mL that were comparable or better than that of FLC (MIC <0.195 to >125 μg/mL). The thioalkoxy TOB analog **210** also displayed good antifungal activity against

the four azole-susceptible and three azole-resistant *C. albicans* strains tested (MIC = 3.9-7.8 μg/mL).

As expected, mechanism of action studies revealed that **209-210** induced apoptosis through a mechanism involving the disruption of fungal cell membranes. Analogs **209-210** were fungicidal against azole-resistant *C. albicans*, displayed 50% hemolytic activity of mouse erythrocytes at 4- to 32-fold and 8- to 32-fold higher levels than their MIC values, respectively, and showed no toxicity against human lung cancer A549 or bronchial epithelial BEAS-2B cell lines. Checkerboard assays revealed that **209-210** exhibited synergy in combination with FLC, ITC, POS, and VRC.[244] An additional study investigating the effect of the linker (*e.g.* thioether, sulfone, triazole, amide, and ether group) at the 6"-OH position of TOB demonstrated that the introduction of a 1,2,3-triazole bearing a C_{12} alkyl chain at C-6" in analog **211** was the most active compound (Fig. 1.29).[245] Overall, the introduction of alkyl chains at the C-6" position of TOB proved a successful strategy for developing, new, promising antifungal agents.

Modification at the C-4" and 6" positions of amphiphilic aminoglycosides as well as modification of the 6'-position of aminoglycosides provided various KANA and one TOB derivatives. Acylation, for example of the C-6' position KANA and TOB furnished carboxamides **212-214** with acyl chains that varied in length from C_6-C_{18} (Fig. 1.30).[246] Overall, the KANA and TOB derivatives displayed poor activity when tested against *A. flavus*; however, analogs **212-214** displayed good activity when tested against nine other fungal strains comprising three *C. albicans*, one *F. graminearium,* one *C. neoformans*, one

Rhodotorula pilimanae, one *Candida rugosa*, one azole-resistant *C. parapsilosis*, and one *C. tropicalis* with MIC values of 4-8 μg/mL that were comparable or better than that of VRC (MIC = 0.125 to ≥256 μg/mL). Analogs containing long acyl chains (C_{16}-C_{18}), such as **213**, caused increased membrane permeabilization relative to analogs with short acyl chains; however, because there was an increase in toxicity in HeLa cells as the chain length increased, it will be important to balance the increase in membrane permeability against hemolysis in assessing these compounds as potential antifungal agents.

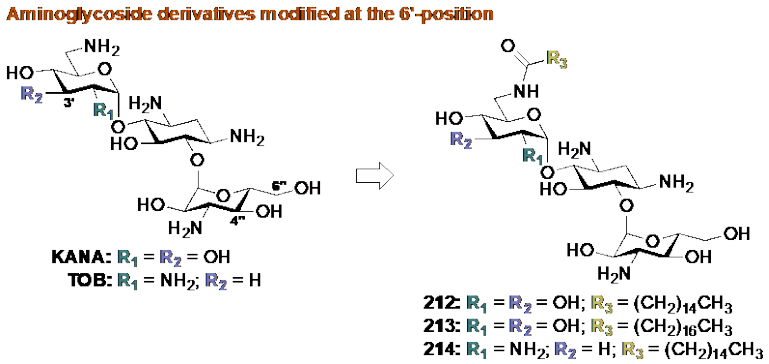

Fig. 1.30. Representative examples of compounds from a new scaffold tested as potential antifungals, which are derivatives of KANA or TOB.

Finally, a study of the conversion of alkylated NEO to mono- or bisbenzimidazole analogs led to eleven NEO derivatives, including a representative NEO analog **215** (Fig. 1.31) that displayed an interesting pattern of antifungal activity.[247-249] Testing against thirteen fungal strains (*i.e.*, four azole-susceptible *C. albicans*, three FLC- and ITC-resistant *C. albicans*, one *C. glabrata*, one *C. krusei*, one *C. parapsilosis*, one *A. flavus*, one *A. nidulans*, and one *A. terreus*) showed that four of the eleven compounds displayed excellent activity against at least one of the thirteen strains. Three of the analogs displayed excellent activity against seven to twelve of the thirteen strains with MIC values of 0.12-1.95 μg/mL that were better

than that of FLC (MIC = 1.95 to >125 μg/mL). In an outcome similar to that seen with compounds **202**-**204** that displayed no antifungal activity, these NEO analogs were inactive against *A. flavus*. Analog **215** displayed fungicidal activity at 1× MIC against *C. albicans* and displayed an inhibitory effect against biofilms of two *C. albicans* strains that was better than or comparable to that of VRC. In cytotoxicity experiments using the A549 and BEAS-2B human cell lines, four out of the eleven NEO derivatives displayed no toxicity at concentrations up to 31 μg/mL for A549, and two of the compounds, including compound **215**, were nontoxic at 15.6 μg/mL in BEAS-2B, a value that was about 10× MIC. This NEO analog **215** also displayed little to no hemolytic activity in murine red blood cells up to 15.6 μg/mL. In a study of sterol composition, compound **215** had no effect on ergosterol biosynthesis and instead, the mechanism of action appeared to be the induction of ROS. With low MIC values, toxicity, and hemolysis, these NEO derivatives warrant additional study.

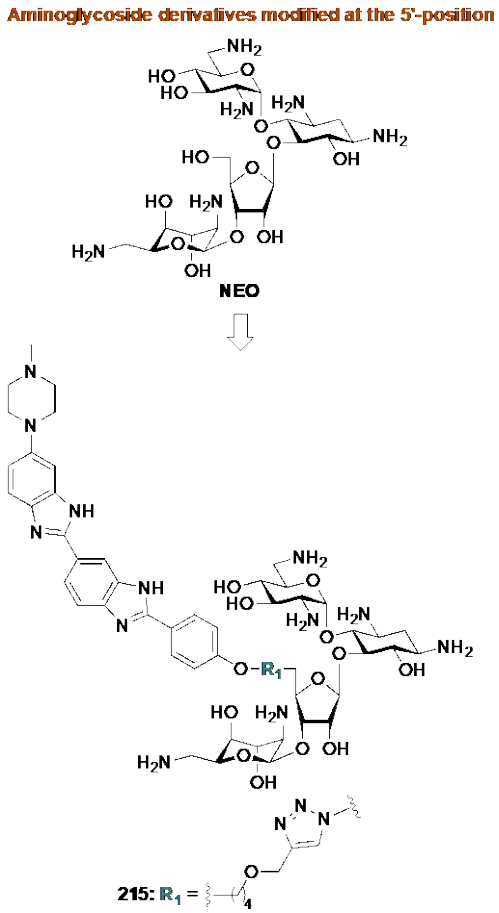

Fig. 1.31. A representative example of compounds from a new scaffold tested as a potential antifungal, which is a derivative of NEO.

1.3.3.2. Probes for determination of mechanism of action of amphiphilic aminoglycosides and azoles

Fluorescent probes provide a valuable window for investigating the mechanism of action of amphiphilic aminoglycosides and azole derivatives.[246, 250-251] To examine visually the mechanism of action of amphiphilic AGs, NEA and TOB were alkylated to afford **216** and **218**, respectively, and subsequently modified either with a fluorescent nitrobenzoxidiazole to yield **217** or with a 7-diethylaminocoumarin to yield **219** (Fig. 1.32A).[250] The availability of these fluorescent analogs facilitated mechanism-of-action studies that established the importance of fungal, plasma-membrane permeabilization for compounds **217** and **219**.

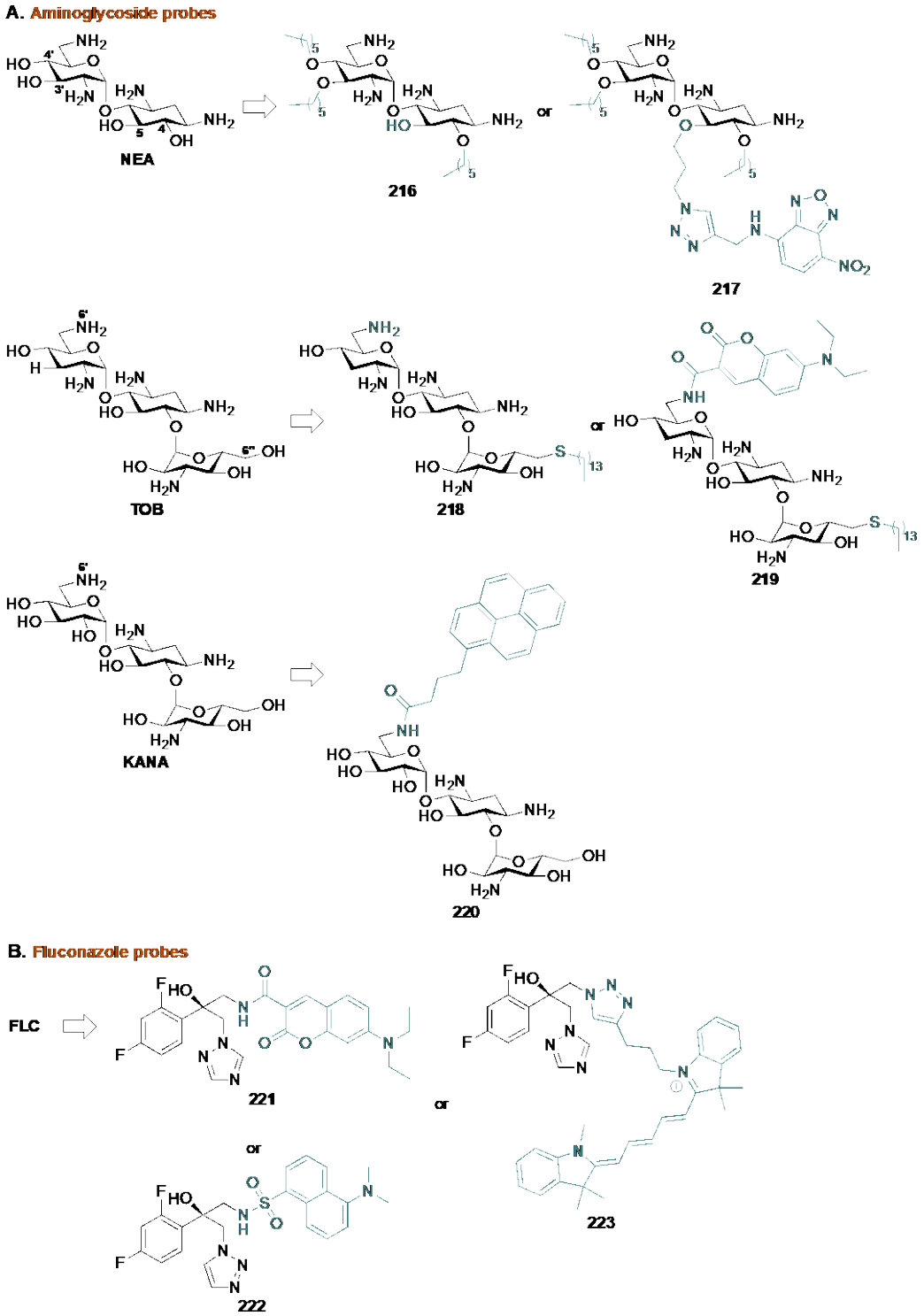

Fig. 1.32. Representative examples of compounds from four new scaffolds tested as potential antifungals, which are **A.** amphiphilic aminoglycosides or **B.** azole derivatives.

The inclusion of a 1-pyrenylbutanoyl fluorescent group at the C-6' position of KANA yielded compound **220** that displayed antifungal activity and facilitated studies of mechanism of action (Fig. 1.32A).[246] Not all fluorescent tags were useful, and the introduction of either a fluorescein or a 2-phenyl-4-quinolinecarbonyl tag at that same position led to inactive compounds that were ineffective probes. Probe **220** indicated that the mechanism of action of these analogs in *F. graminearum* and *C. albicans* was membrane permeabilization. Additional kinetic membrane-permeabilization studies[246] using **220** and propidium iodide showed that the rate of membrane permeabilization for the KANA derivatives from fastest to slowest was fungi, bacteria, and then mammalian cells.

In another study, the synthesis of fluorescent FLC analogs yielded five azole derivatives, such as **221**-**223**, that were active against *Candida* spp. (Fig. 1.32B).[251] In mechanism of action studies, aminocoumarin-based FLC derivative **221** localized to the endoplasmic reticulum, and compounds **222** and **223** localized in the mitochondria of the *Candida* spp. Overall, fluorescent probes provided a direct means for investigating the antifungal mechanism of action of amphiphilic aminoglycosides and azole derivatives.

1.3.3.3. Additional amphiphilic molecules - Quinone amphiphiles

In addition to the amphiphilic AGs, a synthesis of six quinone-based amphiphiles in two to three steps led to dimeric quinones containing a 1,2,3-triazole. The triazole possessed alkyl groups with varying chain lengths (C_1-C_{10}) at the *N*-1 position, as illustrated by the representative analogs **224**-**225** (Fig. 1.33).[252] Alkylation at the *N*-3-position with a C_6 alkyl chain connected the two quinone-based moieties. When tested against one strain of azole-

susceptible *C. albicans*, one strain of azole-resistant *C. albicans*, one strain of *C. neoformans*, and one strain of *R. pilimanae*, compounds **224-225** displayed excellent to good activity with MIC values of 2.0-3.91 μg/mL that were better than that of FLC (MIC = 1.56 to >250 μg/mL). Compounds **224-225** exhibited only slight activity against *A. flavus*, and the other four analogs were inactive. In both *C. albicans* and *F. graminearum*, the mechanism of action of **225** was cell membrane disruption. In cytotoxicity experiments using the human ovarian cancer SKOV3 cell line, five compounds displayed good safety profiles. The quinone-based amphiphiles **224-225** warrant further investigation.

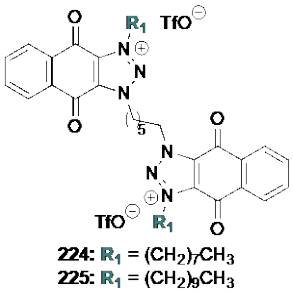

Fig. 1.33. Representative examples of compounds from a new scaffold tested as potential antifungals, which are quinone derivatives.

1.3.3.4. Ebselen derivatives

Ebselen is an organoselenium compound that has a structurally similar sulfur analog called ebsulfur. Because ebselen has several therapeutic applications and a reasonable safety profile in clinical trials,[236] several studies investigated the antifungal properties of these compounds, such as the analogs **226-228** (Fig. 1.34).[253] A study of thirty-two ebsulfur derivatives made three modifications: (1) substitution of the *N*-phenyl of ebselen by mono- and disubstituted phenyl, naphthyl, and nitrogen-containing aromatic heterocycles that slightly increased antifungal activity; (2) substitution of the *N*-phenyl with linear and

branched alkyl chains or with alkyl chains with terminal phenyl or adamantyl groups that dramatically increased activity; and (3) oxidized sulfoxide derivatives that led to a complete loss of activity. When tested against the same thirteen strains as those described above for the NEO derivative **215**, ten of the thirty-two compounds displayed excellent activity against at least ten of the thirteen strains. Seven of these compounds displayed excellent activity against all thirteen strains tested with MIC values of ≤0.02-1.95 μg/mL that were better than that of FLC (MIC = 1.95 to >125 μg/mL). Compound **226** displayed fungistatic activity at 4× MIC against *C. albicans*. Two ebsulfur derivatives were tested against murine red blood cells, and one was found to be safe at up to 15.6 μg/mL and the other at 3.9 μg/mL. In cytotoxicity experiments using HEK-293 and a murine macrophage (J774A.1) cell line, compounds **226-228** were comparable to ebselen with IC_{50} of 10 μg/mL that represented at least a 10-fold difference between the toxic dose to the mammalian cells and the fungal MIC values of the most active compounds. Preliminary mechanism of action studies suggested an induction of ROS production in *C. albicans*. Due to their excellent antifungal activity, additional studies of these compounds appear to offer promising outcomes.

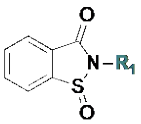

226: $R_1 = (CH_2)_4CH_3$
227: $R_1 = (CH_2)_5CH_3$
228: $R_1 = C(CH_3)_3$

Fig. 1.34. Representative examples of compounds from a new scaffold tested as potential antifungals, which are ebselen derivatives.

1.3.4. Repositioning antifungals as anticancer agents

The converse of studying non-antifungal-related drugs as antifungal agents involves studies in which antifungal agents are repurposed for other ailments, such as cancer[254] or bacterial infections.[255] For example, a study of ITC as a source of antineoplastic agents led to analogs such as **229** (Fig. 1.35).[254] Synthesis of a series of twenty-four ITC derivatives in a convergent, fourteen-step synthesis led to ITC derivatives with modifications at various stereogenic centers and to ITC derivatives in which nitro or amine groups replaced the triazolone. The most active compound that showed promise as an antineoplastic agent was compound **229** that incidentally displayed no antifungal activity due to the lack of the essential, triazole moiety. Although the ultimate outcome of repurposing studies such as this one may be unclear, it seems reasonable to conclude that scaffolds that show success in providing antifungal drugs may also offer avenues for success in other areas of drug discovery.

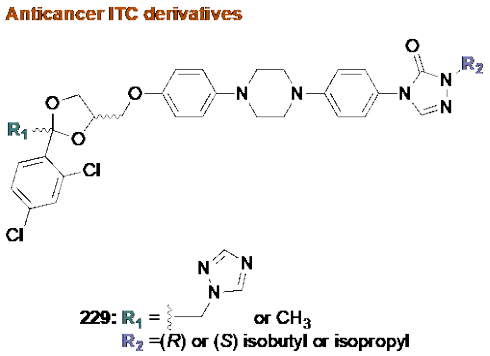

Fig. 1.35. Representative examples of ITC derivatives investigated as potential anticancer agents.

1.3.5. New scaffolds for synergy with azoles

In addition to the aminoglycoside amphiphiles including NEB (**199**; Fig. 1.28), KANA (**202** and **204**; Fig. 1.29), KANB (**205-206**; Fig. 1.29), and TOB (**209-210**; Fig. 1.29), and

in addition to derivatives of 5FC (**70**; Fig. 1.20A), tetrazole (**110b** and **111b**; Fig. 1.23), chalcone (**167-168**; Fig. 1.26), and hydrazone (**113-116**; Fig. 1.24), the repurposing of new scaffolds and investigations of synergistic effects in combination studies with FDA-approved azoles may have a promising future. For example, a combination study of the antifungal activity of the antipsychotic drug, bromperidol **230** (Fig. 1.36) and its derivatives containing C-4 substituted phenyl groups, with a variety of FDA-approved azole antifungal agents led to interesting results.[256] Testing in combination with FLC, ITC, KTC, POS, and VRC against seven strains of *C. albicans*, one *C. glabrata*, and one *A. terreus* indicated that one of the bromperidol compounds **230** showed the good synergy with POS with a 16-fold reduction of MIC values for both compounds. Synergy was also observed with compound **230** and POS with a 32-fold reduction in both MIC values. Time-kill assays of an azole-resistant *C. albicans* strain with compound **230** and POS or VRC revealed fungistatic activity at 8× MIC_{combo} concentrations. The combination of compound **230** and POS or VRC showed an additive effect in fungal biofilms of an azole-resistant *C. albicans* with sessile MIC (SMIC) values of POS or VRC decreased from >32 to 0.5 μg/mL. In cytotoxicity experiments using BEAS-2B, HEK-293, and J774A.1 cell lines, compound **230** was not toxic at up to 8 μg/mL alone, and similar cytotoxicity was observed with POS and VRC with 8 μg/mL of compound **230**. Bromperidol at 32 μg/mL in combination with VRC at any concentration displayed no cytotoxicity and appeared to warrant further study as a useful combination therapy.

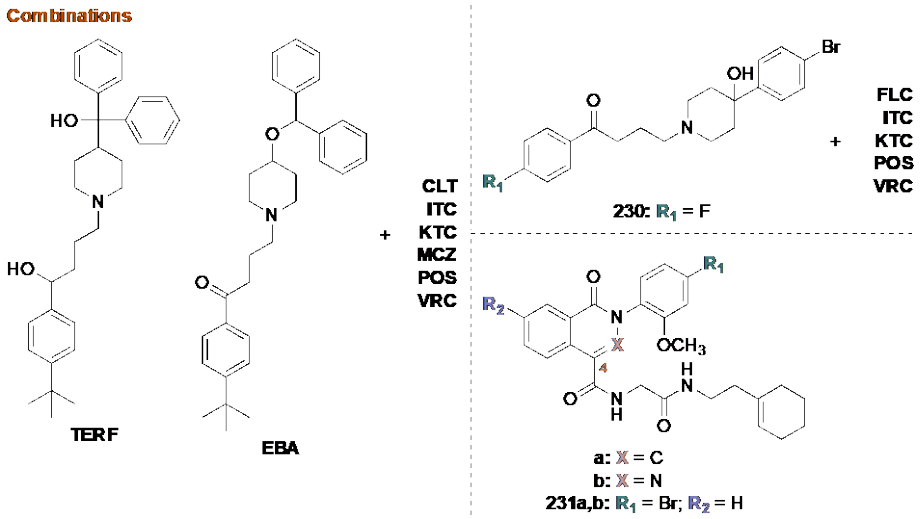

Fig. 1.36. Representative examples of compounds from two new scaffolds tested as potential antifungals, which were used in combination with FDA-approved azoles.

In an attempt to find new solutions to the treatment of drug-resistant *Candida* fungal infections, the repositioning of the antihistamines, TERF and EBA, for antifungal combination synergy studies involved ninety-one different combinations with seven different azoles (TERF and EBA; Fig. 1.36).[257] Testing of these combinations of either TERF or EBA with either CLT, ITC, KTC, MCZ, POS, or VRC against thirteen strains of *Candida* spp. comprising seven *C. albicans* (four of which were resistant to most triazoles), four *C. glabrata*, one *C. krusei*, and one *C. parapsilosis* led to interesting synergistic outcomes. Out of the ninety-one combinations, fifty-one of them were synergistic. The best combination was POS and EBA in which time-kill assays were fungistatic at 4× MIC against *C. albicans* and *C. glabrata*. When tested against fungal biofilms of one strain of azole-sensitive *C. albicans*, one azole-resistant *C. albicans*, and one azole-resistant *C. glabrata*, the combination of POS and EBA displayed synergy as shown by *C. glabrata* $SMIC_{90}$ values of >32 μg/mL and ≥25 μg/mL alone to 0.06 μg/mL and 6.3 μg/mL in combination for POS and EBA, respectively. In cytotoxicity experiments using A549,

BEAS-2B, HEK-293, and human skin keratinocyte (HaCaT) mammalian cell lines, no significant difference was observed in the safety profile of POS and EBA when tested alone or in combination. EBA was found to be safe at up to 6.3 μg/mL in HaCaT cells and 3.1 μg/mL in all other cell lines, while POS was found to be safe at 4 μg/mL for both A549 and HEK-293 and safe to up to 8 μg/mL for the other cell lines. The combination of EBA and POS warrants further investigation.

In another combination study, modifications of isoquinolones and phthalazinones based on a previously identified leading compound **231a,b** (Fig. 1.36)[258] led to three types of derivatives: (1) modifications of the bicyclic core including replacement of the phenyl group with a heterocycle containing various substituents; (2) introduction of a methoxy group at the 2-position of the *N*-phenyl ring that was essential for activity; and (3) modification of the C-4-position with a glycine derivative to afford compound **231a**. Testing against two strains of *C. albicans* in combination with 0.25 μg/mL of FLC produced interesting results in which nine combinations displayed excellent EC_{50} values of 0.001-0.23 μM. Additionally, testing of compounds **231a,b** in combination with FLC against five strains of FLC-resistant *C. albicans* (EC_{50} = 11-170 μM) displayed good to poor activity, and testing against *C. glabrata* or *C. neoformans* var. *grubii* showed no antifungal activity. Even though the compounds did not kill the FLC-susceptible or FLC-resistant *C. albicans* strains, compounds **231a,b** displayed fractional inhibitory concentration indices (FICI) of 0.12-0.17 in combination with FLC, indicating synergy (*Note*: FICI values are used to determine the interaction between two drugs for the purpose of being used in combination. A FICI value <0.5 indicates synergy). These compounds

also displayed antifungal activity in combination with ISA. Cytotoxicity experiments with all twelve derivatives against 3T3 mammalian fibroblasts revealed that they were safe at up to 10 μM. The isoquinolone and phthalazinone derivatives displayed excellent antifungal activity in combination with FLC and warrant additional study as potential antifungal agents.

1.3.6. Isolation and/or derivatization of novel natural products with antifungal activity

1.3.6.1. Isolated natural products

Natural products served as starting points for the development of antifungal agents in the past and will undoubtedly continue to serve as sources of new scaffolds for future, antifungal drug discovery. Unfortunately, in recent years, no new natural products emerged with particularly promising, antifungal activities. For example, the testing of twelve natural products, such as the terpenoid **232** (Fig. 1.37)[259] from the Chinese liverwort, *Tritomaria quinquedentate*, for antifungal activity against five *C. albicans* strains showed that compound **232** possessed a high MIC_{80} of 16 μg/mL against one drug efflux pump-deficient strain of *C. albicans*. However, this natural product also targeted ERG6 and ERG11, decreased the amount of ergosterol in *C. albicans*, and inhibited yeast-to-hyphal formation. Although interesting, the high MIC_{80} value is unlikely to spark much interest in these terpenoids as potential antifungal agents.

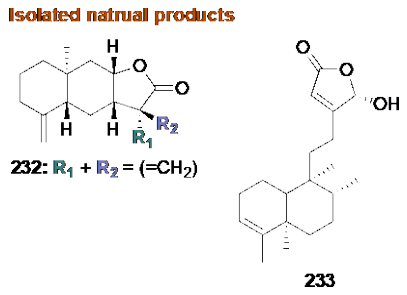

Fig. 1.37. Representative examples of compounds from two new scaffolds tested as potential antifungals, which are isolated natural products.

Similarly, a diterpenoid, **233**, isolated from the evergreen tree, *Polyalthia longifolia* var. *pendula* displayed minimal activity (MIC_{90} value of 50 μM (equivalent to 17.2 μg/mL) to 805 μM) when tested against two strains of *C. albicans*, one *C. glabrata*, one *C. neoformans*, one *A. fumigatus*, one *A. niger*, one *F. oxysporum*, and one *Neurospora crassa* (Fig. 1.37).[260] At concentrations of up to 1200 μM, low hemolytic activity was observed for compound **233**. This compound also inhibited yeast-to-hyphal transition in *C. albicans*. Membrane-permeabilization assays with the isolated compound **233** using fluorescent microscopy in *C. albicans* showed that the mechanism of action was the anticipated, membrane disruption. An increase in intracellular ROS generation was also observed with this compound. This minimal activity and the lack of information regarding cytotoxicity suggests discontinuing additional studies of antifungal activity of these compounds.

1.3.6.2. Natural product derivatives

Semisynthetic natural products often offer a more promising avenue to new antifungals than natural products themselves. For example, two analogs **234-235** of sampangine with simplified structures were synthesized in five steps and were more active and more water soluble than those of the parent natural product (Fig. 1.38).[261] When tested against *C.*

parapsilosis, *C. neoformans*, *A. fumigatus*, *T. rubrum*, and *M. gypseum*, these compounds **234-235** displayed antifungal activity (MIC_{80} values of 0.125-4 μg/mL) that were 4- to 512-fold better than that of sampangine (MIC_{80} values of 2 to >64 μg/mL). When tested against four FLC-resistant strains of *C. albicans*, these compounds displayed MIC_{80} values of 0.5-1 μg/mL in contrast with FLC that had an MIC_{80} value that was >1024 μg/mL. In anti-biofilm studies, compounds **234-235** inhibited *C. albicans* biofilms by 30% at 1 μg/mL and inhibited yeast-to-hyphal formation. In cytotoxicity experiments using *C. elegans* worms, these compounds were non-toxic at concentrations of 128 μg/mL. In summary, these sampangine derivatives showed promise as antifungal agents and optimization of the leading compounds led to a series of 32 sampangine derivatives in five to eight synthetic steps, exemplified by **236-237** (Fig. 1.38).[262] When tested against the same seven strains as those described above for **234-235**, six of the 32 compounds displayed MIC_{80} values of 0.25-2 μg/mL, similar to or better than that of FLC (MIC_{80} = 0.25 to >64 μg/mL) against at least six of the seven strains tested. Compounds **236** and **237** additionally displayed MIC_{80} values of 0.25-1 μg/mL against five FLC-resistant strains of *C. albicans* as well as anti-biofilm activity in *C. albicans* biofilms at concentrations of 6.4-12.8 μg/mL. Both compounds also inhibited yeast-to-hyphal formation at 0.4 μg/mL. In cytotoxicity experiments using *C. elegans*, no toxicity was observed at concentrations up to 100 μg/mL. Additional studies of cytotoxicity experiments using mammalian cells and potential development of resistance to these compounds will further define the very promising activity of these potential antifungal agents.

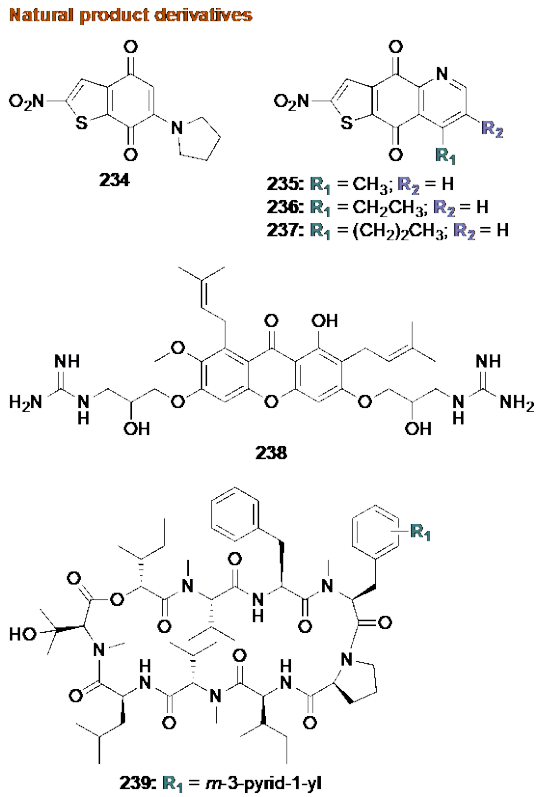

Fig. 1.38. Representative examples of compounds from four new scaffolds tested as potential antifungals, which are derivatives of isolated natural products.

Investigations focused on derivatives of the natural product, α-mangostin, led to thirty-two, semisynthetic α-mangostin derivatives such as **238** (Fig. 1.38)[263]. Analog **238**, displayed excellent to good antifungal activity when tested against one strain of drug-resistant *C. albicans*, five drug-susceptible *C. albicans*, four *F. solani*, two *F. oxysporum*, one *A. brasiliensis*, two *A. flavus*, and two *A. fumigatus* with MIC values of 0.78-6.25 μg/mL that were similar to or better than that of CAS (MIC = 0.10 to >50 μg/mL). In combination studies with TRB, compound **238** displayed synergy against *C. albicans* and fungicidal activity at 4× MIC against drug-resistant *C. albicans*. In a drug-resistance development study, *C. albicans* DF2672R failed to develop drug resistance after twenty-seven passages. In cytotoxicity experiments using human corneal fibroblasts, this

compound was non-toxic at concentrations up to IC_{50} of 64.1 μg/mL. The mechanism of action of compound **238** was increased membrane permeabilization and compound **238** was efficacious in a *C. albicans* murine model of fungal keratitis. Clearly, this compound displayed activities that warrant additional development.

Finally, a three-step synthesis led to twenty-four derivatives of the natural product, aureobasidin A such as analog **239** (Fig. 1.38).[264] Six analogs displayed excellent antifungal activity when tested against *C. albicans* and *A. fumigatus* with MIC values of <0.025-2.5 μg/mL that were better than that of aureobasidin A (MIC <0.05 to >25 μg/mL). Testing of the most active compound **239** against an additional thirty-four fungal strains comprising six *C. albicans*, eight non-*albicans Candida*, *Cryptococcus* spp., *Issatchenkia* spp. (often designated as *C. krusei*), *Saccharomyces* spp., ten *Aspergillus* spp., *Emericella* spp. (sexual form of *Aspergillus*), *Fusarium* spp., *Rhizopus* spp., *Sporothrix* spp., and three *Trichophyton* spp. showed excellent antifungal activity against thirty-one out of the thirty-four strains with MIC = 0.008-2 μg/mL, that was comparable to that of AmB (MIC = 0.004-1 μg/mL). Compound **239** clearly warrants additional study as an antifungal agent in order to understand its mechanism of action, potential for drug resistance, and cytotoxicity.

Overall, many families of compounds have been investigated as potential antifungal agents. Many were found to be promising, while others have informed us of directions that are less desirable. Table 1.3 presents a general summary of all data that were discussed throughout this review.

Table 1.3. Activity of the representative compounds amongst the series prepared.

Family	Cpd #	Candida spp.	Aspergillus spp.	Cryptococcus spp.	Other
Currently used antifungal					
Imidazoles	**1-4**	✓?	×		×
	5-9	✓			
	10-12	✓?	✓		✓
	13	✓ to ~	✓ to ~		✓ to ~
Triazoles	**14-22**	✓	✓		
	23-26	✓	✓	✓	
	27-28	×	×	×	×
	29-37	✓ to ~	✓		
	38-39	×	×	×	×
	40-41	✓	×	×	
	42-62	✓	~	✓	
Polyenes	**63**	~			
	64	✓ to ~			
	65	✓			
	66-67	✓	✓	✓	✓
	68	✓ to ×		✓ to ~	✓ to ~
Echinocandins	**CD101**	✓	✓		
Allylamines	**69**				~
Antimetabolites	**70**	✓			
	71	~ to ×	~ to ×		
	72	×	×		✓
	73-74	~	×		
Natural Products					
Isolated	**232**	×			
	233	×	×	×	×
Derivatives	**234-237**	~	~	~	~
	238	✓ to ~	✓ to ~		✓ to ~
	239	✓	✓	✓	✓

Family	Cpd #	Candida spp.	Aspergillus spp.	Cryptococcus spp.	Other
Novel Scaffolds					
Imidazoles	**75-77**	✓	×	✓	
	78-79	✓	~ to ×	✓	
	80-82	✓ to ×			
Thiazoles	**83-85**			×	✓
	86-94	✓ to ×			
Benzimidazoles	**95-97**	✓ to ~	✓ to ~		
Benzothiazoles	**98-104**	✓	×	✓	
1,2,3-Triazoles	**105**	×			
	106-108	✓ to ×	×		✓
Tetrazoles	**109-112**	✓	×		×
Hydrazones	**113-116**	×			
	117-121	✓			
	122-125	✓ to ~	✓ to ~		
	126-131	✓	✓		✓
Aromatic and heterocyclic	**132-135**				×
	136-137	✓		✓	
	138-142	✓ to ×?	✓ to ×?		
	143-144		✓		
	145-147	×	✓	×	
	148-158	✓	×	✓	
Additional scaffolds	**159-162**	×	✓ to ~		
	163-166	×	✓		~
	167-168	✓			
	169-172	✓	✓		
Repositioning					
AG amphiphiles	**199**	✓ to ×			~
	200-201	✓ to ~			
	202-204		×		×
	205-207	~	✓ to ~		
	208	~		~	
	209-210	~	✓ to ~	✓ to ~	✓ to ~
	211	✓ to ×	✓ to ×	✓	
	212-214	~	×	~	~
	215	✓	✓ to ×		
Quinone amphiphiles	**224-225**	✓ to ~	×	✓ to ~	✓ to ~
Ebselen	**226-228**	✓	✓		

✓	Indicates MIC values of ≤2 μg/mL for the best representative compounds amongst the series prepared.
✓ to ~	Indicates MIC values of ≤2-8 μg/mL for the best representative compounds amongst the series prepared
✓ to ×	Indicates MIC values of ≤2 to ≥15.6 μg/mL for the best representative compounds amongst the series prepared.
~	Indicates MIC values of 3.9-8 μg/mL for the best representative compounds amongst the series prepared.
~ to ×	Indicates MIC values of 3.9 to ≥15.6 μg/mL for the best representative compounds amongst the series prepared.
×	Indicates MIC values of ≥15.6 μg/mL for the best representative compounds amongst the series prepared.
?	Indicates: (i) MIC data were provided without comparable MIC values for the standards from which the compounds were derived or (ii) inconsistencies between units used in the manuscript for the MIC values.

1.4. OVERALL CONCLUSION AND PERSPECTIVE

The first antifungal drug to enter the clinic was AmB in 1959, and the most recent class of antifungals to succeed in the clinic were the echinocandins, beginning with CFG in 2001. The history of antifungal drugs may be short in comparison with agents for other infectious diseases, but antifungal agents currently advancing in preclinical development and in clinical trials represent promising antifungal scaffolds. We share not only our enthusiasm for the recent progress in this area but also our excitement as we learn of the advances that colleagues across the world make in developing new agents as medicines.

For the compounds currently in preclinical studies, the wealth of preliminary studies heralds a growing interest in antifungal development. Although only a few compounds appear to pass the earliest stages of development that are generally limited to MIC values or even just disk diffusion assays, we encourage the use of dilution assays, multiple fungal strains, studies of the potential for drug resistance, hemolysis studies and, of course, animal studies. Those that venture into the investigation of the mechanism of action often explore known mechanisms and we also encourage our colleagues to look for novel mechanisms of action for the new scaffolds under development.

There are scaffolds, as indicated in this review, that show considerable promise and warrant further investigation, particularly using the few available, animal models that will evaluate the true potential of these antifungal agents. There are mouse models for disseminated candidiasis and aspergillosis that mimic the natural progression of disease in humans. For candidiasis, the mice can be infected through gastrointestinal colonization as well as by

intravenous or intraperitoneal injections. To replicate lung disease in aspergillosis, mice are infected with spores using an inhalation inoculation. For more specific disease models, mouse models of disseminated infections have been modified to replicate mucosal *Candida* infections, neonatal *Candida* infections, and fungal biofilms.

Fungal resistance is on the rise. We encourage colleagues to pursue in-depth studies leading to the development of antifungal agents that address this need. While once a minor problem in healthcare, fungal resistance will soon become a major healthcare crisis that will demand our full attention. We hope this review provides a thoughtful summary of the most recent chemical discoveries in the period covering from 2015-2019 and serves as a call-to-action for current and new investigators who desire to help in the fight against fungal diseases.

1.5. AUTHOR CONTRIBUTIONS

E.K.D. wrote and made figures for the introduction (section 1.2) and wrote section 1.3.6. K.C.H. wrote and made figures for section 1.3. S.G.-T. contributed to making all figures, writing, and supervision of research. D.S.W. read and edited the manuscript and contributed to the writing of the abstract and conclusion.

Chapter 2

Synergistic combinations of azoles and antihistamines against *Candida* species *in vitro*

2.1. ABSTRACT

Fungal infections are a major cause of skin and mucosal membrane disease. Immunocompromised individuals, such as those undergoing chemotherapy, are most susceptible to fungal infections. With a growing population of immunocompromised patients, there are many reports of increasing numbers of infections and of fungal strains resistant to current antifungals. One way to treat drug-resistant infections is to administer combinations of drugs to patients. Azoles are the most prescribed antifungals, as they are broad-spectrum and orally bioavailable. Terfenadine (TERF) and ebastine (EBA) are second-generation antihistamines, with EBA being used in many countries. In this study, we explored combinations of seven azole antifungals and two antihistamines (TERF and EBA) against a panel of thirteen *Candida* fungal strains. We found fifty-five out of ninety-one combinations tested of TERF and EBA against the various fungal strains to be synergistic with the azoles. To evaluate the efficiency of these combinations to inhibit fungal growth, we performed time-kill assays. We also investigated the ability of these combinations to disrupt biofilm formation. Finally, we tested the specificity of the combinations towards fungal cells by mammalian cytotoxicity assays. These findings suggest a potential new strategy for targeting drug-resistant *Candida* infections.

2.2. INTRODUCTION

Candida spp. are a normal part of the skin and gastrointestinal microbiome. However, patients who are being treated with broad-spectrum antibiotics, corticosteroids, or immunosuppressants as well as patients with conditions, such as HIV, that compromise the immune system are more susceptible to fungal infections. In addition, patients with diabetes and severe burn wounds are at an increased risk for fungal infections.[265-268] On the skin and mucosal membranes, *Candida* spp. can cause cutaneous infections, which when untreated can lead to invasive infections affecting the eyes, heart, and brain with a high mortality rate.[269-272] In addition, *Candida* spp. are the primary cause of oral thrush and vulvovaginal infections.[273-275]

As *Candida* spp. are eukaryotes, development of antifungal drugs has exploited differences in cell membrane structure. There are four classes of drugs used to treat *Candida* infections. These classes include the azoles, the polyenes, the echinocandins, and the allylamines. The polyenes are broad-spectrum antifungals and include nystatin (NYT) topical cream and amphotericin B (AmB), which is only delivered intravenously. The echinocandins are narrow-spectrum antifungals, and the only approved member of this antifungal family for topical application is micafungin. Terbinafine is the primary example of an allylamine and can be given orally or as a nail lacquer. The azoles are broad-spectrum antifungals that are used to treat *Candida* infections by inhibiting ergosterol biosynthesis.

The azoles are comprised of imidazoles and triazoles. The imidazoles, examples including clotrimazole (CLT), miconazole (MCZ), and ketoconazole (KTC), are used to treat skin

infections while the triazoles, fluconazole (FLC), itraconazole (ITC), posaconazole (POS), and voriconazole (VRC), are used for invasive infections (Fig. 2.1A). For cutaneous infections, treatment with azoles can range from a few days to a few months depending on the severity of the infection and species causing the infection. Treatment can also be extended due to fungal resistance, as there are reports of infections resistant to azoles, especially in non-*albicans Candida* strains.[276-278] With topical treatments, skin irritation can occur as a result of the azoles.[279]

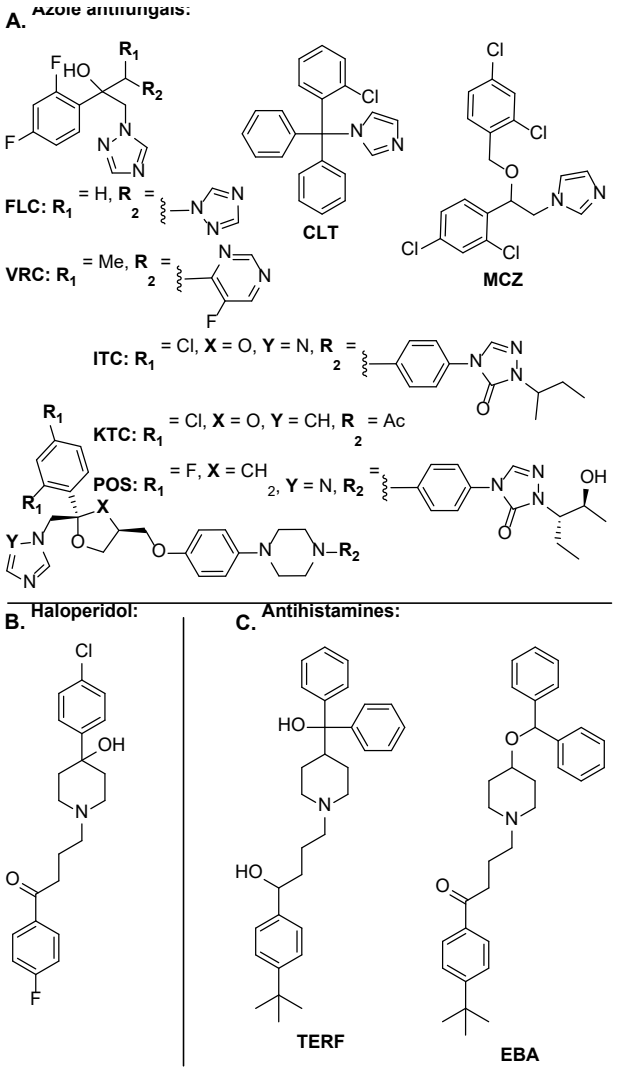

Fig. 2.1. Structures of: **A.** azole antifungals clotrimazole (CLT), fluconazole (FLC), ketoconazole (KTC), itraconazole (ITC), miconazole (MCZ), posaconazole (POS), and voriconazole (VRC), **B.** haloperidol, an antipsychotic, and **C.** antihistamine agents ebastine (EBA) and terfenadine (TERF).

Previous studies have shown the antipsychotic haloperidol (Fig. 2.1B) and its derivatives to act synergistically with azole antifungals *in vitro*.[256, 280] Some antihistamines such as terfenadine (TERF) and ebastine (EBA) have a 4-piperidinol group as well as an acetophenone moiety similar to haloperidol (Fig. 2.1C), but are not able to cross the blood-brain barrier to cause drowsiness, which is an adverse effect of haloperidol.[281] Interestingly,

studies have explored TERF for additional drug activities, including antibacterial and antitumor activity.[282-284]

Based on similarity in structure between TERF, EBA, and haloperidol, we predicted that TERF and EBA would also act synergistically with azole antifungals. The goal of this study is to explore novel combinations of antifungals and antihistamine drugs to discover synergistic antifungal combinations for potential use as topical antifungal treatments. Checkerboard assays were used to calculate the fractional inhibitory concentration indexes (FICI) of combinations. In order to be considered synergistic, a minimum of 4-fold decrease of both individual MIC values while in combination needs to be achieved. With synergistic combinations, the addition of the second drug in this case decreases the MIC of the initial drug. In the case of azole-resistant *Candida* strains, this both improves the efficaciousness of the azole antifungal as well as lowers the dose of needed, which decreases the potential for side-effects. With additive combinations, both drugs exert their effect, however, MIC values remain the same in combination. We investigated two antihistamines, TERF and EBA, by checkerboard dilution assays with seven azole antifungal drugs, CLT, KTC, MCZ, ITC, POS, FLC, and VRC against a panel of 13 *Candida* spp. We then evaluated combinations with successful FICI scores in time-kill assays, biofilm disruption assays, and mammalian cytotoxicity assays to assess the cytotoxicity of the drug combinations with planktonic fungal cells, sessile fungal cells, and mammalian cells, respectively.

2.3. RESULTS

2.3.1. Determination of synergistic azole antifungal and antihistamine combinations by checkerboard assays

In order to establish the concentration ranges to use for combination studies of azoles and antihistamines, we first determined the minimal inhibitory concentration (MIC) values of seven azole antifungals (three imidazoles: CLT, KTC, and MCZ; as well as four triazoles: ITC, POS, FLC, and VRC) and two antihistamine agents (TERF and EBA) individually against thirteen yeast strains (strains *A*-*M*), of which one strain is annotated as FLC sensitive (strain *E*) and all other are considered FLC resistant (Tables 2.1 and 2.2). Many of the strains were susceptible to the imidazole antifungals CLT, KTC, and MCZ (Table 2.1), but showed reduced susceptibility to the triazole antifungals ITC, POS, FLC, and VRC (Table 2.2). The antihistamines did not show any antifungal activity against the thirteen strains tested.

We next investigated the potential synergy of azole and antihistamine combinations by using checkerboard assays (Tables 2.1 and 2.2). Combinations were considered synergistic (SYN) if they displayed FICI ≤ 0.5, additive (ADD) if $0.5 < \text{FICI} \leq 2$, and antagonistic (ANT) if FICI ≥ 4. Under this definition, both drugs need to have at least a four-fold decrease in MIC value when used in combination as compared to their MIC alone to be considered a synergistic combination. As the antihistamines showed no activity against the fungal strains tested, and many fungal strains were resistant to multiple azole antifungals, there are drugs with MIC values greater than the maximum concentration of drugs tested.

In these cases, the maximum concentration of drug tested was considered the MIC_{alone}, which results in increased FICI values.

Table 2.1. Combinational effect of imidazoles with antihistamine compounds against thirteen fungal strains.

TERF								EBA							
Azole	Strain	MIC alone (μg/mL)		MIC combo (μg/mL)		FICI	Interp.	Azole	Strain	MIC alone (μg/mL)		MIC combo (μg/mL)		FICI	Interp.
		Azole	Cpd	Azole	Cpd					Azole	Cpd	Azole	Cpd		
CLT	*A*	16	>42.7	1	21.4	0.56	ADD	**CLT**	*A*	16	>25	16	25	2.00	ADD
	B	1	>42.7	0.5	42.7	1.50	ADD		*B*	1	>25	1	25	2.00	ADD
	C	16	>42.7	0.063	10.7	0.25	SYN		*C*	8	>25	32	25	5.00	ANT
	D	4	>42.7	0.008	21.4	0.50	SYN		*D*	4	>25	>4	>25	2.00	ADD
	E	1	>42.7	0.008	21.4	0.51	ADD		*E*	0.5	>25	1	0.39	2.00	ADD
	F	16	>42.7	4	10.7	0.50	SYN		*F*	16	>25	8	12.5	1.00	ADD
	G	16	>42.7	0.5	10.7	0.28	SYN		*G*	16	>25	8	1.6	0.56	ADD
	H	4	>42.7	0.5	5.3	0.25	SYN		*H*	4	>25	1	6.3	0.50	SYN
	I	4	>42.7	1	2.7	0.31	SYN		*I*	4	>25	8	25	3.00	ADD
	J	4	>42.7	2	5.3	0.62	ADD		*J*	8	>25	8	25	2.00	ADD
	K	4	>42.7	0.031	42.7	1.01	ADD		*K*	4	>25	8	25	3.00	ADD
	L	0.25	>42.7	0.13	42.7	1.50	ADD		*L*	0.25	>25	0.25	25	2.00	ADD
	M	0.25	>42.7	0.25	42.7	2.00	ADD		*M*	0.25	>25	0.016	3.1	0.19	SYN
KTC	*A*	32	>42.7	1	21.4	0.53	ADD	**KTC**	*A*	32	>25	32	25	2.00	ADD
	B	0.25	>42.7	0.25	21.3	1.50	ADD		*B*	0.25	>25	0.13	0.8	0.55	ADD
	C	32	>42.7	0.25	10.7	0.26	SYN		*C*	32	>25	>32	>25	2.00	ADD
	D	16	>42.7	0.063	10.7	0.25	SYN		*D*	>32	>25	>32	>25	2.00	ADD
	E	32	>42.7	0.063	10.7	0.25	SYN		*E*	>32	>25	>32	>25	2.00	ADD
	F	16	>42.7	4	42.7	1.25	ADD		*F*	16	>25	16	25	2.00	ADD
	G	32	>42.7	16	10.7	0.75	ADD		*G*	32	>25	32	>25	2.00	ADD
	H	32	42.7	16	1.3	0.53	ADD		*H*	32	>25	0.25	1.6	0.07	SYN
	I	32	>42.7	2	2.7	0.13	SYN		*I*	32	>25	4	3.1	0.25	SYN
	J	8	>42.7	2	10.7	0.50	SYN		*J*	8	>25	8	25	2.00	ADD
	K	32	>42.7	2	5.3	0.19	SYN		*K*	32	>25	4	12.5	0.63	ADD
	L	2	>42.7	2	42.7	2.00	ADD		*L*	2	>25	2	25	2.00	ADD
	M	0.1	>42.7	0.1	42.7	2.00	ADD		*M*	0.1	>25	0.05	1.6	0.56	ADD
MCZ	*A*	>32	>42.7	1	21.4	0.53	ADD	**MCZ**	*A*	>32	>25	>32	>25	2.00	ADD
	B	2	>42.7	0.13	42.7	1.07	ADD		*B*	2	>25	2	25	2.00	ADD
	C	16	>42.7	0.5	10.7	0.28	SYN		*C*	16	>25	>16	>25	2.00	ADD
	D	8	>42.7	0.13	10.7	0.27	SYN		*D*	8	>25	>16	>25	3.00	ADD
	E	4	>42.7	0.032	10.7	0.26	SYN		*E*	4	>25	2	1.6	0.56	ADD
	F	>32	>42.7	>32	>42.7	2.00	ADD		*F*	>32	>25	>32	>25	2.00	ADD
	G	8	>42.7	0.5	10.7	0.31	SYN		*G*	8	>25	8	>25	2.00	ADD
	H	8	42.7	0.06	10.7	0.26	SYN		*H*	4	>25	0.016	1.6	0.07	SYN
	I	32	>42.7	0.063	10.7	0.25	SYN		*I*	32	>25	>32	>25	2.00	ADD
	J	2	>42.7	0.25	10.7	0.38	SYN		*J*	4	>25	4	25	2.00	ADD
	K	16	>42.7	0.25	5.3	0.14	SYN		*K*	16	>25	16	25	2.00	ADD
	L	4	>42.7	1	42.7	1.25	ADD		*L*	4	>25	>4	>25	2.00	ADD
	M	1	>42.7	1	>42.7	2.00	ADD		*M*	1	>25	0.13	3.1	0.25	SYN

Strains: *A* = *C. albicans* ATCC MYA-1003, *B* = *C. albicans* ATCC 10231, *C* = *C. albicans* ATCC MYA-1237, *D* = *C. albicans,* ATCC MYA-2310, *E* = *C. albicans* ATCC MYA-2876, *F* = *C. albicans* ATCC 64124, *G* = *C. albicans* ATCC 90819, *H* = *C. glabrata* ATCC 2001, *I* = *C. glabrata* clinical isolate 1 (CG1), *J* = *C. glabrata* clinical isolate 2 (CG2), *K* = *C. glabrata* clinical isolate 3 (CG3), *L* = *C. krusei* ATCC 6258, *M* = *C. parapsilosis* ATCC 22019.

Abbreviations used: cpd = compound, CLT = clotrimazole, EBA = ebastine, KTC = ketoconazole, MCZ = miconazole, MIC = minimum inhibitory concentration, TERF = terfenadine.

The FICI cutoff values for determining synergy are: synergistic (SYN) if FICI ≤ 0.5, additive (ADD) if 0.5 < FICI ≤ 4, antagonistic (ANT) if FICI > 4.

Note: Where the highest concentration of a compound or azole drug alone did not achieve optical growth inhibition, the MIC_{alone} value used in the FICI calculation is the highest concentration tested of that compound or azole drug. Combinations were tested in duplicate.

Table 2.2. Combinational effect of triazoles with antihistamine compounds against thirteen fungal strains.

TERF								EBA							
Azole	Strain	MIC alone (μg/mL)		MIC combo (μg/mL)		FICI	Interp.	Azole	Strain	MIC alone (μg/mL)		MIC combo (μg/mL)		FICI	Interp.
		Azole	Cpd	Azole	Cpd					Azole	Cpd	Azole	Cpd		
FLC	*A*	>32	>42.7	>32	>42.7	2.00	ADD	**FLC**	*A*	>32	>25	>32	>25	2.00	ADD
	B	>32	>42.7	32	42.7	2.00	ADD		*B*	>32	>25	>32	>25	2.00	ADD
	C	>32	>42.7	4	21.3	0.63	ADD		*C*	>32	>25	>32	>25	2.00	ADD
	D	>32	>42.7	4	21.3	0.63	ADD		*D*	>32	>25	>32	>25	2.00	ADD
	E	>32	>42.7	4	21.3	0.63	ADD		*E*	>32	>25	>32	>25	2.00	ADD
	F	>32	>42.7	>32	>42.7	2.00	ADD		*F*	>32	>25	>32	>25	2.00	ADD
	G	>32	42.7	8	21.3	0.75	ADD		*G*	>32	>25	>32	>25	2.00	ADD
	H	>32	42.7	16	5.3	0.62	ADD		*H*	>32	>25	8	12.5	0.75	ADD
	I	>32	>42.7	32	42.7	2.00	ADD		*I*	>32	>25	>32	>25	2.00	ADD
	J	>32	>42.7	>32	>42.7	2.00	ADD		*J*	>32	>25	>32	>25	2.00	ADD
	K	>32	>42.7	>32	>42.7	2.00	ADD		*K*	>32	>25	>32	>25	2.00	ADD
	L	>32	>42.7	1	42.7	1.03	ADD		*L*	>32	>25	>32	>25	2.00	ADD
	M	8	>42.7	8	42.7	2.00	ADD		*M*	8	>25	2	3.1	0.37	SYN
ITC	*A*	>32	>42.7	0.13	42.7	1.00	ADD	**ITC**	*A*	>32	>25	>32	>25	2.00	ADD
	B	1	>42.7	0.03	42.7	1.03	ADD		*B*	1	>25	0.5	1.6	0.56	ADD
	C	>32	>42.7	1	21.4	0.53	ADD		*C*	>32	>25	>32	>25	2.00	ADD
	D	>32	>42.7	0.13	10.7	0.25	SYN		*D*	>32	>25	>32	>25	2.00	ADD
	E	>32	>42.7	0.5	10.7	0.27	SYN		*E*	>32	>25	>32	>25	2.00	ADD
	F	>32	>42.7	>32	>42.7	2.00	ADD		*F*	>32	>25	>32	>25	2.00	ADD
	G	>32	>42.7	2	21.4	0.56	ADD		*G*	>32	>25	>32	>25	2.00	ADD
	H	>32	42.7	1	5.3	0.16	SYN		*H*	>32	>25	2	6.3	0.31	SYN
	I	>32	>42.7	1	5.3	0.16	SYN		*I*	>32	>25	>32	>25	2.00	ADD
	J	>32	>42.7	1	42.7	1.03	ADD		*J*	>32	>25	>32	>25	2.00	ADD
	K	>32	>42.7	1	21.4	0.53	ADD		*K*	>32	>25	>32	>25	2.00	ADD
	L	4	>42.7	0.13	42.7	1.03	ADD		*L*	4	>25	4	25	2.00	ADD
	M	1	>42.7	0.25	2.7	0.31	SYN		*M*	1	>25	0.06	3.1	0.18	SYN
POS	*A*	>32	>42.7	0.25	21.3	0.51	ADD	**POS**	*A*	>32	>25	>32	>25	2.00	ADD
	B	1	>42.7	0.25	5.3	0.37	SYN		*B*	1	>25	0.125	3.1	0.25	SYN
	C	>32	>42.7	0.063	21.3	0.50	SYN		*C*	>32	>25	>32	>25	2.00	ADD
	D	>32	>42.7	0.063	10.7	0.25	SYN		*D*	>32	>25	>32	>25	2.00	ADD
	E	>32	>42.7	0.125	10.7	0.25	SYN		*E*	>32	>25	>32	>25	2.00	ADD
	F	>32	>42.7	2	10.7	0.31	SYN		*F*	>32	>25	1	12.5	0.53	ADD
	G	>32	>42.7	0.5	10.7	0.27	SYN		*G*	>32	>25	>32	>25	2.00	ADD
	H	>32	42.7	1	1.3	0.06	SYN		*H*	>32	>25	0.5	0.78	0.05	SYN
	I	>32	>42.7	2	21.4	0.56	ADD		*I*	>32	>25	>32	>25	2.00	ADD
	J	>32	>42.7	1	21.4	0.53	ADD		*J*	>32	>25	>32	>25	2.00	ADD
	K	>32	>42.7	0.5	21.4	0.52	ADD		*K*	>32	>25	>32	>25	2.00	ADD
	L	0.5	42.7	0.125	5.3	0.37	SYN		*L*	2	>25	0.5	3.1	0.37	SYN
	M	0.25	>42.7	0.032	1.3	0.16	SYN		*M*	0.5	>25	0.008	3.1	0.14	SYN
VRC	*A*	>32	>42.7	4	21.3	0.62	ADD	**VRC**	*A*	>32	>25	>32	>25	2.00	ADD
	B	1	>42.7	0.5	42.7	1.50	ADD		*B*	0.5	>25	0.5	>25	2.00	ADD
	C	>32	>42.7	0.063	21.3	0.50	SYN		*C*	>32	>25	>32	>25	2.00	ADD
	D	>32	>42.7	0.25	10.7	0.26	SYN		*D*	>32	>25	>32	>25	2.00	ADD
	E	>32	>42.7	0.063	10.7	0.25	SYN		*E*	>32	>25	>32	>25	2.00	ADD
	F	>32	>42.7	16	10.7	0.75	ADD		*F*	>32	>25	>32	>25	2.00	ADD
	G	>32	>42.7	0.5	5.3	0.14	SYN		*G*	>32	>25	>32	>25	2.00	ADD
	H	>32	42.7	1	1.3	0.06	SYN		*H*	>32	>25	0.5	1.56	0.08	SYN
	I	>32	>42.7	4	5.3	0.25	SYN		*I*	>32	>25	>32	>25	2.00	ADD
	J	8	>42.7	2	21.4	0.75	ADD		*J*	8	>25	4	12.5	1.00	ADD
	K	>32	>42.7	8	5.3	0.37	SYN		*K*	>32	>25	>32	>25	2.00	ADD
	L	0.5	42.7	0.5	42.7	2.00	ADD		*L*	1	>25	1	25	2.00	ADD
	M	0.063	>42.7	>0.063	>42.7	2.00	ADD		*M*	0.065	>25	0.033	3.1	0.62	ADD

Strains: *A* = *C. albicans* ATCC MYA-1003, *B* = *C. albicans* ATCC 10231, *C* = *C. albicans* ATCC MYA-1237, *D* = *C. albicans,* ATCC MYA-2310, *E* = *C. albicans* ATCC MYA-2876, *F* = *C. albicans* ATCC 64124, *G* = *C. albicans* ATCC 90819, *H* = *C. glabrata* ATCC 2001, *I* = *C. glabrata* clinical isolate 1 (CG1), *J* = *C. glabrata* clinical isolate 2 (CG2), *K* = *C. glabrata* clinical isolate 3 (CG3), *L* = *C. krusei* ATCC 6258, *M* = *C. parapsilosis* ATCC 22019.

Abbreviations used: cpd = compound, EBA = ebastine, FLC = fluconazole, ITC = itraconazole, MIC = minimum inhibitory concentration, POS = posaconazole, TERF = terfenadine, VRC = voriconazole.

The FICI cutoff values for determining synergy are: synergistic (SYN) if FICI ≤ 0.5, additive (ADD) if 0.5 < FICI ≤ 4, antagonistic (ANT) if FICI > 4.

Note: Where the highest concentration of a compound or azole drug alone did not achieve optical growth inhibition, the MIC_{alone} value used in the FICI calculation is the highest concentration tested of that compound or azole drug. Combinations were tested in duplicate.

The combination with the best FICI score was POS and EBA against *C. glabrata* (strain *H*) with a FICI value of 0.05. Strain *H* is resistant to both POS and EBA alone, having MIC values of >32 and >25 μg/mL, respectively. In combination, 0.5 μg/mL of POS and 0.78 μg/mL of EBA inhibited the growth of strain *H,* which is a 64-fold decrease in POS and a thirty-two-fold decrease in EBA. Other combinations with FICI values lower than 0.10 included POS and TERF as well as KTC, MCZ, and VRC with EBA, all against *C. glabrata* (strain *H*). While strain *H* appears more susceptible to both antihistamines and these POS and EBA combinations, this is interesting as *C. glabrata* is a species that has intrinsic resistance to many azoles.[285] With strain *H*, there were a total of five SYN combinations with TERF and six with EBA. In contrast, the clinical isolates of *C. glabrata* (CG1-CG3; strain *I-K*) displayed reduced susceptibility, but we observed six SYN combinations with strain *I* (five with TERF, one with EBA), two SYN with strain *J* (two with TERF), and three SYN with strain *K* (three with TERF). It is also notable that five of seven azoles exhibited SYN with EBA with the other non-*albicans Candida*, *C. parapsilosis* (strain *M*). While multiple combinations with EBA produced very low FICI values, overall, TERF displayed more SYN across all the azole antifungals and all fungal strains.

In total, we observed forty-one SYN combinations with TERF and fourteen with EBA. It appears that the synergistic effect of EBA is more strain-dependent. In addition, POS appears to have the best effect with EBA against many strains. For both TERF and EBA, combinations with POS and ITC appear to be very effective against *C. krusei* (strain *L*), *C. parapsilosis* (strain *M*), and *C. glabrata* (strain *H*). TERF and azole combinations exhibited much SYN with *C. albicans* strains, especially in strains *C*, *D*, *E*, and *G*, all of which are

resistant to most triazoles. In contrast to TERF, EBA appeared to be best with *C. parapsilosis* (strain *M*). For a summary of FICI scores, we presented the checkerboard results in heat map style in Tables 2.3 and 2.4.

Table 2.3. FICI values of azole and TERF combinations against a panel of thirteen fungal strains.

		Imidazole			Triazole			
	strain	CLT	KTC	MCZ	FLC	ITC	POS	VRC
Candida albicans spp.	*A*	0.56	0.53	0.53	2.00	1.00	0.51	0.62
	B	1.50	1.50	1.07	2.00	1.03	0.37	1.50
	C	0.25	0.26	0.28	0.63	0.53	0.50	0.50
	D	0.50	0.25	0.27	0.63	0.25	0.25	0.26
	E	0.51	0.25	0.26	0.63	0.27	0.25	0.25
	F	0.50	1.25	2.00	2.00	2.00	0.31	0.75
	G	0.28	0.75	0.31	0.75	0.56	0.27	0.14
non-albicans Candida spp.	*H*	0.25	0.53	0.26	0.62	0.16	0.06	0.06
	I	0.31	0.13	0.25	2.00	0.16	0.56	0.25
	J	0.62	0.50	0.38	2.00	1.03	0.53	0.75
	K	1.01	0.19	0.14	2.00	0.53	0.52	0.37
	L	1.50	2.00	1.25	1.03	1.03	0.37	2.00
	M	2.00	2.00	2.00	2.00	0.31	0.16	2.00

Strains: *A* = *C. albicans* ATCC MYA-1003, *B* = *C. albicans* ATCC 10231, *C* = *C. albicans* ATCC MYA-1237, *D* = *C. albicans,* ATCC MYA-2310, *E* = *C. albicans* ATCC MYA-2876, *F* = *C. albicans* ATCC 64124, *G* = *C. albicans* ATCC 90819, *H* = *C. glabrata* ATCC 2001, *I* = *C. glabrata* clinical isolate 1 (CG1), *J* = *C. glabrata* clinical isolate 2 (CG2), *K* = *C. glabrata* clinical isolate 3 (CG3), *L* = *C. krusei* ATCC 6258, *M* = *C. parapsilosis* ATCC 22019.
The FICI cutoff values for determining synergy are: synergistic (SYN) if FICI ≤ 0.5, additive (ADD) if 0.5 < FICI ≤ 4, antagonistic (ANT) if FICI > 4.
Indicates synergy (SYN, both drugs showed ≥4-fold reduction in MIC value).
Indicates additive effect (ADD).

Table 2.4. FICI values of azole and EBA combinations against a panel of thirteen fungal strains.

		Imidazole			Triazole			
	strain	CLT	KTC	MCZ	FLC	ITC	POS	VRC
Candida albicans spp.	*A*	2.00	2.00	2.00	2.00	2.00	2.00	2.00
	B	2.00	0.55	2.00	2.00	0.56	0.25	2.00
	C	5.00	2.00	2.00	2.00	2.00	2.00	2.00
	D	2.00	2.00	3.00	2.00	2.00	2.00	2.00
	E	2.00	2.00	0.56	2.00	2.00	2.00	2.00
	F	1.00	2.00	2.00	2.00	2.00	0.53	2.00
	G	0.56	2.00	2.00	2.00	2.00	2.00	2.00
non-albicans Candida spp.	*H*	0.50	0.07	0.07	0.75	0.31	0.05	0.08
	I	3.00	0.25	2.00	2.00	2.00	2.00	2.00
	J	2.00	2.00	2.00	2.00	2.00	2.00	1.00
	K	3.00	0.63	2.00	2.00	2.00	2.00	2.00
	L	2.00	2.00	2.00	2.00	2.00	0.37	2.00
	M	0.19	0.56	0.25	0.37	0.18	0.14	0.62

Strains: *A* = *C. albicans* ATCC MYA-1003, *B* = *C. albicans* ATCC 10231, *C* = *C. albicans* ATCC MYA-1237, *D* = *C. albicans,* ATCC MYA-2310, *E* = *C. albicans* ATCC MYA-2876, *F* = *C. albicans* ATCC 64124, *G* = *C. albicans* ATCC 90819, *H* = *C. glabrata* ATCC 2001, *I* = *C. glabrata* clinical isolate 1 (CG1), *J* = *C. glabrata* clinical isolate 2 (CG2), *K* = *C. glabrata* clinical isolate 3 (CG3), *L* = *C. krusei* ATCC 6258, *M* = *C. parapsilosis* ATCC 22019.
The FICI cutoff values for determining synergy are: synergistic (SYN) if FICI ≤ 0.5, additive (ADD) if 0.5 < FICI ≤ 4, antagonistic (ANT) if FICI > 4.
Indicates synergy (SYN, both drugs showed ≥4-fold reduction in MIC value).
Indicates additive effect (ADD).
Indicates antagonistic effect (ANT, both drugs show ≥4-fold increase in MIC value).

2.3.2. Time-dependent killing of fungi with POS and EBA combinations

To examine the efficiency of azole and antihistamine combinations at inhibiting the growth of fungi, we tested the POS and EBA combination against two yeast strains, *C. albicans* ATCC 10231 (strain *B*) and *C. glabrata* ATCC 2001 (strain *H*). As EBA is approved in many countries and as of all the azoles tested POS exhibited the most synergy and had the lowest FICI score with *C. glabrata* (strain *H*), we selected POS and EBA combinations as representatives for the time-kill assays as well as for the cytotoxicity and biofilm studies. To study the synergistic effect of POS and EBA, we tested POS and EBA alone at sub-inhibitory concentrations and compared these to POS and EBA combinations. The specific experiments included no drug (growth control), POS alone at concentration used in $MIC_{combination}$, EBA alone at concentration used in $MIC_{combination}$, POS with EBA at $MIC_{combination}$, and POS with EBA at 4× the $MIC_{combination}$, and the polyenes nystatin (NYT) and AmB at 1× MIC as fungicidal controls. Both strains *B* and *H* showed similar profiles in the relative amounts of colony forming units (CFU) over time (Fig. 2.2). EBA alone did not inhibit fungal growth. The sub-inhibitory concentration of POS partially inhibited the growth of strains *B* and *H*; only reaching 10^8 CFU/mL at 24 h as compared to 10^{13} for each the growth control. In combination at 1× MIC, POS and EBA strongly inhibited fungal growth, limiting the growth to 10^6 CFU/mL through the 24 h time period, but inhibition was not complete. However, at 4× MIC, counts remained between 10^4 and 10^5 CFU/mL throughout the 24-hour time frame, indicating complete inhibition of fungal growth and between 10^2 and 10^3 decrease as compared to POS alone. The POS and EBA combination shows a fungistatic effect while NYT and AmB showed fungicidal activity by decreasing the initial inoculum of 10^5 to 10^1-10^2 CFU/mL by 24 h.

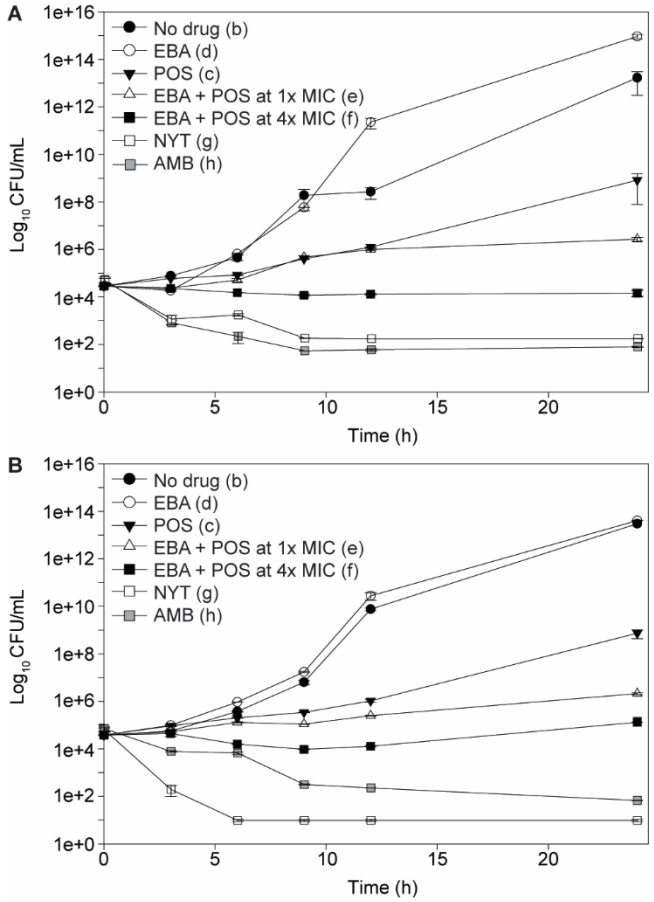

Fig. 2.2. Representative time-kill curves for POS and EBA against **A.** *C. albicans* ATCC 10231 (strain *B*) and **B.** *C. glabrata* ATCC 2001 (strain *H*). Fungal strains were treated with no drug (black circles), EBA (white circle), POS (inverted black triangle), 1× MIC (white triangle), 4× MIC (black square), AmB at 1× MIC (grey square), and NYT at 1× MIC (white square). We further verified the number of CFU/mL at the 24-hour end point by adding resazurin to the cultures. Actively replicating fungal cells metabolize resazurin, which is a blue-purple color, to produce resorufin, which has a pink-orange color. In cultures where there is little to no active cells, the culture remains a blue-purple. Where there is a low number of CFU, the culture appears a red color, and where there are many cells, the culture appears pink to orange. Time-points were plated in duplicate.

2.3.3. Determination of biofilm disruption activity by POS and EBA combinations

To evaluate the ability of POS and EBA combinations to disrupt biofilms (sessile MIC values (SMIC)), a cell viability assay using the water-soluble dye XTT in checkerboard format was performed (Table 2.5 and Fig. 2.3A-F). Two *C. albicans* strains, ATCC 10231 (strain *B*) and ATCC 64124 (strain *F*), and one *C. glabrata* strain, ATCC 2001 (strain *H*), were chosen as representative strains. As free-floating planktonic cells, strain *B* is generally

sensitive to azole antifungals, while both strains *F* and *H* are resistant. Against the biofilms, neither POS nor EBA showed any activity ($SMIC_{90}$ for POS >32 μg/mL and $SMIC_{90}$ for EBA ≥25 μg/mL against strains *B*, *F*, and *H*). When tested in combination, POS with EBA had no activity against both *C. albicans* strains (*B* and *F*). However, POS with EBA showed synergy against *C. glabrata* (strain *H*) ($SMIC_{90}$ combo for POS = 0.06 μg/mL and $SMIC_{90}$ combo for EBA = 6.3 μg/mL). Similarly, both AmB and NYT had no activity against *C. albicans* (strain *B*), but had an $SMIC_{90}$ of 4 μg/mL against *C. glabrata* (strain *H*), while *C. albicans* (strain *F*) biofilm had an $SMIC_{90}$ of 32 μg/mL for AmB and >32 μg/mL for NYT (Table 2.6 and Fig. 2.3

G-I).

Table 2.5. Disruption of biofilm by POS and EBA combination against three fungal strains

Strain	$SMIC_{90}$ alone (μg/μL)		$SMIC_{90}$ combo (μg/μL)		FICI	Interpretation
	Azole	Cpd	Azole	Cpd		
B	>32	>25	>32	>25	2.00	ADD
F	>32	>25	>32	>25	2.00	ADD
H	>32	25	0.06	6.3	0.25	SYN

Strains: *B* = *C. albicans* ATCC 10231, *F* = *C. albicans* ATCC 64124, *H* = *C. glabrata* ATCC 2001.
Abbreviations used: cpd = compound, EBA = ebastine, POS = posaconazole, SMIC = sessile minimum inhibitory concentration.
The FICI cutoff values for determining synergy are: synergistic (SYN) if FICI ≤ 0.5, additive (ADD) if 0.5 < FICI ≤ 4, antagonistic (ANT) if FICI > 4.
Note: In cases where the highest concentration of EBA or azole alone did not achieve complete growth inhibition, the MIC_{alone} value used in the FICI calculation is the highest concentration tested of compound EBA or azole drugs. Combinations were tested in duplicate.

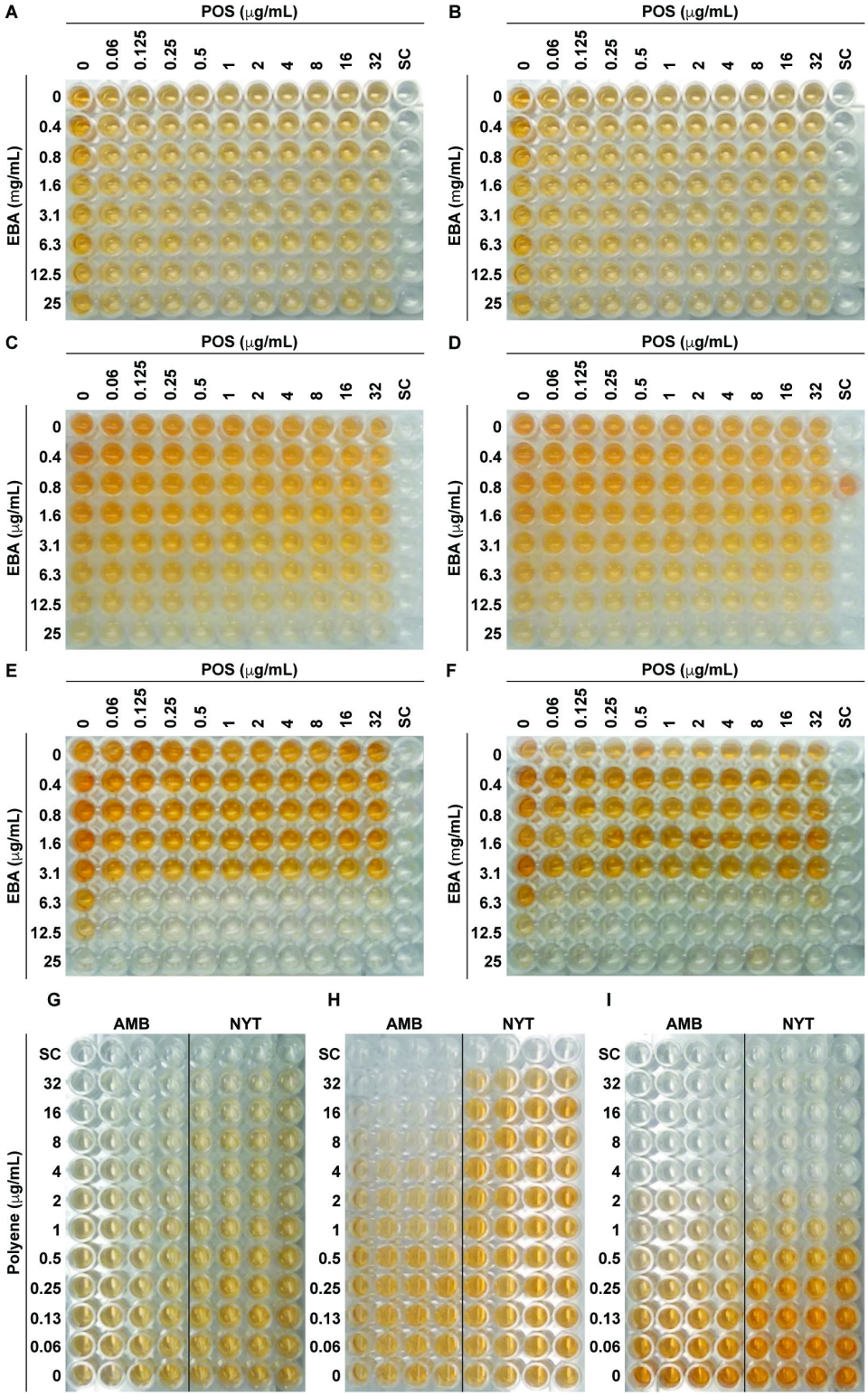

Fig. 2.3. Duplicate 96-well plates showing the anti-biofilm activity of the POS and EBA combinations against **A-B.** *C. albicans* ATCC 10231 (strain *B*), **C-D.** *C. albicans* ATCC 64124 (strain *F*), and **E-F.** *C. glabrata* ATCC 2001 (strain *H*). For comparison to fungicidal control, SMIC of the polyenes AmB and NYT tested in quadruplicate are shown against **G.** *C. albicans* ATCC 10231 (strain *B*), **H.** *C. albicans* ATCC 64124

(strain *F*), and **I.** *C. glabrata* ATCC 2001 (strain *H*). The corresponding data are presented in Table 2.6. SC indicates sterile controls where no fungal cells were added to the wells.

Table 2.6. SMIC values for polyenes against biofilms of three fungal strains

strain	Polyene	$SMIC_{90}$ (μg/mL)
B	AmB	>32
	NYT	>32
F	AmB	32
	NYT	>32
H	AmB	4
	NYT	4

Strains: *B* = *C. albicans* ATCC 10231, *F* = *C. albicans* ATCC 64124, *H* = *C. glabrata* ATCC 2001.
Note: Compounds were tested in duplicate.

2.3.4. Evaluation of mammalian cytotoxicity of POS and EBA combinations

To examine whether the activity of POS and EBA combinations is specific to fungal strains, we used a resazurin cell viability assay to assess the cytotoxic effect of POS and EBA alone and in combination against mammalian cells (Fig. 2.4). For these assays, we used four human cell lines, including lung carcinoma epithelial cells (A549), bronchial epithelial cells (BEAS-2B), embryonic kidney cells (HEK-293), and of course, the keratinocytes (HaCaT), which are most relevant for skin infections. We tested POS within the concentration range of 0.06-16 μg/mL. With POS alone, the maximum concentration with no observed toxicity was 4 μg/mL for HEK-293 and A549, whereas it was 8 μg/mL for HaCaT and BEAS-2B. For EBA alone, we used concentrations ranging from 0.1-25 μg/mL. Complete cell survival was observed up to 6.3 μg/mL for HaCaT and 3.1 μg/mL for all other cell lines. A cytotoxic effect began at 6.3 μg/mL with cell survival of 78 ± 8%, 69 ± 5%, and 70 ± 7% for A549, BEAS-2B, and HEK-293, respectively. At the highest concentration of EBA, 25 μg/mL, we observed near 0% cell survival for all cell lines.

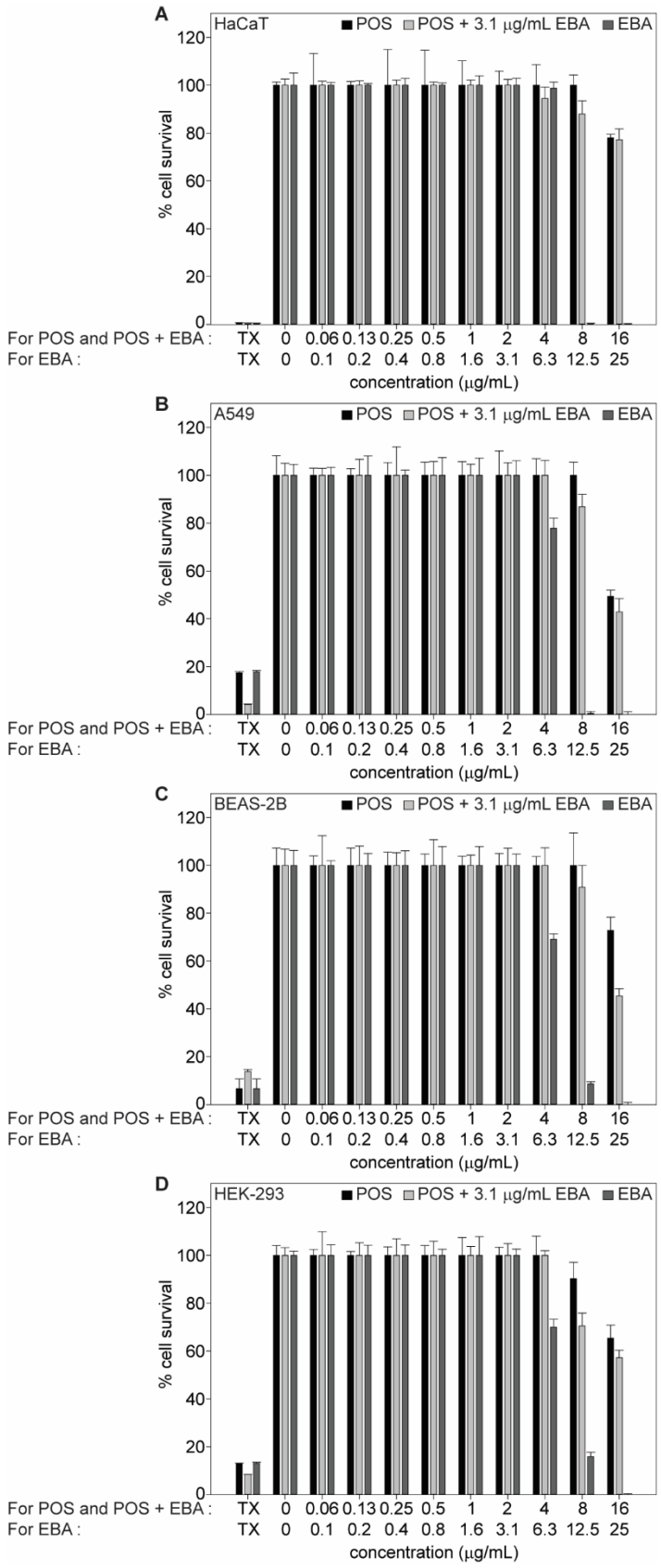
A
HaCaT
POS
POS + 3.1 μg/mL EBA
EBA
% cell survival
For POS and POS + EBA : TX 0 0.06 0.13 0.25 0.5 1 2 4 8 16
For EBA : TX 0 0.1 0.2 0.4 0.8 1.6 3.1 6.3 12.5 25
concentration (μg/mL)
B
A549
C
BEAS-2B
D
HEK-293

Fig. 2.4. Representative cytotoxicity assays against four mammalian cell lines: **A.** HaCaT, **B.** A549, **C.** BEAS-2B, and **D.** HEK-293. Treatments included POS alone (black bars), POS + 3.1 μg/mL EBA (pale gray bars), and EBA alone (dark gray bars). The positive control consisted of cells treated with Triton X-100® (TX, 12.5% *v*/*v*). The negative control consisted of cells treated with DMSO (no drug). Combinations were tested in duplicate.

To examine the effect of POS and EBA combinations on cytotoxicity, we varied the concentration of POS with a constant amount of EBA. Since all cell lines showed no toxicity at 3.1 μg/mL of EBA, we assessed POS with all cell lines in combination with 3.1 μg/mL of EBA (Fig. 2.4C). Cell survival rates of POS + 3.1 μg/mL of EBA was not significantly different as compared to POS alone for all 4 cell lines.

2.4. DISCUSSION

Candida infections primarily affect immunocompromised patients, but they also occur in otherwise healthy adults. It is estimated that 75% of all women will have at least one vulvovaginal infection during their life. Approximately half of vaginal infections are caused by *Candida* species.[286] Out of the cases of candidiasis, a study in China reported that 80.5% of vaginal candidiasis cases over an eight-year period were caused by *C. albicans*, while 18%, 1.2%, and 0.1% were caused by *C. glabrata*, *C. krusei*, and *C. tropicalis*, respectively.[273] We found 55 synergistic combinations of azole antifungals and antihistamines. While these combinations did not reverse FLC resistance, there appeared to be an adjuvant effect with other azole antifungals. While both EBA and TERF showed synergy with azoles against *C. albicans* strains, each also showed synergy against non-*albicans Candida* strains, which have intrinsic resistance to azole antifungals.[277-278, 286] Furthermore, as many skin diseases have similar symptoms, diagnosis of fungal infections without a diagnostic test can be difficult.[287] Due to this difficulty and the associated

irritation from fungal infections, CLT is also formulated with hydrocortisone or betamethasone, a highly potent fluorinated corticosteroid.[288] However, corticosteroids used for prolonged periods and in occlusive environments such as where fungal infections normally occur, can have serious side effects including severe allergic reactions and skin atrophy.[289-290] In addition, as dermatophyte species cause the majority of cutaneous fungal infections and dermatophytes show lower susceptibility to azoles than yeasts, the azole and antihistamine combinations could be explored with dermatophytes.[291-292] If combinations of azoles and antihistamines were shown to be efficacious in animal models and further testing, a topical cream containing an azole and an antihistamine could be an alternative product for the CLT corticosteroid topical cream.

In addition to checkerboard assays, we used time-kill studies to further verify the synergistic interactions between the azoles and antihistamines. We chose two fungal strains and the POS and EBA combination to observe the inhibitory effect of the drug combination over time. The results from the time-kill study do substantiate the synergy observed in the checkerboard assays as the addition of EBA to a sub-inhibitory concentration of POS decreases fungal counts while EBA alone has no effect on fungal growth. Additionally, as azoles are fungistatic against *Candida* spp., we looked at time-kill dynamics to evaluate whether the combinations of azoles and antihistamines remained fungistatic. As the number of CFU/mL remained constant for POS and EBA in combination at 4× MIC while the fungicidal controls, AmB and NYT, decreased counts to $\leq 10^2$ CFU/mL, this suggests that the POS and EBA combinations are fungistatic.

Many fungal strains *in vivo* can form biofilms, especially on implanted medical devices such as joint replacements and urinary catheters.[293-294] Treatment of infections where biofilms occur is more challenging as the biofilms protect fungal cells from the antifungal drugs. In biofilms, fungal cells secrete an oligosaccharide layer that can prevent antifungal drugs from penetrating the biofilm and acting on the fungal cells. Biofilms remaining intact after treatment increases the risk of reoccurring infections.[176, 295] As an additional measure to evaluate the effectiveness of the POS and EBA combinations, we used a biofilm disruption assay to look at the outcome on sessile cells. While we did not observe synergy against *C. albicans* biofilms, which are believed to be a cause of recurrent mucosal infections, we did observe synergy against *C. glabrata* (strain *H*) biofilm.[296-297] The concentration of POS and EBA used to achieve $SMIC_{90}$ against strain *H* had similar concentrations of POS and about 100-fold less concentration of EBA as compared to the 4 μg/mL of AmB and NYT needed to also achieve $SMIC_{90}$. The difference in results between fungal species may be due to differences in the oligosaccharide composition of the biofilms or differences in regulation of efflux pumps.[298-299]

Since we corroborated the synergistic interaction with POS and EBA, we then assessed cytotoxicity. We found that EBA at 3.1 μg/mL in combination with POS has a similar cell survival rates as POS alone, which is non-toxic to the mammalian cells up to at least 16 μg/mL. The concentration of POS alone at which a cytotoxic effect was beginning to be observed, 16 μg/mL, was at significantly higher concentrations of POS than the MIC values for POS alone against sensitive fungal strains, as the MIC values for POS ranged from 0.25-1.0 μg/mL. In synergistic combinations, the MIC values for POS ranged from

0.008-0.5 μg/mL, while MIC values for EBA in synergistic combinations with POS ranged from 0.78-3.1 μg/mL. As the MIC values for POS and EBA in synergistic combinations are the same as or lower than the concentrations of drugs in combination where no cytotoxic effect was observed, it suggests that POS and EBA combinations would be safe to use.

The known targets for EBA and TERF are the histamine H1 receptors.[103] In addition, TERF, and to a lesser extent EBA, is known to inhibit the human cardiac hERG potassium channel at high concentrations. While fungi also have potassium channels, there is no known orthologue to hERG in fungi.[300] The mechanism of action of the antifungal activity is uncertain for TERF and EBA. However, other groups have proposed mechanisms of action for TERF with regards to the other activities it exhibits. While we did not test TERF for cytotoxicity, reports show that TERF and its derivative have strong antitumor activity, suggesting that TERF would be cytotoxic at the concentrations tested.[301-303] *In vitro*, TERF sensitized cancer cells to doxorubicin by a proposed mechanism of inhibiting P-glycoprotein.[282] Other studies have proposed TERF as a CYP2J2, inhibitor, which also plays a role in apoptosis and inhibiting cancer cells.[283] Furthermore, TERF and its derivatives show antibacterial activity against *Staphylococcus aureus*, which may be partially due to inhibition of type II topoisomerases.[284] Less work has been done to identify secondary targets of EBA, but one study showed *in silico* evidence as an ATPase inhibitor.[304] As TERF and EBA are structurally similar, we expect that both compounds would have similar targets, but the specific targets for each remains unclear. This will be the topic of future studies outside of the scope of the current work.

In sum, we evaluated the effectiveness of combinations of seven azole antifungals and two antihistamines, EBA and TERF, against a wide panel of fungal strains. We found that both TERF and EBA exhibited synergy in combination with azole antifungals. The majority of synergy was observed with POS and VRC and specific strains of *Candida*. More synergistic combinations were observed with TERF than EBA, however, the POS and EBA combination with *C. glabrata* (strain *H*) had the lowest FICI value. By time-kill studies we found that POS and EBA at 1× MIC were fungistatic. The POS and EBA combination was also found to be synergistic against biofilms of *C. glabrata* (strain *H*), but not against those of *C. albicans* (strains *B* and *F*). Finally, we showed that POS and EBA combinations were not toxic to mammalian cells.

2.5. EXPERIMENTAL

2.5.1. Antifungal and antihistamine agents used for combination studies

The antifungal agents fluconazole (FLC), itraconazole (ITC), posaconazole (POS), and voriconazole (VRC) were purchased from AK Scientific (Union City, CA, USA). The remaining antifungal agents amphotericin B (AmB), clotrimazole (CLO), ketoconazole (KTC), miconazole (MCZ), and nystatin (NYT) were purchased from Sigma-Aldrich (St. Louis, MO, USA). The antihistamines used were terfenadine (TERF, Sigma-Aldrich, St. Louis, MO, USA) and ebastine (EBA, VWR, Atlanta, GA, USA). All compounds (>98% purity) were dissolved in DMSO and stored at -20 °C (Sigma-Aldrich, St. Louis, MO, USA) for use in assays. It is to note that all other chemicals used for the various experiments

were purchased from Sigma-Aldrich (St. Louis, MO, USA) and used without any further purification.

2.5.2. Fungal strains, mammalian cell lines, and their culture conditions

The *Candida albicans* strains ATCC MYA-1003 (strain *A*), ATCC MYA-1237 (strain *C*), ATCC MYA-2310 (strain *D*), and ATCC 90819 (strain *G*) were purchased from the American Type Culture Collection (ATCC, Manassas, VA, USA). The remaining *C. albicans* strains, including ATCC 10231 (strain *B*), ATCC MYA-2876 (strain *E*), and ATCC 64124 (strain *F*) were a generous gift from Dr. Jon Y. Takemoto (Utah State University, Logan, UT, USA). The non-*albicans Candida* fungi *C. glabrata* ATCC 2001 (strain *H*), *C. krusei* ATCC 6258 (strain *L*), and *C. parapsilosis* ATCC 22019 (strain *M*) were also purchased from ATCC. The *C. glabrata* clinical isolates, CG1 (strain *I*), CG2 (strain *J*), and CG3 (strain *K*) were a wonderful gift from Dr. Nathan P. Wiederhold (The University of Texas, San Antonio, TX, USA). All *Candida* strains were grown at 35 °C on potato dextrose agar plates (PDA, catalog # 110130, EMD Millipore, Billerica, MA, USA). Liquid cultures of the yeast strains were grown in yeast extract peptone dextrose (YEPD) broth at 35 °C.

The human embryonic kidney cell line HEK-293 and the human lung carcinoma epithelial cells A549 were purchased from ATCC. The human bronchial epithelial cells BEAS-2B were a generous gift from Prof. David K. Orren (University of Kentucky, Lexington, KY). Immortalized human keratinocytes HaCaT were an amiable gift from Prof. Hollie Swanson (University of Kentucky, Lexington, KY). All mammalian cells were cultured in

Dulbecco's Modified Eagle's Medium (DMEM, catalog # 11965-092, Thermo Fisher Scientific, Waltham, MA) supplemented with 10% fetal bovine serum (FBS; from ATCC) and 1% penicillin/streptomycin (from ATCC) at 37 °C with 5% CO_2.

2.5.3. Determination of minimum inhibitory concentration (MIC) values

MIC values were recorded for all antifungals and antihistamines in order to determine the concentration range of compounds to be used in the checkerboard assays. All antifungal agents were screened in the range of 0.063-32 μg/mL. The antihistamines, EBA and TERF, are less soluble in ddH_2O and therefore were tested starting at the maximal concentration where no precipitation was observed, 42.7 μg/mL for TERF (0.08-42.7 μg/mL) and 25 μg/mL for EBA (0.05-25 μg/mL). Compound stocks for all antifungal agents and EBA were dissolved in DMSO at a concentration of 5 mg/mL while TERF was dissolved in DMSO at 10 mg/mL.

The MIC assays were done using the broth microdilution method as described in CLSI document M27-A3 with minor modifications.[305] Inocula were prepared by picking a colony from a PDA plate stored at 4 °C. The colonies were grown in YEPD medium overnight at 35 °C with shaking at 200 rpm. In a 96-well plate compounds were diluted lengthwise along the plate in serial 2-fold dilutions in the RPMI 1640 medium. The yeast cultures were diluted in RPMI 1640 medium to an OD_{600} within the range of 0.12 and 0.15 (~1×10^6 cells/mL). The fungal cells were further diluted by taking 25 μL of fungal cells and adding them to 10 mL of RPMI 1640 medium before adding 100 μL to plate (200 μL total volume). The plates were incubated at 35 °C for 48 h. Visual inspection of the wells for no growth

was used to determine the MIC. All compounds were tested in duplicate with the maximum concentration of DMSO <1% (Tables 2.1 and 2.2).

2.5.4. Combination studies of azoles and antihistamines by checkerboard assays

Checkerboard assays were done as previously described to determine the fractional inhibitory concentration index (FICI) (Tables 2.1 and 2.2 and 2.3-2.4).[305-306] 2-fold dilutions of the azole drug were made in RPMI 1640 medium lengthwise along the plate. (*Note*: In order to confirm that diluting in RPMI 1640 medium gave the same MIC and FICI results as performing the experiments by doing the serial 2-fold dilutions in DMSO, we selected 4 azoles to test in combination with TERF and EBA against *C. glabrata* ATCC 2001 (strain *H*) (Table 2.7). We found that both serial 2-fold dilution methods gave the same results). For the antihistamine, 2-fold serial dilutions were made in sterile tubes with RPMI 1640 medium, then aliquoted into the plate. The drug concentration used in the checkerboards was 2- or 4-fold higher concentrations than the measured individual MIC values. The maximum drug concentration tested for the azoles was 32 μg/mL, while 25 μg/mL was maximal for EBA, and 42.7 μg/mL for TERF. The maximal amount was used in the checkerboard assays if complete inhibition was not observed in the MIC assays. Inocula were prepared diluting overnight cultures in RPMI 1640 medium to an OD_{600} between 0.12 and 0.15 (~1×10^6 cells/mL). Cells were then further diluted by taking 25 μL of cell suspension and adding to 10 mL of RPMI 1640 medium. After the drugs were added to the plate with 100 μL of medium, 100 μL of fungal cells were added. Plates were incubated at 35 °C for 48 h and visual inspection was used to determine wells with no growth. All experiments were carried out in duplicate. The FICI was calculated based on

the formula below. The combinational effect of the 2 tested compounds were considered synergistic (SYN) if FICI ≤ 0.5, additive (ADD) if 0.5 < FICI ≤ 4, and antagonistic if FICI > 4 (Tables 2.1 and 2.2 and 2.3-2.4).[307]

$$\text{FICI} = \frac{MIC\ of\ azole_{combo}}{MIC\ of\ azole_{alone}} + \frac{MIC\ of\ antihistamine_{combo}}{MIC\ of\ antihistamine_{alone}}$$

Table 2.7. Selected combinations of azoles and antihistamines against *C. glabrata* ATCC 2001 (strain *H*).

TERF							EBA						
Azole	MIC alone (μg/mL)		MIC combo (μg/mL)		FICI	Interp.	Azole	MIC alone (μg/mL)		MIC combo (μg/mL)		FICI	Interp.
	Azole	Cpd	Azole	Cpd				Azole	Cpd	Azole	Cpd		
CLT	4	>42.7	0.5	5.3	0.25	SYN	**CLT**	4	>25	1	6.3	0.50	SYN
	4	**>42.7**	**0.5**	**2.7**	**0.19**	**SYN**		**4**	**>25**	**0.25**	**1.6**	**0.13**	**SYN**
MCZ	8	42.7	0.06	10.7	0.26	SYN	**MCZ**	4	>25	0.016	1.6	0.07	SYN
	4	**>42.7**	**0.13**	**2.7**	**0.10**	**SYN**		**4**	**>25**	**0.063**	**3.1**	**0.14**	**SYN**
POS	>32	42.7	1	1.3	0.06	SYN	**POS**	>32	>25	0.5	0.78	0.05	SYN
	>32	**>42.7**	**0.5**	**2.7**	**0.08**	**SYN**		**>32**	**>25**	**0.25**	**1.6**	**0.07**	**SYN**
VRC	>32	42.7	1	1.3	0.06	SYN	**VRC**	>32	>25	0.5	1.6	0.08	SYN
	>32	**>42.7**	**0.5**	**2.7**	**0.08**	**SYN**		**>32**	**>25**	**0.25**	**1.6**	**0.07**	**SYN**

[a] The non-bold data are the same as in Tables 1 and 2 (from experiments performed by diluting in RPMI medium), whereas the data in bold are those resulting from experiments performed by diluting in DMSO. When compared, it is clear that both methods result in the same MIC values.
Note: Combinations were tested in duplicate.

2.5.5. Time-kill assays

Time-kill assays were used to assess the inhibitory efficiency of the POS and EBA combination against two yeast strains, *C. albicans* ATCC 10231 (strain *B*) and *C. glabrata* ATCC 2001 (strain *H*). The protocol for time-kill assays followed methods previously described with minor modifications.[244, 308] Yeast cultures were grown overnight in YEPD medium at 35 °C with shaking at 200 rpm. A working stock of fungal cells was made by diluting cultures in 1640 medium to an OD_{600} of 0.125 (~1×10^6 CFU/mL). From the working stock, 100 μL of cells was added to 4.9 mL of RPMI 1640 medium in sterile culture tubes, making the starting fungal cell concentration ~1×10^5 CFU/mL. Drug was then added to the fungal cells. The treatment conditions included sterile control, growth

control, EBA, POS, EBA and POS combination at 1× MIC, EBA and POS combination at 4× MIC, as well as AmB and NYT at their respective 1× MIC as fungicidal controls. The concentration of EBA and POS alone were the same concentration used in the combination at 1× MIC treatment. Treated fungal cultures were incubated in the culture tubes at 35 °C with 200 rpm shaking for 24 h. Samples were aliquoted from the different treatments at regular time points (0, 3, 6, 9, 12, and 24 h) and plated in duplicate. For each time point, cultures were vortexed, 100 μL of culture was aspirated, and 10-fold serial dilutions were made in sterile ddH_2O. From the appropriate dilutions, 100 μL of fungal suspension was spread on PDA plates and incubated at 35 °C for 48 h before colony counts were determined. Only plates containing between 30 and 300 colonies were counted making 30 CFU/mL the limit of detection. At 24 h, 50 μL of 1 mM resazurin in phosphate buffered saline (PBS) was added to the treatments and incubated at 35 °C with 200 rpm shaking for 2 h in the dark for visual inspection. As resazurin (blue-purple) is metabolized by the cells to produce resorufin (pink-orange), the addition of resazurin is used as a qualitative measure to confirm the relative growth of the fungal cells in the different treatment conditions (Fig. 2.2). Experiments were performed in duplicate.

2.5.6. Biofilm disruption assays

Biofilm disruption assays were performed to assess the effectiveness of the POS and EBA combination against sessile yeast cells for 3 representative yeast strains, *C. albicans* ATCC 10231 (strain *B*), *C. albicans* ATCC 64124 (strain *F*), and *C. glabrata* ATCC 2001 (stain *H*). Biofilm assays were performed in 96-well plates using XTT [2,3-bis(2-methoxy-4-nitro-5-sulfophenyl)-2H-tetrazolium-5-carboxanilide] to measure the viability of the

biofilm as previously described.[309] An overnight culture of yeast was grown at 35 °C in YEPD medium with shaking at 200 rpm. The overnight culture was diluted in RPMI 1640 medium to an OD_{600} between 0.12 and 0.15 to make a working stock. Working stock was transferred to the 96-well plate in 100 μL aliquots, leaving one column empty for the sterile control. The plates were incubated at 37 °C for 24 h to allow formation of the biofilm. The medium and planktonic cells from the plate were then aspirated. Wells were washed with 100 μL of PBS 3 time to remove any remaining planktonic cells off of the biofilm. After washing, RPMI 1640 medium and drug were added to the plate, in a similar fashion to that described in the checkerboard assays. POS was tested in the concentration range of 0.06-32 μg/mL with EBA at concentrations of 0.39-25 μg/mL in checkerboard format. As controls, the AmB and NYT SMIC were also tested in the range of 0.06-32 μg/mL (Table 2.6). Plates were incubated at 37 °C for 24 h. Finally, the plates were washed 3 times with PBS before adding 100 μL of XTT dye. The XTT was prepared by dissolving XTT at 0.5 mg/mL concentration in sterile PBS. Before adding to a plate, 1 μL of 10 mM menadione in acetone was added to 10 mL of the 0.5 mg/mL solution of XTT. After addition of XTT (containing menadione), the plates were incubated at 3 h at 37 °C in the dark. 80 μL of liquid from each well was transferred to a new plate. Plates were then read with a SpectraMax M5 plate reader (Molecular Devices, Sunnyvale, CA, USA) for absorbance at 450 nm. For these experiments, we determined the $SMIC_{90}$, which is defined as the drug concentration required to inhibit the metabolic activity of biofilm by 90% compared to the growth control. The $SMIC_{90}$ values were used to calculate the FICI as described above (Table 2.5). The plates used to determine the $SMIC_{90}$ are provided in Fig. 2.3. Each assay was performed in duplicate.

2.5.7. Mammalian cytotoxicity assays

To examine whether the inhibitory effect of the antifungal and antihistamine combinations is specific to fungal cells, the combinations were tested with four mammalian cell lines: A459, BEAS-2B, HEK-293, and HaCaT. POS and EBA alone were tested against each cell line to measure their cytotoxic effect by using a resazurin cell viability assay as previously described with minor modifications.[310] The assays were done in 96-well plates. A549 and BEAS-2B cells were plated at a density of 3×10^3 cells/mL, HaCaT were plated at 2×10^4 cells/mL, and HEK-293 cells were plated at 1×10^4 cells/mL as determined by using a hemacytometer. POS was tested in concentrations ranging from 0.06 to 16 μg/mL and EBA was tested in the range of 0.10 to 25 μg/mL. In order to test the cytotoxic effect of the azole and antihistamine combinations, the highest concentration of EBA that did not show any cytotoxic effect when used alone (3.1 μg/mL of EBA for all cell lines) was used with varying concentrations of POS (Fig. 2.4). It is important to note that testing xenobiotics at sub-IC_{50} concentrations can result in increase in cell growth, resulting in >100% cell survival in the treatment groups.[244, 311-314] In instances where >100% cell survival was observed, as custom in this field of research, we displayed the data as 100% cell survival. All assays were done in quadruplicate.

2.6. AUTHOR CONTRIBUTIONS

E.K.D performed all experiments, made figures, and wrote the manuscript. S.G.-T. contributed in the supervision of research, writing, figure-making, and editing of the manuscript.

Chapter 3

Distorted gold(I)-phosphine complexes as antifungal agents

3.1. ABSTRACT

Fungi cause serious nosocomial infections including candidiasis and aspergillosis, some of which display reduced susceptibility to current antifungals. Inorganic compounds have been found beneficial against various medical ailments, but have yet to be applied to fungal infections. Here, we explore the activity of linear and square-planar gold(I)-phosphine complexes against a panel of twenty-eight fungal strains including *Candida* spp., *Cryptococcus* spp., *Aspergillus* spp., and *Fusarium* spp. Notably, two square-planar gold(I) complexes with excellent broad-spectrum activity display potent antifungal effects against strains of *Candida auris*, an emerging multidrug-resistant fungus that presents a serious global health threat. To characterize the biological activity of these gold(I) complexes, we used a series of time-kill studies, cytotoxicity, and hemolysis assays, as well as whole cell uptake and development of resistance studies.

3.2. INTRODUCTION

Fungal infections are deadly for patients with conditions that weaken the immune system,[13] as demonstrated by mortality rates exceeding 50% for systemic fungal infections.[12] Those most affected include patients (i) with acquired immune deficiency syndrome, (ii) having received recent chemotherapy, (iii) having had an organ transplant, as well as (iv) with underlying lung disease such as chronic obstructive pulmonary disorder and asthma.[12-13]

These systemic fungal infections are primarily caused by only a few fungal genera, specifically *Candida*[72] and *Aspergillus*.[315]

For treatment of fungal infections, there are three classes of antifungal agents that can be used. One class, the polyenes, includes the widely used antifungal therapy, amphotericin B (AmB). While effective in treating a broad spectrum of infections, treatment is often associated with severe side effects. The second class, the azoles, specifically fluconazole (FLC) and voriconazole (VRC), are a first line of defense against fungal infections, but can cause drug-drug interactions. The third class is the echinocandins, which includes caspofungin (CFG). The echinocandins, are narrow-spectrum and can only be administered by intravenous catheter. What is of concern is the ability of fungi to be intrinsically resistant to antifungal agents. Examples include *Candida glabrata*[316] to the echinocandins and the emerging pathogen, *Candida auris*, which in some cases is resistant to all three drug classes.[317-318] *C. auris* is currently attracting attention due to recent outbreaks of resistant *C. auris* infections in the USA.[1-3] In addition, infections can develop decreased susceptibility to antifungal agents during treatment. With a limited armament of antifungal agents, there is a need for new classes of agents.

In agriculture, metal salts (*e.g.*, copper salts[319]) are widely used as fungicides to improve food production. As medicines, inorganic compounds have been predominantly developed as anticancer agents (*e.g.*, cisplatin).[320] These metal complexes typically consist of either platinum, ruthenium, silver, or copper. As anticancer agents, these compounds have been successful, but typically have problems with toxicity[321] and associated acquired

resistance.[322] More recently gold(I) phosphine and gold(III) complexes have gained attention as anticancer agents[323] as well as antimicrobials.[324-325]

The arthritis drug, auranofin (Fig. 3.1), is an exemplary gold complex that has been used in the clinic since 1983. It can be administered orally and has been shown to be well-tolerated at a 6 mg daily dose in patients (www.fda.gov/drugsatfda). Auranofin is believed to block inflammation in arthritis by regulating the secretion levels of various cytokines.[326] In recent years, reports looking at repurposing auranofin as an antimicrobial agent against bacteria[327-330] and fungi have been published.[280, 331-333] In fact, auranofin is currently in clinical trials for cancer, HIV, amoebiasis, and tuberculosis.[334-335] As an anticancer and antimicrobial agent, auranofin acts to inhibit thioredoxin reductase.[336-337] With no known inorganic antifungals on the market, auranofin speaks to the promise of using gold scaffolds to investigate and develop novel antifungal agents.

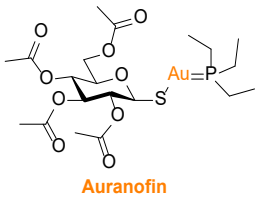

Fig. 3.1. Structure of auranofin.

Our group has a long-standing interest in the development of antifungal agents. In the past, we have used different strategies to develop antifungals, including the development of azole analogues,[183-184, 338] combinations of antifungal drugs,[244, 256-257] and synthesis and biological evaluation of new scaffolds.[205, 211-212, 245, 253] We previously developed gold complexes as potential anticancer agents.[339-340] We were intrigued to see if the applications

of gold complexes could be expanded to include antifungal activity. Herein, we present the antifungal activity of six distorted gold(I)-phosphine complexes, **1-6** (Fig. 3.2) not derived or related in structure to auranofin, against yeast, molds, and yeast biofilms. We then confirm the activity of the two best complexes, **4** and **6**, in time-kill studies. To evaluate the efficacy of complexes **4** and **6**, we use both cytotoxicity studies against four mammalian cell lines as well as hemolysis assay with both murine and human red blood cells. We also present whole cell uptake assays and development of resistance studies. The gold complexes with square-planar geometry appear to show great promise for future development as antifungal agents. As there are currently no metal complexes that have been thoroughly investigated for antifungal activity, our distorted gold(I)-phosphine complexes are innovative in the field of antifungal development.

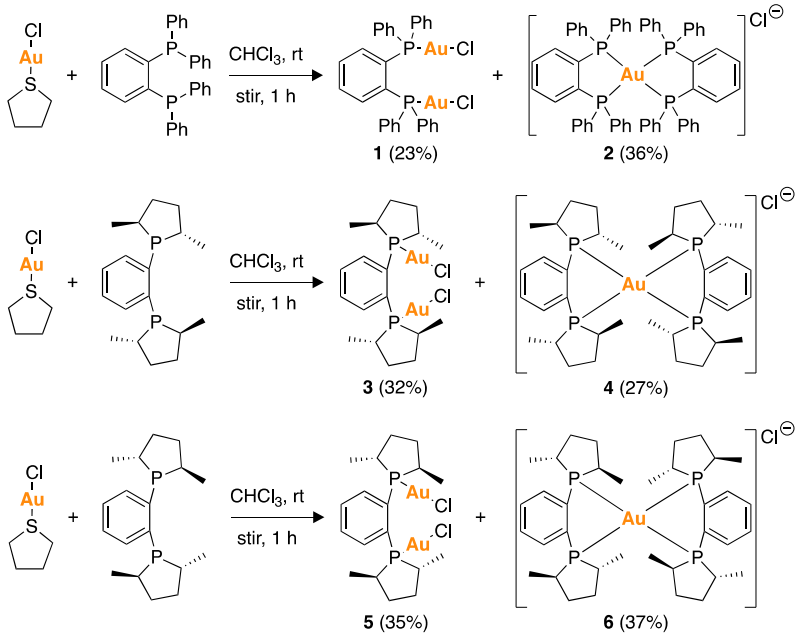

Fig. 3.2. Synthetic schemes showing the preparation of the Au complexes **1**-**6**.

3.3. RESULTS AND DISCUSSION

3.3.1. Design, chemical synthesis, and X-ray crystallography

For this study we wanted to create gold(I) complexes that could be easily prepared in a single synthetic step (Fig. 3.2). The reaction of three commercially available phosphorus ligands with AuCl(THT) (prepared by the reaction of tetrahydrothiophene and tetrachloroauric acid ($HAuCl_4 \cdot 3H_2O$))[341] in chloroform at room temperature afforded mixtures of linear gold(I) complexes **1**, **3**, and **5** and their square-planar gold(I) complex counterparts **2**, **4**, and **6** in 23-37% yield, which could be easily separated by silica gel flash chromatography. To expand the availability of chiral gold(I) complexes, which are limited and underexplored for biological applications, we used both the achiral bis(diphenylphosphino)benzene ligand and chiral ligands such as the 1,2-bis[(2*S*,5*S*)-2,5-dimethylphospholano]benzene and 1,2-bis[(2*R*,5*R*)-2,5-dimethylphospholano]benzene. The structures of compounds **1-6** were confirmed by ^{1}H, ^{13}C, and ^{31}P NMR spectroscopy, mass spectrometry, as well as RP-HPLC for purity determination. Additionally, the structures of compounds **3**, **4**, **5**, and **6** were confirmed by X-ray crystallography. Single crystals of complexes were grown by vapor diffusion (Fig. 3.3). Crystal structures for the known compounds **1**[342] and **2**[343] had already been solved. The structures of complexes **3** and **5** were consistent with linear geometry for classical gold(I) complexes. Furthermore, complexes **4** and **6** were characterized by a distorted square-planar arrangement around the gold(I) center as observed in gold complexes with bisphosphine ligands. In all cases, the gold(I) center is coordinated to bidentate ligands with phosphorus donors; **3** and **5** have one chloride ion bound to the gold(I) center, while **4** and **6** have all donors as phosphorus

atoms. Typically, Au–P distances vary from 2.229-2.239 Å and Au–Cl distances are in the range of 2.286-2.292 Å.

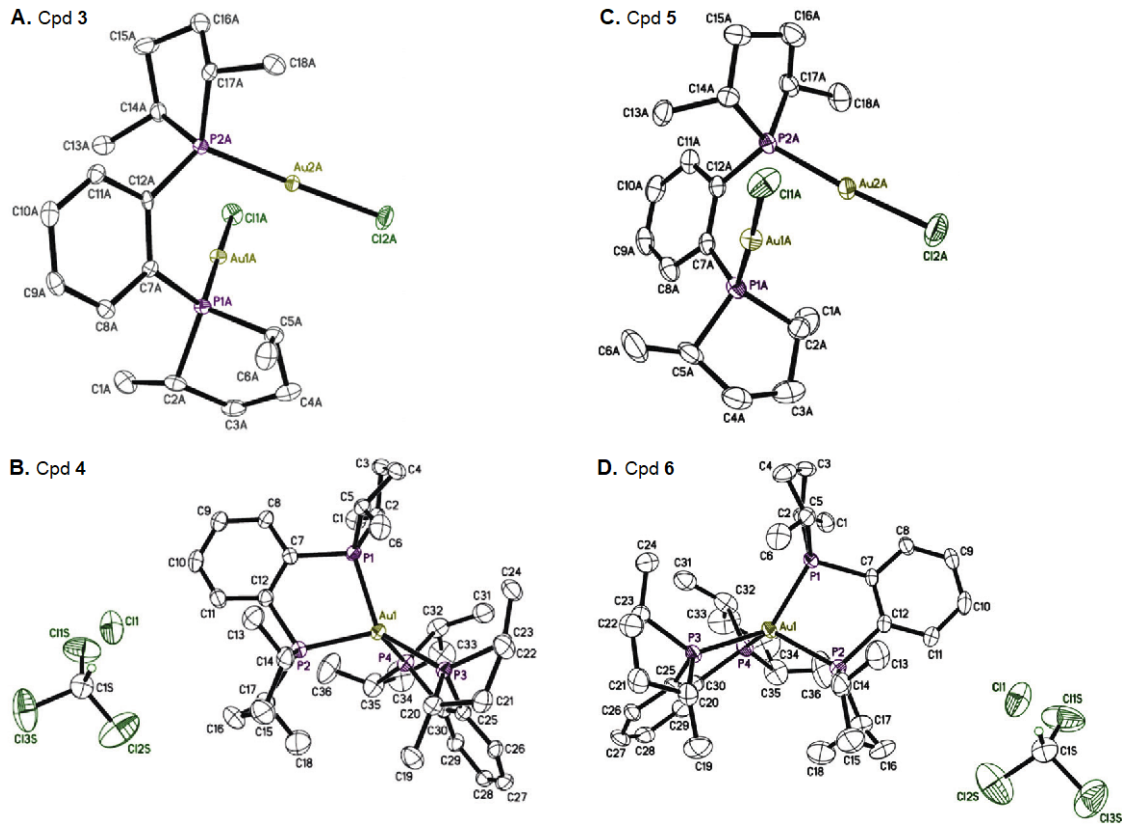

Fig. 3.3. X-ray crystal structures of compounds **A. 3**, **B. 4**, **C. 5**, and **D. 6**. Ellipsoids are drawn at 50% probability level. Hydrogen atoms bound to carbon atoms are omitted for clarity. For compounds **4** and **6**, the molecules co-crystallized with a molecule of $CHCl_3$.

3.3.2. Determination of minimum inhibitory concentration (MIC) values of compounds 1-6 against twenty-eight fungal strains

For all biological studies, we used auranofin as a control as it is one of the only metal complexes that is an FDA-approved drug, is well-tolerated in patients, and has some reported antimicrobial activity, and may have a similar cellular target at the gold(I)-phosphine complexes. As there are currently no metal complexes that have been thoroughly investigated for antifungal activity, our distorted gold(I)-phosphine complexes are

innovative in the field of antifungal development. For most biological assays, we also used the current FDA-approved antifungal AmB as a positive control.

Compounds **1-6** were first tested in MIC value determination assays against a panel of twenty fungal strains (Table 3.1). The panel consisted of seven *Candida albicans* (strains *A*-*G*), five non-*albicans Candida* (one *C. glabrata* (strain *H*), one *C. krusei* (strain *I*), one *C. parapsilosis* (strain *J*), and two *C. auris* (strains *K* and *L*)), four *Cryptococcus neoformans* (strains *M*-*P*), three *Aspergillus* (strains *Q*-*S*), as well as one *Fusarium graminearum* (strain *T*). These strains were chosen as they represent pathogens causing systemic infections. Furthermore, this panel includes many (five out of seven) *C. albicans* strains designated as fluconazole-resistant by the American Type Culture Collection (ATCC, see legend of Table 3.1). We observed that auranofin had no antifungal activity against *Candida* spp., while it displayed MIC values of 0.06 to 7.8 μg/mL against all four *C. neoformans* and two of the three *Aspergillus* strains tested, which agrees with other reports of its activity.[332] We found that compounds **4** and **6** displayed excellent activity against *Candida* spp. and *Cryptococcus* spp. with MIC values against seventeen strains in the range of 0.06 to 1.95 μg/mL, which were generally better than MIC values for AmB. Compounds **4** and **6** also displayed good to excellent activity (MIC values of 1.95 to 7.8 μg/mL) against all filamentous fungi, the *Aspergillus* spp. and *Fusarium* spp., which was much better than that of AmB (MIC values 7.8-31.3 μg/mL). Compound **3**, on the other hand, was found to be completely inactive against all fungal strains tested, except for *C. neoformans* (strain *M*). Compounds **1**, **2**, and **5** were inactive against both *Aspergillus* spp. and *Fusarium* spp. and most of the non-*albicans Candida* strains tested, whereas they

displayed some activity in the range of 0.12 to 7.8 μg/mL against a few strains of *C. albicans* and *C. neoformans*. From these data, we concluded that linear gold(I) complexes (*i.e.*, **1**, **3**, and **5**) and achiral square-planar gold(I) complexes (*i.e.*, **2**) were poor antifungals that should not be further pursued, whereas the chiral square-planar gold(I) complexes (*i.e.*, **4** and **6**) showed great promise as antifungals and deserved further investigation.

Table 3.1. MIC values in μg/mL (*Note:* MIC values are also provided in μM into parentheses) for compounds **1-6**, auranofin, and AmB against various fungal strains.

		Compound #							
Strains		**1**	**2**	**3**	**4**	**5**	**6**	Auranofin	AmB
Candida albicans	*A*	3.9 (4.3)	15.6 (13.9)	31.3 (40.6)	0.98 (1.2)	3.9 (5.1)	0.49 (0.6)	>31.3 (>46.1)	0.98 (1.1)
	B	15.6 (17.1)	15.6 (13.9)	>31.3 (40.6)	1.95 (2.3)	31.3 (40.6)	0.98 (1.2)	>31.3 (>46.1)	1.95 (2.1)
	C	0.49 (5.4)	15.6 (13.9)	>31.3 (40.6)	0.98 (1.2)	15.6 (20.2)	0.98 (1.2)	>31.3 (>46.1)	3.9 (4.2)
	D	7.8 (8.6)	7.8 (6.9)	31.3 (40.6)	0.98 (1.2)	7.8 (10.1)	0.49 (0.6)	>31.3 (>46.1)	7.8 (8.4)
	E	7.8 (8.6)	7.8 (6.9)	31.3 (40.6)	0.98 (1.2)	15.6 (20.2)	0.49 (0.6)	>31.3 (>46.1)	3.9 (4.2)
	F	7.8 (8.6)	7.8 (6.9)	31.3 (40.6)	0.98 (1.2)	15.6 (20.2)	0.49 (0.6)	>31.3 (>46.1)	3.9 (4.2)
	G	7.8 (8.6)	7.8 (6.9)	31.3 (40.6)	0.98 (1.2)	7.8 (10.1)	0.49 (0.6)	>31.3 (>46.1)	0.98 (1.1)
Non-*albicans* *Candida*	*H*	7.8 (8.6)	7.8 (6.9)	>31.3 (>40.6)	1.95 (2.3)	15.6 (20.2)	0.98 (0.6)	>31.3 (>46.1)	3.9 (4.2)
	I	15.6 (17.1)	15.6 (13.9)	>31.3 (>40.6)	1.95 (2.3)	31.3 (40.6)	0.98 (0.6)	31.3 (46.1)	3.9 (4.2)
	J	15.6 (17.1)	7.8 (6.9)	>31.3 (>40.6)	0.98 (1.2)	15.6 (20.2)	0.49 (0.6)	>31.3 (>46.1)	3.9 (4.2)
	K	>31.3 (>34.3)	>31.3 (>27.8)	>31.3 (>40.6)	3.9 (4.6)	>31.3 (>40.6)	1.95 (2.3)	>31.3 (>46.1)	1.95 (2.1)
	L	>31.3 (>34.3)	>31.3 (>27.8)	>31.3 (>40.6)	7.8 (9.2)	>31.3 (>40.6)	1.95 (2.3)	>31.3 (>46.1)	1.95 (2.1)
Cryptococcus	*M*	0.98 (1.1)	3.9 (3.5)	1.95 (2.5)	0.98 (1.2)	0.12 (0.2)	0.25 (0.3)	≤0.06 (≤0.1)	>31.3 (>33.9)
	N	3.9 (4.3)	3.9 (3.5)	>31.3 (>40.6)	0.98 (1.2)	15.6 (20.2)	0.49 (0.6)	3.9 (5.7)	0.98 (1.1)
	O	3.9 (4.3)	3.9 (3.5)	31.3 (40.6)	0.98 (1.2)	7.8 (10.1)	0.49 (0.6)	7.8 (11.5)	1.95 (2.1)
	P	15.6 (17.1)	3.9 (3.5)	>31.3 (>40.6)	0.98 (1.2)	7.8 (10.1)	0.49 (0.6)	3.9 (5.7)	0.98 (1.1)
Aspergillus	*Q*	>31.3 (>34.3)	>31.3 (>27.8)	>31.3 (>40.6)	3.9 (4.6)	>31.3 (>40.6)	3.9 (4.6)	3.9 (5.7)	15.6 (16.9)
	R	>31.3 (>34.3)	>31.3 (>27.8)	>31.3 (>40.6)	1.95 (2.3)	>31.3 (>40.6)	3.9 (4.6)	7.8 (11.5)	7.8 (8.4)
	S	>31.3 (>34.3)	>31.3 (>27.8)	>31.3 (>40.6)	7.8 (9.2)	>31.3 (>40.6)	7.8 (9.2)	>31.3 (>46.1)	31.3 (33.8)
Fusarium	*T*	>31.3 (>34.3)	31.3 (27.8)	>31.3 (>40.6)	3.9 (4.6)	>31.3 (>40.6)	3.9 (4.6)	>31.3 (>46.1)	7.8 (8.4)

***Candida albicans* strains:** *A* = *C. albicans* ATCC MYA-1003(R), *B* = *C. albicans* ATCC 10231(R), *C* = *C. albicans* ATCC MYA-1237(R), *D* = *C. albicans* ATCC MYA-2310(S), *E* = *C. albicans* ATCC MYA-2876(S), *F* = *C. albicans* ATCC 64124(R), *G* = *C. albicans* ATCC 90819(R). NOTE: (S) and (R) are indicating strains that are reported to be sensitive (S) and resistant (R) to fluconazole by the ATCC.
Non-*albicans* *Candida* strains: *H* = *C. glabrata* ATCC 2001, *I* = *C. krusei* ATCC 6258, *J* = *C. parapsilosis* ATCC 22019, *K* = *C. auris* AR Bank # 0384, *L* = *C. auris* AR Bank # 0390.
***Cryptococcus* strains:** *M* = *C. neoformans* ATCC MYA-85, *N* = *C. neoformans* CN1, *O* = *C. neoformans* CN2, *P* = *C. neoformans* CN3.
***Aspergillus* strains:** *Q* = *A. nidulans* ATCC 38163, *R* = *A. terreus* ATCC MYA-3633, *S* = *A. flavus* ATCC MYA-3631.
***Fusarium* strain:** *T* = *F. graminearum* 053.
Abbreviations: AmB = amphotericin B; MIC = minimum inhibitory concentration.
Note: Compounds were tested in duplicate.

	MIC ≤1.95 μg/mL (excellent antifungal activity)
	MIC = 3.9 - 7.8 μg/mL (good antifungal activity)
	MIC ≥15.6 μg/mL (poor antifungal activity)

As *C. auris* is an emerging drug-resistant pathogen, we included two *C. auris* strains in our initial panel (strains *K* and *L*) (Table 3.1). As compounds **4** and **6** displayed good and excellent activity against these two *C. auris* strains, respectively, we expanded our panel and tested compounds **4** and **6**, and AmB with an additional eight *C. auris* strains (strains I-VIII) from the Centers for Disease Control (CDC) Antibiotic Resistance Bank[51] (Table 3.2). We observed that both compounds **4** and **6** had excellent antifungal activity (MIC values 0.98 to 1.95 μg/mL) against almost all *C. auris* strains.

Table 3.2. MIC values in μg/mL (*Note:* MIC values are also provided in μM into parentheses) for compounds **4**, **6**, and AmB against a panel of *C. auris* strains.

	Compound #					
Strains	**4**	**6**	AmB	CFG	FLC†	VRC†
I	0.98 (1.2)	0.98 (1.2)	1.95 (2.1)	<0.98 (<0.9)	0.49 (1.6)	0.06 (0.2)
II	1.95 (2.3)	0.98 (1.2)	0.98 (1.1)	<0.98 (<0.9)	0.49 (1.6)	0.06 (0.2)
III	1.95 (2.3)	3.9 (4.6)	1.95 (2.1)	1.95 (1.8)	62.5 (204.1)	1.95 (5.6)
IV	1.95 (2.3)	1.95 (2.3)	1.95 (2.1)	<0.98 (<0.9)	>62.5 (>204.1)	3.9 (11.2)
V	1.95 (2.3)	3.9 (4.6)	1.95 (2.1)	7.8 (7.1)	>62.5 (>204.1)	3.9 (11.2)
VI	1.95 (2.3)	1.95 (2.3)	1.95 (2.1)	31.3 (28.6)	0.98 (3.2)	0.06 (0.2)
VII	1.95 (2.3)	1.95 (2.3)	1.95 (2.1)	31.3 (28.6)	>62.5 (>204.1)	0.49 (1.4)
VIII	1.95 (2.3)	1.95 (2.3)	1.95 (2.1)	7.8 (7.1)	>62.5 (>204.1)	0.98 (2.8)
*K**	3.9 (4.6)	1.95 (2.3)	1.95 (2.1)	1.95 (1.8)	31.3 (102.2)	0.24 (0.7)
*L**	7.8 (9.2)	1.95 (2.3)	1.95 (2.1)	7.8 (7.1)	>62.5 (>204.1)	0.49 (1.4)

***C. auris* strains:** I = *C. auris* AR Bank # 0381, II = *C. auris* AR Bank # 0382, III = *C. auris* AR Bank # 0383, IV = *C. auris* AR Bank # 0385, V = *C. auris* AR Bank # 0386, VI = *C. auris* AR Bank # 0387, VII = *C. auris* AR Bank # 0388, VIII = *C. auris* AR Bank # 0389, *K* = *C. auris* AR Bank # 0384, *L* = *C. auris* AR Bank # 0390.
Abbreviations: AmB = amphotericin B; CFG = caspofungin; FLC = fluconazole; MIC = minimum inhibitory concentration; VRC = voriconazole.
*Note: values presented for strains *K* and *L*, which are new to this manuscript, are also presented in Table 3.1, but are also displayed here for ease of comparison.
†MIC-2 values are presented for azoles. MIC-0 values are presented for all other compounds.
Note: Compounds were tested in duplicate.

MIC ≤1.95 μg/mL (excellent antifungal activity)
MIC = 3.9 - 7.8 μg/mL (good antifungal activity)
MIC ≥15.6 μg/mL (poor antifungal activity)

3.3.3. Time-kill assays for compounds 4 and 6

With the very promising antifungal activity results for compounds **4** and **6**, we next examined their killing kinetics. Time-kill assays were done with four representative *Candida* strains, one *C. albicans* (strain *B*), one *C. glabrata* (strain *H*), and two *C. auris*

(strains *K* and *L*) (Fig. 3.4). Compounds **4** and **6** were tested at both their 1× and 2× MIC values, and AmB at 1× MIC was used as a known fungicidal control. Both compounds significantly decreased fungal colony forming units (CFU) by 10^2 CFU/mL by the 3 h time point and did not increase over the 24 h time period, which indicated that compounds **4** and **6** are fungicidal. This pattern was very similar to AmB. With *C. albicans* (strain *B*), compound **4** at 1× MIC reached the limit of detection at 9 h and compound **6** at 2× MIC at 3 h. With *C. glabrata* (strain *H*), both compounds at 2× MIC were at the limit of detection by 24 h. For *C. auris* (strain *K*), compound **4** failed to reach the limit of detection by 24 h, but compound **6** at 1× MIC reached the limit at 6 h. However, with *C. auris* (strain *L*) both compounds **4** and **6** at 1× MIC reached the limit of detection by 3 h and remained under the limit of detection, while AmB reached the limit of detection at 9 h before the CFU/mL began to return to the original yeast cell concentration.

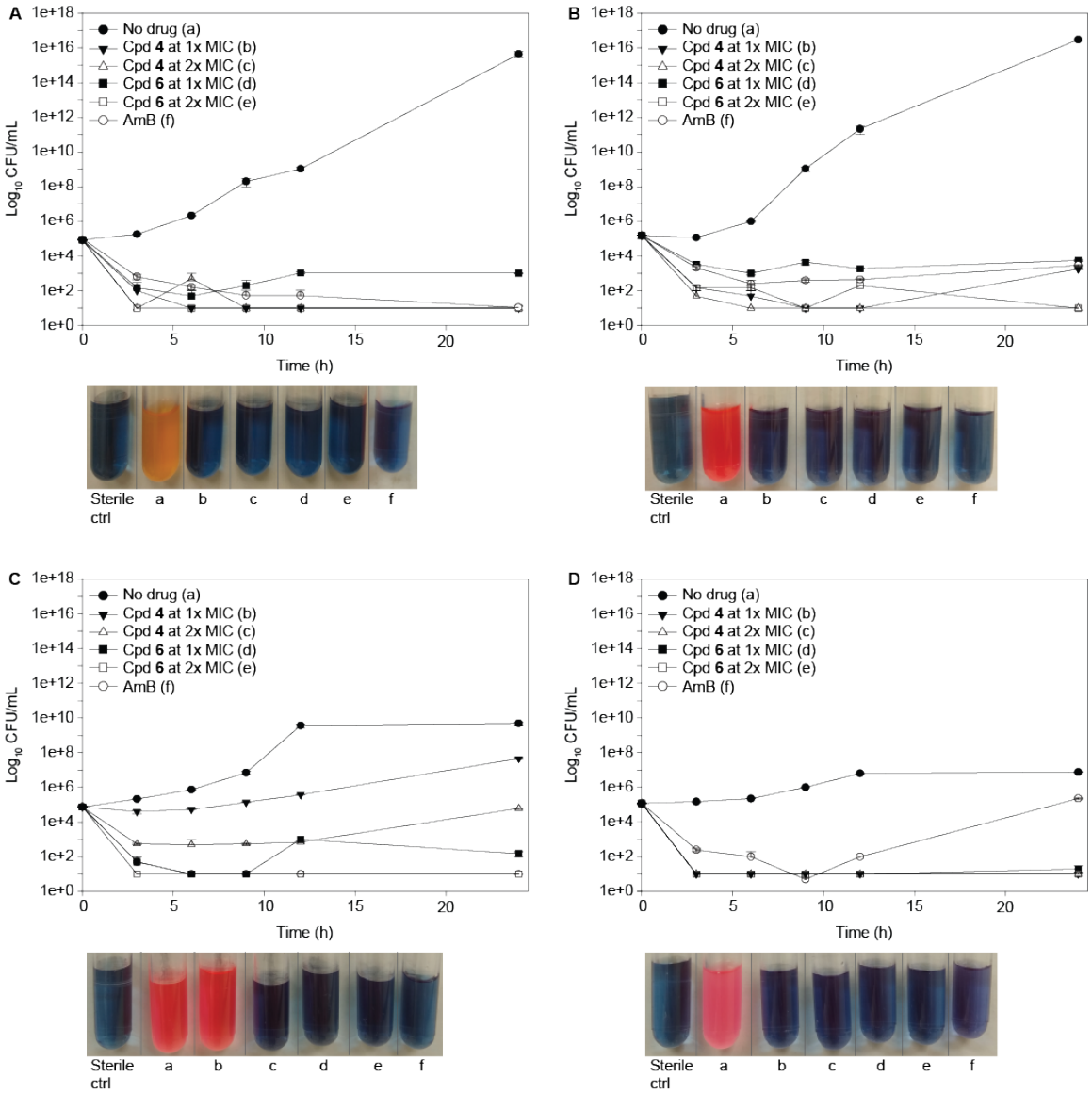

Fig. 3.4. Representative time-kill curves for compounds **4**, **6**, and AmB against **A.** *C. albicans* ATCC 10231 (strain *B*) and **B.** *C. glabrata* ATCC 2001 (strain *H*), **C.** *C. auris* AR Bank # 0384 (strain *K*), and **D.** *C. auris* AR Bank # 0390 (strain *L*). Fungal strains were treated with no drug (black circles), compound **4** at 1× MIC (black triangle), compound **4** at 2× MIC (white triangle), compound **6** at 1× MIC (black square), compound **6** at 2× MIC (white square), and AmB at 1× MIC (white circle). At the 24-hour end point, resazurin was added to the cultures to qualitatively measure the CFU/mL. Resazurin, which is a blue-purple color, is metabolized by viable cells to produce resorufin, which has a pink-orange color. Cultures with little to no cells remain a blue-purple color while dense cultures appear pink or orange. Time-points samples were done in duplicate.

3.3.4. Prevention of biofilm formation and disruption of pre-formed biofilm assays for compounds 4 and 6

Biofilms are well-known in the world of bacteria to cause difficult to treat and reoccurring infections by a multitude of species including *Staphylococcus aureus*, *Escherichia coli*, and *Pseudomonas aeruginosa*.[344-345] There is an extensive number of fungal strains known to form biofilms, but biofilm formation on catheters, prostheses, and other medical devices in healthcare associated infections are mainly limited to *Candida* spp.[346-349] The ability of compounds **4** and **6** to both prevent and disrupt biofilm formation is important for prophylactic treatment and to stop the spread of a fungal infection. However, it is regarded that it is more challenging to disrupt a pre-formed biofilm as the large, sugary extracellular matrix that is the key characteristic of biofilms, can prevent many drugs from reaching the fungal cells.[350] Furthermore, in biofilms, fungal cells can upregulate efflux pumps to prevent the action of any drugs that do reach the fungal cells through the extracellular matrix.[351] We measured the ability of compounds **4** and **6**, auranofin, and AmB to both prevent biofilm formation and to disrupt pre-formed biofilms of *C. albicans* (strain *B*), *C. glabrata* (strain *H*), and *C. auris* (strains *K* and *L*) (Table 3.3 and Figs. 3.5 and 3.6). As the biofilm assay is a colorimetric assay and it is difficult to achieve 100% disruption of biofilms, we report the sessile MIC_{90} ($SMIC_{90}$), which is the concentration of compound at which there is a 90% decrease in metabolic activity as compared to untreated biofilm. Both compounds **4** and **6** showed similar results with both fungal strains tested. $SMIC_{90}$ values in prevention of biofilm formation assays were 1- to 2-fold higher than with planktonic cells. When tested against a pre-formed biofilm, compound **4** had a $SMIC_{90}$ of 7.8 μg/mL with both strains and compound **6** had a $SMIC_{90}$ of 3.9 μg/mL with both strains.

These $SMIC_{90}$ results were 4-fold higher than the MIC results for the same *Candida* strains with planktonic cells. Interestingly, auranofin with *C. albicans* (strain *B*) achieved the same $SMIC_{90}$ as compound **4**, but was inactive against *C. glabrata* (strain *H*). These values for auranofin are similar to a value reported for auranofin against the biofilm of one *C. albicans* strain.[331] In contrast, AmB had $SMIC_{90}$ values of 7.8 μg/mL and 31.3 μg/mL against *C. glabrata* (strain *H*) and *C. albicans* (strain *B*), respectively, which were 2- and 32-fold higher than its MIC values against the same strains in liquid culture.

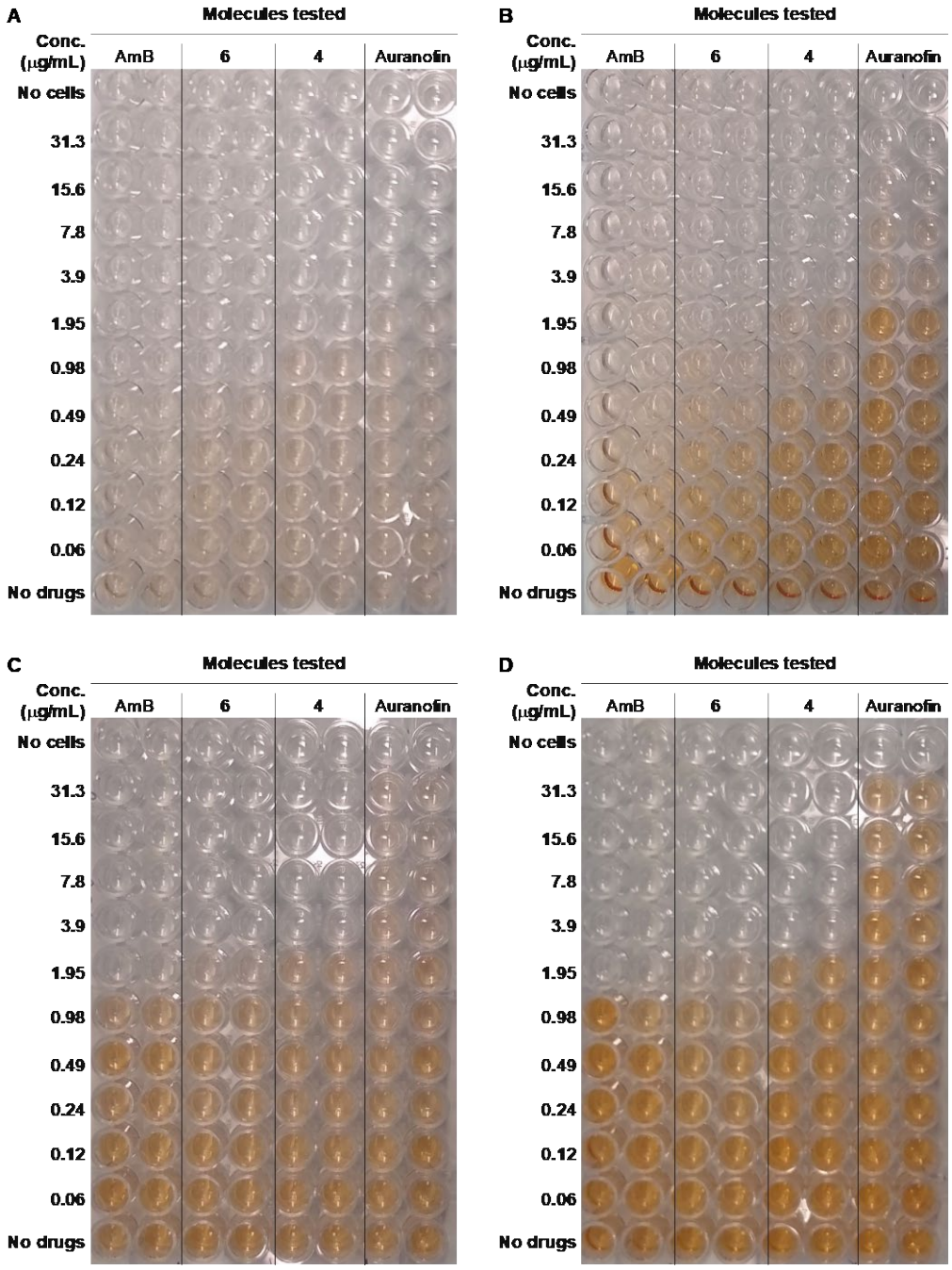

Fig. 3.5. Prevention of biofilm formation of **A.** *C. albicans* ATCC 10231 (strain *B*), **B.** *C. glabrata* ATCC 2001 (strain *H*), **C.** *C. auris* AR Bank # 0384 (strain *K*), and **D.** *C. auris* AR Bank # 0390 (strain *L*) treated at 0 h with auranofin, **6**, **4**, and AmB. Compounds were tested in duplicate. XTT dye is metabolized by fungal cells to produce an orange color. The corresponding data are presented in Table 3.3.

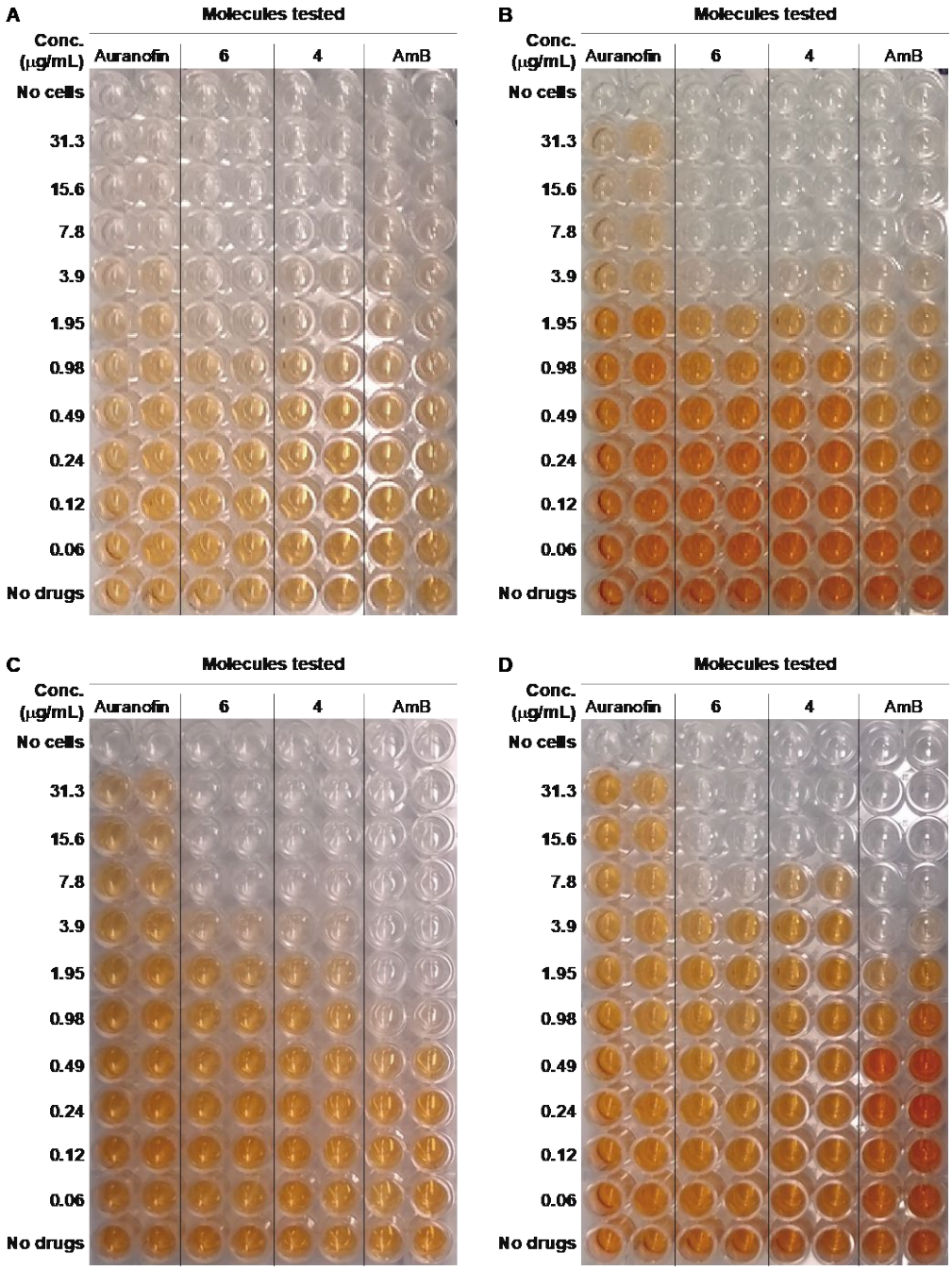

Fig. 3.6. Disruption of pre-formed biofilms of **A.** *C. albicans* ATCC 10231 (strain *B*), **B.** *C. glabrata* ATCC 2001 (strain *H*), **C.** *C. auris* AR Bank # 0384 (strain *K*), and **D.** *C. auris* AR Bank # 0390 (strain *L*) treated at 24 h with auranofin, **6**, **4**, and AmB. Compounds were tested in duplicate. XTT dye is metabolized by fungal cells to produce an orange color. The corresponding data are presented in Table 3.3.

It is promising that both compounds **4** and **6** have good activity against biofilms of *Candida* spp. There have been reports that compared planktonic and sessile MIC values of other

FDA-approved antifungal agents, which demonstrate the reduced susceptibility of biofilms to antifungal agents.[348, 352] Of the currently used antifungal agents, AmB and echinocandins have the best efficacy with biofilms with $SMIC_{90}$ in the range of 0.5-128 μg/mL (4- to 128-fold increase from MIC) and 0.03-8 μg/mL (2- to 16-fold increase from MIC), respectively. For the azoles, itraconazole and posaconazole have some efficacy against biofilms with 1- to 256-fold increases in MIC against biofilms. However, VRC and FLC have no efficacy with $SMIC_{90}$ exceeding 512 μg/mL. Additionally, new investigational antifungal molecules that have been reported to be active against *C. albicans* biofilms, include azole derivatives and benzimidazole containing compounds. For the azole derivatives, seven econazole derivatives were reported with minimum biofilm inhibiting concentrations at or near 8 μg/mL[178] (2- to 16-fold increase in MIC) and alkylated azole derivatives displayed $SMIC_{80}$ values of 15.6-31.3 μg/mL.[184] Other investigational molecules with activity against biofilms included three neomycin B-benzimidazole hybrid molecules with $SMIC_{80}$ values of 7.8-15.6 μg/mL[247] (2- to 4-fold increase in MIC). *Candida* biofilms are known to be key virulence factors in mucosal membrane infections (*i.e.*, thrush and vulvovaginal infections)[353-355] and *Candida* clinical isolates from bloodstream infections can form biofilms as well. Of the bloodstream isolates, it is estimated that approximately 20% of *C. albicans* strains were able to form biofilm *in vitro*, with that percentage increasing to near 70% for non-*albicans Candida*.[167, 356-357] With few other antifungals displaying antibiofilm activity, the 4-fold difference that we observed is highly promising.

Table 3.3. Prevention of biofilm formation and disruption of a pre-formed biofilm by compounds **4**, **6**, auranofin, and AmB against four fungal strains.			
		Biofilm prevention	Pre-formed biofilm
Strain	Compound	$SMIC_{90}$ (μg/mL)	$SMIC_{90}$ (μg/mL)
B	**4**	3.9	7.8
	6	0.98	3.9
	Auranofin	7.8	7.8
	AmB	0.98	31.3
H	**4**	3.9	7.8
	6	1.95	3.9
	Auranofin	31.3	>31.3
	AmB	0.98	7.8
K	**4**	3.9	7.8
	6	3.9	7.8
	Auranofin	>31.3	>31.3
	AmB	1.95	1.95
L	**4**	3.9	15.6
	6	3.9	7.8
	Auranofin	>31.3	>31.3
	AmB	1.95	7.8
Strains: *B* = *C. albicans* ATCC 10231, *H* = *C. glabrata* ATCC 2001, *K* = *C. auris* AR Bank # 0384, *L* = *C. auris* AR Bank # 0390. *Note*: Compounds were tested in duplicate.			

3.3.5. Mammalian cytotoxicity assays for compounds 4 and 6

For the gold complexes to progress further into the drug development process, the gold complex activity should be specific to fungal cells and not be toxic to mammalian cells. Therefore, we tested compounds **4** and **6** as well as the control auranofin against four mammalian cell lines: human adenocarcinoma (A549), bronchial epithelial (BEAS-2B), human embryonic kidney (HEK-293), and murine macrophage (J774A.1) (Fig. 3.7). Excluding auranofin with J774A.1, we observed <50% cell survival at 7.8 μg/mL with no cell survival at 15.6 μg/mL for both compounds **4** and **6** and auranofin. Auranofin, displayed IC_{50} values of 0.5-3.0 μM against A549, BEAS-2B, and HEK-293 cell lines, which agrees with other published values against cisplatin-sensitive cell lines.[339] For J774A.1, the IC_{50} value for auranofin was significantly higher at 16.2 μM. As J774A.1 is a macrophage cell line, auranofin may have had an anti-inflammatory effect that stimulated

cell metabolism, which could account for the higher IC_{50} value. There is interest in repurposing auranofin as an antimicrobial, however, auranofin does not appear to be promising as an antifungal. Auranofin displayed poor activity against *Candida* spp. (MIC >31.3 μg/mL) and only good activity against two *Aspergillus* spp. (MIC = 3.9 and 7.8 μg/mL). For compound **4**, IC_{50} values were very similar for BEAS-2B, HEK-293, and J774A.1 (1.5-2.0 μM) and somewhat higher for A549 (4.5 μM). The MIC values for compounds **4** and **6** against eighteen of the *Candida* spp. are in the range of 0.49-1.95 μg/mL, which are concentrations at which there is toxicity observed for the mammalian cells. Overall, compounds **4** and **6** displayed somewhat better selectivity to kill fungi over mammalian cells than the FDA approved drug, auranofin. Despite this result, there is room to improve these gold complexes to increase the therapeutic window by reducing mammalian cell toxicity.

Reports have suggested that gold complexes bind to thioredoxin reductase in bacteria and mammalian cells,[336-337] but there is some evidence to suggest that gold complexes could inhibit mitochondrial function in fungi.[333] Future studies for the gold complexes, out of scope for this proof-of-concept work, should seek to answer whether these square planar gold complexes bind thioredoxin reductase or mitochondrial enzymes, which if so, could lead to more in depth structure activity studies to decrease cytotoxicity. For other reported gold complexes which were investigated for anti-cancer activity, IC_{50} values for complexes comprised of (1*R*,2*R*)-(+)-1,2-diaminocyclohexane ligands ranged from 1.2-14.8 μM against cancer cell lines, and were >100 μM against a human normal lung fibroblast cell line, MRC5.[339] Another square-planar gold(I)-phosphine complex displayed IC_{50} values of

0.3-9.2 μM.[358] In this report, IC_{50} values ranged from 0.55-0.83 μM against two cancer cell lines for both compounds **4** and **6**. Interestingly, an achiral version of these complexes was reported to be insoluble. Furthermore, in a preliminary study with a xenograft model, compounds **4** and **6** were tolerated in mice at a dose of 2 mg/kg (100% survival) or 8 mg/kg (83% and 67% survival, respectively), which suggests an acceptable level of toxicity at lower doses.

Table 3.4. IC_{50} (μM) for mammalian cell lines.

Compound #	A549	BEAS-2B	HEK-293	J774A.1
4	4.5 ± 0.6	2.0 ± 0.3	1.9 ± 0.7	1.5 ± 0.1
6	2.5 ± 0.2	4.9 ± 0.3	5.7 ± 0.5	1.5 ± 0.1
Auranofin	0.5 ± 0.1	1.3 ± 0.1	3.0 ± 0.2	16.2 ± 0.9

Note: Compounds were tested in quadruplicate.

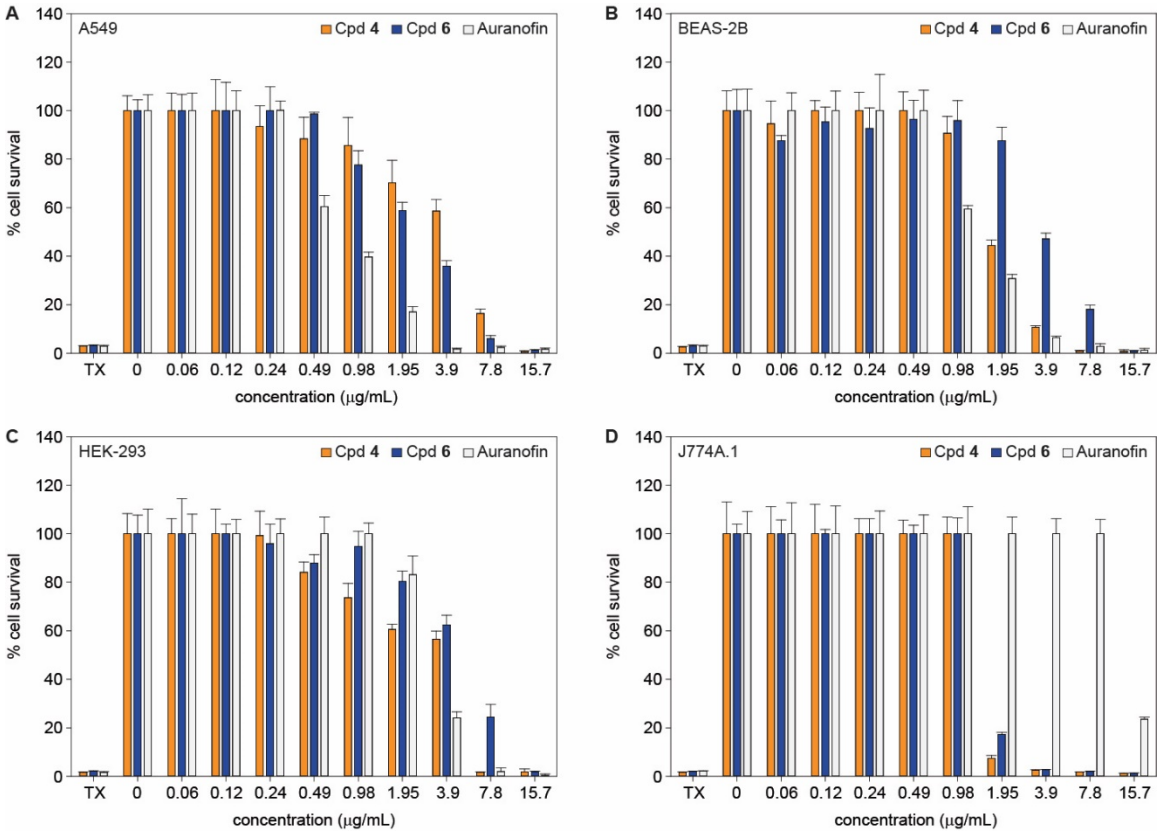

Fig. 3.7. Evaluation of cytotoxicity for compound **4** (orange), compound **6** (blue), and auranofin (white) with **A.** A549, **B.** BEAS-2B, **C.** HEK-293, and **D.** J774A.1 cell lines. Controls include treatment with Triton-X®

(TX, 1% *v/v*, positive control) and 0.5% DMSO (negative control). *Note*: values >100% were normalized to 100%. Compounds were tested in quadruplicate.

3.3.6. Measurement of hemolysis for compounds 4 and 6

To expand upon the cytotoxicity results, we obtained both murine and human red blood cells (RBCs) to evaluate the hemolytic activity of compounds **4** and **6** as compared to both auranofin and AmB, as well as to the detergent, Triton-X® (positive control) (Fig. 3.8). Some drugs, especially those containing both hydrophobic and hydrophilic components, can disrupt cell membranes to cause hemolysis.[359] Examples of drugs that are known to be hemolytic include AmB as well as cisplatin. With AmB, to minimize hemolytic activity a lipid formulation has been developed.[360] The results are similar for both murine and human RBCs, however, the murine RBCs appear more prone to hemolysis as compounds **4** and **6** displayed 13% and 60% hemolysis, respectively, at 3.9 μg/mL and less than 5% with human RBCs. We observed that both compounds **4** and **6** displayed hemolytic activity at 7.8 μg/mL. AmB exhibited somewhat better values with 30-60% hemolysis at 7.8 μg/mL and 100% hemolysis at 15.6 μg/mL. In contrast, auranofin displayed no hemolytic activity at 15.6 μg/mL. With MIC values for compounds **4** and **6** typically in the range of 0.49-1.95 μg/mL for *Candida* spp., there is a 1- to 2-fold therapeutic window, which is not perfect when comparing to the desired 10-fold therapeutic window.

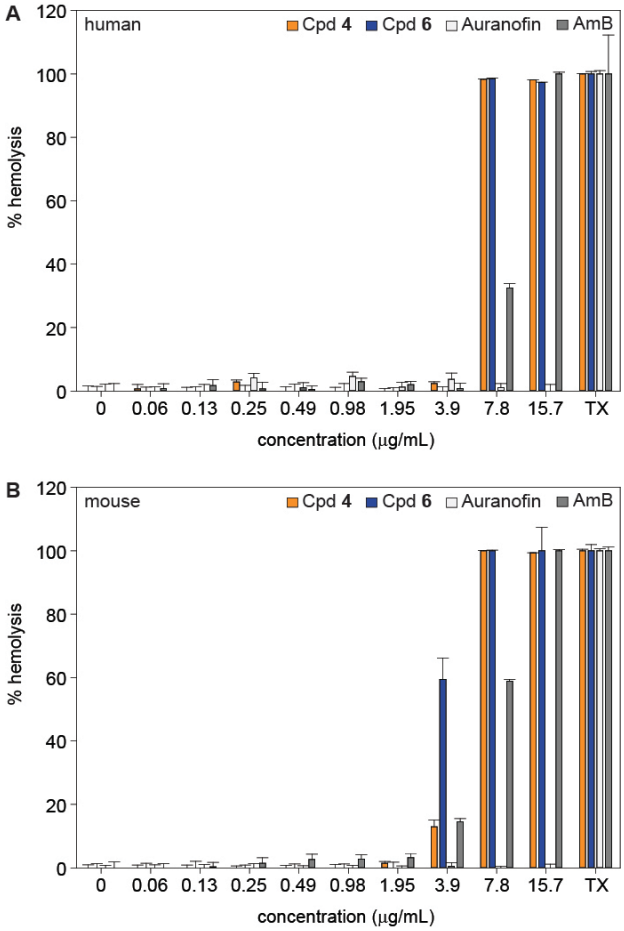

Fig. 3.8. Hemolytic activity of compound **4** (orange), compound **6** (blue), auranofin (white), and AmB (grey) against **A.** human and **B.** murine red blood cells. Positive control is Triton-X® (TX, 1% *v*/*v*). Compounds were tested in quadruplicate.

3.3.7. Whole cell uptake assay for compounds 4 and 6

To gain some insight into whether compounds **4** and **6** have an intracellular or extracellular target, the uptake of gold into the cell was measured using Inductively Coupled Plasma Optical Emission Spectroscopy (ICP-OES, Fig. 3.9). Uptake was measured with 100 million yeast cells (Note: this is 2-3× more cells than in MIC and time-kill studies) after 30 minutes treatment with 10 μM (~5× MIC for compounds **4** and **6** against strain *B* and *H*, respectively; ~10× MIC for compounds **4** and **6** against strain *H* and *B*, respectively) compound. These conditions were chosen to have a significant number of cells for analysis,

a saturating amount of compound (note that 10 μM was required to achieve saturation), and at a time-point within the doubling time of the yeast. Both compounds exhibited very similar uptake by *C. albicans* (strain *B*) and *C. glabrata* (strain *H*) of ~17 pmol/million cells. However, the uptake when 5× MIC was used was higher than when 10× MIC was used. With the values for gold uptake in the pmol/million cells range, there appears to be a relatively low amount of gold uptake per cell, but there are no reports of similar uptake studies in yeast to compare to. However, we do observe uptake and these values correspond to approximately 15% and 20% of total gold content for compounds **4** and **6**, respectively. It is possible that by the 30-minute end point there is some lysis of the fungal cells, especially with 10× MIC, which would decrease uptake values. These results do suggest that the compounds enter the yeast cell by facilitated diffusion or active transport as with passive diffusion higher dosing of compound (*e.g.*, saturating amount) corresponds to greater cell uptake. We previously published gold(III) complexes that we investigated as anticancer agents, where we measured gold uptake in OVCAR8 cells.[339] We found that gold(III) complexes that included a single chloride anion had improved uptake over similar complexes with perchlorate anions, with relative uptake of ~300-400 and ~200 pmol/million cells, respectively. These values were significantly lower than the ~1300 pmol/million cells uptake of auranofin in the OVCAR8 cell. The uptake values for compounds **4** and **6** in fungi appear significantly lower than the values measured for other complexes with the mammalian cells, but are similar when the difference in cell volume and incubation time between yeast and mammalian cells is considered.[361-362] Therefore, it is still unclear, but within reason for the gold complexes to have an intracellular target. Conceivably, the structurally complex cell wall of fungus composed of chitin, glucans, and

glycoproteins may contribute to the limited uptake of the cationic gold complexes investigated. Further studies will focus on developing neutral complexes and complexes that benefit from active transport.

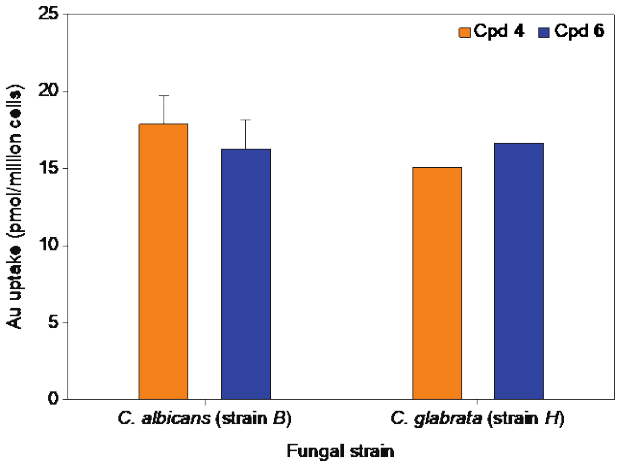

Fig. 3.9. Whole cell uptake of 10 μM of compound **4** (orange) and compound **6** (blue) by **A.** *C. albicans* ATCC 10231 (strain *B*) and **B.** *C. glabrata* ATCC 2001 (strain *H*) after 30 min treatment. Compounds were tested in duplicate.

3.3.8. Development of fungal resistance for compounds 4 and 6

Fungal drug resistance can be caused by mutation of the target protein (observed with azoles and echinocandins),[83-84] overexpression of the target protein (observed with azoles),[73-74] the use of efflux pumps (observed with azoles),[86-90] or increased filamentation to decrease drug uptake (observed with AmB).[127, 131] In order to assess the potential for the development of fungal resistance, we determined MIC values of compounds **4** and **6** as well as AmB as a control over fifteen serial passages with *C. albicans* (strain *B*) and *C. glabrata* (strain *H*) (Fig. 3.10). We observed no significant changes in MIC values for our compounds over the course of this study. The gold complexes are likely to display different mechanisms of action in fungi that can circumvent resistance pathways.

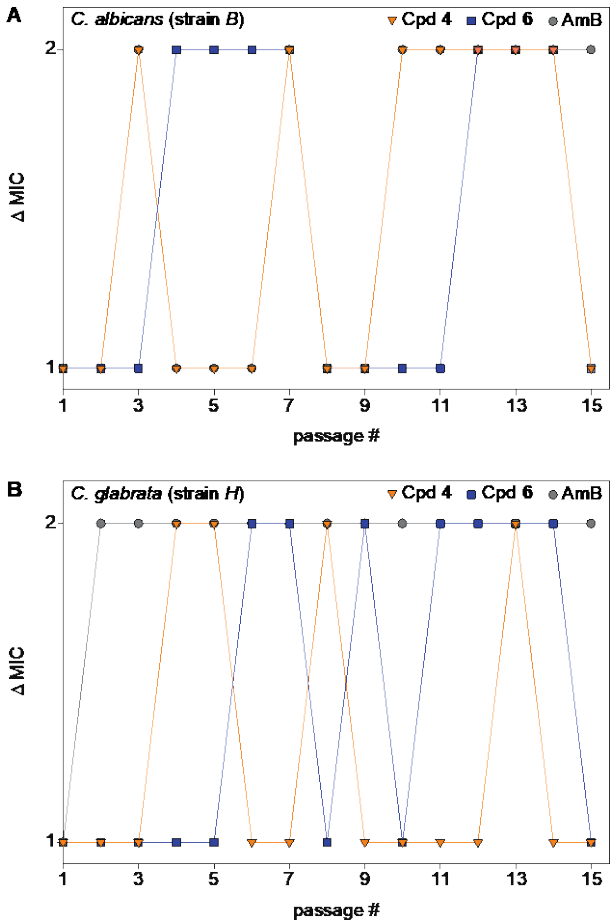

Fig. 3.10. Changes in MIC values of **A.** *C. albicans* ATCC 10231 (strain *B*) and **B.** *C. glabrata* ATCC 2001 (strain *H*) treated with compound **4** (orange), compound **6** (blue), and AmB (grey) over fifteen serial passages. MICs were done in duplicate.

3.4. CONCLUSIONS

In summary, we synthesized three linear gold(I)-phosphine complexes and three corresponding square-planar gold(I) complexes and explored their antifungal activity. Two square-planar complexes, **4** and **6**, displayed excellent antifungal activity against a panel of twenty-one *Candida* strains which included *C. albicans*, *C. glabrata*, *C. krusei*, *C. parapsilosis*, and *C. auris* as well as four *C. neoformans* Furthermore, these square-planar complexes displayed good activity against four filamentous strains of *Aspergillus* spp., and

Fusarium spp. In addition, compounds **4** and **6** displayed good activity against *Candida* spp. biofilms. When tested against mammalian cells, the gold complexes displayed limited improvement in selectivity index over the FDA-approved drugs AmB and auranofin. Finally, by development of resistance studies of compounds **4** and **6** in *Candida* spp., it was found that *Candida* spp. have a low chance of developing resistance to these gold complexes. Future studies will work to decrease the toxic effect to mammalian cells and to substantiate the mechanism of action of the gold complexes in fungi.

3.5. EXPERIMENTAL

3.5.1. Chemistry

3.5.1.1. Materials and instrumentation

Tetrahydrothiophene (THT) was from Sigma-Aldrich and used without further purification or drying. Tetrachloroauric acid ($HAuCl_4 \cdot 3H_2O$) was purchased from Oakwood and used as received. THT and $HAuCl_4 \cdot 3H_2O$ were used to prepare AuCl(THT) as previously reported.[341] All phosphorus ligands used: 1,2-bis(diphenylphosphino)benzene, 1,2-bis[(2*S*,5*S*)-2,5-dimethylphospholano]benzene, and 1,2-bis[(2*R*,5*R*)-2,5-dimethylphospholano]benzene were purchased from Sigma-Aldrich and used as received. ACS grade solvents were purchased from Pharmco-Aaper and used without further purification or drying. Deuterated solvents were purchased from Cambridge Isotope Laboratories and used as received. Silica gel for column chromatography (Silicycle, P/N: R10030B SiliaFlash®F60, Size: 40-63 μm, Canada) was purchased from Silicycle. Aluminum backed silica-gel plates (20 × 20 cm^2) were purchased from Silicycle (TLA-R10011B-323) and utilized for analytical thin-layer chromatography (TLC).

All reactions were insensitive to air or moisture, as a result, they were carried out under standard atmospheric conditions without air-sensitive techniques or drying agents. Reactions were carried out in round-bottom flasks or scintillation vials equipped with Teflon-coated magnetic stir bars for stirring non-homogenous reaction mixtures. Reactions were monitored by NMR and TLC, and the TLC plates visualized under short-wavelength light (254 nm) or stained with iodine on Silica. All compound purification was performed using silica-gel chromatography, employing CombiFlash® Rf+ Lumen, Teledyne ISCO. Filtrations were carried out using medium-porosity ceramic funnels. Removal of solvents in vacuo was performed using a Büchi rotary evaporator and further drying was achieved by Schlenk line at ~120 mTorr using a dynamic vacuum pump.

^{1}H, ^{13}C (^{1}H-decoupled), and ^{31}P (^{1}H-decoupled) NMR spectra were recorded on a Varian Unity 400 MHz NMR spectrometer with a Spectro Spin superconducting magnet at the University of Kentucky NMR facility in the Department of Chemistry. Chemical shifts in ^{1}H and ^{13}C NMR spectra were internally referenced to solvent signals (^{1}H NMR: $CDCl_3$ at δ = 7.26 ppm; ^{13}C NMR: $CDCl_3$ at δ = 77.16 ppm), and those in ^{31}P NMR spectra, which were run in $CDCl_3$, were externally referenced to 85% H_3PO_4 in D_2O at δ = 0 ppm.

High-resolution mass spectra (HRMS) were obtained using a direct flow injection (injection volume = 1 μL) method with ElectroSpray Ionization (ESI) on a Waters Q-TOF Premier instrument in the positive mode. The optimized conditions were as follows: capillary = 3000 kV, cone = 35, source temperature = 120 °C, and desolvation temperature

= 350 °C. Mass spectrometry experiments and analysis were conducted at the Chemical Instrumentation Center at Boston University.

In addition to spectroscopic characterization, the purity of all compounds was assessed by RP-HPLC using an Agilent Technologies 1100 series HPLC instrument and an Agilent Phase Eclipse Plus C18 column (4.6 mm × 100 mm; 3.5 μm particle size). All compounds were found to be ≥97% pure.

3.5.1.2. Synthesis and characterization of compounds 1-6

Synthesis of the known compounds [1,2-bis(diphenylphosphino)benzene]digold(I) (1)[342] and bis-[1,2-bis(diphenylphosphino)benzene]gold(I) (2)[343]

Under normal atmospheric conditions, in a 25 mL round bottom flask was placed AuCl(THT) (58.7 mg, 0.183 mmol). $CHCl_3$ (10.0 mL) was added and the solution (white suspension) was stirred at room temperature for 2-3 min. To the solution was added 1,2-bis(diphenylphosphino)benzene (80.2 mg, 0.180 mmol). The solution turned yellow instantly. The solution was stirred for about 1 h and monitored by TLC using 5:95/MeOH:CH_2Cl_2 as an eluent. Separation of compounds **1** and **2** was achieved *via* flash chromatography using CombiFlash® Rf+ Lumen with 5:95/MeOH:CH_2Cl_2.

*Characterization of compound **1***: White solid (37 mg, 23%); R_f 0.8 in 5:95/MeOH:CH_2Cl_2; ^{1}H NMR (400 MHz, $CDCl_3$, Fig. 3.A1 "Disclaimer: All figures are presented for Chapter 3 are presented in Appendix A and are listed as Fig. 3.A#") δ 7.56-7.46 (m, 6H), 7.46-7.35 (m, 16H), 7.25-7.16 (m, 2H); ^{13}C NMR (101 MHz, $CDCl_3$, Fig. 3.A2) δ 137.12, 137.05,

136.97, 134.81, 134.74, 134.67, 132.35, 131.90, 131.87, 131.84, 129.60, 129.54, 129.48, 128.91, 128.60, 128.28; ^{31}P NMR (162 MHz, $CDCl_3$, Fig. 3.A3) δ 24.60; HRMS (ESI) (*m*/*z*): calcd. for $C_{30}H_{24}Au_2Cl_2P_2$ $[M\text{-}Cl]^+$: 875.0373, found: 875.0408 Δ = 3.9998 (Fig. 3.A4). Purity was demonstrated to be 97% by RP-HPLC: R_t = 8.82 min using the following method: Flow rate: 1 mL/min; λ = 260 nm; Eluent A = H_2O with 0.1% TFA; Eluent B = MeCN with 0.05% formic acid; Elution program: 0 to 100% B over 10 min followed by 100 to 0% B over 5 min and 4 additional min at 0% B (Fig. 3.A5).

Characterization of compound ***2***: Yellow solid (68 mg, 36%); R_f 0.2 in 5:95/MeOH:CH_2Cl_2; ^{1}H NMR (400 MHz, $CDCl_3$, Fig. 3.A6) δ 7.57-7.25 (m, 20H), 7.13-6.87 (m, 28H); ^{13}C NMR (101 MHz, $CDCl_3$, Fig. 3.A7) δ 142.13, 134.52, 134.37, 132.56, 132.44, 132.37, 132.33, 132.29, 132.25, 132.21, 132.18, 131.72, 130.40, 129.13, 129.11, 129.08, 129.06, 129.03, 129.01, 128.89, 128.86, 128.74; ^{31}P NMR (162 MHz, $CDCl_3$, Fig. 3.A8) δ 21.17; HRMS (ESI) (*m*/*z*): calcd. for $C_{60}H_{48}AuClP_4$ $[M\text{-}Cl]^+$: 1089.2372, found: 1089.2357 Δ = 1.3771 (Fig. 3.A9). Purity was demonstrated to be 100% by RP-HPLC: R_t = 10.78 min using the following method: Flow rate: 1 mL/min; λ = 260 nm; Eluent A = H_2O with 0.1% TFA; Eluent B = MeOH with 0.1% TFA; Elution program: 0 to 100% B over 5 min, stay at 100% B for 10 min, followed by 100 to 0% B over 4 min (Fig. 3.A10).

Synthesis of [1,2-bis[(2*S*,5*S*)-2,5-dimethylphospholano]benzene]digold(I) (3) and bis-[1,2-bis[(2*S*,5*S*)-2,5-dimethylphospholano]benzene]gold(I) (4)

Compounds **3** and **4** were synthesized and separated following the procedure described for the preparation of compounds 1 and 2 using AuCl(THT) (64.6 mg, 0.202 mmol) and 1,2-bis[(2*S*,5*S*)-2,5-dimethyl-1-phospholano]benzene (58.6 mg, 0.191 mmol).

*Characterization of compound **3***: White solid (47 mg, 32%); R_f 0.8 in 5:95/MeOH:CH_2Cl_2; ^{1}H NMR (400 MHz, $CDCl_3$, Fig. 3.A11) δ 7.73-7.64 (m, 4H), 3.60 (sextet, *J* = 7.6 Hz, 2H), 2.99-2.85 (m, 2H), 2.53-2.38 (m , 2H), 2.30-2.13 (m, 2H), 1.92-1.77 (m, 2H), 1.57-1.44 (m, 2H), 1.37 (dd, *J* = 20.6, 6.7 Hz, 6H), 1.06 (dd, *J* = 17.2, 7.2 Hz, 6H); ^{13}C NMR (101 MHz, $CDCl_3$, Fig. 3.A12) δ 134.45, 134.39, 134.33, 132.19, 131.61, 131.58, 131.56, 37.20, 37.03, 37.01, 36.97, 36.84, 36.79, 36.61, 35.56, 35.54, 33.99, 33.92, 33.85, 19.59, 19.56, 19.52, 19.47, 19.42; ^{31}P NMR (162 MHz, $CDCl_3$, Fig. 3.A13) δ 43.96; HRMS (ESI) (*m*/*z*): calcd. for $C_{18}H_{28}Au_2Cl_2P_2$ $[M\text{-}Cl]^+$: 735.0686, found: 735.0671 Δ = 2.0406 (Fig. 3.A14). Purity was demonstrated to be 97% by RP-HPLC: R_t = 7.94 min using the following method: Flow rate: 1 mL/min; λ = 260 nm; Eluent A = H_2O with 0.1% TFA; Eluent B = MeCN with 0.05% formic acid; Elution program: 0 to 100% B over 10 min followed by 100 to 0% B over 5 min and 4 additional min at 0% B (Fig. 3.A15).

*Characterization of compound **4***: Yellow solid (44 mg, 27%); R_f 0.4 in 5:95/MeOH:CH_2Cl_2; ^{1}H NMR (400 MHz, $CDCl_3$, Fig. 3.A16) δ 7.75-7.67 (m, 4H), 7.60-7.54 (m, 4H), 2.71-2.46 (m, 8H), 2.35-2.13 (m, 8H), 1.87-1.72 (m, 4H), 1.62-1.49 (m, 4H), 1.19 (td, *J* = 10.6, 6.9 Hz, 12H), 0.81-0.71 (m, 12H); ^{13}C NMR (101 MHz, $CDCl_3$, Fig. 3.A17) δ 142.52, 142.36, 142.20, 133.34, 133.31, 133.29, 130.67, 40.56, 40.48, 40.40, 37.71, 37.65, 37.59, 36.06, 35.84, 21.47, 21.41, 21.36, 14.49; ^{31}P NMR (162 MHz, $CDCl_3$,

Fig. 3.A18) δ 38.34; HRMS (ESI) (*m*/*z*): calcd. for $C_{36}H_{56}AuClP_4$ $[M-Cl]^+$: 809.2998, found: 809.3016 Δ = 2.2241 (Fig. 3.A19). Purity was demonstrated to be 98% by RP-HPLC: R_t = 10.81 min using the following method: Flow rate: 1 mL/min; λ = 260 nm; Eluent A = H_2O with 0.1% TFA; Eluent B = MeCN with 0.05% formic acid; Elution program: 0 to 100% B over 10 min followed by 100 to 0% B over 5 min and 4 additional min at 0% B (Fig. 3.A20).

Synthesis of the known compounds[1,2-bis[(2R,5*R*)-2,5-dimethylphospholano]benzene]digold(I) (5)[363] and of bis-[1,2-bis[(2*R*,5*R*)-2,5-dimethylphospholano]benzene]gold(I) (6)

Compounds **5** and **6** were synthesized and separated following the procedure described for the preparation of compounds **1** and **2** using AuCl(THT) (61.9 mg, 0.193 mmol) and 1,2-bis[(2*R*,5*R*)-2,5-dimethylphospholano]benzene (60.1 mg, 0.196 mmol).

Characterization of compound ***5***: White powder (35 mg, 35%); R_f 0.8 in 5:95/MeOH:CH_2Cl_2; ^{1}H NMR (400 MHz, $CDCl_3$, Fig. 3.A21) δ 7.73-7.64 (m, 4H), 3.61 (sextet, *J* = 7.7 Hz, 2H), 2.99-2.86 (m, 2H), 2.54-2.38 (m, 2H), 2.30-2.12 (m, 2H), 1.92-1.76 (m, 2H), 1.56-1.44 (m, 2H), 1.37 (dd, *J* = 20.6, 6.8 Hz, 6H), 1.06 (dd, *J* = 17.2, 7.2 Hz, 6H); ^{13}C NMR (101 MHz, $CDCl_3$, Fig. 3.A22) δ 134.62, 134.56, 134.49, 131.75, 131.72, 131.70, 37.37, 37.20, 37.19, 37.16, 37.02, 36.99, 36.81, 35.73, 35.71, 35.69, 34.17, 34.10, 34.03, 19.73, 19.71, 19.68, 19.63, 19.57; ^{31}P NMR (162 MHz, $CDCl_3$, Fig. 3.A23) δ 43.96; HRMS (ESI) (*m*/z): calcd. for $C_{18}H_{28}Au_2Cl_2P_2$ $[M-Cl]^+$: 735.0686, found: 735.0697 Δ = 1.4965 (Fig. 3.A24). Purity was demonstrated to be 97% by RP-HPLC: R_t =

7.86 min using the following method: Flow rate: 1 mL/min; λ = 260 nm; Eluent A = H_2O with 0.1% TFA; Eluent B = MeCN with 0.05% formic acid; Elution program: 0 to 100% B over 10 min followed by 100 to 0% B over 5 min and 4 additional min at 0% B (Fig. 3.A25).

Characterization of compound ***6***: Yellow powder (71 mg, 37%); R_f 0.2 in 5:95/MeOH:CH_2Cl_2; ^{1}H NMR (400 MHz, $CDCl_3$, Fig. 3.A26) δ 7.74-7.66 (m, 4H), 7.60-7.53 (m, 4H), 2.71-2.44 (m, 8H), 2.35-2.13 (m, 8H), 1.86-1.72 (m, 4H), 1.61-1.48 (m, 4H), 1.18 (td, J = 10.5, 6.8 Hz, 12H), 0.80-0.71 (m, 12H); ^{13}C NMR (101 MHz, $CDCl_3$, Fig. 3.A27) δ 142.34, 133.32, 133.29, 133.27, 130.66, 40.54, 40.46, 40.39, 37.69, 37.63, 37.56, 36.04, 35.82, 21.45, 21.39, 21.34, 14.47; ^{31}P NMR (162 MHz, $CDCl_3$, Fig. 3.A28) δ 38.24; HRMS (ESI) (*m*/*z*): calcd. for $C_{36}H_{56}AuClP_4$ $[M\text{-}Cl]^+$: 809.2998, found: 809.3025 Δ = 3.3362 (Fig. 3.A29). Purity was demonstrated to be 97% by RP-HPLC: R_t = 10.81 min using the following method: Flow rate: 1 mL/min; λ = 260 nm; Eluent A = H_2O with 0.1% TFA; Eluent B = MeCN with 0.05% formic acid; Elution program: 0 to 100% B over 10 min followed by 100 to 0% B over 5 min and 4 additional min at 0% B (Fig. 3.A30).

3.5.1.3. X-ray crystallography of compounds 3-6

The single crystal of compound **3** was grown at 4 °C by vapor diffusion of Et_2O into a CH_2Cl_2 solution and compounds **4**, **5**, and **6** were grown at room temperature by vapor diffusion of Et_2O into $CDCl_3$ solutions. Suitable crystals were selected by microscopic examination through crossed polarizers, mounted on a fine glass fibre in polyisobutene oil, and cooled to 90 K under a stream of nitrogen. A Bruker D8 Venture diffractometer with

graded-multilayer focused MoKα X-rays (λ = 0.71073 Å) was used to collect the diffraction data from the crystals. The raw data were integrated, scaled, merged and corrected for Lorentz-polarization effects using the APEX3 package.[364-365] Space group determination and structure solution and refinement were carried out with SHELXT, and SHELXL,[366-367] respectively. All non-hydrogen atoms were refined with anisotropic displacement parameters. Hydrogen atoms were placed at calculated positions and refined using a riding model with their isotropic displacement parameters (U_{iso}) set to either $1.2U_{iso}$ or $1.5U_{iso}$ of the atom to which they were attached. The structures, deposited in the Cambridge Structural Database (deposition number = 1889869 (**3**), 1889576 (**4**), 1889577 (**5**), and 1916580 (**6**)), were checked for missed higher symmetry, twinning, and overall quality with PLATON,[368] an R-tensor,[369] and finally validated using CheckCIF.[368] The X-ray structures of compounds **3-6** are presented in Fig. 3.3 and the corresponding structure refinement data in Table 3.5.

Table 3.5. Crystal data and structure refinement for compound **3-6**.				
	Compound **3**	Compound **4**	Compound **5**	Compound **6**
Empirical formula	$C_{18}H_{28}Au_2Cl_2P_2$	$C_{37}H_{57}AuCl_4P_4$[a]	$C_{18}H_{28}Au_2Cl_2P_2$	$C_{37}H_{57}AuCl_4P_4$[a]
Molecular weight	771.18	964.47	771.18	964.47
Temperature	90.0(2) K	220(2) K	180(2) K	220(2) K
Wavelength	0.71073 Å	0.71073 Å	0.71073 Å	0.71073 Å
Crystal system, space group	Orthorhombic, $P2_12_12_1$	Orthorhombic, $P2_12_12_1$	Orthorhombic, $P2_12_12_1$	Orthorhombic, $P2_12_12_1$
Unit cell dimensions	a = 16.3388(9) Å, α = 90° b = 16.3413(9) Å, β = 90° c = 16.4154(8) Å, γ = 90°	a = 12.6939(5) Å, α = 90° b = 16.5334(8) Å, β = 90° c = 20.1529(8) Å, γ = 90°	a = 16.1576(3) Å, α = 90° b = 16.3885(3) Å, β = 90° c = 16.7778(4) Å, γ = 90°	a = 12.7646(3) Å, α = 90° b = 16.4972(3) Å, β = 90° c = 20.0823(5) Å, γ = 90°
Volume	4382.9(4) $Å^3$	4229.6(3) $Å^3$	4442.74(16) $Å^3$	4228.93(16) $Å^3$
Z, Calculated density	8, 2.337 Mg/m^3	4, 1.515 Mg/m^3	8, 2.306 Mg/m^3	4, 1.515 Mg/m^3
Absorption coefficient	13.763 mm^{-1}	3.907 mm^{-1}	13.577 mm^{-1}	3.908 mm^{-1}
F(000)	2864	1944	2864	1944
Crystal size	0.100 × 0.080 × 0.040 mm	0.140 × 0.100 × 0.070 mm	0.220 × 0.200 × 0.160 mm	0.120 × 0.090 × 0.090 mm
Theta range for data collection	2.777 to 27.506°	3.110 to 28.819°	2.728 to 27.492°	2.861 to 27.505°
Limiting indices	$-21 \leq h \leq 21$, $-21 \leq k \leq 21$, $-21 \leq l \leq 21$	$-17 \leq h \leq 17$, $-22 \leq k \leq 22$, $-27 \leq l \leq 27$	$-20 \leq h \leq 20$, $-21 \leq k \leq 21$, $-21 \leq l \leq 21$	$-16 \leq h \leq 16$, $-21 \leq k \leq 21$, $-26 \leq l \leq 26$
Reflections collected / unique	64860 / 10048 [R(int) = 0.0440]	98447 / 11027 [R(int) = 0.0479]	74012 / 10159 [R(int) = 0.0314]	78808 / 9679 [R(int) = 0.0411]
Completeness to theta = 25.242	99.8%	99.7%	99.8%	99.8%
Absorption correction	Semi-empirical from equivalents	Semi-empirical from equivalents	Semi-empirical from equivalents	Semi-empirical from equivalents
Max. and min. transmission	0.746 and 0.431	0.746 and 0.609	0.491 and 0.284	0.746 and 0.665
Refinement method	Full-matrix least-squares on F^2	Full-matrix least-squares on F^2	Full-matrix least-squares on F^2	Full-matrix least-squares on F^2
Data / restraints / parameters	10048 / 386 / 442	11027 / 488 / 456	10159 / 36 / 442	9679 / 488 / 454
Goodness-of-fit on F^2	1.069	1.112	1.048	1.060
Final R indices [I > 2σ(I)]	$R_1 = 0.0213$, $wR_2 = 0.0409$	$R_1 = 0.0262$, $wR_2 = 0.0571$	$R_1 = 0.0149$, $wR_2 = 0.0309$	$R_1 = 0.0298$, $wR_2 = 0.0660$
R indices (all data)	$R_1 = 0.0246$, $wR_2 = 0.0417$	$R_1 = 0.0332$, $wR_2 = 0.0594$	$R_1 = 0.0160$, $wR_2 = 0.0312$	$R_1 = 0.0346$, $wR_2 = 0.0681$
Absolute structure parameter	0.007(3)	0.016(5)	0.009(2)	0.008(3)
Extinction coefficient	0.000064(19)	0.00047(11)	0.00049(2)	N/A
Largest diff. peak and hole	1.971 and -1.017 e. $Å^{-3}$	0.816 and -0.573 e. $Å^{-3}$	1.007 and -1.056 e. $Å^{-3}$	1.138 and -0.676 e. $Å^{-3}$
[a] The empirical formula includes a molecule of $CHCl_3$.				

3.5.2. Biochemistry and microbiology

3.5.2.1. Biochemical/biological reagents and instrumentation

The American Type Culture Collection (ATCC) *Candida albicans* strains, including 10231 (strain *B*), MYA-2876 (strain *E*), and 64124 (strain *F*), were a generous gift from Dr. Jon Y. Takemoto (Utah State University, Logan, UT, USA). The rest of the *C. albicans* strains, including MYA-1003 (strain *A*), MYA-1237 (strain *C*), MYA-2310 (strain *D*), 90819

(strain *G*), and as well as the non-*albicans Candida* fungi *C. glabrata* ATCC 2001 (strain *H*), *C. krusei* ATCC 6258 (strain *I*), *C. parapsilosis* ATCC 22019 (strain *J*), and *Cryptococcus neoformans* ATCC MYA-85 (strain *M*) were purchased from the American Type Culture Collection (ATCC, Manassas, VA, USA). A panel of *Candida auris* strains were acquired from the CDC & FDA Antibiotic Resistance Isolate Bank (CDC, Atlanta, GA, USA), which included *C. auris* AR Bank # 0381-0390 (strains *K*, *L*, and I-VIII). *C. neoformans* clinical isolates CN1-CN3 (strains *N*-*P*) were generously provided by Dr. Nathan Wiederhold (University of Texas, San Antonio, TX, USA). The filamentous fungi *Aspergillus nidulans* ATCC 38163 (strain *Q*) and *Fusarium graminearum* 053 (strain *T*) were kind gifts from Prof. Jon S. Thorson (University of Kentucky, Lexington, KY) and Prof. Lisa Vaillancourt (University of Kentucky, Lexington, KY, USA), while the *Aspergillus terreus* ATCC MYA-3633 (strain *R*) and *Aspergillus flavus* ATCC MYA-3631 (strain *S*) were purchased from the ATCC. Yeast strains were cultured at 35 °C in yeast extract peptone dextrose (YEPD) broth. *Aspergillus* spp. strains were cultured on potato dextrose agar (PDA, catalog # 110130, EMD Millipore, Billerica, MA, USA) at 28 °C before the spores were harvested. All fungal experiments were carried out in RPMI 1640 medium (catalog # R6504, Sigma-Aldrich, St. Louis, MO, USA) buffered to pH 7.0 with 0.165 M MOPS buffer (Sigma-Aldrich, St. Louis, MO, USA).

For cytotoxicity assays, the human embryonic kidney cell line (HEK-293) was purchased from the ATCC. The human bronchial epithelial cell line (BEAS-2B), the human lung carcinoma cell line (A549), and the mouse macrophage cell line (J774A.1) were generous gifts from Prof. David K. Orren (University of Kentucky, Lexington, KY), Prof. Markos

Leggas (University of Kentucky, Lexington, KY), and Prof. David J. Feola (University of Kentucky, Lexington, KY), respectively. A549, HEK-293, and BEAS-2B cells were cultured in Dulbecco's Modified Eagle's Medium (DMEM, catalog # VWRL0100, VWR, Chicago, IL) supplemented with 10% fetal bovine serum (FBS; from ATCC) and 1% penicillin/streptomycin (from ATCC) at 37 °C with 5% CO_2. The J774A.1 cells were cultured in DMEM (catalog # 30-2002, ATCC, Manassas, VA), which was also supplemented with FBS and antibiotics and grown at 37 °C with 5% CO_2.

Instrumentation for fungal assays with yeast were the V-1200 spectrophotometer (VWR, Radnor, PA, USA) and the SpectraMax M5 plate reader (Molecular Devices, Sunnyvale, CA, USA) for biofilm, cytotoxicity, and hemolysis assays. For the whole cell uptake assay, Inductively Coupled Plasma Optical Emission Spectroscopy (ICP-OES, Agilent, Santa Clara, CA, USA). The known antifungal drugs, amphotericin B (AmB, VWR, Chicago, IL, USA), caspofungin (CFG, Sigma-Aldrich, St. Louis, MO, USA), fluconazole (FLC, AK Scientific, Union City, CA, USA), voriconazole (VRC, AK Scientific, Union City, CA, USA), and the antirheumatic drug, auranofin (Santa Cruz Biotechnology, Dallas, TX, USA) were used as positive controls.

3.5.2.2. Determination of minimum inhibitory concentration (MIC) values of compounds 1-6

The individual minimum inhibitory concentration (MIC) values of compounds **1-6** were measured for each fungal strain. The MIC values were determined using the broth microdilution method[305] in sterile 96-well plates. Concentrations of compound tested were

0.06-31.3 μg/mL. For testing, compounds were dissolved in DMSO at a concentration of 5 mg/mL allowing the highest concentration of DMSO to be 0.63% in the assay. Serial two-fold dilutions of compound were made horizontally across the plate in 100 μL of RPMI 1640 medium. For yeast, the overnight culture was diluted into RPMI 1640 (25 μL of a fungal stock with OD_{600} of 0.12-0.15 into 10 mL of RPMI 1640 medium, resulting in final inoculum size around 1-5×10^3 CFU/mL) and added to the plate (100 μL per well), making a final volume of 200 μL total per well. Similarly, for *Aspergillus* spp. and *F. graminearum* 053, spores were diluted in RPMI 1640 to 5×10^5 spores/mL then 100 μL of stock was seeded in each well.[370] The MIC-0 value of each compound was determined by visual inspection, MIC-2 values were measured *via* optical density reading at 600 nm. For *Candida* spp., plates were incubated for 48 h at 35 °C, for *Cryptococcus* spp. and *Aspergillus* spp. were incubated for 72 h at 35 °C, and *F. graminearum* 053 was incubated at room temperature for 5 days. MIC values for CFG were read at 24 h (Tables 3.1 and 3.2).

3.5.2.3. Time-kill assays for compounds 4 and 6

To assess the time-dependent inhibition of compounds **4** and **6** against four yeast strains, *C. albicans* ATCC 10231 (strain *B*), *C. glabrata* ATCC 2001 (strain *H*), *C. auris* AR Bank # 0384 (strain *K*), and *C. auris* AR Bank # 0390 (strain *L*) we performed time-kill assays. The protocol for time-kill assays followed methods previously described with minor modifications.[256, 308] Overnight cultures were grown in YEPD medium at 35 °C with shaking at 200 rpm. The overnight cultures were diluted in RPMI 1640 medium to an OD_{600} of 0.125 (~1×10^6 CFU/mL). Then, 200 μL of cells were added to 4.8 mL of RPMI 1640

medium in sterile culture tubes to afford a fungal cell concentration ~1×10^5 CFU/mL. Compounds were then added to the fungal cells. The treatment conditions included sterile control (negative control), growth control, compound **4** at 1× MIC, **4** at 2× MIC, **6** at 1× MIC, **6** at 2× MIC, as well as AmB at 1× MIC as a positive control. Treated fungal cultures were incubated in the culture tubes at 35 °C with 200 rpm shaking for 24 h. Samples were aliquoted from the different treatments at regular time points (0, 3, 6, 9, 12, and 24 h) and plated in duplicate onto PDA plates. For each time point, cultures were vortexed, 100 μL of culture was aspirated, and 10-fold serial dilutions were made in sterile ddH_2O. From the appropriate dilutions, 100 μL of fungal suspension was spread on agar plates and incubated at 35 °C for 48 h before colony counts were determined. Only plates containing between 30 and 300 colonies were counted, making 30 CFU/mL the limit of detection. At 24 h, 50 μL of sterile 2 mM resazurin in phosphate buffered saline (PBS) was added to the treatments and incubated at 35 °C with 200 rpm shaking for 2 h in the dark for visual inspection. As resazurin (blue-purple) is metabolized by the cells to produce resorufin (pink-orange), the addition of resazurin is used as a qualitative measure to confirm the relative growth of the fungal cells in the different treatment conditions (Fig. 3.4).

3.5.2.4. Prevention of biofilm formation and disruption of pre-formed biofilm assays for compounds 4 and 6

To evaluate the ability of the gold complexes to prevent formation of biofilms and also their ability to disrupt pre-formed biofilms, we conducted assays for compounds **4** and **6** against sessile yeast cells for four representative yeast strains, *C. albicans* ATCC 10231 (strain *B*), *C. glabrata* ATCC 2001 (stain *H*), *C. auris* AR Bank # 0384 (strain *K*), and *C.*

auris AR Bank # 0390 (strain *L*). All biofilm assays were performed in 96-well plates using XTT [2,3-bis(2-methoxy-4-nitro-5-sulfophenyl)-2H-tetrazolium-5-carboxanilide] to measure the viability of the biofilm as previously described.[309, 371] An overnight culture of yeast was grown at 35 °C in YEPD medium with shaking at 200 rpm before dilution in RPMI 1640 medium to an OD_{600} between 0.12 and 0.15. For biofilm prevention assays, serial dilutions of compounds were made in 100 μL of RPMI as in the MIC assays and 100 μL of fungal suspension with OD_{600} of 0.12-0.15 was added. For assays with a pre-formed biofilm, 100 μL of fungal cells were aliquoted in a 96-well plate, leaving one column empty for the sterile control. After 24 h incubation at 37 °C, visible biofilms had formed in the well. The biofilm was washed three times with 100 μL of PBS. After washing, RPMI 1640 medium and compound were added to the plate, in a similar fashion to that described for the MIC values. All compounds were tested in the concentration range of 0.06-31.3 μg/mL and AmB and auranofin were included as controls. Plates were incubated at 37 °C for 24 h. Finally, the plates were washed three times with PBS before adding 100 μL of XTT dye. The XTT was prepared by dissolving XTT at 0.5 mg/mL concentration in sterile PBS. Before adding to a plate, 1 μL of 10 mM menadione in acetone was added to 10 mL of the 0.5 mg/mL solution of XTT. After addition of XTT (containing menadione), the plates were incubated for 3 h at 37 °C in the dark. 80 μL of liquid from each well was transferred to a new plate and then with the plate reader for absorbance at 450 nm. For these experiments, we determined the sessile MIC ($SMIC_{90}$), which is defined as the compound concentration required to inhibit the metabolic activity of biofilm by 90% compared to the growth control (Table 3.3). The plates used to determine the $SMIC_{90}$ values are provided

in Fig. 3.5 (prevention of biofilm formation) and Fig. 3.6 (disruption of pre-formed biofilm). Each assay was performed in duplicate.

3.5.2.5. Mammalian cytotoxicity assays for compounds 4 and 6

To examine whether the compounds are safe for human cells, cytotoxicity assays were done against four mammalian cell lines: HEK-293, A549, BEAS-2B, and J774A.1 cells. Compounds **4** and **6** as well as auranofin were tested against each cell line to measure their cytotoxic effect by using a resazurin cell viability assay as previously described with minor modifications.[244, 372] The assays were done in 96-well plates and cell counts were made using a hemacytometer. HEK-293 and J774A.1 cells were plated at 1×10^4 cells/mL while A549 and BEAS-2B were plated at 3×10^3 cells/mL. Compounds were tested in concentrations ranging from 0.06 to 15.6 μg/mL with final concentration of DMSO at 0.5% (Fig. 3.7). It is important to note that testing xenobiotics at sub-IC_{50} concentrations can result in increase in cell growth, resulting in >100% cell survival in the treatment groups.[244, 311-314] In instances where >100% cell survival was observed, we displayed the data as 100% cell survival in Fig. 3.7. We are providing the data with observed % in Fig. 3.11. All assays were done in quadruplicate.

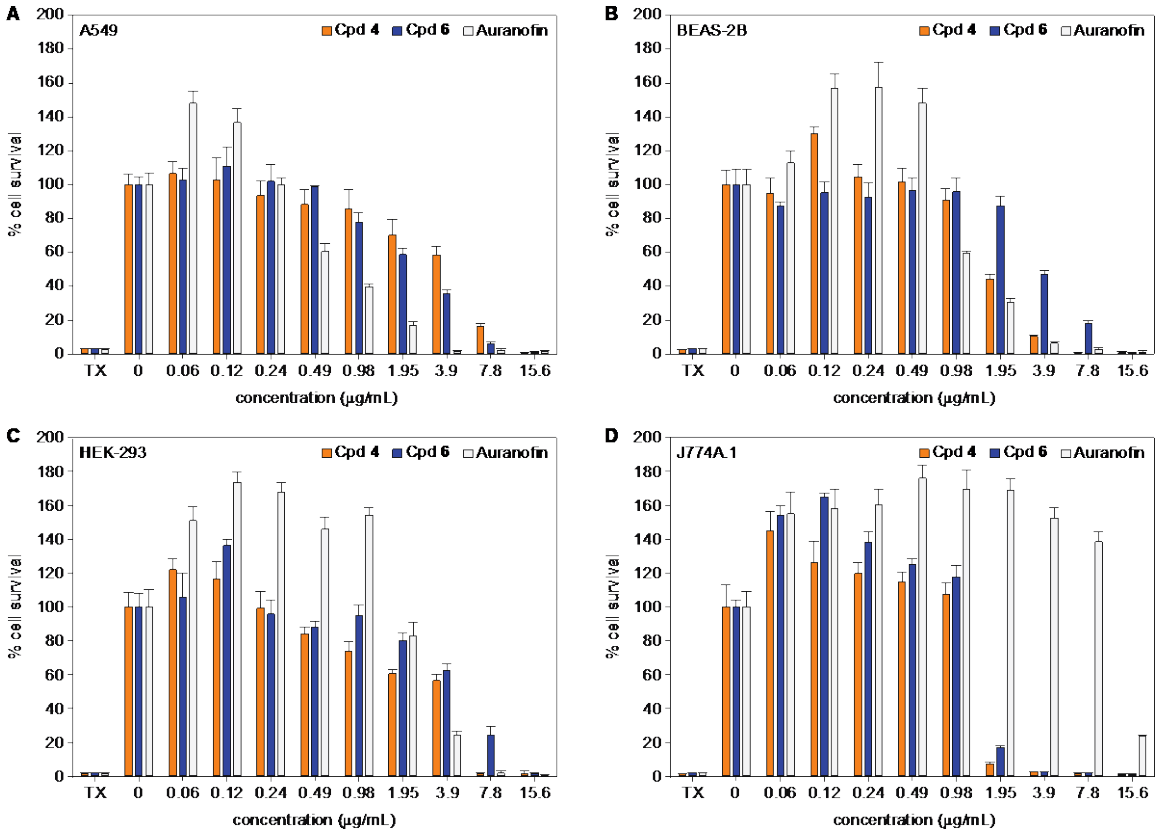

Fig. 3.11. Evaluation of cytotoxicity for compound **4** (orange), compound **6** (blue), and auranofin (white) with **A.** A549, **B.** BEAS-2B, **C.** HEK-293, and **D.** J774A.1 cell lines. Controls include treatment with Triton-X® (TX, 1% *v/v*, positive control) and 0.5% DMSO (negative control).

3.5.2.6. Measurement of hemolysis for compounds 4 and 6

To extend on the cytotoxicity results, compounds **4** and **6** along with auranofin and AmB, were tested for their ability to lyse red blood cells (RBCs). Both human and murine RBCs were provided in a citrate-treated tube on ice and the hemolysis assay was done as previously described with minor modifications and in similar fashion to cytotoxicity assays.[253, 373-374] The RBCs were washed three times in PBS by resuspending 0.5 mL of RBCs in 5 mL PBS and pelleting at 1,000 rpm for 7 min. The RBCs were resuspended in PBS to achieve a cell concentration of on the order of 10^7 cells/mL. Compounds were dissolved at concentration of 3.14 mg/mL (200×) in DMSO. Serial double dilutions were made in DMSO. A 1:100 dilution of compound in PBS was added to 100 µL of RBCs in a

96-well plate (total volume of 200 μL). Compounds were tested in the range of 0.06-15.6 μg/mL in quadruplicate with 0.5% DMSO and ~5×10^6 RBCs per tube. The RBCs were also treated with 1% Triton-X® (positive control) and PBS (negative control). The RBCs were treated for 30 min at 37 °C and the absorbance was read at 595 nm. Hemolysis is visually observed by a decrease in optical density of the wells (turbid, dark red to transparent pink). Percent hemolysis (Fig. 3.8) was calculated using this equation after subtraction of the background absorbance (positive control):

$$\% \text{ Hemolysis} = \frac{\text{absorbance of sample}}{\text{absorbance of RBC+PBS (negative control)}} \times 100$$

3.5.2.7. Whole cell uptake assay for compounds 4 and 6

To gain insight into the mechanism of action of these compounds, we measured the uptake of the gold-containing compounds into the yeast cells. Compounds **4** and **6** were each tested with *C. albicans* ATCC 10231 (strain *B*) and *C. glabrata* ATCC 2001 (strain *H*) in independent triplicates following protocols for whole cell uptake assays as previously described with minor modifications.[339, 375-376] A single colony was used to inoculate 3 mL of YEPD, which was grown overnight at 35 °C with 200 rpm shaking. Overnight culture was diluted into 100 mL of YEPD to an OD_{600} of ~0.075 and grown at 35 °C with 200 rpm shaking for 4-6 h until the culture reached an OD_{600} of ~0.3 indicating logarithmic phase growth. The cells were pelleted by centrifugation at 500 ×g for 5 min at room temperature and diluted in RPMI to 10^8 cells/mL in RPMI 1640 medium as determined by counting with a hemacytometer. 1 mL of fungal suspension was aliquoted into a 12 mL culture tube. Treatment conditions included 10 μM compound, growth control (no compound), medium

with compound (no cells), and 10 μM (8.5 μL) compound for ICP-OES analysis (100% signal). Each treatment was tested in duplicate at 35 °C with 200 rpm shaking. After 30 min of treatment, cells were pelleted by centrifugation at 3,000 rpm (~1,000 ×g) for 5 min. Cell pellets were washed twice with 1 mL of ice-cold PBS. Cell pellets were digested in 0.5 mL of concentrated HCl and added to 4.5 mL of ddH_2O (10% final concentration of HCl). Samples were analyzed for gold content using ICP-OES. Data presented (Fig. 3.9) shows values for 10μM compound after subtraction of values for media with compound.

3.5.2.8. Development of fungal resistance for compounds 4 and 6

To assess the rate at which fungal strains can develop resistance to the gold compounds, fungal cells were repeatedly exposed to sub-inhibitory amounts of compound and the MIC values for each sub-culture were monitored. The procedure for the development of resistance assay was modified for fungal cells following the reported method.[373] MIC assays were done as described above for compounds **4**, **6**, and AmB against *C. albicans* ATCC 10231 (strain *B*) and *C. glabrata* ATCC 2001 (strain *H*). Overnight cultures were inoculated from fungal cells exposed to ½ the MIC concentration for each compound. This was repeated for 15 subcultures (Fig. 3.10).

3.6. AUTHOR CONTRIBUTIONS

E.K.D. and S.G.-T. designed all the biochemical and biological studies. S.G.A. and J.H.K. designed the synthesis of compounds **1**-**6**. E.K.D. performed all biochemical and biological experiments. J.H.K. synthesized compounds **1**-**6** and characterized the compounds. S.P. solved the X-ray structures of compounds **3**-**6**. E.K.D. and S.G.-T. wrote the manuscript

and Appendix A and made all figures, with help from Dr. Nishad Thamban Chandrika in making the final figures for the NMR spectra and HPLC traces. All authors provided feedback on the manuscript and Appendix A and have given approval to the final version of the manuscript and Appendix A.

3.7. ACKNOWLEDGEMENTS

This work was supported in part by a University of Kentucky Igniting Research Collaborations pilot grant, funded by the Vice President for Research and College Deans (to S.G.-T. and S.G.A.) and startup funds from the University of Kentucky (to S.G.-T. and S.G.A.). We would also like to thank the University of Kentucky's Environmental Research Training Laboratory (ERTL) for their assistance with the ICP-OES, Prof. Sidney Whiteheart for providing the red blood cells for the hemolysis studies, and Dr. Norman Lee of the Chemical Instrumentation Center at Boston University for mass spectrometry analysis. Crystallography at the University of Kentucky is supported by NSF MRI award CHE1625732 (to S.P.).

Chapter 4

Broad-spectrum antifungal agents: Fluorinated aryl- and heteroaryl-substituted hydrazones

4.1. ABSTRACT

Fluorinated aryl- and heteroaryl-substituted monohydrazones displayed excellent broad-spectrum activity against various fungal strains, including a panel of clinically relevant *Candida auris* strains relative to a control antifungal agent, voriconazole (VRC). These monohydrazones displayed less hemolysis of murine red blood cells than that of VRC at the same concentrations, possessed fungicidal activity in a time-kill study, and exhibited no mammalian cell cytotoxicity. In addition, these monohydrazones prevented the formation of biofilms that otherwise block antibiotic effectiveness and did not trigger the development of resistance when exposed to *C. auris* AR Bank # 0390 over 15 passages.

4.2. INTRODUCTION

Nosocomial fungal infections[314, 377-380] represent continuing threats to medical advances conjoined with immunosuppression and often afflict nursing home residents or hospitalized patients undergoing transplantation,[381-384] antiviral,[385] and antineoplastic therapies.[386-387] In addition, the emergence of new strains of fungal pathogens that resist[277, 388-389] current drug therapies and possess high mortality rates compound these ongoing threats.[390-391] Appearing first in 2009 in Japan,[392] *Candida auris* represents an archetypical, fungal infection that presents challenges in terms of its diagnosis[393-394] and its treatment because some strains are resistant to the three available classes of current antifungals: the azoles

(*e.g.*, fluconazole (FLC) and voriconazole (VRC)), the echinocandins (*e.g.*, caspofungin (CFG)), and the polyenes (*e.g.*, amphotericin B (AmB)). Front-page articles in *The New York Times*[1-3, 395-397] delineate the dangers that *C. auris* represents and call for research to address this healthcare problem at a time of declining investment in antimicrobial drug development within the pharmaceutical industry.[398]

Paramount among the challenges facing investigators intent on antifungal drug development are the issues of potency, breadth of selectivity, biofilm penetration or prevention, cytotoxicity including erythrocyte hemolysis, and the development of resistance. Despite this gamut of hurdles, the complexity of fungal cell architecture offers an array of as yet, unexplored targets for drug development. Prior efforts by multiple investigators focused on antifungal agents[205, 212, 253, 390, 399] possessing chemically diverse scaffolds including aminoglycosides,[238, 241-244, 246-247] benzimidazoles,[205, 212, 400] azoles,[183-184, 338, 401-403] haloperidols,[256, 404] gold(I) complexes,[405] and ebselen/ebsulfur.[253, 406-407] We now report the development of fluorinated, diaryl- and heterodiaryl-substituted hydrazones as compounds that meet these challenges and represent a new class of potential agents for the selective treatment of candidiasis.[408-412] Of particular interest, these new agents show particular promise for the treatment of *C. auris* infections that now afflict an increasing number of patients in nursing homes and hospitals.[413-414]

We previously reported the development of bishydrazones **I** and **II** (Fig. 4.1) bearing either *N*-amidino or *N*-aryl groups, respectively, as potential antibacterial and antifungal agents.[211] Subsequent structure-activity studies revealed that alkoxy-substituted, aryl

groups attached to bishydrazones **III** with biphenyl linkers had greater potency as *in vitro* antifungal agents than as antibacterial agents, possessed minimal toxicity, and exhibited no resistance through multiple generations.[212] Further work disclosed that no particular advantage accrued to symmetrical bishydrazones relative to comparable monohydrazones in which an aryl or heteroaryl group replaced the biphenyl linker in **III**. The monohydrazones **IV** (*i.e.*, compounds **1-7** in Fig. 4.2) bearing fluorinated aryl or heteroaryl groups possessed not only the positive spectrum of drug attributes seen for the bishydrazones **III** but also surprising potency and selectivity for ten fungal strains in the *C. auris* family.

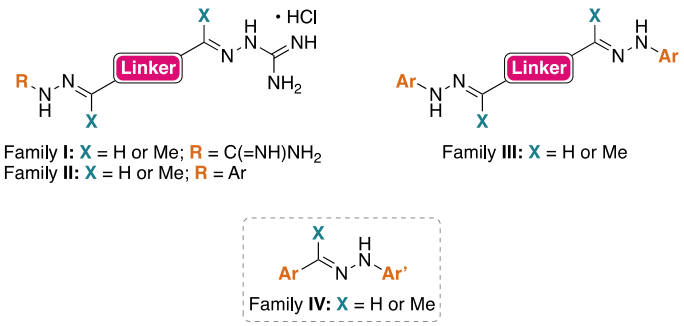

Fig. 4.1. General structures of *N*-aryl and *N*-amidino-substituted bishydrazones (families **I-III**), as well as monohydrazones (family **IV**) studies herein. The square represents the hydrocarbon platform separating these hydrazone groups in families **I-III**.

4.3. RESULTS AND DISCUSSION

4.3.1. Synthesis

The synthesis of 35 family **IV** monohydrazones in seven series (**1-7**), each comprised of six compounds with varied R_2 groups (**a-f**) entailed the condensation of either substituted aldehydes (*i.e.*, benzaldehyde, 3-fluorobenzaldehyde, 4-fluorobenzaldehyde, 4-chlorobenzaldehyde, 4-methoxybenzaldehyde, 2,4-difluorobenzaldehyde) or

acetophenone with 1-2 equivalents of substituted phenylhydrazines at 80 °C to yield **1a-7f** in 26-98% yields (Fig. 4.2).

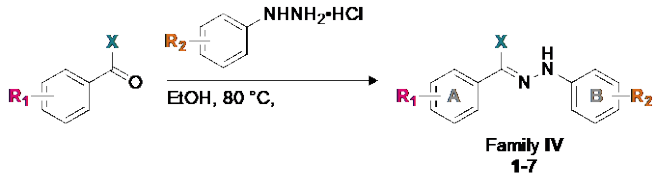

1a: R_1 = H, X = H, R_2 = H (66%)	**4c**: R_1 = *p*-Cl, X = H, R_2 = *p*-F (87%)
1b: R_1 = H, X = H, R_2 = *m*-F (x)	**4d**: R_1 = *p*-Cl, X = H, R_2 = *p*-Cl (83%)
1c: R_1 = H, X = H, R_2 = *p*-F (46%)	**4e**: R_1 = *p*-Cl, X = H, R_2 = *p*-OMe (94%)
1d: R_1 = H, X = H, R_2 = *p*-Cl (47%)	**4f**: R_1 = *p*-Cl, X = H, R_2 = *o,p*-diF (84%)
1e: R_1 = H, X = H, R_2 = *p*-OMe (62%)	**5a**: R_1 = *p*-OMe, X = H, R_2 = H (66%)
1f: R_1 = H, X = H, R_2 = *o,p*-diF (78%)	**5b**: R_1 = *p*-OMe, X = H, R_2 = *m*-F (x)
2a: R_1 = *m*-F, X = H, R_2 = H (96%)	**5c**: R_1 = *p*-OMe, X = H, R_2 = *p*-F (98%)
2b: R_1 = *m*-F, X = H, R_2 = *m*-F (92%)	**5d**: R_1 = *p*-OMe, X = H, R_2 = *p*-Cl (87%)
2c: R_1 = *m*-F, X = H, R_2 = *p*-F (88%)	**5e**: R_1 = *p*-OMe, X = H, R_2 = *p*-OMe (49%)
2d: R_1 = *m*-F, X = H, R_2 = *p*-Cl (82%)	**5f**: R_1 = *p*-OMe, X = H, R_2 = *o,p*-diF (89%)
2e: R_1 = *m*-F, X = H, R_2 = *p*-OMe (96%)	**6a**: R_1 = *o,p*-diF, X = H, R_2 = H (94%)
2f: R_1 = *m*-F, X = H, R_2 = *o,p*-diF (94%)	**6b**: R_1 = *o,p*-diF, X = H, R_2 = *m*-F (95%)
3a: R_1 = *p*-F, X = H, R_2 = H (84%)	**6c**: R_1 = *o,p*-diF, X = H, R_2 = *p*-F (91%)
3b: R_1 = *p*-F, X = H, R_2 = *m*-F (x)	**6d**: R_1 = *o,p*-diF, X = H, R_2 = *p*-Cl (82%)
3c: R_1 = *p*-F, X = H, R_2 = *p*-F (91%)	**6e**: R_1 = *o,p*-diF, X = H, R_2 = *p*-OMe (x)
3d: R_1 = *p*-F, X = H, R_2 = *p*-Cl (81%)	**6f**: R_1 = *o,p*-diF, X = H, R_2 = *o,p*-diF (97%)
3e: R_1 = *p*-F, X = H, R_2 = *p*-OMe (x)	**6g**: R_1 = *o,p*-diF, X = H, R_2 = *o,m*-diF (96%)
3f: R_1 = *p*-F, X = H, R_2 = *o,p*-diF (98%)	**6h**: R_1 = *o,p*-diF, X = H, R_2 = *m,m*-diF (95%)
4a: R_1 = *p*-Cl, X = H, R_2 = H (79%)	**7a**: R_1 = H, X = Me, R_2 = H (26%)
4b: R_1 = *p*-Cl, X = H, R_2 = *m*-F (89%)	**7f**: R_1 = H, X = Me, R_2 = *o,p*-diF (77%)

Fig. 4.2. Synthetic scheme for the preparation of compounds **1a-7f** in family **IV**.

4.3.2. Antifungal activity by determination of minimum inhibitory concentration (MIC) values

To provide comparable data for monohydrazones in family **IV** relative to their previously reported counterparts, namely the bishydrazones in family **III**, we first tested the 35 monohydrazones **1a-7f** against a panel of seven strains (*A*-*G*) of *Candida albicans*: ATCC 10231(R) (*A*), ATCC 64124(R) (*B*), ATCC MYA-2876(S) (*C*), ATCC 90819(R) (*D*), ATCC MYA-2310(S) (*E*), ATCC MYA-1237(R) (*F*), and ATCC MYA-1003(R) (*G*) (Table 4.1). We also explored their activity against a panel of three non-*albicans Candida* strains: *Candida glabrata* ATCC 2001 (*H*), *Candida krusei* ATCC 6258 (*I*), and *Candida parapsilosis* ATCC 22019 (*J*) (Table 4.1). Throughout this study, we employed a range of concentrations varying from 0.03 to 31.3 μg/mL for monohydrazones **1a-7f**, as well as for

the commercially available, positive antifungal controls, amphotericin B (AmB), caspofungin (CFG), fluconazole (FLC), and voriconazole (VRC). In Table 4.1, MIC-0 values (*i.e.*, no visible growth) were reported for monohydrazones **1a-7f** and for the positive controls AmB and CFG, and MIC-2 values (*i.e.*, 50% growth inhibition) were reported for FLC and VRC against all fungal strains tested. Herein, we defined antifungal activity as excellent (≤1.95 μg/mL), good (3.9-7.8 μg/mL), or poor (≥15.6 μg/mL) based on MIC values, and we utilized a color scheme (excellent, green; good, yellow; and poor, pink) to provide an overall visual picture of the performance of individual monohydrazones *versus* positive controls.

Table 4.1. MIC values (μg/mL) determined for compounds **1a-7a** as well as the antifungal controls AmB, CFG, FLC, and VRC against seven *Candida albicans* strains (*A-G*) and three non-*albicans Candida* strains (*H-J*). The LogP values calculated in ChemDraw and Molinspiration are also provided.

Cpd #	**LogP value**		**Strain**									
	ChemDraw	Molinspiration	*A*	*B*	*C*	*D*	*E*	*F*	*G*	*H*	*I*	*J*
1a	3.42	4.76	0.49	7.8	3.9	3.9	7.8	7.8	1.95	15.6	0.98	7.8
1c	3.58	4.93	0.49	7.8	3.9	7.8	31.3	7.8	1.95	15.6	1.95	7.8
1d	3.98	5.44	0.98	3.9	3.9	7.8	15.6	1.95	1.95	3.9	0.98	7.8
1e	3.29	4.82	0.98	3.9	3.9	7.8	15.6	3.9	1.95	3.9	1.95	31.3
1f	3.73	5.02	0.49	3.9	7.8	7.8	3.9	1.95	3.9	3.9	0.49	7.8
2a	3.58	4.90	0.98	7.8	7.8	7.8	15.6	7.8	3.9	15.6	3.9	7.8
2b	3.73	5.04	0.49	0.98	1.95	3.9	1.95	15.6	1.95	3.9	1.95	3.9
2c	3.73	5.07	0.06	7.8	0.98	15.6	3.9	3.9	15.6	7.8	3.9	7.8
2d	4.13	5.58	1.95	3.9	3.9	3.9	0.98	3.9	1.95	1.95	3.9	3.9
2e	3.45	4.96	1.95	7.8	3.9	7.8	1.95	3.9	1.95	15.6	0.12	31.3
2f	3.89	5.16	0.24	15.6	3.9	7.8	7.8	15.6	0.98	7.8	0.98	7.8
3a	3.58	4.93	0.24	1.95	1.95	1.95	0.98	1.95	0.98	3.9	0.24	3.9
3c	3.73	5.09	0.12	7.8	1.95	15.6	7.8	3.9	15.6	15.6	3.9	7.8
3d	4.13	5.61	7.8	7.8	1.95	7.8	15.6	7.8	1.95	3.9	1.95	31.3
3f	3.89	5.18	0.12	1.95	3.9	1.95	15.6	1.95	0.98	3.9	0.49	7.8
4a	3.98	5.44	0.98	7.8	3.9	15.6	31.3	7.8	1.95	>31.3	1.95	15.6
4b	4.13	5.58	0.49	7.8	1.95	7.8	3.9	7.8	1.95	15.6	0.49	7.8
4c	4.13	5.61	0.49	7.8	3.9	31.3	7.8	7.8	1.95	15.6	15.6	7.8
4d	4.53	6.12	3.9	3.9	7.8	15.6	31.3	7.8	3.9	7.8	7.8	31.3
4e	3.85	5.50	0.98	15.6	15.6	15.6	7.8	7.8	15.6	7.8	7.8	31.3
4f	4.29	5.70	0.98	7.8	7.8	15.6	31.3	7.8	3.9	15.6	0.98	15.6
5a	3.29	4.82	0.98	>31.3	>31.3	15.6	>31.3	>31.3	>31.3	>31.3	>31.3	>31.3
5c	3.45	4.98	0.98	1.95	1.95	3.9	0.98	1.95	0.98	3.9	0.24	3.9
5d	3.85	5.50	0.12	3.9	3.9	1.95	15.6	7.8	1.95	1.95	0.49	7.8
5e	3.16	4.88	15.6	7.8	3.9	15.6	15.6	3.9	3.9	31.3	3.9	>31.3
5f	3.61	5.08	0.49	0.24	3.9	0.98	3.9	0.98	0.49	1.95	0.24	1.95
6a	3.73	5.02	0.98	7.8	3.9	3.9	7.8	7.8	3.9	15.6	0.98	7.8
6b	3.89	5.16	0.98	0.98	7.8	15.6	0.98	7.8	0.49	3.9	0.12	7.8
6c	3.89	5.18	0.24	15.6	1.95	15.6	7.8	7.8	0.98	15.6	1.95	15.6
6d	4.29	5.70	0.49	1.95	0.98	15.6	1.95	3.9	0.98	1.95	1.95	7.8
6f	4.05	5.27	0.98	7.8	3.9	3.9	7.8	7.8	1.95	7.8	0.98	7.8
6g	4.05	5.27	0.12	31.3	1.95	15.6	7.8	15.6	31.3	31.3	1.95	7.8
6h	4.05	5.27	0.06	15.6	0.98	15.6	3.9	3.9	7.8	7.8	0.98	3.9
7a	2.98	5.21	7.8	>31.3	>31.3	>31.3	31.3	>31.3	1.95	31.3	15.6	>31.3
7f	3.3	5.46	0.24	0.49	0.98	>31.3	0.98	7.8	0.49	31.3	0.98	3.9
AmB[a]			3.9	3.9	1.95	0.98	1.95	3.9	3.9	1.95	3.9	1.95
CFG[a]			0.98	0.24	0.06	0.12	0.12	0.24	0.49	0.06	0.49	1.95
FLC[a]			62.5	>125	15.6	>125	>125	62.5	62.5	>31.3	>31.3	1.95
VRC[a]			0.24	3.9	1.95	1.95	0.98	7.8	1.95	0.06	0.12	0.03

Strains: *A* = *C. albicans* ATCC 10231, *B* = *C. albicans* ATCC 64124, *C* = *C. albicans* ATCC MYA-2876(S), *D* = *C. albicans* ATCC 90819(R), *E* = *C. albicans* ATCC MYA-2310(S), *F* = *C. albicans* ATCC MYA-1237(R), *G* = *C. albicans* ATCC MYA-1003(R), *H* = *C. glabrata* ATCC 2001, *I* = *C. krusei* ATCC 6258, and *J* = *C. parapsilosis* ATCC 22019. NOTE: Here, the (S) and (R) indicate that ATCC reports these strains to be susceptible (S) and resistant (R) to itraconazole (ITC) and FLC. Known antifungal agents: AmB = amphotericin B, CFG = caspofungin, FLC = fluconazole, and VRC = voriconazole. MIC-0 values are reported for compounds **1a-7f**, AmB, and CFG; and MIC-2 values are reported for azoles. Compounds were tested in duplicate.

[a] These values were previously reported in ref [247], and are here for comparison purpose.

MIC ≤1.95 μg/mL (excellent antifungal activity)

MIC = 3.9-7.8 μg/mL (good antifungal activity)

MIC ≥15.6 μg/mL (poor antifungal activity)

From a quick glance at the data reported in Table 4.1, we observed that compounds **5a** and **7a** generally displayed poor activity against the ten strains (*A-J*) tested, and we excluded them from additional biological studies besides additional MIC values determination. The 33 remaining monohydrazones synthesized displayed excellent to good activity against

these ten fungal strains. A detailed analysis of the seven series (*i.e.*, series **1-7**) led to the following conclusions. Monohydrazones **1a-1f** with no substituents in the benzylidine portion of the monohydrazones (*i.e.*, R_1 = H; Fig. 4.2) displayed excellent to good activity against strains *A-J* (0.49-7.8 μg/mL) with the exception of compounds **1a** (MIC = 15.6 μg/mL against *H*), **1c** (MIC ≥15.6 μg/mL against *E* and *H*), **1d** (MIC = 15.6 μg/mL against *E*), and **1e** (MIC ≥15.6 μg/mL against *E* and *J*). Monohydrazones **2a-2f** with *meta*-fluorobenzylidene structures (*i.e.*, R_1 = *m*-F; Fig. 4.2) displayed excellent to good activity (0.06-7.8 μg/mL) against all fungal strains tested with exception of compounds **2a**, **2b**, **2c**, **2e**, and **2f** against strains *E* and *H* (15.6 μg/mL), strain *F* (15.6 μg/mL), strains *D* and *G* (15.6 μg/mL), strains *H* and *J* (15.6 and 31.3 μg/mL), and strains *B* and *F* (15.6 μg/mL), respectively. Monohydrazones **3a**, **3c**, **3d**, and **3f** with *para*-fluorobenzylidene structures (*i.e.*, R_1 = *p*-F; Fig. 4.2) displayed excellent to good activity against strains *A-J* (0.12-7.8 μg/mL), but compounds **3c**, **3d**, and **3f** displayed poor activity (15.6-31.3 μg/mL) against strains (*D*, *G*, and *H*), strains (*E* and *J*), and strain *E*, respectively. In the case of monohydrazones **4a-4f** with *para*-chlorobenzylidene structures (*i.e.*, R_1 = *p*-Cl; Fig. 4.2), these compounds displayed excellent to good activity against strains *A-C*, *F*, *G*, and *I* (0.49-7.8 μg/mL) with the exception of compounds **4c** and **4e**, which displayed poor activity against strains *I*, and strains *B*, *C*, and *G,* respectively. In the case of monohydrazones **5a-5f** with *para*-methoxybenzylidene structures (*i.e.*, R_1 = *p*-OMe; Fig. 4.2), compounds **5c**, **5d**, and **5f** exhibited excellent to good activity (0.24-7.8 μg/mL) against the whole panel of 10 fungal strains tested, with the exception of compound **5d** against strain *E* (15.6 μg/mL). Compound **5e** displayed good activty against strains *B*, *C*, *F*, *G*, and *I* (3.9-7.8 μg/mL). In the case of monohydrazones **6a-6h** with *ortho,para*-difluorobenzylidene

structures (*i.e.*, R_1 = *o,p*-diF; Fig. 4.2) compounds **6a**, **6b**, **6d**, **6f**, and **6h** exhibited excellent to good activity (0.06-7.8 μg/mL) against strains *A-J* with the exception of compounds **6a**, **6b**, **6d**, and **6h** against strain *H* (15.6 μg/mL), strain *D* (15.6 μg/mL), strain *D* (15.6 μg/mL), and strains (*B* and *D*) (15.6 μg/mL), respectively. Compounds **6c** and **6g** exhibited excellent to good activity against strains (*A*, *C*, *E-G*, and *I*) (0.24-7.8 μg/mL) and strains (*A*, *C*, *E*, *I*, and *J*) (0.12-7.8 μg/mL), respectively. Finally, monohydrazone **7f** with a 1-phenylethylidene structure (*i.e.*, R_1 = H; Fig. 4.2) displayed excellent to good activity (0.24-7.8 μg/mL) against strains *A-C*, *E-G*, *I*, and *J*. In summary, perhaps best grasped from the green and yellow colors in Table 4.1, a comparison with the FDA-approved antifungal agents, AmB, CFG, FLC, and VRC with some of these monohydrazones revealed that monohydrazones exhibited comparable or superior activity against strains *A*, *B*, *F*, *G*, and *I*.

We next explored the activity of representatives monohydrazones (*i.e.*, **1a**, **1c**, **1d**, **1e**, **1f**, **2b**, **2d**, **2f**, **4c**, **4d**, **5e**, **6b**, and **7a**) against three *Aspergillus* strains: *Aspergillus flavus* ATCC MYA-3631 (*K*), *Aspergillus nidulans* ATCC 38163 (*L*), and *Aspergillus terreus* ATCC MYA-3633 (*M*) (Table 4.2). We found all of the representative monohydrazones tested to be generally inactive as antifungal agents against *Aspergillus* strains. As a result, we decided against testing the remaining 22 compounds against these three *Aspergillus* strains. From all of the observations made on compounds **1a-7f**, we concluded that compounds **1d**, **2b**, **2d**, **2e**, **3a**, **3f**, **4b**, **5c**, **5d**, **5f**, **6b**, **6c, 6d**, and **7f** displayed better overall activity. It is important to point out that these compounds maintained better activity against the FLC-resistant *C. albicans* strain.

Table 4.2. MIC values (μg/mL) determined for compounds **1a-7a** as well as the antifungal controls AmB, CFG, FLC, and VRC against three *Aspergillus* spp.

	Filamentous fungi		
Cpd #	*K*	*L*	*M*
1a	>31.3	7.8	>31.3
1c	>31.3	7.8	>31.3
1d	>31.3	31.3	>31.3
1e	>31.3	31.3	>31.3
1f	>31.3	31.3	>31.3
2b	>31.3	7.8	>31.3
2d	>31.3	15.6	>31.3
2f	>31.3	7.8	>31.3
4c	>31.3	7.8	>31.3
4d	>31.3	>31.3	>31.3
5e	>31.3	>31.3	>31.3
6b	>31.3	>31.3	>31.3
7a	>31.3	>31.3	>31.3
AmB[a]	15.6	15.6	3.9
CFG[a]	>31.3	>31.3	>31.3
FLC[a]	62.5	62.5	62.5
VRC[a]	0.24	0.12	0.12

Strains: *K* = *A. flavus* ATCC MYA-3631, *L* = *A. nidulans* ATCC 38163, and *M* = *A. terreus* ATCC MYA-3633. Known antifungal agents: AmB = amphotericin B, CFG = caspofungin, FLC = fluconazole, and VRC = voriconazole. MIC-0 values are reported for compounds **1a-7f** as well as AmB and CFG, whereas MIC-2 values are reported for azoles. Compounds were tested in duplicate.

[a] These values were previously reported in ref [247], and are here for comparison purpose.

MIC ≤1.95 μg/mL (excellent antifungal activity)

MIC = 3.9-7.8 μg/mL (good antifungal activity)

MIC ≥15.6 μg/mL (poor antifungal activity)

Based on the promising antifungal activities observed in Table 4.1, we selected seven of the best compounds (*i.e.*, **2b**, **3f**, **4b**, **5f**, **6b**, **6d**, and **7f**) and two of the worse (*i.e.*, **5a** and **7a** as negative controls) for further testing against a panel of ten *C. auris* strains (AR Bank # 0381-0390) and ten other fungal strains including three *Candida duobushaemulonii* strains (AR Bank # 0391, AR Bank # 0392, and AR Bank # 0394), two *Candida haemulonii* strains (AR Bank # 0393, and AR Bank # 0395), two *Saccharomyces cerevisiae* strains (AR Bank # 0399 and AR Bank # 0400), and one each of the following strains: *Kodameae ohmeri* (AR Bank # 0396), *Candida krusei* (AR Bank # 0397), and *Candida lusitaniae* (AR Bank # 0398) (Table 4.3). Using a concentration range of 0.015-31.3 μg/mL for the nine selected monohydrazones and using AmB, CFG, FLC, and VRC as positive controls, we obtaind MIC-0 values (*i.e.*, no visible growth) for the monohydrazones and the control AmB, and the MIC-2 values (*i.e.*, 50% growth inhibition) for CFG, FLC and VRC.

Monohydrazones **2b**, **3f**, **4b**, **5f**, **6d**, and **7f** displayed excellent to good activity against (0.015-7.8 μg/mL) all 20 strains tested. Compound **6b** exhibited excellent to good activity (0.24-7.8 μg/mL) against most of the strains tested, with the exception of strains AR Bank # 0383-0385, AR Bank # 0387, AR Bank # 0389, AR Bank # 0399, and AR Bank # 0400 (15.6-31.3 μg/mL). As expected based on their poor activity against *C. albicans*, compounds **5a** and **7a** displayed poor activity against the ten *C. auris* strains tested. However, compound **5a** displayed excellent to good activity (0.12-7.8 μg/mL) against *C. duobushaemulonii*, *C. haemulonii*, *S. cerevisiae*, *K. ohmeri*, *C. krusei*, and *C. lusitaniae*. On the other hand, compound **7a** only displayed excellent activity (0.49-0.98 μg/mL) against strains AR Bank # 0393, AR Bank # 0395, and AR Bank # 0397. Overall, as shown in Table 4.3, the most active monohydrazones, namely **2b**, **3f**, **4b**, **5f**, **6b**, **6d**, and **7f**, displayed excellent activity against a panel of ten *C. auris* (AR Bank # 0381-0390) and ten other fungal strains (AR Bank # 0391-0400). Excluding the *C. auris* strains, monohydrazones **5a** and **7a** showed promise against other *K. ohmeri* and other *Candida* strains.

Table 4. 3. MIC values (µg/mL) determined for compounds **1a-7a** as well as the antifungal controls AmB, CFG, FLC, and VRC against ten *Candida auris* strains (AR Bank # 0381-0390) and ten other fungal strains (AR Bank # 391-0400).

Strain	**AR #**	**Cpd #**									**Controls**			
		2b	**3f**	**4b**	**5a**	**5f**	**6b**	**6d**	**7a**	**7f**	AmB	CFG	FLC	VRC
C. auris	0381	0.49	0.24	0.24	31.3	0.24	3.9	0.98	31.3	0.24	0.98	≤0.06	0.49	0.06
	0382	0.12	0.24	0.24	3.9	0.49	1.95	0.98	31.3	0.49	1.95	≤0.06	0.49	0.06
	0383	0.49	1.95	0.49	31.3	0.98	15.6	1.95	>31.3	7.8	3.9	≤0.06	62.6	1.95
	0384	3.9	3.9	1.95	>31.3	3.9	15.6	3.9	>31.3	7.8	1.95	0.12	31.3	0.24
	0385	0.49	0.49	0.49	>31.3	0.98	15.6	0.98	>31.3	0.98	3.9	≤0.06	62.6	1.95
	0386	0.24	0.24	0.24	7.8	0.24	1.95	0.24	31.3	0.49	0.98	≤0.06	>62.6	3.9
	0387	0.12	0.12	0.12	31.3	0.12	15.6	0.49	31.3	0.12	1.95	≤0.06	>62.6	3.9
	0388	0.12	0.12	0.12	15.6	0.12	7.8	0.49	>31.3	0.12	1.95	≤0.06	0.98	0.06
	0389	0.12	0.12	0.12	15.6	0.24	15.6	0.98	>31.3	≤0.06	0.98	≤0.06	>62.6	0.49
	0390	0.98	1.95	0.98	15.6	1.95	7.8	7.8	>31.3	1.95	1.95	≤0.06	>62.6	0.98
C. duobushaemulonii	0391	0.12	0.12	0.12	0.98	0.12	0.98	0.12	3.9	0.12	0.98	0.06	>62.6	>31.3
C. duobushaemulonii	0392	0.49	1.95	0.49	0.24	0.06	0.49	0.24	7.8	>3.9	3.9	0.06	62.6	>31.3
C. haemulonii	0393	0.24	0.24	0.49	0.24	0.24	0.98	0.12	0.98	0.24	1.95	0.12	>62.6	31.3
C. duobushaemulonii	0394	0.12	0.12	0.12	3.9	0.98	7.8	0.12	31.3	0.49	0.98	0.06	62.6	>31.3
C. haemulonii	0395	0.12	0.12	0.12	0.12	0.12	0.24	0.24	0.49	0.12	3.9	0.12	>62.6	3.9
K. ohmeri	0396	0.49	0.49	0.98	0.24	0.49	0.98	0.98	3.9	0.98	1.95	0.12	7.8	0.06
C. krusei	0397	0.015	0.03	0.015	0.12	0.03	0.24	0.06	0.49	0.015	0.49	0.12	>62.6	3.9
C. lusitaniae	0398	1.95	3.9	1.95	1.95	0.98	3.9	0.98	31.3	3.9	3.9	0.12	1.95	0.06
S. cerevisiae	0399	1.95	3.9	1.95	7.8	0.98	31.3	0.98	31.3	3.9	1.95	0.12	1.95	0.24
S. cerevisiae	0400	1.95	1.95	1.95	3.9	0.98	15.6	0.98	15.6	1.95	1.95	0.24	3.9	0.12

Known antifungal agents: AmB = amphotericin B, CFG = caspofungin, FLC = fluconazole, and VRC = voriconazole. MIC-0 values are reported for compounds **1a-7f** as well as AmB. MIC-2 values are reported for CFG at 24 h and for the azoles, FLC and VRC, at 48 h. Compounds were tested in duplicate.

MIC ≤1.95 µg/mL (excellent antifungal activity)
MIC = 3.9-7.8 µg/mL (good antifungal activity)
MIC ≥15.6 µg/mL (poor antifungal activity)

4.3.3. Structure-activity relationship (SAR) analysis

The substitution pattern and identity of the substituent(s) in rings A (R_1) and B (R_2) had a considerable influence on the activity of these monohydrazones. When investigating the effect of the R_2 substituent while keeping R_1 constant (*i.e.*, comparing the monohydrazones within each series), we observed that when R_1 = H (series **1**, Fig. 4.2), the introduction of either *o*,*p*-diF (**1f**), *p*-Cl (**1d**), or H (**1a**) as R_2 substituents resulted in better antifungal activity than other substituents (*i.e.*, *m*-F, *p*-F and *p*-OMe). For series **2** (R_1 = *m*-F), compounds **2b**, **2d**, and **2e** that displayed excellent activity had *m*-F, *p*-Cl, and *p*-OMe as R_2 substituents. In addition, when the R_1 groups = *p*-F, *p*-Cl, or *p*-OMe (series **3**, series **4**, or series **5**, Fig. 4.2), the most active monohydrazones in each series (*i.e.*, (**3a**, **3f**, and **3d**), (**4b**, **4a**, and **4c**), and (**5f**, **5c**, and **5d**)) possessed (H, *o*,*p*-diF, and *p*-Cl), (*m*-F, H, and *p*-F), and (*o*,*p*-diF, *m*-F, and *p*-Cl) as R_2 substituents, respectively. In series **6** (R_1 = *o*,*p*-diF), the R_2 substituents *p*-Cl (**6d**), *m*-F (**6b**), and *o*,*p*-diF (**6f**) resulted in better activity than the

activity observed with other substituents (*i.e.*, H, *p*-F, *p*-OMe, *o,m*-diF, and *m,m*-diF). In general, we observed that in each series (**1-6**), the majority of the most active monohydrazones had either *p*-Cl (**d**) and/or *o,p*-diF (**f**) as R_2 substituents.

When looking at the effect of the R_1 substituent while keeping R_2 constant (*i.e.*, comparing **1a-6a**, **1b-6b**, etc.), we found that the monohydrazones displaying the best antifungal activity generally did not have the same R_1 substituents. In the case of compounds with R_2 = H (**1a**, **2a**, **3a**, **4a**, **5a**, and **6a**), the most active compounds **3a**, **1a**, and **6a** had *p*-F, H, and *o,p*-diF as R_1 substituents. For monohydrazones with R_2 = *m*-F (**b**), the introduction of *m*-F and *o,p*-diF as R_1 substituents resulted in compounds **2b** and **6b** with better overall antifungal activity than those with other substitution patterns. The most active compounds in the case of monohydrazones with R_2 = *p*-F, compounds **5c**, **6c**, and **1c** possessed *p*-OMe, *o,p*-diF, and H as R_1 substituents. When R_2 group = *p*-Cl, the most active compounds **6d**, **5d**, and **2d** possessed *o,p*-diF, *p*-OMe, and *m*-F as R_1 substituents. In addition, for compounds with R_2 = *p*-OMe or *o,p*-diF the most active monohydrazones had *m*-F or H (**2e** and **1e**), and *p*-OMe, *p*-F, and *o,p*-diF (**5f**, **3f**, and **6f**) as R_1 substituents. Overall, we observed that most of the monohydrazones with the best antifungal activity with diverse R_2 groups were from series **6** with R_1 = *o,p*-diF with the sole exception of the monohydrazone with R_2 = *p*-OMe (**6e**).

Since the monohydrazones with *o,p*-diF groups as either R_1 or R_2 substituent displayed broad-spectrum activity against the fungal strains tested, we explored the effect of R_2 = *o,m*-diF and *m,m*-diF substituents on antifungal activity. The monohydrazones **6g** (R_1 =

o,*p*-diF, R_2 = *o*,*m*-diF) and **6h** (R_1 = *o*,*p*-diF, R_2 = *m*,*m*-diF) were compared to **6f** (R_1 = *o*,*p*-diF, R_2 = *o*,*p*-diF). In both cases, the introduction of *o*,*m*-diF and *m*,*m*-diF as R_2 substituents led to a decrease in activity profile against the whole panel of fungal strains compared to the *o,p*-diF analogue **6f**. Next, we explored the effect of regioisomers by comparing series **2** (R_1 = *m*-F) with series **3** (R_1 = *p*-F). We observed that the compounds **3a** (R_1 = *p*-F, R_2 = H) and **3f** (R_1 = *p*-F, R_2 = *o*,*p*-diF) performed better than their counterparts **2a** (R_1 = *m*-F, R_2 = H) and **2f** (R_1 = *m*-F, R_2 = *o*,*p*-diF), whereas compounds **2c** (R_1 = *m*-F, R_2 = *p*-F) and **2d** (R_1 = *m*-F, R_2 = *p*-Cl) displayed better activity compared to **3c** (R_1 = *p*-F, R_2 = *p*-F) and **3d** (R_1 = *p*-F, R_2 = *p*-Cl). From the data reported above, we were unable to point to the superiority of one regioisomeric series over another. We then evaluated the impact of the specific halogen on antifungal activity by comparing series **3** and series **4** (*p*-F *vs* *p*-Cl). Compounds **3a** (R_1 = *p*-F, R_2 = H), **3d** (R_1 = *p*-F, R_2 = *p*-Cl), and **3f** (R_1 = *p*-F, R_2 = *o*,*p*-diF) exhibited better broad-spectrum activity against various strains than their corresponding counterparts **4a** (R_1 = *p*-Cl, R_2 = H), **4d** (R_1 = *p*-Cl, R_2 = *p*-Cl), and **4f** (R_1 = *p*-Cl, R_2 = *o*,*p*-diF). In this case, monohydrazones where R_1 = *p*-F performed significantly better their counterparts where R_1 = *p*-Cl. Finally, we explored the effect of a methyl group (where X = Me) on the monohydrazone activity by comparing **7a** with **1a** and **1f** with **7f**. The addition of a methyl group in compound **1a** (where X = H) resulted in compound **7a** (where X = Me) with decreased antifungal activity against all the strains tested. In contrast, when we compared **1f** with **7f**, the addition of methyl group resulted in a considerable increase in antifungal activity. Overall, compounds **3a**, **5f**, **6d**, **5c**, **2b**, **3f**, **7f**, **6b**, **5d**, **1d**, **2d**, **2e**, **4b**, and **6c** displayed the broadest spectrum of activity based on their MIC values.

4.3.4. Hemolysis assay

Potency and SAR development are only one facet of antimicrobial drug development. Since the monohydrazones displayed potency and broad-spectrum antifungal activity, it was additionally important to establish that these agents showed selectivity for fungal cells over mammalian cells. Thus, we investigated the hemolytic activity for the most promising monohydrazones **2b**, **3f**, **4b**, **5f**, **6d**, and **7f**, as well as controls AmB and VRC against murine red blood cells (mRBCs) (Fig. 4.3 and Table 4.4). Monohydrazones **3f** and **6d** displayed <10% and <68% hemolysis at concentrations of 31.3 μg/mL which are 2- to 1043-fold higher than their overall MIC values. Monohydrazones **2b** and **5f** displayed lower hemolysis levels (<9% at 15.6 μg/mL) than those observed for **7f** (<21% at 15.6 μg/mL). These hemolysis values for **2b**, **5f**, and **7f** were again 1- to 1040-fold higher than the overall MIC values reported for these compounds. Finally, monohydrazone **4b** displayed <62% at 15.6 μg/mL (1- to 1040-fold of its overall MIC values). Overall, the monohydrazones **2b**, **3f**, **5f**, **6d**, and **7f** displayed little to no hemolysis of mRBCs at either concentrations either 15.6 or 31.3 μg/mL that lie well above their MIC values.

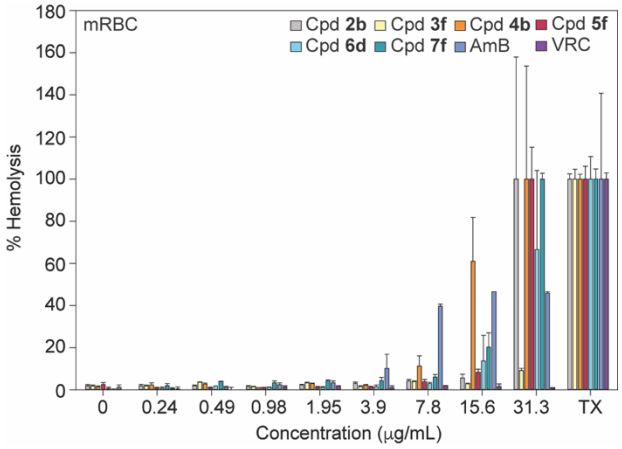

Fig. 4.3. 2D bar graph normalized at 100% depicting the dose-dependent hemolytic activity of monohydrazones **2b**, **3f**, **4b**, **5f**, **6d**, **7f**, as well as AmB and VRC against mRBCs. mRBCs were treated and

incubated for 1 h at 37 °C with monohydrazones, AmB, and VRC at concentrations ranging from 0.24 to 31.3 μg/mL. Triton X-100® (TX) (1% *v/v*) was used as a positive control (100% hemolysis). Compounds were tested in quadruplicate. *Note*: The corresponding non-normalized data are presented in Fig. 4.9.

Table 4.4. Percentage of hemolysis caused by compounds **2b**, **3f**, **4b**, **5f**, **6d**, and **7f**, as well as controls AmB and VRC against murine red blood cells (mRBCs) with the error bars (± SDEV).

Cpd #	**Concentration (μg/mL)**									
	TX	**0**	**0.24**	**0.49**	**0.98**	**1.95**	**3.9**	**7.8**	**15.6**	**31.3**
2b	100 ± 3	2.1 ± 0.3	1.9 ± 0.7	1.9 ± 0.3	1.5 ± 0.4	2.2 ± 0.4	3.0 ± 0.7	4.1 ± 0.7	5.6 ± 2	120 ± 60
3f	100 ± 5	3.5 ± 0.4	1.9 ± 0.4	3.6 ± 0.1	1.5 ± 0.2	3.2 ± 0.4	1.6 ± 0.3	3.9 ± 0.3	2.8 ± 0.3	9.1 ± 1
4b	100 ± 2	2.9 ± 0.6	2.4 ± 0.9	2.7 ± 0.5	1.0 ± 0.1	2.9 ± 0.3	2.1 ± 0.3	11 ± 5	61 ± 20	210 ± 50
5f	100 ± 6	0.85 ± 0.5	0.97 ± 0.2	0.93 ± 0.3	1.1 ± 0.2	1.3 ± 0.3	1.4 ± 0.2	3.8 ± 1	8.3 ± 1	110 ± 20
6d	100 ± 10	1.3 ± 0.3	0.78 ± 0.6	1.8 ± 0.0	1.2 ± 0.1	1.2 ± 0.2	1.5 ± 0.9	2.9 ± 0.6	13.7 ± 10	67 ± 40
7f	100 ± 5	3.0 ± 0.5	1.9 ± 1	3.9 ± 0.2	3.3 ± 1	4.2 ± 0.4	4.4 ± 1	6.0 ± 1	20 ± 7	100 ± 3
AmB	100 ± 5	1.2 ± 0.4	0.93 ± 0.6	2.0 ± 0.8	4.0 ± 1	5.5 ± 2	17 ± 1	67 ± 2	79 ± 0.1	78 ± 1
VRC	100 ± 3	-1.2 ± 0.4	0.46 ± 0.9	0.23 ± 1	1.4 ± 0.5	1.7 ± 0.1	1.0 ± 0.8	1.8 ± 0.2	1.6 ± 1	0.83 ± 0.3

Note: Compounds tested in quadruplicate.

4.3.5. Cytotoxicity

It was also important to consider the toxicity of these monohydrazones towards mammalian cell lines. The toxicity profile of compounds **2b**, **3f**, **4b**, **5f**, **6d**, and **7f**, as well as controls AmB and VRC (within a concentration range of 0.12-31.3 μg/mL) was investigated against three mammalian cell lines A549, J774A.1, and HEK-293 (Fig. 4.4). When tested against all three mammalian cell lines at 31.3 μg/mL, none of the monohydrazones tested displayed toxicity (with the exception of **4b** against J774A.1, which displayed 86% cell survival at that concentration). The excellent MIC values of these monohydrazones combined with the fact that none of them exhibited toxicity to mammalian cell lines at the highest concentration provided still further evidence that these agents warranted additional biological evaluation.

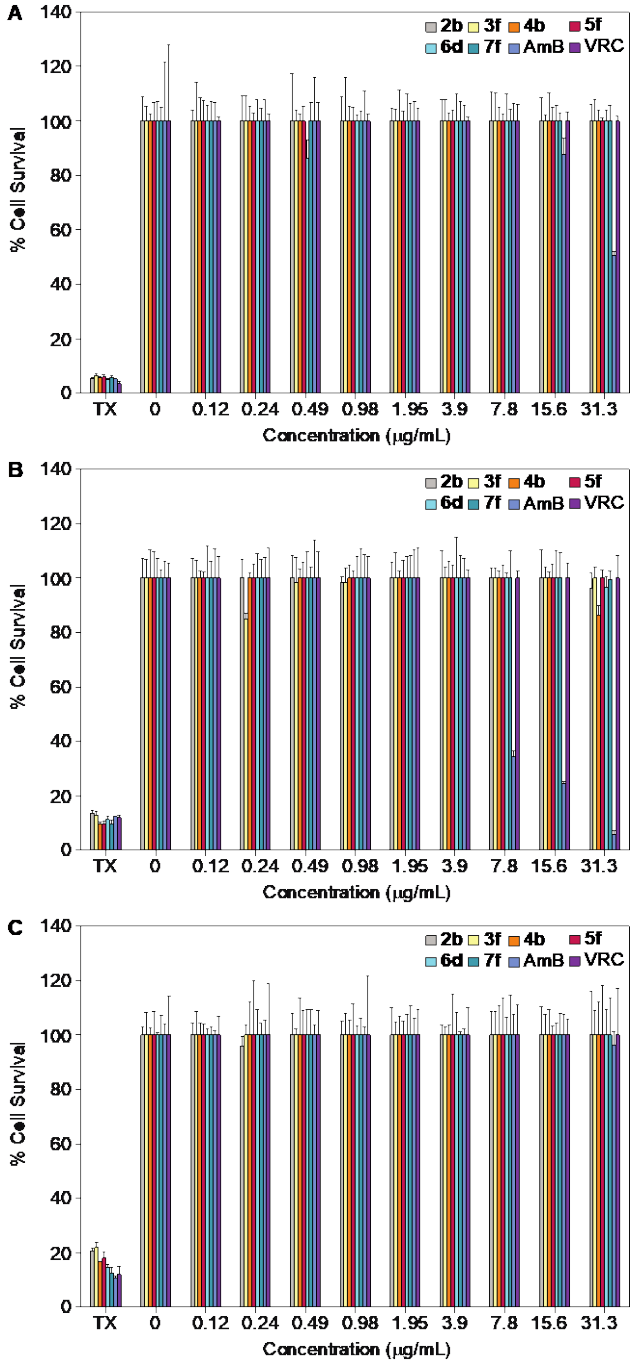

Fig. 4.4. 2D bar graph normalized at 100% depicting the dose-dependent cytotoxic activity of monohydrazones **2b**, **3f**, **4b**, **5f**, **6d**, **7f**, as well as AmB and VRC against **A.** A549, **B.** J774A.1, and **C.** HEK-293 cell lines. *Note*: For Triton X-100® (TX) the eight bars are colored differently which corresponds to colors of the respective compounds for which TX was used as a positive control. Compounds were tested in quadruplicate. *Note*: The corresponding non-normalized data are presented in Fig. 4.10.

4.3.6. Time-kill studies

A time-kill kinetics assay was used to determine whether the monohydrazones are fungistatic and simply inhibit growth, or are fungicidal and kill the fungal cells. Compounds **2b, 3f, 4b, 5f, 6d,** and **7f** were tested at ½×, 1×, and 4× MIC against *C. albicans* ATCC 10231 (strain *A*) to observe the dose-dependent effect and also to account for any normal variations in MIC values (Figs. 4.5 and 4.6). In addition, AmB at 1× MIC and VRC at 1× MIC-0 against *C. albicans* ATCC (strain *A*) were also evaluated for comparison purposes. Fungicidal activity is defined as at least a three $\log_{10}$-fold decrease in colony forming units (CFU), and this level of decrease is observed with the monohydrazones at the 1× MIC concentration for compound **2b** at the ½× concentration, compounds **2b**, **4f**, and **5f** at the 1× concentration, and all tested at the 4× concentration. CFU counts were confirmed by adding the metabolic dye resazurin at the 24 h time point and observing the amount of color change over the following two days where no growth is indicated by a blue color (Fig. 4.6, panel A). By 72 h, only four sample tubes with *C. albicans* remain blue and these samples include **2b** at 4×, **5f** at 1× and 4×, and **7f** at 4×. A screen with the resazurin was performed with *C. auris* AR Bank # 0384 and # 0390 (Fig. 4.6, panels B and C). Except for compound **6d**, which had growth at 72 h at the 1× concentration, all monohydrazones at 1× and 4× concentrations inhibited *C. auris* growth up to 72 h. The fungicidal activity at and above MICs shows the potential of the monohydrazones to clear, not just halt, a fungal infection.

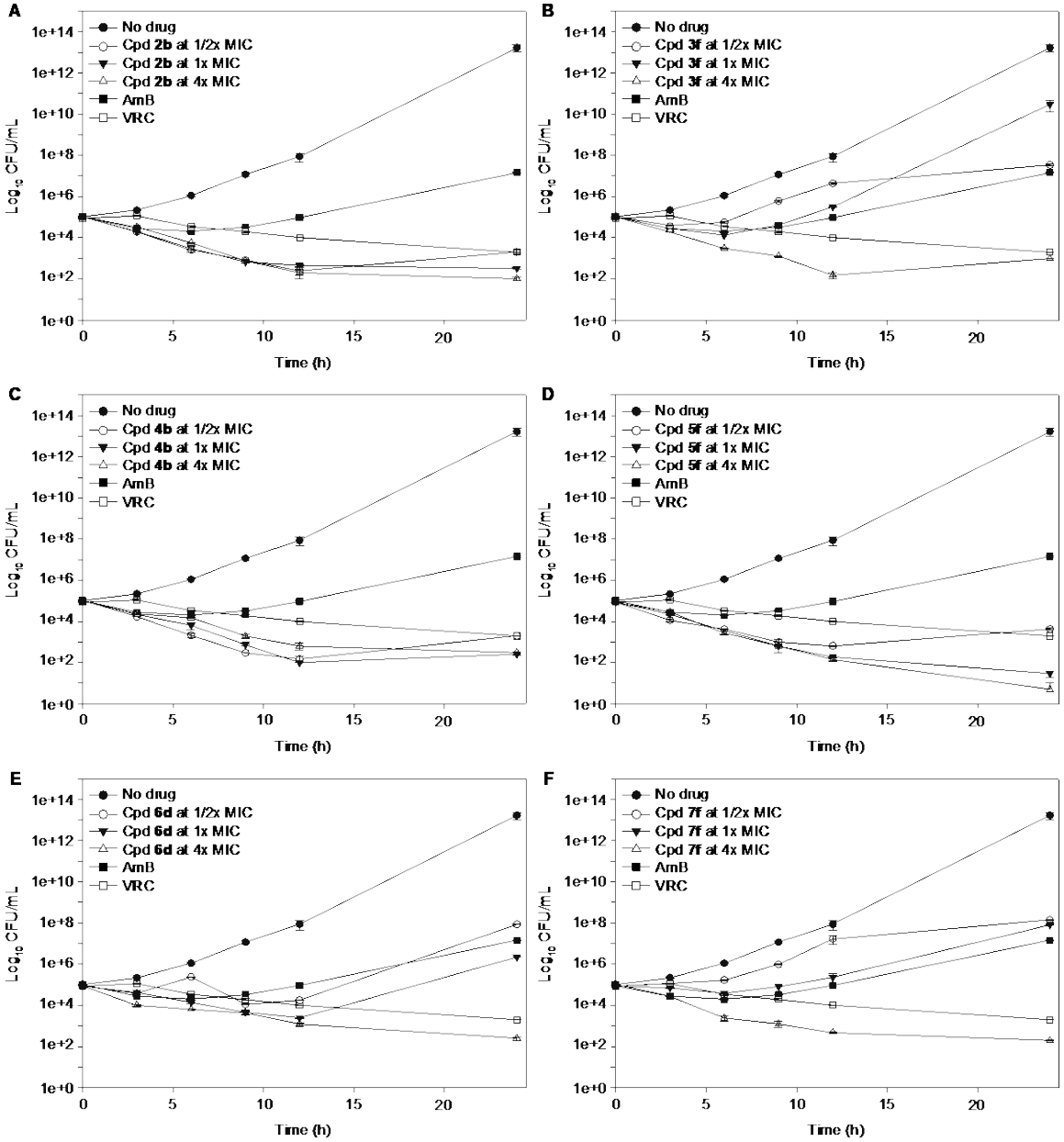

Fig. 4.5. Time-killing kinetics for compounds **A. 2b**, **B. 3f**, **C. 4b**, **D. 5f**, **E. 6d**, and **F. 7f** at ½×, 1×, and 4× MIC as well as AmB 1× MIC and VRC at 1× MIC-0 against *C. albicans* ATCC (strain *A*). To confirm CFU counts, the metabolic dye, resazurin, was added at 24 h. Time-points samples were plated in duplicate.

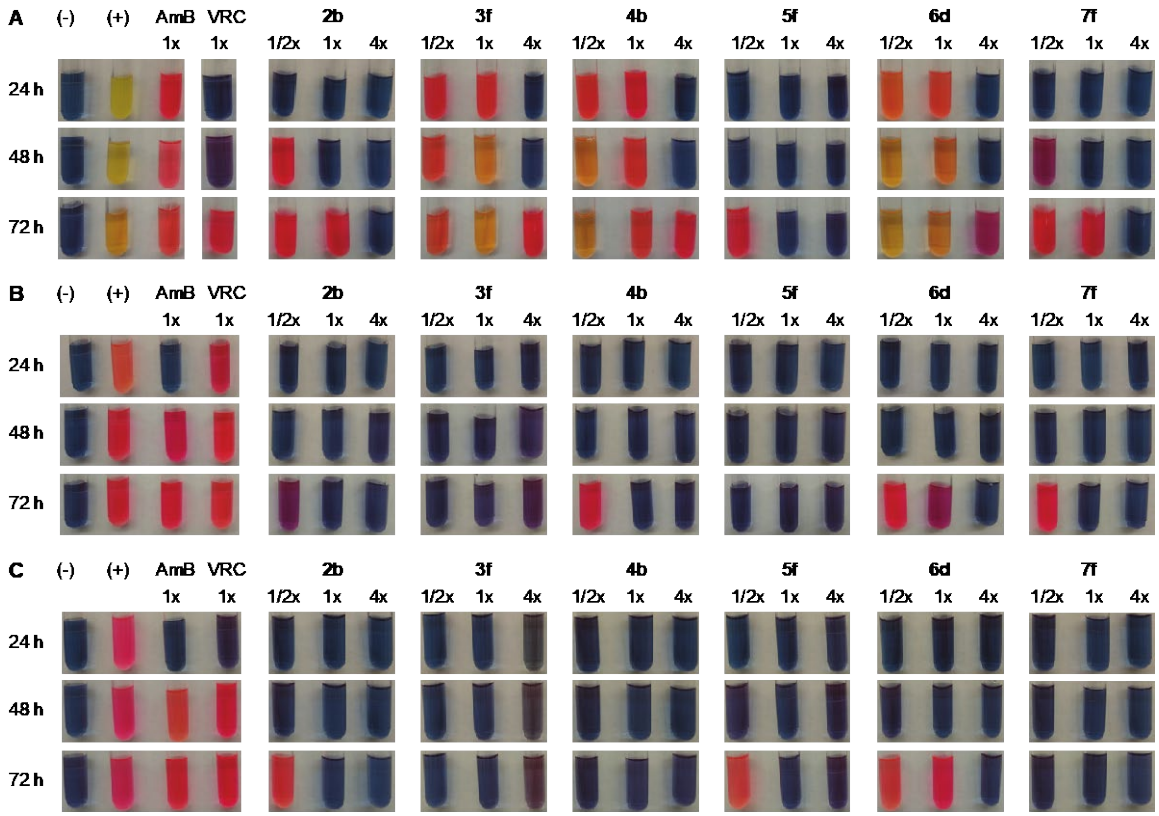

Fig. 4.6. Sample tubes for monohydrazones **2b**, **3f**, **4b**, **5f**, **6d**, and **7f** at ½×, 1×, and 4× MICs, as well as AmB and VRC at ½×, 1× MIC-0 after the addition of resazurin at 24 h, 48 h, and 72 h (relative to the treatment start time) against **A.** *C. albicans* ATCC 10231 (strain *A*), **B.** *C. auris* AR Bank # 0384, and **C.** *C. auris* AR Bank # 0390. Resazurin (blue) is metabolized by the yeast and color change is relative to CFU counts (blue < purple < red < pink < orange < yellow) *Note*: The corresponding kinetic data for *C. albicans* ATCC (strain *A*) are presented in Fig. 4.5.

4.3.7. Antibiofilm activity

Fungal biofilms[390] are a protective mechanism that allow fungal cells to survive harsh conditions including those that may exist within the human body. These biofilms commonly occur, for example, on medical devices such as catheters. Once biofilms are formed, it is significantly more difficult to eliminate the fungal cells than in their absence. The ability of compounds **2b**, **3f**, **4b**, **5f**, **6d**, and **7f**, as well as controls AmB and VRC were assessed against *C. albicans* ATCC 10231 (strain *A*), *C. auris* AR Bank # 0384, and

C. auris AR Bank # 0390 in two biofilm studies: (i) prevention of biofilm formation and (ii) destruction of pre-formed biofilms.

Prevention of biofilm formation. A large fungal load was exposed to the monohydrazones at time 0 h to evaluate the ability of the compounds to prevent *Candida* biofilm formation (Table 4.5, Fig. 4.7). We determined the sessile MIC (SMIC) for 50% and 90% inhibition of biofilm formation as compared to the no drug control. Monohydrazones **2b** and **4b** displayed excellent activity similar to VRC with $SMIC_{50}$ values of 1.95 μg/mL against *C. albicans* ATCC 10231 (strain *A*, which is 4-fold greater than the MIC. Monohydrazones **5f** and **6d** also had good activity against *C. albicans* with $SMIC_{50}$ of 7.8 and 3.9 μg/mL, respectively, and **7f** also had some activity as well. Two monohydrazones, **4b** and **7f**, displayed good activity against one *C. auris* strain, *C. auris* AR Bank # 0384, with $SMIC_{50}$ values of 7.8 μg/mL. Monohydrazones **2b**, **5f**, and **6d** also displayed poor activity against *C. auris* AR Bank # 0384 while compounds **4b**, **5f**, **6d**, and **7f** displayed poor activity against *C. auris* AR Bank # 0390 with $SMIC_{50}$ values of 15.6 μg/mL. Monohydrazones **4b** and **6d** were the most promising as they display $SMIC_{90}$ values of 7.8 μg/mL against *C. albicans* (16-fold greater than MIC) and 15.6-31.3 μg/mL against the *C. auris* strains which is 4- to 16-fold greater than their MIC values against the same strains.

Table 4.5. $SMIC_{50}$ and $SMIC_{90}$ values (μg/mL) for prevention of biofilm formation determined for compounds **2b**, **3f**, **4b**, **5f**, **6d**, **7f** as well as the antifungal controls AmB and VRC against three fungal strains.

		$SMIC_{50}$ (μg/mL)							
Strain		**2b**	**3f**	**4b**	**5f**	**6d**	**7f**	AmB	VRC
C. albicans ATCC 10231 (*A*)	$SMIC_{50}$	1.95	31.3	1.95	7.8	3.9	15.6	0.12	1.95
	$SMIC_{90}$	31.3	>31.3	7.8	31.3	7.8	15.6	0.98	3.9
C. auris AR Bank # 0384	$SMIC_{50}$	15.6	31.3	7.8	15.6	15.6	7.8	1.95	3.9
	$SMIC_{90}$	31.3	>31.3	15.6	31.3	15.6	15.6	7.8	>31.3
C. auris AR Bank # 0390	$SMIC_{50}$	31.3	>31.3	15.6	15.6	15.6	15.6	1.95	1.95
	$SMIC_{90}$	31.3	>31.3	15.6	31.3	31.3	31.3	3.9	15.6

Note: Compounds were tested in duplicate.

MIC ≤1.95 μg/mL (excellent antifungal activity)

MIC = 3.9-7.8 μg/mL (good antifungal activity)

MIC ≥15.6 μg/μL (poor antifungal activity)

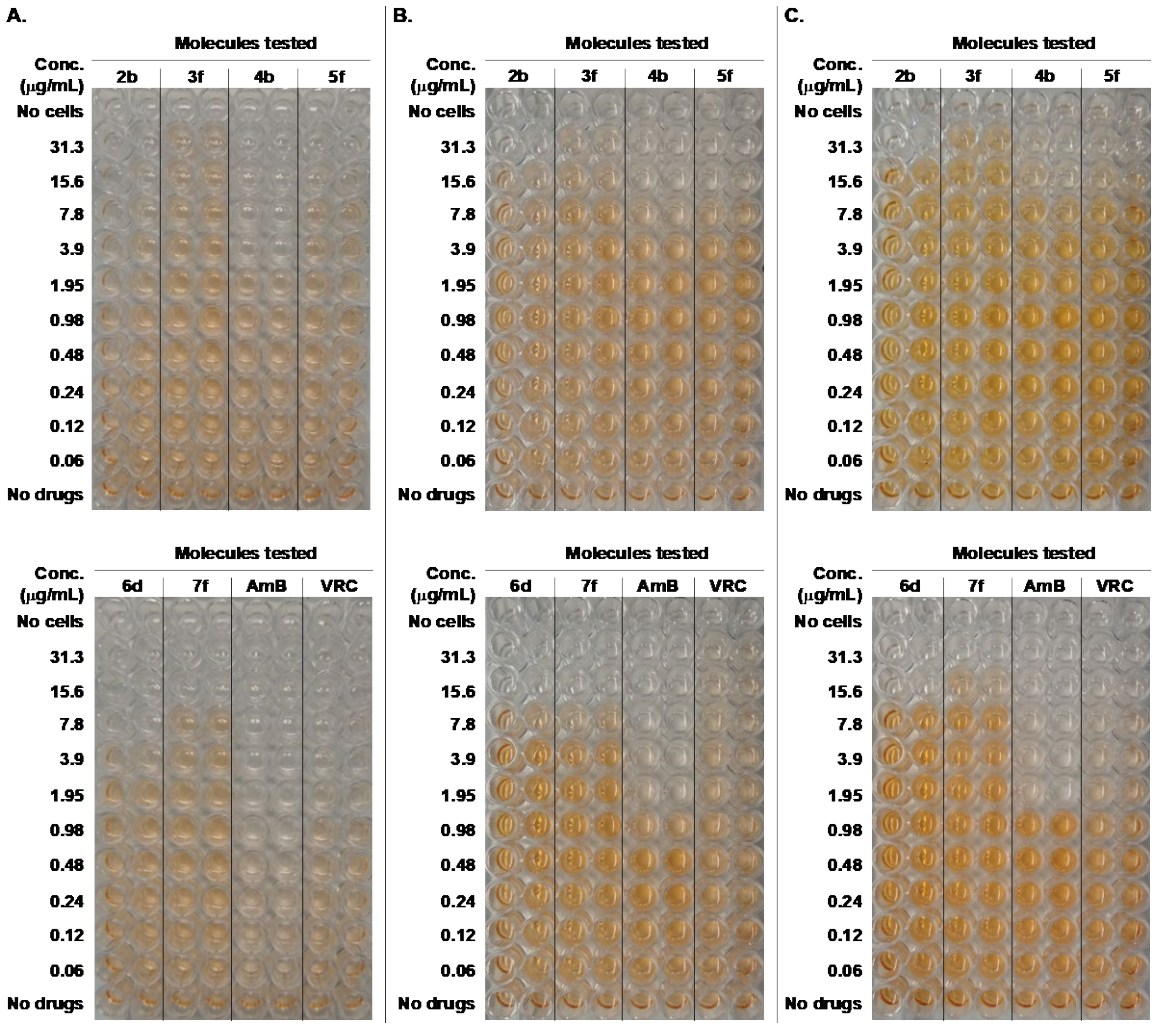

Fig. 4.7. Prevention of biofilm formation of **A.** *C. albicans* ATCC 10231 (strain *A*), **B.** *C. auris* AR Bank # 0384, and **C.** *C. auris* AR Bank # 0390 treated at 0 h with **2b**, **3f**, **4b**, **5f**, **6d**, **7f**, AmB, and VRC. XTT dye is metabolized by fungal cells to produce an orange color. Compounds were tested in duplicate. The corresponding data are presented in Table 4.5.

Destruction of pre-formed biofilms. Although the monohydrazones were able to prevent biofilm formation, we also evaluated their ability to destroy a pre-formed biofilm (treatment after 24 h) (Table 4.6). Overcoming the problem of a biofilm presents is challenging, and reflecting this challenge, we report $SMIC_{50}$ values because no monohydrazones were able to decrease biofilm activity by 90%. Against *C. albicans* ATCC 10231 (strain *A*), compounds **4b** and **7f** display $SMIC_{50}$ values of 31.3 μg/mL, which matched the value for VRC. Against both *C. auris* strains, compounds **2b**, **4b**, and **6d** displayed $SMIC_{50}$ values of 15.6-31.3 μg/mL, which were better than VRC. Overall, compounds **4b** and **6d** performed the best against biofilms. In both the *prevention of biofilm formation* and *destruction of a pre-formed biofilm* assays, the monohydrazones appear to have similar activity to VRC, but very little activity compared to AmB.

Table 4.6. $SMIC_{50}$ values (μg/mL) for destruction of a pre-formed biofilm determined for compounds **2b**, **3f**, **4b**, **5f**, **6d**, **7f** as well as the antifungal controls AmB and VRC against three fungal strains.

	$SMIC_{50}$ (μg/mL)							
Strain	**2b**	**3f**	**4b**	**5f**	**6d**	**7f**	AmB	VRC
C. albicans ATCC 10231 (*A*)	>31.3	>31.3	31.3	>31.3	>31.3	31.3	0.24	31.3
C. auris AR Bank # 0384	15.6	>31.3	31.3	>31.3	15.6	>31.3	0.98	>31.3
C. auris AR Bank # 0390	31.3	>31.3	15.6	>31.3	15.6	>31.3	1.95	>31.3

Note: Compounds were tested in duplicate.

MIC ≤1.95 μg/mL (excellent antifungal activity)

MIC ≥15.6 μg/μL (poor antifungal activity)

4.3.8. Resistance development

To evaluate the potential of fungi to develop resistance to the monohydrazones, we repeatedly exposed *C. auris* AR Bank # 0390 to the monohydrazones at ½× MIC to simulate fungal drug exposure in a clinical setting (Fig. 4.8). Compounds **2b**, **3f**, **4b**, **5f**, and **6d**, as well as controls AmB were investigated. Compound **7f** was not included due to degradation of the compound when kept in solution. While normal variations in MIC values occurred, no significant changes in MIC values were observed as the MIC values

remained within 8-fold of the original MIC value. Considering the generally long duration of treatment with antifungal drugs, this is a promising result that suggests that a fungal strain is not likely to develop resistance to the monohydrazones, even after repeated exposures.

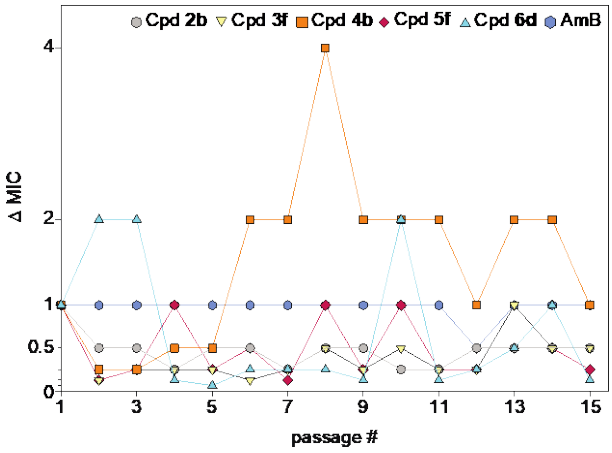

Fig. 4.8. Graph illustrating fold changes in MIC values (Δ MIC) over fifteen serial passages for monohydrazones **2b**, **3f**, **4b**, **5f**, **6d**, as well as AmB against *C. auris* AR Bank # 0390. *Note*: starting MIC values were 0.24, 0.49, 0.49, 0.49, 1.95, and 0.98 μg/mL, respectively. MICs were done in duplicate.

4.4. CONCLUSIONS

In summary, we developed a synthesis of substituted monohydrazones **1a-7f**, and performed a detailed study of antifungal activity of the compounds **1a-7f** against a panel of seven strains of *C. albicans* and three strains of non-*albicans Candida*. Commercially available antifungal agents, AmB, CFG, FLC, and VRC were used as positive controls. This SAR studies identified compounds **3a**, **5f**, **6d**, **5c**, **2b**, **3f**, **7f**, **6b**, **5d**, **1d**, **2d**, **2e**, **4b**, and **6c** as having the broadest spectrum of activity based on their MIC values. The seven best compounds (**2b**, **3f**, **4b**, **5f**, **6b**, **6d**, and **7f**) and two of the worse (**5a** and **7a** to serve as negative controls) were further tested against a panel of ten *C. auris* and ten other fungal strains. The monohydrazones **2b**, **3f**, **4b**, **5f**, **6d**, and **7f** displayed excellent to good activity

(0.015-7.8 μg/mL) against all 20 strains tested. In comparison with the FDA-approved drug VRC, monohydrazones **2b**, **3f**, **5f**, **6d**, and **7f** displayed little to no hemolysis of mRBCs at concentrations of either 15.6 or 31.3 μg/mL. In addition, none of the monohydrazones **2b**, **3f**, **5f**, **6d**, and **7f** exhibited toxicity against three mammalian cell lines, A549, J774A.1, and HEK-293. A time-kill assay over a 24 h period using compounds **2b, 3f, 4b, 5f, 6d,** and **7f** against *C. albicans* ATCC 10231 (strain *A*) indicated the monohydrazones were fungicidal at and/or above their MIC values. Compounds **2b**, **3f**, **4b**, **5f**, **6d**, and **7f**, as well as controls AmB and VRC were assessed against *C. albicans* ATCC 10231 (strain *A*), *C. auris* AR Bank # 0384, and *C. auris* AR Bank # 0390 in two biofilm studies: (i) prevention of biofilm formation and (ii) destruction of pre-formed biofilms. The monohydrazones were able to prevent the formation of biofilm against these representative strains. When exposed to compounds **2b**, **3f**, **4b**, **5f**, and **6d** over 15 passages, *C. auris* AR Bank # 0390 developed no resistance. In conclusion, the fluorinated aryl-and heteroaryl-substituted monohydrazones reported herein display promise as a new family of antifungal agents.

4.5. EXPERIMENTAL

4.5.1. Chemistry

Materials and instrumentation. The chemicals used in this study were purchased from Sigma-Aldrich (St. Louis, MO), AK Scientific (Union City, CA), Acros Organics (New Jersey, NJ), TCI America (Portland, OR), Oakwood Chemicals (Estill, SC), Combi-Blocks (San Diego, CA), Accela Chembio (San Diego, CA), and Chem-Impex (Wood Dale, IL), and used without any further purification. Chemical reactions were monitored by TLC (Merck, Silica gel 60 F254) and visualization was achieved using UV light. Compounds

were purified by SiO_2 flash chromatography (Dynamic Adsorbents Inc., Flash SiO_2 gel 32-63μ) or by filtration of pure solids. ^1H and ^{13}C NMR spectra were recorded at 500 MHz or 400 MHz (for ^1H) and 100 MHz (for ^{13}C) on Agilent VNMRS-500 and MR-400 spectrometers, respectively, using deuterated solvents as specified. Chemical shifts (δ) are given in parts per million (ppm). Coupling constants (*J*) are given in Hertz (Hz), and conventional abbreviations used for signal shape are as follows: d, doublet; dd, doublet of doublets; ddd, doublet of doublet of doublets; dt, doublet of triplets; m, multiplet; s, singlet; t, triplet; td, triplet of doublets; tt, triplet of triplets. Liquid chromatography-mass spectrometry (LCMS) was carried out using an Agilent 1200 series Quaternary LC system equipped with a diode array detector, and Agilent EC-C18 column (100 mm × 3.0 mm, 4 μm). LCMS $[M + H]^+$ signals were consistent with the expected molecular weights for all the reported compounds. Purity of the compounds was further confirmed to be ≥95% by LCMS by using following method: Flow rate = 0.4 mL/min; λ = 254 nm; column = Agilent EC-C18, 100 mm × 3.0 mm, 4 μm; eluents: A = H_2O + 0.1% formic acid, C = MeCN + 0.1% formic acid; gradient profile: starting from 5% C, increasing from 5% to 95% C over 21 min, decreasing from 95% to 5% over 6 min. Prior to each injection, the LCMS column was equilibrated for 8 min with 5% C. We were not able to purify compounds **1b**, **3b**, **3e**, **5b**, and **6e** and therefore we did not include them in any of the biological assays performed in this study.

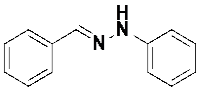

Preparation of compound 1a (SGT1288). To a solution of benzaldehyde (600 mg, 5.65 mmol) in EtOH (8 mL), phenylhydrazine (0.67 mL, 6.78 mmol) was added. The reaction mixture was stirred at 80 °C for 1 h and the

resulting solution was filtered. The residue obtained was washed with hot EtOH (15 mL) to afford compound **1a** (742 mg, 66%) as a white solid: ^{1}H NMR (400 MHz, $(CD_3)_2SO$, Fig. 4.B1 "Disclaimer: All figures are presented for Chapter 3 are presented in Appendix B and are listed as Fig. 4.B#") δ 10.32 (s, 1H), 7.86 (s, 1H), 7.64 (dd, J_1 = 8.1 Hz, J_2 = 1.1 Hz, 2H), 7.38 (t, J = 8.0 Hz, 2H), 7.28 (tt, J_1 = 7.4 Hz, J_2 = 1.2 Hz, 1H), 7.21 (dd, J_1 = 8.6 Hz, J_2 = 7.2 Hz, 2H), 7.06 (dd, J_1 = 8.6 Hz, J_2 = 1.2 Hz, 2H), 6.74 (tt, J_1 = 7.3 Hz, J_2 = 1.2 Hz, 1H); ^{13}C NMR (100 MHz, $(CD_3)_2SO$, Fig. 4.B2) δ 145.3, 136.4, 135.8, 129.1, 128.6, 127.9, 125.6, 118.7, 112.0; ; *m/z* calcd for $C_{13}H_{12}N_2$ 196.1; found 197.1 $[M+H]^+$. Purity of the compound was further confirmed by LCMS: R_t = 18.55 min (99% pure; Fig. 4.B3).

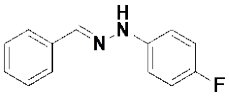

Preparation of compound 1c (SGT1289). To a solution of benzaldehyde (600 mg, 5.65 mmol) in EtOH (8 mL), 4-fluorophenylhydrazine hydrochloride (1.10 g, 6.78 mmol) was added. The reaction mixture was stirred at 80 °C for 1 h and, to the resulting solution, H_2O (15 mL) was added. The residue obtained was filtered and washed with cold EtOH (15 mL) to afford compound **1c** (562 mg, 46%) as a pink solid: ^{1}H NMR (400 MHz, $(CD_3)_2SO$, Fig. 4.B4) δ 10.31 (s, 1H), 7.85 (s, 1H), 7.66-7.61 (m, 2H), 7.38 (t, J = 7.2 Hz, 2H), 7.28 (tt, J_1 = 7.3 Hz, J_2 = 1.4 Hz, 1H), 7.06 (s, 2H), 7.05 (s, 2H); ^{13}C NMR (100 MHz, $(CD_3)_2SO$, Fig. 4.B5) δ 163.2 (d, J = 232.4 Hz), 142.0 (d, J = 1.8 Hz), 136.5, 135.7, 128.6, 127.9, 125.6, 115.6 (d, J = 22.1 Hz), 112.9 (d, J = 7.4 Hz); *m/z* calcd for $C_{13}H_{11}FN_2$ 214.1; found 215.2 $[M+H]^+$. Purity of the compound was further confirmed by LCMS: R_t = 18.72 min (96% pure; Fig. 4.B6).

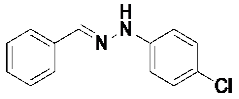

Preparation of compound 1d (SGT1280). To a solution of benzaldehyde (0.29 mL, 2.82 mmol) in EtOH (10 mL), 4-chlorophenylhydrazine hydrochloride (607 mg, 3.39 mmol) was added. The reaction mixture was stirred at 80 °C for 1 h and, to the resulting solution, H_2O (25 mL) was added. The residue obtained was filtered and dried to afford compound **1d** (307 mg, 47%) as a pink solid: ^{1}H NMR (400 MHz, $(CD_3)_2SO$, Fig. 4.B7) δ 10.46 (s, 1H), 7.87 (s, 1H), 7.67-7.62 (m, 2H), 7.42-7.36 (m, 2H), 7.30 (tt, J_1 = 7.4 Hz, J_2 = 1.2 Hz, 1H), 7.24 (d, J = 8.8 Hz, 2H), 7.06 (d, J = 8.8 Hz, 2H); ^{13}C NMR (100 MHz, $(CD_3)_2SO$, Fig. 4.B8) δ 144.2, 137.3, 135.5, 128.9, 126.6, 128.1, 125.8, 121.9, 113.4; *m/z* calcd for $C_{13}H_{11}ClN_2$ 230.1; found 231.1 $[M+H]^+$. Purity of the compound was further confirmed by LCMS: R_t = 20.08 min (96% pure; Fig. 4.B9).

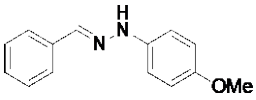

Preparation of compound 1e (SGT1281). To a solution of benzaldehyde (0.29 mL, 2.82 mmol) in EtOH (10 mL), 4-methoxyphenylhydrazine hydrochloride (592 mg, 3.39 mmol) was added. The reaction mixture was stirred at 80 °C for 1 h and, to the resulting solution, H_2O (25 mL) was added. The residue obtained was filtered and dried to afford compound **1e** (396 mg, 62%) as a pink solid: ^{1}H NMR (500 MHz, $(CD_3)_2SO$, Fig. 4.B10) δ 10.11 (s, 1H), 7.80 (s, 1H), 7.63-7.59 (m, 2H), 7.39-7.34 (m, 2H), 7.26 (tt, J_1 = 7.4 Hz, J_2 = 1.3 Hz, 1H), 7.00 (d, J = 9.0 Hz, 2H), 6.84 (d, J = 9.0 Hz, 2H), 3.69 (s, 3H); ^{13}C NMR (100 MHz, $(CD_3)_2SO$, Fig. 4.B11) δ 152.6, 139.4, 136.1, 135.2, 128.6, 127.6, 125.4, 114.6, 113.0, 55.3; *m/z* calcd for $C_{14}H_{14}N_2O$ 226.1; found 227.1 $[M+H]^+$. Purity of the compound was further confirmed by LCMS: R_t = 17.95 min (95% pure; Fig. 4.B12).

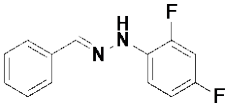

Preparation of compound 1f (SGT1279). To a solution of benzaldehyde (0.29 mL, 2.82 mmol) in EtOH (10 mL), 2,4-difluorophenylhydrazine hydrochloride (613 mg, 3.39 mmol) was added. The reaction mixture was stirred at 80 °C for 1 h and, to the resulting solution, H_2O (25 mL) was added. The residue obtained was filtered and dried to afford compound **1f** (510 mg, 78%) as a pink solid: ^{1}H NMR (400 MHz, $(CD_3)_2SO$, Fig. 4.B13) δ 10.20 (s, 1H), 8.11 (s, 1H), 7.67-7.62 (m, 2H), 7.50 (td, J_1 = 9.4 Hz, J_2 = 6.0 Hz, 1H), 7.42-7.37 (m, 2H), 7.32 (tt, J_1 = 7.2 Hz, J_2 = 1.4 Hz, 1H), 7.21 (ddd, J_1 = 11.9 Hz, J_2 = 8.9 Hz, J_3 = 2.8 Hz, 1H), 7.03-6.96 (m, 1H); ^{13}C NMR (100 MHz, $(CD_3)_2SO$, Fig. 4.B14) δ 154.7 (dd, J_1 = 235.9 Hz, J_2 = 10.8 Hz), 148.3 (dd, J_1 = 241.3 Hz, J_2 = 12.0 Hz), 139.4, 135.5, 130.5 (dd, J_1 = 9.9 Hz, J_2 = 3.0 Hz), 128.7, 128.3, 125.9, 114.1 (dd, J_1 = 8.7 Hz, J_2 = 4.6 Hz), 111.4 (dd, J_1 = 21.6 Hz, J_2 = 3.4 Hz), 103.8 (dd, J_1 = 26.8 Hz, J_2 = 22.2 Hz); *m/z* calcd for $C_{13}H_{10}F_2N_2$ 232.1; found 233.1 $[M+H]^+$. Purity of the compound was further confirmed by LCMS: R_t = 19.47 min (99% pure; Fig. 4.B15).

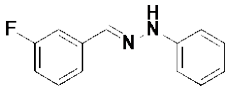

Preparation of compound 2a (SGT1296). To a solution of 3-fluorobenzaldehyde (0.21 mL, 2.08 mmol) in EtOH (10 mL), phenylhydrazine (0.24 mL, 2.50 mmol) was added. The reaction mixture was stirred at 80 °C for 1 h and, to the resulting solution, H_2O (40 mL) was added. The residue obtained was filtered and dried to afford compound **2a** (412 mg, 96%) as an off-white solid: ^{1}H NMR (500 MHz, $(CD_3)_2SO$, Fig. 4.B16) δ 10.48 (s, 1H), 7.84 (s, 1H), 7.48-7.38 (m, 3H), 7.24-7.20 (m, 2H), 7.12-7.06 (m, 3H), 6.77 (tt, J_1 = 7.3 Hz, J_2 = 1.1 Hz, 1H); ^{13}C NMR (100

MHz, $(CD_3)_2SO$, Fig. 4.B17) δ 162.6 (d, J = 241.7 Hz), 145.0, 138.5 (d, J = 8.0 Hz), 134.9 (d, J = 3.2 Hz), 130.6 (d, J = 8.5 Hz), 129.1, 121.9 (d, J = 2.6 Hz), 119.1, 114.4 (d, J = 21.4 Hz), 112.1, 111.4 (d, J = 22.4 Hz); *m/z* calcd for $C_{13}H_{11}FN_2$ 214.1; found 215.1 $[M+H]^+$. Purity of the compound was further confirmed by LCMS: R_t = 18.86 min (97% pure; Fig. 4.B18).

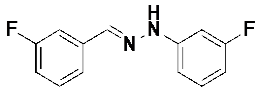

Preparation of compound 2b (SGT1374). To a solution of 3-fluorobenzaldehyde (0.21 mL, 2.01 mmol) in EtOH (12 mL), 3-fluorophenylhydrazine hydrochloride (390 mg, 2.4 mmol) was added. The reaction mixture was stirred at 90 °C for 100 min and, to the resulting solution, H_2O (50 mL) was added and stirred for 12 h. The residue obtained was filtered and dried to afford compound **2b** (429 mg, 92%) as a reddish-brown solid: ^1H NMR (500 MHz, $(CD_3)_2SO$, Fig. 4.B19) δ 10.68 (s, 1H), 7.87 (s, 1H), 7.52-7.43 (m, 2H), 7.42 (td, J_1 = 8.0 Hz, J_2 = 5.7 Hz, 1H), 7.23 (td, J_1 = 8.1 Hz, J_2 = 6.8 Hz, 1H), 7.15-7.10 (m, 1H), 6.90 (dt, J_1 = 11.7 Hz, J_2 = 2.3 Hz, 1H), 6.84 (ddd, J_1 = 8.2 Hz, J_2 = 2.1 Hz, J_3 = 0.9 Hz, 1H), 6.57-6.51 (m, 1H); ^{13}C NMR (100 MHz, $(CD_3)_2SO$, Fig. 4.B20) δ 164.2 (d, J = 80.1 Hz), 161.8 (d, J = 82.4 Hz), 147.0 (d, J = 11.0 Hz), 138.2 (d, J = 8.0 Hz), 136.2 (d, J = 3.2 Hz), 130.7 (d, J = 10.0 Hz), 130.6 (d, J = 8.4 Hz), 122.2 (d, J = 2.6 Hz), 114.8 (d, J = 21.4 Hz), 111.8 (d, J = 22.4 Hz), 108.3 (d, J = 2.2 Hz), 105.2 (d, J = 21.5 Hz), 98.7 (d, J = 26.1 Hz); *m/z* calcd for $C_{13}H_{10}F_2N_2$ 232.1; found 233.1 $[M+H]^+$. Purity of the compound was further confirmed by LCMS: R_t = 19.16 min (90% pure; Fig. 4.B21).

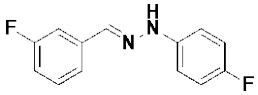

Preparation of compound 2c (SGT1386). To a solution of 3-fluorobenzaldehyde (0.09 mL, 0.81 mmol) in EtOH (8 mL), 4-fluorophenylhydrazine hydrochloride (157 mg, 0.97 mmol) was added. The reaction mixture was stirred at 90 °C for 2 h and, to the resulting solution, H_2O (50 mL) was added and stirred for 2 h. The residue obtained was filtered and dried to afford compound **2c** (166 mg, 88%) as a peach solid: ^{1}H NMR (500 MHz, $(CD_3)_2SO$, Fig. 4.B22) δ 10.49 (s, 1H), 7.82 (s, 1H), 7.48-7.43 (m, 2H), 7.39 (td, J_1 = 7.9 Hz, J_2 = 5.7 Hz, 1H), 7.12-7.09 (m, 1H), 7.07 (s, 2H), 7.06 (d, J = 1.0 Hz, 2H); ^{13}C NMR (100 MHz, CD_3OD, Fig. 4.B23) δ 164.6 (d, J = 242.5 Hz), 158.3 (d, J = 134.2 Hz), 143.2 (d, J = 2.0 Hz), 140.2 (d, J = 7.9 Hz), 136.3 (d, J = 3.3 Hz), 131.3 (d, J = 8.3 Hz), 123.0 (d, J = 2.7 Hz), 116.4 (d, J = 22.6 Hz), 115.4 (d, J = 21.9 Hz), 114.3 (d, J = 7.4 Hz), 112.5 (d, J = 22.8 Hz); *m/z* calcd for $C_{13}H_{10}F_2N_2$ 232.1; found 233.2 $[M+H]^+$. Purity of the compound was further confirmed by LCMS: R_t = 19.11 min (95% pure; Fig. 4.B24).

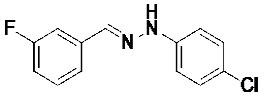

Preparation of compound 2d (SGT1375). To a solution of 3-fluorobenzaldehyde (0.21 mL, 2.01 mmol) in EtOH (12 mL), 4-chlorophenylhydrazine hydrochloride (430 mg, 2.4 mmol) was added. The reaction mixture was stirred at 90 °C for 1.5 h and, to the resulting solution, H_2O (50 mL) was added and stirred for 3 h. The residue obtained was filtered and dried to afford compound **2d** (412 mg, 82%) as a brown solid: ^{1}H NMR (500 MHz, $(CD_3)_2SO$, Fig. 4.B25) δ 10.61 (s, 1H), 7.85 (s, 1H), 7.50-7.45 (m, 2H), 7.42 (td, J_1 = 8.0 Hz, J_2 = 5.8 Hz, 1H), 7.25 (d, J = 8.9 Hz, 2H), 7.15-7.11 (m, 1H), 7.09 (d, J = 8.9 Hz, 2H); ^{13}C NMR (100 MHz, $(CD_3)_2SO$, Fig. 4.B26) δ 162.5 (d, J = 241.8 Hz), 143.9, 138.3 (d, J = 7.9 Hz), 135.7 (d, J = 3.2 Hz), 130.6

(d, J = 8.4 Hz), 128.9, 122.3, 122.0 (d, J = 2.6 Hz), 114.7 (d, J = 21.3 Hz), 113.6, 111.6 (d, J = 22.4 Hz); *m/z* calcd for $C_{13}H_{10}ClFN_2$ 248.1; found 249.0 $[M+H]^+$. Purity of the compound was further confirmed by LCMS: R_t = 20.30 min (99% pure; Fig. 4.B27).

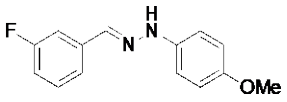

Preparation of compound 2e (SGT1399). To a solution of 3-fluorobenzaldehyde (0.09 mL, 0.81 mmol) in EtOH (8 mL), 4-methoxyphenylhydrazine hydrochloride (211 mg, 1.21 mmol) was added. The reaction mixture was stirred at 90 °C for 90 min and, to the resulting solution, H_2O (50 mL) was added and stirred for 40 min. The residue obtained was filtered and dried to afford compound **2e** (190 mg, 96%) as a pale yellow solid: ^{1}H NMR (500 MHz, $(CD_3)_2SO$, Fig. 4.B28) δ 10.30 (s, 1H), 7.78 (s, 1H), 7.45-7.37 (m, 3H), 7.10-7.04 (m, 1H), 7.03 (d, J = 8.9 Hz, 2H), 6.85 (d, J = 9.0 Hz, 2H), 3.69 (s, 3H); ^{13}C NMR (100 MHz, CD_3OD, Fig. 4.B29) δ 165.1 (d, J = 242.1 Hz), 155.5, 141.3, 141.0 (d, J = 7.9 Hz), 135.8 (d, J = 3.3 Hz), 131.7 (d, J = 8.4 Hz), 123.2 (d, J = 2.7 Hz), 116.2, 115.6 (d, J = 22.1 Hz), 115.0, 112.8 (d, J = 22.7 Hz), 56.6; *m/z* calcd for $C_{14}H_{13}FN_2O$ 244.1; found 245.1 $[M+H]^+$. Purity of the compound was further confirmed by LCMS: R_t = 18.36 min (98% pure; Fig. 4.B30).

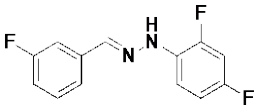

Preparation of compound 2f (SGT1373). To a solution of 3-fluorobenzaldehyde (0.21 mL, 2.01 mmol) in EtOH (12 mL), 2,4-difluorophenylhydrazine hydrochloride (433 mg, 2.4 mmol) was added. The reaction mixture was stirred at 90 °C for 70 min and, to the resulting solution, H_2O (50 mL) was added and stirred for 2 h. The residue obtained was filtered and dried to afford compound **2f** (475 mg, 94%) as a tan solid: ^{1}H NMR (500 MHz, $(CD_3)_2SO$, Fig. 4.B31) δ 10.37 (s,

1H), 8.09 (s, 1H), 7.53 (td, J_1 = 9.4 Hz, J_2 = 6.0 Hz, 1H), 7.51-7.47 (m, 1H), 7.47-7.40 (m, 2H), 7.22 (ddd, J_1 = 11.9 Hz, J_2 = 8.9 Hz, J_3 = 2.8 Hz, 1H), 7.16-7.11 (m, 1H), 7.03-6.97 (m, 1H); ^{13}C NMR (100 MHz, $(CD_3)_2SO$, Fig. 4.B32) δ 162.6 (d, J = 241.8 Hz), 154.9 (dd, J_1 = 236.1 Hz, J_2 = 10.9 Hz), 148.4 (dd, J_1 = 241.6 Hz, J_2 = 11.9 Hz), 138.2 (d, J = 7.9 Hz), 137.8 (d, J = 3.4 Hz), 130.6 (d, J = 8.4 Hz), 130.1 (dd, J_1 = 9.9 Hz, J_2 = 3.0 Hz), 122.3 (d, J = 2.7 Hz), 114.9 (d, J = 21.6 Hz), 114.4 (dd, J_1 = 8.8 Hz, J_2 = 4.5 Hz), 111.6 (d, J = 22.3 Hz), 111.4 (dd, J_1 = 21.6 Hz, J_2 = 3.4 Hz), 103.8 (dd, J_1 = 26.8 Hz, J_2 = 22.1 Hz); *m/z* calcd for $C_{13}H_9F_3N_2$ 250.1; found 251.1 $[M+H]^+$. Purity of the compound was further confirmed by LCMS: R_t = 19.71 min (99% pure; Fig. 4.B33).

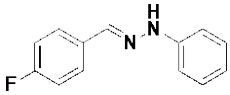

Preparation of compound 3a (SGT1417). To a solution of 4-fluorobenzaldehyde (0.09 mL, 0.81 mmol) in EtOH (8 mL), phenylhydrazine (0.12 mL, 1.21 mmol) was added. The reaction mixture was stirred at 90 °C for 1.5 h and, to the resulting solution, H_2O (50 mL) was added and stirred for 1.5 h. The residue obtained was filtered and dried to afford compound **3a** (146 mg, 84%) as a light pink solid: ^{1}H NMR (500 MHz, $(CD_3)_2SO$, Fig. 4.B34) δ 10.33 (s, 1H), 7.85 (s, 1H), 7.69 (dd, J_1 = 8.8 Hz, J_2 = 5.7 Hz, 2H), 7.22 (dd, J_1 = 9.0 Hz, J_2 = 4.3 Hz, 2H), 7.20 (dd, J_1 = 7.3 Hz, J_2 = 2.2 Hz, 2H), 7.05 (dd, J_1 = 8.7 Hz, J_2 = 1.3 Hz, 2H), 6.74 (tt, J_1 = 7.3 Hz, J_2 = 1.2 Hz, 1H); ^{13}C NMR (100 MHz, CD_3OD, Fig. 4.B35) δ 164.0 (d, J = 244.8 Hz), 146.9, 136.6 (d, J = 12.3 Hz), 134.1 (d, J = 29.6 Hz), 130.0, 128.5 (d, J = 8.1 Hz), 120.2, 116.4 (d, J = 22.2 Hz), 113.3; *m/z* calcd for $C_{13}H_{11}FN_2$ 214.1; found 215.1 $[M+H]^+$. Purity of the compound was further confirmed by LCMS: R_t = 18.75 min (99% pure; Fig. 4.B36).

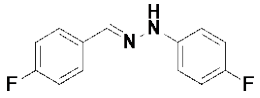

Preparation of compound 3c (SGT1385). To a solution of 4-fluorobenzaldehyde (0.09 mL, 0.81 mmol) in EtOH (8 mL), 4-fluorophenylhydrazine hydrochloride (157 mg, 0.97 mmol) was added. The reaction mixture was stirred at 90 °C for 2 h and, to the resulting solution, H_2O (50 mL) was added and stirred for 2 h. The residue obtained was filtered and dried to afford compound **3c** (171 mg, 91%) as a light peach solid: ^{1}H NMR (500 MHz, $(CD_3)_2SO$, Fig. 4.B37) δ 10.34 (s, 1H), 7.84 (s, 1H), 7.69 (dd, J_1 = 8.7 Hz, J_2 = 5.7 Hz, 2H), 7.22 (app. t, J = 8.9 Hz, 2H), 7.06 (d, J = 2.9 Hz, 2H), 7.05 (br s, 2H); ^{13}C NMR (100 MHz, $(CD_3)_2SO$, Fig. 4.B38) δ 161.9 (d, J = 244.0 Hz), 155.9 (d, J = 232.9 Hz), 142.0 (d, J = 1.8 Hz), 135.4, 132.4 (d, J = 3.0 Hz), 127.5 (d, J = 8.1 Hz), 115.7 (d, J = 1.5 Hz), 115.5, 112.9 (d, J = 7.5 Hz); *m/z* calcd for $C_{13}H_{10}F_2N_2$ 232.1; found 233.1 $[M+H]^+$. Purity of the compound was further confirmed by LCMS: R_t = 18.93 min (98% pure; Fig. 4.B39).

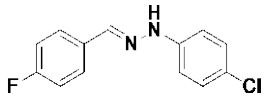

Preparation of compound 3d (SGT1380). To a solution of 4-fluorobenzaldehyde (0.21 mL, 2.01 mmol) in EtOH (12 mL), 4-chlorophenylhydrazine hydrochloride (430 mg, 2.4 mmol) was added. The reaction mixture was stirred at 90 °C for 80 min and, to the resulting solution, H_2O (50 mL) was added and stirred for 2 h. The residue obtained was filtered and dried to afford compound **3d** (405 mg, 81%) as a tan solid: ^{1}H NMR (500 MHz, $(CD_3)_2SO$, Fig. 4.B40) δ 10.46 (s, 1H), 7.86 (s, 1H), 7.70 (dd, J_1 = 8.7 Hz, J_2 = 5.7 Hz, 2H), 7.24 (d, J = 8.9 Hz, 2H), 7.21 (d, J = 8.9 Hz, 2H), 7.06 (d, J = 8.9 Hz, 2H); ^{13}C NMR (100 MHz, $(CD_3)_2SO$, Fig. 4.B41) δ 162.0 (d, J = 244.2 Hz), 144.2, 136.2, 132.2 (d, J = 3.0 Hz), 128.9, 127.6 (d, J = 8.1 Hz), 122.0, 115.6 (d, J = 21.7 Hz), 113.4; *m/z* calcd for $C_{13}H_{10}ClFN_2$ 248.1; found 249.1

[M+H]$^+$. Purity of the compound was further confirmed by LCMS: R_t = 20.30 min (99% pure; Fig. 4.B42).

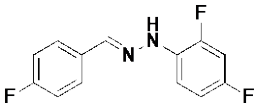

Preparation of compound 3f (SGT1379). To a solution of 4-fluorobenzaldehyde (0.21 mL, 2.01 mmol) in EtOH (12 mL), 2,4-difluorophenylhydrazine hydrochloride (433 mg, 2.4 mmol) was added. The reaction mixture was stirred at 90 °C for 70 min and, to the resulting solution, H_2O (50 mL) was added and stirred for 4 h. The residue obtained was filtered and dried to afford compound **3f** (493 mg, 98%) as a tan solid: ^{1}H NMR (500 MHz, $(CD_3)_2SO$, Fig. 4.B43) δ 10.20 (s, 1H), 8.10 (s, 1H), 7.69 (dd, J_1 = 8.7 Hz, J_2 = 5.7 Hz, 2H), 7.49 (td, J_1 = 9.4 Hz, J_2 = 6.0 Hz, 1H), 7.23 (t, J = 8.9 Hz, 2H), 7.19 (dd, J_1 = 8.9 Hz, J_2 = 2.8 Hz, 1H), 7.02-6.96 (m, 1H); ^{13}C NMR (100 MHz, $(CD_3)_2SO$, Fig. 4.B44) δ 162.1 (d, J = 244.4 Hz), 154.7 (dd, J_1 = 235.9 Hz, J_2 = 11.0 Hz), 148.4 (dd, J_1 = 241.3 Hz, J_2 = 11.9 Hz), 138.2, 132.1 (d, J = 3.0 Hz), 130.4 (dd, J_1 = 10.0 Hz, J_2 = 3.0 Hz), 127.8 (d, J = 8.2 Hz), 115.6 (d, J = 21.7 Hz), 114.1 (dd, J_1 = 8.8 Hz, J_2 = 4.6 Hz), 111.4 (dd, J_1 = 21.6 Hz, J_2 = 3.4 Hz), 103.8 (dd, J_1 = 26.8 Hz, J_2 = 22.1 Hz); *m/z* calcd for $C_{13}H_9F_3N_2$ 250.1; found 251.1 [M+H]$^+$. Purity of the compound was further confirmed by LCMS: R_t = 19.74 min (98% pure; Fig. 4.B45).

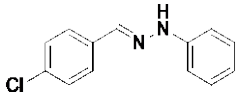

Preparation of compound 4a (SGT1287). To a solution of 4-chlorobenzaldehyde (1.0 g, 7.11 mmol) in EtOH (10 mL), phenylhydrazine (0.77 mL, 7.83 mmol) was added. The reaction mixture was stirred at 80 °C for 1 h and the resulting solution was filtered. The residue obtained was washed with hot EtOH (25 mL) to afford compound **4a** (1.29 g, 79%) as a white solid: ^{1}H NMR (500

MHz, $(CD_3)_2SO$, Fig. 4.B46) δ 10.43 (s, 1H), 7.84 (s, 1H), 7.66 (d, J = 8.6 Hz, 2H), 7.43 (d, J = 8.6 Hz, 2H), 7.21 (dd, J_1 = 8.6 Hz, J_2 = 7.2 Hz, 2H), 7.06 (dd, J_1 = 8.8 Hz, J_2 = 1.2 Hz, 2H), 6.76 (tt, J_1 = 7.3 Hz, J_2 = 1.2 Hz, 1H); ^{13}C NMR (100 MHz, $(CD_3)_2SO$, Fig. 4.B47) δ 145.1, 135.0, 134.8, 132.1, 129.1, 128.6, 127.1, 118.9, 112.1; *m/z* calcd for $C_{13}H_{11}ClN_2$ 230.1; found 231.1 $[M+H]^+$. Purity of the compound was further confirmed by LCMS: R_t = 20.19 min (96% pure; Fig. 4.B48).

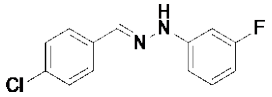

Preparation of compound 4b (SGT1360). To a solution of 4-chlorobenzaldehyde (165 mg, 1.17 mmol) in EtOH (7 mL), 3-fluorophenylhydrazine hydrochloride (229 mg, 1.41 mmol) was added. The reaction mixture was stirred at 80 °C for 1 h and, to the resulting solution, H_2O (35 mL) was added. The residue obtained was filtered and dried to afford compound **4b** (258 mg, 89%) as a pink solid: ^1H NMR (500 MHz, $(CD_3)_2SO$, Fig. 4.B49) δ 10.63 (s, 1H), 7.86 (s, 1H), 7.69 (d, J = 8.5 Hz, 2H), 7.44 (d, J = 8.5 Hz, 2H), 7.23 (td, J_1 = 8.2 Hz, J_2 = 6.8 Hz, 1H), 6.87 (dt, J_1 = 11.7 Hz, J_2 = 2.2 Hz, 1H), 6.83 (ddd, J_1 = 8.2 Hz, J_2 = 2.1 Hz, J_3 = 0.9 Hz, 1H), 6.56-6.51 (m, 1H); ^{13}C NMR (100 MHz, $(CD_3)_2SO$, Fig. 4.B50) δ 163.4 (d, J = 239.4 Hz), 147.1 (d, J = 11.0 Hz), 136.3, 134.4, 132.5, 130.7 (d, J = 10.1 Hz), 128.7, 127.4, 108.2 (d, J = 2.2 Hz), 105.0 (d, J = 21.3 Hz), 98.6 (d, J = 26.1 Hz); *m/z* calcd for $C_{13}H_{10}ClFN_2$ 248.1; found 249.1 $[M+H]^+$. Purity of the compound was further confirmed by LCMS: R_t = 20.45 min (97% pure; Fig. 4.B51).

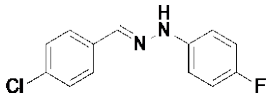

Preparation of compound 4c (SGT1361). To a solution of 4-chlorobenzaldehyde (250 mg, 1.78 mmol) in EtOH (10 mL), 4-

fluorophenylhydrazine hydrochloride (346 mg, 2.13 mmol) was added. The reaction mixture was stirred at 80 °C for 1 h and, to the resulting solution, H_2O (45 mL) was added. The residue obtained was filtered and dried to afford compound **4c** (381 mg, 87%) as an off-white solid: ^{1}H NMR (500 MHz, $(CD_3)_2SO$, Fig. 4.B52) δ 10.42 (s, 1H), 7.82 (s, 1H), 7.66 (d, J = 8.5 Hz, 2H), 7.43 (d, J = 8.5 Hz, 2H), 7.07-7.04 (m, 4H); ^{13}C NMR (100 MHz, $(CD_3)_2SO$, Fig. 4.B53) δ 156.0 (d, J = 233.1 Hz), 141.8 (d, J = 1.9 Hz), 135.0, 134.8, 132.1, 128.6, 127.1, 115.6 (d, J = 22.2 Hz), 113.0 (d, J = 7.4 Hz); *m/z* calcd for $C_{13}H_{10}ClFN_2$ 248.1; found 249.1 M+H]$^+$. Purity of the compound was further confirmed by LCMS: R_t = 20.33 min (97% pure; Fig. 4.B54).

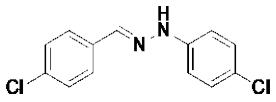

Preparation of compound 4d (SGT1291). To a solution of 4-chlorobenzaldehyde (250 mg, 1.78 mmol) in EtOH (10 mL), 4-chlorophenylhydrazine hydrochloride (382 mg, 2.13 mmol) was added. The reaction mixture was stirred at 80 °C for 1 h and, to the resulting solution, H_2O (35 mL) was added. The residue obtained was filtered and dried to afford compound **4d** (393 mg, 83%) as a pink solid: ^{1}H NMR (500 MHz, $(CD_3)_2SO$, Fig. 4.B55) δ 10.56 (s, 1H), 7.85 (s, 1H), 7.67 (d, J = 8.5 Hz, 2H), 7.44 (d, J = 8.5 Hz, 2H), 7.25 (d, J = 8.8 Hz, 2H), 7.07 (d, J = 8.8 Hz, 2H); ^{13}C NMR (100 MHz, $(CD_3)_2SO$, Fig. 4.B56) δ 144.0, 135.9, 134.5, 132.3, 128.9, 128.7, 127.3, 122.2, 113.5; *m/z* calcd for $C_{13}H_{10}Cl_2N_2$ 264.0; found 265.1 [M+H]$^+$. Purity of the compound was further confirmed by LCMS: R_t = 21.84 min (99% pure; Fig. 4.B57).

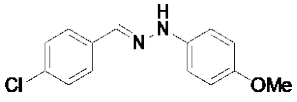

Preparation of compound 4e (SGT1371). To a solution of 4-cholorobenzaldehyde (100 mg, 0.71 mmol) in EtOH (8 mL), 4-

methoxyphenylhydrazine hydrochloride (149 mg, 0.85 mmol) was added. The reaction mixture was stirred at 90 °C for 1 h and, to the resulting solution, H_2O (45 mL) was added. The residue obtained was filtered and dried to afford compound **4e** (174 mg, 94%) as a yellow solid: ^{1}H NMR (500 MHz, $(CD_3)_2SO$, Fig. 4.B58) δ 10.25 (s, 1H), 7.77 (s, 1H), 7.63 (d, J = 8.6 Hz, 2H), 7.41 (d, J = 8.6 Hz, 2H), 7.00 (d, J = 9.0 Hz, 2H), 6.84 (d, J = 9.0 Hz, 2H), 3.69 (s, 3H); ^{13}C NMR (100 MHz, $(CD_3)_2SO$, Fig. 4.B59) δ 152.8, 139.1, 135.1, 133.8, 131.7, 128.6, 126.9, 114.6, 113.1, 55.3; *m/z* calcd for $C_{14}H_{13}ClN_2O$ 260.1; found 261.1 $[M+H]^+$. Purity of the compound was further confirmed by LCMS: R_t = 19.63 min (98% pure; Fig. 4.B60).

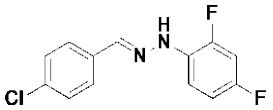

Preparation of compound 4f (SGT1359). To a solution of 4-chlorobenzaldehyde (250 mg, 1.78 mmol) in EtOH (10 mL), 2,4-difluorophenylhydrazine hydrochloride (385 mg, 2.13 mmol) was added. The reaction mixture was stirred at 80 °C for 1 h and, to the resulting solution, H_2O (35 mL) was added. The residue obtained was filtered and dried to afford compound **4f** (395 mg, 84%) as an off-white solid: ^{1}H NMR (500 MHz, $(CD_3)_2SO$, Fig. 4.B61) δ 10.31 (s, 1H), 8.08 (s, 1H), 7.67 (d, J = 8.6 Hz, 2H), 7.50 (td, J_1 = 9.4 Hz, J_2 = 6.0 Hz, 1H), 7.45 (d, J = 8.6 Hz, 2H), 7.21 (ddd, J_1 = 11.9 Hz, J_2 = 8.9 Hz, J_3 = 2.8 Hz, 1H), 7.02-6.97 (m, 1H); ^{13}C NMR (100 MHz, $(CD_3)_2SO$, Fig. 4.B62) δ 154.8 (dd, J_1 = 235.0 Hz, J_2 = 10.9 Hz), 148.4 (dd, J_1 = 241.4 Hz, J_2 = 12.0 Hz), 137.9, 134.5, 132.6, 130.2 (dd, J_1 = 9.9 Hz, J_2 = 3.0 Hz), 128.7, 127.4, 114.2 (dd, J_1 = 8.8 Hz, J_2 = 4.5 Hz), 111.4 (dd, J_1 = 21.6 Hz, J_2 = 3.4 Hz), 103.8 (dd, J_1 = 26.8 Hz, J_2 = 22.1 Hz); *m/z* calcd for $C_{13}H_9ClF_2N_2$ 266.0; found 267.1 $[M+H]^+$.

Purity of the compound was further confirmed by LCMS: R_t = 21.04 min (100% pure; Fig. 4.B63).

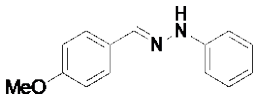

Preparation of compound 5a (SGT1284). To a solution of 4-methoxybenzaldehyde (2.0 g, 14.7 mmol) in EtOH (20 mL), phenylhydrazine (1.45 mL, 14.7 mmol) was added. The reaction mixture was stirred at 90 °C for 1 h and the solid formed was filtered. The product obtained was recrystallized in hot EtOH (8 mL) to afford compound **5a** (2.21 g, 66%) as white solid: ^{1}H NMR (400 MHz, $(CD_3)_2SO$, Fig. 4.B64) δ 10.14 (s, 1H), 7.81 (s, 1H), 7.58 (d, J = 8.8 Hz, 2H), 7.19 (dd, J_1 = 8.5 Hz, J_2 = 7.2 Hz, 2H), 7.03 (dd, J_1 = 8.5 Hz, J_2 = 1.2 Hz, 2H), 6.96 (d, J = 8.8 Hz, 2H), 6.71 (tt, J_1 = 7.2 Hz, J_2 = 1.2 Hz, 1H), 3.78 (s, 3H); ^{13}C NMR (100 MHz, $(CD_3)_2SO$, Fig. 4.B65) δ 159.3, 145.6, 136.6, 129.0, 128.5, 127.0, 118.3, 114.2, 111.8, 55.2; *m/z* calcd for $C_{14}H_{14}N_2O$ 226.1; found 227.1 $[M+H]^+$. Purity of the compound was further confirmed by LCMS: R_t = 16.40 min (99% pure; Fig. 4.B66).

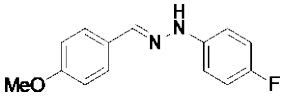

Preparation of compound 5c (SGT1398). To a solution of 4-methoxybenzaldehyde (0.08 mL, 0.73 mmol) in EtOH (8 mL), 4-fluorophenylhydrazine hydrochloride (179 mg, 1.10 mmol) was added. The reaction mixture was stirred at 90 °C for 100 min and, to the resulting solution, H_2O (50 mL) was added and stirred for 150 min. The residue obtained was filtered and dried to afford compound **5c** (175 mg, 98%) as an off-white solid: ^{1}H NMR (500 MHz, $(CD_3)_2SO$, Fig. 4.B67) δ 10.12 (s, 1H), 7.81 (s, 1H), 7.58 (d, J = 8.8 Hz, 2H), 7.04 (d, J = 7.1 Hz, 2H), 7.02 (d, J = 3.9 Hz, 2H), 6.95 (d, J = 8.8 Hz, 2H), 3.78 (s, 3H); ^{13}C NMR (100 MHz, $(CD_3)_2SO$,

Fig. 4.B68) δ 159.3, 155.6 (d, J = 232.2 Hz), 142.3 (d, J = 1.8 Hz), 136.7, 128.4, 127.0, 115.5 (d, J = 22.2 Hz), 114.1, 112.7 (d, J = 7.4 Hz), 55.2; *m/z* calcd for $C_{134}H_{13}FN_2O$ 244.1; found 245.1 $[M+H]^+$. Purity of the compound was further confirmed by LCMS: R_t = 18.46 min (97% pure; Fig. 4.B69).

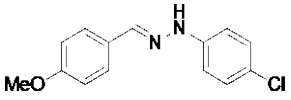

Preparation of compound 5d (SGT1367). To a solution of 4-methoxybenzaldehyde (0.22 mL, 1.84 mmol) in EtOH (10 mL), 4-chlorophenylhydrazine hydrochloride (394 mg, 2.20 mmol) was added. The reaction mixture was stirred at 80 °C for 1 h and, to the resulting solution, H_2O (45 mL) was added. The residue obtained was filtered and dried to afford compound **5d** (417 mg, 87%) as a pink solid: ^{1}H NMR (500 MHz, $(CD_3)_2SO$, Fig. 4.B70) δ 10.27 (s, 1H), 7.82 (s, 1H), 7.58 (d, J = 8.8 Hz, 2H), 7.22 (d, J = 8.9 Hz, 2H), 7.02 (d, J = 8.9 Hz, 2H), 6.95 (d, J = 8.8 Hz, 2H), 3.78 (s, 3H); ^{13}C NMR (100 MHz, $(CD_3)_2SO$, Fig. 4.B71) δ 159.5, 144.5, 137.4, 128.8, 128.2, 127.2, 121.5, 114.2, 113.2, 55.2; *m/z* calcd for $C_{14}H_{13}ClN_2O$ 260.1; found 261.1 $[M+H]^+$. Purity of the compound was further confirmed by LCMS: R_t = 19.71 min (97% pure; Fig. 4.B72).

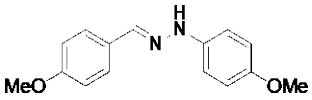

Preparation of compound 5e (SGT1290). To a solution of 4-methoxybenzaldehyde (0.22 mL, 1.84 mmol) in EtOH (10 mL), 4-methoxyphenylhydrazine hydrochloride (385 mg, 2.20 mmol) was added. The reaction mixture was stirred at 80 °C for 1 h and, to the resulting solution, H_2O (35 mL) was added. The residue obtained was filtered and dried to afford compound **5e** (235 mg, 49%) as a yellow solid: ^{1}H NMR (500 MHz, $(CD_3)_2SO$, Fig. 4.B73) δ 9.90 (s, 1H), 7.76 (s, 1H), 7.55

(d, J = 8.8 Hz, 2H), 6.97 (d, J = 8.9 Hz, 2H), 6.94 (d, J = 8.8 Hz, 2H), 6.82 (d, J = 8.9 Hz, 2H), 3.77 (s, 3H), 3.68 (s, 3H); ^{13}C NMR (100 MHz, $(CD_3)_2SO$, Fig. 4.B74) δ 159.1, 152.3, 139.7, 135.5, 128.7, 126.8, 114.6, 114.1, 112.8, 55.3, 55.1; *m/z* calcd for $C_{15}H_{16}N_2O_2$ 256.1; found 257.2 $[M+H]^+$. Purity of the compound was further confirmed by LCMS: R_t = 17.54 min (99% pure; Fig. 4.B75).

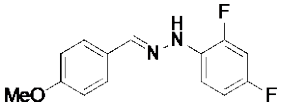

Preparation of compound 5f (SGT1366). To a solution of 4-methoxybenzaldehyde (0.22 mL, 1.84 mmol) in EtOH (10 mL), 2,4-difluorophenylhydrazine hydrochloride (397 mg, 2.20 mmol) was added. The reaction mixture was stirred at 80 °C for 1 h and, to the resulting solution, H_2O (45 mL) was added. The residue obtained was filtered and dried to afford compound **5f** (429 mg, 89%) as a pink solid: ^{1}H NMR (500 MHz, $(CD_3)_2SO$, Fig. 4.B76) δ 9.99 (s, 1H), 8.06 (s, 1H), 7.58 (d, J = 8.8 Hz, 2H), 7.46 (td, J_1 = 9.4 Hz, J_2 = 6.0 Hz, 1H), 7.18 (ddd, J_1 = 11.9 Hz, J_2 = 8.9 Hz, J_3 = 2.9 Hz, 1H), 7.00-6.98 (m, 1H), 6.96 (d, J = 8.8 Hz, 2H), 3.78 (s, 3H); ^{13}C NMR (100 MHz, $(CD_3)_2SO$, Fig. 4.B77) δ 159.6, 154.4 (dd, J_1 = 235.3 Hz, J_2 = 10.9 Hz), 148.3 (dd, J_1 = 241.0 Hz, J_2 = 12.0 Hz), 139.6, 130.8 (dd, J_1 = 9.9 Hz, J_2 = 3.0 Hz), 128.2, 127.3, 114.2, 113.9 (dd, J_1 = 8.7 Hz, J_2 = 4.7 Hz), 111.3 (dd, J_1 = 21.4 Hz, J_2 = 3.4 Hz), 103.7 (dd, J_1 = 26.7 Hz, J_2 = 22.1 Hz), 55.2; *m/z* calcd for $C_{14}H_{12}F_2N_2O$ 262.1; found 263.1 $[M+H]^+$. Purity of the compound was further confirmed by LCMS: R_t = 19.21 min (99% pure; Fig. 4.B78).

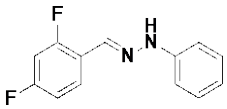

Preparation of compound 6a (SGT1294). To a solution of 2,4-difluorobenzaldehyde (0.19 mL, 1.76 mmol) in EtOH (10 mL),

phenylhydrazine (0.21 mL, 2.11 mmol) was added. The reaction mixture was stirred at 80 °C for 1 h and, to the resulting solution, H_2O (40 mL) was added. The residue obtained was filtered and dried to afford compound **6a** (381 mg, 94%) as a pink solid: ^{1}H NMR (500 MHz, $(CD_3)_2SO$, Fig. 4.B79) δ 10.54 (s, 1H), 7.97 (s, 1H), 7.96 (td, J_1 = 8.8 Hz, J_2 = 6.7 Hz, 1H), 7.28 (ddd, J_1 = 11.4 Hz, J_2 = 9.2 Hz, J_3 = 2.5 Hz, 1H), 7.25-7.20 (m, 2H), 7.15-7.10 (m, 1H), 7.07-7.04 (m, 2H), 6.77 (tt, J_1 = 7.3 Hz, J_2 = 1.1 Hz, 1H); ^{13}C NMR (100 MHz, $(CD_3)_2SO$, Fig. 4.B80) δ 161.8 (dd, J_1 = 221.3 Hz, J_2 = 12.2 Hz), 159.3 (dd, J_1 = 223.9 Hz, J_2 = 12.4 Hz), 144.9, 129.1, 127.9 (dd, J_1 = 3.8 Hz, J_2 = 2.0 Hz), 126.7 (dd, J_1 = 9.6 Hz, J_2 = 5.0 Hz), 120.2 (dd, J_1 = 10.3 Hz, J_2 = 3.8 Hz), 119.1, 112.2 (dd, J_1 = 21.7 Hz, J_2 = 3.4 Hz), 112.1, 104.1 (t, J = 25.7 Hz); *m/z* calcd for $C_{13}H_{10}F_2N_2$ 232.1; found 233.1 $[M+H]^+$. Purity of the compound was further confirmed by LCMS: R_t = 19.45 min (99% pure; Fig. 4.B81).

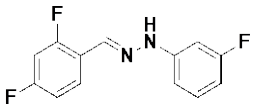

Preparation of compound 6b (SGT1363). To a solution of 2,4-difluorobenzaldehyde (0.19 mL, 1.76 mmol) in EtOH (10 mL), 3-fluorophenylhydrazine hydrochloride (343 mg, 2.11 mmol) was added. The reaction mixture was stirred at 80 °C for 1 h and, to the resulting solution, H_2O (45 mL) was added. The residue obtained was filtered and dried to afford compound **6b** (418 mg, 95%) as an off-white solid: ^{1}H NMR (500 MHz, $(CD_3)_2SO$, Fig. 4.B82) δ 10.75 (s, 1H), 8.02-7.96 (td, J_1 = 8.7 Hz, J_2 = 6.7 Hz, 1H), 8.00 (s, 1H), 7.29 (ddd, J_1 = 11.2 Hz, J_2 = 9.3 Hz, J_3 = 2.5 Hz, 1H), 7.24 (td, J_1 = 8.2 Hz, J_2 = 6.8 Hz, 1H), 7.16-7.11 (m, 1H), 6.88 (dt, J_1 = 11.7 Hz, J_2 = 2.3 Hz, 1H), 6.81 (ddd, J_1 = 8.2 Hz, J_2 = 2.1 Hz, J_3 = 0.9 Hz, 1H), 6.58-6.53 (m, 1H); ^{13}C NMR (100 MHz, $(CD_3)_2SO$, Fig. 4.B83) δ 163.4 (d, J = 239.5 Hz), 162.1 (dd, J_1 =

227.7 Hz, J_2 = 12.5 Hz), 159.6 (dd, J_1 = 230.1 Hz, J_2 = 12.4 Hz), 146.9 (d, J = 11.0 Hz), 130.8 (d, J = 10.0 Hz), 129.3 (dd, J_1 = 3.8 Hz, J_2 = 1.9 Hz), 127.1 (dd, J_1 = 9.8 Hz, J_2 = 4.9 Hz), 119.8 (dd, J_1 = 10.2 Hz, J_2 = 3.8 Hz), 112.3 (dd, J_1 = 21.7 Hz, J_2 = 3.4 Hz), 108.2 (d, J = 2.2 Hz), 105.2 (d, J = 21.4 Hz), 104.2 (t, J = 25.6 Hz), 98.6 (d, J = 26.1 Hz); *m/z* calcd for $C_{13}H_9F_3N_2$ 250.1; found 251.1 $[M+H]^+$. Purity of the compound was further confirmed by LCMS: R_t = 19.85 min (95% pure; Fig. 4.B84).

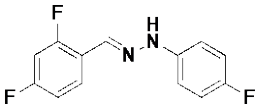

Preparation of compound 6c (SGT1364). To a solution of 2,4-difluorobenzaldehyde (0.19 mL, 1.76 mmol) in EtOH (10 mL), 4-fluorophenylhydrazine hydrochloride (343 mg, 2.11 mmol) was added. The reaction mixture was stirred at 80 °C for 1 h and, to the resulting solution, H_2O (45 mL) was added. The residue obtained was filtered and dried to afford compound **6c** (401 mg, 91%) as a yellow solid: ^{1}H NMR (500 MHz, $(CD_3)_2SO$, Fig. 4.B85) δ 10.54 (s, 1H), 7.98-7.92 (td, J_1 = 8.7 Hz, J_2 = 6.7 Hz, 1H), 7.96 (s, 1H), 7.28 (ddd, J_1 = 11.5 Hz, J_2 = 9.3 Hz, J_3 = 2.6 Hz, 1H), 7.13 (td, J_1 = 8.4 Hz, J_2 = 2.6 Hz, 1H), 7.10-7.04 (m, 4H); ^{13}C NMR (100 MHz, $(CD_3)_2SO$, Fig. 4.B86) δ 161.8 (dd, J_1 = 222.5 Hz, J_2 = 12.4 Hz), 159.4 (dd, J_1 = 225.2 Hz, J_2 = 12.3 Hz), 156.1 (d, J = 233.2 Hz), 141.6 (d, J = 1.9 Hz), 128.0 (dd, J_1 = 5.7 Hz, J_2 = 2.4 Hz), 126.8 (dd, J_1 = 9.6 Hz, J_2 = 5.0 Hz), 120.1 (dd, J_1 = 10.3 Hz, J_2 = 3.8 Hz), 115.7 (d, J = 22.3 Hz), 113.0 (d, J = 7.4 Hz), 112.2 (dd, J_1 = 21.7 Hz, J_2 = 3.4 Hz), 104.1 (t, J = 25.6 Hz); *m/z* calcd for $C_{13}H_9F_3N_2$ 250.1; found 251.1 $[M+H]^+$. Purity of the compound was further confirmed by LCMS: R_t = 19.61 min (96% pure; Fig. 4.B87).

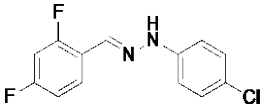

Preparation of compound 6d (SGT1362). To a solution of 2,4-difluorobenzaldehyde (0.19 mL, 1.76 mmol) in EtOH (10 mL), 4-chlorophenylhydrazine hydrochloride (378 mg, 2.11 mmol) was added. The reaction mixture was stirred at 80 °C for 1 h and, to the resulting solution, H_2O (45 mL) was added. The residue obtained was filtered and dried to afford compound **6d** (384 mg, 82%) as a brown solid: ^{1}H NMR (500 MHz, $(CD_3)_2SO$, Fig. 4.B88) δ 10.67 (s, 1H), 7.98 (s, 1H), 7.96 (td, J_1 = 8.8 Hz, J_2 = 6.7 Hz, 1H), 7.29 (ddd, J_1 = 11.3 Hz, J_2 = 9.3 Hz, J_3 = 2.6 Hz, 1H), 7.26 (d, J = 8.9 Hz, 2H), 7.16-7.10 (m, 1H), 7.06 (d, J = 8.9 Hz, 2H); ^{13}C NMR (100 MHz, $(CD_3)_2SO$, Fig. 4.B89) δ 162.0 (dd, J_1 = 226.6 Hz, J_2 = 12.4 Hz), 159.5 (dd, J_1 = 229.1 Hz, J_2 = 12.4 Hz), 143.9, 129.0, 128.9 (dd, J_1 = 3.8 Hz, J_2 = 1.9 Hz), 126.9 (dd, J_1 = 9.7 Hz, J_2 = 4.8 Hz), 122.4, 119.9 (dd, J_1 = 10.5 Hz, J_2 = 3.8 Hz), 113.5, 112.3 (dd, J_1 = 21.6 Hz, J_2 = 3.4 Hz), 104.2 (t, J = 25.6 Hz); *m/z* calcd for $C_{13}H_9ClF_2N_2$ 266.0; found 267.1 $[M+H]^+$. Purity of the compound was further confirmed by LCMS: R_t = 20.50 min (100% pure; Fig. 4.B90).

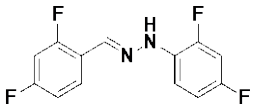

Preparation of compound 6f (SGT1293). To a solution of 2,4-difluorobenzaldehyde (0.19 mL, 1.76 mmol) in EtOH (10 mL), 2,4-difluorophenylhydrazine hydrochloride (349 mg, 1.94 mmol) was added. The reaction mixture was stirred at 80 °C for 1 h and, to the resulting solution, H_2O (50 mL) was added. The residue obtained was filtered and dried to afford compound **6f** (458 mg, 97%) as an off-white solid: ^{1}H NMR (500 MHz, $(CD_3)_2SO$, Fig. 4.B91) δ 10.42 (s, 1H), 8.25 (s, 1H), 7.98 (td, J_1 = 8.7 Hz, J_2 = 6.7 Hz, 1H), 7.50 (td, J_1 = 9.3 Hz, J_2 = 5.9 Hz, 1H), 7.29 (ddd, J_1 = 11.4 Hz, J_2 = 9.2 Hz, J_3 = 2.5 Hz, 1H), 7.22 (ddd, J_1 = 11.8 Hz, J_2 = 8.8 Hz, J_3 = 2.8

Hz, 1H), 7.17-7.11 (m, 1H), 7.03-6.96 (m, 1H); ^{13}C NMR (100 MHz, $(CD_3)_2SO$, Fig. 4.B92) δ 162.1 (dd, J_1 = 228.3 Hz, J_2 = 12.4 Hz), 159.6 (dd, J_1 = 230.9 Hz, J_2 = 12.4 Hz), 154.9 (dd, J_1 = 236.0 Hz, J_2 = 10.9 Hz), 148.4 (dd, J_1 = 241.6 Hz, J_2 = 12.1 Hz), 131.0 (d, J = 21.7 Hz), 130.1 (dd, J_1 = 9.9 Hz, J_2 = 3.0 Hz), 127.0 (dd, J_1 = 9.7 Hz, J_2 = 4.9 Hz), 119.9 (dd, J_1 = 10.3 Hz, J_2 = 3.9 Hz), 114.2 (dd, J_1 = 8.8 Hz, J_2 = 4.5 Hz), 112.3 (dd, J_1 = 21.6 Hz, J_2 = 3.4 Hz), 111.4 (dd, J_1 = 21.7 Hz, J_2 = 3.4 Hz), 104.2 (t, J = 25.6 Hz), 103.9 (dd, J_1 = 26.9 Hz, J_2 = 22.1 Hz); *m/z* calcd for $C_{13}H_8F_4N_2$ 268.1; found 269.1 $[M+H]^+$. Purity of the compound was further confirmed by LCMS: R_t = 20.39 min (99% pure; Fig. 4.B93).

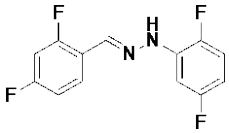

Preparation of compound 6g (SGT1384). To a solution of 2,4-difluorobenzaldehyde (0.08 mL, 0.70 mmol) in EtOH (8 mL), 2,5-difluorophenylhydrazine hydrochloride (122 mg, 0.84 mmol) was added. The reaction mixture was stirred at 90 °C for 3.25 h and, to the resulting solution, H_2O (50 mL) was added and stirred for 2.75 h. The residue obtained was filtered and dried to afford compound **6g** (181 mg, 96%) as a peach solid: ^{1}H NMR (500 MHz, $(CD_3)_2SO$, Fig. 4.B94) δ 10.67 (s, 1H), 8.31 (s, 1H), 8.06 (td, J_1 = 8.8 Hz, J_2 = 6.7 Hz, 1H), 7.30 (ddd, J_1 = 11.3 Hz, J_2 = 9.3 Hz, J_3 = 2.6 Hz, 1H), 7.26 (ddd, J_1 = 10.7 Hz, J_2 = 6.6 Hz, J_3 = 3.2 Hz, 1H), 7.18 (ddd, J_1 = 11.4 Hz, J_2 = 8.9Hz, J_3 = 5.0 Hz, 1H), 7.16-7.11 (m, 1H), 6.59-6.53 (m, 1H); ^{13}C NMR (100 MHz, $(CD_3)_2SO$, Fig. 4.B95) δ 162.3 (dd, J_1 = 232.2 Hz, J_2 = 12.2 Hz), 159.9 (dd, J_1 = 234.8 Hz, J_2 = 12.4 Hz), 159.2 (dd, J_1 = 236.3 Hz, J_2 = 1.7 Hz), 145.2 (dd, J_1 = 234.1 Hz, J_2 = 2.2 Hz), 134.5 (t, J = 118.3 Hz), 132.3 (dd, J_1 = 4.1 Hz, J_2 = 1.9 Hz), 127.4 (dd, J_1 = 9.7 Hz, J_2 = 4.7 Hz), 119.6 (dd, J_1 = 10.3 Hz, J_2 = 3.7 Hz), 116.0 (dd,

J_1 = 20.3 Hz, J_2 = 10.5 Hz), 112.3 (dd, J_1 = 21.6 Hz, J_2 = 3.3 Hz), 104.3 (dd, J_1 = 15.6 Hz, J_2 = 8.3 Hz), 104.1 (dd, J_1 = 14.6 Hz, J_2 = 7.2 Hz), 100.5 (dd, J_1 = 29.4 Hz, J_2 = 3.8 Hz); *m/z* calcd for $C_{13}H_8F_4N_2$ 268.1; found 269.1 $[M+H]^+$. Purity of the compound was further confirmed by LCMS: R_t = 20.32 min (99% pure; Fig. 4.B96).

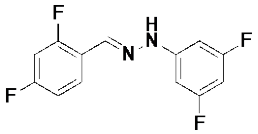

Preparation of compound 6h (SGT1383). To a solution of 2,4-difluorobenzaldehyde (0.08 mL, 0.70 mmol) in EtOH (8 mL), 3,5-difluorophenylhydrazine hydrochloride (152 mg, 0.84 mmol) was added. The reaction mixture was stirred at 90 °C for 2 h and, to the resulting solution, H_2O (50 mL) was added and stirred for 3.5 h. The residue obtained was filtered and dried to afford compound **6h** (179 mg, 95%) as a peach solid: ^{1}H NMR (500 MHz, $(CD_3)_2SO$, Fig. 4.B97) δ 10.92 (s, 1H), 8.01 (s, 1H), 8.02 (td, J_1 = 8.7 Hz, J_2 = 6.7 Hz, 1H), 7.31 (ddd, J_1 = 11.4 Hz, J_2 = 9.3 Hz, J_3 = 2.6 Hz, 1H), 7.14 (td, J_1 = 8.6 Hz, J_2 = 2.5Hz, 1H), 6.68 (dd, J_1 = 10.0 Hz, J_2 = 2.4 Hz, 2H), 6.52 (tt, J_1 = 9.5 Hz, J_2 = 2.4 Hz, 1H); ^{13}C NMR (100 MHz, $(CD_3)_2SO$, Fig. 4.B98) δ 164.0 (dd, J_1 = 241.0 Hz, J_2 = 15.7 Hz), 162.3 (dd, J_1 = 233.0 Hz, J_2 = 12.3 Hz), 159.8 (dd, J_1 = 235.3 Hz, J_2 = 12.2 Hz), 147.6 (t, J = 13.7 Hz), 130.6 (dd, J_1 = 3.8 Hz, J_2 = 1.9 Hz), 127.4 (dd, J_1 = 9.7 Hz, J_2 = 4.7 Hz), 119.5 (dd, J_1 = 10.3 Hz, J_2 = 3.7 Hz), 112.3 (dd, J_1 = 21.7 Hz, J_2 = 3.3 Hz), 104.2 (t, J = 25.6 Hz), 95.0 (d, J = 29.2 Hz), 93.6 (t, J = 26.4 Hz); *m/z* calcd for $C_{13}H_8F_4N_2$ 268.1; found 269.1 $[M+H]^+$. Purity of the compound was further confirmed by LCMS: R_t = 20.34 min (95% pure; Fig. 4.B99).

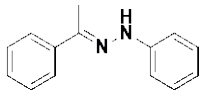

Preparation of compound 7a (SGT1292). To a solution of acetophenone (0.49 mL, 4.16 mmol) in EtOH (12 mL), phenylhydrazine

(0.49 mL, 4.99 mmol) was added. The reaction mixture was stirred at 80 °C for 1 h and, to the resulting solution, H_2O (30 mL) was added. The residue obtained was filtered and dried to afford compound **7a** (228 mg, 26%) as a dark grey solid: ^{1}H NMR (500 MHz, $(CD_3)_2SO$, Fig. 4.B100) δ 9.25 (s, 1H), 7.80-7.77 (m, 2H), 7.40-7.34 (m, 2H), 7.29 (tt, J_1 = 7.2 Hz, J_2 = 1.2 Hz, 1H), 7.25-7.18 (m, 4H), 6.75 (tt, J_1 = 6.5 Hz, J_2 = 1.9 Hz, 1H), 2.25 (s, 3H); ^{13}C NMR (100 MHz, $(CD_3)_2SO$, Fig. 4.B101) δ 146.1, 140.4, 139.2, 128.9, 128.2, 127.4, 125.1, 118.8, 112.8, 12.8; *m/z* calcd for $C_{14}H_{14}N_2$ 210.1; found 211.1 $[M+H]^+$.

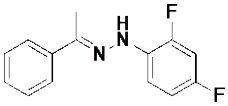

Preparation of compound 7f (SGT1295). To a solution of acetophenone (0.24 mL, 2.08 mmol) in EtOH (7 mL), 2,4-difluorophenylhydrazine hydrochloride (451 mg, 2.50 mmol) was added. The reaction mixture was stirred at 80 °C for 1 h and, to the resulting solution, H_2O (40 mL) was added. The residue obtained was filtered and dried to afford compound **7f** (396 mg, 77%) as a brown solid: ^{1}H NMR (500 MHz, $(CD_3)_2SO$, Fig. 4.B102) δ 8.61 (s, 1H), 7.82-7.79 (m, 2H), 7.56 (td, J_1 = 9.3 Hz, J_2 = 6.0 Hz, 1H), 7.42-7.37 (m, 2H), 7.35-7.31 (m, 1H), 7.22 (ddd, J_1 = 11.8 Hz, J_2 = 8.8 Hz, J_3 = 2.8 Hz, 1H), 7.04-6.98 (m, 1H), 2.30 (s, 3H); ^{13}C NMR (100 MHz, $(CD_3)_2SO$, Fig. 4.B103) δ 155.2 (dd, J_1 = 236.2 Hz, J_2 = 10.8 Hz), 149.4 (dd, J_1 = 242.5 Hz, J_2 = 11.8 Hz), 145.1, 138.8, 131.3 (dd, J_1 = 9.7 Hz, J_2 = 3.0 Hz), 128.3, 128.1, 125.5, 115.7 (dd, J_1 = 8.8 Hz, J_2 = 4.5 Hz), 111.2 (dd, J_1 = 21.6 Hz, J_2 = 3.4 Hz), 103.8 (dd, J_1 = 26.7 Hz, J_2 = 22.4 Hz), 13.0; *m/z* calcd for $C_{14}H_{12}F_2N_2$ 246.1; found 247.1 $[M+H]^+$.

4.5.2. Biochemistry and microbiology

Biochemical/biological reagents and instrumentation. The American Type Culture Collection (ATCC) *Candida albicans* strains, including 10231 (strain *A*), 64124 (strain *B*), and MYA-2876(S) (strain *C*), were a generous gift from Dr. Jon Y. Takemoto (Utah State University, Logan, UT, USA). The rest of the *C. albicans* strains, including 90819(R) (strain *D*), MYA-2310(S) (strain *E*), MYA-1237(R) (strain *F*), and MYA-1003(R) (strain *G*), as well as the non-*albicans Candida* fungi *C. glabrata* ATCC 2001 (strain *H*), *C. krusei* ATCC 6258 (strain *I*), and *C. parapsilosis* ATCC 22019 (strain *J*) were purchased from the American Type Culture Collection (ATCC, Manassas, VA, USA). A panel of *Candida auris* strains was acquired from the CDC & FDA Antibiotic Resistance Isolate Bank (CDC, Atlanta, GA, USA), which included *C. auris* (AR Bank # 0381-0390), *Candida duobushaemulonii* (AR Bank # 0391, 0392, and 0394), *Candida haemulonii* (AR Bank # 0393 and 0395), *Kodameae ohmeri* (AR Bank # 0396), *Candida krusei* (AR Bank # 0397), *Candida lusitaniae* (AR Bank # 0398), and *Saccharomyces cerevisiae* (AR Bank # 0399 and 0400). The filamentous fungi *Aspergillus nidulans* ATCC 38163 (strain *L*) was a kind gift from Prof. Jon S. Thorson (University of Kentucky, Lexington, KY), while the *Aspergillus flavus* ATCC MYA-3631 (strain *K*) and *Aspergillus terreus* ATCC MYA-3633 (strain *M*) were purchased from the ATCC. Yeast strains (strains *A*-*J* and AR Bank # 0381-0400) were cultured at 35 °C in yeast extract peptone dextrose (YEPD) broth. *Aspergillus* spp. strains *K*-*M* were cultured on potato dextrose agar (PDA, catalog # 110130, EMD Millipore, Billerica, MA, USA) at 28 °C before the spores were harvested. All fungal experiments were carried out in RPMI 1640 medium (catalog # R6504, Sigma-Aldrich, St.

Louis, MO, USA) buffered to pH 7.0 with 0.165 M MOPS buffer (Sigma-Aldrich, St. Louis, MO, USA).

For cytotoxicity assays, the human lung carcinoma cell line, A549, and the mouse macrophage cell line, J774A.1, were provided by Profs. Markos Leggas (University of Kentucky, Lexington, KY) and David J. Feola (University of Kentucky, Lexington, KY), respectively. The human embryonic kidney cell line, HEK-293, was bought from the ATCC. The A549 and HEK-293 cells were grown in Dulbecco's Modified Eagle's Medium (DMEM, catalog # VWRL0100, VWR, Chicago, IL) supplemented with 10% fetal bovine serum (FBS; from ATCC) and 1% penicillin/streptomycin (from ATCC) at 37 °C with 5% CO_2. The J774A.1 cells were grown at 37 °C with 5% CO_2 in DMEM (catalog # 30-2002, ATCC, Manassas, VA) supplemented with FBS and antibiotics.

Instrumentation for fungal assays with yeast were the V-1200 spectrophotometer (VWR, Radnor, PA, USA) and the SpectraMax M5 plate reader (Molecular Devices, Sunnyvale, CA, USA) for biofilm, cytotoxicity, and hemolysis assays. The known antifungal drugs, amphotericin B (AmB, VWR, Chicago, IL, USA), caspofungin (CFG, Sigma-Aldrich, St. Louis, MO, USA), fluconazole, (FLC, AK Scientific, Union City, CA, USA) and voriconazole (VRC, AK Scientific, Union City, CA, USA) were used as positive controls.

Determination of minimum inhibitory concentration (MIC) values. The individual minimum inhibitory concentration (MIC) values of compounds **1a-7f** were measured for each fungal strain. The MIC values were determined using the broth microdilution method

in sterile 96-well plates.[305] Concentrations of compound tested were 0.06-31.3 μg/mL against strains *A-M* (Tables 4.1 and 4.2). In cases where MIC values were at or below, 0.06 μg/mL, compounds were then tested in the range of 0.015-7.8 μg/mL. The select compounds, **2b**, **3f**, **4b**, **5a**, **5f**, **6b**, **6d**, **7a**, and **7f** were also tested against the 20 strains from the CDC antibiotic resistance bank (Table 4.3). For testing, compounds were dissolved in DMSO at a concentration of 5 mg/mL allowing the highest concentration of DMSO to be 0.63% in the assay. Serial two-fold dilutions of compound were made horizontally across the plate in 100 μL of RPMI 1640 medium. For yeast, the overnight culture was diluted into RPMI 1640 (25 μL of a fungal stock with OD_{600} of 0.12-0.15 into 10 mL of RPMI 1640 medium, resulting in final inoculum size around 1-5×10^3 CFU/mL) and added to the plate (100 μL per well), making a final volume of 200 μL total per well. Similarly, for *Aspergillus* spp., spores were diluted in RPMI 1640 to 5×10^5 spores/mL, then 100 μL of stock was seeded in each well.[370] The MIC value of each compound was determined by visual inspection (MIC-0). The known antifungal drugs, AmB, CFG, FLC, and VRC were used as controls. In Table 4.1, the MIC-0 values were determined for compounds **1a-7f** as well as AmB and CFG, whereas MIC-2 values were reported for FLC and VRC. For *C. auris* and other related *Candida* strains (AR Bank # 0381-0400, Table 4.3) the MIC-0 was reported for AmB, while for CFG, FLC, and VRC, the MIC-2 was recorded. For yeast, plates were incubated for 48 h at 35 °C, except for with CFG, which was read at 24 h. *Aspergillus* spp. were incubated for 72 h at 35 °C. Control values reported for *C. albicans*, non-albicans *Candida*, and *Aspergillus* strains (Tables 4.1 and 4.2) MIC values for AmB, CFG, FLC, and VRC had been previously reported[247] and were included for comparison purpose.

Hemolysis assays. Hemolytic activity of compounds **2b**, **3f**, **4b**, **5f**, **6d**, **7f**, as well as AmB and VRC was assessed using methods previously reported with minor modifications.[374] 2 mL of citrate-treated murine red blood cells (mRBCs) were obtained and suspended 10 mL of sterile PBS. mRBCs were washed thrice by spinning at 500×g for 7 min. After washing, mRBCs were counted using a hemacytometer and diluted in PBS to 5×10^7 cells/mL. Serial dilutions of compounds were made in PBS in 96-well plates (100 μL volume) in similar fashion as described for MIC assays (Fig. 4.3). Plates also contained a positive control (1% Triton-X®, TX), a negative control (DMSO), and wells with no mRBCs to account for any background absorbance. After compounds were added to the plate, 100 μL of mRBCs were added to each well and plates were incubated at 37 °C for 30 min. After incubation, plates were spun at 500×g for 7 min. 100 μL of supernatant was then transferred to a new 96-well plate and the absorbance at 500 nm was read using a spectrophotometer. Percent hemolysis was calculated using the following equation after subtraction of the background absorbance. These data are presented in Fig. 4.3 and Table 4.4 (normalized to 100%) as well as Fig. 4.9 (non-normalized).

$$\%\ \text{hemolysis} = \frac{\text{Abs}_{500}\ \text{of compound}}{\text{Abs}_{500}\ \text{of TX}} \times 100$$

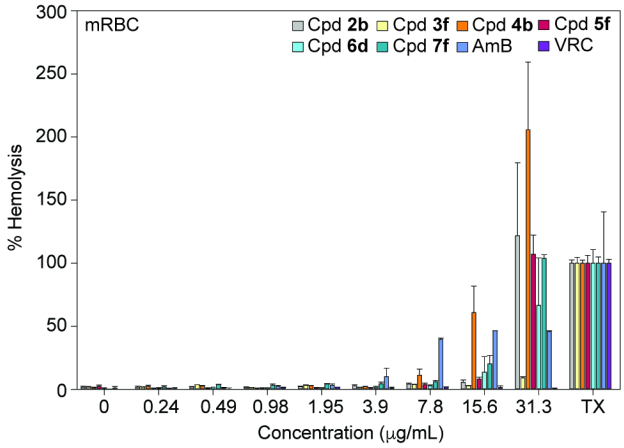

Fig. 4.9. Non-normalized 2D bar graph depicting the dose-dependent hemolytic activity of monohydrazones **2b**, **3f**, **4b**, **5f**, **6d**, **7f**, as well as AmB and VRC against mRBCs. mRBCs were treated and incubated for 1 h at 37 °C with monohydrazones, AmB, and VRC at concentrations ranging from 0.24 to 31.3 μg/mL. Triton X-100® (TX) (1% *v/v*) was used as a positive control (100% hemolysis). *Note*: The corresponding data normalized at 100% are presented in Fig. 4.3 and Table 4.4.

Mammalian cytotoxicity assays. Cytotoxicity assays were performed as previously described[244] with slight modifications. A549, J774A.1, and HEK-293 cells were first thawed from stocks and grown in Dulbecco's modified Eagles's medium (DMEM) containing 10% fetal bovine serum (FBS) and 1% antibiotics. The adherent cells (A549 and HEK-293) were then trypsinized with 0.05% trypsin-0.53 mM EDTA and resuspended in fresh DMEM medium. Once the cells were 80% confluent, they were transferred to a 96-well microtitier plate at density of 5000 cells/well for A549 and 10,000 cells/well for HEK-293 and J774A.1. The 96-well plates were incubated 37 °C with 5% CO_2 overnight. Fresh powder of compounds **2b**, **3f**, **4b**, **5f**, **6d**, and **7f**, as well as controls AmB and VRC were prepared as 6.26 mg/mL stock solutions in biological DMSO (200× the highest final concentration). The stock solutions were diluted in 1.5 mL eppendorf tubes to achieve concentrations of 6.26-0.024 mg/mL (200×). 5 μL of these 200× compound stock solutions was then added to 495 μL of DMEM medium in 1.5 mL eppendorf tubes to obtain concentrations of 62.6-0.24 μg/mL (2×). The medium in the 96-well plates containing the

cells was aspirated and replaced by fresh DMEM medium (100 μL). The serially diluted monohydrazones **2b**, **3f**, **4b**, **5f**, **6d**, and **7f**, as well as controls AmB and VRC were added to the 96-well plates (μL) to obtain final concentrations of 31.3-0.12 μg/mL. The 96-well plates were further incubated for 24 h at 37 °C with 5% CO_2 overnight. To evaluate cell survival, each well was treated with 10 μL (25 mg/L) of resazurin sodium salt (Sigma-Aldrich, St. Louis, MO, USA) and was incubated for another 6 h. Metabolically active cells can convert resazurin to the highly fluorescent dye, resorufin, and be detected at λ_{560} excitation and λ_{590} emission using a SpectraMax M5 plate reader (Molecular Devices, San Jose, CA, USA). Triton X-100® (1%, *v*/*v*) was used as positive control, the negative control consisted of cells treated with the delivery vehicle (0.05% DMSO), and the blank control only had medium with 0.05% DMSO without cells. The percentage survical rates were calculated by using the following formula:

$$\%\ \text{cell survival} = \frac{[(\text{fluorescence}_{\text{sample}}) - (\text{fluorescence}_{\text{background}})]}{[(\text{fluorescence}_{\text{negative control}}) - (\text{fluorescence}_{\text{background}})]} \times 100$$

Experiments were done in quadruplicate. The 100% normalized data are reported in Fig. 4.4 and the corresponding non-normalized data are reported in Fig 4.10.

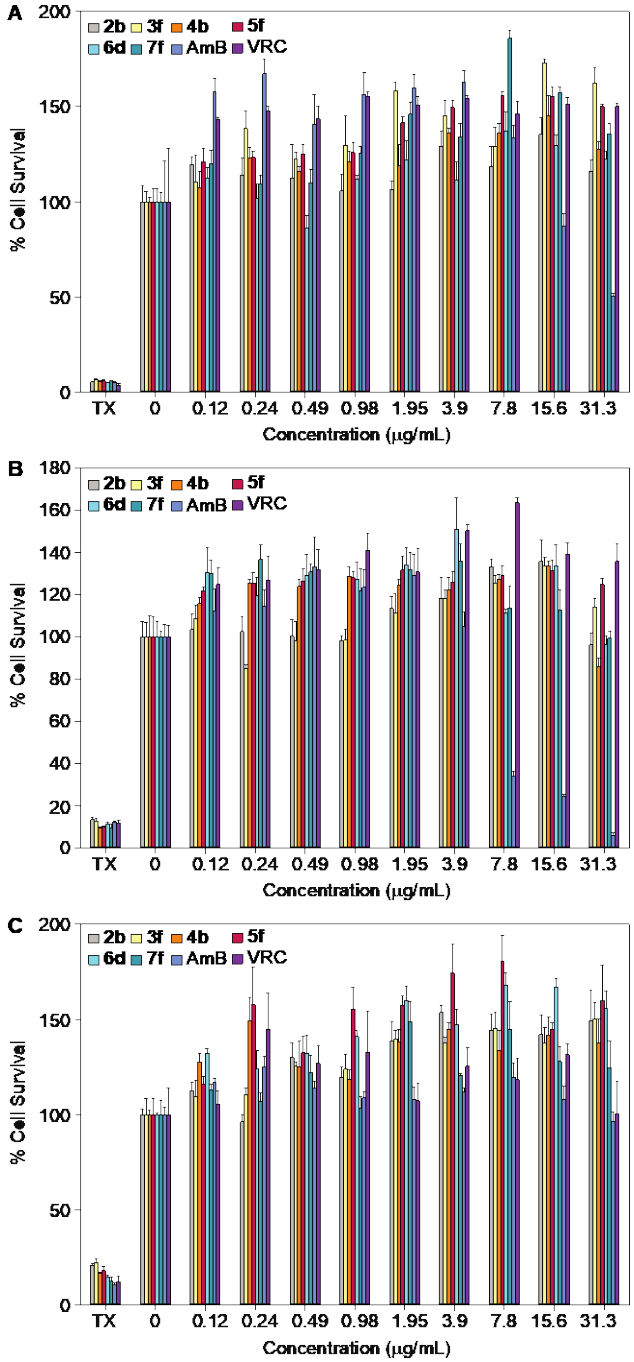

Fig. 4.10. Non-normalized 2D bar graph depicting the dose-dependent hemolytic activity of monohydrazones **2b**, **3f**, **4b**, **5f**, **6d**, **7f**, as well as AmB and VRC against mRBCs. mRBCs were treated and incubated for 1 h at 37 °C with monohydrazones, AmB, and VRC at concentrations ranging from 0.24 to 31.3 µg/mL. Triton X-100® (TX) (1% *v/v*) was used as a positive control (100% hemolysis). *Note*: The corresponding data normalized at 100% are presented in Fig. 4.3 and Table 4.4.

Time-kill assays. Time-killing kinetics were assessed for compounds **2b**, **3f**, **4b**, **5f**, **6d**, **7f**, as well as AmB and VRC against *C. albicans* ATCC 10231 (strain *A*) to evaluate whether the compounds act in a fungistatic or fungicidal manner (Figs. 4.5 and 4.6). In addition to this, the six compounds plus controls were screened against *C. auris* AR # 0384 and *C. auris* AR # 0390 (Fig. 4.6). For all experiments, 3 mL of YEPD medium was inoculated and grown overnight at 35 °C with 200 rpm shaking. In the morning, the overnight culture was diluted in RPMI 1640 medium to an OD_{600} between 0.120 and 0.125 and aliquoted 5 mL into each sample tube and after compound was added, tubes were incubated at 35 °C with 200 rpm shaking. Each compound was tested at ½×, 1×, and 4× MICs. For the known antifungal agents, AmB was tested at 1× MIC concentration and VRC was tested at 1× MIC-0 concentration for *C. albicans* ATCC (strain *A*, 0.98 μg/mL) and 31.3 μg/mL for both *C. auris* strains as the MIC-0 value was ≥31.3 μg/mL. For the kinetic analysis, 100 μL samples were taken at 0, 3, 6, 9, 12, and 24 h, serial 10-fold dilutions were made in sterile H_2O, and 100 μL from the appropriate dilutions were plated on PDA plates and incubated at 48 h at 35 °C. After 48 h, the number of colony forming units (CFU) on each plate were recorded and plates containing between 30 and 300 CFU were used for data analysis. At the 24 h time point, 50 μL of 25 mg/L resazurin was added to the sample tubes and incubated in the dark at 35 °C with 200 rpm shaking for 2 h. The color change observed with the resazurin was used to confirm colony counts. For the time-kill screen with the two *C. auris* strains (Fig. 4.6), sample tubes were prepared in the same manner as above. Samples were vortexed occasionally over the 24 h period and resazurin was added at 24 h to show the relative growth. After the initial 24 h period, all sample tubes were incubated at 35 °C with no shaking and the color was recorded at 48 h and 72 h in

addition to the initial 24 h time point to observe if any growth occurred outside of the 24 h experimental period.

Biofilm assays. Two variations of the biofilm assay were performed to determine the sessile MIC (SMIC) values of compounds **2b**, **3f**, **4b**, **5f**, **6d**, **7f**, as well as AmB and VRC against *C. albicans* ATCC 10231 (strain *A*) as well as *C. auris* AR Bank # 0384 and AR Bank # 0390. Both biofilm assays followed previous protocols and utilized XTT [2,3-bis(2-methoxy-4-nitro-5-sulfophenyl)-2H-tetrazolium-5-carboxanilide] to assess viability of fungal biofilms after treatment. Assays were performed in similar fashion to the MIC assays for plate setup and compound concentrations using procedures as previously described.[309] For the first biofilm assay, *prevention of biofilm formation*, serial dilutions of compound were made in RPMI 1640 medium (100 μL) and fungal suspension (OD_{600} ~0.15) was added to the compounds (200 μL total). Plates were sealed with parafilm and incubated at 37 °C for 48 h. At 48 h, the plates were washed thrice with 200 μL of sterile phosphate buffered saline (PBS) before the addition of XTT. We reported both the $SMIC_{50}$ and $SMIC_{90}$ which are the concentrations of compound at which 50% and 90% inhibition of biofilm activity compared to growth control were observed, respectively (Table 4.5, Fig. 4.7). For the second assay, *destruction of a pre-formed biofilm*, 100 μL per well of fungal suspension was aliquoted into a 96-well plate and incubated at 37 °C for 24 h. At 24 h, the wells were washed thrice with 100 μL sterile PBS. Serial dilutions of compounds were made in RPMI 1640 medium in the plate (200 μL total). The treated biofilms were sealed with parafilm and incubated at 37 °C. At 24 h, the plates were washed thrice with 200 μL PBS before XTT was added (Table 4.6, Fig. 4.11). Directly before use, 1 μL of 10 mM

menadione in acetone (per 10 mL XTT) was added to XTT (0.5 mg/mL in sterile PBS). 100 μL of XTT was aliquoted to each well and allowed to incubate in the dark for 3 h at 37 °C before being read on the spectrophotometer (λ = 450 nm). As no obvious biofilm inhibition was observed, we reported the $SMIC_{50}$. Each assay was performed in duplicate.

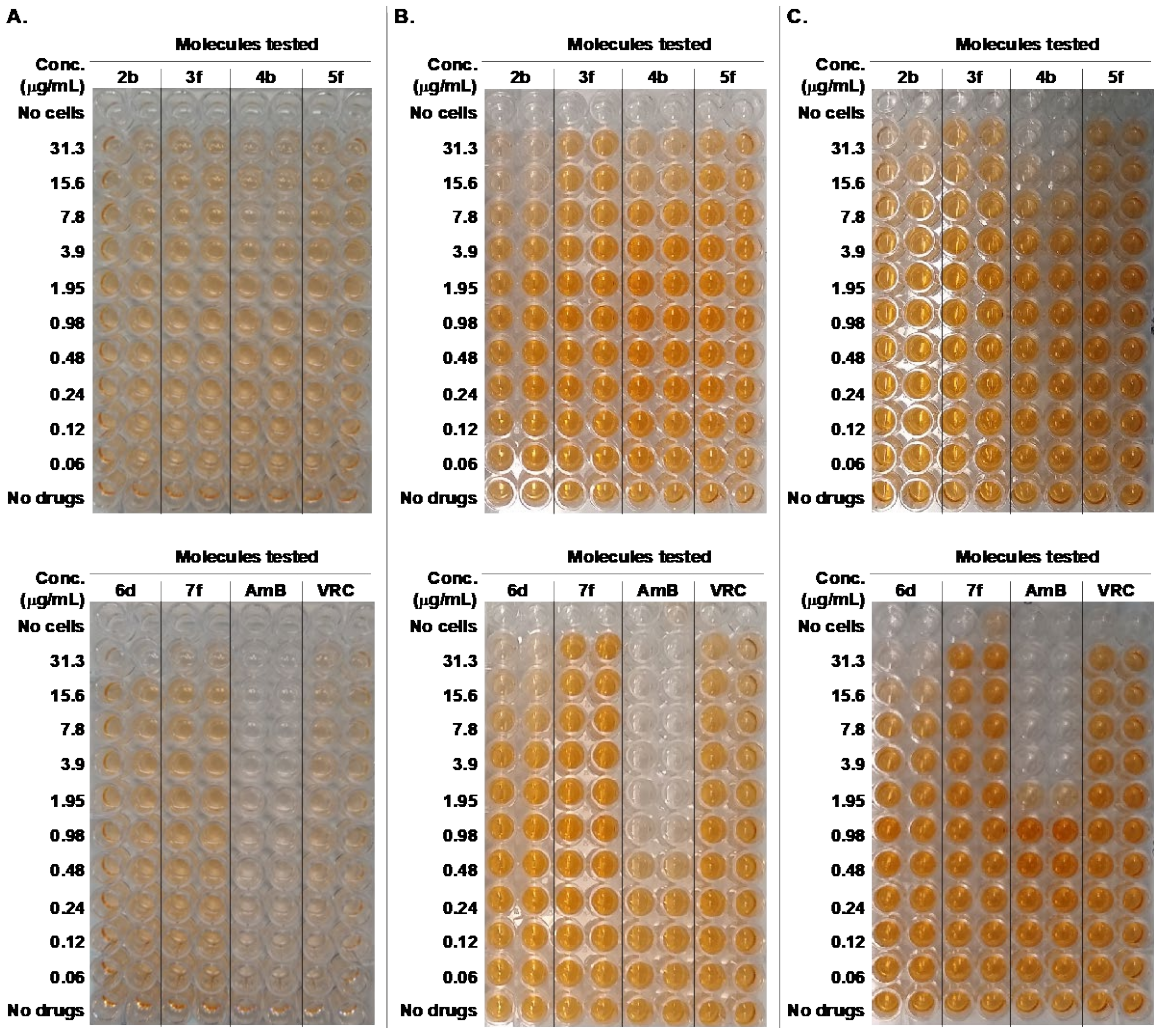

Fig. 4.1. Destruction of a pre-formed biofilm of **A.** *C. albicans* ATCC 10231 (strain *A*), **B.** *C. auris* AR Bank # 0384, and **C.** *C. auris* AR Bank # 0390 treated at 24 h with **2b**, **3f**, **4b**, **5f**, **6d**, **7f**, AmB, and VRC. XTT dye is metabolized by fungal cells to produce an orange color. The corresponding data are presented in Table 4.6.

Development of fungal resistance. To evaluate the likelihood that fungal strain can develop resistance, the change in the MIC of compounds **2b**, **3f**, **4b**, **5f**, **6d**, as well as AmB over 15 serial passages was monitored with *C. auris* AR Bank # 0390 (Fig. 4.8). The procedure was followed from the previously recorded method with little modifications.[373] MIC assays were performed as described above. For the serial passages, cells were selected from a well representing ½ the MIC concentration and used to start an overnight culture for the following MIC.

4.6. AUTHOR CONTRIBUTIONS

N.T.C. synthesized compound **1a-1f**, **2a**, **4a-4f**, **5a**, **5d-5f**, and **6a-6f**. N.T.C. characterized all compounds, performed cytotoxicity and hemolysis experiments, and made figures for experiments performed, and wrote the text and Appendix B. K.R.B. synthesized compounds **2b-2f**, **3a-3f**, **5c**, and **6g-6h**. E.K.D. performed MIC, biofilm, development of resistance, and hemolysis assays, and wrote text and made figures for experiments performed. N.T.C., E.K.D., S.G.-T., and D.S.W. contributed to writing of the manuscript. N.T.C., S.K., D.S.W., and S.G.-T. conceptualized the idea.

4.7. ACKNOWLEDGMENTS

The work was supported by startup funds from the College of Pharmacy at the University of Kentucky (to S.G.-T). D.S.W. was supported by NIH R01 CA172379, the Office of the Dean of the College of Medicine, the Markey Cancer Center, the Center for Pharmaceutical Research and Innovation (CPRI) in the College of Pharmacy, Department of Defense (DoD) Idea Development Award (PC150326P2), NIH P20 RR020171 from the National

Institute of General Medical Sciences, NIH P20 GM130456, and the National Center for Advancing Translational Science (UL1 TR000117 and UL1 TR001998). This manuscript's contents are solely the responsibility of the authors and do not necessarily represent the official views of the NIH, NSF, NIGMS, or the DoD. We also thank Sarah A. Foree for help with determining some MIC values as a part of the University of Kentucky SURP. We are also grateful to writers at *The New York Times* who sparked our interest in finding treatments for *Candida auris* and whose commitment to discovery and the truth matches our own.

Chapter 5

Additional ongoing research

5.1. INTRODUCTION

This section presents five projects that were conceptualized during my time as a graduate student, but are incomplete at this time. Four projects explore the utility of an adjuvant approach to combat antimicrobial resistance. The first three projects, "fexofenadine and azole antifungal combinations," "ebastine and non-azole antifungal combinations," and "antihistamine and antibiotic combinations" are inspired by the work on antihistamine and azole combinations presented in Chapter 2. The fourth project "additional gold (I)-phosphine complexes" includes data for two different families of gold(I)-phosphine complexes related to the complexes presented in Chapter 3. And the final project, "monohydrazides" gives preliminary biological data for a series of compounds closely related to those presented in Chapter 4.

5.2. RESULTS AND DISCUSSION

5.2.1. Fexofenadine and azole antifungal combinations

We previously showed in Chapter 2 that combinations of azoles and antihistamines were synergistic against *Candida* spp.[257] These combinations were important because fungi, including *Candida* spp., develop resistance to azoles so that the antifungals are no longer effective. The antihistamine terfenadine (TERF, Fig. 5.1) was previously approved by the FDA. At the time of its approval, TERF was well regarded as was one of the first second-

generation antihistamines, which do not cause drowsiness. Another second-generation antihistamine, ebastine (EBA, Fig. 5.1), has not been approved in the U.S. The major downside to using these two antihistamines, specifically with the azoles, is that there are drug-drug interactions. The azoles inhibit cytochrome P450 (CYP) proteins[283] responsible for the metabolism of both TERF and EBA into their active metabolites, fexofenadine (FEX) and carebastine, respectively. The CYP inhibition results in toxic levels of TERF and EBA in the blood, leading to human *ether-à-go-go-related gene* (hERG) inhibition and potentially fatal heart arrythmia.

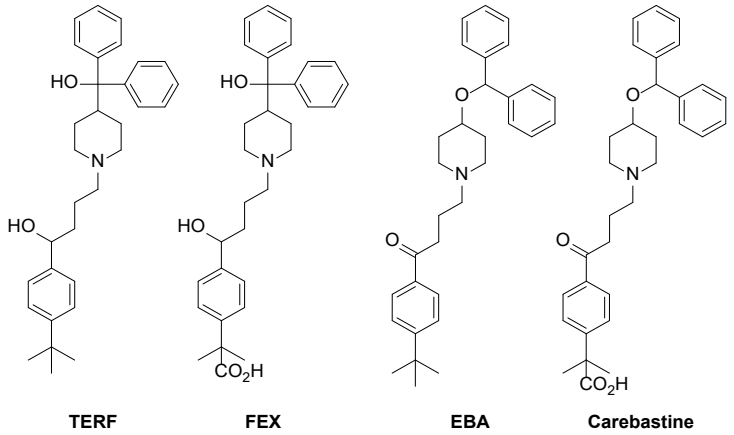

Fig. 5.1. Structures of the antihistamines terfenadine (TERF), fexofenadine (FEX), ebastine (EBA), and carebastine.

In Chapter 2, we observed synergy of TERF with all azole antifungals, except with fluconazole (FLC). Less synergy was observed with EBA and it appeared synergy was dependent on the fungal strain. Compared to TERF, FEX has an added hydroxyl group and is not able to cause hERG inhibition. FEX is currently approved by the FDA and is sold under the brand name Allegra®. To avoid drug-drug interactions, combinations with azoles and FEX were investigated for synergistic antifungal activity.

Combinations of FEX with posaconazole (POS) or voriconazole (VRC) were tested against four yeast strains (Table 5.1). The combination of FEX and POS displayed an FICI of 0.63 against *C. albicans* ATCC 10231 (strain *B*) indicating some positive interactions. However, it was apparent that FEX displayed no true synergistic effect against fungi. As no significant positive interactions were observed, combination with FEX were no longer explored. A similar outcome would be predicted for the active metabolite of EBA, carebastine.

Table 5.1. Combinational effect of FEX with POS or VRC against a variety of fungal strains.

Azole	Strain	MIC alone (µg/mL)		MIC combo (µg/mL)		FICI	Interp.	Azole	Strain	MIC alone (µg/mL)		MIC combo (µg/mL)		FICI	Interp.
		Azole	FEX	Azole	FEX					Azole	FEX	Azole	FEX		
POS	*B*	1	>128	0.5	16	0.63	pSYN	**VRC**	*B*	1	>128		128	2.00	ADD
	F	>32	>128	>32	>128	2.00	ADD		*F*	>32	>128	>32	>128	2.00	ADD
	G	>32	>128	>32	>128	2.00	ADD		*G*	>32	>128	>32	>128	2.00	ADD
	H	>32	>128	>32	>128	2.00	ADD		*H*	>32	>128	>32	>128	2.00	ADD

Strains: *A* = *C. albicans* ATCC MYA-1003, *B* = *C. albicans* ATCC 10231, *C* = *C. albicans* ATCC MYA-1237, *D* = *C. albicans,* ATCC MYA-2310, *E* = *C. albicans* ATCC MYA-2876, *F* = *C. albicans* ATCC 64124, *G* = *C. albicans* ATCC 90819, *H* = *C. glabrata* ATCC 2001, *I* = *C. glabrata* clinical isolate 1 (CG1), *J* = *C. glabrata* clinical isolate 2 (CG2), *K* = *C. glabrata* clinical isolate 3 (CG3), *L* = *C. krusei* ATCC 6258, *M* = *C. parapsilosis* ATCC 22019.
The FICI cutoff values for determining synergy are: synergistic (SYN) if FICI ≤ 0.5, additive (ADD) if 0.5 < FICI ≤ 4, antagonistic (ANT) if FICI > 4.
Note: Where the highest concentration of a compound or azole drug alone did not achieve optical growth inhibition, the MIC_{alone} value used in the FICI calculation is the highest concentration tested of that compound or azole drug. Combinations were tested in duplicate.
Indicates partial synergy (pSYN, both drugs showed reduction in MIC values and one drug showed ≥2-fold reduction in MIC value).
Indicates weak additive effect (ADD, neither of the drugs showed ≥2-fold reduction in MIC value).

5.2.2. Ebastine and non-azole antifungal combinations

The second strategy to repurpose antihistamines as antifungals was to explore combinations with the other two main classes of antifungals, the polyenes (*e.g.* amphotericin B (AmB) and nystatin (NYT)) and the echinocandins (*e.g.* caspofungin (CFG)). Neither of these antifungals are CYP inhibitors and therefore combinations with these are not expected to result in major side effects such as hERG inhibition and heart problems. Combinations of EBA and antifungals were all tested against four yeast strains

(Table 5.2). Both polyenes, AmB and NYT, displayed some positive interactions with EBA as both polyene combinations exhibited pSYN against two to three yeast strains. However, no synergistic combinations were observed. For CFG, synergy was observed with all four yeast strains. To explore whether the combination of EBA and CFG also had activity against filamentous fungi, the combination was tested against one *A. terreus* strain (strain *L*), but the combination was additive.

Table 5.2. Combinations of EBA with the antifungals AmB, NYT, and CFG against a panel of fungi.

Polyenes								Echinocandins							
Azole	Strain	MIC alone (μg/mL)		MIC combo (μg/mL)		FICI	Interp.	Azole	Strain	MIC alone (μg/mL)		MIC combo (μg/mL)		FICI	Interp.
		Azole	EBA	Azole	EBA					Azole	EBA	Azole	EBA		
AmB	*B*	3.9	>25	3.9	25	2.00	ADD	**CFG**	*B*	1	>25	0.016	6.3	0.27	SYN
	F	3.9	>25	3.9	25	2.00	ADD		*F*	0.5	>25	0.063	6..3	0.38	SYN
	G	0.98	>25	0.49	3.1	0.62	pSYN		*G*	1	>25	0.016	6.3	0.27	SYN
	H	1.95	>25	0.98	1.6	0.57	pSYN		*H*	>32	>25	1	3.1	0.16	SYN
									L	>32	>25	>32	>25	2.00	ADD
NYT	*B*	8	>25	4	3.1	0.62	pSYN								
	F	8	>25	4	0.8	0.53	pSYN								
	G	2	>25	2	25	2.00	ADD								
	H	4	>25	2	1.6	0.56	pSYN								

Strains: *B* = *C. albicans* ATCC 10231, *F* = *C. albicans* ATCC 64124, *G* = *C. albicans* ATCC 90819, *H* = *C. glabrata* ATCC 2001, *L*= *A. terreus* ATCC MYA-3633.
The FICI cutoff values for determining synergy are: synergistic (SYN) if FICI ≤ 0.5, additive (ADD) if 0.5 < FICI ≤ 4, antagonistic (ANT) if FICI > 4.
Note: Where the highest concentration of a compound or azole drug alone did not achieve optical growth inhibition, the MIC_{alone} value used in the FICI calculation is the highest concentration tested of that compound or azole drug. Combinations were tested in duplicate.

	Indicates synergy (SYN, both drugs showed ≥4-fold reduction in MIC value).
	Indicates partial synergy (pSYN, both drugs showed reduction in MIC values and one drug showed ≥2-fold reduction in MIC value).
	Indicates weak additive effect (ADD, neither of the drugs showed ≥2-fold reduction in MIC value).

Some parameters that may influence whether synergistic interactions are observed and to what extent with CFG are in what MIC assay procedure is followed. For one, there is the paradoxical effect with CFG *in vitro* where to a certain concentration, CFG inhibits fungal growth and after a second point at a higher concentration of CFG, fungal growth is no longer inhibited likely due to a stress response.[147] Due to this and the fungistatic nature of CFG, CFG MIC standard protocol in the CSLI standards is to read the MIC-1 at 24 h. However, for other antifungals, such as the polyenes, the MIC-0 at 48 h is measured. And

in between, the MIC-1 of azoles are measured at 48 h. Here, the MIC-0 at 48 h is reported for all combinations, which cause higher MIC_{combo} values. However, maybe these should be compared to MIC-1 at 24 h values of CFG instead of MIC-0 at 48 h. It would be interesting to see the FICI values then as the paradoxical effect elevates MIC values, especially at 48 h. As the EBA and CFG combination appears synergistic, it would be useful to further expand the study to other *Candida* strains, including *C. auris*. It would also be necessary to include the other echinocandins, anidulafungin and micafungin.

5.2.3. Antihistamine and antibiotic combinations

As the antihistamines EBA and TERF displayed synergistic activity with the azole antifungals, it was hypothesized that the antihistamines may also act as an adjuvant with antibiotics against bacteria. Some investigations have already demonstrated that TERF possesses some antibacterial activity against Gram-positive bacteria[284] while FEX does not.[415] Furthermore, the only class of antibiotics that are CYP inhibitors and would have drug-drug interactions with the antihistamines are the macrolides. Therefore, one antibiotic each from various classes were selected. Antibiotic classes represented are the β-lactams (ampicillin, AMP), the quinolones (ciprofloxacin, CIP), trimethoprim (TRI), tetracycline (TET), and aminoglycosides (tobramycin, TOB). The glycopeptide (vancomycin, VAN) was also included for Gram-positive strains.

TERF combinations were tested against two Gram-positive and two Gram-negative strains (Table 5.3). Only an additive effect was observed with *VRE* and *K. pneumoniae*. Some cases of partial synergy were observed against *B. anthracis* and *E. cloacae*. While *S. aureus*

has not been tested, TERF by itself does exhibit MIC values of 16 and 20 μg/mL against the two Gram-positive strains, *B. anthracis* and *VRE*, respectively. It is interesting to observe that in the cases of partial synergy against *B. anthracis*, the MIC_{combo} value for TERF remains constant while the MIC_{combo} decreased by 4-fold for the antibiotic.

Table 5.3. Combinational effect of antibiotics (AB) with the antihistamine, TERF, against a variety of bacterial strains.

Gram-positive								Gram-negative							
Azole	Strain	MIC alone (μg/mL)		MIC combo (μg/mL)		FICI	Interp.	Azole	Strain	MIC alone (μg/mL)		MIC combo (μg/mL)		FICI	Interp.
		AB	TERF	AB	TERF					AB	TERF	AB	TERF		
VRE	AMP	>32	20	32	20	2.00	ADD	*K. pne*	AMP	>32	>40	>32	>40	2.00	ADD
	CIP	>2	20	2	20	2.00	ADD		CIP	0.03	>40	0.03	40	2.00	ADD
	TRI	>32	20	32	20	2.00	ADD		TRI	>32	>40	>32	>40	2.00	ADD
	TET	32	20	32	20	2.00	ADD		TET	1	>40	1	40	2.00	ADD
	TOB	>32	20	32	20	2.00	ADD		TOB	1	>40	1	40	2.00	ADD
B. ant	AMP	>32	16	8	8	0.75	pSYN	*E. clo*	AMP	>32	>40	>32	>40	2.00	ADD
	CIP	4	16	4	16	2.00	ADD		CIP	0.06	>40	0.03	20	1.00	ADD*
	TRI	>32	16	>32	16	2.00	ADD		TRI	>32	>40	4	40	1.13	ADD*
	TET	0.5	16	0.13	16	0.75	pSYN		TET	2	>40	1	40	1.50	ADD*
	TOB	>32	16	>32	16	2.00	ADD		TOB	2	>40	1	5	0.63	pSYN

Antibiotics (AB): AMP = ampicillin, CIP = ciprofloxacin, TRI = trimethoprim, TET = tetracycline, TOB = tobramycin, VAN = vancomycin.
Gram-positive: *B. ant* = *Bacillus anthracis* Sterne strain, *VRE* = Vancomycin-resistant *Enterococcus*
Gram-negative = *E. clo* = *Enterobacter cloacae* ATCC 13047, *K. pne* = *Klebsiella pneumonia* ATCC 27736.
The FICI cutoff values for determining synergy are: synergistic (SYN) if FICI ≤ 0.5, additive (ADD) if 0.5 < FICI ≤ 4, antagonistic (ANT) if FICI > 4.
Note: Where the highest concentration of a compound or azole drug alone did not achieve optical growth inhibition, the MIC_{alone} value used in the FICI calculation is the highest concentration tested of that compound or azole drug. Combinations were tested in duplicate.

Indicates partial synergy (pSYN, both drugs showed reduction in MIC values and one drug showed ≥2-fold reduction in MIC value).
Indicates strong additive effect (ADD*, only one drug showed ≥2-fold reduction in MIC value).
Indicates weak additive effect (ADD, neither of the drugs showed ≥2-fold reduction in MIC value).

Combinations with EBA were tested against three Gram-positive and five Gram-negative strains (Table 5.4). EBA by itself had antibacterial activity against *B. anthracis* and *VRE*. Some combinations with partial synergy were displayed against Gram-positive bacteria, while combinations against Gram-negative were widely additive. The only exception with the Gram-negative bacteria and the only combinations to exhibit synergistic interactions were with EBA against the *E. coli* strain. Overall, both antihistamines, EBA and TERF, appear to have some antibiotic activity by themselves against Gram-positive bacteria, but are not synergistic with antibiotics.

Table 5.4. Combinational effect of antibiotics (AB) with the antihistamine, EBA, against a variety of bacterial strains.

Gram-positive								Gram-negative							
Strain	AB	MIC alone (µg/mL)		MIC combo (µg/mL)		FICI	Interp.	Strain	AB	MIC alone (µg/mL)		MIC combo (µg/mL)		FICI	Interp.
		AB	EBA	AB	EBA					AB	EBA	AB	EBA		
B. ant	AMP	>32	6.3	32	3.1	1.50	ADD*	*E. coli*	AMP	8	25	2	12.5	1.00	ADD*
	CIP	8	6.3	4	3.1	1.00	ADD*		CIP	0.004	>25	0.004	25	2.00	ADD
	TRI	>32	6.3	32	6.3	2.00	ADD		TRI	>32	25	0.13	12.5	0.50	SYN
	TET	0.13	6.3	0.02	3.1	0.65	pSYN		TET	1	>25	0.25	6.3	0.50	SYN
	TOB	>32	6.3	32	6.3	2.00	ADD		TOB						
	VAN	1	6.3	0.25	3.1	0.75	pSYN		VAN						
S. aur	AMP	0.13	>25	0.06	6.3	0.75	pSYN	*E. clo*	AMP	>32	>25	>32	>25	2.00	ADD
	CIP	0.25	>25	0.25	25	2.00	ADD		CIP	0.06	>25	0.06	25	2.00	ADD
	TRI	>32	>25	>32	>25	2.00	ADD		TRI	>32	>25	>32	>25	2.00	ADD
	TET	1	>25	0.25	12.5	0.75	pSYN		TET	2	>25	2	25	2.00	ADD
	TOB	0.5	>25	0.5	25	2.00	ADD		TOB	2	>25	2	25	2.00	ADD
	VAN	0.5	>25	0.5	25	2.00	ADD		VAN						
VRE	AMP	>32	6.3	32	6.3	2.00	ADD	*K. pne*	AMP	>32	>25	>32	>25	2.00	ADD
	CIP	>0.06	6.3	0.06	6.3	2.00	ADD		CIP	>0.06	>25	>0.06	>25	2.00	ADD
	TRI	>32	6.3	32	6.3	2.00	ADD		TRI	>32	>25	>32	>25	2.00	ADD
	TET	0.5	6.3	0.06	3.1	0.62	pSYN		TET	>8	>25	>8	>25	2.00	ADD
	TOB	>32	6.3	>32	6.3	2.00	ADD		TOB						
	VAN	1	6.3	0.25	3.1	0.75	pSYN		VAN						
S. epi	AMP							*S. ent*	AMP	4	>25	2	1.6	0.56	pSYN
	CIP								CIP	>0.06	>25	>0.06	>25	2.00	ADD
	TRI								TRI	>32	>25	>32	>25	2.00	ADD
	TET								TET	8	>25	8	25	2.00	ADD
	TOB								TOB						
	VAN								VAN						
L. mon	AMP							*P. aer*	AMP	>32	>25	>32	>25	2.00	ADD
	CIP								CIP	0.5	>25	0.5	25	2.00	ADD
	TRI								TRI	>32	>25	>32	>25	2.00	ADD
	TET								TET	8	>25	8	25	2.00	ADD
	TOB								TOB	1	>25	1	25	2.00	ADD
	VAN								VAN						

Antibiotics (AB): AMP = ampicillin, CIP = ciprofloxacin, TRI = trimethoprim, TET = tetracycline, TOB = tobramycin, VAN = vancomycin.
Gram-positive: *B. ant* = *Bacillus anthracis* Sterne strain, *L. mon* = *Listeria monocytogenes* ATCC 19115, *S. aur* = *Staphylococcus aureus* ATCC 25923, *S. epi* = *Staphylococcus epidermidis* ATCC 12228, *VRE* = Vancomycin-resistant *Enterococcus*
Gram-negative = *E. clo* = *Enterobacter cloacae* ATCC 13047, E. *coli* = *Escherichia coli* MC1060, *K. pne* = *Klebsiella pneumoniae* ATCC 27736, *P. aer* = *Pseudomonas aeruginosa* Boston 41501 ATCC 27853, *S. ent* = *Salmonella enterica* ATCC 14028.
The FICI cutoff values for determining synergy are: synergistic (SYN) if FICI ≤ 0.5, additive (ADD) if 0.5 < FICI ≤ 4, antagonistic (ANT) if FICI > 4.
Note: Where the highest concentration of a compound or azole drug alone did not achieve optical growth inhibition, the MIC_{alone} value used in the FICI calculation is the highest concentration tested of that compound or azole drug. Combinations were tested in duplicate.

	Indicates synergy (SYN, both drugs showed ≥4-fold reduction in MIC value).
	Indicates partial synergy (pSYN, both drugs showed reduction in MIC values and one drug showed ≥2-fold reduction in MIC value).
	Indicates strong additive effect (ADD*, only one drug showed ≥2-fold reduction in MIC value).
	Indicates weak additive effect (ADD, neither of the drugs showed ≥2-fold reduction in MIC value).

5.2.4. Additional gold(I)-phosphine complexes

The gold(I)-phosphine complexes discussed in Chapter 3 displayed good to excellent antifungal activity against a broad range of fungal species.[405] Other gold(I)-phosphine complexes were obtained from the Awuah laboratory for antifungal testing (Fig. 5.2).

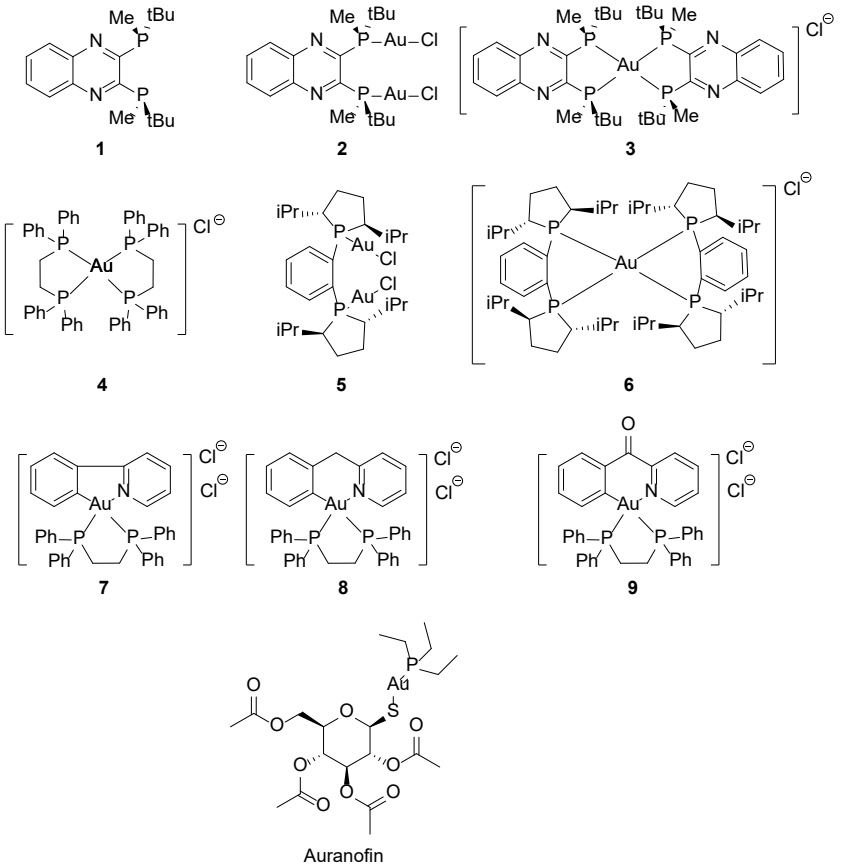

Fig. 5.2. Structures of cpds **1-9** and auranofin.

5.2.4.1. Minimum inhibitory concentration assays

All compounds were initially tested against a panel of six fungal strains including three *C. albicans*, one *C. parapsilosis*, and two *Aspergillus* spp. Compounds **2** and **3** were also tested against a larger panel including thirteen *Candida* and *Aspergillus* strains (Table 5.5).

For the first scaffold, the ligand (cpd **1**) and the linear molecule (cpd **2**) displayed no antifungal activity while the square planar complex (cpd **3**) had excellent antifungal activity against *Candida* spp. with activity similar to the known antifungal AmB. Against *Aspergillus* spp., cpd **3** displayed some activity, but only poor activity. This corresponds to

the trends observed in Chapter 2. Below, cpd **3** was evaluated in cytotoxicity, hemolysis, disruption of a pre-formed biofilm, and development of resistance assays as this work was done alongside the testing in Chapter 2. Other analogues should be synthesized and tested. Additional testing for cpd **3** would be in a time-kill assay to see if it is fungicidal.

With the second scaffold, compounds tested included both the linear cpd **5** and its corresponding square planar complex cpd **6**. In this case, both compounds were inactive against all six fungal strains, similar to auranofin. Auranofin here is used as a standard as it is an older FDA approved medicine for rheumatoid arthritis and has more recently been investigated for being repurposed as an antimicrobial agent and shows some promise as an antibacterial.[326-330] This scaffold does not warrant further investigation as an antifungal. Instead, cpds **5** and **6** should be checked for antibacterial activity.

The third scaffold consisting of cpds **7-9**, displayed good antifungal activity. Compound **8** displayed the best antifungal activity with MIC values of 0.98-1.95 μg/mL against *Candida* spp. similar to cpd **3** and AmB. It is also important to note that cpd **8** displayed the best activity of all nine compounds and AmB against *Aspergillus* spp. Compound **7** also displayed good activity against *Candida* spp., but had MIC values of 1.95-3.9 μg/mL, which is 2-fold greater than for cpd **8**. Compound **9** also displayed considerably good MIC values against *Candida* spp., but were in the range of 3.9-7.8 μg/mL, which is 4-fold greater than cpd **8**. In addition, a fourth scaffold, cpd **4**, also exhibits good activity against *Candida albicans*, however, not as good as the third scaffold. This third scaffold, cpds **7-9**, warrant further investigation including the synthesis of more analogues for a more in-depth SAR

study. Cpds **7** and **9** were also included in cytotoxicity studies below. Further biological testing with MIC testing against *C. auris* strains, as well as biofilm, time-kill, and development of resistance studies would be beneficial.

Table 5.5. MIC values in µg/mL for compounds **1-9** against various fungal strains.

Strains		Compound										
		1	**2**	**3**	**4**	**5**	**6**	**7**	**8**	**9**	**Auranofin**	**AmB**
Candida albicans	*A*	>31.3	15.6	0.98	NT	NT	NT	NT	NT	NT	>31.3	0.98
	B	>31.3	>31.3	0.98	NT	NT	NT	NT	NT	NT	>31.3	3.9
	C	>31.3	31.3	1.95	NT	NT	NT	NT	NT	NT	>31.3	3.9
	D	NT	>31.3	1.95	7.8	>31.3	31.3	3.9	1.95	7.8	>31.3	7.8
	E	>31.3	>31.3	0.98	NT	NT	NT	NT	NT	NT	>31.3	3.9
	F	NT	>31.3	0.98	7.8	31.3	15.6	1.95	0.98	3.9	>31.3	3.9
	G	>31.3	>31.3	1.95	7.8	31.3	15.6	3.9	1.95	3.9	>31.3	0.98
Non-*albicans Candida*	*H*	>31.3	31.3	0.98	NT	NT	NT	NT	NT	NT	>31.3	1.95
	I	NT	>31.3	1.95	NT	NT	NT	NT	NT	NT	31.3	3.9
	J	NT	>31.3	0.98	15.6	>31.3	>31.3	3.9	1.95	3.9	>31.3	0.98
Aspergillus	*K*	NT	>31.3	15.6	15.6	>31.3	>31.3	7.8	1.95	15.6	3.9	>31.3
	L	NT	31.3	7.8	31.3	>31.3	>31.3	15.6	3.9	15.6	7.8	>31.3
	M	NT	>31.3	>31.3	NT	NT	NT	NT	NT	NT	>31.3	>31.3

***Candida albicans* strains:** *A = C. albicans* ATCC MYA-1003, *B = C. albicans* ATCC 10231, *C = C. albicans* ATCC MYA-1237, *D = C. albicans,* ATCC MYA-2310, *E = C. albicans* ATCC MYA-2876, *F = C. albicans* ATCC 64124, *G = C. albicans* ATCC 90819.
Non-*albicans Candida* strains: *H = C. glabrata* ATCC 2001, *I = C. krusei* ATCC 6258, *J = C. parapsilosis* ATCC 22019.
***Aspergillus* strains:** *K = A. nidulans* ATCC 38163, *L = A. terreus* ATCC MYA-3633, *M = A. flavus* ATCC MYA-3631.
Note: Compounds were tested in duplicate.

	MIC ≤1.95 µg/mL (excellent antifungal activity)
	MIC = 3.9-7.8 µg/mL (good antifungal activity)
	MIC ≥15.6 µg/mL (poor antifungal activity)

5.2.4.2. Cytotoxicity

To establish a therapeutic window for these gold(I)-phosphine complexes, cpds **3**, **5**, **7**, **8**, and **9** were selected for cytotoxicity testing along with auranofin as a known standard (Fig. 5.3). Compound **3** and auranofin were tested against four cell lines: human adenocarcinoma (A549), a human bronchial epithelial (BEAS-2B), human embryonic kidney (HEK-293), and mouse macrophage (J774A.1) cell lines. Less than 50% cell survival is observed with the A549, BEAS-2B, and HEK-293 cell lines for cpd **3** at and above 7.8 µg/mL and at 3.9 µg/mL with the J774A.1 cell line. This demonstrates an approximate 2- to 4-fold therapeutic window. Therefore, cpd **3** is less selective for the *Candida* spp. than desired.

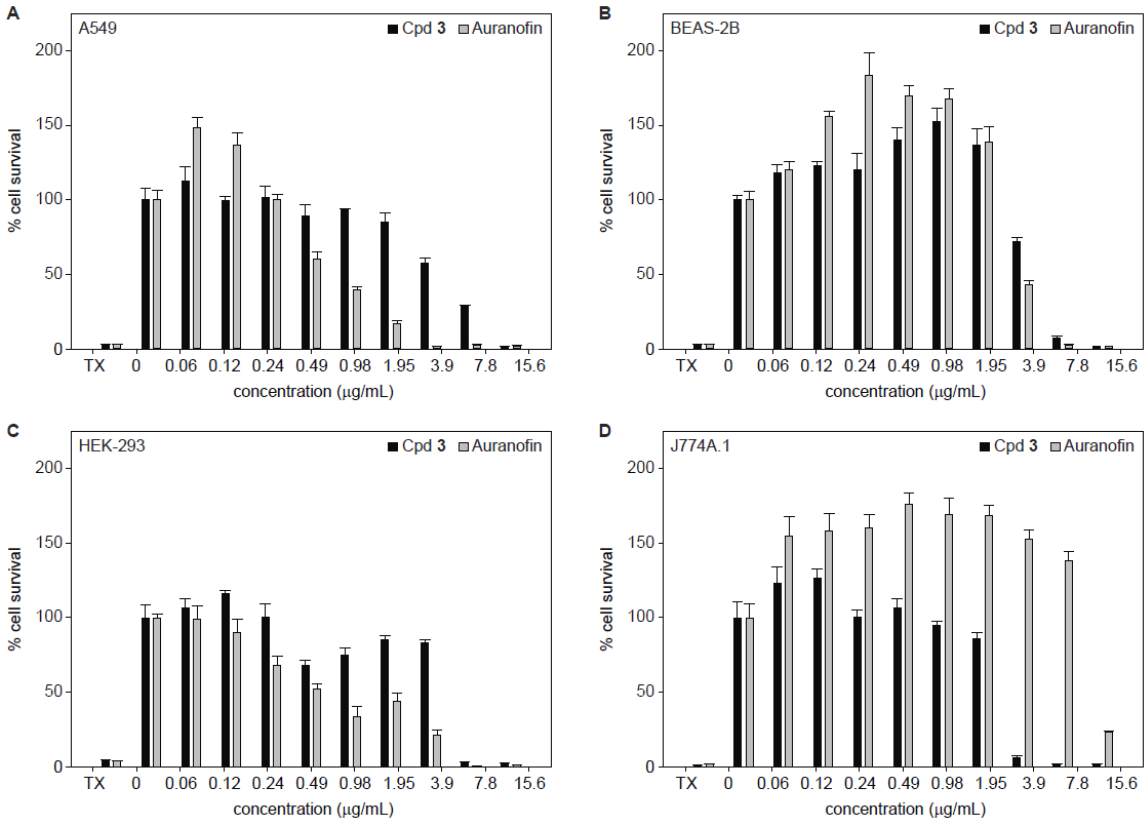

Fig. 5.3. Evaluation of cytotoxicity for cpd **3** and auranofin with **A.** A549, **B.** BEAS-2B, **C.** HEK-293, and **D.** J774A.1 cell lines. Controls include treatment with Triton-X® (TX, 1% *v/v*, positive control) and 0.5% DMSO (negative control). Compounds were tested in quadruplicate.

For the other gold(I)-phosphine complexes, cpds **5**, **7**, **8**, and **9**, all four compounds display at least 50% cell survival against the A549 cell line with cpds **7** and **9** exhibiting near 100% cell survival (Fig. 5.4). When tested with HEK-293, all four compounds display greater than 50% cell survival up to 7.8 µg/mL. At 15.6 µg/mL cpds **8** and **9** have near 100% cell survival, cpd **7** is near 50% and cpd **5** is less than 50%. Compounds **7**, **8**, and **9** all display an approximate 4-fold therapeutic window, although cpds **7** and **8** had the greatest cell survival and two lowest MIC values. Compound **9** has greater than 50% cell survival at 15.6 µg/mL for both cell lines, but MIC values also at 3.9-15.6 µg/mL, which is 2-fold higher than cpds **7** and **8**.

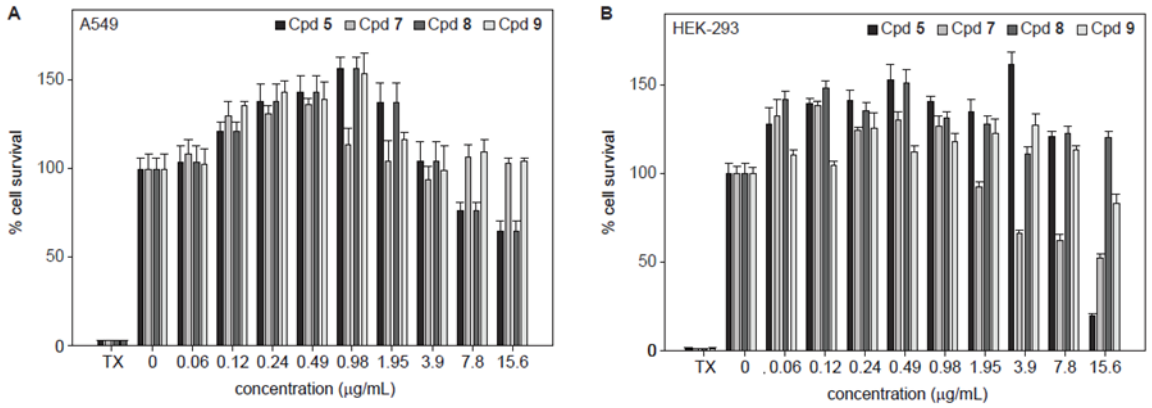

Fig. 5.4. Evaluation of cytotoxicity for cpds **5**, **7**, **8**, and **9** with **A.** A549 and **B.** HEK-293 cell lines. Controls include treatment with Triton-X® (TX, 1% *v/v*, positive control) and 0.5% DMSO (negative control). Compounds were tested in quadruplicate.

5.2.4.3. Hemolysis

In addition to cytotoxicity testing, cpd **3** was examined for hemolytic activity with both human and murine red blood cells (Fig. 5.5). Here, auranofin and AmB are used as known standards. AmB is known to exhibit hemolytic activity and in this experiment, significant hemolytic activity was observed beginning at 3.9 μg/mL. Compound **3** displays increased hemolytic activity with 100% hemolysis for both human and mouse red blood cells at 7.8 μg/mL, which is only 2- to 4- fold greater than MIC values with *Candida* spp.

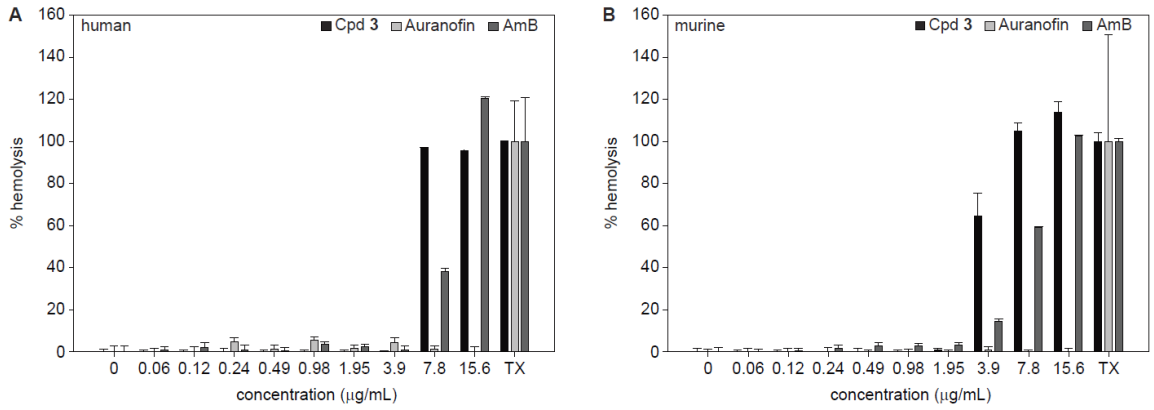

Fig. 5.5. Evaluation of hemolytic activity for cpd **3**, auranofin, and AmB with **A.** human RBCs and **B.** murine RBCs. Controls include treatment with Triton-X® (TX, 1% *v/v*, positive control) and 0.5% DMSO (negative control). Compounds were tested in quadruplicate.

5.2.4.4. Disruption of a pre-formed biofilm

To further evaluate the antifungal potential of cpd **3**, we tested the ability of cpd **3** and the ligand, cpd **1**, to disrupt a pre-formed biofilm (Table 5.6, Fig. 5.6). The ligand was inactive against *C. glabrata* ATCC 2001 (strain *H*) and not tested against *C. albicans* ATCC 10231 (strain *B*). Compound **3** was somewhat more effective at disrupting the biofilm of *C. glabrata* ATCC 2001 (strain *H*) with an $SMIC_{90}$ value of 7.8 μg/mL, which is only 2-fold greater than AmB against the same biofilm and 8-fold greater than the MIC value for cpd **3** against the same strain. Against *C. albicans* ATCC 10231 (strain *B*) cpd **3** exhibited poor activity when considering the $SMIC_{90}$ value, however, the $SMIC_{50}$ value of 1.95 μg/mL is the same $SMIC_{50}$ value as AmB. Further testing of the antibiofilm activity of cpd **3** should include a *C. auris* strain and also a prevention of biofilm formation assay.

Table 5.6. Disruption of a pre-formed biofilm by compounds **1**, **3**, auranofin, and AmB against two fungal strains.			
Strain	Compound	$SMIC_{50}$ (μg/mL)	$SMIC_{90}$ (μg/mL)
B	**1**		
	3	1.95	15.6
	Auranofin	3.9	15.6
	AmB	1.95	>31.3
H	**1**	>31.3	>31.3
	3	3.9	7.8
	Auranofin	3.9	>31.3
	AmB	0.49	3.9
Strains: *B* = *C. albicans* ATCC 10231, *H* = *C. glabrata* ATCC 2001. *Note*: Compounds were tested in duplicate.			
	MIC ≤1.95 μg/mL (excellent antifungal activity)		
	MIC = 3.9-7.8 μg/mL (good antifungal activity)		
	MIC ≥15.6 μg/mL (poor antifungal activity)		

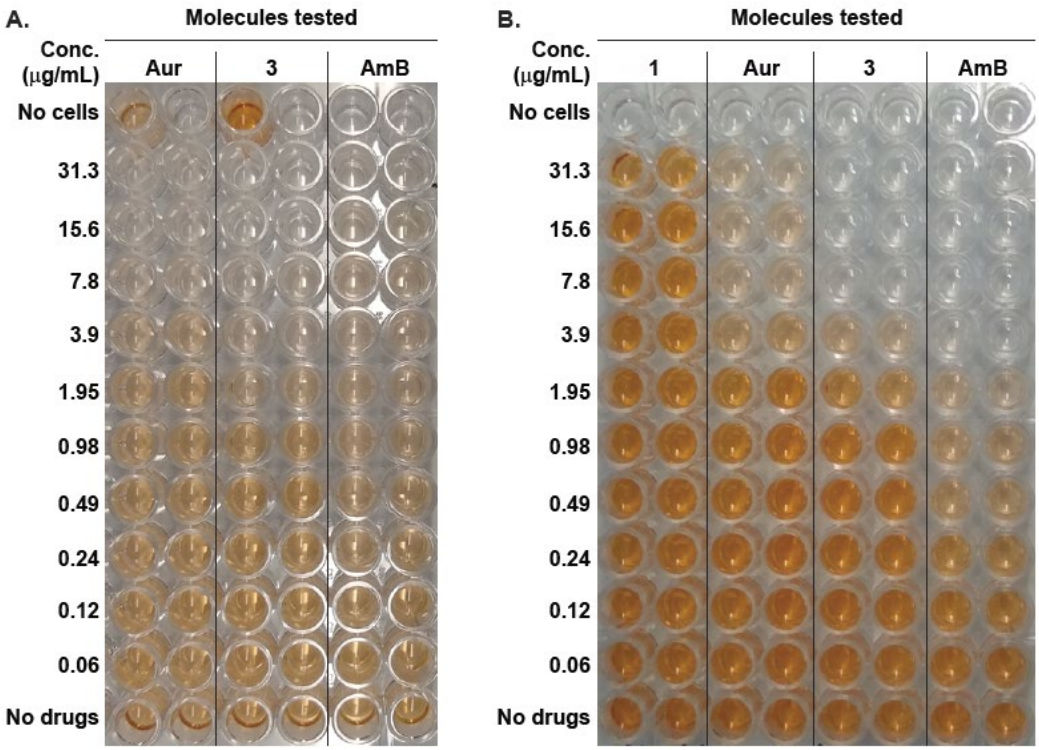

Fig. 5.6. Disruption of a pre-formed biofilm for cpd **1**, auranofin, cpd **3**, and AmB against **A.** *C. albicans* ATCC 10231 (strain *B*) and **B.** *C. glabrata* ATCC 2001 (strain *H*). Compounds were tested in duplicate.

5.2.4.5. Development of resistance

To evaluate whether yeast can develop resistance to cpd **3** during continued exposure, a development of resistance assay was performed against *C. albicans* ATCC 10231 (strain *B*) and *C. glabrata* ATCC 2001 (strain *H*) (Fig. 5.7). Against both strains, neither cpd **3**

nor the control, AmB, exhibited MIC changes greater than 2-fold suggesting that the yeast are not able to develop resistance.

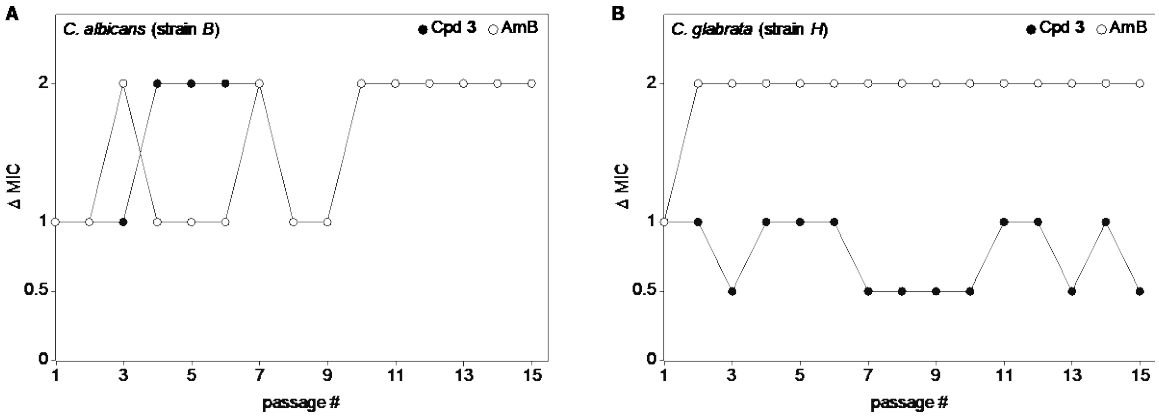

Fig. 5.7. Fold-change in MIC values of cpd **3** and AmB over 15 passages against **A**. *C. albicans* ATCC 10231 (strain *B*) and **B.** *C. glabrata* ATCC 2001 (strain *H*). MICs were tested in duplicate.

5.2.5. Monohydrazides

A sample of hydrazide analogues of the monohydrazone from Chapter 4 were synthesized and tested for their antifungal activity. We are currently in the process of expanding the library of monohydrazides for a full SAR analysis. The monohydrazides, for drug design purposes, improve upon the monohydrazones as the hydrazide is less prone to being metabolized.

5.2.5.1. Synthesis

At this point, twenty-two monohydrazides have been synthesized towards this project (Fig. 5.8.) as well as a fluorescent analogue and a biotinylated analogue. Synthesis involves starting with one of three molecules (2,4-difluorobenzoic acid, picolinic acid, or pyrazinoic acid) and doing a condensation with a substituted phenylhydrazine (*i.e.*, 3-fluorobenzyl hydrazine, 4-fluorobenzyl hydrazine, 4-chlorobenzyl hydrazine, 4-methoxybenzyl

hydrazine, 2,4-difluorobenzyl hydrazine). Synthesis of a full library of compounds for a SAR study is in progress and characterization of the monohydrazides will be reported in a manuscript in due course.

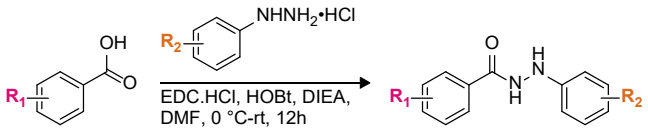

Fig. 5.8. General synthetic scheme for the monohydrazides, cpds **10-32** (the structures of the compounds are shown in Tables 5.7-5.9).

5.2.5.2. Minimum inhibitory concentration assays

Compounds **10-16** were initially tested against a few fungal strains and observed to have excellent activity. Therefore, cpds **10-16** testing was expanded to a panel of ten *C. auris* strains (Table 5.7) and ten related drug-resistance *Candida* strains (Table 5.8). Compound demonstrated excellent activity against most *Candida* strains with MIC values ranging from 0.12-3.9 μg/mL. The only exception is cpd **12** which was investigated to identify a location on the monohydrazide where a probe could successfully be linked.

Table 5.7. MIC values in µg/mL for compounds **10-16** against ten *C. auris* strains.

		AR Bank #									
Cpd #	Structure	0381	0382	0383	0384	0385	0386	0387	0388	0389	0390
10	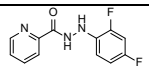	0.49	0.49	0.49	0.49	0.49	0.49	0.12	0.12	0.24	0.12
11	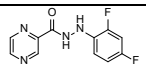	3.9	1.95	0.98	3.9	0.98	0.49	0.49	0.49	0.49	0.98
12	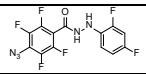	31.3	3.9	7.8	7.8	3.9	3.9	7.8	>31.3	3.9	7.8
13	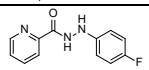	0.98	1.95	1.95	3.9	0.98	0.49	0.98	0.98	0.49	0.98
14	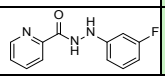	0.49	0.98	1.95	1.95	0.98	0.49	0.49	0.49	0.12	0.24
15	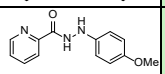	1.95	1.95	1.95	3.9	0.98	0.24	0.49	0.49	0.24	0.12
16	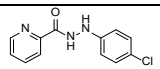	1.95	3.9	1.95	1.95	1.95	0.98	1.95	1.95	0.98	1.95
AmB		0.98	0.98	1.95	1.95	1.95	0.98	0.98	1.95	1.95	1.95

Note: Compounds were tested in duplicate.

MIC ≤1.95 µg/mL (excellent antifungal activity)
MIC = 3.9-7.8 µg/mL (good antifungal activity)
MIC ≥15.6 µg/mL (poor antifungal activity)

Table 5.8. MIC values in µg/mL for compounds **10-16** against ten *C. auris*-related strains.

		AR Bank #									
Cpd #	Structure	0391	0392	0393	0394	0395	0396	0397	0398	0399	0400
10	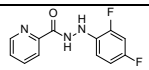	0.12	0.49	0.49	3.9	0.24	0.98	0.03	1.95	0.49	0.49
11	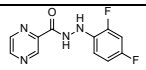	0.49	0.24	0.24	7.8	1.95	0.98	1.95	3.9	7.8	1.95
12	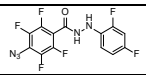	3.9	3.9	0.98	7.8	0.49	0.49	0.24	7.8	31.3	3.9
13	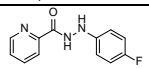	0.49	0.49	0.24	0.24	0.12	0.24	0.24	1.95	3.9	1.95
14	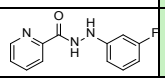	0.49	0.24	0.12	0.49	≤0.06	0.24	0.24	0.98	1.95	1.95
15	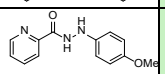	0.98	0.98	0.49	0.98	0.49	0.49	0.49	0.98	1.95	0.98
16	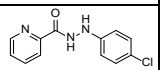	0.98	0.98	0.49	0.40	0.12	0.24	0.24	0.98	0.98	0.98
AmB		7.8	7.8	15.6	0.98	3.9	1.95	0.49	3.9	15.6	1.95

Strains: AR Bank # 0391, 0392, 0394 = *C. duobushaemulonii*; 0393, 0395 = *C. haemulonii*; 0396 = *K. ohmeri*; 0397 = *C. krusei*; 0398 = *C. lusitaniae*; 0399, 0400 = *S. cerevisiae.*

Note: Compounds were tested in duplicate.

MIC ≤1.95 µg/mL (excellent antifungal activity)
MIC = 3.9-7.8 µg/mL (good antifungal activity)
MIC ≥15.6 µg/mL (poor antifungal activity)

As compounds **10**, **11**, and **13-16** all displayed excellent activity against the twenty strains tested, which are known to be drug-resistant, more monohydrazides were synthesized to include cpds **17-32**. Again, all compounds exhibit good to excellent activity with only a few instances of poor activity against a *C .auris* strains. There is not a clear trend on any effect of the R_2 substituents. Compounds with picoline do appear to be better than pyrazine acid which is better than 2,4-difluoro. For this study, synthesis of the remaining library, MIC testing against the full panel of *C. albicans* and non-*albicans Candida*, biofilm, time-kill, cytotoxicity, hemolysis, and development of resistance assays are remaining.

Table 5.9. MIC values in µg/mL for compounds **17-32** against three *Candida* spp. strains.

		Strains					Strains		
Cpd #	Structure	*B*	0384	0390	Cpd #	Structure	*B*	0384	0390
17	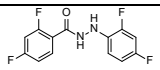	1.95	15.6	7.8	**14**	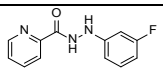	0.06	1.95	0.24
10	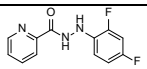	0.12	0.49	0.12	**25**	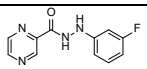	0.24	0.98	0.98
11	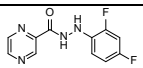	0.24	3.9	0.98	**15**	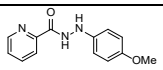	0.12	3.9	0.12
12	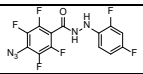	0.24	7.8	7.8	**26**	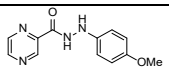	0.49	0.48	0.49
18	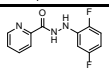	0.12	0.24	0.98	**27**	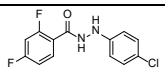	1.95	7.8	>31.3
19	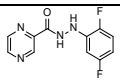	0.24	0.48	1.95	**16**	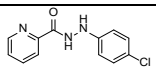	0.12	1.95	1.95
20	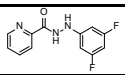	≤0.06	0.24	0.49	**28**	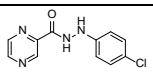	0.98	1.95	3.9
21	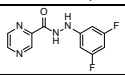	0.24	0.48	1.95	**29**	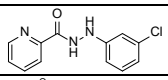	0.12	0.98	0.98
22	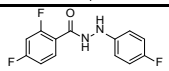	0.49	1.95	1.95	**30**	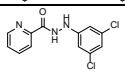	0.24	7.8	1.95
13	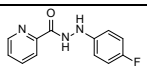	0.12	3.9	0.98	**31**	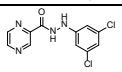	0.24	1.95	0.98
23	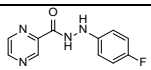	0.24	0.48	0.98	**32**	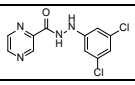	0.49	15.6	7.8

Strains: *B* = *C. albicans* ATCC 10231, 0384 = *C. auris* AR Bank # 0384, 0390 = *C. auris* AR Bank # 0390.
Note: Compounds were tested in duplicate.

	MIC ≤1.95 µg/mL (excellent antifungal activity)
	MIC = 3.9-7.8 µg/mL (good antifungal activity)
	MIC ≥15.6 µg/mL (poor antifungal activity)

5.2.5.3. Probing the target of monohydrazides

We have developed two potential approaches to elucidate the target within the fungal cell for the monohydrazides and their mechanism of action. Both approaches require chemical modification of the monohydrazide molecule to add a probe, either a fluorescent or biotin molecule, which acts to detect the monohydrazide within the cell or after cell lysis.

5.2.5.3.1. Analogue for fluorescence microscopy

The probe was synthesized in the Watt laboratory and given for MIC testing to ensure that antifungal activity was retained (Fig. 5.9). The MIC of the probe was tested against four fungal strains and shown to be active with good activity (Table 5.10). The probe will next be fed to the yeast and imaged using a fluorescent microscope. The goal of the probe is to determine the relative area in the cell where the molecule is congregating, and this may be useful in identifying a protein target. In addition, microscopy will be used to observe if treatment with monohydrazides causes any changes in yeast cell morphology.

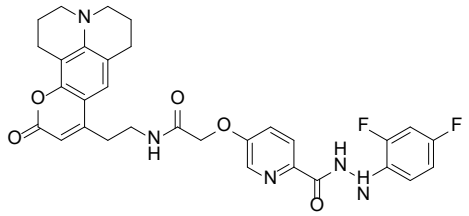

Fig. 5.9. Structure of the fluorescent probe, cpd **33**

Table 5.10. MIC values for cpd **33** against four *Candida* strains.		
	Strain	MIC (µg/mL)
Candida albicans	*B*	0.98
	F	3.9
Candida auris	0384	3.9
	0390	1.95
Strains: *B* = *C. albicans* ATCC 10231, *F* = C. *albicans* ATCC 64124, 0384 = *C. auris* AR Bank # 0384, 0390 = *C. auris* AR Bank # 0390. *Note*: Compound was tested in duplicate.		
	MIC ≤1.95 µg/mL (excellent antifungal activity)	
	MIC = 3.9-7.8 µg/mL (good antifungal activity)	

5.2.5.3.2. Biotinylated analogue for pull-down assay

The second strategy is to use a biotinylated analogue in a pulldown assay to isolate protein to which the monohydrazides bind. The biotinylated analogue, cpd **39**, was acquired from the Watt laboratory. The probe as well as its intermediates in the synthetic were tested for antifungal activity (Table 5.11). As the molecule becomes larger the MIC values increase. Fortunately, the biotinylated analogue does retain antifungal activity with a MIC value of 1.95 µg/mL against *C. albicans* ATCC 10231 (strain *B*). As the biotinylated probe still has moderate antifungal activity, it can be used in a pull-down assay to try to identify a protein target.

Table 5.11. MIC values for cpds **34-39** against one *C. albicans* strains		
Cpd #	Structure	Strain *B*
34	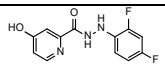	≤0.06
35	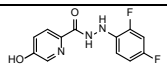	≤0.06
36	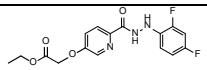	0.12
37	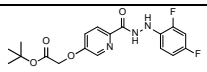	0.24
38	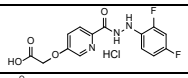	0.98
39	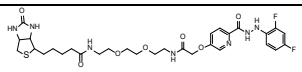	1.95
AmB		3.9
Strains: *B* = *C. albicans* ATCC 10231. *Note*: Compounds were tested in duplicate.		
	MIC ≤1.95 µg/mL (excellent antifungal activity)	
	MIC = 3.9-7.8 µg/mL (good antifungal activity)	

5.3. EXPERIMENTAL

5.3.1. Strains and culture conditions

For fungal assays, the *Candida albicans* strains, including MYA-1003 (strain *A*), MYA-1237 (strain *C*), MYA-2310 (strain *D*), 90819 (strain *G*), and as well as the non-*albicans Candida* fungi *C. glabrata* ATCC 2001 (strain *H*), *C. krusei* ATCC 6258 (strain *I*), *C. parapsilosis* ATCC 22019 (strain *J*) were purchased from the American Type Culture Collection (ATCC, Manassas, VA, USA). The remaining *C. albicans* strains, including 10231 (strain *B*), MYA-2876 (strain *E*), and 64124 (strain *F*), were a generous gift from Dr. Jon Y. Takemoto (Utah State University, Logan, UT, USA). A panel of *Candida auris* strains were acquired from the CDC & FDA Antibiotic Resistance Isolate Bank (CDC, Atlanta, GA, USA), which included *C. auris* AR Bank # 0381-0390. The filamentous fungi *Aspergillus nidulans* ATCC 38163 (strain *K*) was a kind gifts from Prof. Jon S. Thorson (University of Kentucky, Lexington, KY), while the *Aspergillus terreus* ATCC MYA-3633 (strain *L*) and *Aspergillus flavus* ATCC MYA-3631 (strain *M*) were purchased from the ATCC. Yeast strains were cultured at 35 °C in yeast extract peptone dextrose (YEPD) broth. *Aspergillus* spp. strains were cultured on potato dextrose agar (PDA, catalog # 110130, EMD Millipore, Billerica, MA, USA) at 28 °C before the spores were harvested. All fungal experiments were carried out in RPMI 1640 medium (catalog # R6504, Sigma-Aldrich, St. Louis, MO, USA) buffered to pH 7.0 with 0.165 M MOPS buffer (Sigma-Aldrich, St. Louis, MO, USA).

Bacterial strains used included five Gram-positive and five Gram-negative strains. Gram-positive strains included *Bacillus anthracis* Sterne strain, *Listeria monocytogenes* ATCC 19115, *Staphylococcus aureus* ATCC 25923, *Staphylococcus epidermidis* ATCC 12228, and vancomycin-resistant *Enterococcus* (VRE). Gram-negative strains consisted of *Enterobacter cloacae* ATCC 13047, *Escherichia coli* MC1060, *Klebsiella pneumoniae* ATCC 27736, *Pseudomonas aeruginosa* Boston 41501 ATCC 27853, and *Salmonella enterica* ATCC 14028. Bacteria were grown at 37 on Mueller Hinton (MH) medium (Sigma-Aldrich, St. Louis, MO, USA). *VRE* was a gift from Prof. David H. Sherman (University of Michigan, Ann Arbor, MI, USA). *L. monocytogenes* ATCC 19115, *S. enterica* ATCC 14028, *K. pneumoniae* ATCC 27736, and *E. coli* MC1061 were a kindly provided by Prof. Paul J. Hergenrother (University of Illinois at Urbana-Champaign, Champaign, IL, USA). *E. cloacae* ATCC 13047, *S. epidermidis* ATCC 12228 were a kind gift from Prof. Dev P. Arya (Clemson University, Clemson, SC, USA).

For cytotoxicity assays, the human embryonic kidney cell line (HEK-293) was purchased from the ATCC. The human bronchial epithelial cell line (BEAS-2B), the human lung carcinoma cell line (A549), and the mouse macrophage cell line (J774A.1) were generous gifts from Prof. David K. Orren (University of Kentucky, Lexington, KY), Prof. Markos Leggas (University of Kentucky, Lexington, KY), and Prof. David J. Feola (University of Kentucky, Lexington, KY), respectively. A549, HEK-293, and BEAS-2B cells were cultured in Dulbecco's Modified Eagle's Medium (DMEM, catalog # VWRL0100, VWR, Chicago, IL) supplemented with 10% fetal bovine serum (FBS; from ATCC) and 1% penicillin/streptomycin (from ATCC) at 37 °C with 5% CO_2. The J774A.1 cells were

cultured in DMEM (catalog # 30-2002, ATCC, Manassas, VA), which was also supplemented with FBS and antibiotics and grown at 37 °C with 5% CO_2.

Instrumentation for fungal assays with yeast were the V-1200 spectrophotometer (VWR, Radnor, PA, USA) and the SpectraMax M5 plate reader (Molecular Devices, Sunnyvale, CA, USA) for biofilm, cytotoxicity, and hemolysis assays. The known antifungal drugs, amphotericin B (AmB, VWR, Chicago, IL, USA), caspofungin (CFG, Sigma-Aldrich, St. Louis, MO, USA), fluconazole (FLC, AK Scientific, Union City, CA, USA), voriconazole (VRC, AK Scientific, Union City, CA, USA), and the antirheumatic drug, auranofin (Santa Cruz Biotechnology, Dallas, TX, USA) were used as positive controls. All other chemicals were supplied from Sigma-Aldrich (St. Louis, MO, USA).

5.3.2. Minimum inhibitory concentration assays.

The individual minimum inhibitory concentration (MIC) values for all compounds were measured using the broth microdilution method[305] in sterile 96-well plates as in Chapters 3, 4, and 5. Compound stocks were made to be 5 mg/mL in DMSO and diluted by serial two-fold dilution in the assay to final concentrations of 0.06-31.3 μg/mL. For yeast, the overnight culture was diluted into RPMI 1640 (25 μL of a fungal stock with OD_{600} of 0.12-0.15 into 10 mL of RPMI 1640 medium, resulting in final inoculum size around $1\text{-}5\times10^3$ CFU/mL) and added to the plate (100 μL per well), making a final volume of 200 μL total per well. Similarly, for *Aspergillus* spp., spores were diluted in RPMI 1640 to 5×10^5 spores/mL then 100 μL of stock was seeded in each well.[370] The MIC value of each compound was determined by visual inspection. For *Candida* spp., plates were incubated

for 48 h at 35 °C and *Aspergillus* spp. were incubated for 72 h at 35 °C (Table 5.5, Table 5.7-5.11).

5.3.3. Checkerboard assays

Checkerboard assays for fungal strains were performed as described in Chapter 2. Compounds (antifungals and antibiotics) were serially diluted lengthwise in RPMI-1640 in a 96-well plate. The antihistamines were serially diluted in culture tubes before being added to the 96-well plate with serial dilutions going along the width of the plate. The antifungals POS, VRC, AmB, CFG, and NYT were tested in the range of 0.06-32 μg/mL as well as the antibiotics AMP, CIP, TET, TRI, TOB, and VAN. EBA was tested in the range of 0.4-25 μg/mL and TERF was tested from 0.8-40 μg/mL except with *B. anthracis* where TERF was tested in the range of 0.5-32 μg/mL. Yeasts suspensions were prepared as described above for MIC assays. For bacterial strains, the same experimental setup was used. The overnight bacterial culture was diluted 1:1000 in MH medium. The inoculum is then incubated at 37 °C with 200 rpm rotation for 2-4 h until the OD_{600} is approximately 0.4. The culture is then diluted 1:1000 into MH medium and 100 mL per well is added to the 96-well plate. Bacterial plates are incubated at 37 °C for 24 h. All experiments were done in duplicate (Table 5.1-5.4).

5.3.4. Cytotoxicity

To examine the selectivity index for fungal cells compared to mammalian cells, cytotoxicity assays were performed as described in Chapter 3. Four mammalian cell lines, HEK-293, A549, BEAS-2B, and J774A.1 cells, were used for testing cpds **3**, **5**, **7**, **8**, and **9**

as well as auranofin. HEK-293 and J774A.1 cells were plated at 1×10^4 cells/mL while A549 and BEAS-2B were plated at 3×10^3 cells/mL. Compound stocks were dissolved in DMSO at 3.14 mg/mL and diluted in DMSO before being further diluted in DMEM and added to the 96-well plate with final concentrations ranging from 0.06 to 15.6 μg/mL (Fig. 5.3 and 5.4). All assays were done in quadruplicate.

5.3.5. Hemolysis

To extend on the cytotoxicity results, cpds **3** along with auranofin and AmB, were tested for their ability to lyse red blood cells (RBCs). Both human and murine RBCs were provided in a citrate-treated tube on ice and the hemolysis assay was done as previously described in Chapter 3 and in similar fashion to cytotoxicity assays. The RBCs were washed three times in PBS before being resuspended in PBS to achieve a cell concentration of on the order of 10^7 cells/mL. Stock concentration of compound were dissolved in DMSO at 3.14 mg/mL. Serial double dilutions were made in DMSO before being diluted in PBS and added to a 96-well plate to afford final concentrations of 0.06-15.6 μg/mL. Compounds were tested in quadruplicate with ~5×10^6 RBCs per well. The RBCs were also treated with 1% Triton-X® (positive control) and PBS (negative control). The RBCs were treated for 30 min at 37 °C and the absorbance was read at 595 nm. Hemolysis is visually observed by a decrease in optical density of the wells (turbid, dark red to transparent pink). Percent hemolysis (Fig. 5.5) was calculated using this equation after subtraction of the background absorbance (positive control):

$$\%\ \text{Hemolysis} = \frac{\text{absorbance of sample}}{\text{absorbance of RBC+PBS (negative control)}} \times 100$$

5.3.6. Disruption of a pre-formed biofilm

The biofilm assay for cpds **1**, **3**, auranofin, and AmB against *C. albicans* ATCC 10231 (strain *B*) and *C. glabrata* ATCC 2001 (strain *H*) was performed as described in Chapter 3. An overnight fungal culture was diluted to an OD_{600} of 0.15 in RPMI-1640 medium. 100 μL of fungal suspension was added per well to a 96-well plate and incubated for 24 at 37 °C. The plate was then washed thrice with 100 mL PBS before the addition of fresh RPMI-1640. Serial dilution of compounds was performed in the same fashion as described for MIC assays. Plates were again incubated for 24 at 37 °C. Finally, the plate was washed thrice with PBS before XTT was added and incubated at 37 °C for 3 h. Absorbance readings were read at 490 nm. All compounds were tested in duplicate and the SMIC was calculated as compared to the growth control (Table 5.6., Fig. 5.6).

5.3.7. Development of resistance

The development of resistance assay for cpd **3** was performed as described in Chapter 3. AmB and cpd **3** were tested in the concentration range of 0.06-31.3 μg/mL using the MIC format described above with *C. albicans* ATCC 10231 (strain *B*) and *C. glabrata* ATCC 2001 (strain *H*). Fungal suspension from the ½ × MIC wells were selected to inoculate the overnight culture for the following passage. This procedure was repeated for 15 passages (Fig. 5.7).

5.4. AUTHOR CONTRIBUTIONS

The gold(I)-phosphine complexes, cpds **1-9**, were synthesized by Dr. Jong Hyun Kim in the Awuah laboratory (Dept. of Chemistry, University of Kentucky) Prof. Samuel G. Awuah., Dr. Jong Hyun Kim, and Prof. Sylvie Garneau-Tsodikova. conceptualized the design of the gold complexes. The monohydrazides, cpds **10-32**, were synthesized by Dr. Nishad Thamban-Chandrika in the Garneau-Tsodikova Laboratory (Dept. of Pharmaceutical Sciences, University of Kentucky). The modified monohydrazides, cpds **33-39**, were synthesized by Dr. Stefan Kwiatkowski in the Watt laboratory (Dept. of Pharmaceutical Sciences, University of Kentucky). Prof. Sylvie Garneau-Tsodikova, Prof. David S. Watt, Dr. Stefan Kwiatkowski, and Dr. Nishad Thamban-Chandrika designed and conceptualized the monohydrazides. Emily K. Dennis performed biological experiments with help from Sarah C. Foree for the MIC data for cpds **4-9** and biofilm assay for cpd **3**. Emily K. Dennis analyzed data, wrote text, and made tables and figures presented here.

Chapter 6

Conclusion and future directions

6.1. A COMBINATIONAL APPROACH

The first approach taken in this work was to use combinations of azole antifungals and the antihistamines terfenadine (TERF) and ebastine (EBA) against a panel of *Candida* strains, covered in Chapter 1. While this is also a repurposing approach, the main goal of this project was to use the antihistamines as an adjuvant for the azole antifungals, specifically against fungal strains that demonstrate intrinsic or acquired resistance to the azoles. In this study, we observed that TERF displayed poor antifungal activity by itself and out of ninety-one total combinations tested, fourty-one were synergistic with TERF and fourteen synergistic with EBA. In Chapter 5, combinations of TERF and/or EBA with polyenes, echinocandins, and/or antibiotics were discussed. Of these combinations, the only synergistic combination was EBA and caspofungin (CFG). While some studies have suggested that antihistamines may inhibit efflux pumps[299] and affect sterol metabolism,[416-417] the mechanism of action of the antihistamine antifungal activity is still unclear. By themselves, combinations of azole antifungals and antihistamines use an adjuvant approach to increasing the azole susceptibility of azole-resistant *Candida* strains, similar to clavulanic acid and amoxicillin for bacterial infections. The azoles are an important class of antifungals and used in a synergistic combination would improve efficacy of the azoles and likely reduce toxic hepatic side effects. Currently, a combination of AmB and 5FC is used for drug-resistant infections, but synergistic combination with azoles would extend

treatment options for these drug-resistant infections. If identifying a specific target would open doors to new target-based studies for the discovery of novel antifungals, which may lead to more success in identifying new classes of antifungal therapeutics.

6.2. GOLD(I)-PHOSPHINE COMPLEXES

The second approach explored the gold(I)-phosphine complexes, which had been reported as an anticancer agent,[323, 339-340] but not yet as an antifungal agent. We showed that two square-planar gold(I)-phosphine complexes displayed excellent antifungal activity, similar to AmB, against a broad range of fungal species not limited to *Candida* spp., and including *C. auris*. Furthermore, this was the only scaffold tested that had good activity against *Aspergillus* spp, of which there are fewer drug available for treatment.The promising activity of the gold complexes was comparable to AmB, however, there does not appear to be the desired 8-fold therapeutic window to suggest that the complexes would be safe. As gold(I)-phosphine complexes have shown some selectivity for cancer cell lines, future cytotoxicity studies should include normal cell lines. New generations of antifungal gold(I)-phosphine complexes should strive to increase their selectivity for fungal cells. As is, the gold complexes could have potential use for applications on surfaces to mitigate toxicity concerns. In Chapter 5, four other gold(I)-phosphine scaffold are discussed, two of which show good antifungal activity. In addition to finding new scaffolds with less toxicity, future goals for this project is to identify the cellular target for these complexes. Gold(I)-phosphine complexes have been reported to inhibit thioredoxin reductase in the mitochondria,[336-337] but that activity has not been tested yet with complexes discussed here and it is possible there is another mechanism of action.

6.3. MONOHYDRAZONES

And finally, as a third approach we were inspired by bis(*N,N'*-arylhydrazones)[212] which exhibited good antifungal activity, but poor solubility and decided to eliminate half of the molecule to afford the monohydrazones. The monohydrazones displayed good activity against *C. albicans* and surprisingly somewhat better activity against *C. auris*. *In vitro*, the monohydrazones displayed better MIC activity than AmB with *C. auris* and related strains and exhibited less toxicity in hemolysis and cytotoxicity assays. The monohydrazones also performed similarly to VRC in biofilm, hemolysis, and cytotoxicity studies, but have the added benefit of being more potent antifungals and having fungicidal activity. This next steps for this project are already in progress, as discussed in Chapter 5, with the monohydrazides and the fluorescent and biotinylated analogues. Determining the cellular target of these molecules and progressing them into animal models are warranted.

6.4. GENERAL APPROACHES TO ANTIMICROBIAL DRUG DISCOVERY

The story of Alexander Fleming and the discovery of the antibiotic penicillin is well known, but what about the first antifungals? The first medicine to be approved specifically as an antifungal was nystatin (NYT), which was isolated in 1949 and patented in 1957.[418] The discovery of NYT was a collaboration between Elizabeth Lee Hazen and Rachel Fuller Brown who worked for the Division of Laboratories and Research of the New York State Department of Health. Hazen collected Actinomycete samples and screened them for antifungal activity while Brown extracted and purified the active compound. Their discovery, NYT, itself was not an immediate success as it also showed toxicity and was

generally unsafe for use with systemic fungal infections, however, it is currently used topically today. This was a critical discovery as it caught the attention of pharmaceutical companies and provided a platform for more research. This soon resulted in the discovery of the gold standard of antifungals, amphotericin B (AmB), which entered the clinic in 1959.[4] The studies in this dissertation, like with NYT, hope to discover a novel antifungal that can be used clinically, but are also meant to be the starting collaboration that finds a starting point for new and useful antifungals.

The various projects within this dissertation are completely new antifungals. And while we use known antifungals as controls so we can compare potency and selectivity of the drugs *in vitro*, these molecules are likely have different mechanisms of action and cannot be directly compared to current antifungals. We take a screening approach to identify a unique, active scaffold, but lack a clear protein target. A more direct approach to antifungal discovery would be to have a specific target in mind and future work is to identify those targets as this would allow for more efficient identification of lead compounds and further optimization modification of compounds. However, the screening approach appears to be the most common method for antifungal discovery at this point. Other considerations in antifungal discovery is the method of eliminating an infection and if it is necessary to have fungicidal antifungal agents. Some fields within the broader antifungal discovery include immunotherapy[419] and molecules that prevent fungal adhesion.[420] While many patients that suffer from fungal infections are immunocompromised, alternate therapeutic strategies such as these may be lackluster, there may be other patients where these strategies may be beneficial for prevention of infection.

APPENDIX A

Compound characterization for Chapter 3 figures 3.A1-3.A30 which includes ^{1}H, ^{13}C NMR, and ^{31}P spectra as well as HRMS (ESI) and HPLC traces.

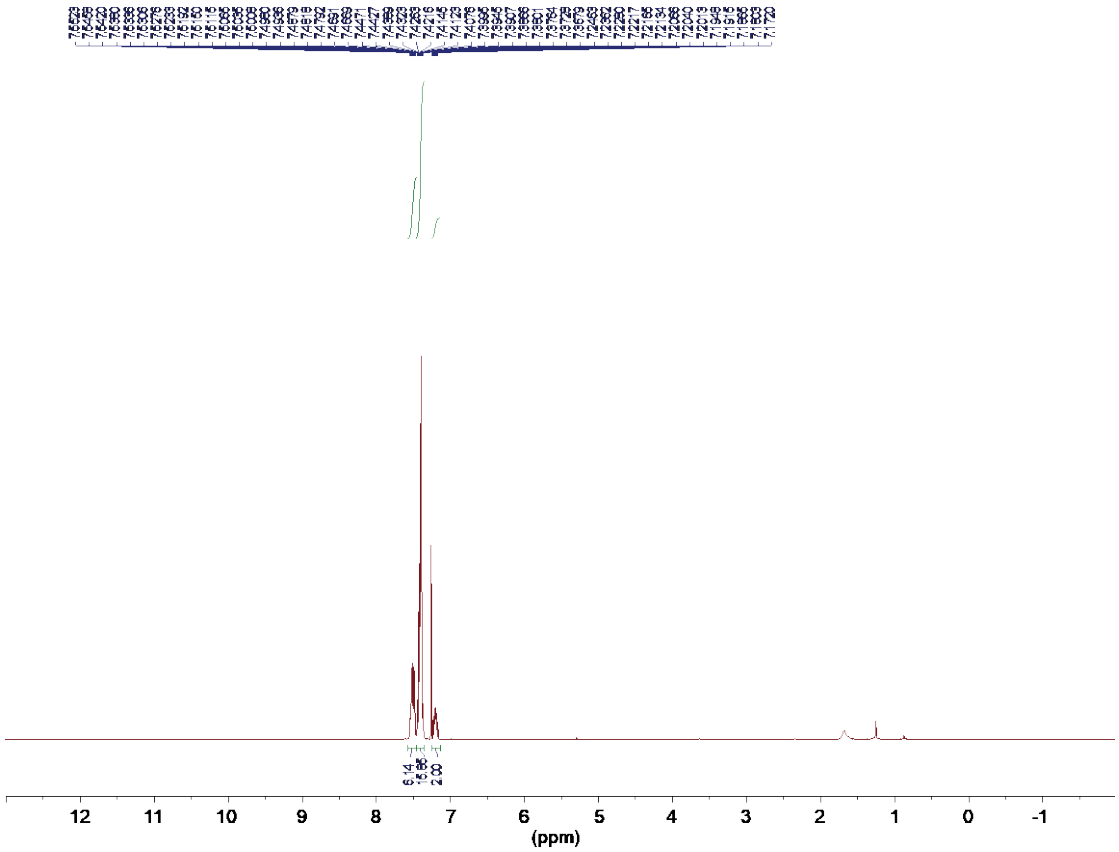

Fig. 3.A1: ^{1}H NMR of compound **1** in $CDCl_3$ at 298K.

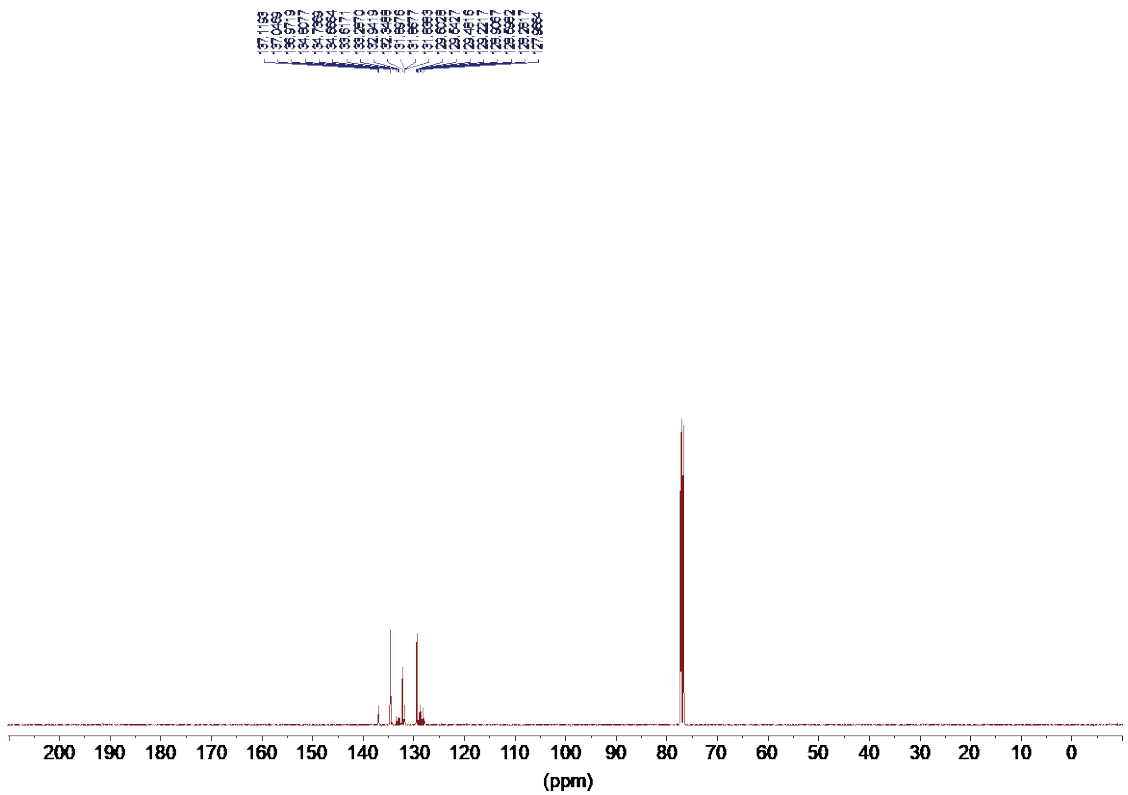

Fig. 3.A2: ^{13}C NMR of compound **1** in $CDCl_3$ at 298K.

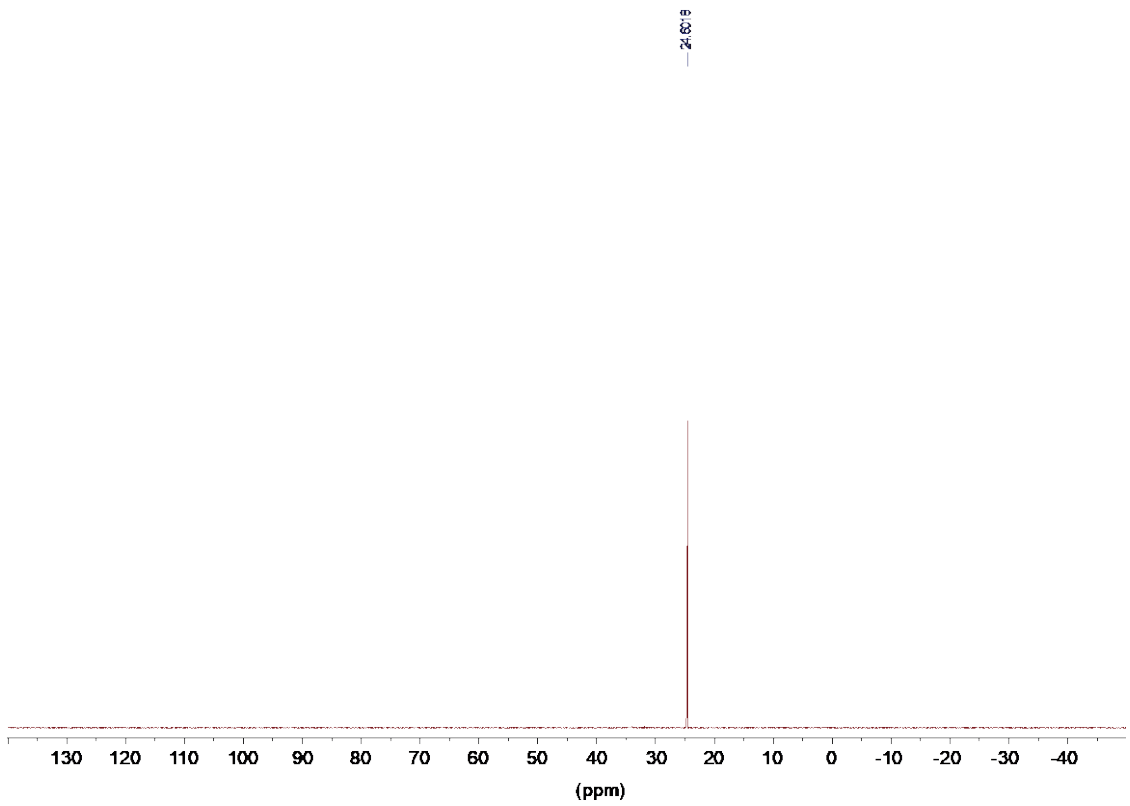

Fig. 3.A3: ^{31}P NMR of compound **1** in $CDCl_3$ at 298K.

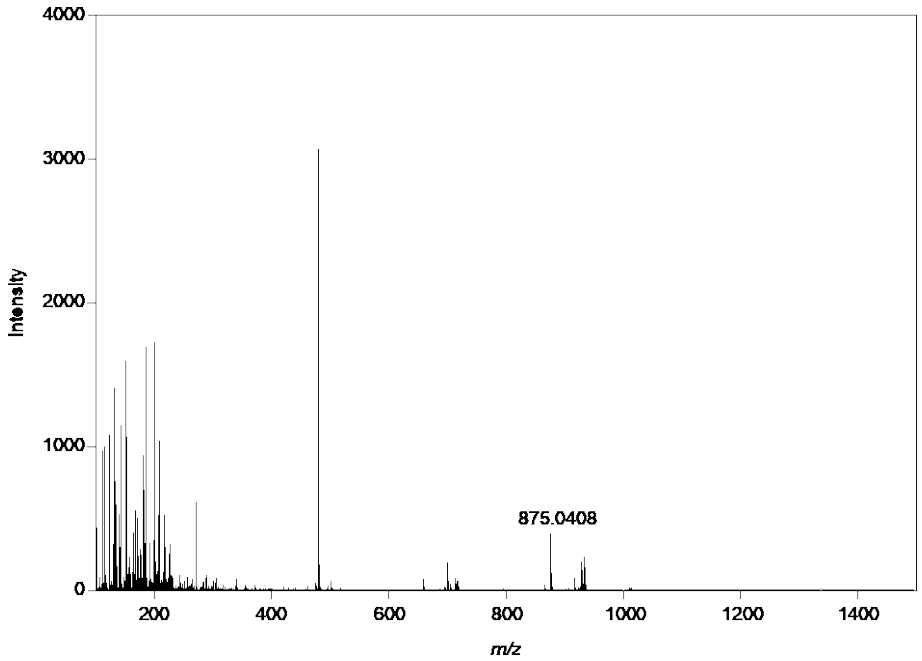

Fig. 3.A4: HRMS (ESI) of compound **1**.

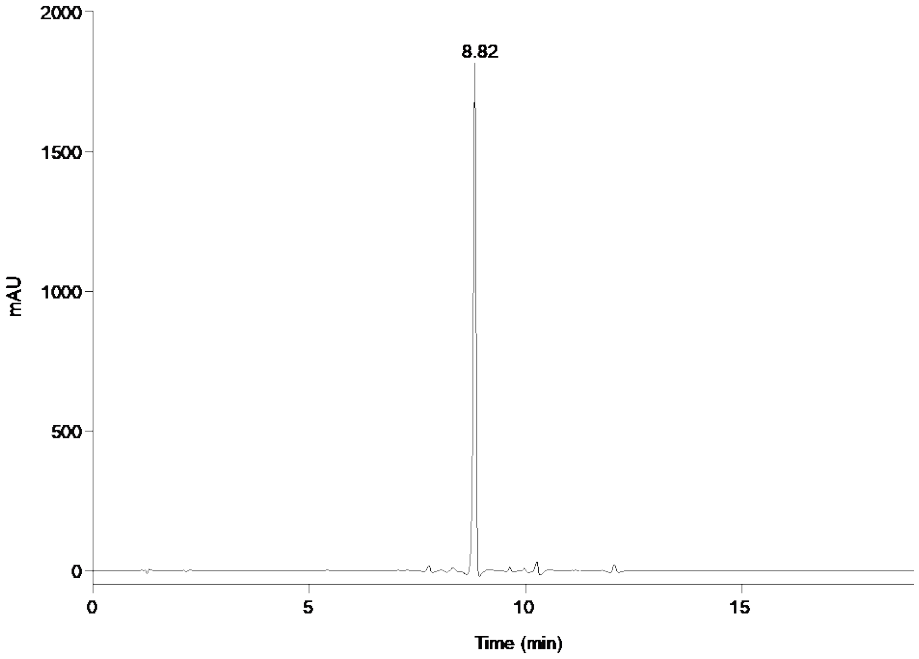

Fig. 3.A5: HPLC trace for compound **1**. R_t = 8.82. Purity = 97%.

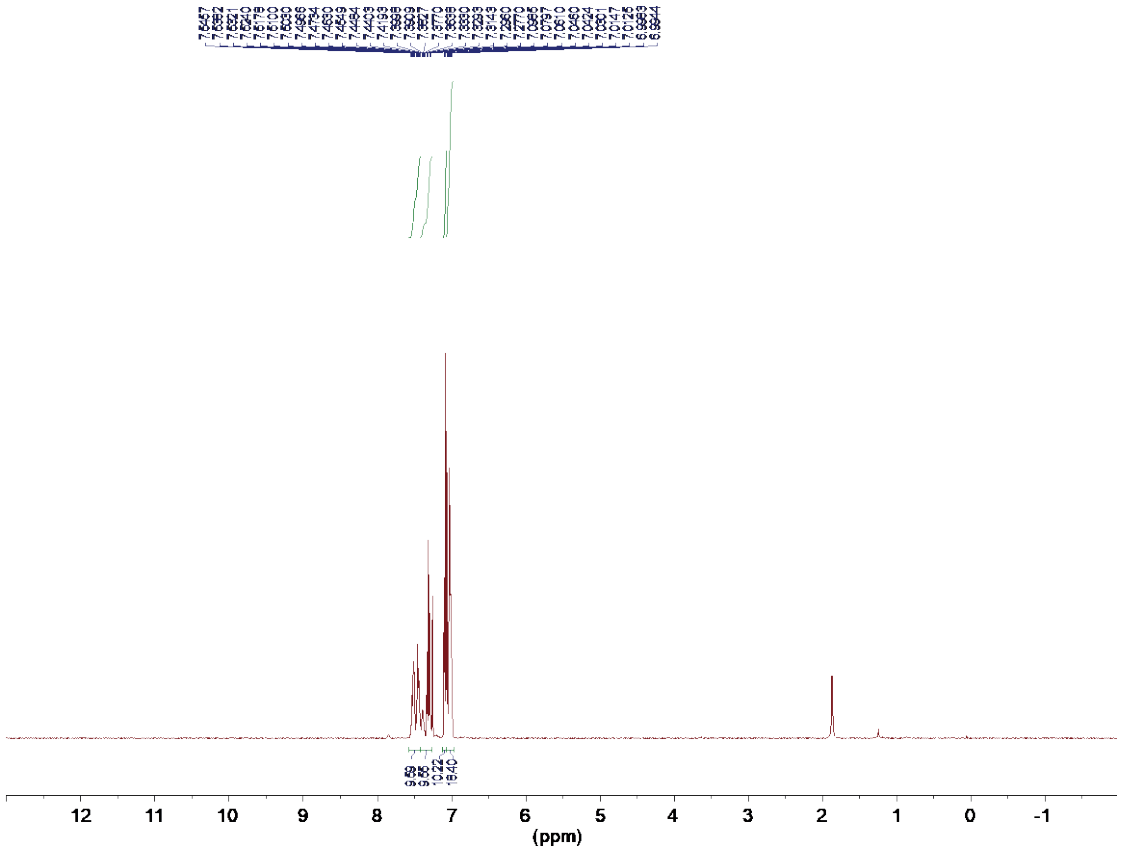

Fig. 3.A6: ^{1}H NMR of compound **2** in $CDCl_3$ at 298K.

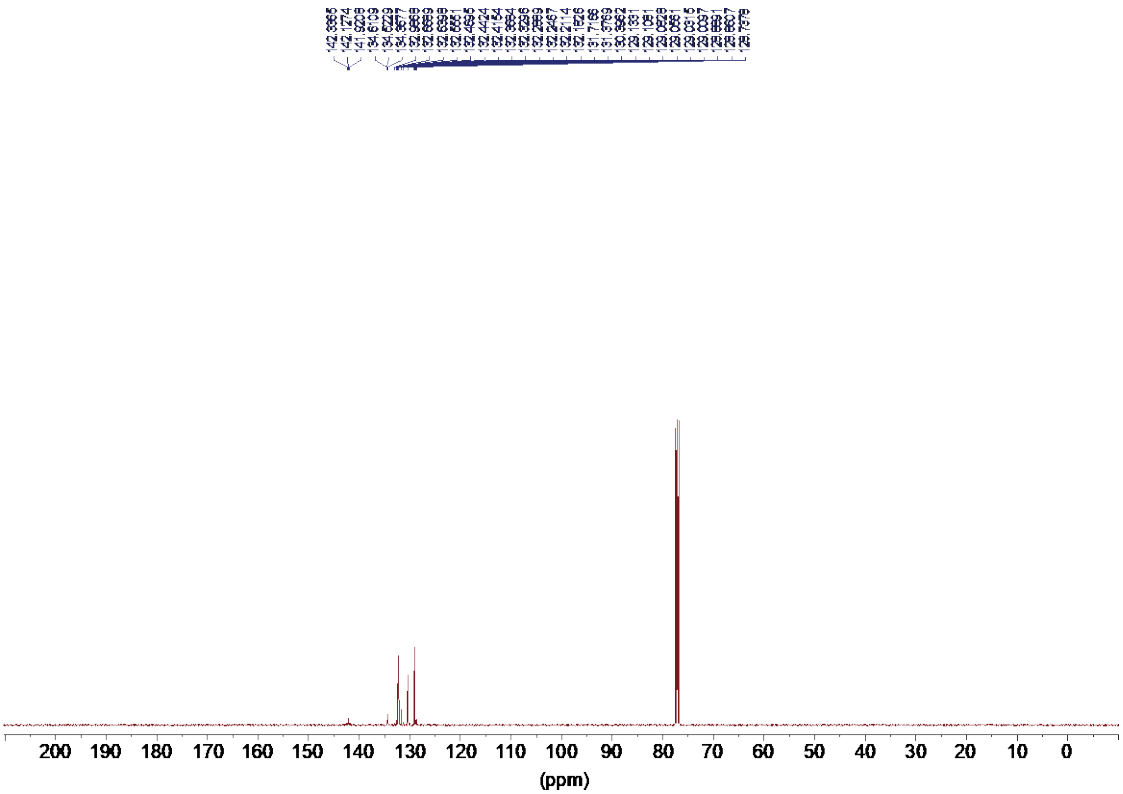

Fig. 3.A7: ^{13}C NMR of compound **2** in $CDCl_3$ at 298K.

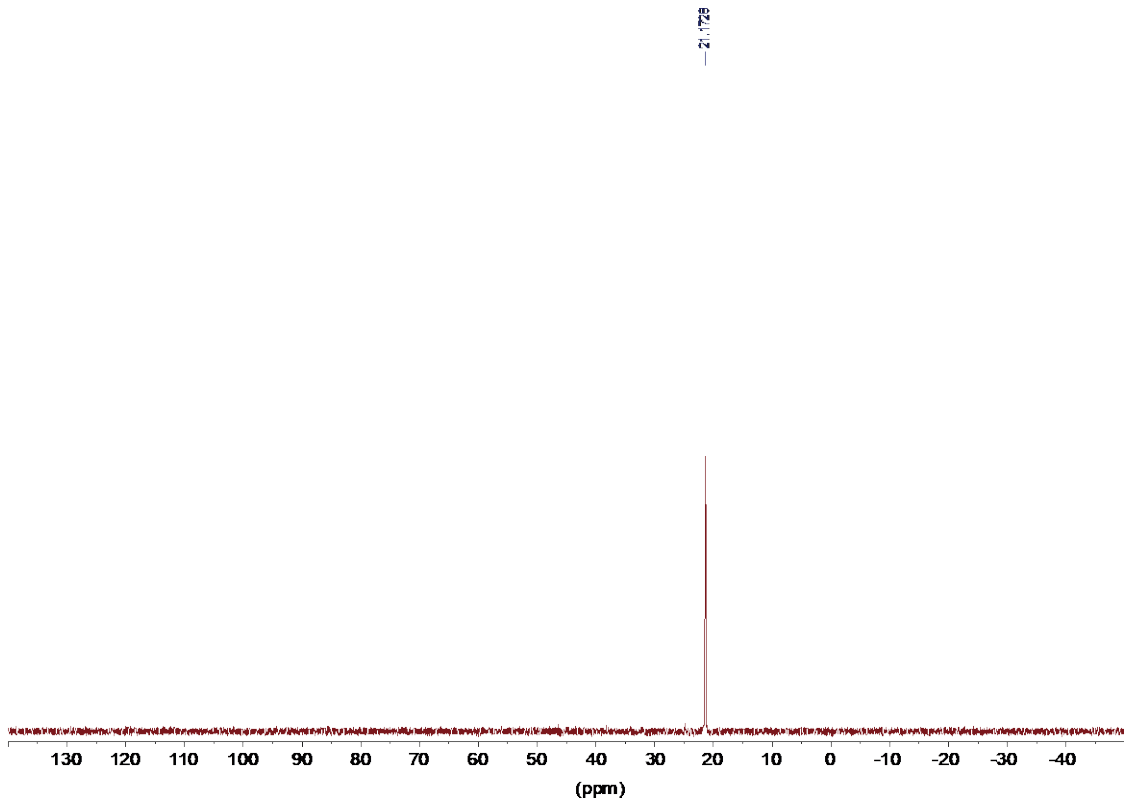

Fig. 3.A8: ^{31}P NMR of compound **2** in $CDCl_3$ at 298K.

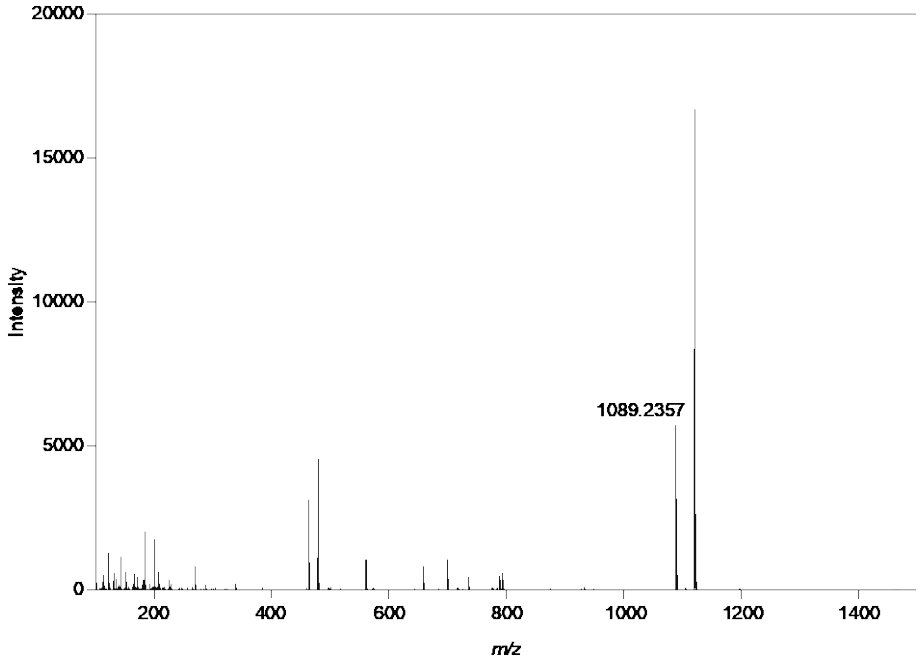

Fig. 3.A9: HRMS (ESI) of compound **2**.

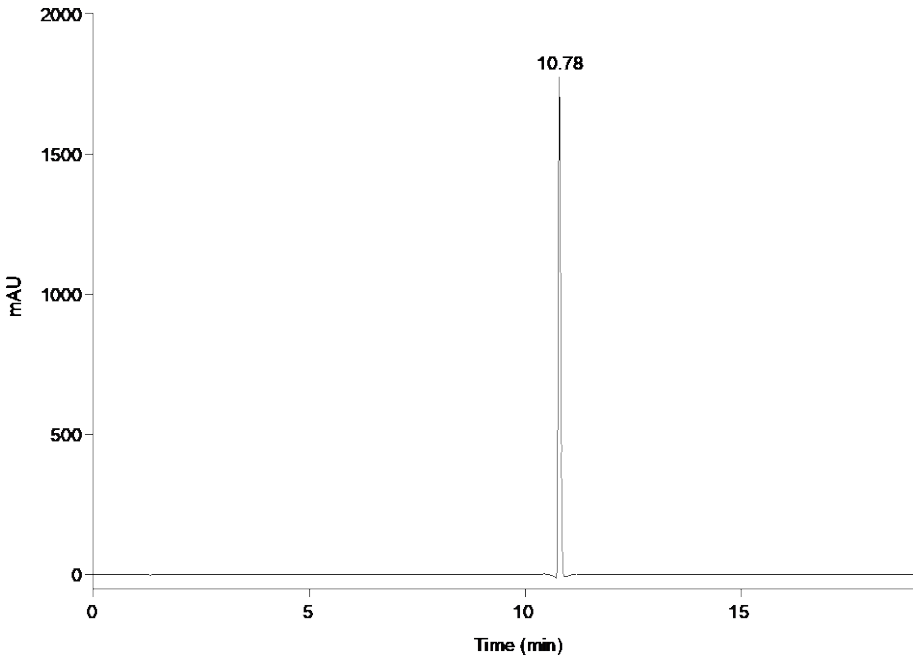

Fig. 3.A10: HPLC trace for compound **2**. R_t = 10.78. Purity = 100%.

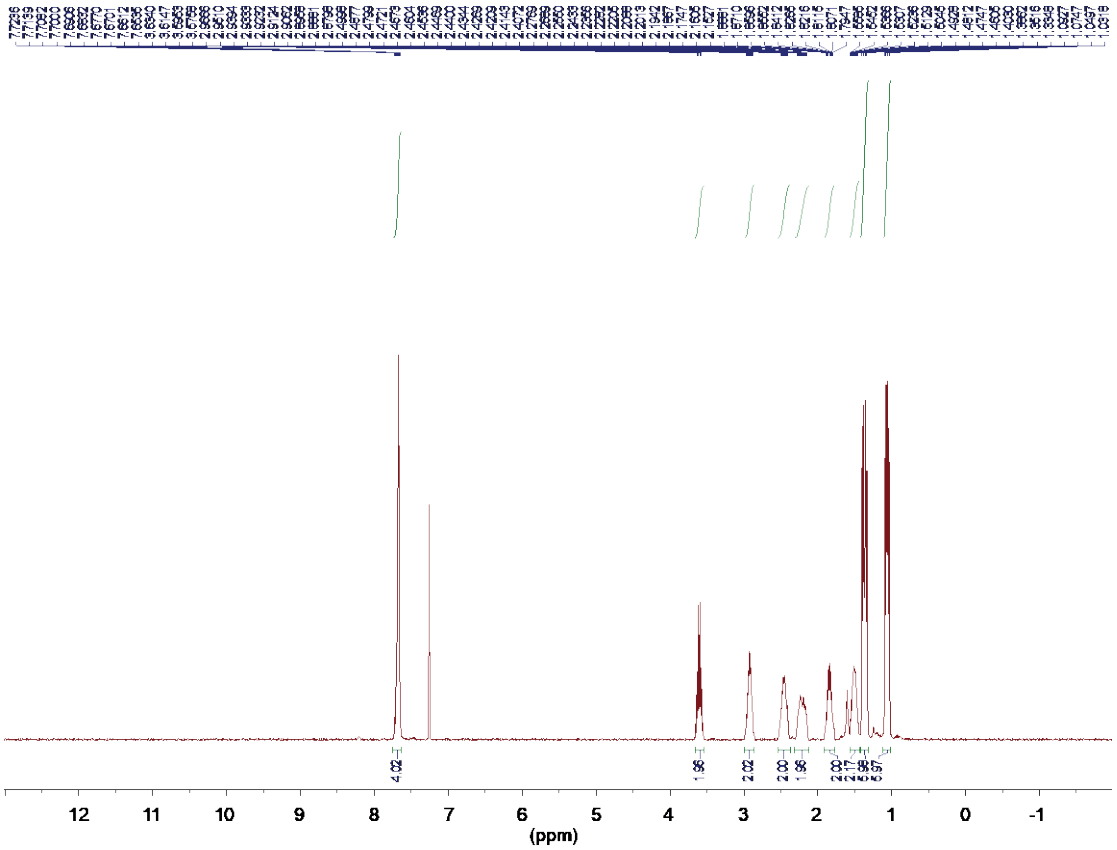

Fig. 3.A11: ^{1}H NMR of compound **3** in $CDCl_3$ at 298K.

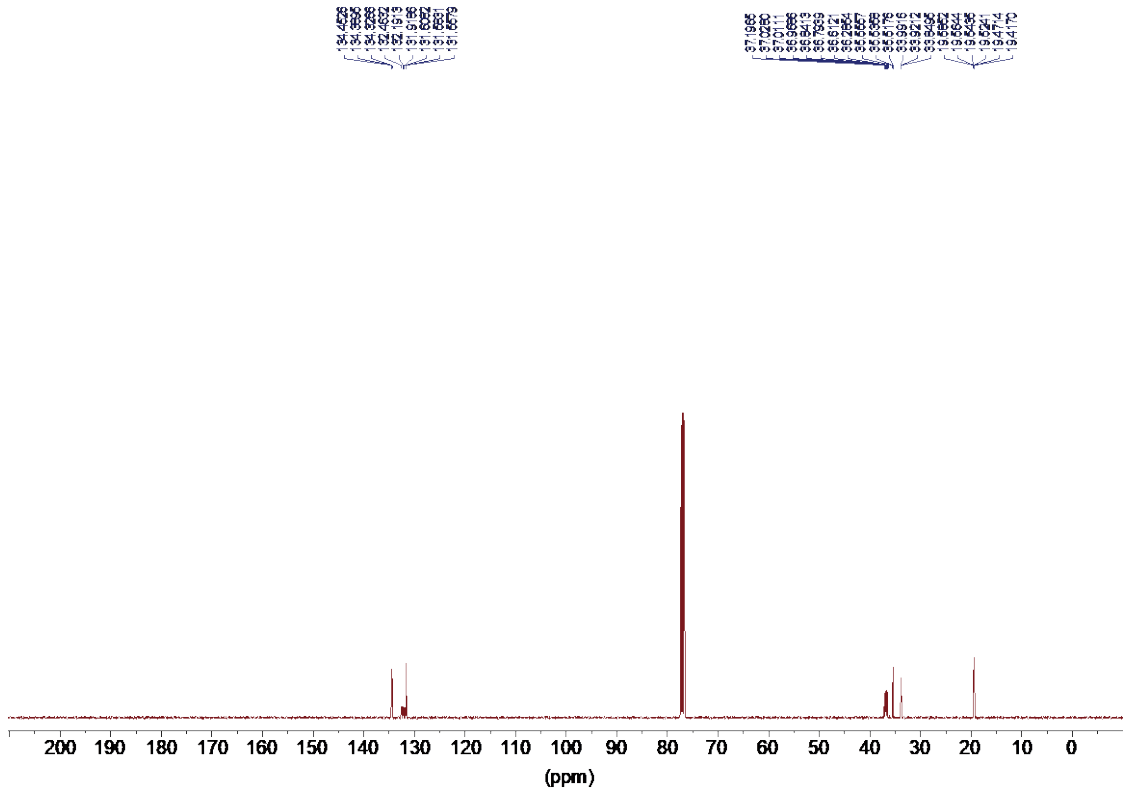

Fig. 3.A12: ^{13}C NMR of compound **3** in $CDCl_3$ at 298K.

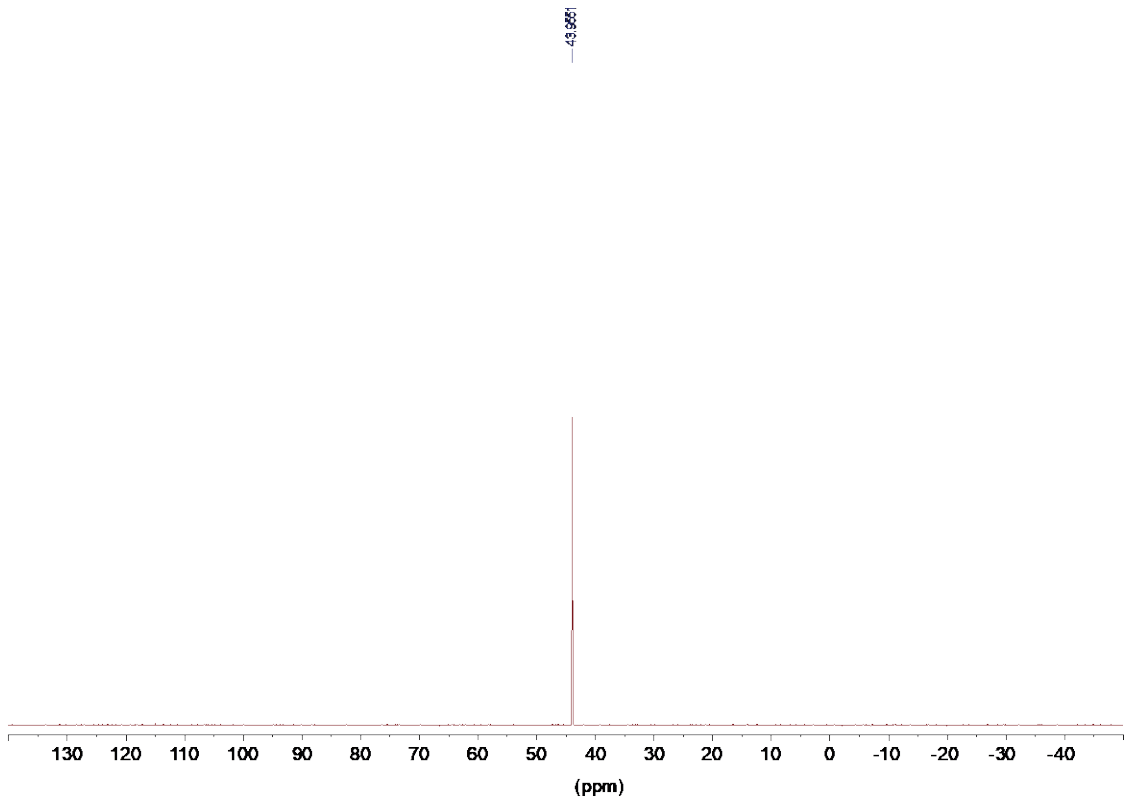

Fig. 3.A13: ^{31}P NMR of compound **3** in $CDCl_3$ at 298K.

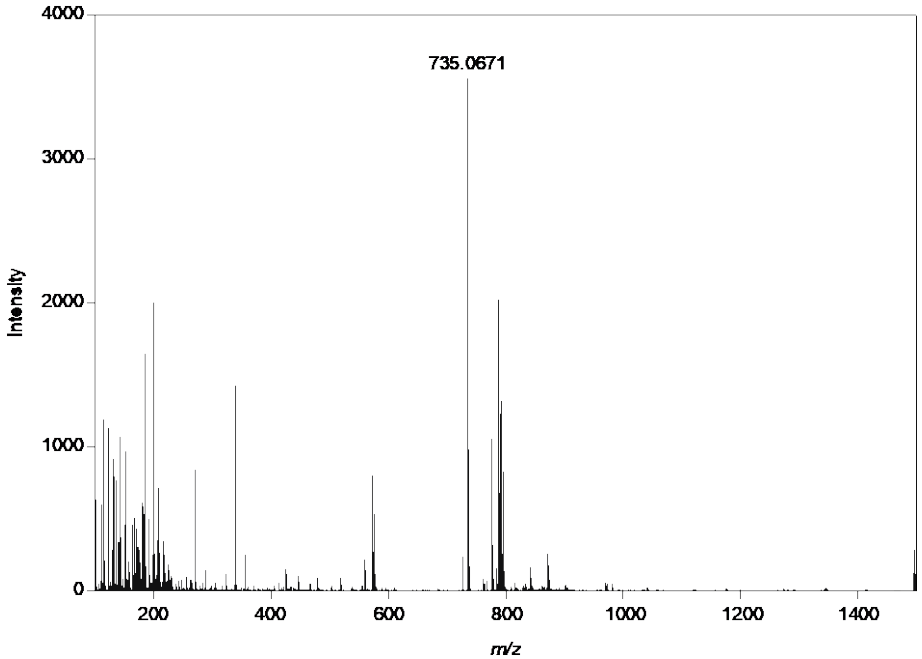

Fig. 3.A14: HRMS (ESI) of compound **3**.

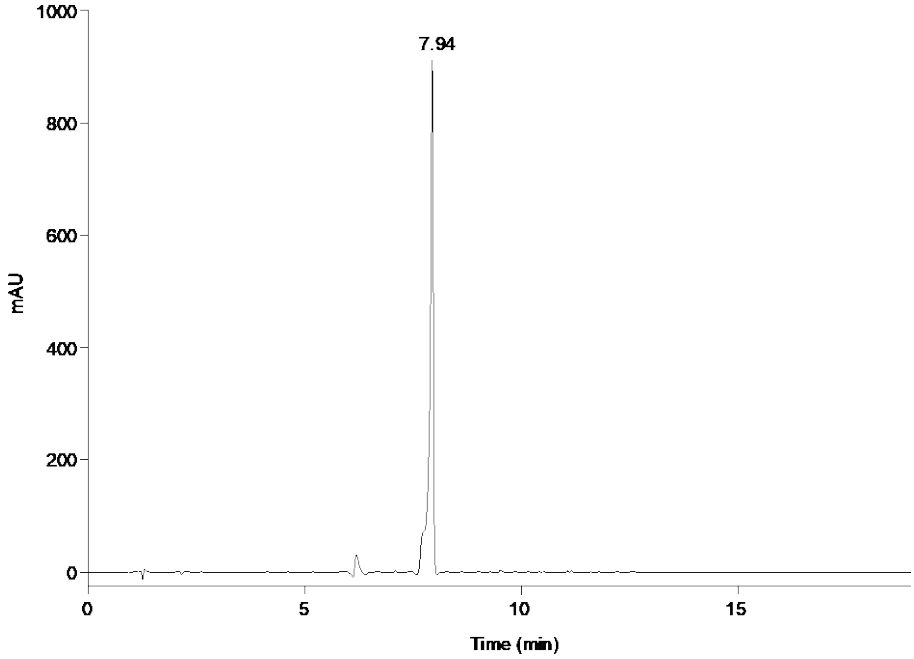

Fig. 3.A15: HPLC trace for compound **3**. R_t = 7.94. Purity = 97%.

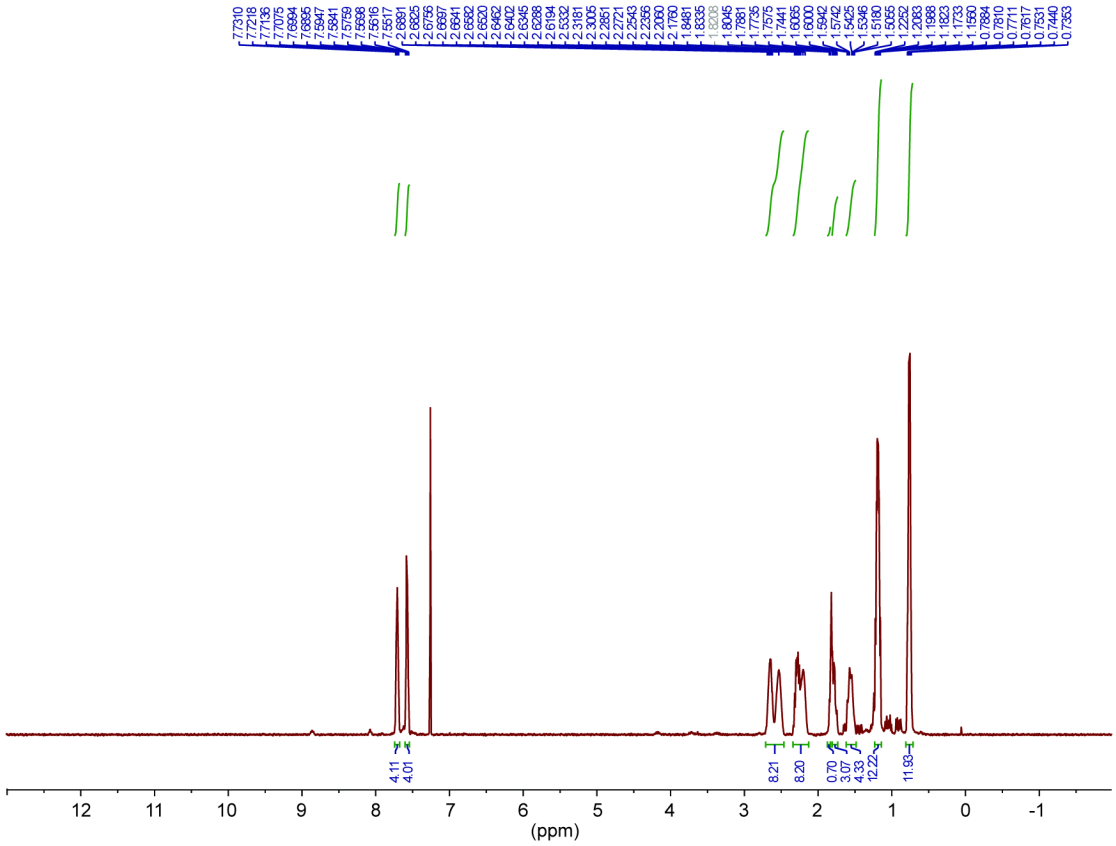

Fig. 3.A16: ^{1}H NMR of compound **4** in $CDCl_3$ at 298K.

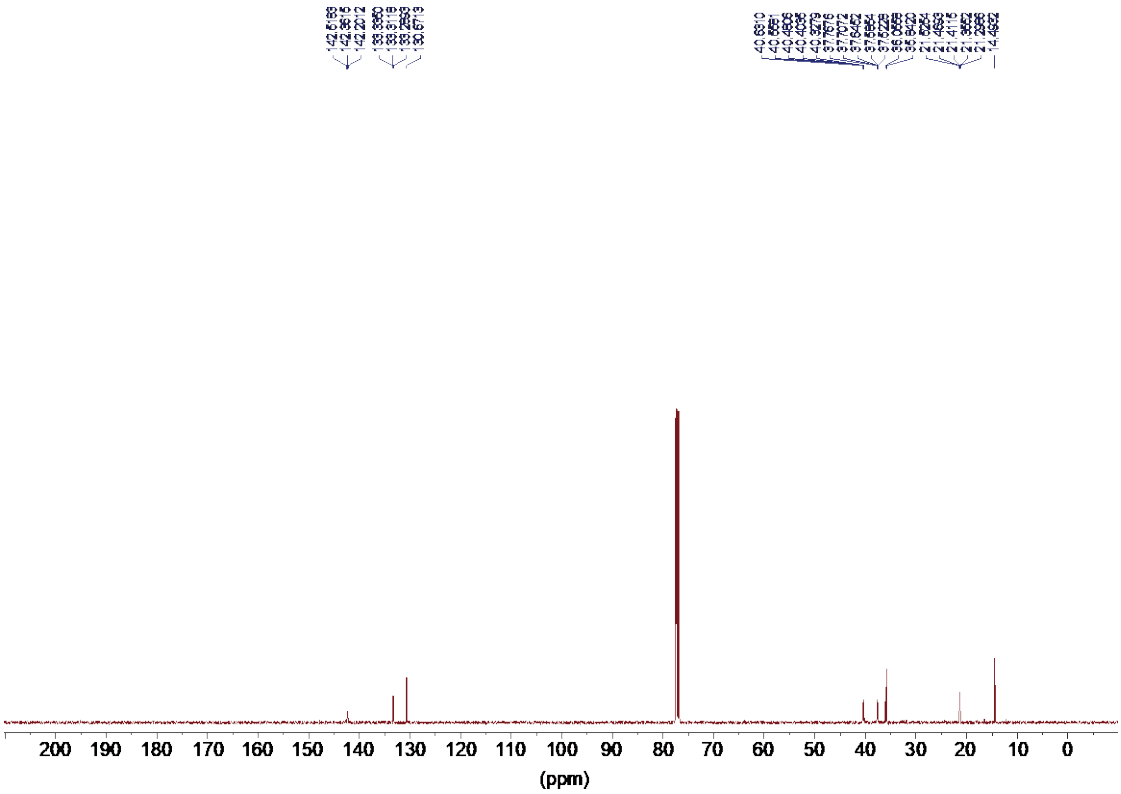

Fig. 3.A17: ^{13}C NMR of compound **4** in $CDCl_3$ at 298K.

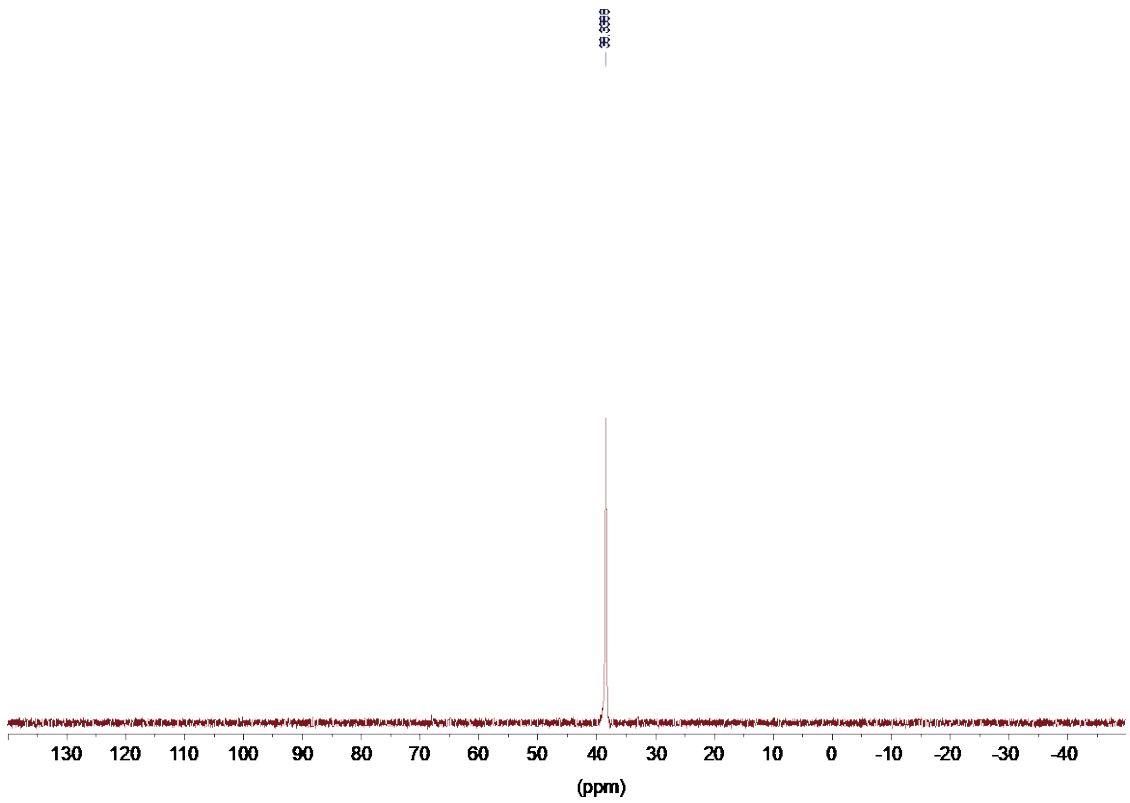

Fig. 3.A18: ^{31}P NMR of compound **4** in $CDCl_3$ at 298K.

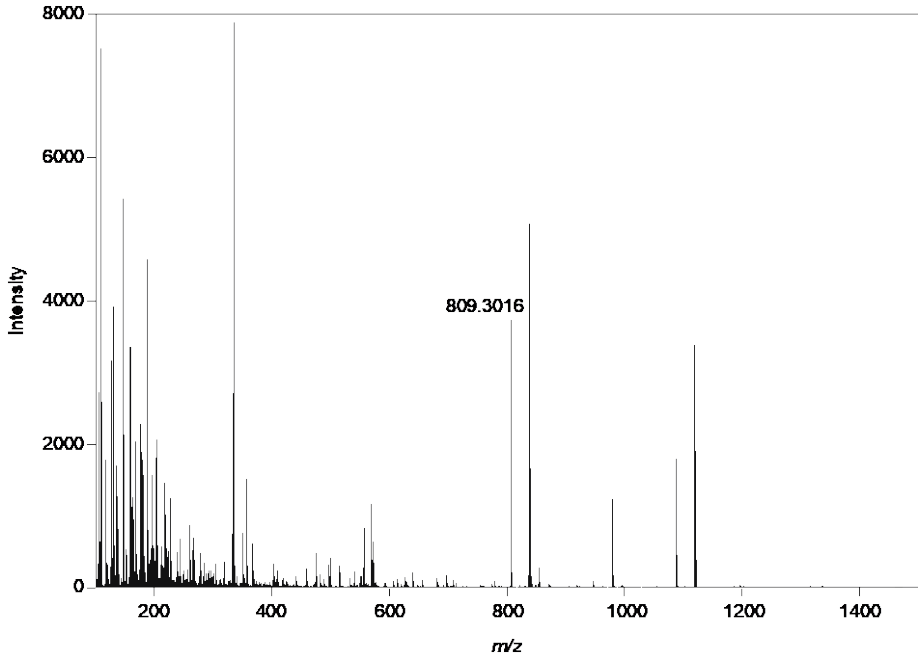

Fig. 3.A19: HRMS (ESI) of compound **4**.

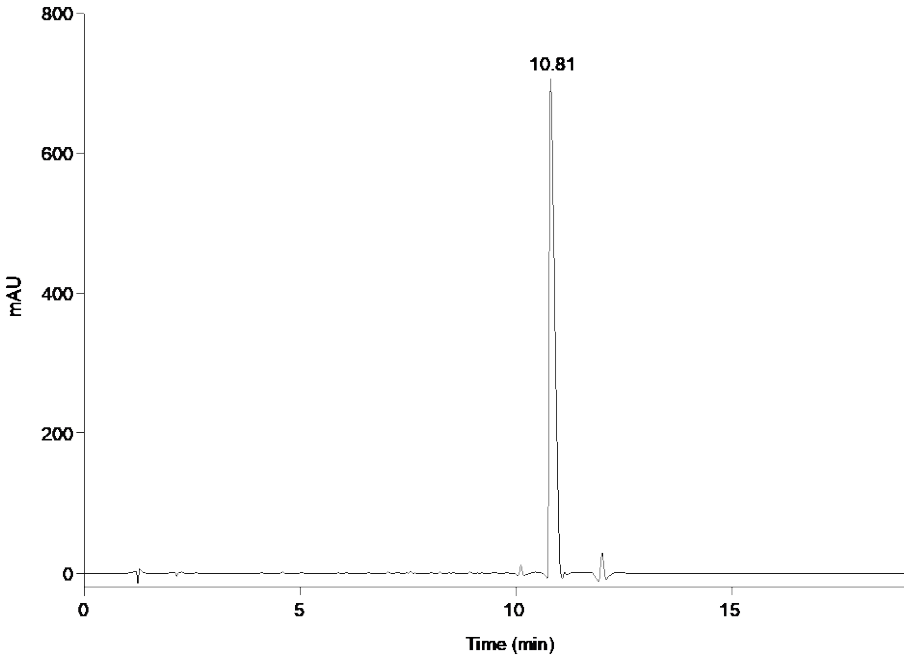

Fig. 3.A20: HPLC trace for compound **4**. R_t = 10.81. Purity = 98%.

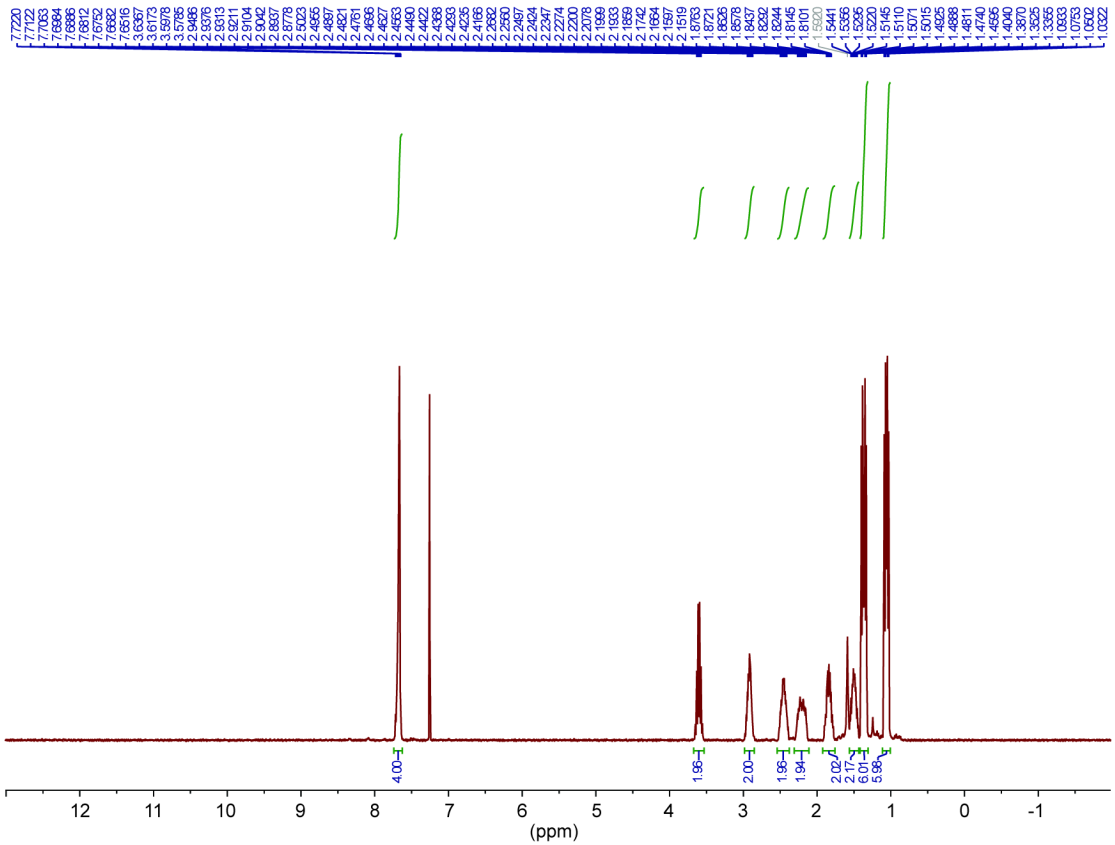

Fig. 3.A21: ^{1}H NMR of compound **5** in $CDCl_3$ at 298K.

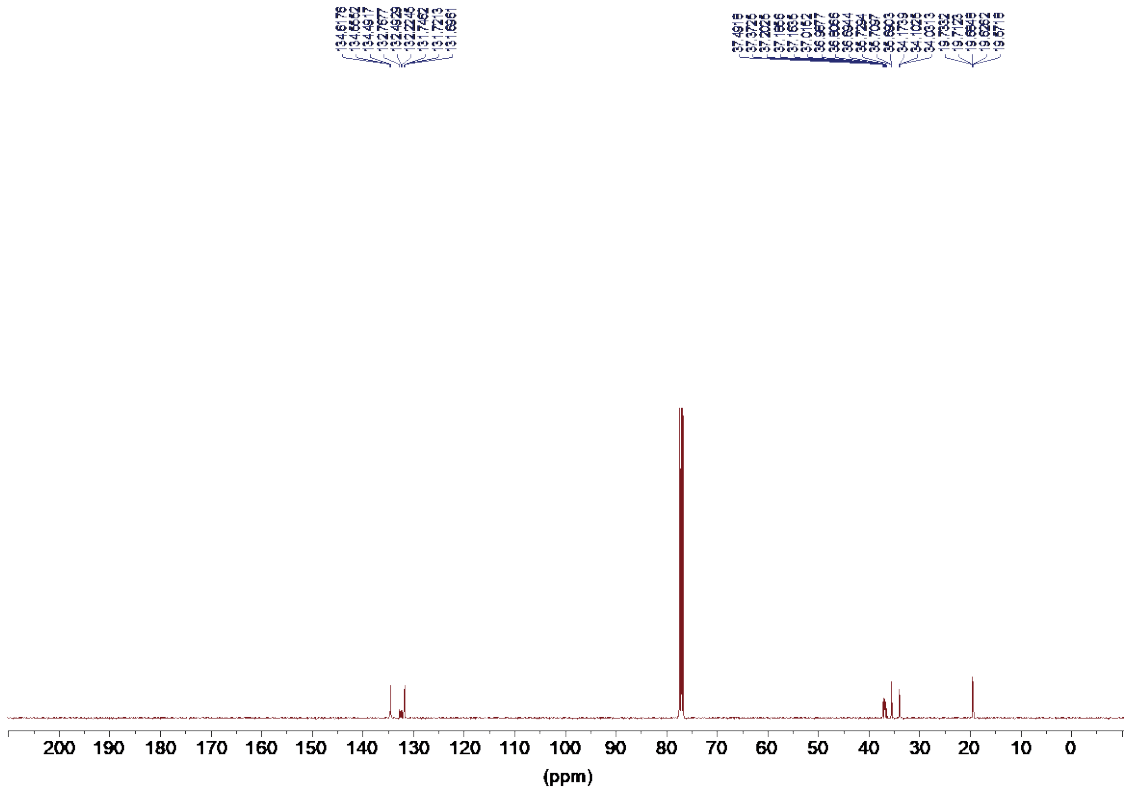

Fig. 3.A22: ^{13}C NMR of compound **5** in $CDCl_3$ at 298K.

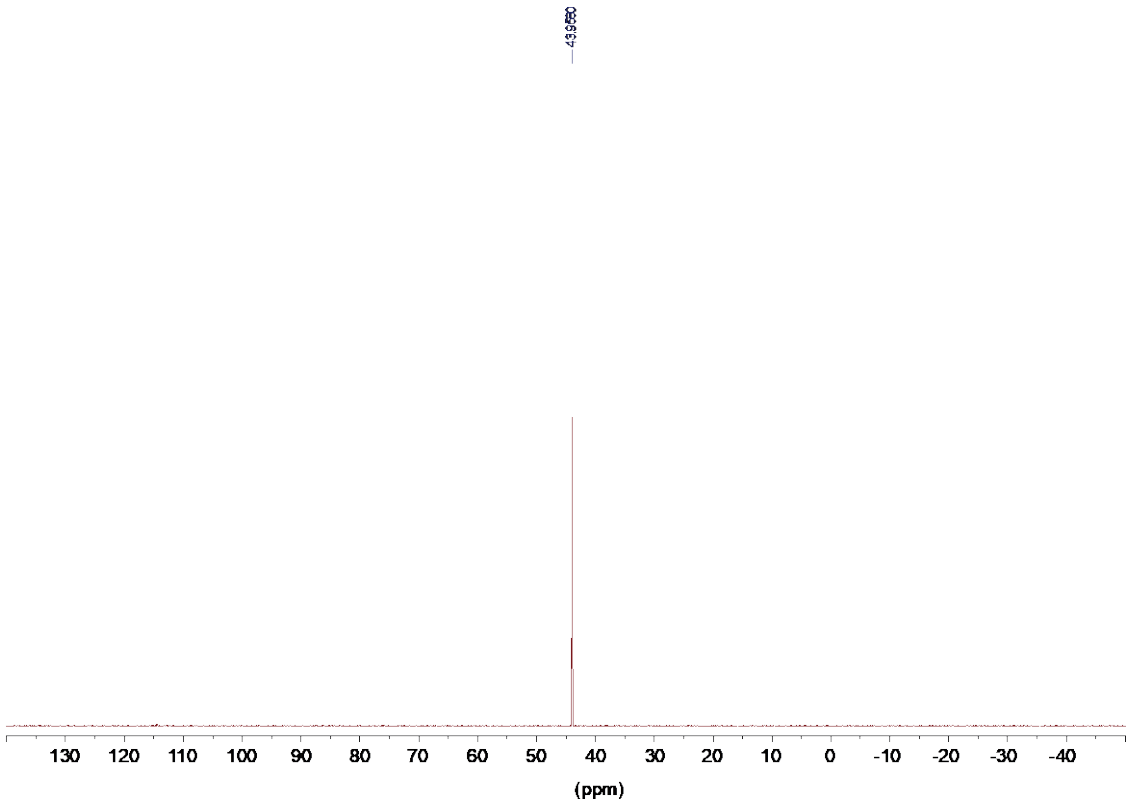

Fig. 3.A23: ^{31}P NMR of compound **5** in $CDCl_3$ at 298K.

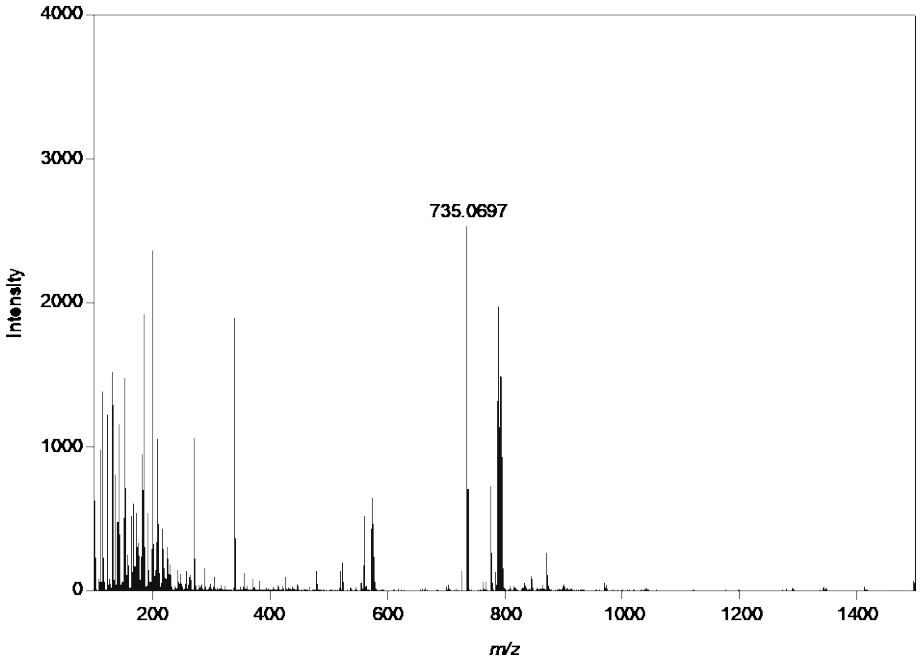

Fig. 3.A24: HRMS (ESI) of compound **5**.

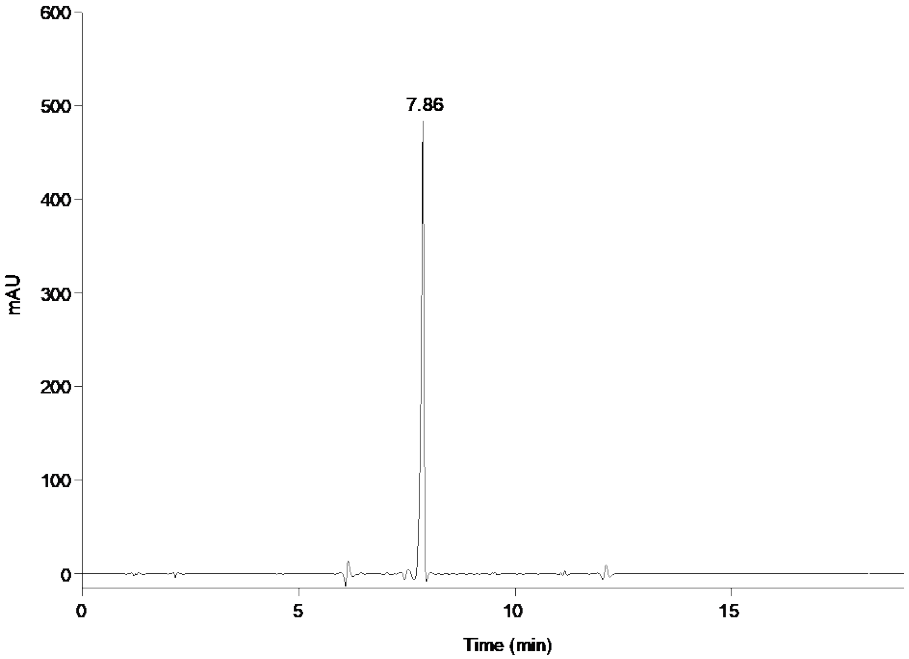

Fig. 3.A25: HPLC trace for compound **5**. R_t = 7.86. Purity = 97%.

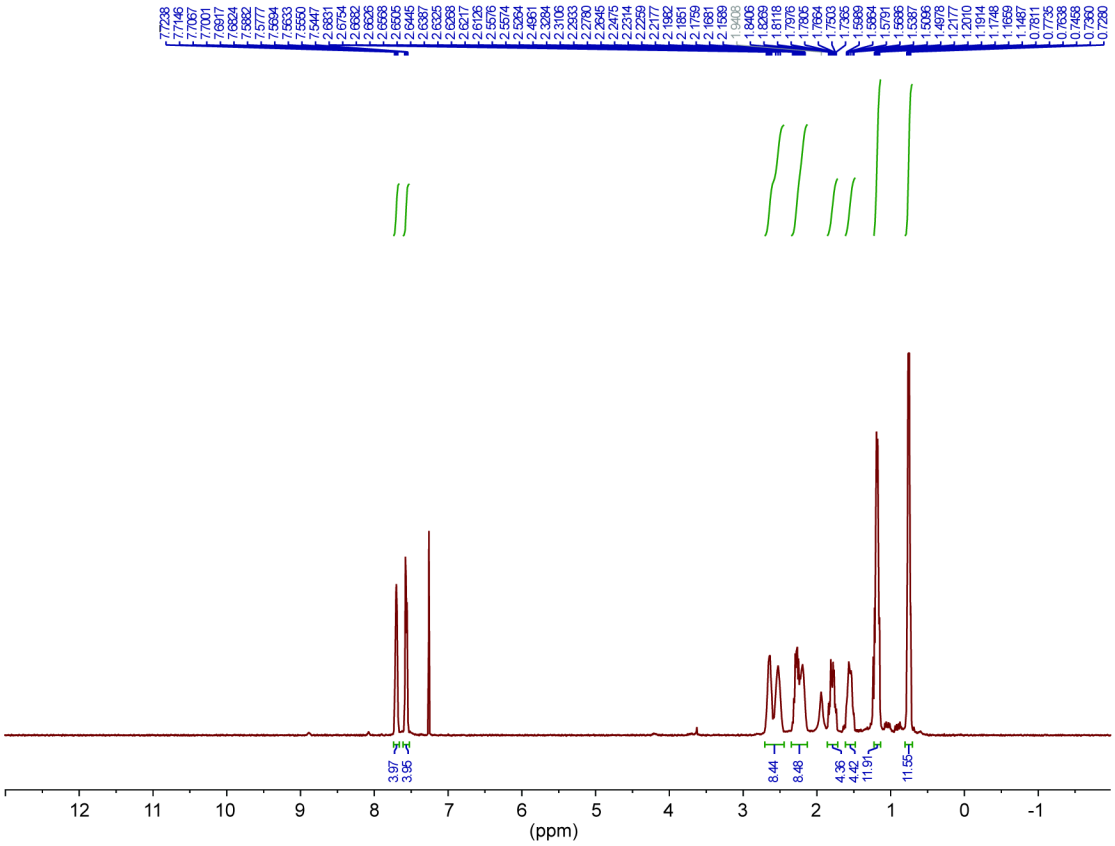

Fig. 3.A26: ^{1}H NMR of compound **6** in $CDCl_3$ at 298K.

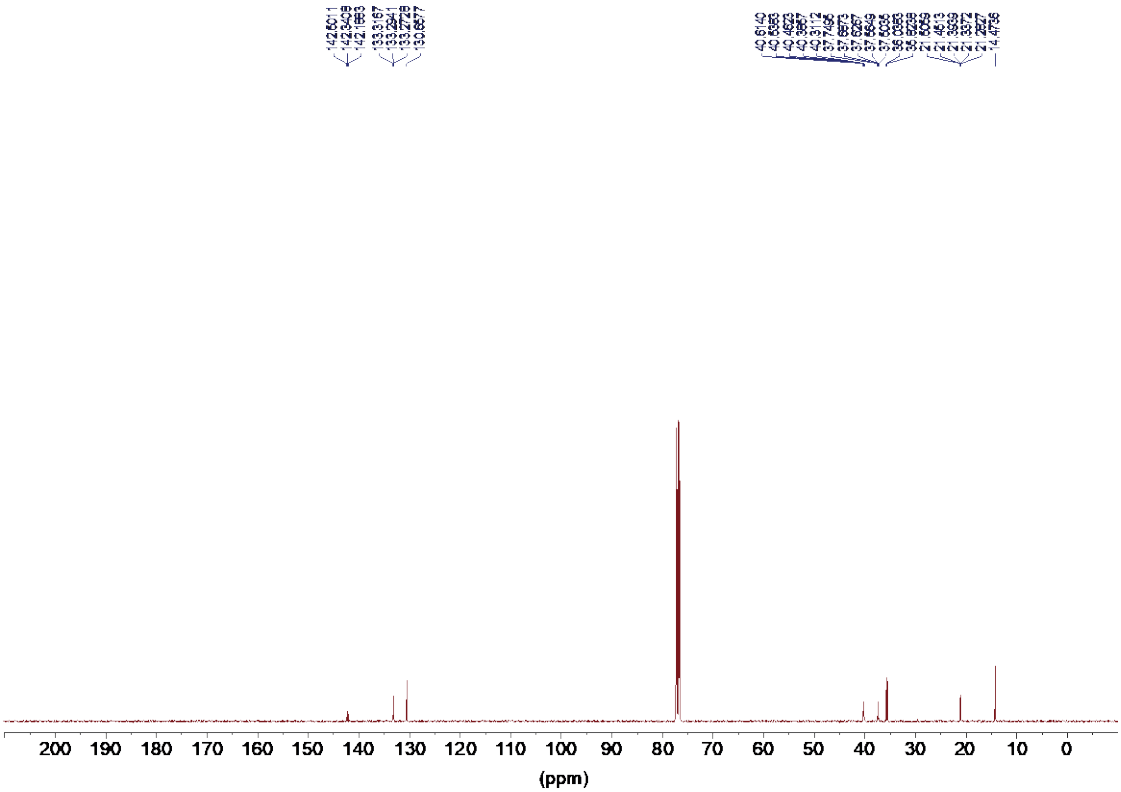

Fig. 3.A27: ^{13}C NMR of compound **6** in $CDCl_3$ at 298K.

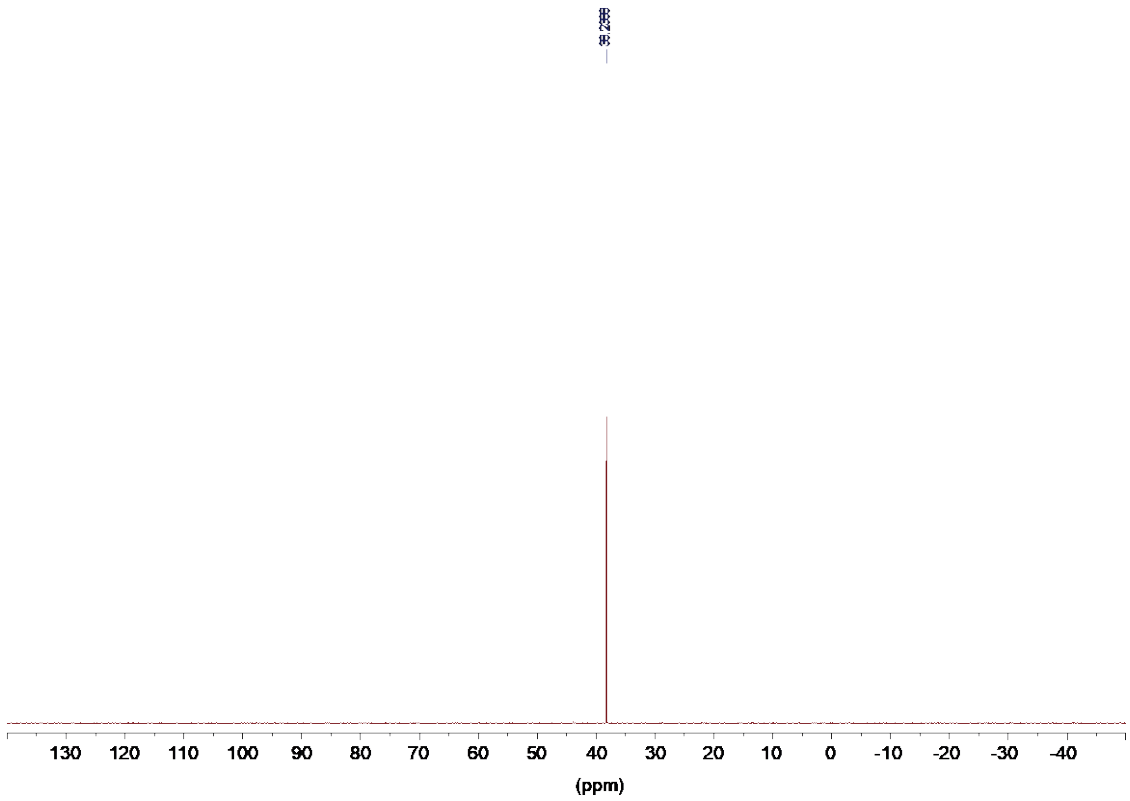

Fig. 3.A28: ^{31}P NMR of compound **6** in $CDCl_3$ at 298K.

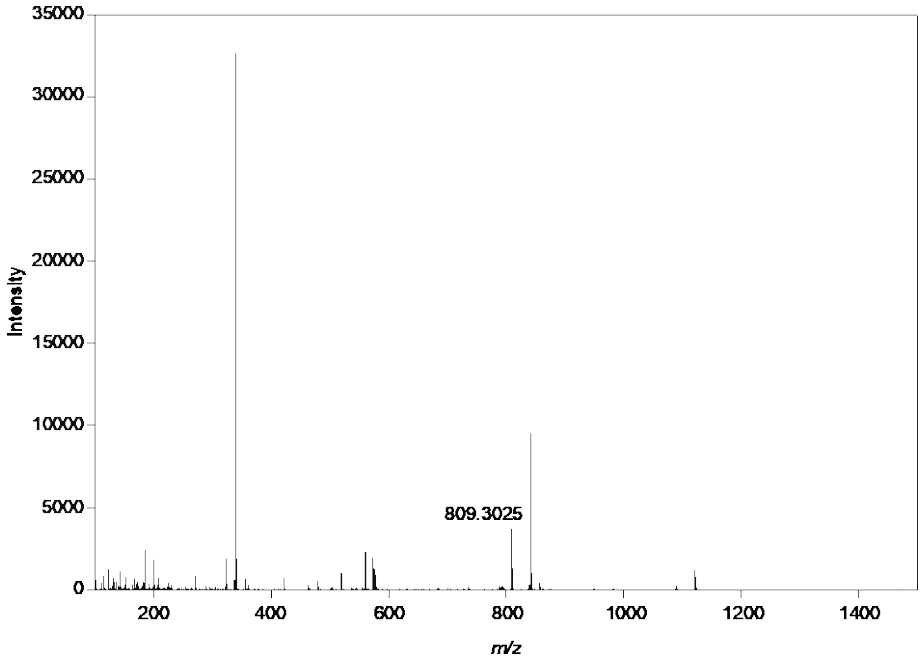

Fig. 3.A29: HRMS (ESI) of compound **6**.

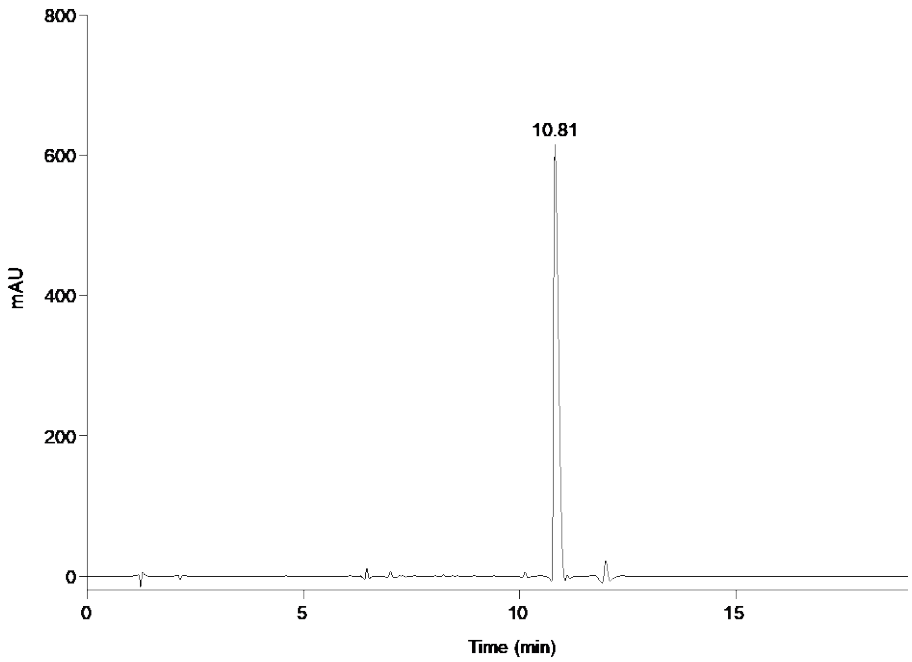

Fig. 3.A30: HPLC trace for compound **6**. R_t = 10.81. Purity = 97%.

APPENDIX B

Compound characterization for Chapter 4 figures 4.A1-4.B103 which includes ^{1}H and ^{13}C NMR spectra as well as HPLC traces.

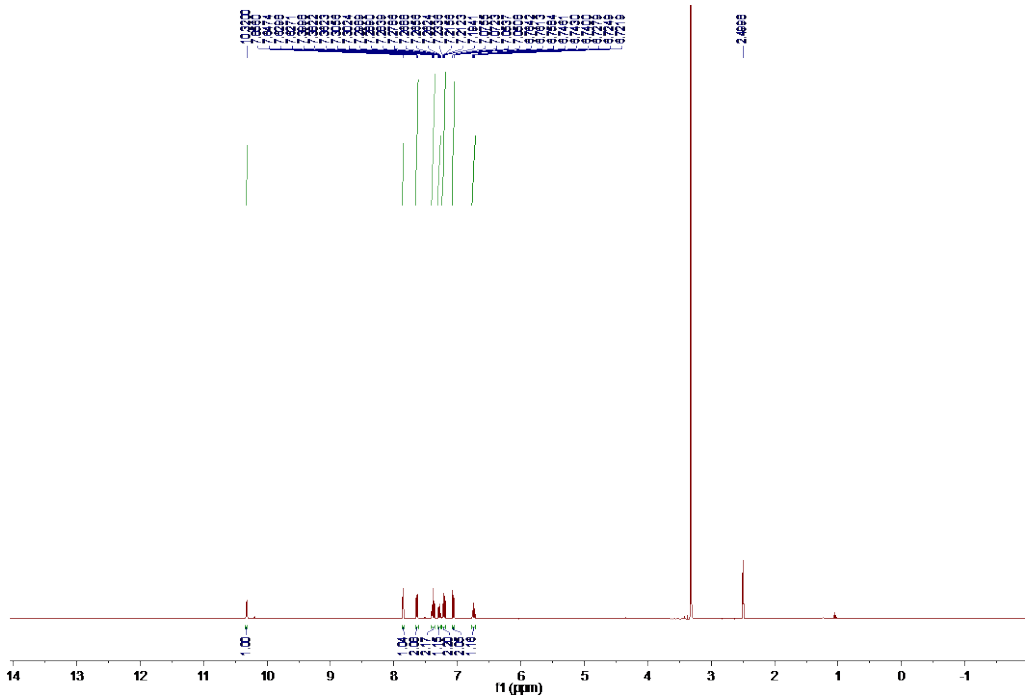

Fig. 4.B1. ^{1}H NMR spectrum for compound **1a** in $(CD_3)_2SO$ (400 MHz).

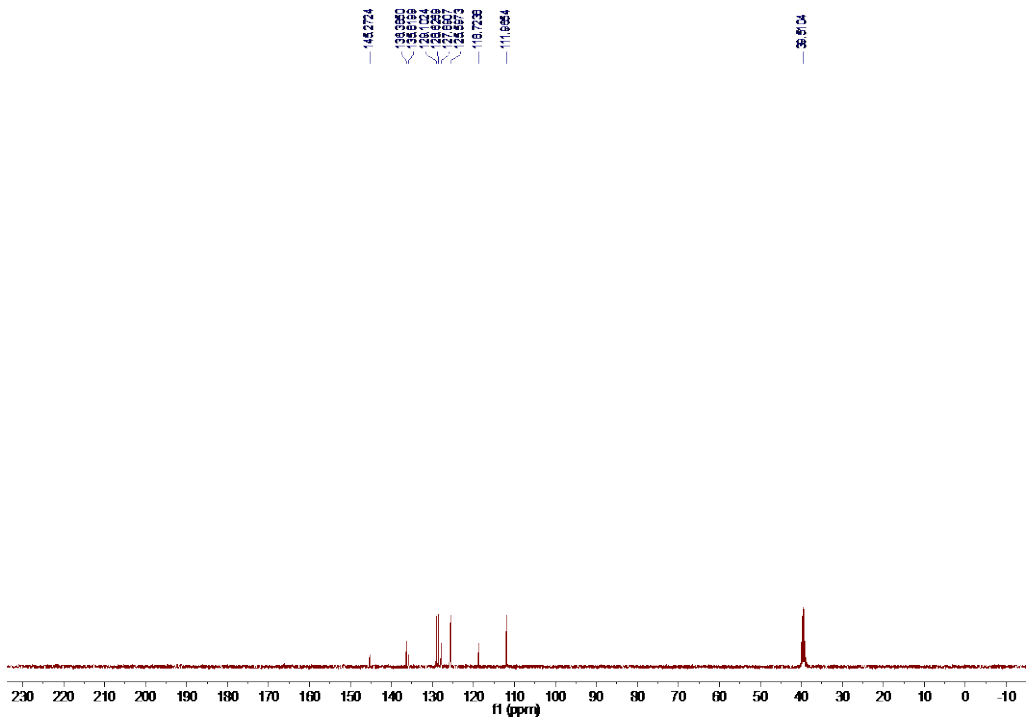

Fig. 4.B2. ^{13}C NMR spectrum for compound **1a** in $(CD_3)_2SO$ (100 MHz).

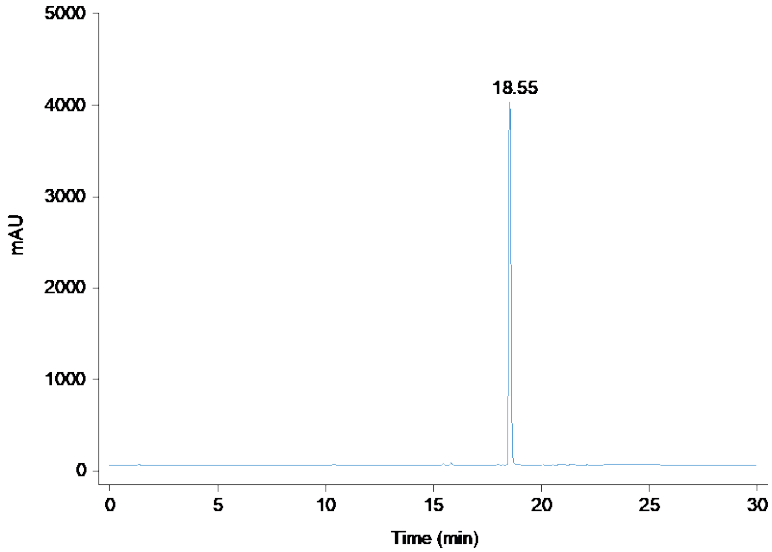

Fig. 4.B3. LCMS trace for compound **1a**. R_t = 18.55 min. Purity: 99%.

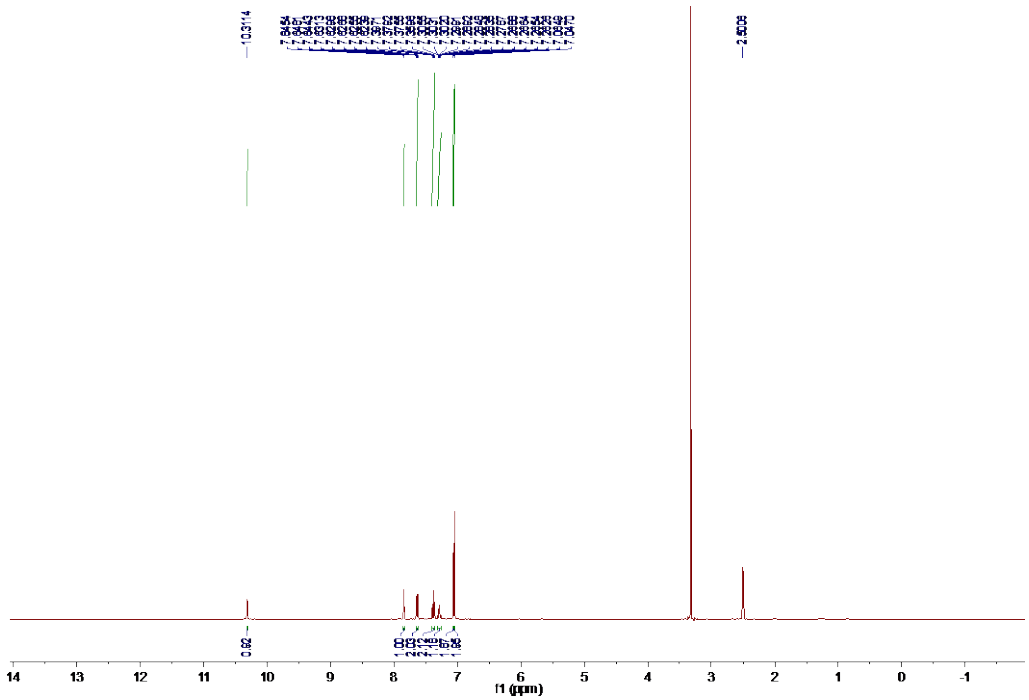

Fig. 4.B4. ^{1}H NMR spectrum for compound **1c** in $(CD_3)_2SO$ (400 MHz).

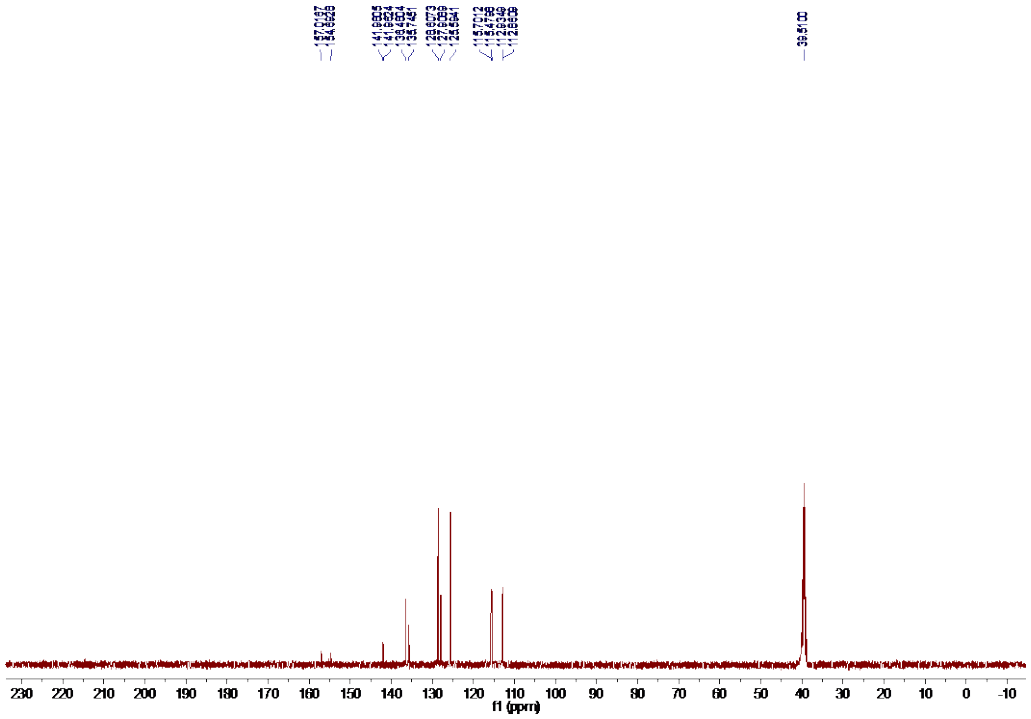

Fig. 4.B5. ^{13}C NMR spectrum for compound **1c** in $(CD_3)_2SO$ (100 MHz).

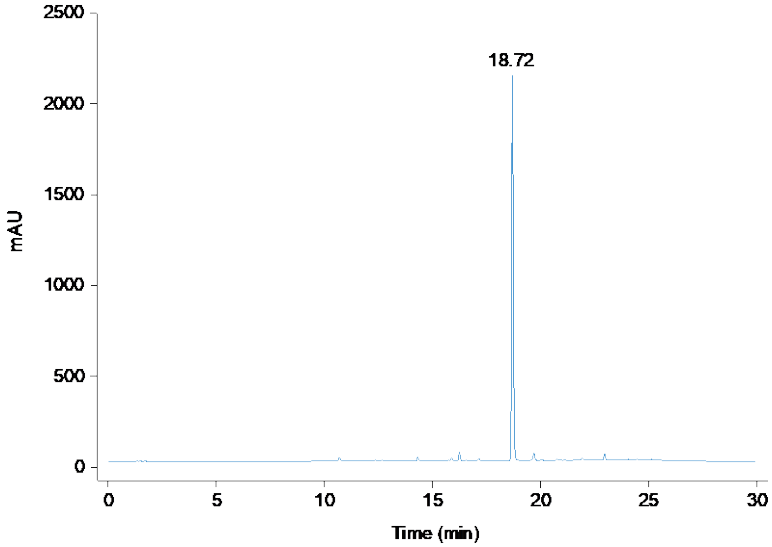

Fig. 4.B6. LCMS trace for compound **1c**. R_t = 18.72 min. Purity: 96%.

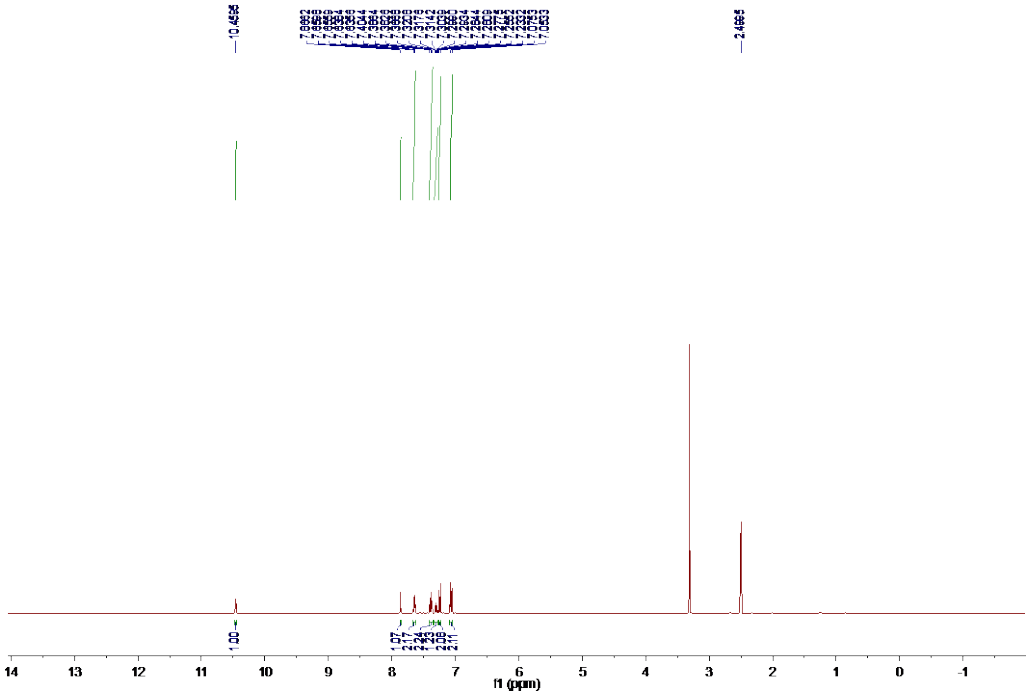

Fig. 4.B7. ^{1}H NMR spectrum for compound **1d** in $(CD_3)_2SO$ (400 MHz).

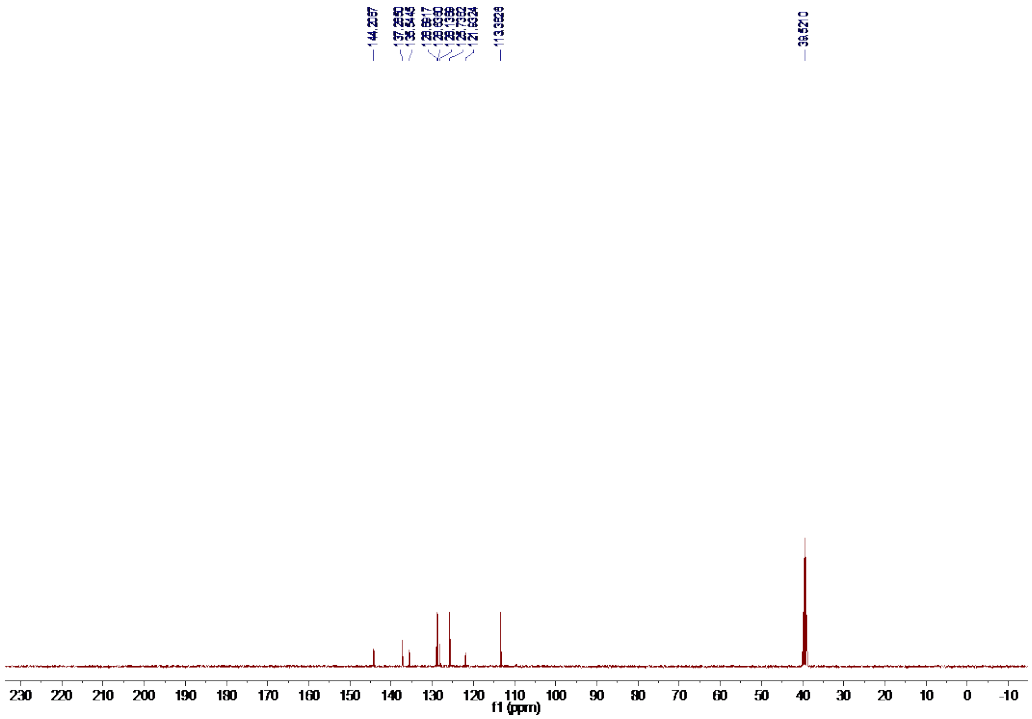

Fig. 4.B8. ^{13}C NMR spectrum for compound **1d** in $(CD_3)_2SO$ (100 MHz).

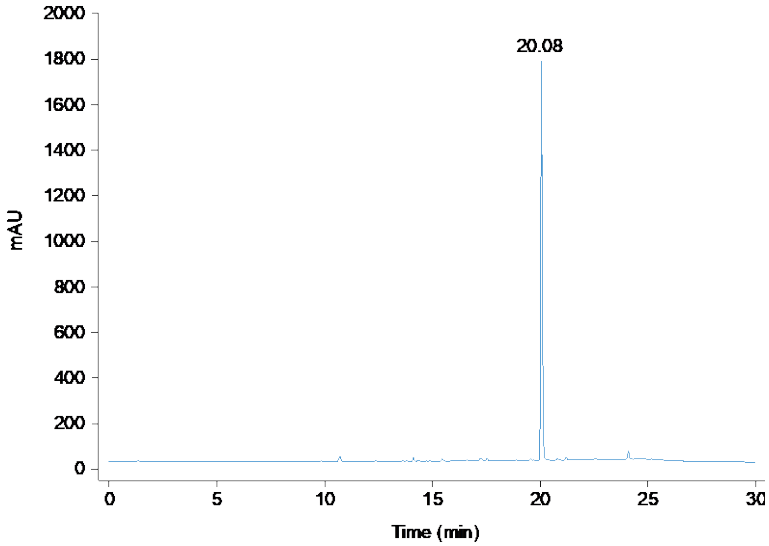

Fig. 4.B9. LCMS trace for compound **1d**. R_t = 20.08 min. Purity: 96%.

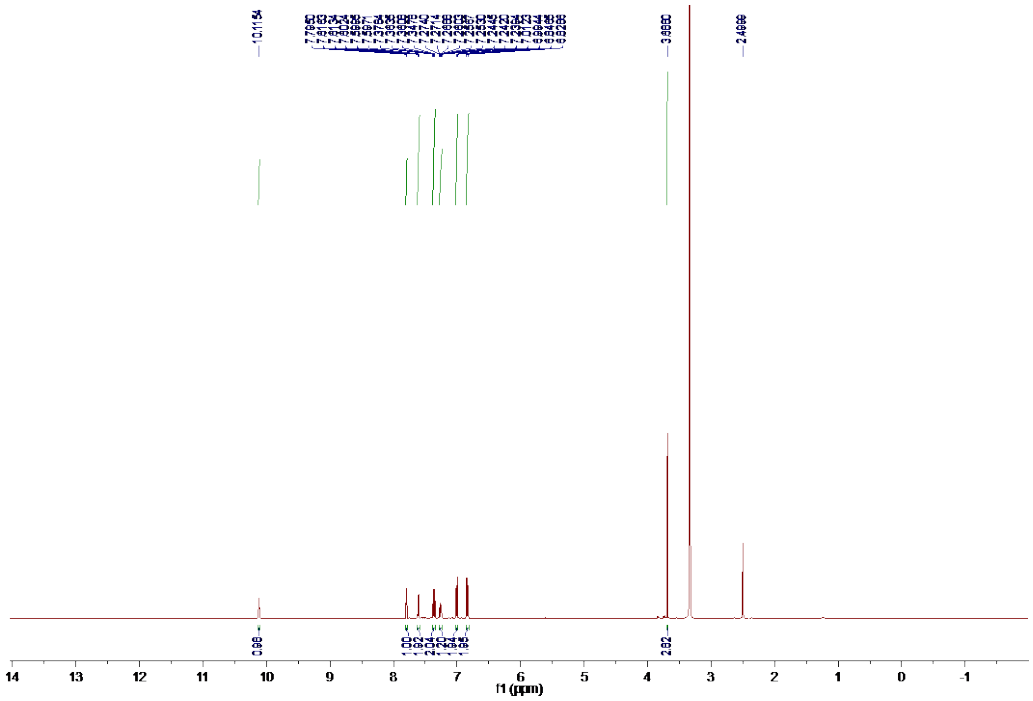

Fig. 4.B10. ^{1}H NMR spectrum for compound **1e** in $(CD_3)_2SO$ (500 MHz).

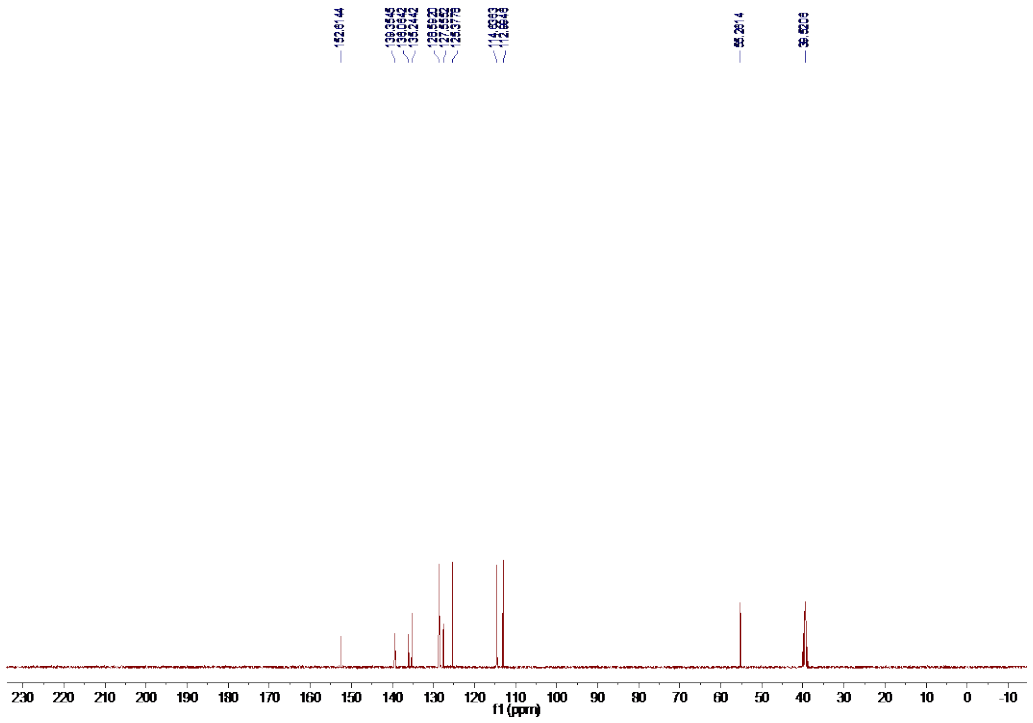

Fig. 4.B11. ^{13}C NMR spectrum for compound **1e** in $(CD_3)_2SO$ (100 MHz).

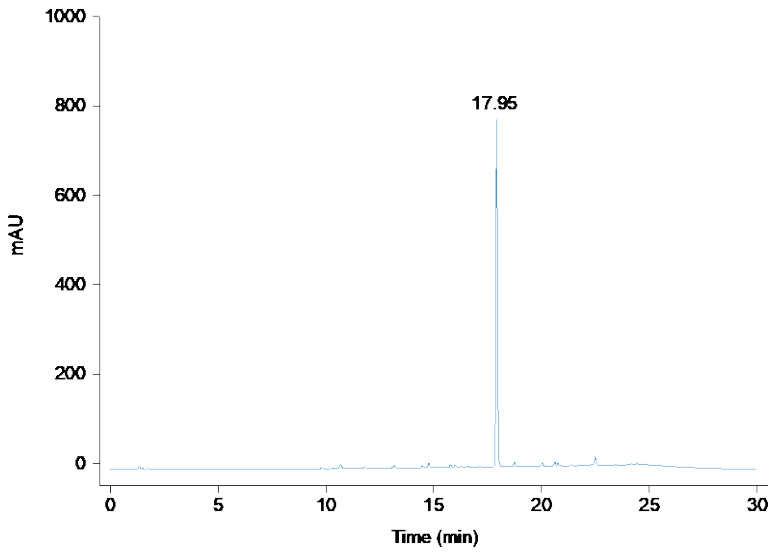

Fig. 4.B12. LCMS trace for compound **1e**. R_t = 17.95 min. Purity: 95%.

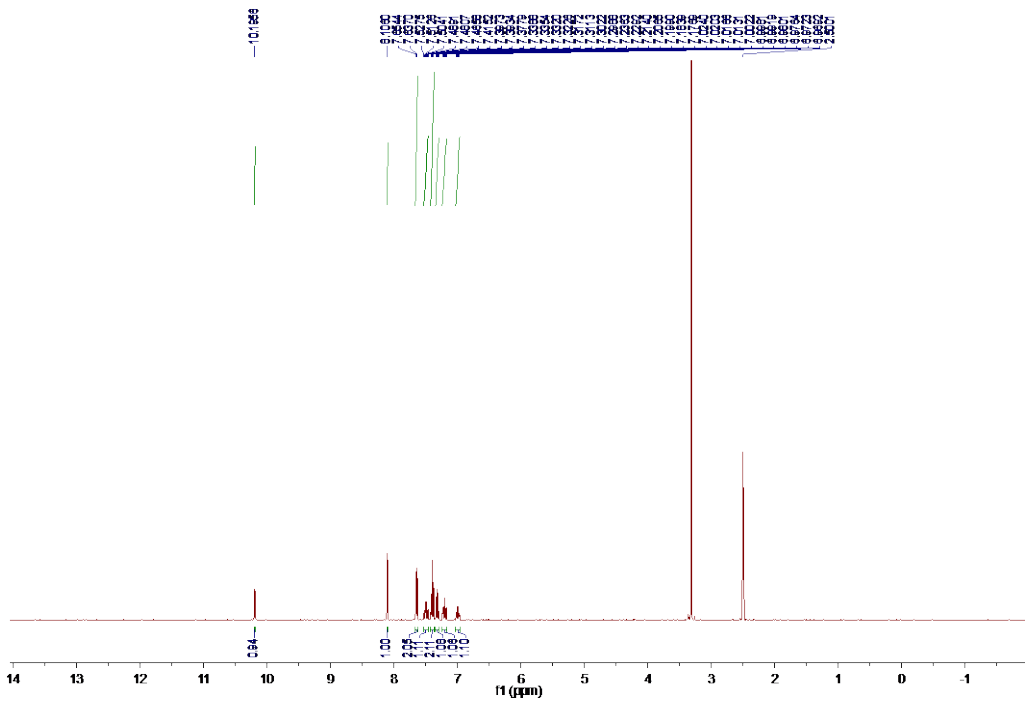

Fig. 4.B13. ^{1}H NMR spectrum for compound **1f** in $(CD_3)_2SO$ (400 MHz).

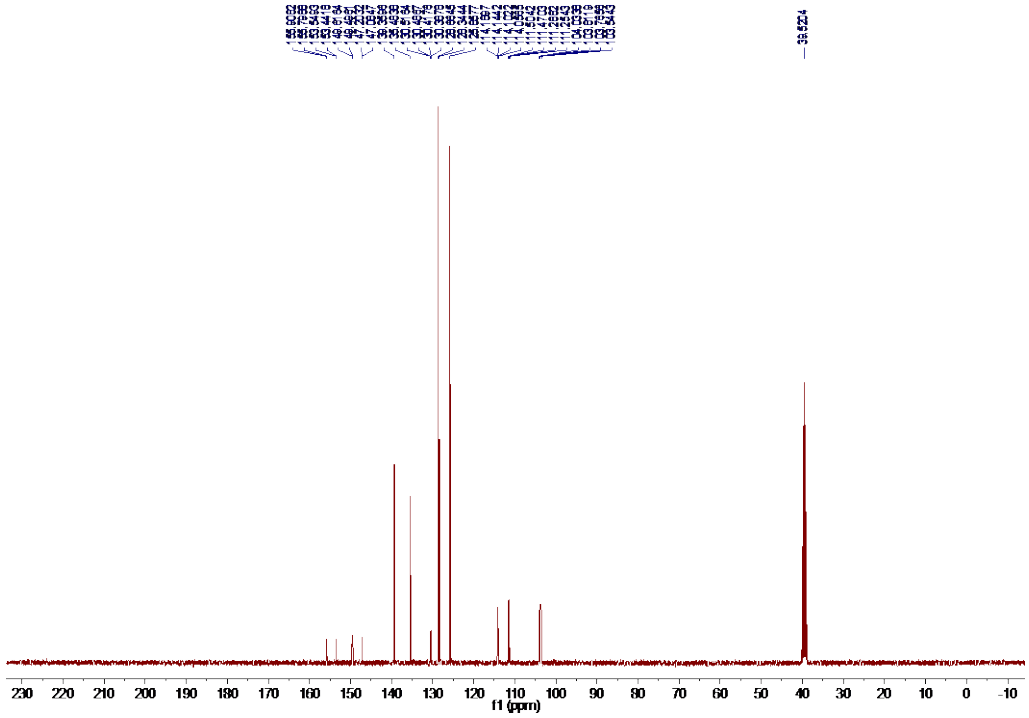

Fig. 4.B14. ^{13}C NMR spectrum for compound **1f** in $(CD_3)_2SO$ (100 MHz).

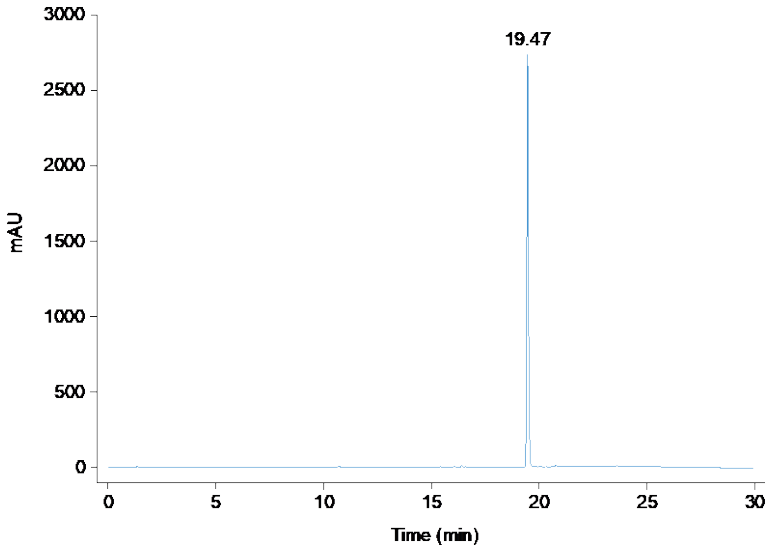

Fig. 4.B15. LCMS trace for compound **1f**. R_t = 19.47 min. Purity: 99%.

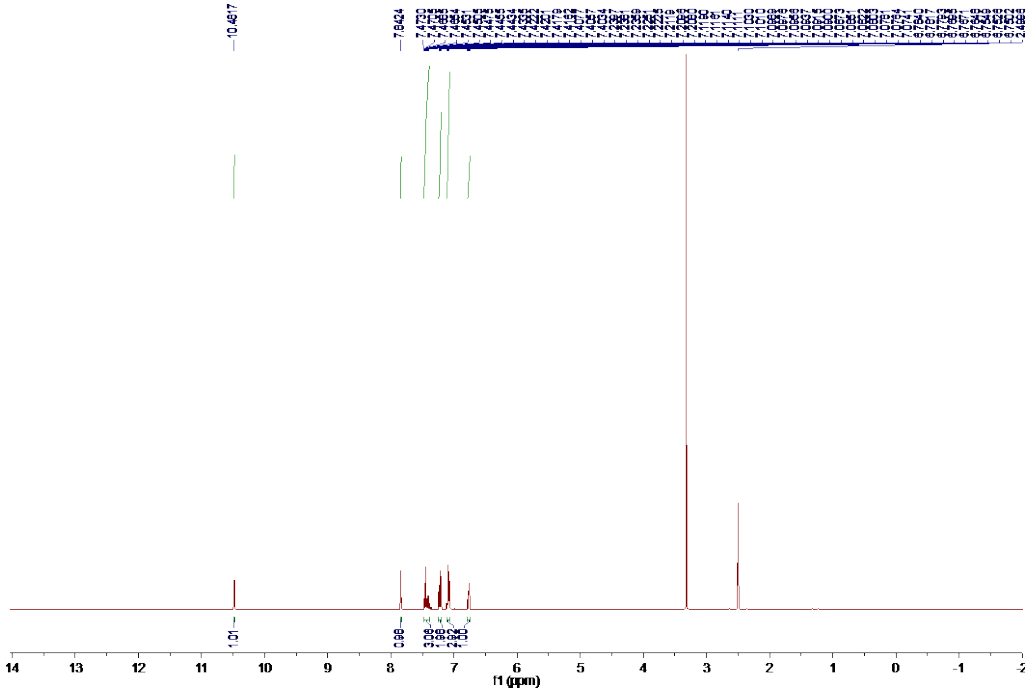

Fig. 4.B16. ^{1}H NMR spectrum for compound **2a** in $(CD_3)_2SO$ (500 MHz).

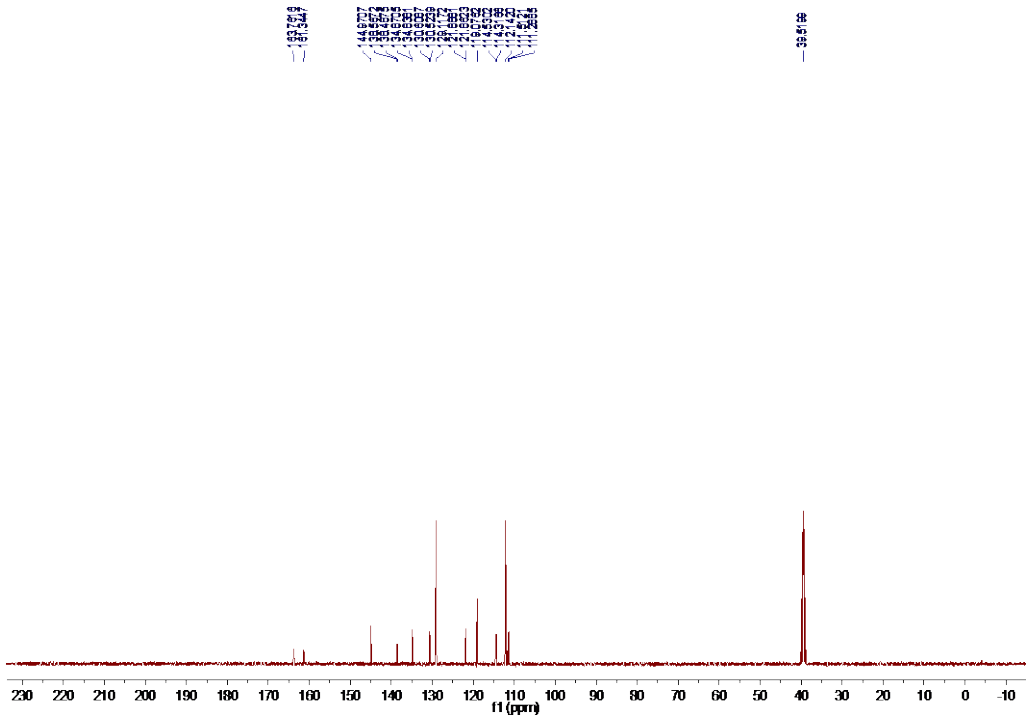

Fig. 4.B17. ^{13}C NMR spectrum for compound **2a** in $(CD_3)_2SO$ (100 MHz).

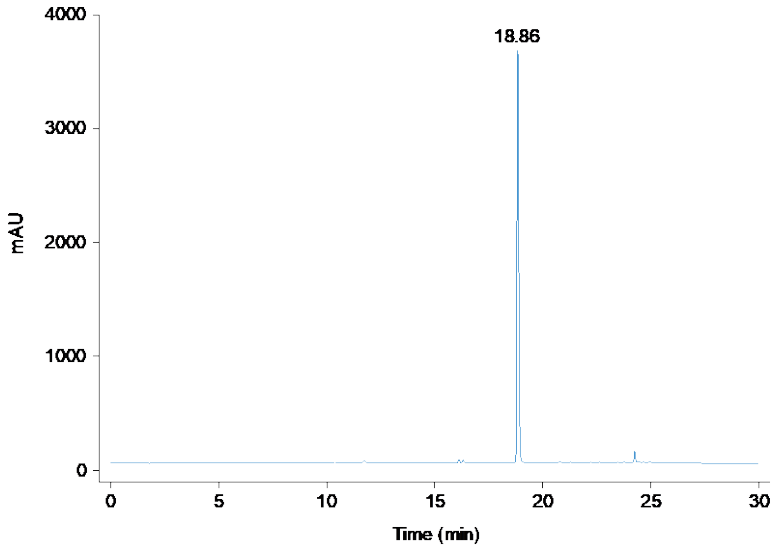

Fig. 4.B18. LCMS trace for compound **2a**. R_t = 18.86 min. Purity: 97%.

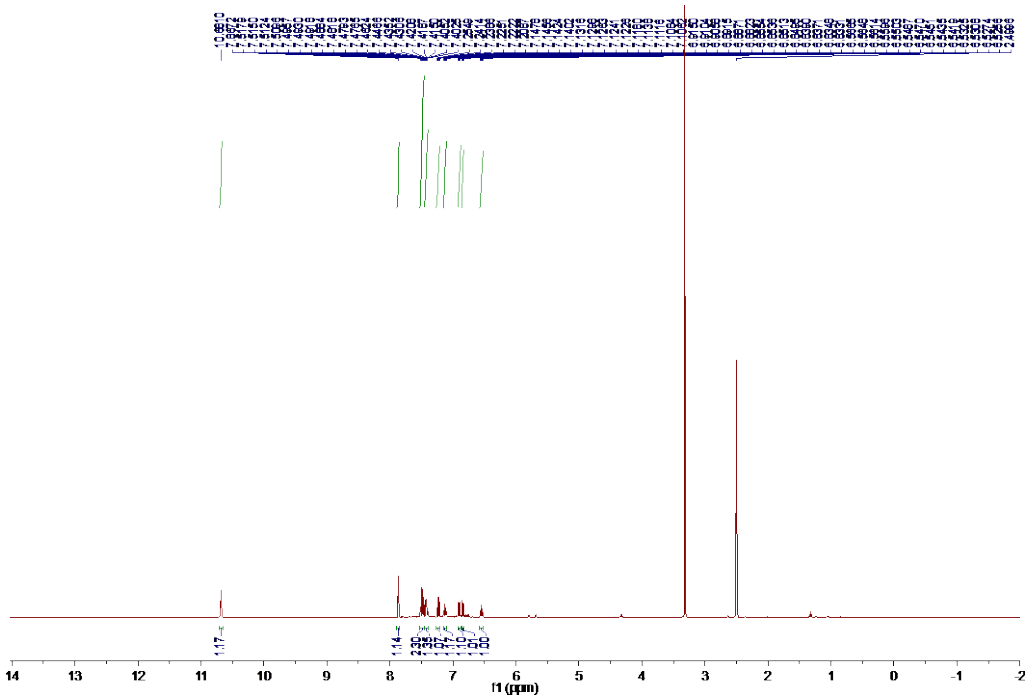

Fig. 4.B19. ^{1}H NMR spectrum for compound **2b** in $(CD_3)_2SO$ (500 MHz).

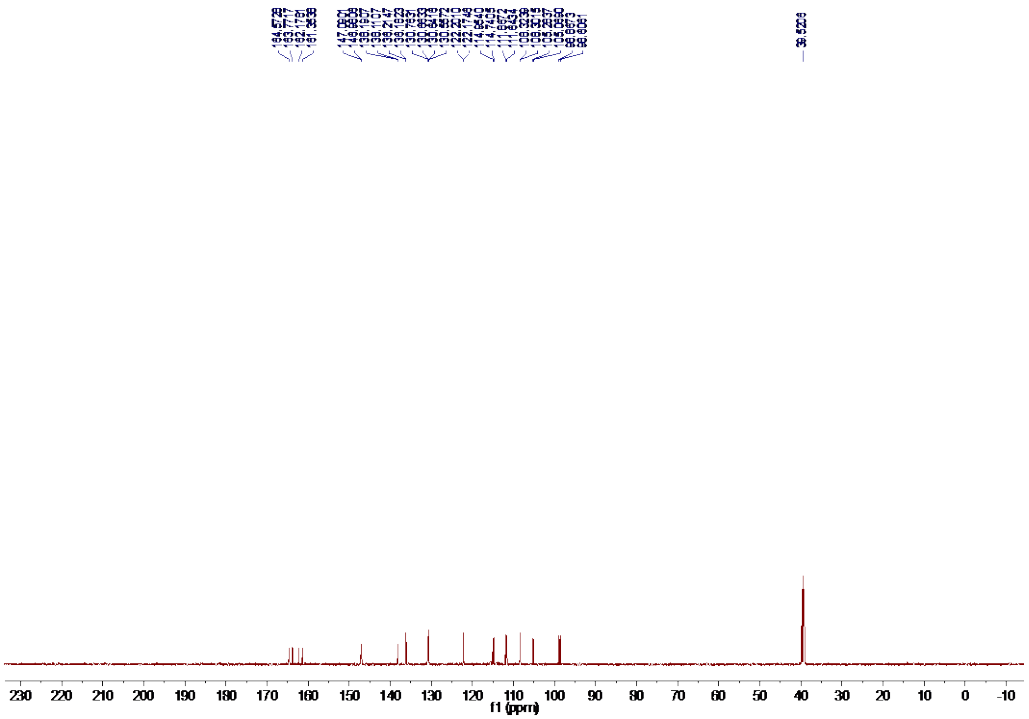

Fig. 4.B20. ^{13}C NMR spectrum for compound **2b** in $(CD_3)_2SO$ (100 MHz).

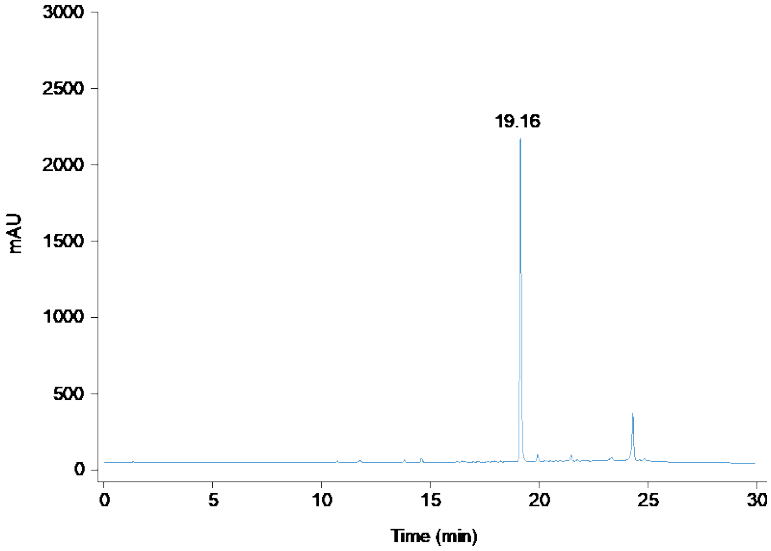

Fig. 4.B21. LCMS trace for compound **2b**. R_t = 19.16 min. Purity: 90%.

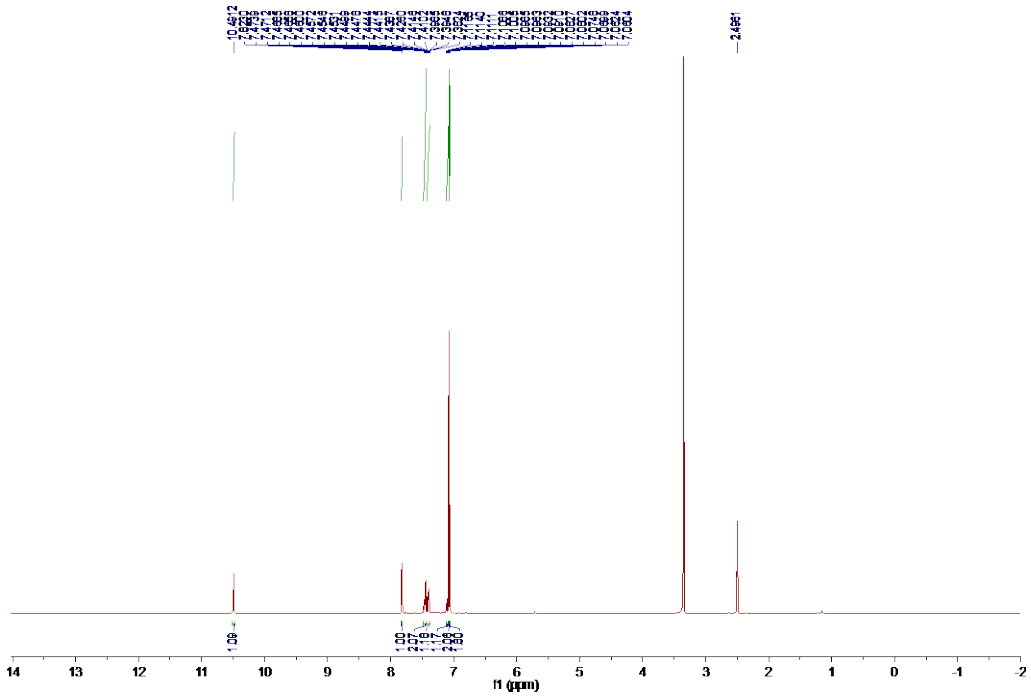

Fig. 4.B22. ^{1}H NMR spectrum for compound **2c** in $(CD_3)_2SO$ (500 MHz).

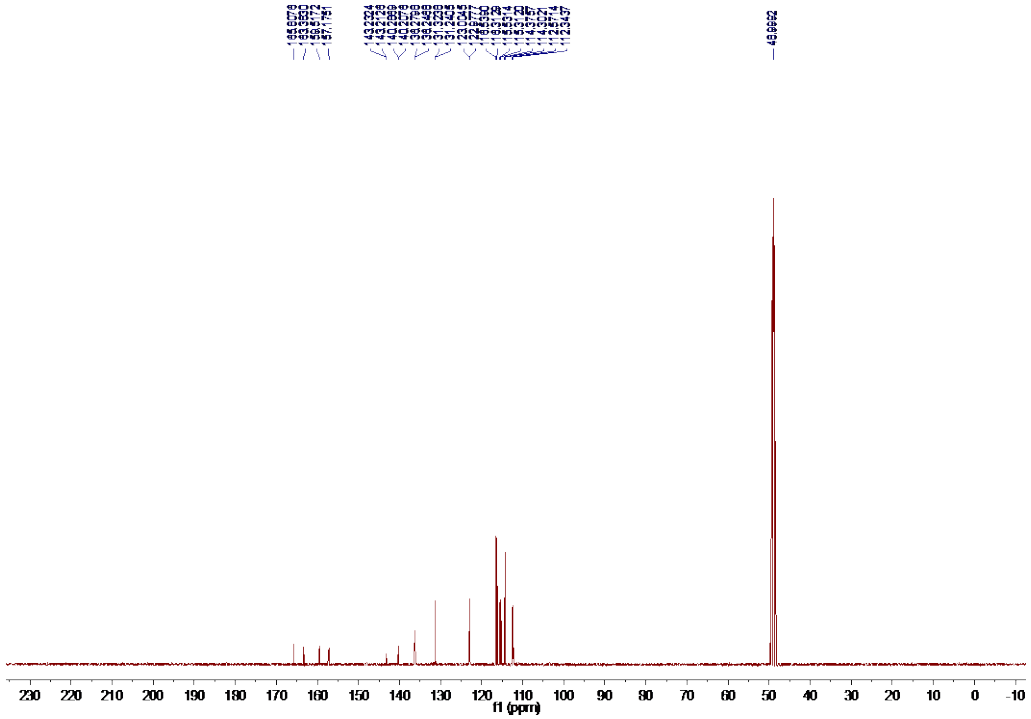

Fig. 4.B23. ^{13}C NMR spectrum for compound **2c** in CD_3OD (100 MHz).

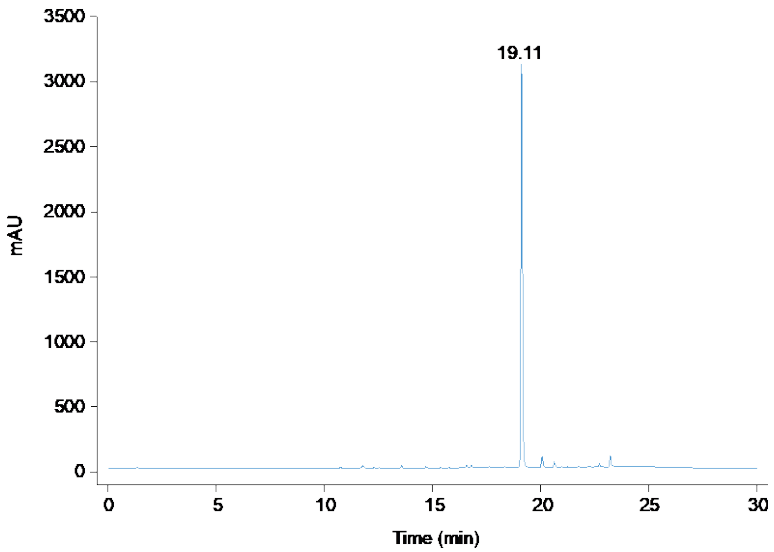

Fig. 4.B24. LCMS trace for compound **2c**. R_t = 19.11 min. Purity: 95%.

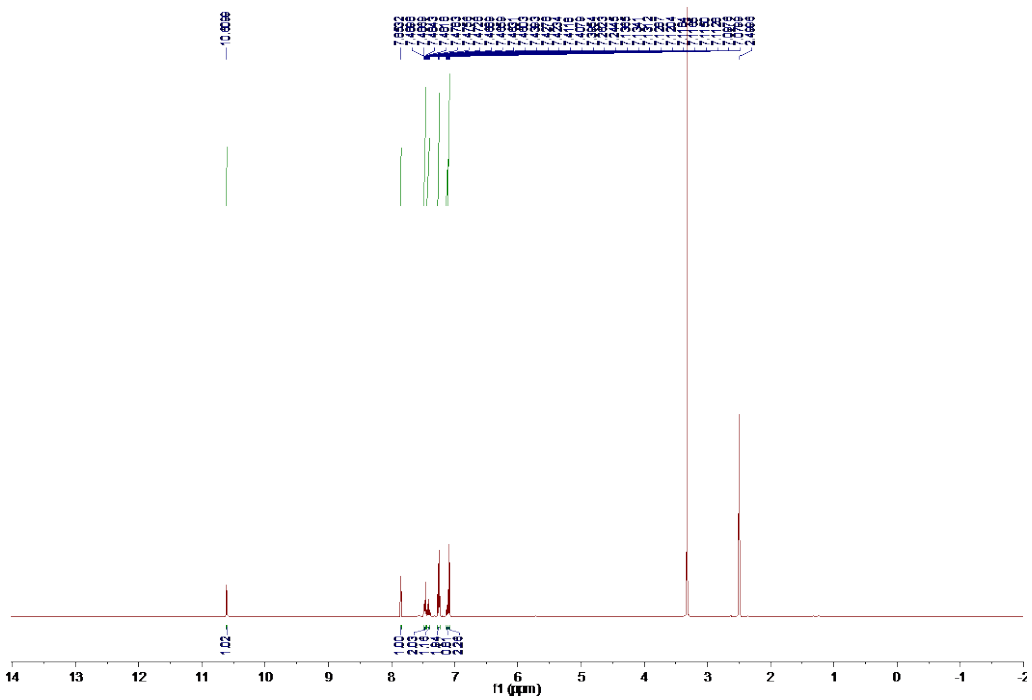

Fig. 4.B25. ^{1}H NMR spectrum for compound **2d** in $(CD_3)_2SO$ (500 MHz).

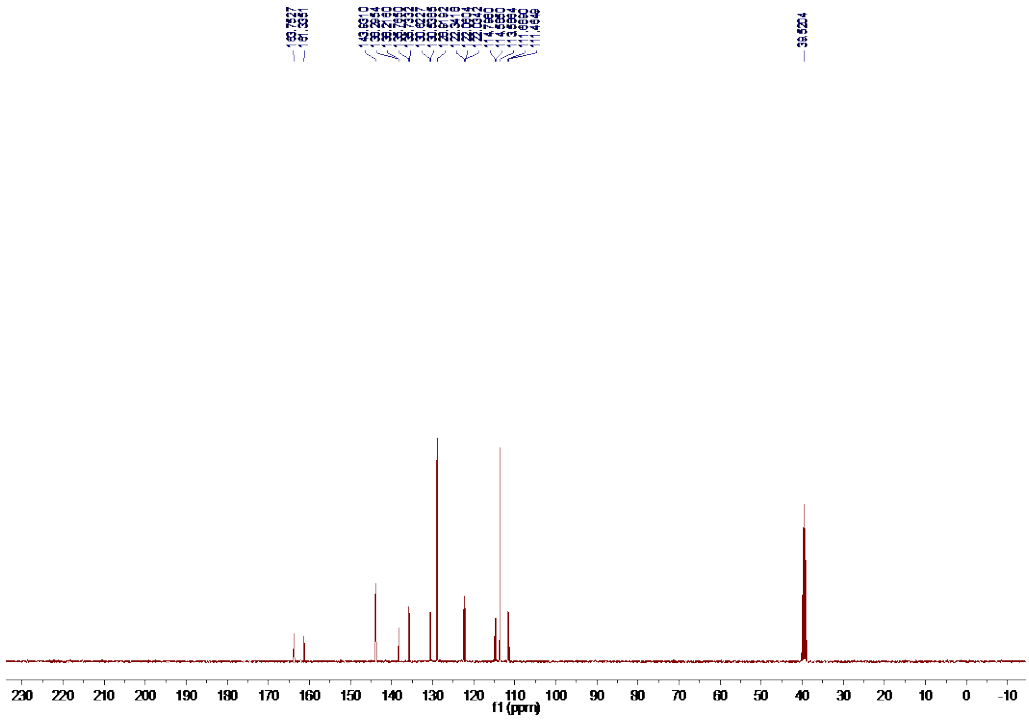

Fig. 4.B26. ^{13}C NMR spectrum for compound **2d** in $(CD_3)_2SO$ (100 MHz).

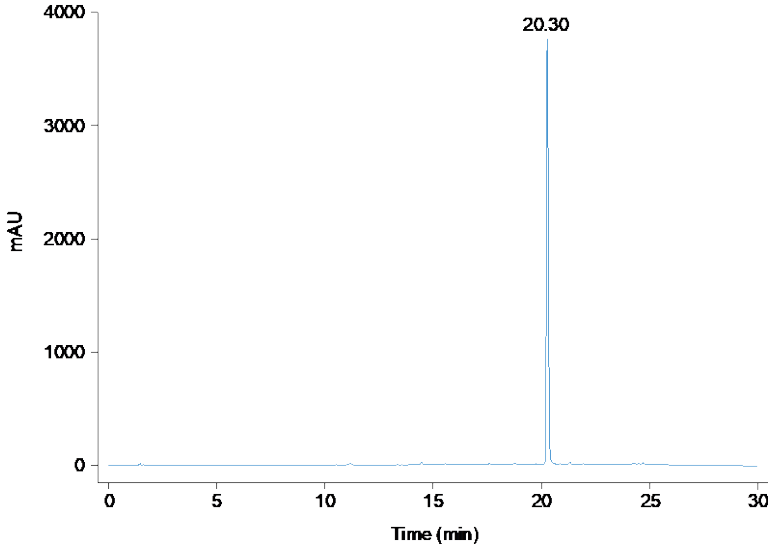

Fig. 4.B27. LCMS trace for compound **2d**. R_t = 20.30 min. Purity: 99%.

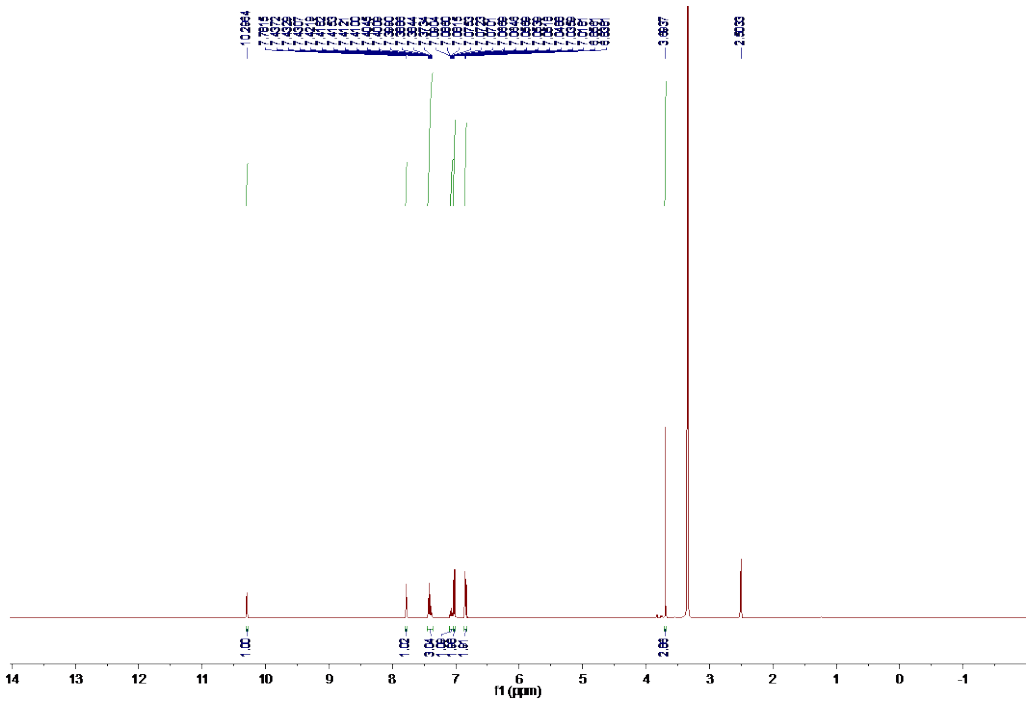

Fig. 4.B28. ^{1}H NMR spectrum for compound **2e** in $(CD_3)_2SO$ (500 MHz).

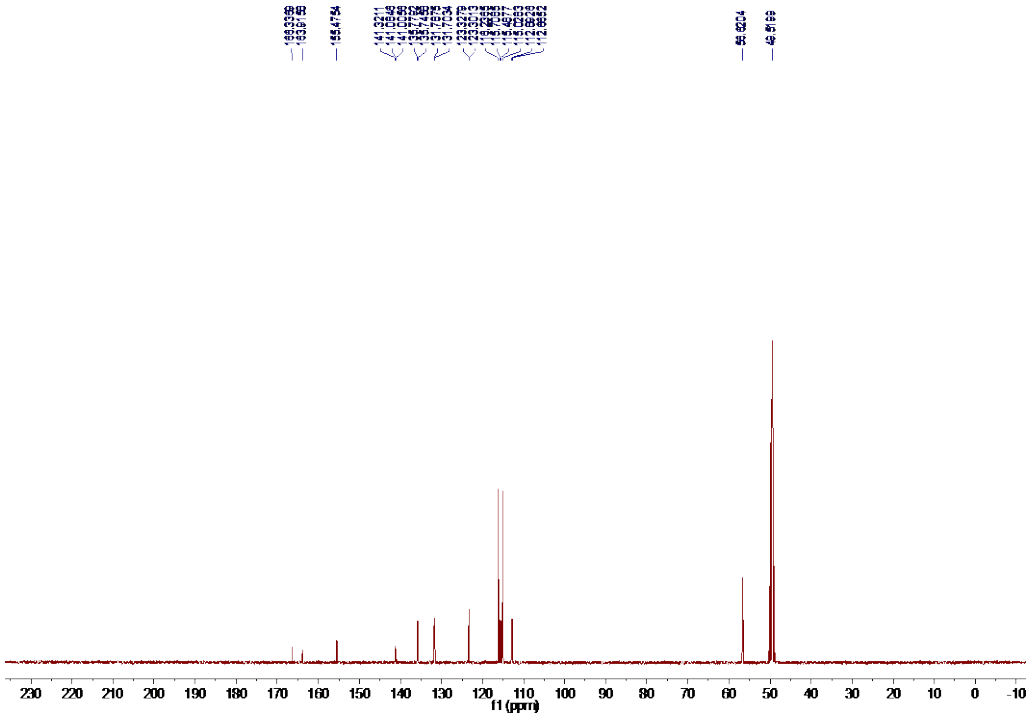

Fig. 4.B29. ^{13}C NMR spectrum for compound **2e** in CD_3OD (100 MHz).

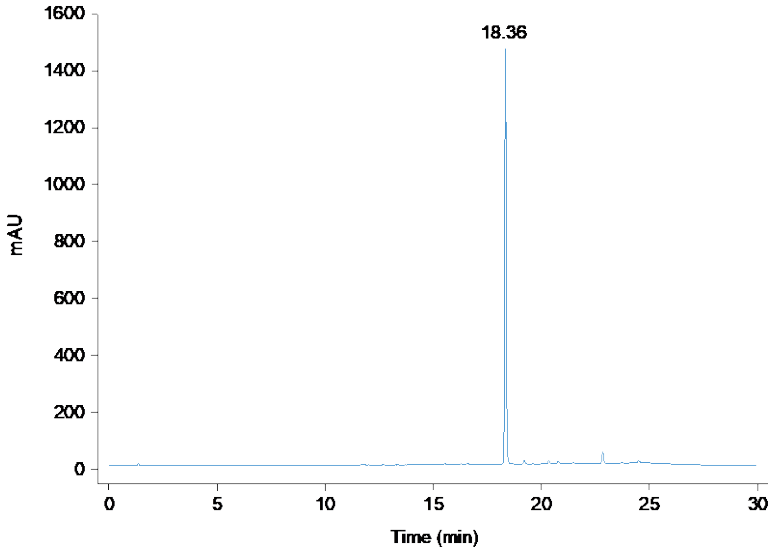

Fig. 4.B30. LCMS trace for compound **2e**. R_t = 18.36 min. Purity: 98%.

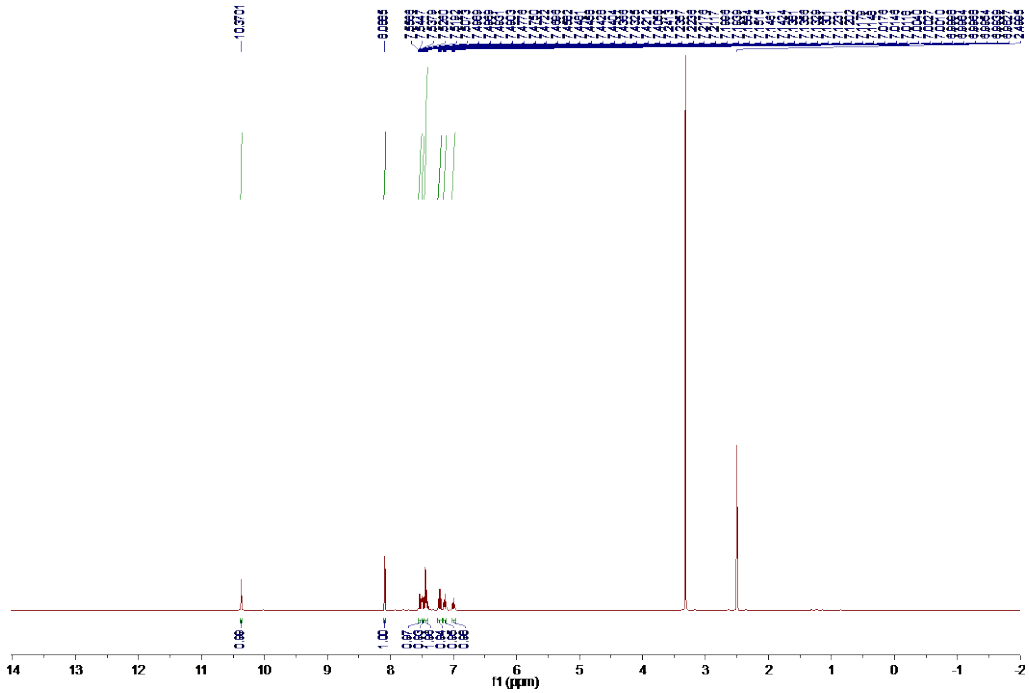

Fig. 4.B31. ^{1}H NMR spectrum for compound **2f** in $(CD_3)_2SO$ (500 MHz).

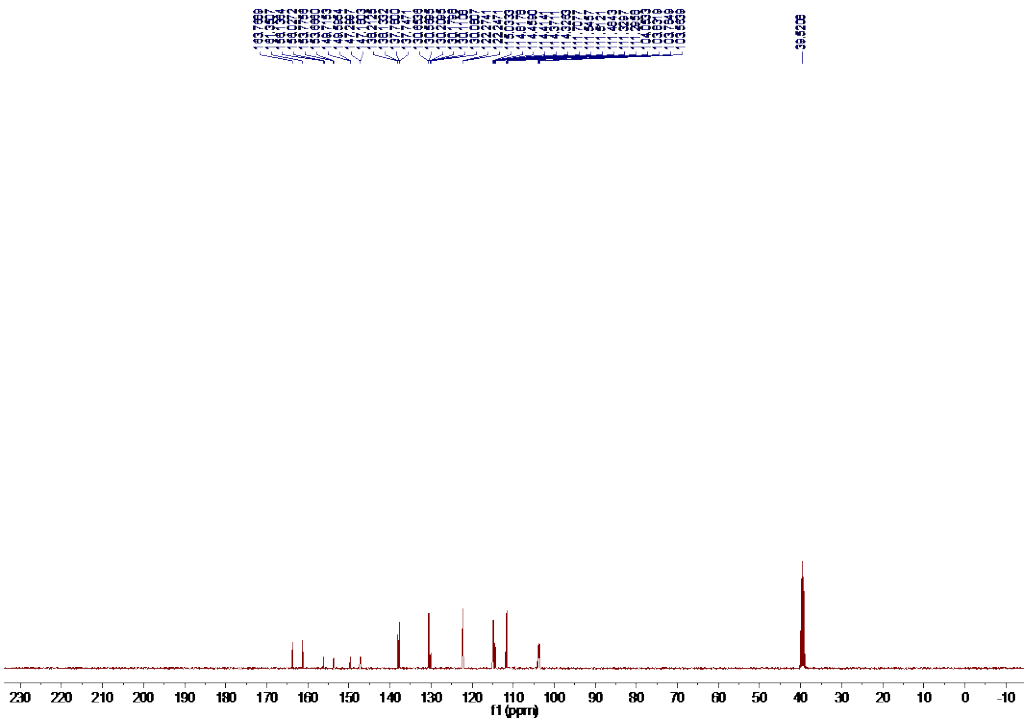

Fig. 4.B32. ^{13}C NMR spectrum for compound **2f** in $(CD_3)_2SO$ (100 MHz).

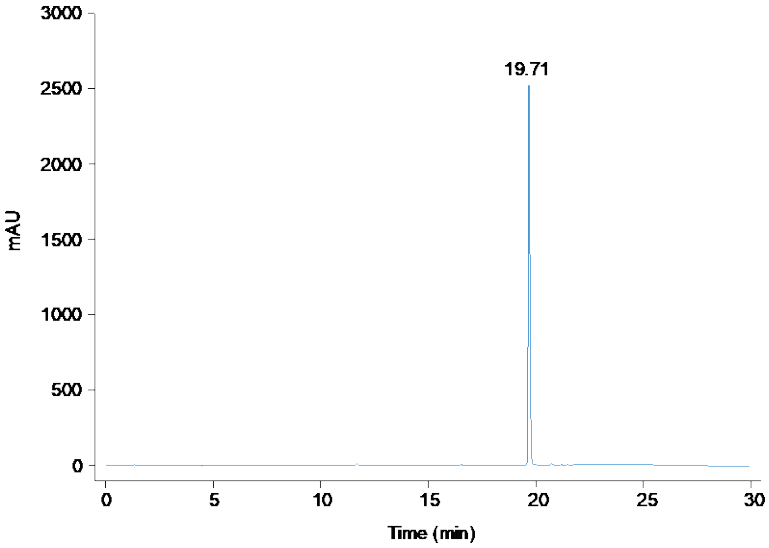

Fig. 4.B33. LCMS trace for compound **2f**. R_t = 19.71 min. Purity: 99%.

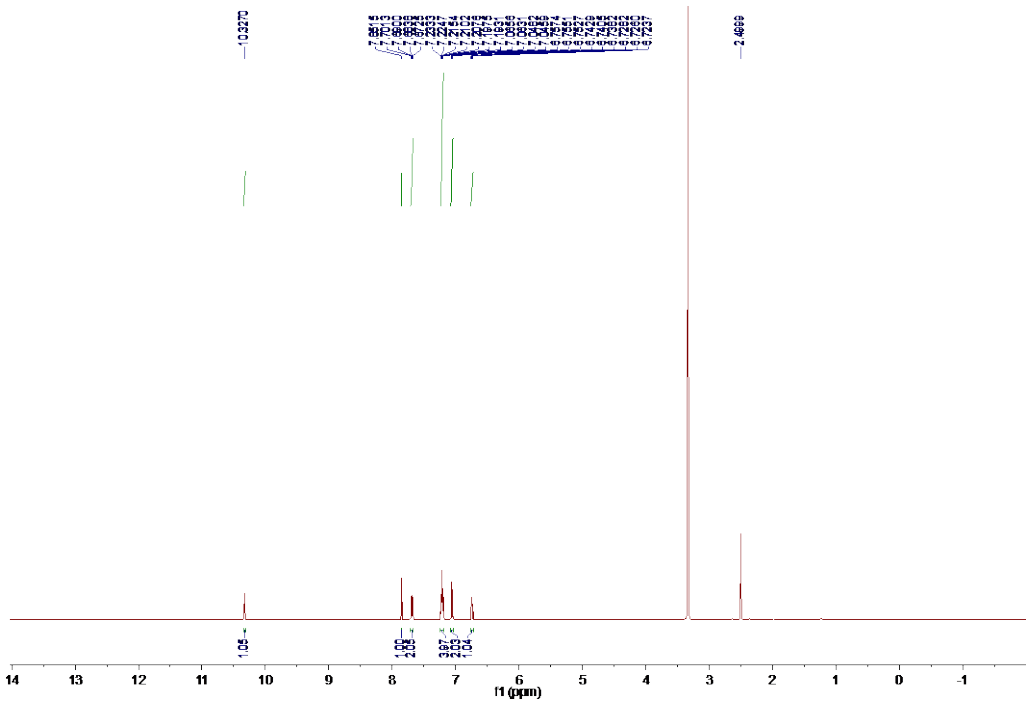

Fig. 4.B34. ^{1}H NMR spectrum for compound **3a** in $(CD_3)_2SO$ (500 MHz).

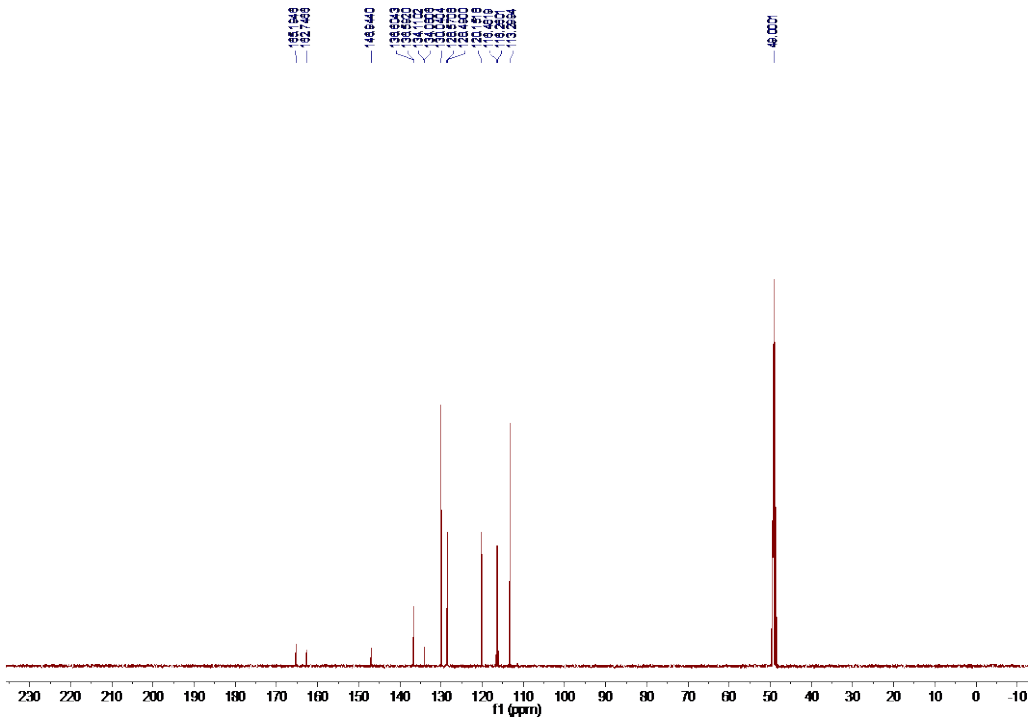

Fig. 4.B35. ^{13}C NMR spectrum for compound **3a** in CD_3OD (100 MHz).

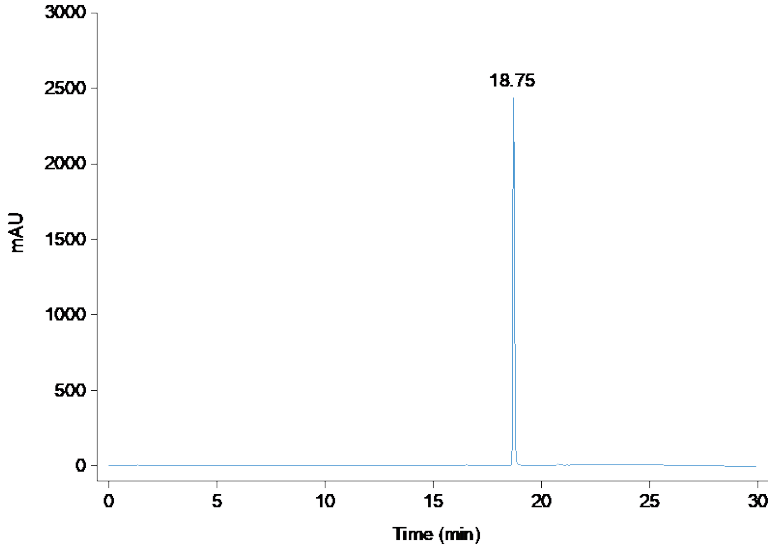

Fig. 4.B36. LCMS trace for compound **3a**. R_t = 18.75 min. Purity: 99%.

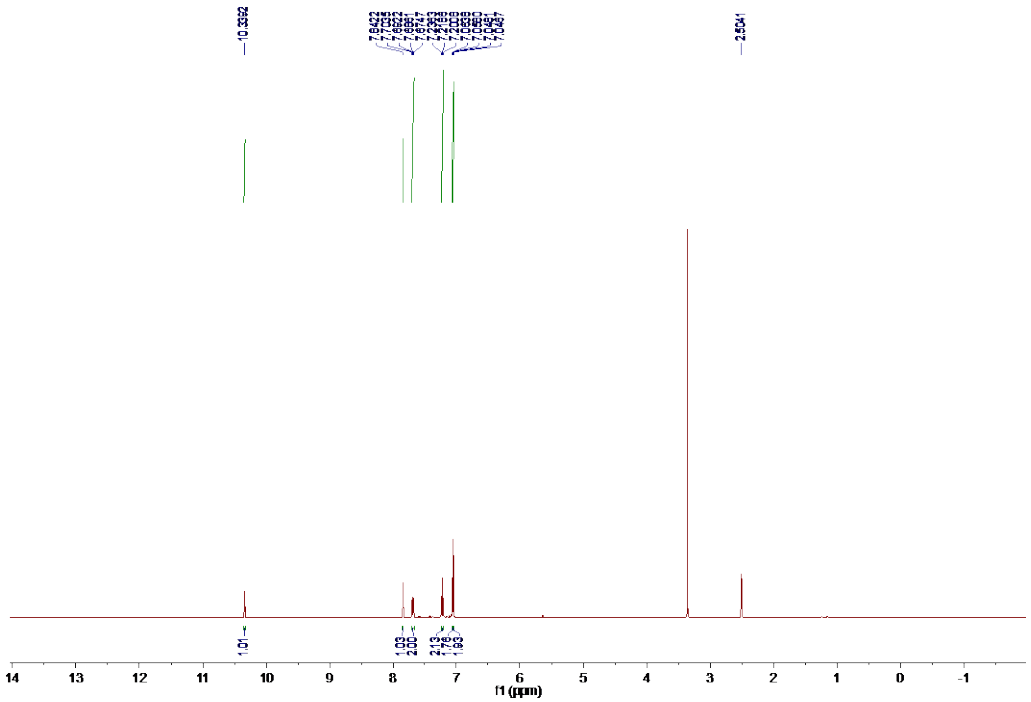

Fig. 4.B37. ^{1}H NMR spectrum for compound **3c** in $(CD_3)_2SO$ (500 MHz).

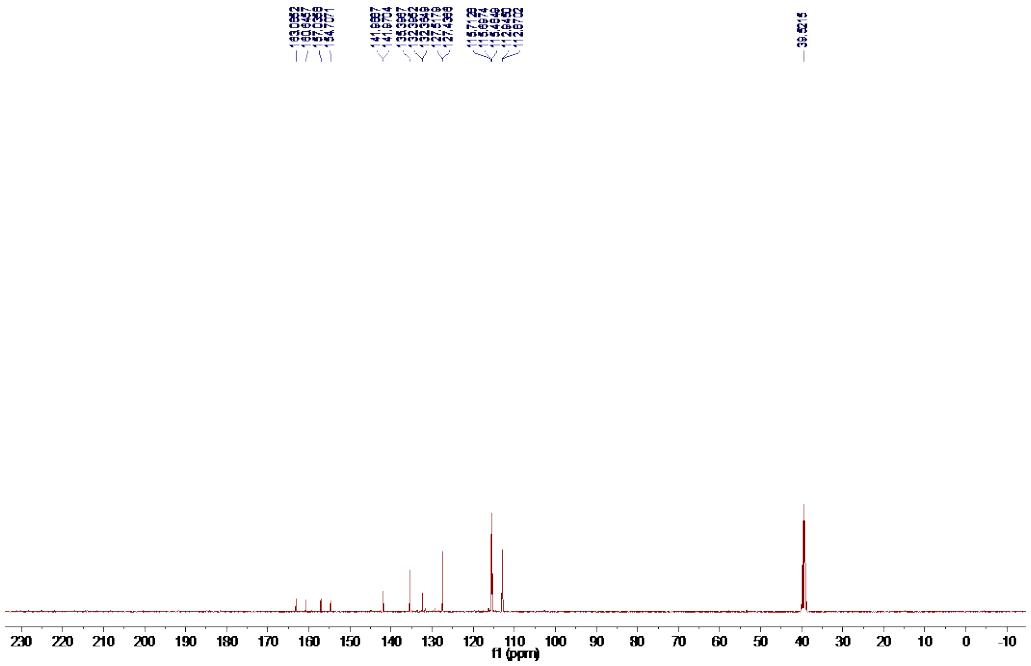

Fig. 4.B38. ^{13}C NMR spectrum for compound **3c** in $(CD_3)_2SO$ (100 MHz).

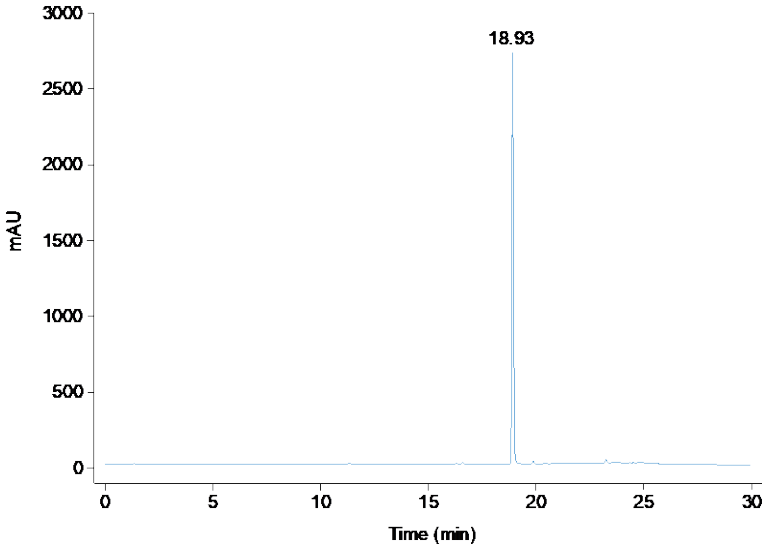

Fig. 4.B39. LCMS trace for compound **3c**. R_t = 18.93 min. Purity: 98%.

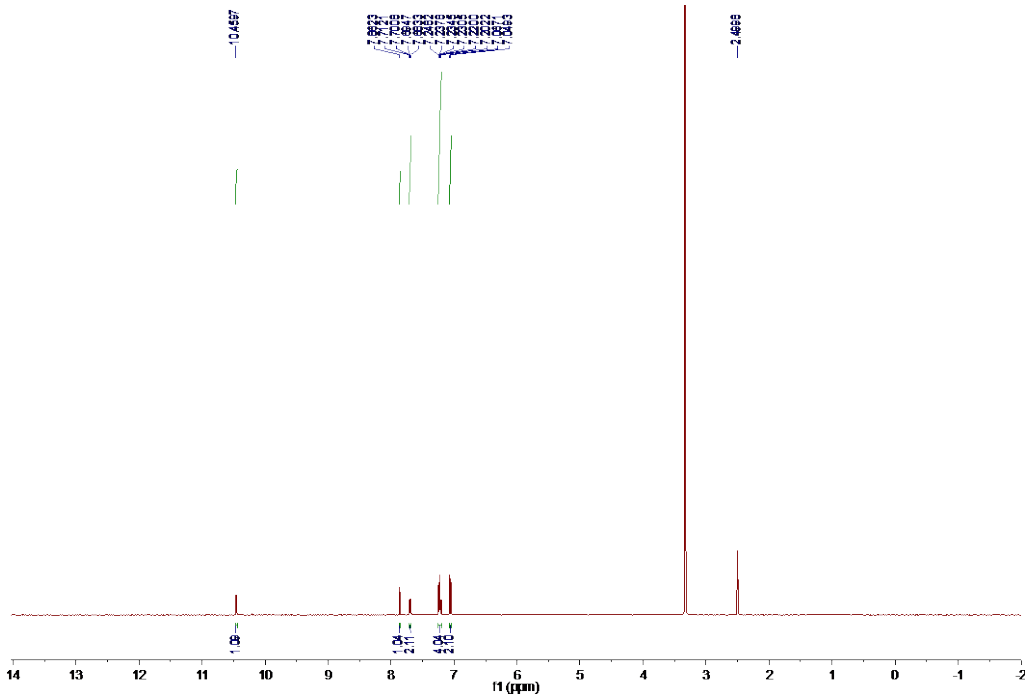

Fig. 4.B40. ^{1}H NMR spectrum for compound **3d** in $(CD_3)_2SO$ (500 MHz).

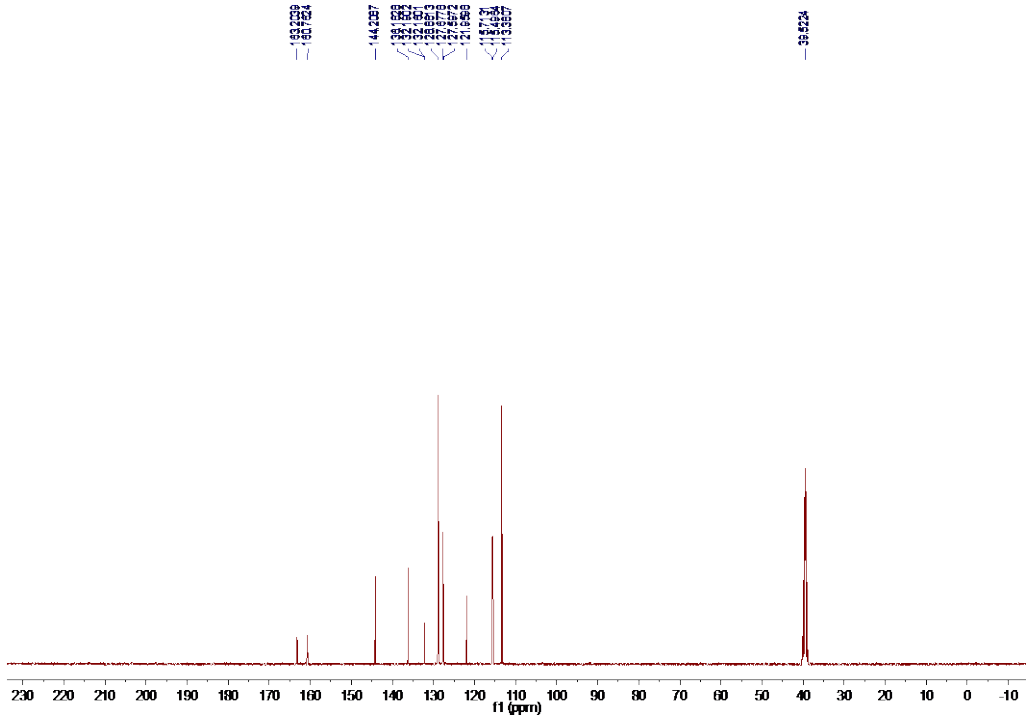

Fig. 4.B41. ^{13}C NMR spectrum for compound **3d** in $(CD_3)_2SO$ (100 MHz).

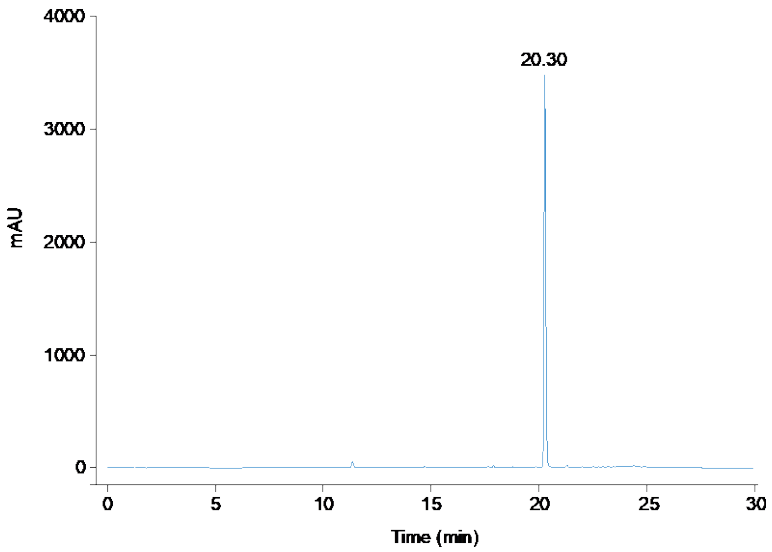

Fig. 4.B42. LCMS trace for compound **3d**. R_t = 20.30 min. Purity: 99%.

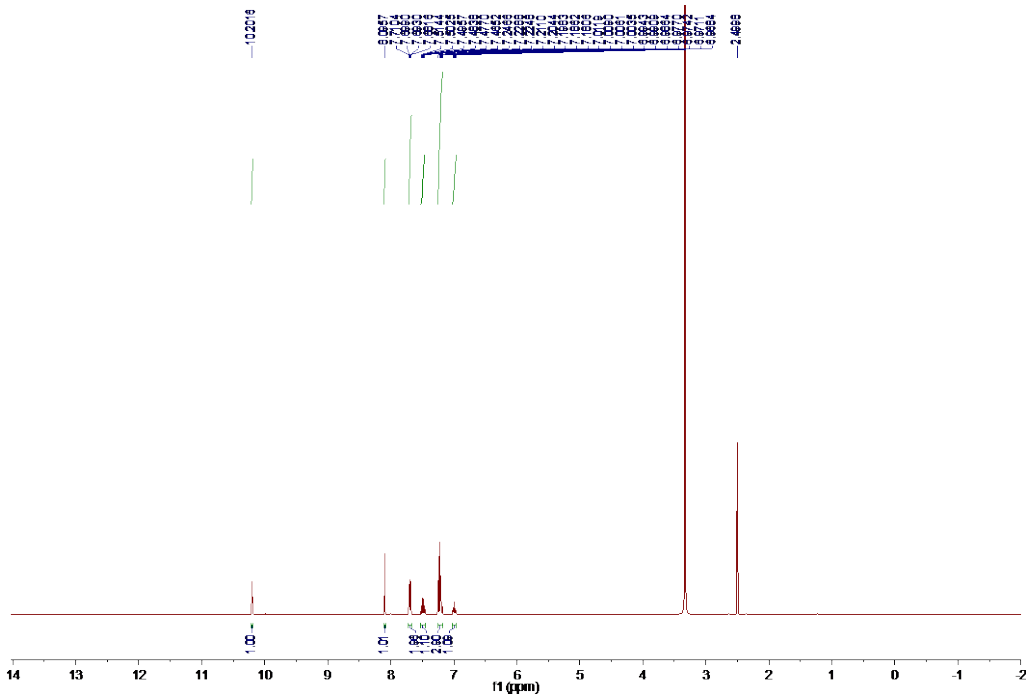

Fig. 4.B43. ^{1}H NMR spectrum for compound **3f** in $(CD_3)_2SO$ (500 MHz).

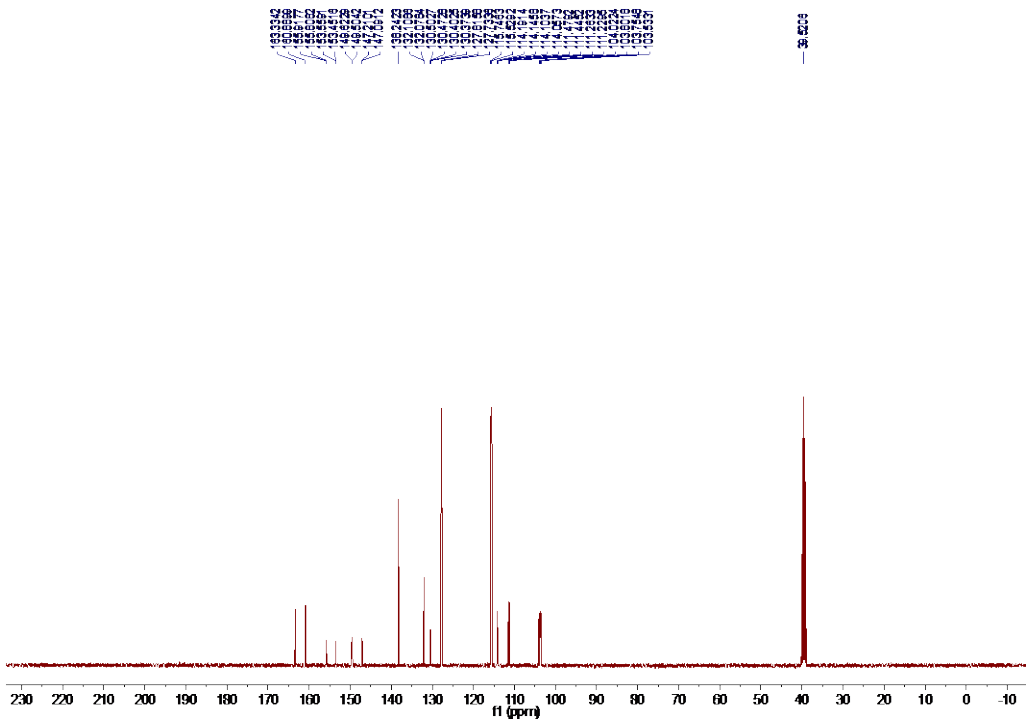

Fig. 4.B44. ^{13}C NMR spectrum for compound **3f** in $(CD_3)_2SO$ (100 MHz).

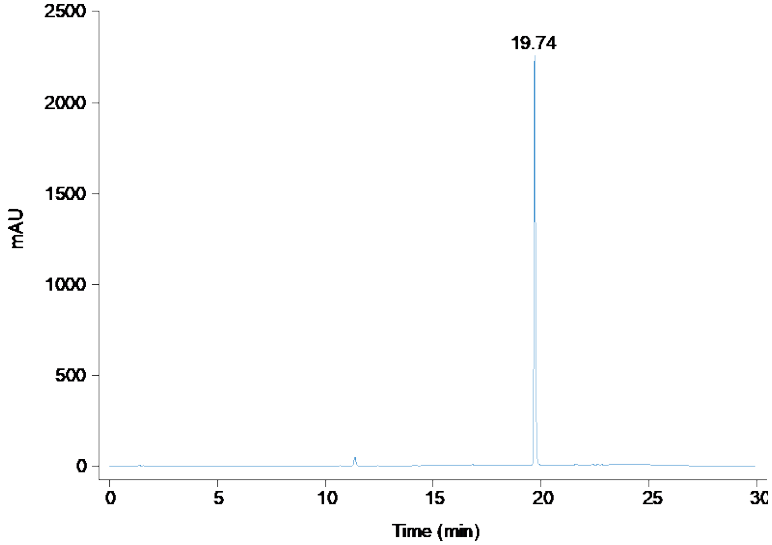

Fig. 4.B45. LCMS trace for compound **3f**. R_t = 19.74 min. Purity: 98%.

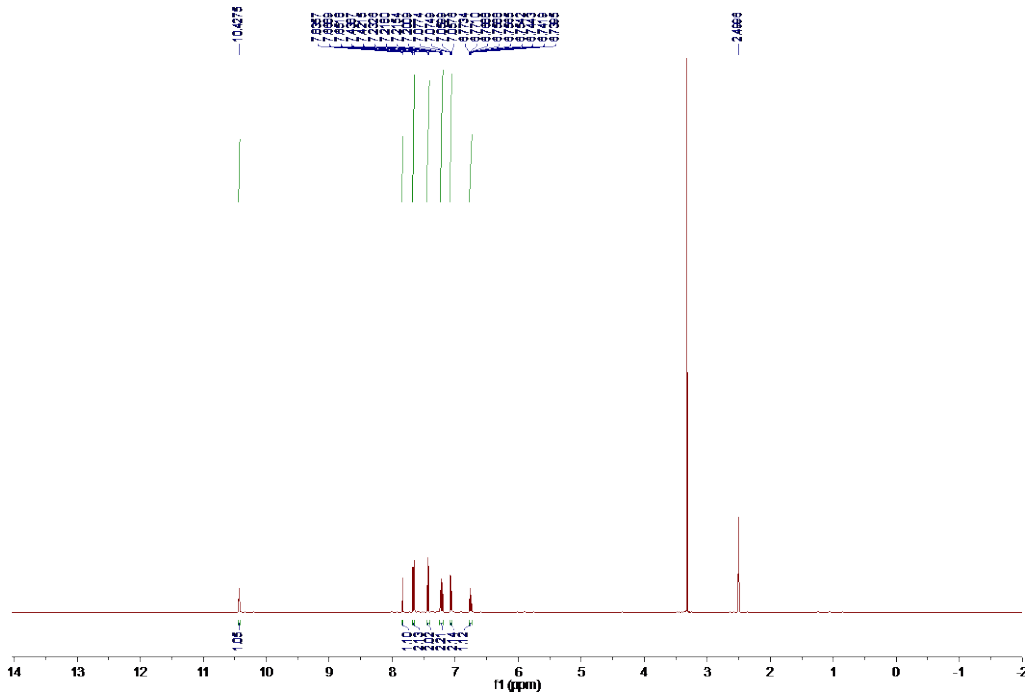

Fig. 4.B46. ^{1}H NMR spectrum for compound **4a** in $(CD_3)_2SO$ (500 MHz).

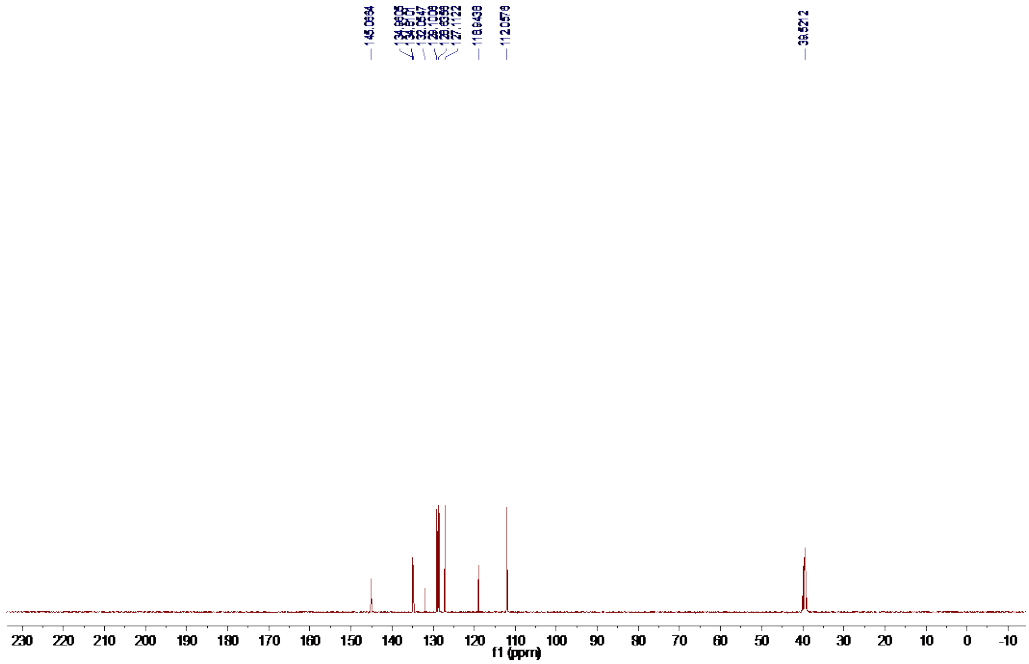

Fig. 4.B47. ^{13}C NMR spectrum for compound **4a** in $(CD_3)_2SO$ (100 MHz).

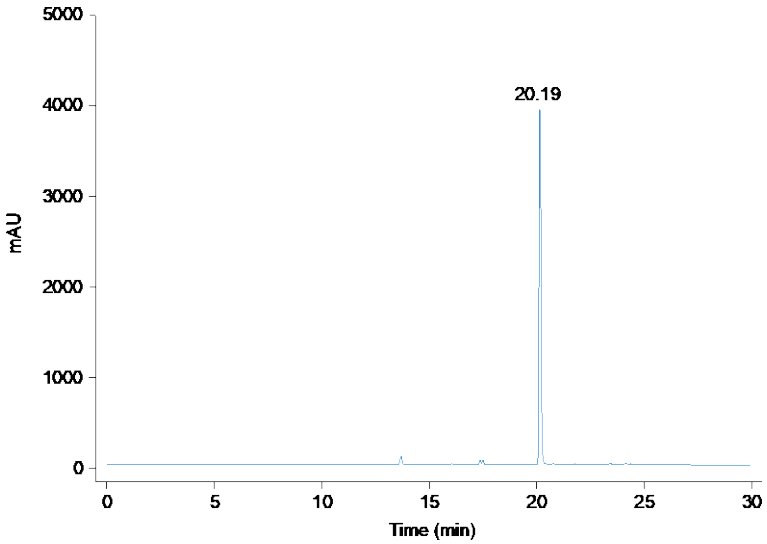

Fig. 4.B48. LCMS trace for compound **4a**. R_t = 20.19 min. Purity: 96%.

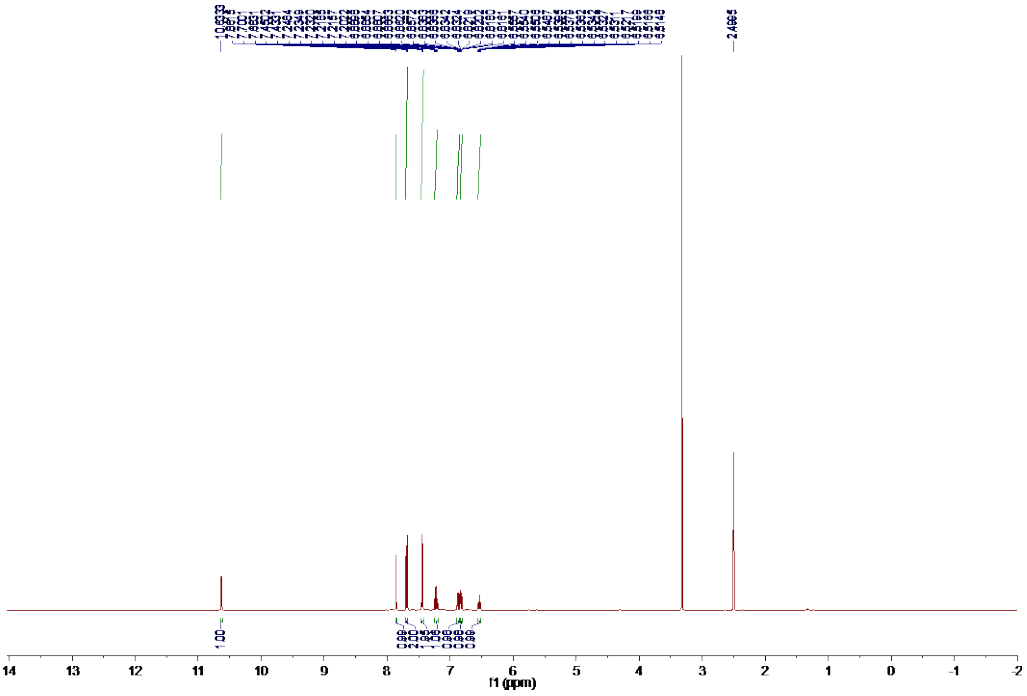

Fig. 4.B49. ^{1}H NMR spectrum for compound **4b** in $(CD_3)_2SO$ (500 MHz).

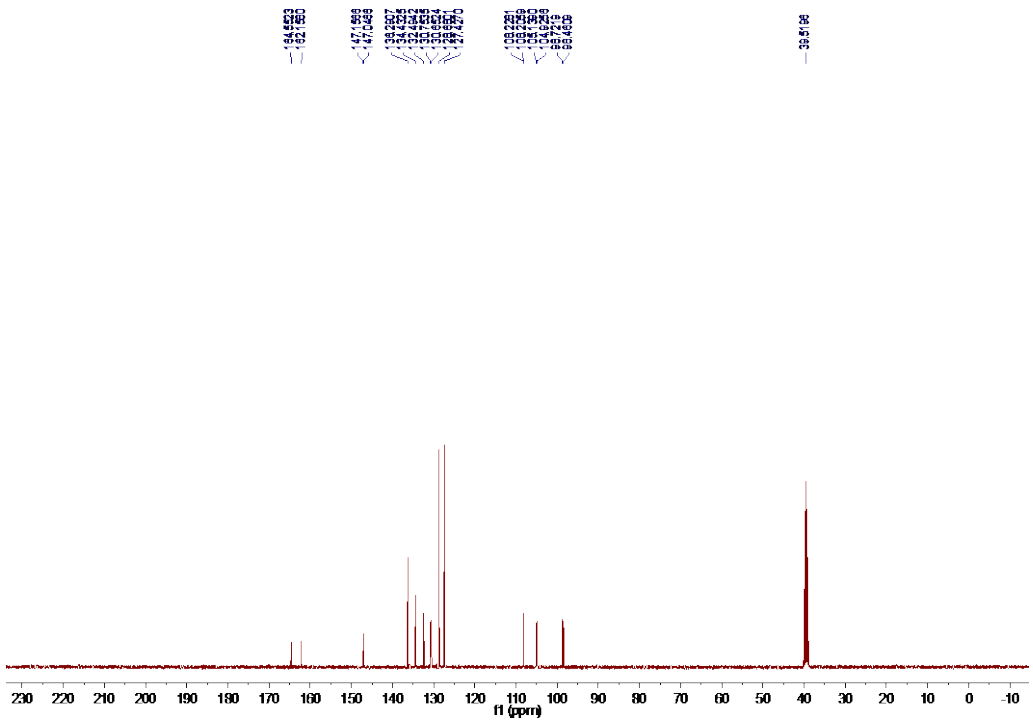

Fig. 4.B50. ^{13}C NMR spectrum for compound **4b** in $(CD_3)_2SO$ (100 MHz).

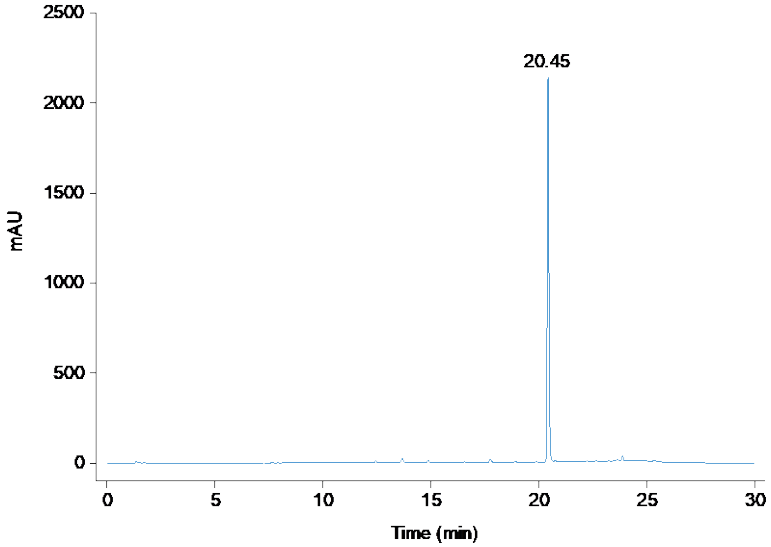

Fig. 4.B51. LCMS trace for compound **4b**. R_t = 20.45 min. Purity: 97%.

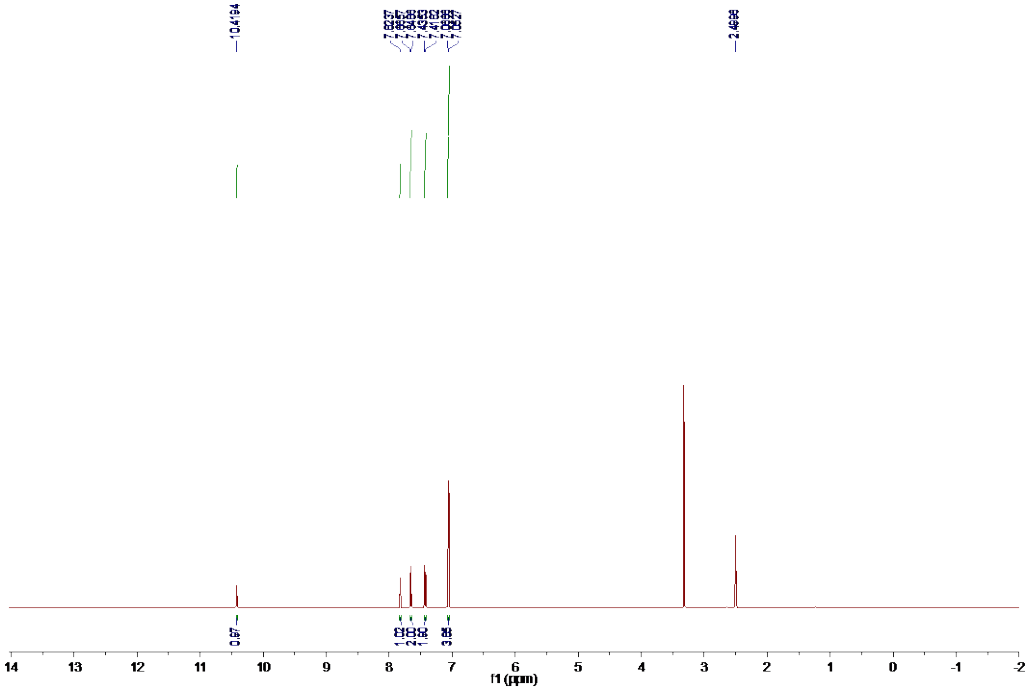

Fig. 4.B 52. ^{1}H NMR spectrum for compound **4c** in $(CD_3)_2SO$ (500 MHz).

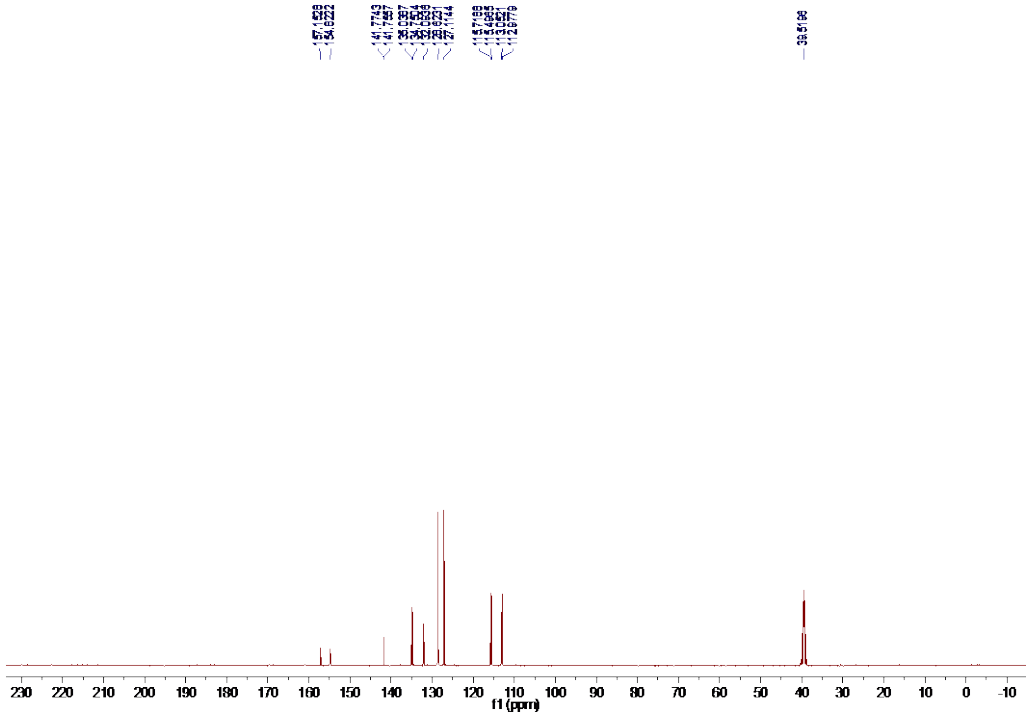

Fig. 4.B53. ^{13}C NMR spectrum for compound **4c** in $(CD_3)_2SO$ (100 MHz).

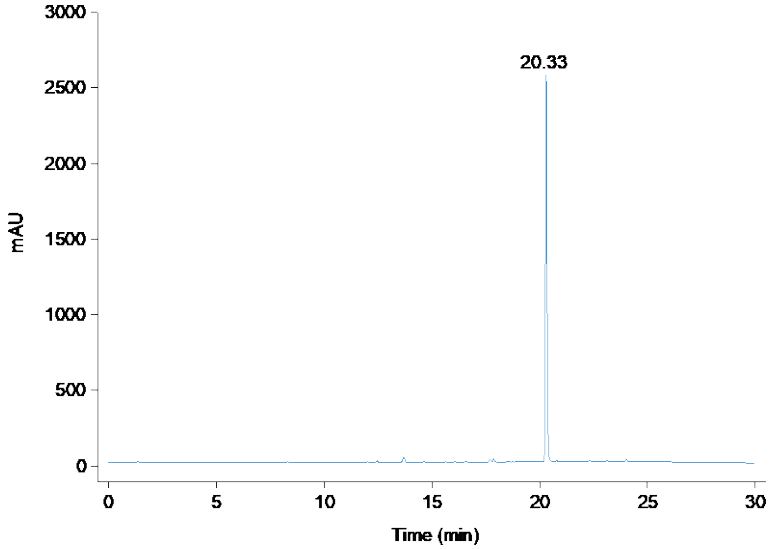

Fig. 4.B54. LCMS trace for compound **4c**. R_t = 20.33 min. Purity: 97%.

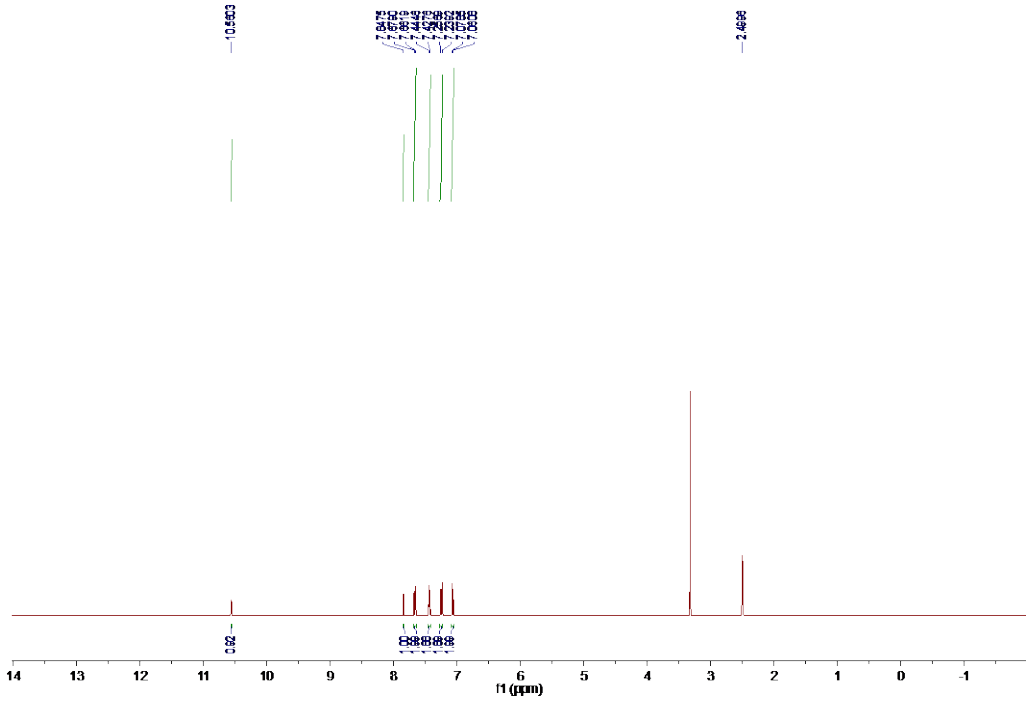

Fig. 4.B55. ^{1}H NMR spectrum for compound **4d** in $(CD_3)_2SO$ (500 MHz).

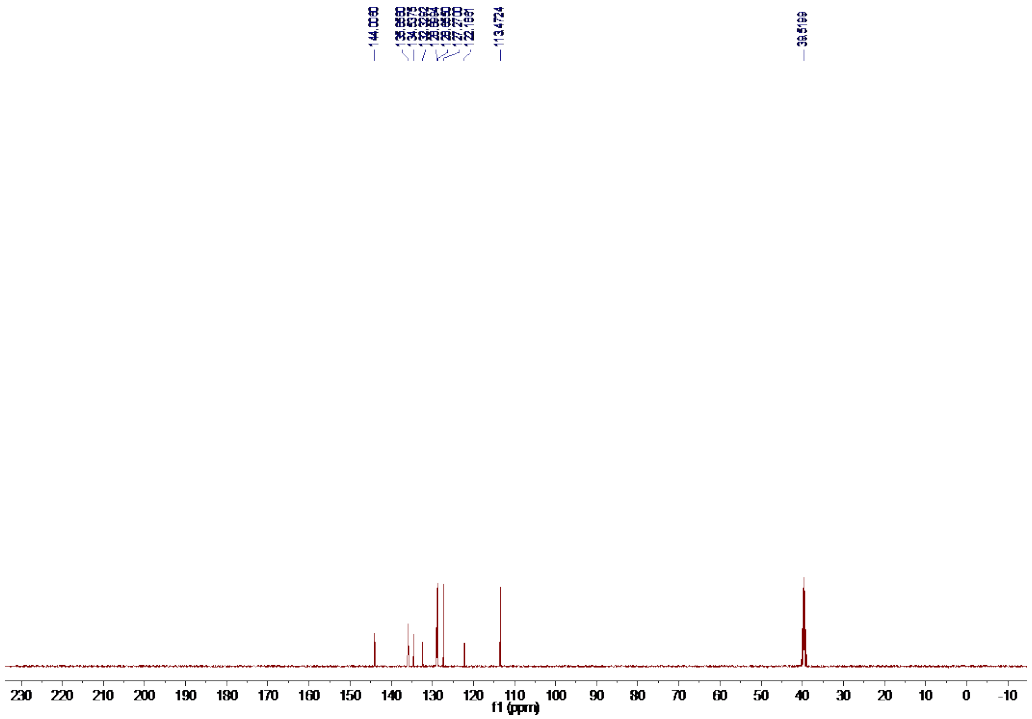

Fig. 4.B56. ^{13}C NMR spectrum for compound **4d** in $(CD_3)_2SO$ (100 MHz).

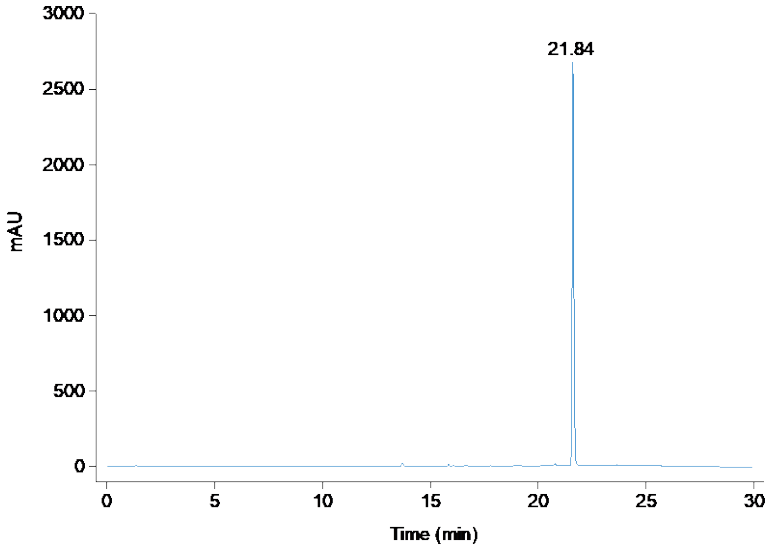

Fig. 4.B57. LCMS trace for compound **4d**. R_t = 21.84 min. Purity: 99%.

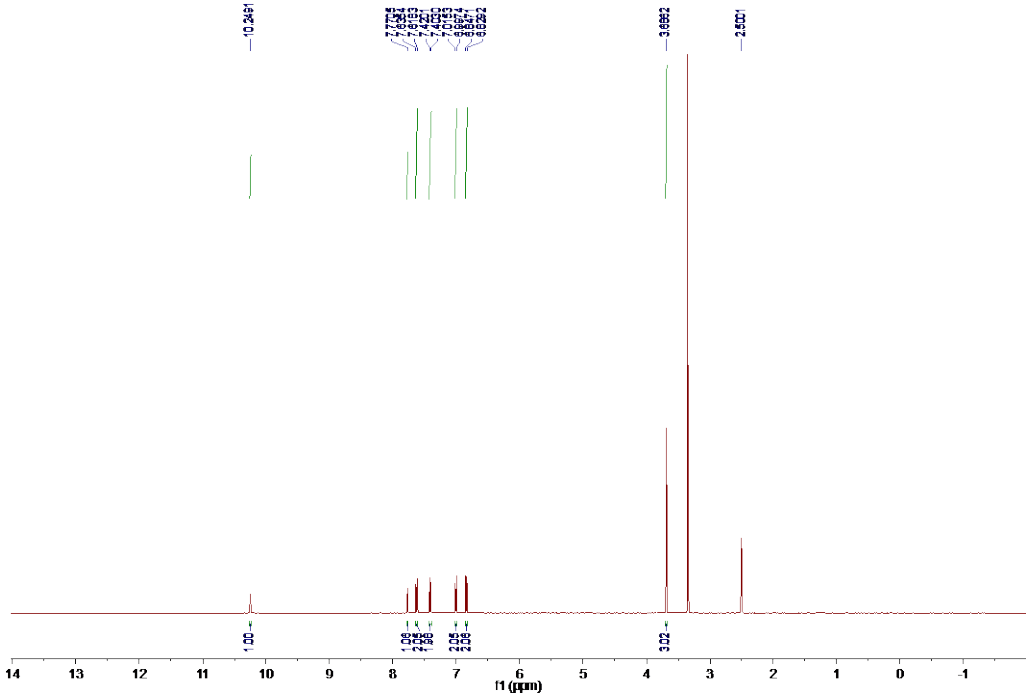

Fig. 4.B58. ^{1}H NMR spectrum for compound **4e** in $(CD_3)_2SO$ (500 MHz).

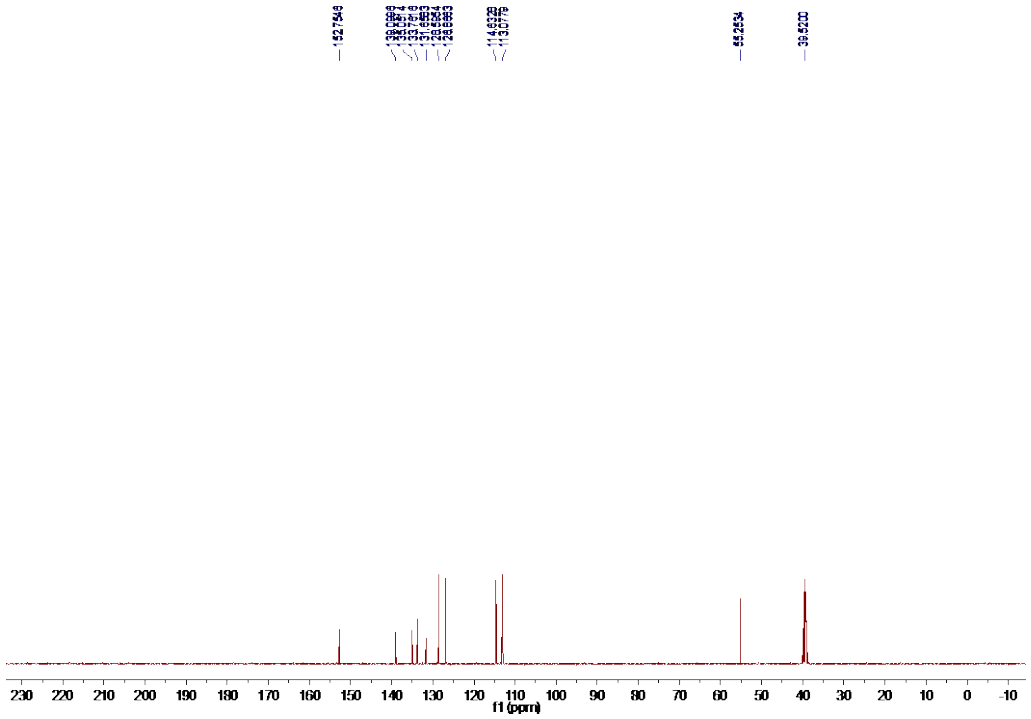

Fig. 4.B59. ^{13}C NMR spectrum for compound **4e** in $(CD_3)_2SO$ (100 MHz).

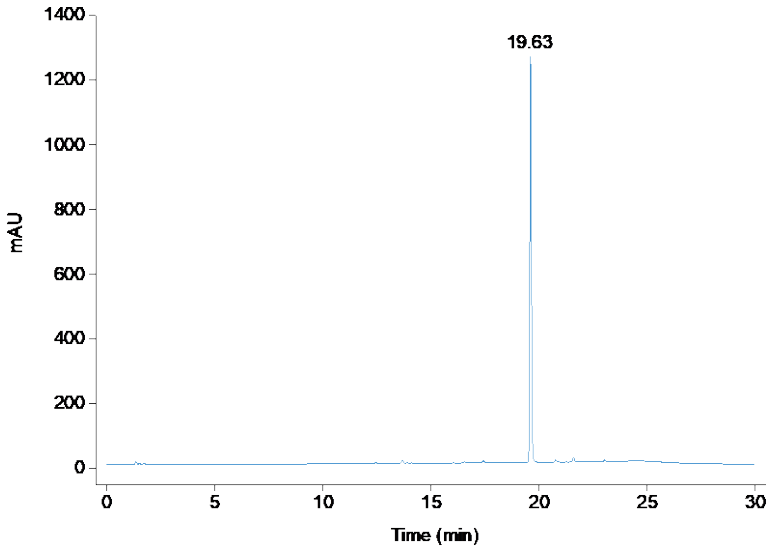

Fig. 4.B60. LCMS trace for compound **4e**. R_t = 19.63 min. Purity: 98%.

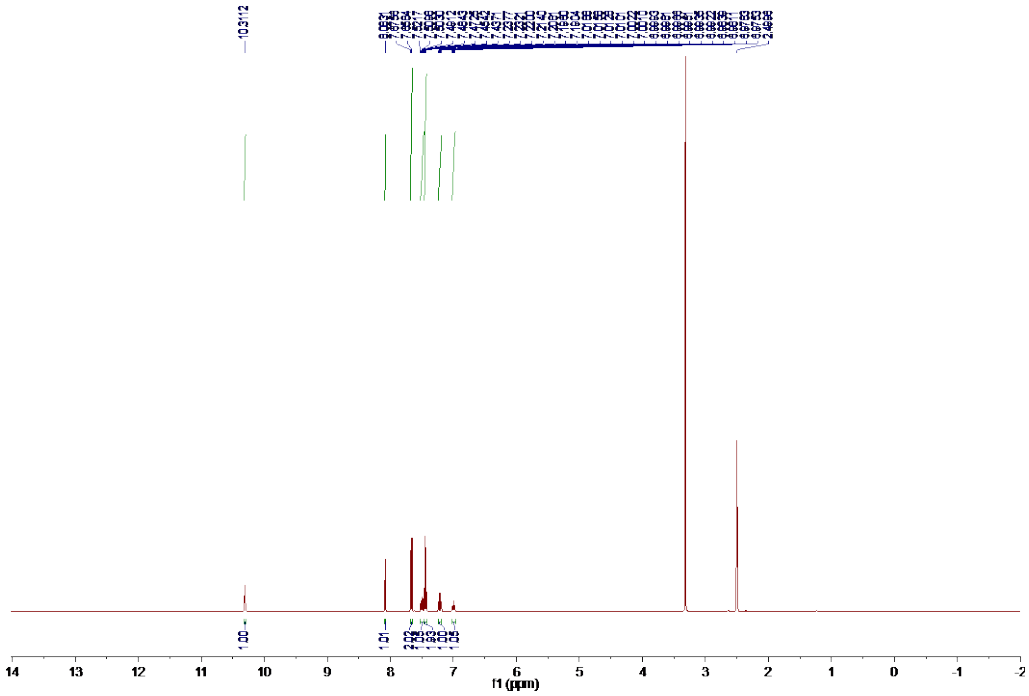

Fig. 4.B61. ^{1}H NMR spectrum for compound **4f** in $(CD_3)_2SO$ (500 MHz).

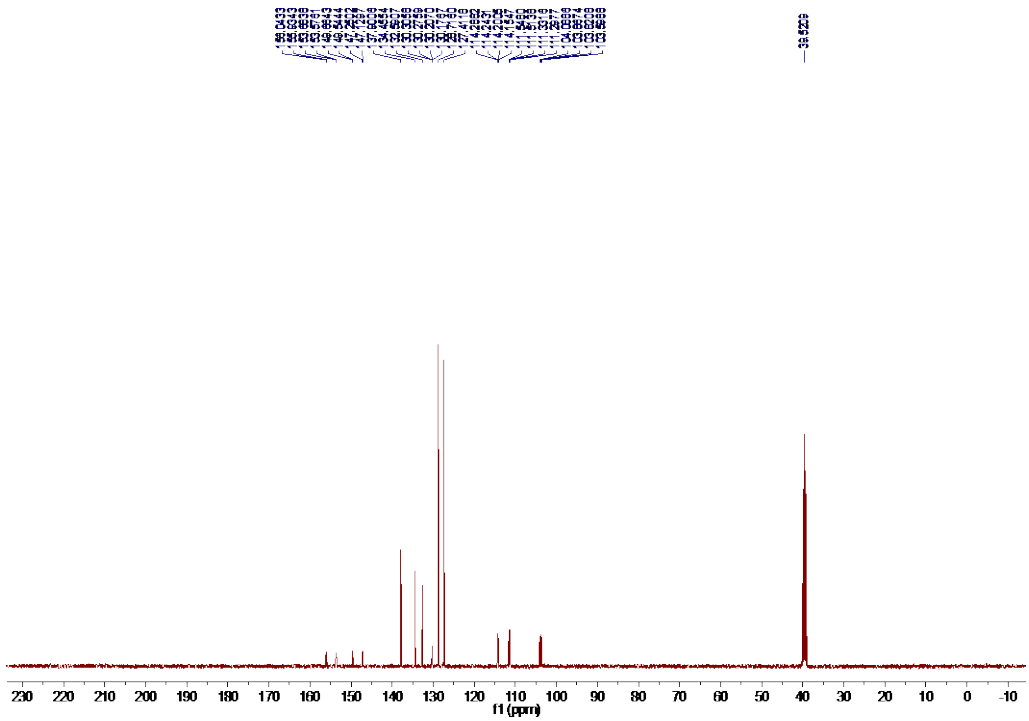

Fig. 4.B62. ^{13}C NMR spectrum for compound **4f** in $(CD_3)_2SO$ (100 MHz).

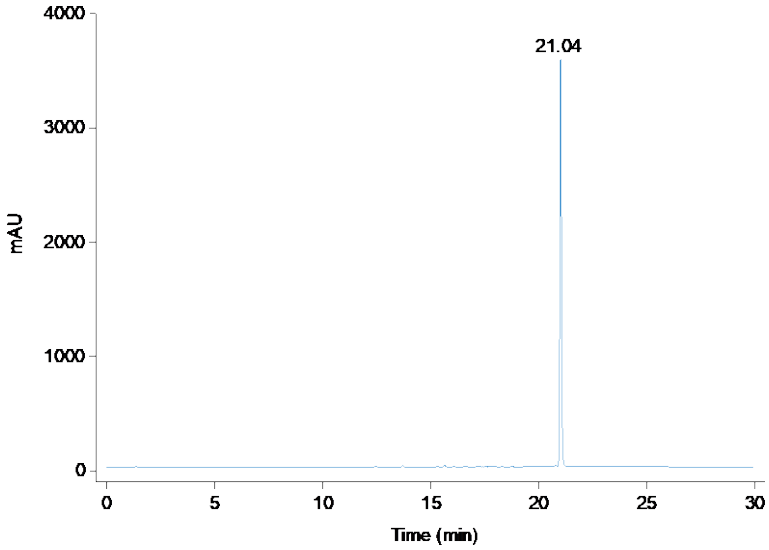

Fig. 4.B63. LCMS trace for compound **4f**. R_t = 21.04 min. Purity: 100%.

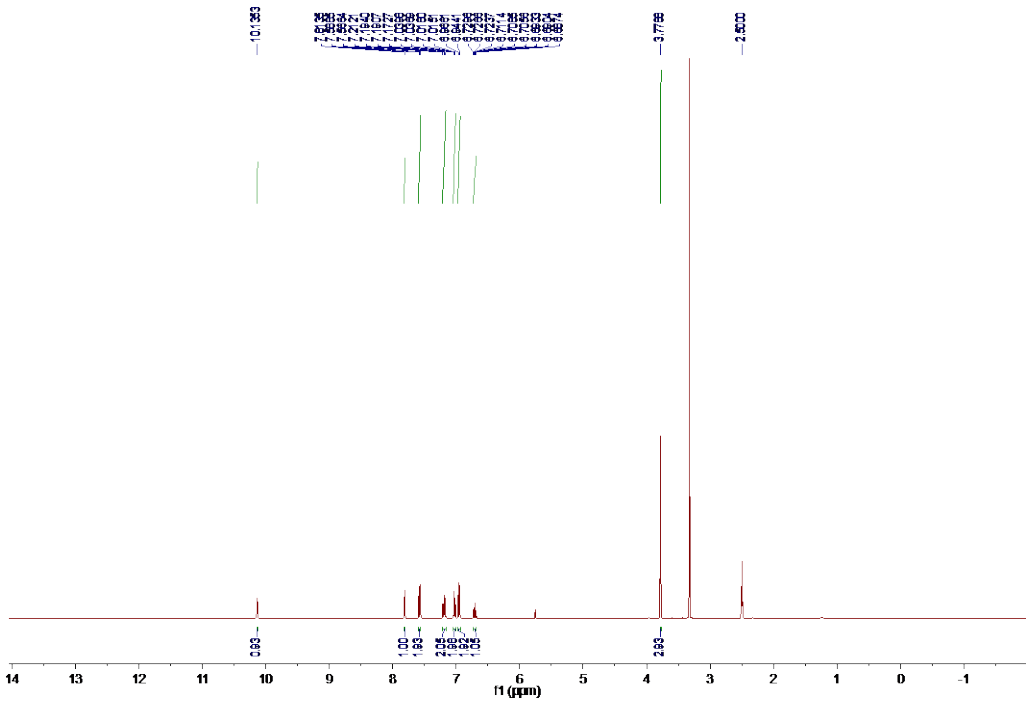

Fig. 4.B64. ^{1}H NMR spectrum for compound **5a** in $(CD_3)_2SO$ (400 MHz).

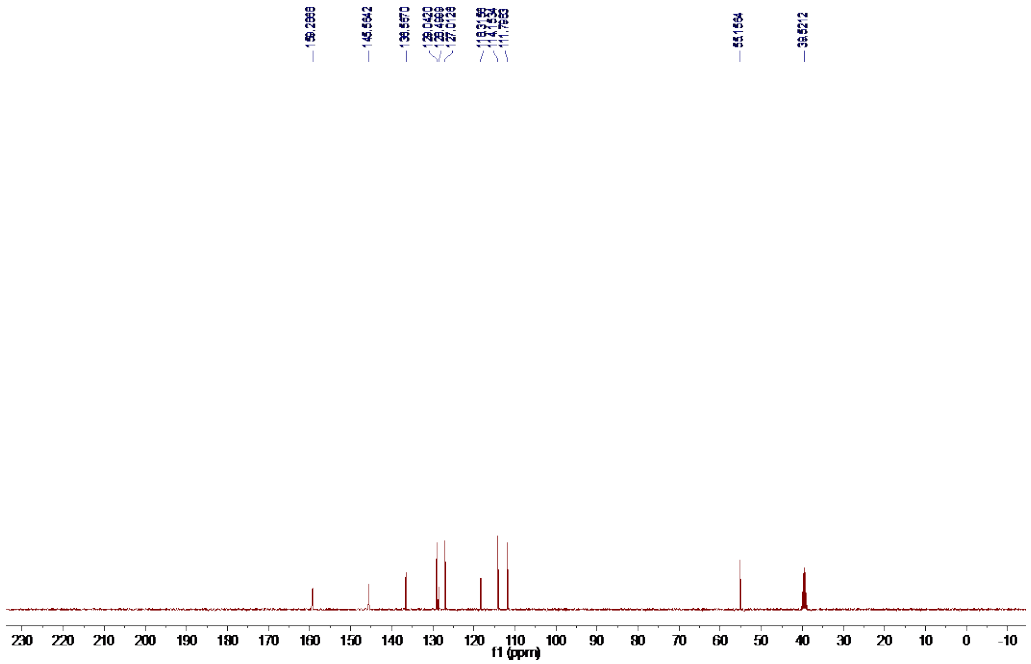

Fig. 4.B65. ^{13}C NMR spectrum for compound **5a** in $(CD_3)_2SO$ (100 MHz).

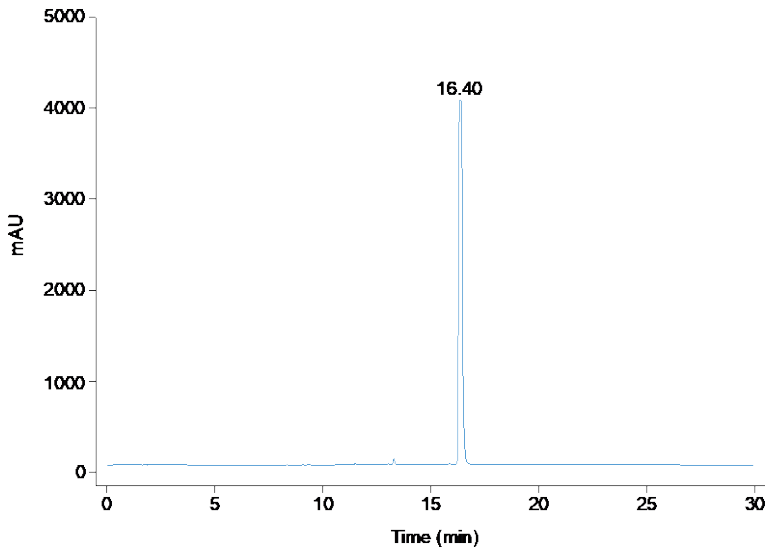

Fig. 4.B66. LCMS trace for compound **5a**. R_t = 16.40 min. Purity: 99%.

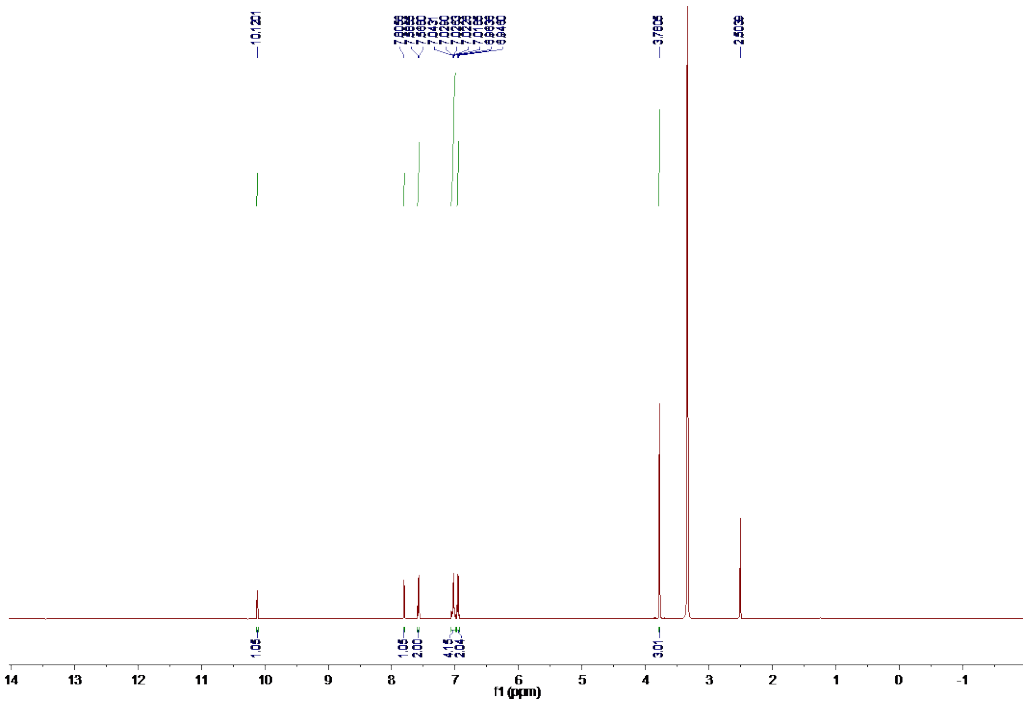

Fig. 4.B67. ^{1}H NMR spectrum for compound **5c** in $(CD_3)_2SO$ (500 MHz).

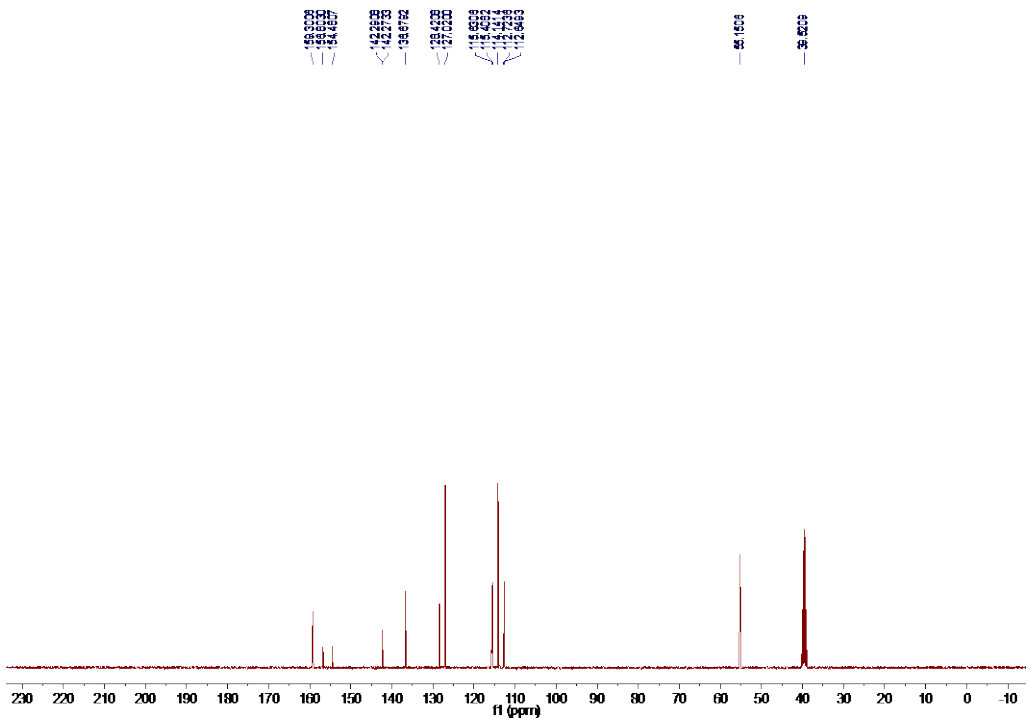

Fig. 4.B68. ^{13}C NMR spectrum for compound **5c** in $(CD_3)_2SO$ (100 MHz).

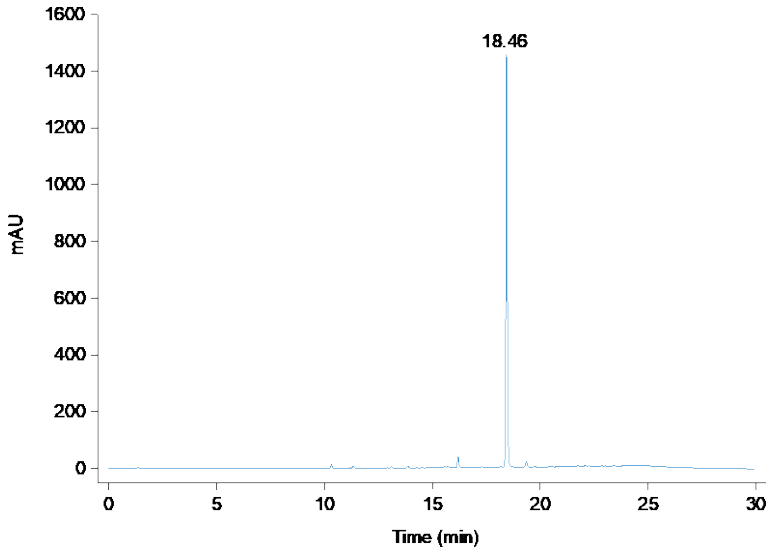

Fig. 4.B69. LCMS trace for compound **5c**. R_t = 18.46 min. Purity: 97%.

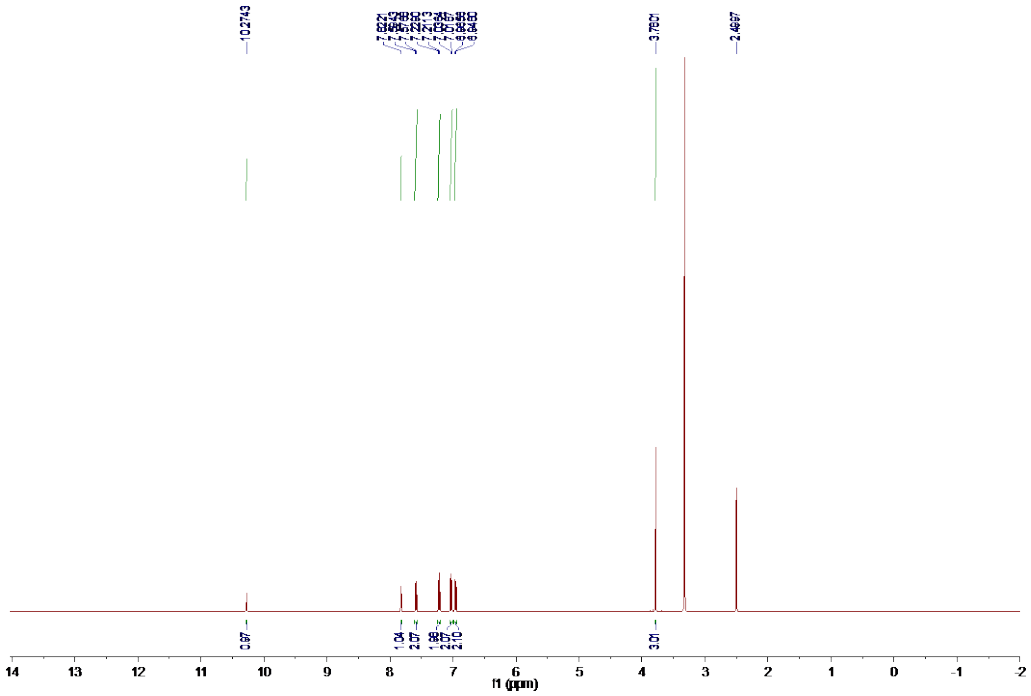

Fig. 4.B70. ^{1}H NMR spectrum for compound **5d** in $(CD_3)_2SO$ (500 MHz).

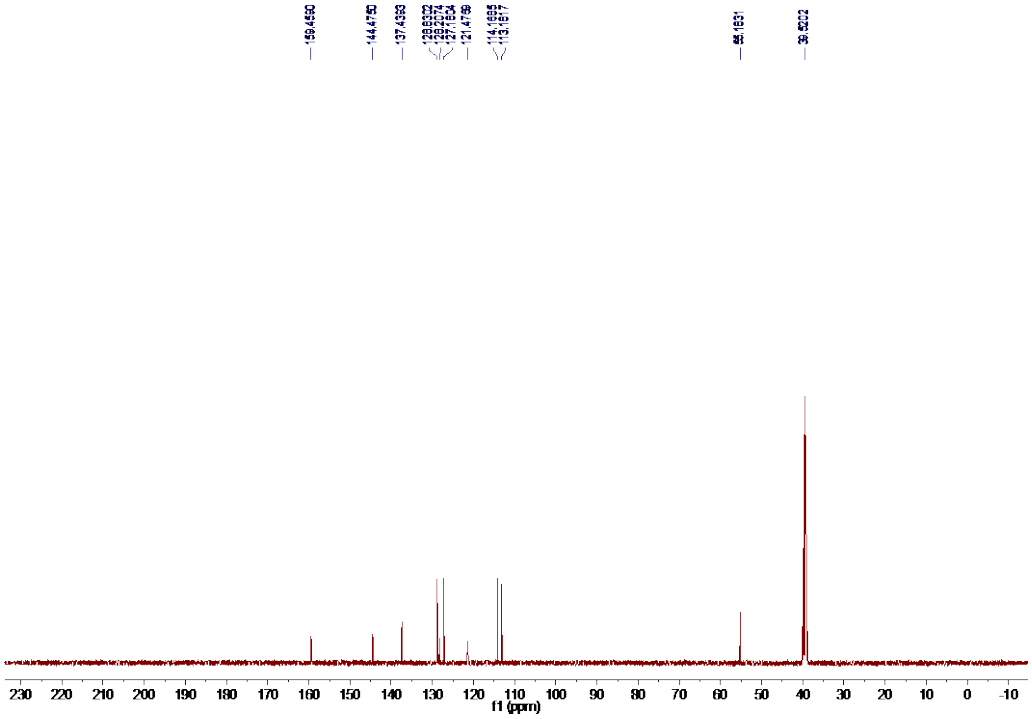

Fig. 4.B71. ^{13}C NMR spectrum for compound **5d** in $(CD_3)_2SO$ (100 MHz).

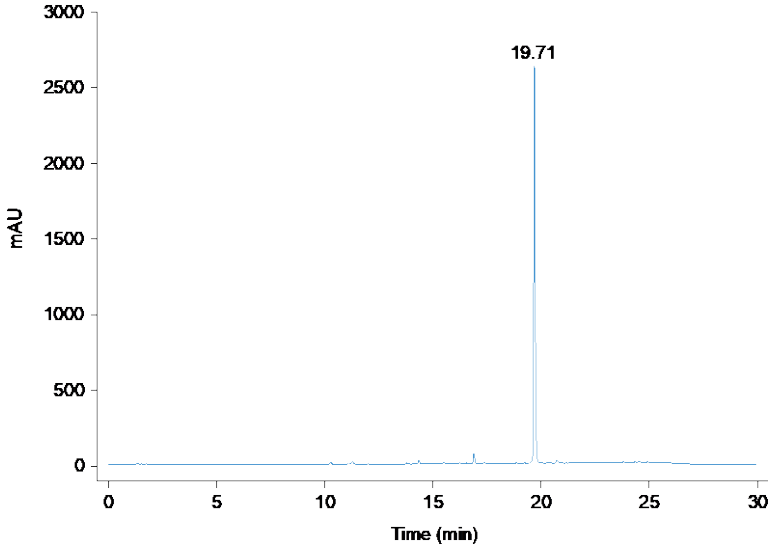

Fig. 4.B72. LCMS trace for compound **5d**. R_t = 19.71 min. Purity: 97%.

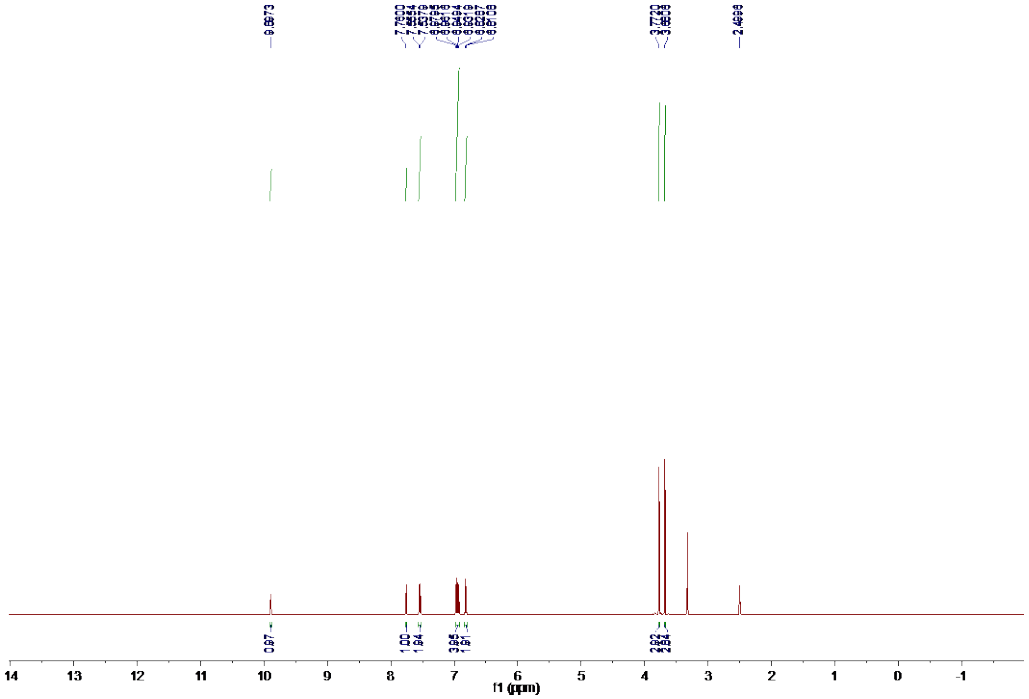

Fig. 4.B73. ^{1}H NMR spectrum for compound **5e** in $(CD_3)_2SO$ (500 MHz).

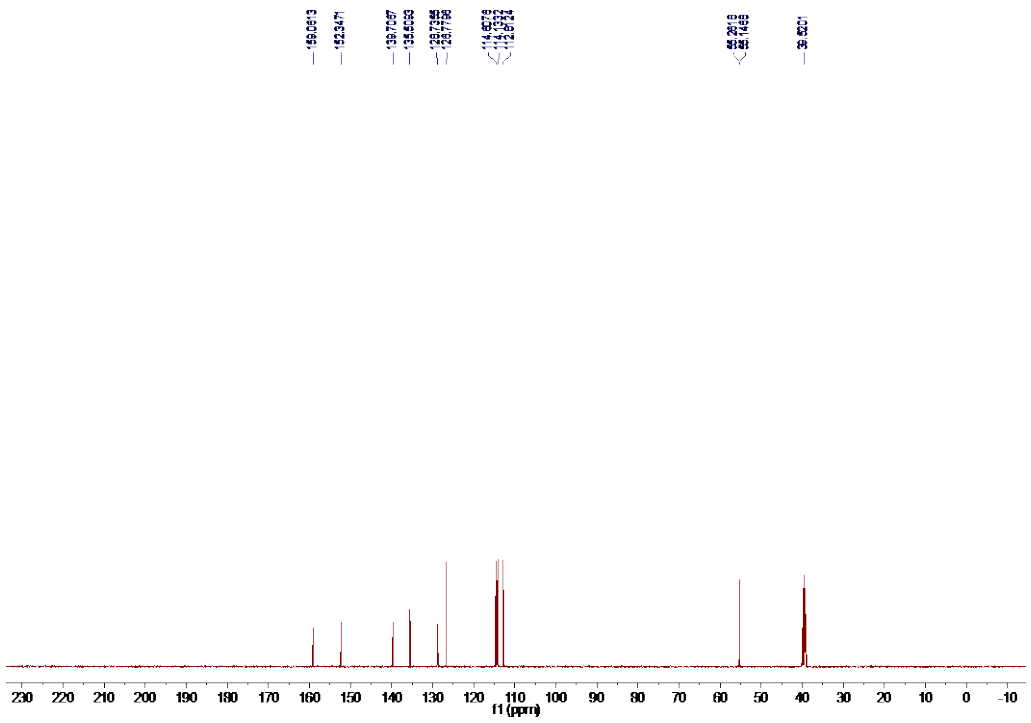

Fig. 4.B74. ^{13}C NMR spectrum for compound **5e** in $(CD_3)_2SO$ (100 MHz).

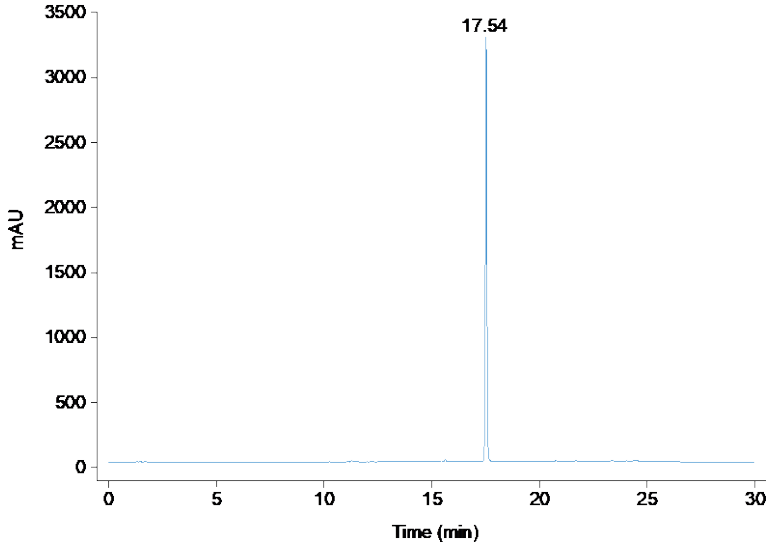

Fig. 4.B75. LCMS trace for compound **5e**. R_t = 17.54 min. Purity: 99%.

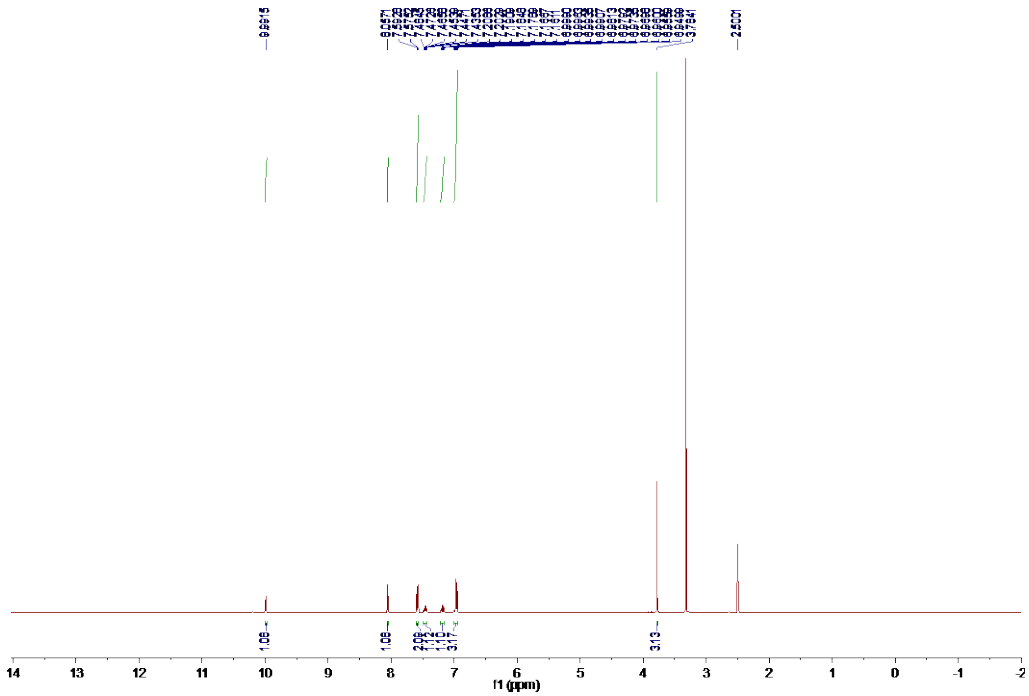

Fig. 4.B76. ^{1}H NMR spectrum for compound **5f** in $(CD_3)_2SO$ (500 MHz).

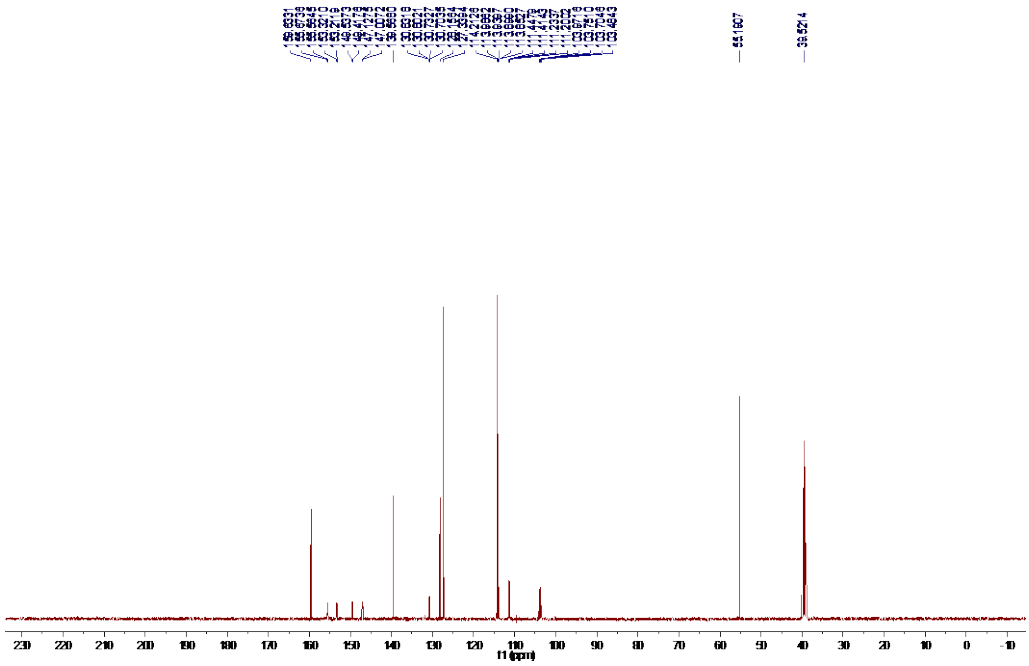

Fig. 4.B77. ^{13}C NMR spectrum for compound **5f** in $(CD_3)_2SO$ (100 MHz).

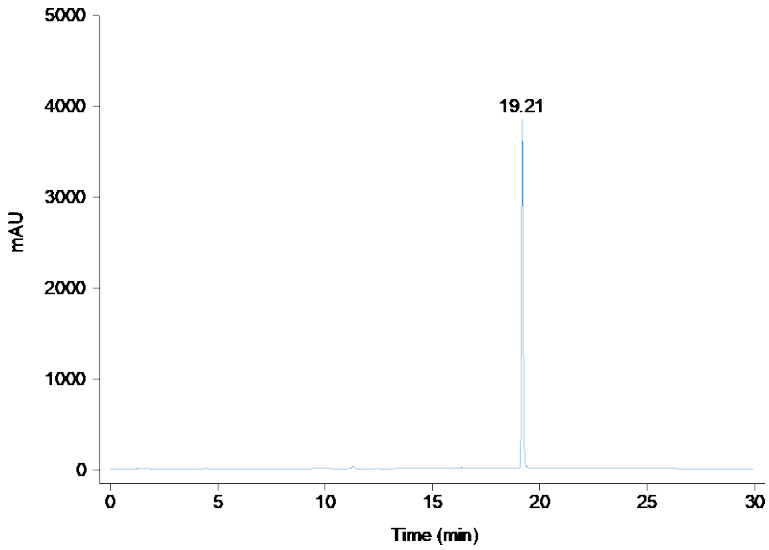

Fig. 4.B78. LCMS trace for compound **5f**. R_t = 19.21 min. Purity: 99%.

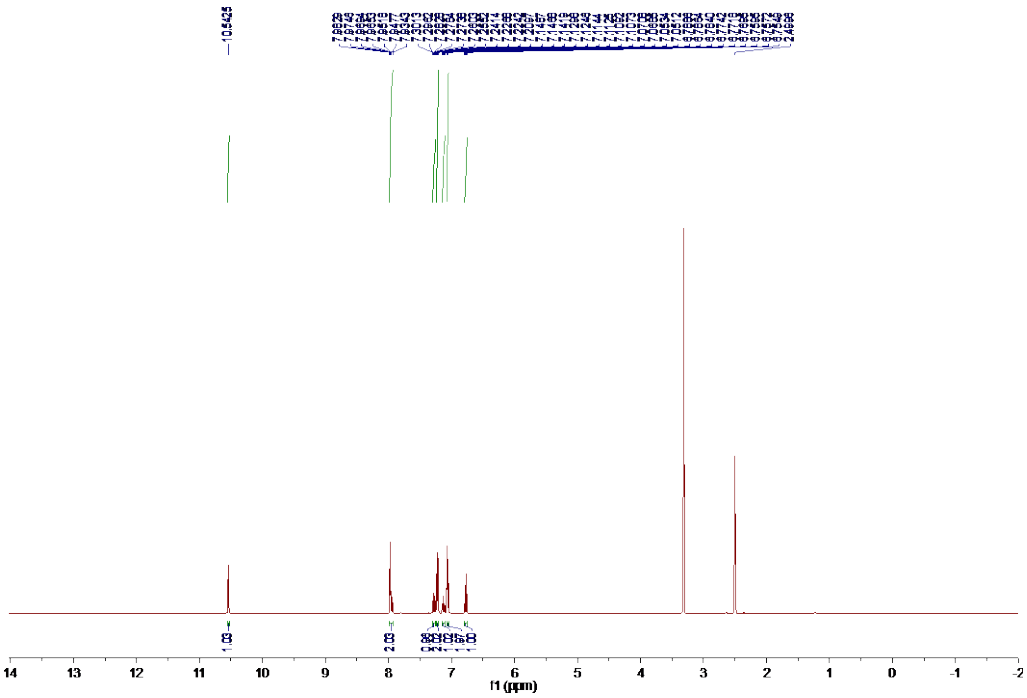

Fig. 4.B79. ^{1}H NMR spectrum for compound **6a** in $(CD_3)_2SO$ (400 MHz).

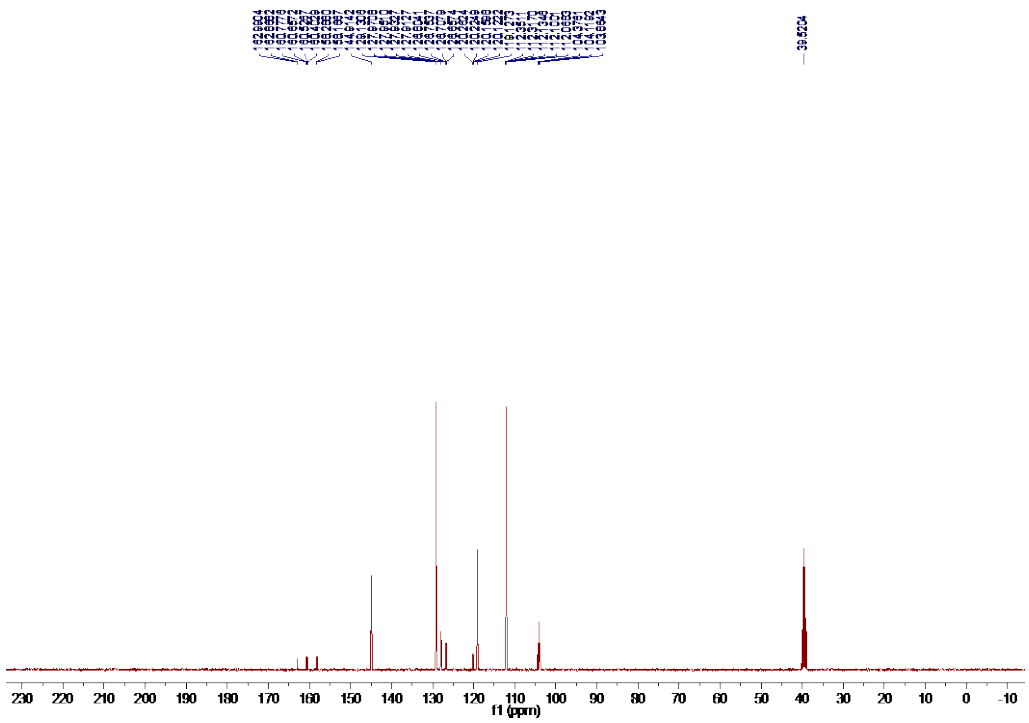

Fig. 4.B80. ^{13}C NMR spectrum for compound **6a** in $(CD_3)_2SO$ (100 MHz).

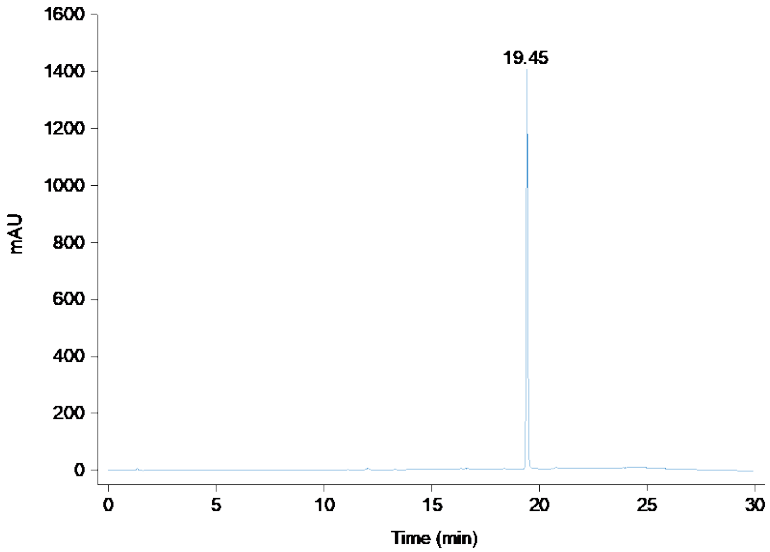

Fig. 4.B81. LCMS trace for compound **6a**. R_t = 19.45 min. Purity: 99%.

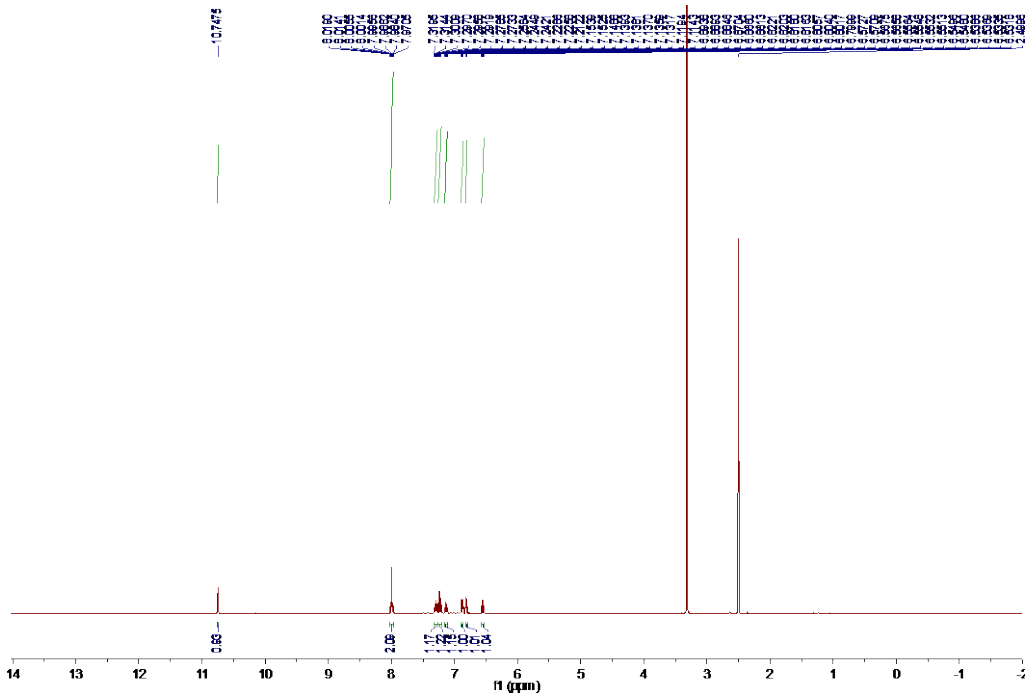

Fig. 4.B82. ^{1}H NMR spectrum for compound **6b** in $(CD_3)_2SO$ (500 MHz).

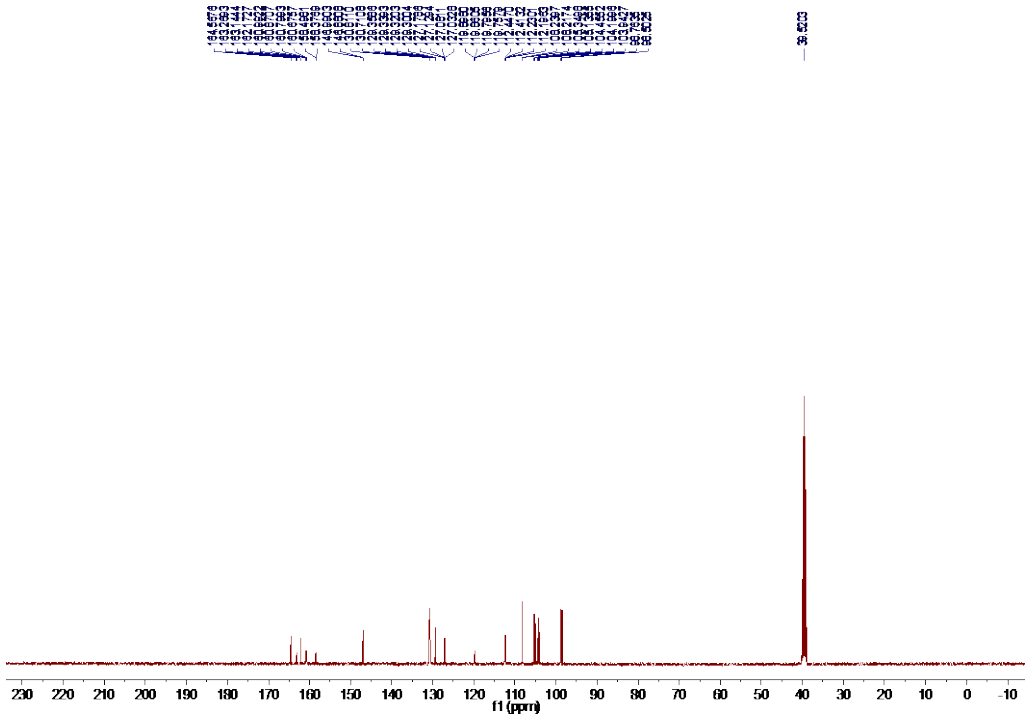

Fig. 4.B83. ^{13}C NMR spectrum for compound **6b** in $(CD_3)_2SO$ (100 MHz).

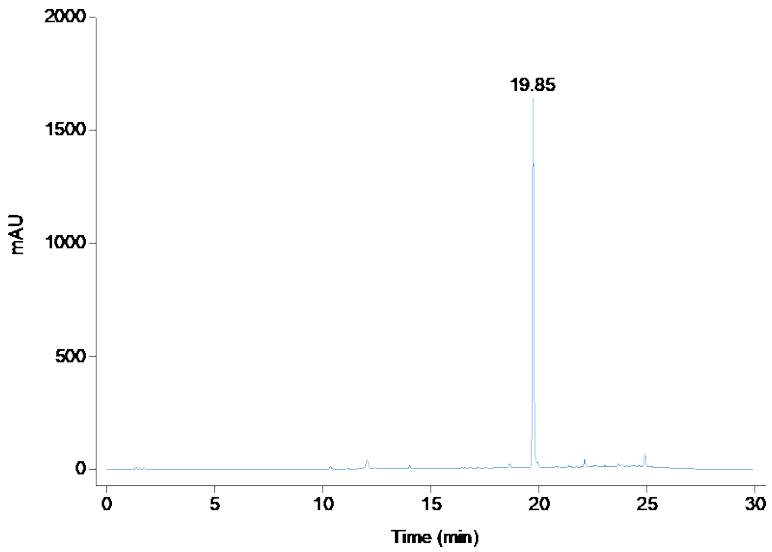

Fig. 4.B84. LCMS trace for compound **6b**. R_t = 19.85 min. Purity: 95%.

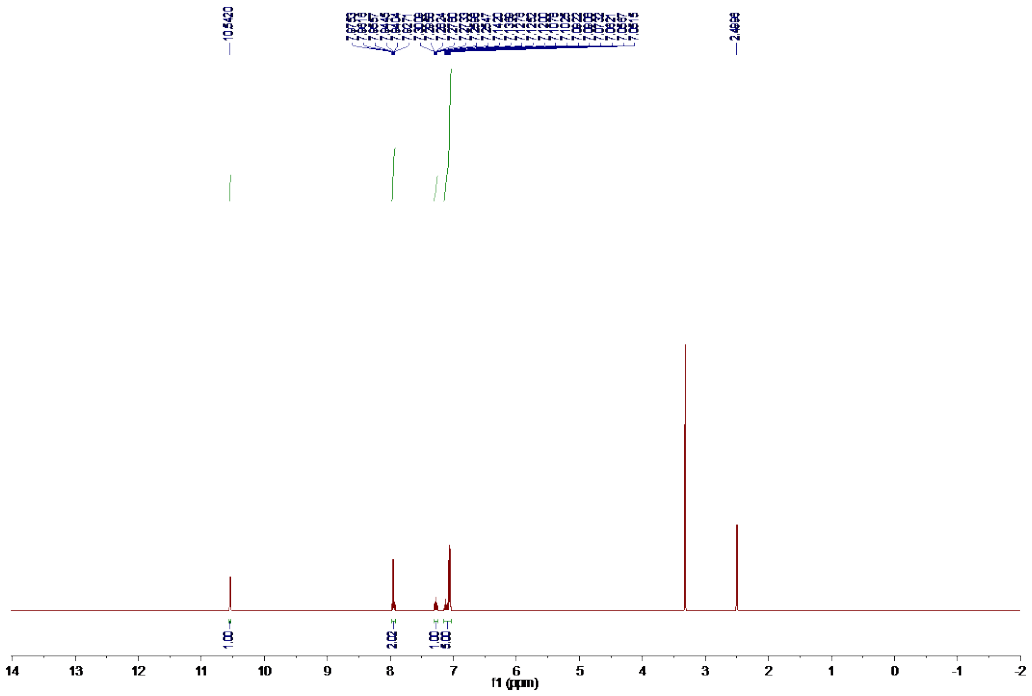

Fig. 4.B85. ^{1}H NMR spectrum for compound **6c** in $(CD_3)_2SO$ (500 MHz).

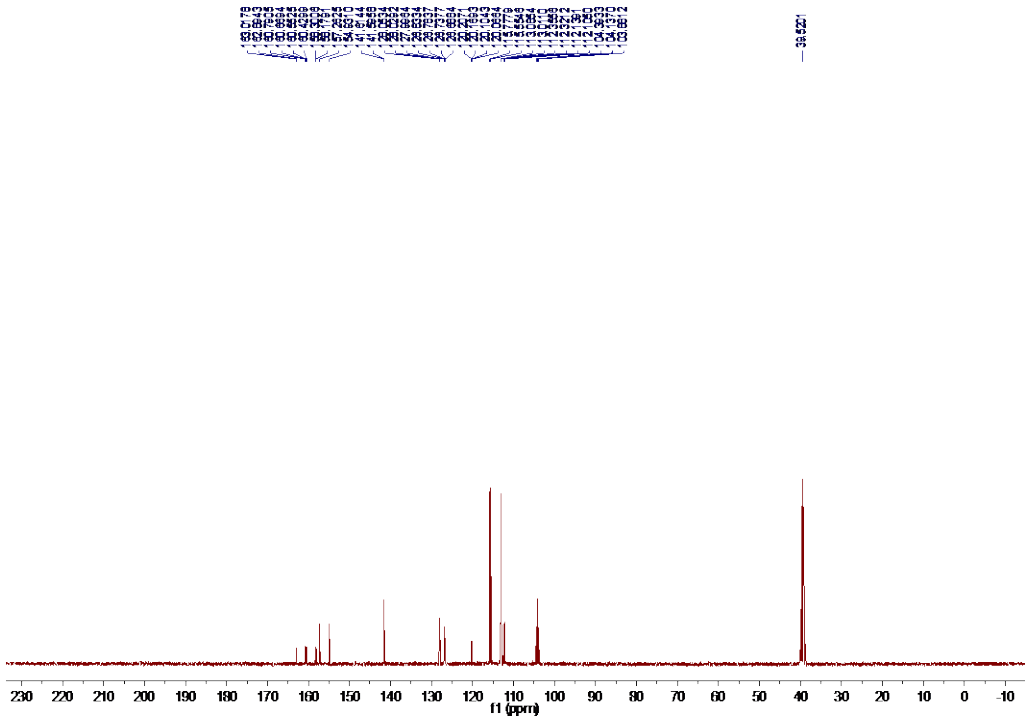

Fig. 4.B86. ^{13}C NMR spectrum for compound **6c** in $(CD_3)_2SO$ (100 MHz).

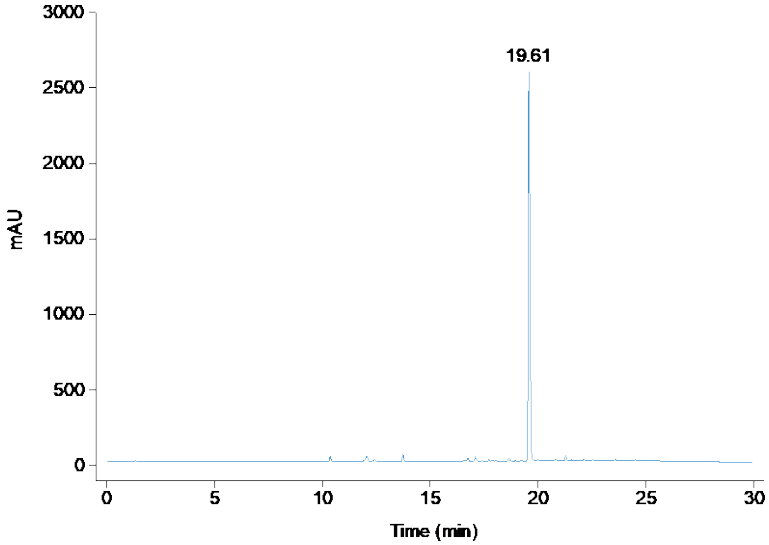

Fig. 4.B87. LCMS trace for compound **6c**. R_t = 19.61 min. Purity: 96%.

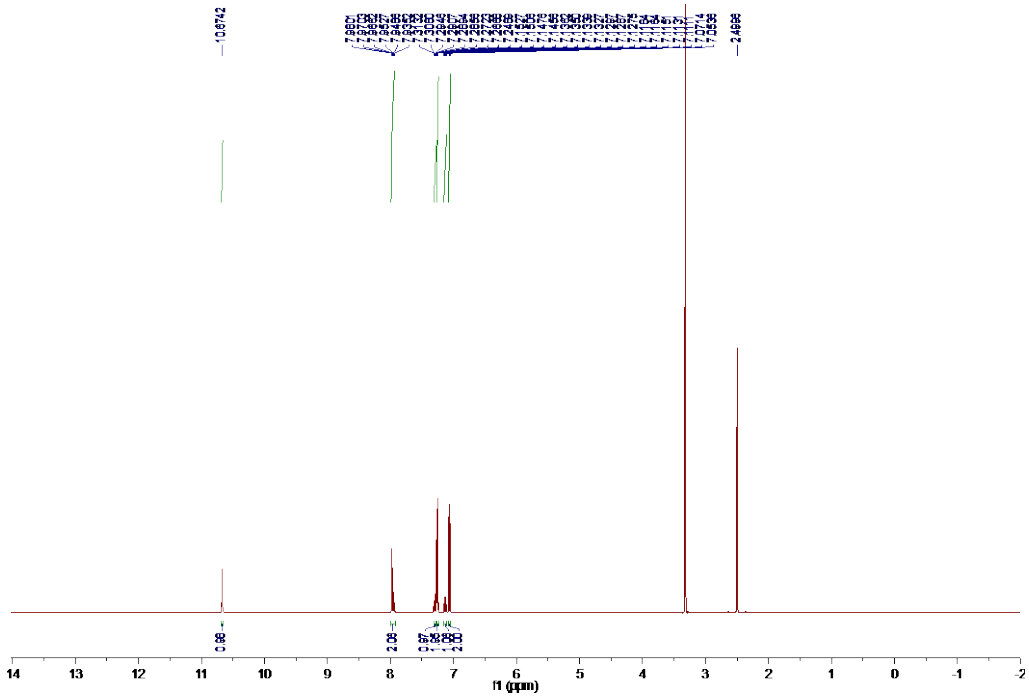

Fig. 4.B88. ^{1}H NMR spectrum for compound **6d** in $(CD_3)_2SO$ (500 MHz).

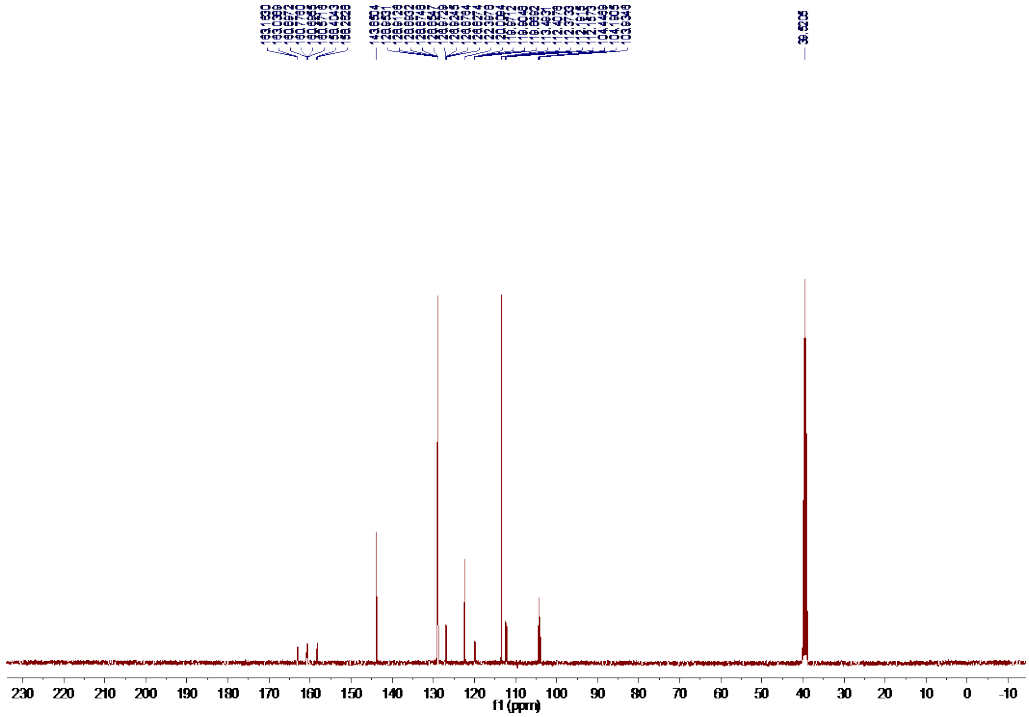

Fig. 4.B89. ^{13}C NMR spectrum for compound **6d** in $(CD_3)_2SO$ (100 MHz).

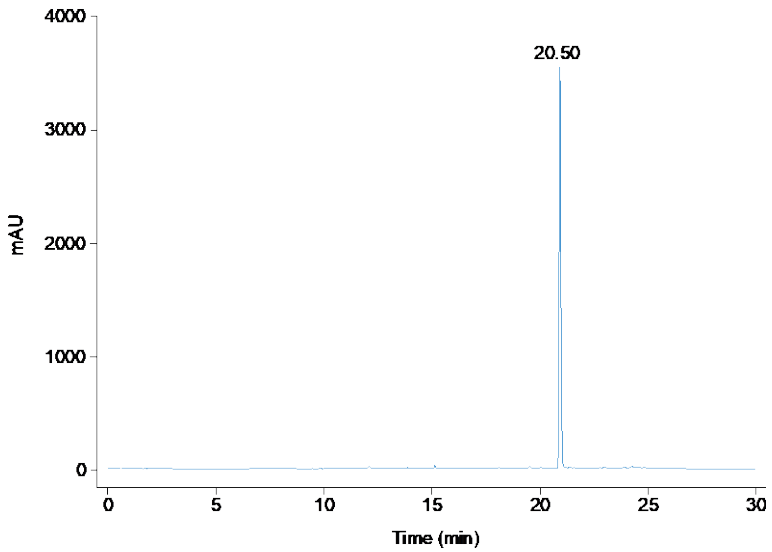

Fig. 4.B90. LCMS trace for compound **6d**. R_t = 20.50 min. Purity: 100%.

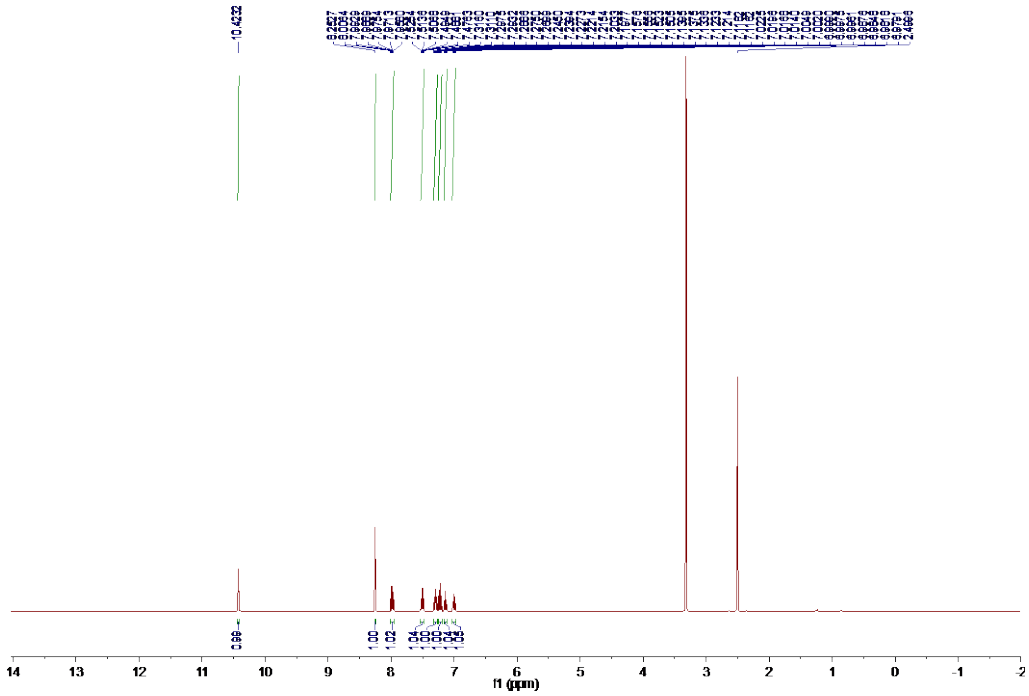

Fig. 4.B91. ^{1}H NMR spectrum for compound **6f** in $(CD_3)_2SO$ (500 MHz).

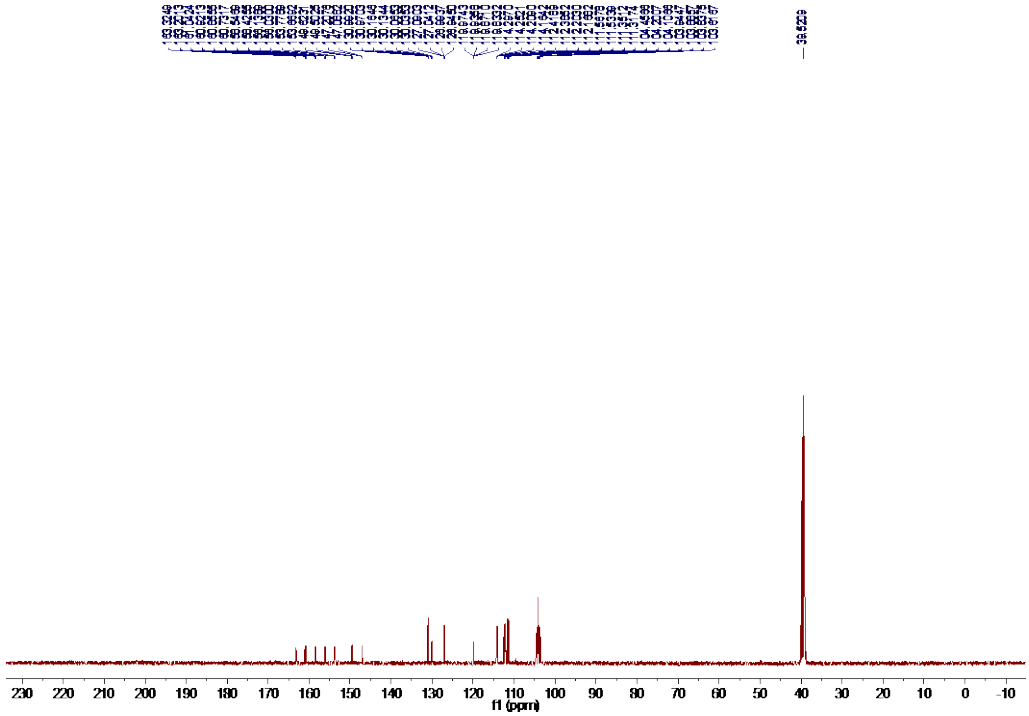

Fig. 4.B92. ^{13}C NMR spectrum for compound **6f** in $(CD_3)_2SO$ (100 MHz).

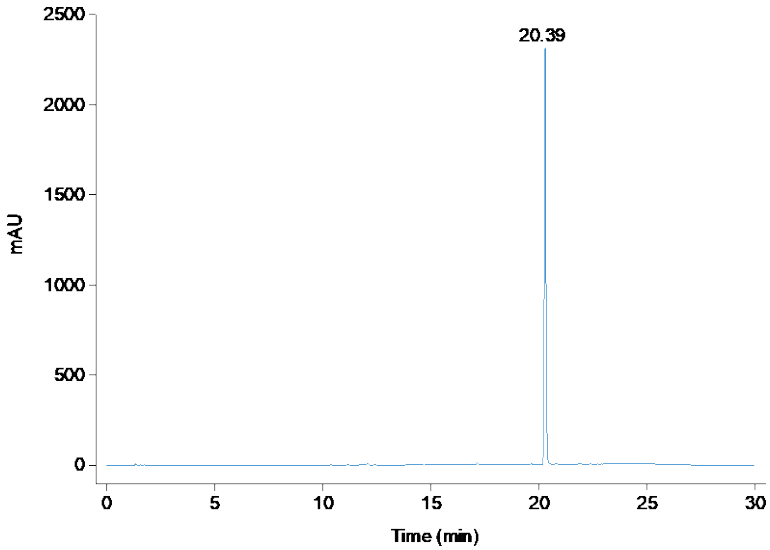

Fig. 4.B93. LCMS trace for compound **6f**. R_t = 20.39 min. Purity: 99%.

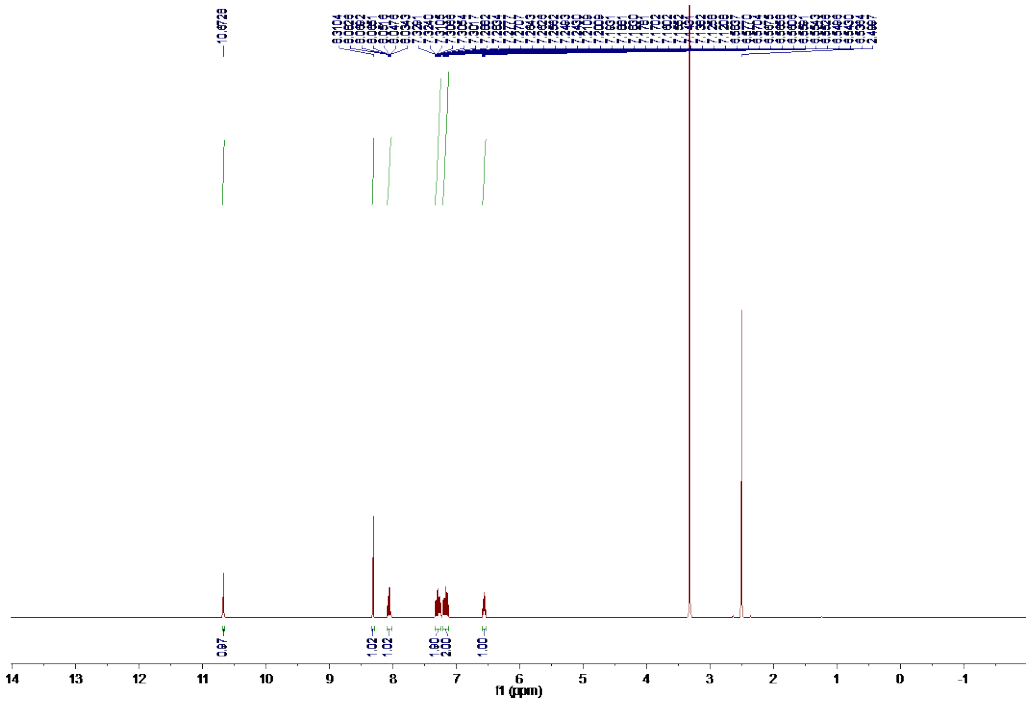

Fig. 4.B94. ^{1}H NMR spectrum for compound **6g** in $(CD_3)_2SO$ (500 MHz).

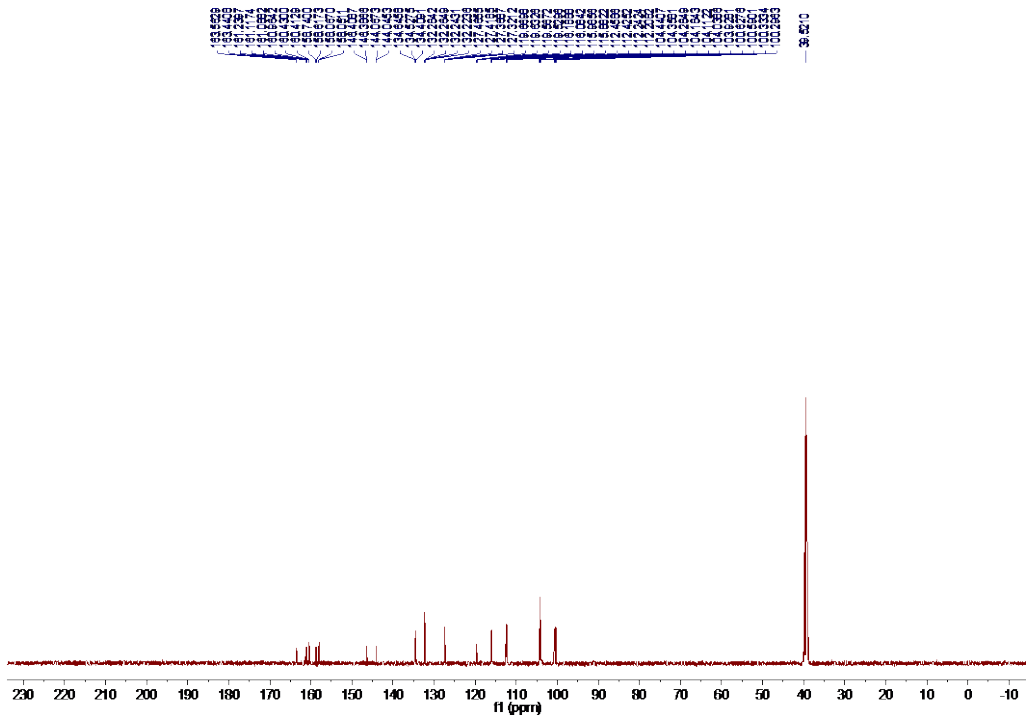

Fig. 4.B95. ^{13}C NMR spectrum for compound **6g** in $(CD_3)_2SO$ (100 MHz).

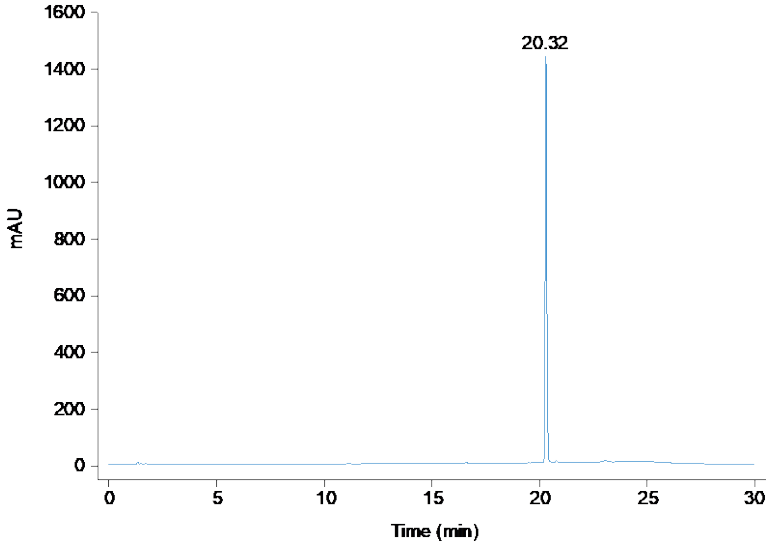

Fig. 4.B96. LCMS trace for compound **6g**. R_t = 20.32 min. Purity: 99%.

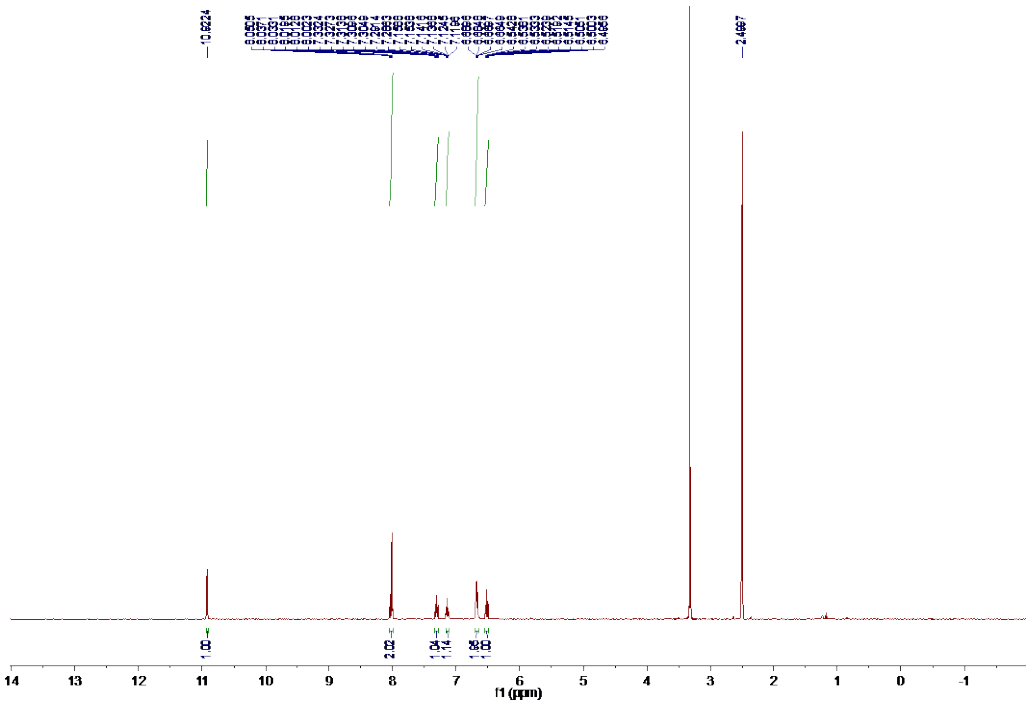

Fig. 4.B97. ^{1}H NMR spectrum for compound **6h** in $(CD_3)_2SO$ (500 MHz).

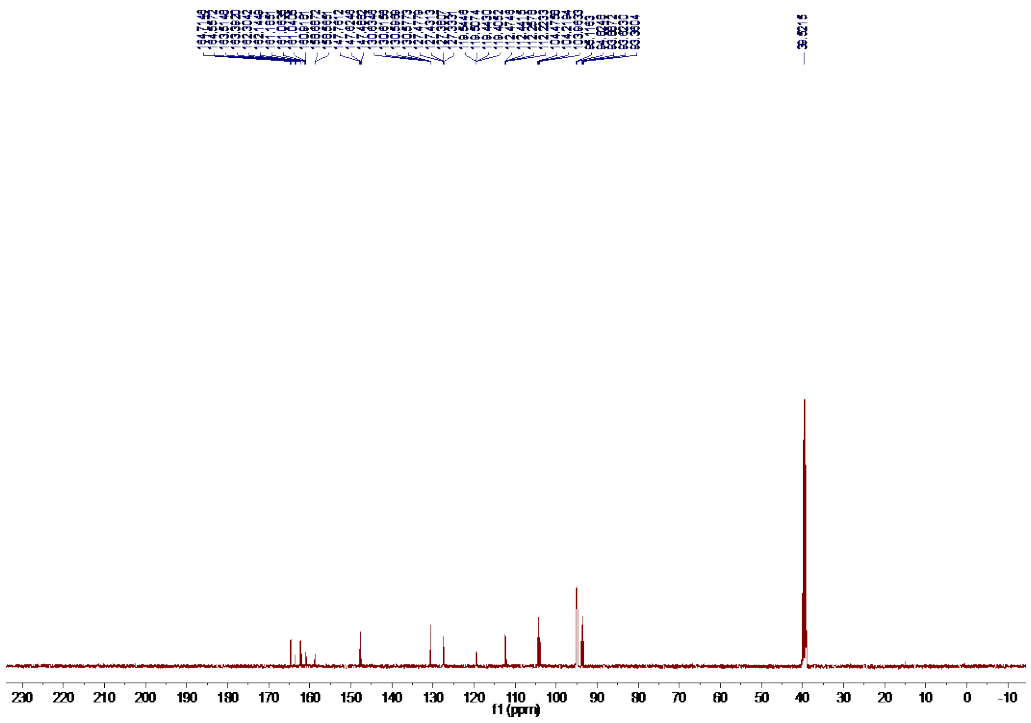

Fig. 4.B98. ^{13}C NMR spectrum for compound **6h** in $(CD_3)_2SO$ (100 MHz).

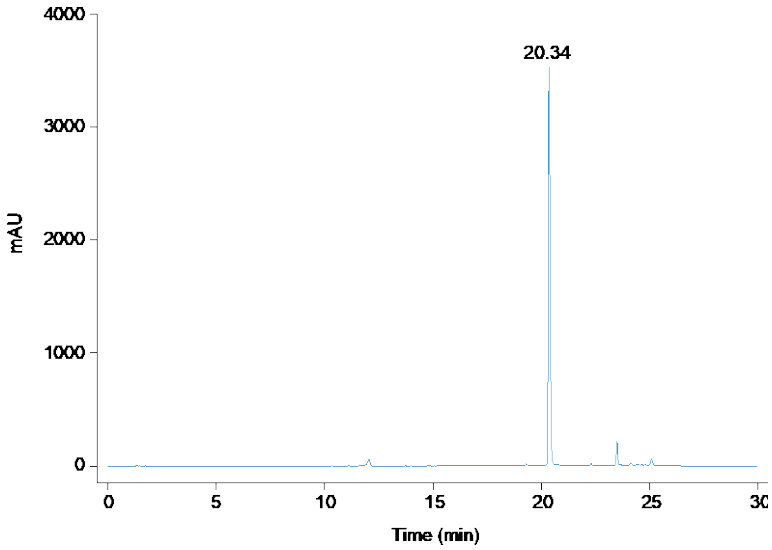

Fig. 4.B99. LCMS trace for compound **6h**. R_t = 20.34 min. Purity: 95%.

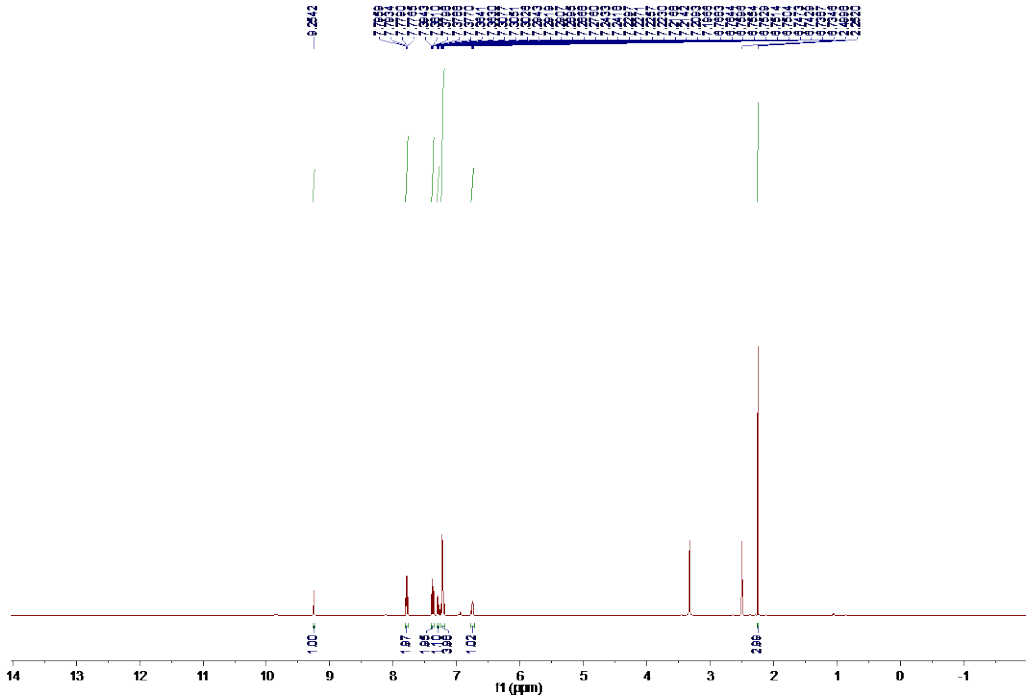

Fig. 4.B100. ^{1}H NMR spectrum for compound **7a** in $(CD_3)_2SO$ (500 MHz).

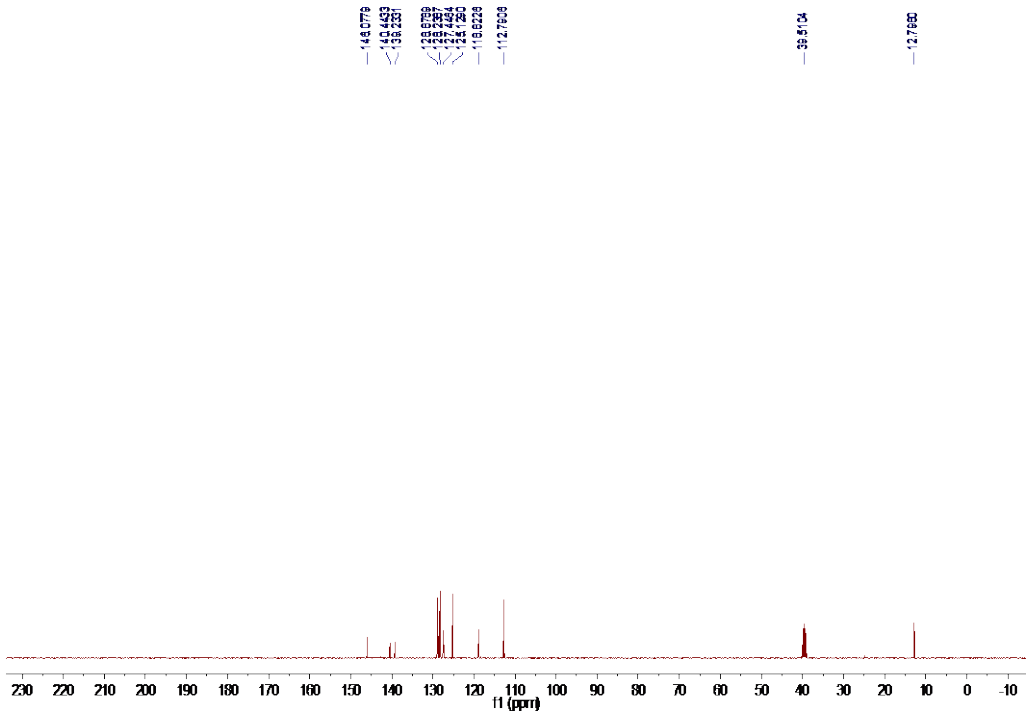

Fig. 4.B101. ^{13}C NMR spectrum for compound **7a** in $(CD_3)_2SO$ (100 MHz).

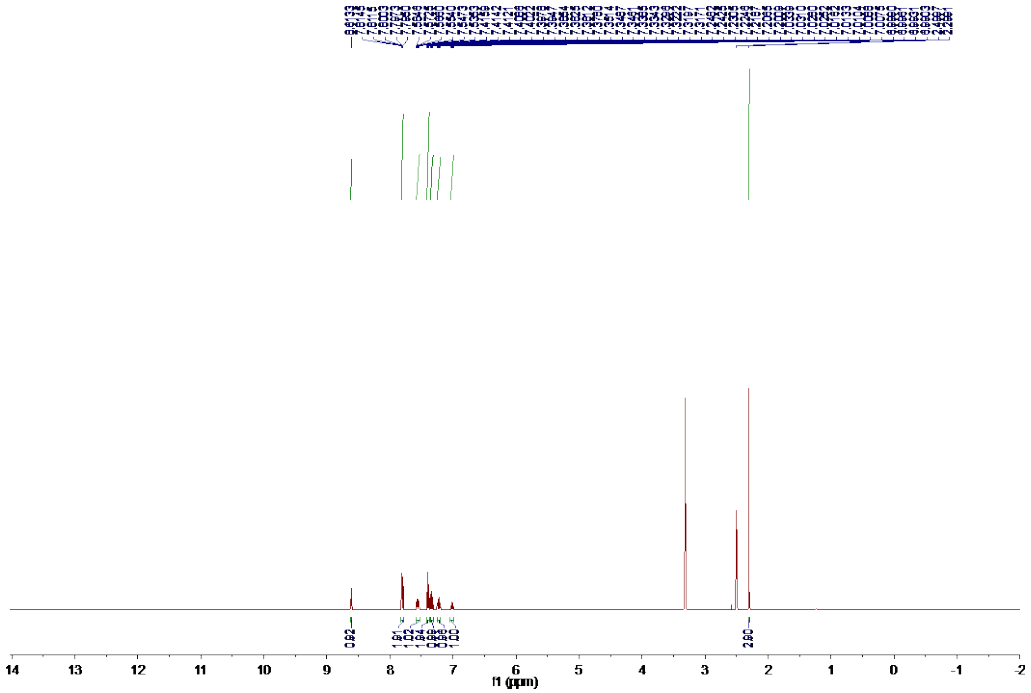

Fig. 4.B102. ^{1}H NMR spectrum for compound **7f** in $(CD_3)_2SO$ (500 MHz).

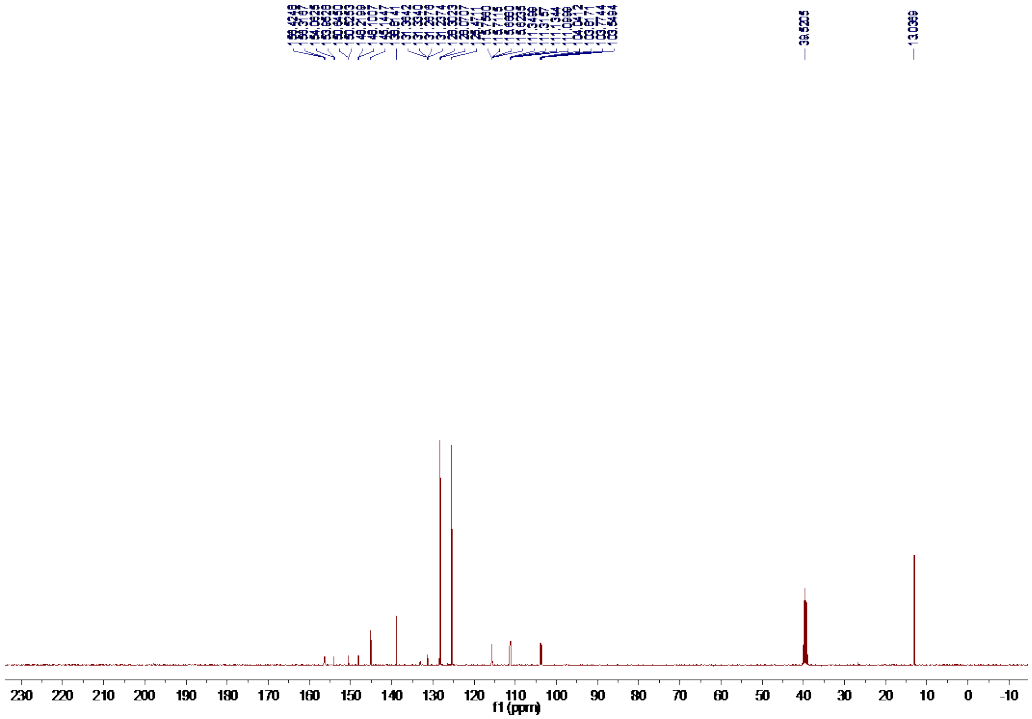

Fig. 4.B103. ^{13}C NMR spectrum for compound **7f** in $(CD_3)_2SO$ (100 MHz).

REFERENCES

1. Richtel, M., To fight deadly *Candida auris*, New York State proposes new tactics. May 23, 2019. *The New York Times* 2019.
2. Richtel, M., *Candida auris*: The fungus nobody wants to talk about. April 8, 2019. *The New York Times* 2019.
3. Richtel, M., How a Chicago woman fell victim to *Candida auris*, a drug-resistant fungus. *The New York Times* **2019**, April 17, 2019.
4. Dutcher, J. D., The discovery and development of amphotericin B. *Dis. Chest* **1968,** *54*, Suppl 1:296-298.
5. Scorzoni, L.; de Paula, E. S. A. C.; Marcos, C. M.; Assato, P. A.; de Melo, W. C.; de Oliveira, H. C.; Costa-Orlandi, C. B.; Mendes-Giannini, M. J.; Fusco-Almeida, A. M., Antifungal therapy: New advances in the understanding and treatment of mycosis. *Front. Microbiol.* **2017,** *8*, 36.
6. Campoy, S.; Adrio, J. L., Antifungals. *Biochem. Pharmacol.* **2017,** *133*, 86-96.
7. Fuentefria, A. M.; Pippi, B.; Dalla Lana, D. F.; Donato, K. K.; de Andrade, S. F., Antifungals discovery: An insight into new strategies to combat antifungal resistance. *Lett. Appl. Microbiol.* **2018,** *66* (1), 2-13.
8. Perfect, J. R., The antifungal pipeline: A reality check. *Nat. Rev. Drug Discov.* **2017,** *16* (9), 603-616.
9. Wiederhold, N. P., The antifungal arsenal: Alternative drugs and future targets. *Int. J. Antimicrob. Agents* **2018,** *51* (3), 333-339.

10. Liu, N.; Wang, C.; Su, H.; Zhang, W.; Sheng, C., Strategies in the discovery of novel antifungal scaffolds. *Future Med. Chem.* **2016,** *8* (12), 1435-1454.

11. Pianalto, K. M.; Alspaugh, J. A., New horizons in antifungal therapy. *J Fungi (Basel)* **2016,** *2* (4), e26.

12. Brown, G. D.; Denning, D. W.; Gow, N. A.; Levitz, S. M.; Netea, M. G.; White, T. C., Hidden killers: Human fungal infections. *Sci. Transl. Med.* **2012,** *4* (165), 165rv13.

13. Bongomin, F.; Gago, S.; Oladele, R. O.; Denning, D. W., Global and multi-national prevalence of fungal diseases-estimate precision. *J. Fungi (Basel)* **2017,** *3* (4), 57.

14. Gow, N. A. R.; Latge, J. P.; Munro, C. A., The fungal cell wall: Structure, biosynthesis, and function. *Microbiol. Spectr.* **2017,** *5* (3).

15. Li, Z.; Nielsen, K., Morphology changes in human fungal pathogens upon interaction with the host. *J. Fungi (Basel)* **2017,** *3* (4), 66.

16. Kwon-Chung, K. J., Taxonomy of fungi causing mucormycosis and entomophthoramycosis (zygomycosis) and nomenclature of the disease: Molecular mycologic perspectives. *Clin. Infect. Dis.* **2012,** *54 Suppl 1*, S8-S15.

17. Ryan, K. J., *Sherris Medical Microbiology*. McGraw-Hill: New York, 2018.

18. Colley, T.; Alanio, A.; Kelly, S. L.; Sehra, G.; Kizawa, Y.; Warrilow, A. G. S.; Parker, J. E.; Kelly, D. E.; Kimura, G.; Anderson-Dring, L.; Nakaoki, T.; Sunose, M.; Onions, S.; Crepin, D.; Lagasse, F.; Crittall, M.; Shannon, J.; Cooke, M.; Bretagne, S.; King-Underwood, J.; Murray, J.; Ito, K.; Strong, P.; Rapeport, G., *In vitro* and *in vivo* antifungal profile of a novel and long-acting inhaled azole, PC945,

on *Aspergillus fumigatus* infection. *Antimicrob. Agents Chemother.* **2017,** *61* (5), e02280-16.

19. Colley, T.; Sehra, G.; Chowdhary, A.; Alanio, A.; Kelly, S. L.; Kizawa, Y.; Armstrong-James, D.; Fisher, M. C.; Warrilow, A. G. S.; Parker, J. E.; Kelly, D. E.; Kimura, G.; Nishimoto, Y.; Sunose, M.; Onions, S.; Crepin, D.; Lagasse, F.; Crittall, M.; Shannon, J.; McConville, M.; King-Underwood, J.; Naylor, A.; Bretagne, S.; Murray, J.; Ito, K.; Strong, P.; Rapeport, G., *In vitro* and *in vivo* efficacy of a novel and long-acting fungicidal azole, PC1244, on *Aspergillus fumigatus* infection. *Antimicrob. Agents Chemother.* **2018,** *62* (5), e01941-17.

20. Brand, S. R.; Degenhardt, T. P.; Person, K.; Sobel, J. D.; Nyirjesy, P.; Schotzinger, R. J.; Tavakkol, A., A phase 2, randomized, double-blind, placebo-controlled, dose-ranging study to evaluate the efficacy and safety of orally administered VT-1161 in the treatment of recurrent vulvovaginal candidiasis. *Am. J. Obstet. Gynecol.* **2018,** *218* (6), 624 e1-624 e9.

21. Wiederhold, N. P.; Shubitz, L. F.; Najvar, L. K.; Jaramillo, R.; Olivo, M.; Catano, G.; Trinh, H. T.; Yates, C. M.; Schotzinger, R. J.; Garvey, E. P.; Patterson, T. F., The novel fungal CYP51 inhibitor VT-1598 is efficacious in experimental models of central nervous system coccidioidomycosis caused by *Coccidioides posadasii* and *Coccidioides immitis*. *Antimicrob. Agents Chemother.* **2018,** *62* (4), e02258-17.

22. Warrilow, A. G.; Hull, C. M.; Parker, J. E.; Garvey, E. P.; Hoekstra, W. J.; Moore, W. R.; Schotzinger, R. J.; Kelly, D. E.; Kelly, S. L., The clinical candidate VT-

1161 is a highly potent inhibitor of *Candida albicans* CYP51 but fails to bind the human enzyme. *Antimicrob. Agents Chemother.* **2014,** *58* (12), 7121-7127.

23. Lockhart, S. R.; Fothergill, A. W.; Iqbal, N.; Bolden, C. B.; Grossman, N. T.; Garvey, E. P.; Brand, S. R.; Hoekstra, W. J.; Schotzinger, R. J.; Ottinger, E.; Patterson, T. F.; Wiederhold, N. P., The investigational fungal Cyp51 inhibitor VT-1129 demonstrates potent *in vitro* activity against *Cryptococcus neoformans* and C*ryptococcus gattii*. *Antimicrob Agents Chemother* **2016,** *60* (4), 2528-2531.

24. Nielsen, K.; Vedula, P.; Smith, K. D.; Meya, D. B.; Garvey, E. P.; Hoekstra, W. J.; Schotzinger, R. J.; Boulware, D. R., Activity of VT-1129 against *Cryptococcus neoformans* clinical isolates with high fluconazole MICs. *Med. Mycol.* **2017,** *55* (4), 453-456.

25. Hargrove, T. Y.; Garvey, E. P.; Hoekstra, W. J.; Yates, C. M.; Wawrzak, Z.; Rachakonda, G.; Villalta, F.; Lepesheva, G. I., Crystal structure of the new investigational drug candidate VT-1598 in complex with *Aspergillus fumigatus* sterol 14alpha-demethylase provides insights into its broad-spectrum antifungal activity. *Antimicrob. Agents Chemother.* **2017,** *61* (7), e00570-17.

26. Matsumori, N.; Sawada, Y.; Murata, M., Mycosamine orientation of amphotericin B controlling interaction with ergosterol: Sterol-dependent activity of conformation-restricted derivatives with an amino-carbonyl bridge. *J. Am. Chem. Soc.* **2005,** *127* (30), 10667-10675.

27. Kim, H. J.; Han, C. Y.; Park, J. S.; Oh, S. H.; Kang, S. H.; Choi, S. S.; Kim, J. M.; Kwak, J. H.; Kim, E. S., Nystatin-like *Pseudonocardia* polyene B1, a novel

disaccharide-containing antifungal heptaene antibiotic. *Sci. Rep.* **2018,** *8* (1), 13584.

28. Bruheim, P.; Borgos, S. E.; Tsan, P.; Sletta, H.; Ellingsen, T. E.; Lancelin, J. M.; Zotchev, S. B., Chemical diversity of polyene macrolides produced by *Streptomyces noursei* ATCC 11455 and recombinant strain ERD44 with genetically altered polyketide synthase NysC. *Antimicrob. Agents Chemother.* **2004,** *48* (11), 4120-4129.

29. Hamill, R. J., Amphotericin B formulations: a comparative review of efficacy and toxicity. *Drugs* **2013,** *73* (9), 919-934.

30. Hope, W. W.; Tabernero, L.; Denning, D. W.; Anderson, M. J., Molecular mechanisms of primary resistance to flucytosine in *Candida albicans*. *Antimicrob. Agents. Chemother.* **2004,** *48* (11), 4377-4386.

31. Trevino-Rangel Rde, J.; Villanueva-Lozano, H.; Hernandez-Rodriguez, P.; Martinez-Resendez, M. F.; Garcia-Juarez, J.; Rodriguez-Rocha, H.; Gonzalez, G. M., Activity of sertraline against *Cryptococcus neoformans*: *in vitro* and *in vivo* assays. *Med. Mycol.* **2016,** *54* (3), 280-286.

32. Rossato, L.; Loreto, E. S.; Zanette, R. A.; Chassot, F.; Santurio, J. M.; Alves, S. H., *In vitro* synergistic effects of chlorpromazine and sertraline in combination with amphotericin B against *Cryptococcus neoformans* var. *grubii*. *Folia Microbiol. (Praha)* **2016,** *61* (5), 399-403.

33. Denning, D. W., Echinocandin antifungal drugs. *Lancet* **2003,** *362* (9390), 1142-1151.

34. Berkow, E. L.; Angulo, D.; Lockhart, S. R., *In vitro* activity of a novel glucan synthase inhibitor, SCY-078, against clinical isolates of *Candida auris*. *Antimicrob. Agents Chemother.* **2017,** *61* (7), e00435-17.

35. Wring, S. A.; Randolph, R.; Park, S.; Abruzzo, G.; Chen, Q.; Flattery, A.; Garrett, G.; Peel, M.; Outcalt, R.; Powell, K.; Trucksis, M.; Angulo, D.; Borroto-Esoda, K., Preclinical pharmacokinetics and pharmacodynamic target of SCY-078, a first-in-class orally active antifungal glucan synthesis inhibitor, in murine models of disseminated candidiasis. *Antimicrob. Agents Chemother.* **2017,** *61* (4), e02068-16.

36. Ghannoum, M.; Long, L.; Larkin, E. L.; Isham, N.; Sherif, R.; Borroto-Esoda, K.; Barat, S.; Angulo, D., Evaluation of the antifungal activity of the novel oral glucan synthase inhibitor SCY-078, singly and in combination, for the treatment of invasive aspergillosis. *Antimicrob. Agents Chemother.* **2018,** *62* (6), e00244-18.

37. Larkin, E.; Hager, C.; Chandra, J.; Mukherjee, P. K.; Retuerto, M.; Salem, I.; Long, L.; Isham, N.; Kovanda, L.; Borroto-Esoda, K.; Wring, S.; Angulo, D.; Ghannoum, M., The emerging pathogen *Candida auris*: Growth phenotype, virulence factors, activity of antifungals, and effect of SCY-078, a novel glucan synthesis inhibitor, on growth morphology and biofilm formation. *Antimicrob. Agents Chemother.* **2017,** *61* (5), e02396-16.

38. Scorneaux, B.; Angulo, D.; Borroto-Esoda, K.; Ghannoum, M.; Peel, M.; Wring, S., SCY-078 is fungicidal against *Candida* species in time-kill studies. *Antimicrob. Agents Chemother.* **2017,** *61* (3), e01961-16.

39. Schell, W. A.; Jones, A. M.; Borroto-Esoda, K.; Alexander, B. D., Antifungal activity of SCY-078 and standard antifungal agents against 178 clinical isolates of

resistant and susceptible *Candida* species. *Antimicrob. Agents Chemother.* **2017,** *61* (11), e01102-17.

40. Jimenez-Ortigosa, C.; Perez, W. B.; Angulo, D.; Borroto-Esoda, K.; Perlin, D. S., De novo acquisition of resistance to SCY-078 in *Candida glabrata* Involves FKS mutations that both overlap and are distinct from those conferring echinocandin resistance. *Antimicrob. Agents Chemother.* **2017,** *61* (9), e00833-17.

41. Oliver, J. D.; Sibley, G. E. M.; Beckmann, N.; Dobb, K. S.; Slater, M. J.; McEntee, L.; du Pre, S.; Livermore, J.; Bromley, M. J.; Wiederhold, N. P.; Hope, W. W.; Kennedy, A. J.; Law, D.; Birch, M., F901318 represents a novel class of antifungal drug that inhibits dihydroorotate dehydrogenase. *Proc. Natl. Acad. Sci., U. S. A.* **2016,** *113* (45), 12809-12814.

42. Wiederhold, N. P.; Law, D.; Birch, M., Dihydroorotate dehydrogenase inhibitor F901318 has potent *in vitro* activity against *Scedosporium* species and *Lomentospora prolificans*. *J. Antimicrob. Chemother.* **2017,** *72* (7), 1977-1980.

43. Hope, W. W.; McEntee, L.; Livermore, J.; Whalley, S.; Johnson, A.; Farrington, N.; Kolamunnage-Dona, R.; Schwartz, J.; Kennedy, A.; Law, D.; Birch, M.; Rex, J. H., Pharmacodynamics of the orotomides against *Aspergillus fumigatus*: New opportunities for treatment of multidrug-resistant fungal disease. *MBio* **2017,** *8* (4), e01157-17.

44. Buil, J. B.; Rijs, A.; Meis, J. F.; Birch, M.; Law, D.; Melchers, W. J. G.; Verweij, P. E., *In vitro* activity of the novel antifungal compound F901318 against difficult-to-treat *Aspergillus* isolates. *J. Antimicrob. Chemother.* **2017,** *72* (9), 2548-2552.

45. Watanabe, N. A.; Miyazaki, M.; Horii, T.; Sagane, K.; Tsukahara, K.; Hata, K., E1210, a new broad-spectrum antifungal, suppresses *Candida albicans* hyphal growth through inhibition of glycosylphosphatidylinositol biosynthesis. *Antimicrob. Agents Chemother.* **2012,** *56* (2), 960-971.

46. Zhao, M.; Lepak, A. J.; VanScoy, B.; Bader, J. C.; Marchillo, K.; Vanhecker, J.; Ambrose, P. G.; Andes, D. R., *In vivo* pharmacokinetics and pharmacodynamics of APX001 against *Candida* spp. in a neutropenic disseminated candidiasis mouse model. *Antimicrob. Agents Chemother.* **2018,** *62* (4), e02542-17.

47. Zhao, Y.; Lee, M. H.; Paderu, P.; Lee, A.; Jimenez-Ortigosa, C.; Park, S.; Mansbach, R. S.; Shaw, K. J.; Perlin, D. S., Significantly improved pharmacokinetics enhances *in vivo* efficacy of APX001 against echinocandin- and multidrug-resistant *Candida* isolates in a mouse model of invasive candidiasis. *Antimicrob. Agents Chemother.* **2018,** *62* (10), e00425-18.

48. Hager, C. L.; Larkin, E. L.; Long, L.; Zohra Abidi, F.; Shaw, K. J.; Ghannoum, M. A., *In vitro* and *in vivo* evaluation of the antifungal activity of APX001A/APX001 against *Candida auris*. *Antimicrob. Agents Chemother.* **2018,** *62* (3), e02319-17.

49. Wiederhold, N. P.; Najvar, L. K.; Fothergill, A. W.; McCarthy, D. I.; Bocanegra, R.; Olivo, M.; Kirkpatrick, W. R.; Everson, M. P.; Duncanson, F. P.; Patterson, T. F., The investigational agent E1210 is effective in treatment of experimental invasive candidiasis caused by resistant *Candida albicans*. *Antimicrob. Agents Chemother.* **2015,** *59* (1), 690-692.

50. Castanheira, M.; Duncanson, F. P.; Diekema, D. J.; Guarro, J.; Jones, R. N.; Pfaller, M. A., Activities of E1210 and comparator agents tested by CLSI and EUCAST

broth microdilution methods against *Fusarium* and *Scedosporium* species identified using molecular methods. *Antimicrob. Agents Chemother.* **2012,** *56* (1), 352-357.

51. Pfaller, M. A.; Duncanson, F.; Messer, S. A.; Moet, G. J.; Jones, R. N.; Castanheira, M., *In vitro* activity of a novel broad-spectrum antifungal, E1210, tested against *Aspergillus* spp. determined by CLSI and EUCAST broth microdilution methods. *Antimicrob. Agents Chemother.* **2011,** *55* (11), 5155-5158.

52. Miyazaki, M.; Horii, T.; Hata, K.; Watanabe, N. A.; Nakamoto, K.; Tanaka, K.; Shirotori, S.; Murai, N.; Inoue, S.; Matsukura, M.; Abe, S.; Yoshimatsu, K.; Asada, M., *In vitro* activity of E1210, a novel antifungal, against clinically important yeasts and molds. *Antimicrob. Agents Chemother.* **2011,** *55* (10), 4652-4658.

53. Hata, K.; Horii, T.; Miyazaki, M.; Watanabe, N. A.; Okubo, M.; Sonoda, J.; Nakamoto, K.; Tanaka, K.; Shirotori, S.; Murai, N.; Inoue, S.; Matsukura, M.; Abe, S.; Yoshimatsu, K.; Asada, M., Efficacy of oral E1210, a new broad-spectrum antifungal with a novel mechanism of action, in murine models of candidiasis, aspergillosis, and fusariosis. *Antimicrob. Agents Chemother.* **2011,** *55* (10), 4543-4551.

54. Gebremariam, T.; Alkhazraji, S.; Alqarihi, A.; Jeon, H. H.; Gu, Y.; Kapoor, M.; Shaw, K. J.; Ibrahim, A. S., APX001 is effective in the treatment of murine invasive pulmonary aspergillosis. *Antimicrob. Agents Chemother.* **2019,** *63* (2), e01713-18.

55. Zhao, M.; Lepak, A. J.; Marchillo, K.; Vanhecker, J.; Sanchez, H.; Ambrose, P. G.; Andes, D. R., APX001 pharmacokinetic/pharmacodynamic target determination against A*spergillus fumigatus* in an *in vivo* model of invasive pulmonary aspergillosis. *Antimicrob. Agents Chemother.* **2019,** *63* (4), e02372-18.

56. Takahata, S.; Kubota, N.; Takei-Masuda, N.; Yamada, T.; Maeda, M.; Alshahni, M. M.; Abe, S.; Tabata, Y.; Maebashi, K., Mechanism of action of ME1111, a novel antifungal agent for topical treatment of onychomycosis. *Antimicrob. Agents Chemother.* **2016,** *60* (2), 873-880.

57. Tabata, Y.; Takei-Masuda, N.; Kubota, N.; Takahata, S.; Ohyama, M.; Kaneda, K.; Iida, M.; Maebashi, K., Characterization of antifungal activity and nail penetration of ME1111, a new antifungal agent for topical treatment of onychomycosis. *Antimicrob. Agents Chemother.* **2016,** *60* (2), 1035-1039.

58. Ghannoum, M.; Isham, N.; Long, L., *In vitro* antifungal activity of ME1111, a new topical agent for onychomycosis, against clinical isolates of dermatophytes. *Antimicrob. Agents Chemother.* **2015,** *59* (9), 5154-5158.

59. Kubota-Ishida, N.; Takei-Masuda, N.; Kaneda, K.; Nagira, Y.; Chikada, T.; Nomoto, M.; Tabata, Y.; Takahata, S.; Maebashi, K.; Hui, X.; Maibach, H. I., *In vitro* human onychopharmacokinetic and pharmacodynamic analyses of ME1111, a new topical agent for onychomycosis. *Antimicrob. Agents Chemother.* **2018,** *62* (1), e00779-17.

60. Nakamura, I.; Yoshimura, S.; Masaki, T.; Takase, S.; Ohsumi, K.; Hashimoto, M.; Furukawa, S.; Fujie, A., ASP2397: A novel antifungal agent produced by *Acremonium persicinum* MF-347833. *J. Antibiot.* **2017,** *70* (1), 45-51.

61. Hu, Y.; Zhu, B., Study on genetic engineering of *Acremonium chrysogenum*, the cephalosporin C producer. *Synth. Syst. Biotechnol.* **2016,** *1* (3), 143-149.

62. Arendrup, M. C.; Jensen, R. H.; Cuenca-Estrella, M., *In vitro* activity of ASP2397 against *Aspergillus* isolates with or without acquired azole resistance mechanisms. *Antimicrob. Agents Chemother.* **2016,** *60* (1), 532-536.

63. Chabrier-Rosello, Y.; Gerik, K. J.; Koselny, K.; DiDone, L.; Lodge, J. K.; Krysan, D. J., *Cryptococcus neoformans* phosphoinositide-dependent kinase 1 (PDK1) ortholog is required for stress tolerance and survival in murine phagocytes. *Eukaryot. Cell* **2013,** *12* (1), 12-22.

64. Koselny, K.; Green, J.; DiDone, L.; Halterman, J. P.; Fothergill, A. W.; Wiederhold, N. P.; Patterson, T. F.; Cushion, M. T.; Rappelye, C.; Wellington, M.; Krysan, D. J., The celecoxib derivative AR-12 has broad-spectrum antifungal activity i*n vitro* and improves the activity of fluconazole in a murine model of cryptococcosis. *Antimicrob. Agents Chemother.* **2016,** *60* (12), 7115-7127.

65. Baxter, B. K.; DiDone, L.; Ogu, D.; Schor, S.; Krysan, D. J., Identification, *in vitro* activity and mode of action of phosphoinositide-dependent-1 kinase inhibitors as antifungal molecules. *ACS Chem. Biol.* **2011,** *6* (5), 502-510.

66. Koselny, K.; Green, J.; Favazzo, L.; Glazier, V. E.; DiDone, L.; Ransford, S.; Krysan, D. J., Antitumor/antifungal celecoxib derivative AR-12 is a non-nucleoside inhibitor of the ANL-family adenylating enzyme acetyl CoA synthetase. *ACS Infect. Dis.* **2016,** *2* (4), 268-280.

67. Morici, P.; Fais, R.; Rizzato, C.; Tavanti, A.; Lupetti, A., Inhibition of *Candida albicans* biofilm formation by the synthetic lactoferricin derived peptide hLF1-11. *PLoS One* **2016,** *11* (11), e0167470.

68. Uppuluri, P.; Singh, S.; Alqarihi, A.; Schmidt, C. S.; Hennessey, J. P., Jr.; Yeaman, M. R.; Filler, S. G.; Edwards, J. E.; Ibrahim, A. S., Human anti-Als3p antibodies are surrogate markers of NDV-3A vaccine efficacy against recurrent vulvovaginal candidiasis. *Front. Immunol.* **2018,** *9*, 1349.

69. Shubitz, L. F.; Trinh, H. T.; Perrill, R. H.; Thompson, C. M.; Hanan, N. J.; Galgiani, J. N.; Nix, D. E., Modeling nikkomycin Z dosing and pharmacology in murine pulmonary coccidioidomycosis preparatory to phase 2 clinical trials. *J. Infect. Dis.* **2014,** *209* (12), 1949-1954.

70. Pfaller, M. A.; Messer, S. A.; Georgopapadakou, N.; Martell, L. A.; Besterman, J. M.; Diekema, D. J., Activity of MGCD290, a Hos2 histone deacetylase inhibitor, in combination with azole antifungals against opportunistic fungal pathogens. *J. Clin. Microbiol.* **2009,** *47* (12), 3797-3804.

71. Pachl, J.; Svoboda, P.; Jacobs, F.; Vandewoude, K.; van der Hoven, B.; Spronk, P.; Masterson, G.; Malbrain, M.; Aoun, M.; Garbino, J.; Takala, J.; Drgona, L.; Burnie, J.; Matthews, R.; Mycograb Invasive Candidiasis Study, G., A randomized, blinded, multicenter trial of lipid-associated amphotericin B alone versus in combination with an antibody-based inhibitor of heat shock protein 90 in patients with invasive candidiasis. *Clin. Infect. Dis.* **2006,** *42* (10), 1404-1413.

72. Lockhart, S. R.; Iqbal, N.; Cleveland, A. A.; Farley, M. M.; Harrison, L. H.; Bolden, C. B.; Baughman, W.; Stein, B.; Hollick, R.; Park, B. J.; Chiller, T., Species identification and antifungal susceptibility testing of *Candida* bloodstream isolates from population-based surveillance studies in two U.S. cities from 2008 to 2011. *J. Clin. Microbiol.* **2012,** *50* (11), 3435-3442.

73. Franz, R.; Kelly, S. L.; Lamb, D. C.; Kelly, D. E.; Ruhnke, M.; Morschhauser, J., Multiple molecular mechanisms contribute to a stepwise development of fluconazole resistance in clinical *Candida albicans* strains. *Antimicrob. Agents Chemother.* **1998,** *42* (12), 3065-3072.

74. Feng, W.; Yang, J.; Xi, Z.; Qiao, Z.; Lv, Y.; Wang, Y.; Ma, Y.; Wang, Y.; Cen, W., Mutations and/or overexpressions of *ERG4* and *ERG11* genes in clinical azoles-resistant isolates of *Candida albicans*. *Microb. Drug Resist.* **2017,** *23* (5), 563-570.

75. Berger, S.; El Chazli, Y.; Babu, A. F.; Coste, A. T., Azole resistance in *Aspergillus fumigatus*: A consequence of antifungal use in agriculture? *Front. Microbiol.* **2017,** *8*, 1024.

76. Astvad, K. M.; Jensen, R. H.; Hassan, T. M.; Mathiasen, E. G.; Thomsen, G. M.; Pedersen, U. G.; Christensen, M.; Hilberg, O.; Arendrup, M. C., First detection of TR46/Y121F/T289A and TR34/L98H alterations in *Aspergillus fumigatus* isolates from azole-naive patients in Denmark despite negative findings in the environment. *Antimicrob. Agents Chemother.* **2014,** *58* (9), 5096-5101.

77. Tangwattanachuleeporn, M.; Minarin, N.; Saichan, S.; Sermsri, P.; Mitkornburee, R.; Gross, U.; Chindamporn, A.; Bader, O., Prevalence of azole-resistant *Aspergillus fumigatus* in the environment of Thailand. *Med. Mycol.* **2017,** *55* (4), 429-435.

78. Sabino, R.; Carolino, E.; Verissimo, C.; Martinez, M.; Clemons, K. V.; Stevens, D. A., Antifungal susceptibility of 175 *Aspergillus* isolates from various clinical and environmental sources. *Med. Mycol.* **2016,** *54* (7), 740-756.

79. Toyotome, T.; Fujiwara, T.; Kida, H.; Matsumoto, M.; Wada, T.; Komatsu, R., Azole susceptibility in clinical and environmental isolates of *Aspergillus fumigatus* from eastern Hokkaido, Japan. *J. Infect. Chemother.* **2016,** *22* (9), 648-650.

80. Meis, J. F.; Chowdhary, A.; Rhodes, J. L.; Fisher, M. C.; Verweij, P. E., Clinical implications of globally emerging azole resistance in *Aspergillus fumigatus*. *Philos. Trans. R. Soc. Lond. B. Biol. Sci.* **2016,** *371* (1709), 20150460.

81. Chowdhary, A.; Sharma, C.; van den Boom, M.; Yntema, J. B.; Hagen, F.; Verweij, P. E.; Meis, J. F., Multi-azole-resistant *Aspergillus fumigatus* in the environment in Tanzania. *J. Antimicrob. Chemother.* **2014,** *69* (11), 2979-2983.

82. Prigitano, A.; Esposto, M. C.; Romano, L.; Auxilia, F.; Tortorano, A. M., Azole-resistant *Aspergillus fumigatus* in the Italian environment. *J. Glob. Antimicrob. Resist.* **2018,** *16*, 220-224.

83. Mane, A.; Vidhate, P.; Kusro, C.; Waman, V.; Saxena, V.; Kulkarni-Kale, U.; Risbud, A., Molecular mechanisms associated with fluconazole resistance in clinical *Candida albicans* isolates from India. *Mycoses* **2016,** *59* (2), 93-100.

84. Hargrove, T. Y.; Friggeri, L.; Wawrzak, Z.; Qi, A.; Hoekstra, W. J.; Schotzinger, R. J.; York, J. D.; Guengerich, F. P.; Lepesheva, G. I., Structural analyses of *Candida albicans* sterol 14alpha-demethylase complexed with azole drugs address the molecular basis of azole-mediated inhibition of fungal sterol biosynthesis. *J. Biol. Chem.* **2017,** *292* (16), 6728-6743.

85. Alvarez-Rueda, N.; Fleury, A.; Loge, C.; Pagniez, F.; Robert, E.; Morio, F.; Le Pape, P., The amino acid substitution N136Y in *Candida albicans* sterol 14alpha-

demethylase is involved in fluconazole resistance. *Med. Mycol.* **2016,** *54* (7), 764-775.

86. Flowers, S. A.; Colon, B.; Whaley, S. G.; Schuler, M. A.; Rogers, P. D., Contribution of clinically derived mutations in ERG11 to azole resistance in *Candida albicans*. *Antimicrob. Agents Chemother.* **2015,** *59* (1), 450-460.

87. Goldman, G. H.; da Silva Ferreira, M. E.; dos Reis Marques, E.; Savoldi, M.; Perlin, D.; Park, S.; Godoy Martinez, P. C.; Goldman, M. H.; Colombo, A. L., Evaluation of fluconazole resistance mechanisms in *Candida albicans* clinical isolates from HIV-infected patients in Brazil. *Diagn. Microbiol. Infect. Dis.* **2004,** *50* (1), 25-32.

88. Teo, J. Q.; Lee, S. J.; Tan, A. L.; Lim, R. S.; Cai, Y.; Lim, T. P.; Kwa, A. L., Molecular mechanisms of azole resistance in *Candida* bloodstream isolates. *BMC Infect. Dis.* **2019,** *19* (1), 63.

89. Rosana, Y.; Yasmon, A.; Lestari, D. C., Overexpression and mutation as a genetic mechanism of fluconazole resistance in *Candida albicans* isolated from human immunodeficiency virus patients in Indonesia. *J. Med. Microbiol.* **2015,** *64* (9), 1046-1052.

90. Siikala, E.; Rautemaa, R.; Richardson, M.; Saxen, H.; Bowyer, P.; Sanglard, D., Persistent *Candida albicans* colonization and molecular mechanisms of azole resistance in autoimmune polyendocrinopathy-candidiasis-ectodermal dystrophy (APECED) patients. *J. Antimicrob. Chemother.* **2010,** *65* (12), 2505-2513.

91. Kheirollahi, M.; Khosravi, F.; Ashouri, S.; Ahmadi, A., Existence of mutations in the homeodomain-encoding region of NKX2.5 gene in Iranian patients with tetralogy of Fallot. *J. Res. Med. Sci.* **2016,** *21*, 24.

92. Loffler, J.; Kelly, S. L.; Hebart, H.; Schumacher, U.; Lass-Florl, C.; Einsele, H., Molecular analysis of cyp51 from fluconazole-resistant *Candida albicans* strains. *FEMS Microbiol. Lett.* **1997,** *151* (2), 263-268.

93. Favre, B.; Didmon, M.; Ryder, N. S., Multiple amino acid substitutions in lanosterol 14alpha-demethylase contribute to azole resistance in *Candida albicans*. *Microbiology* **1999,** *145 (Pt 10)*, 2715-2725.

94. Chau, A. S.; Mendrick, C. A.; Sabatelli, F. J.; Loebenberg, D.; McNicholas, P. M., Application of real-time quantitative PCR to molecular analysis of *Candida albicans* strains exhibiting reduced susceptibility to azoles. *Antimicrob. Agents Chemother.* **2004,** *48* (6), 2124-2131.

95. Morio, F.; Loge, C.; Besse, B.; Hennequin, C.; Le Pape, P., Screening for amino acid substitutions in the *Candida albicans* Erg11 protein of azole-susceptible and azole-resistant clinical isolates: New substitutions and a review of the literature. *Diagn. Microbiol. Infect. Dis.* **2010,** *66* (4), 373-384.

96. Sanglard, D.; Ischer, F.; Koymans, L.; Bille, J., Amino acid substitutions in the cytochrome P-450 lanosterol 14alpha-demethylase (CYP51A1) from azole-resistant *Candida albicans* clinical isolates contribute to resistance to azole antifungal agents. *Antimicrob. Agents Chemother.* **1998,** *42* (2), 241-253.

97. Peron, I. H.; Reichert-Lima, F.; Busso-Lopes, A. F.; Nagasako, C. K.; Lyra, L.; Moretti, M. L.; Schreiber, A. Z., Resistance surveillance in *Candida albicans*: A five-year antifungal susceptibility evaluation in a Brazilian university hospital. *PLoS One* **2016,** *11* (7), e0158126.

98. Wang, H.; Kong, F.; Sorrell, T. C.; Wang, B.; McNicholas, P.; Pantarat, N.; Ellis, D.; Xiao, M.; Widmer, F.; Chen, S. C., Rapid detection of *ERG11* gene mutations in clinical *Candida albicans* isolates with reduced susceptibility to fluconazole by rolling circle amplification and DNA sequencing. *BMC Microbiol.* **2009,** *9*, 167.

99. Choi, M. J.; Won, E. J.; Shin, J. H.; Kim, S. H.; Lee, W. G.; Kim, M. N.; Lee, K.; Shin, M. G.; Suh, S. P.; Ryang, D. W.; Im, Y. J., Resistance mechanisms and clinical features of fluconazole-nonsusceptible *Candida tropicalis* isolates compared with fluconazole-less-susceptible isolates. *Antimicrob. Agents Chemother.* **2016,** *60* (6), 3653-3661.

100. Xu, Y.; Chen, L.; Li, C., Susceptibility of clinical isolates of *Candida* species to fluconazole and detection of *Candida albicans* ERG11 mutations. *J. Antimicrob. Chemother.* **2008,** *61* (4), 798-804.

101. Martel, C. M.; Parker, J. E.; Bader, O.; Weig, M.; Gross, U.; Warrilow, A. G.; Kelly, D. E.; Kelly, S. L., A clinical isolate of *Candida albicans* with mutations in ERG11 (encoding sterol 14alpha-demethylase) and ERG5 (encoding C22 desaturase) is cross resistant to azoles and amphotericin B. *Antimicrob. Agents Chemother.* **2010,** *54* (9), 3578-3583.

102. Yang, L.; Su, M. Q.; Ma, Y. Y.; Xin, Y. J.; Han, R. B.; Zhang, R.; Wen, J.; Hao, X. K., Epidemiology, species distribution, antifungal susceptibility, and ERG11 mutations of *Candida* species isolated from pregnant Chinese Han women. *Genet. Mol. Res.* **2016,** *15* (2).

103. Hu, L.; Du, X.; Li, T.; Song, Y.; Zai, S.; Hu, X.; Zhang, X.; Li, M., Genetic and phenotypic characterization of *Candida albicans* strains isolated from infectious disease patients in Shanghai. *J. Med. Microbiol.* **2015,** *64* (Pt 1), 74-83.

104. Lamb, D. C.; Kelly, D. E.; White, T. C.; Kelly, S. L., The R467K amino acid substitution in Candida albicans sterol 14alpha-demethylase causes drug resistance through reduced affinity. *Antimicrob. Agents Chemother.* **2000,** *44* (1), 63-67.

105. Feng, L. J.; Wan, Z.; Wang, X. H.; Li, R. Y.; Liu, W., Relationship between antifungal resistance of fluconazole resistant *Candida albicans* and mutations in *ERG11* gene. *Chin. Med. J.* **2010,** *123* (5), 544-548.

106. White, T. C.; Holleman, S.; Dy, F.; Mirels, L. F.; Stevens, D. A., Resistance mechanisms in clinical isolates of *Candida albicans*. *Antimicrob. Agents Chemother.* **2002,** *46* (6), 1704-1713.

107. Strzelczyk, J. K.; Slemp-Migiel, A.; Rother, M.; Golabek, K.; Wiczkowski, A., Nucleotide substitutions in the *Candida albicans* ERG11 gene of azole-susceptible and azole-resistant clinical isolates. *Acta Biochim. Pol.* **2013,** *60* (4), 547-552.

108. Manastir, L.; Ergon, M. C.; Yucesoy, M., Investigation of mutations in Erg11 gene of fluconazole resistant *Candida albicans* isolates from Turkish hospitals. *Mycoses* **2011,** *54* (2), 99-104.

109. Xiang, M. J.; Liu, J. Y.; Ni, P. H.; Wang, S.; Shi, C.; Wei, B.; Ni, Y. X.; Ge, H. L., Erg11 mutations associated with azole resistance in clinical isolates of *Candida albicans*. *FEMS Yeast Res.* **2013,** *13* (4), 386-393.

110. Ying, Y.; Zhao, Y.; Hu, X.; Cai, Z.; Liu, X.; Jin, G.; Zhang, J.; Zhang, J.; Liu, J.; Huang, X., *In vitro* fluconazole susceptibility of 1,903 clinical isolates of *Candida*

albicans and the identification of ERG11 mutations. *Microb. Drug Resist.* **2013,** *19* (4), 266-273.

111. Zhang, L.; Yang, H. F.; Liu, Y. Y.; Xu, X. H.; Ye, Y.; Li, J. B., Reduced susceptibility of *Candida albicans* clinical isolates to azoles and detection of mutations in the *ERG11* gene. *Diagn. Microbiol. Infect. Dis.* **2013,** *77* (4), 327-329.

112. Kakeya, H.; Miyazaki, Y.; Miyazaki, H.; Nyswaner, K.; Grimberg, B.; Bennett, J. E., Genetic analysis of azole resistance in the Darlington strain of *Candida albicans*. *Antimicrob. Agents Chemother.* **2000,** *44* (11), 2985-2990.

113. Perea, S.; Lopez-Ribot, J. L.; Kirkpatrick, W. R.; McAtee, R. K.; Santillan, R. A.; Martinez, M.; Calabrese, D.; Sanglard, D.; Patterson, T. F., Prevalence of molecular mechanisms of resistance to azole antifungal agents in *Candida albicans* strains displaying high-level fluconazole resistance isolated from human immunodeficiency virus-infected patients. *Antimicrob. Agents Chemother.* **2001,** *45* (10), 2676-2684.

114. Choi, Y. J.; Kim, Y. J.; Yong, D.; Byun, J. H.; Kim, T. S.; Chang, Y. S.; Choi, M. J.; Byeon, S. A.; Won, E. J.; Kim, S. H.; Shin, M. G.; Shin, J. H., Fluconazole-resistant *Candida parapsilosis* bloodstream isolates with Y132F mutation in *ERG11* gene, South Korea. *Emerg. Infect. Dis.* **2018,** *24* (9), 1768-1770.

115. Chowdhary, A.; Prakash, A.; Sharma, C.; Kordalewska, M.; Kumar, A.; Sarma, S.; Tarai, B.; Singh, A.; Upadhyaya, G.; Upadhyay, S.; Yadav, P.; Singh, P. K.; Khillan, V.; Sachdeva, N.; Perlin, D. S.; Meis, J. F., A multicentre study of antifungal susceptibility patterns among 350 *Candida auris* isolates (2009-17) in

India: Role of the *ERG11* and *FKS1* genes in azole and echinocandin resistance. *J. Antimicrob. Chemother.* **2018,** *73* (4), 891-899.

116. Healey, K. R.; Kordalewska, M.; Jimenez Ortigosa, C.; Singh, A.; Berrio, I.; Chowdhary, A.; Perlin, D. S., Limited ERG11 mutations identified in isolates of *Candida auris* directly contribute to reduced azole susceptibility. *Antimicrob. Agents Chemother.* **2018,** *62* (10), e01427-18.

117. Hou, X.; Lee, A.; Jimenez-Ortigosa, C.; Kordalewska, M.; Perlin, D. S.; Zhao, Y., Rapid detection of ERG11-associated azole resistance and FKS-associated echinocandin resistance in *Candida auris*. *Antimicrob. Agents Chemother.* **2019,** *63* (1), e01811-18.

118. Tan, J.; Zhang, J.; Chen, W.; Sun, Y.; Wan, Z.; Li, R.; Liu, W., The A395T mutation in *ERG11* gene confers fluconazole resistance in *Candida tropicalis* causing candidemia. *Mycopathologia* **2015,** *179* (3-4), 213-218.

119. Spettel, K.; Barousch, W.; Makristathis, A.; Zeller, I.; Nehr, M.; Selitsch, B.; Lackner, M.; Rath, P. M.; Steinmann, J.; Willinger, B., Analysis of antifungal resistance genes in *Candida albicans* and *Candida glabrata* using next generation sequencing. *PLoS One* **2019,** *14* (1), e0210397.

120. Marichal, P.; Koymans, L.; Willemsens, S.; Bellens, D.; Verhasselt, P.; Luyten, W.; Borgers, M.; Ramaekers, F. C. S.; Odds, F. C.; Vanden Bossche, H., Contribution of mutations in the cytochrome P450 14alpha-demethylase (Erg11p, Cyp51p) to azole resistance in *Candida albicans*. *Microbiology* **1999,** *145 (Pt 10)*, 2701-2713.

121. Kwon, Y. J.; Shin, J. H.; Byun, S. A.; Choi, M. J.; Won, E. J.; Lee, D.; Lee, S. Y.; Chun, S.; Lee, J. H.; Choi, H. J.; Kee, S. J.; Kim, S. H.; Shin, M. G., *Candida auris*

clinical isolates from South Korea: Identification, antifungal susceptibility, and genotyping. *J. Clin. Microbiol.* **2019,** *57* (4), e01624-18.

122. Xisto, M. I.; Caramalho, R. D.; Rocha, D. A.; Ferreira-Pereira, A.; Sartori, B.; Barreto-Bergter, E.; Junqueira, M. L.; Lass-Florl, C.; Lackner, M., Pan-azole-resistant *Candida tropicalis* carrying homozygous erg11 mutations at position K143R: A new emerging superbug? *J. Antimicrob. Chemother.* **2017,** *72* (4), 988-992.

123. Jin, L.; Cao, Z.; Wang, Q.; Wang, Y.; Wang, X.; Chen, H.; Wang, H., MDR1 overexpression combined with ERG11 mutations induce high-level fluconazole resistance in *Candida tropicalis* clinical isolates. *BMC Infect. Dis.* **2018,** *18* (1), 162.

124. Jensen, R. H.; Astvad, K. M.; Silva, L. V.; Sanglard, D.; Jorgensen, R.; Nielsen, K. F.; Mathiasen, E. G.; Doroudian, G.; Perlin, D. S.; Arendrup, M. C., Stepwise emergence of azole, echinocandin and amphotericin B multidrug resistance *in vivo* in *Candida albicans* orchestrated by multiple genetic alterations. *J. Antimicrob. Chemother.* **2015,** *70* (9), 2551-2555.

125. Walsh, T. J.; Petraitis, V.; Petraitiene, R.; Field-Ridley, A.; Sutton, D.; Ghannoum, M.; Sein, T.; Schaufele, R.; Peter, J.; Bacher, J.; Casler, H.; Armstrong, D.; Espinel-Ingroff, A.; Rinaldi, M. G.; Lyman, C. A., Experimental pulmonary aspergillosis due to *Aspergillus terreus*: Pathogenesis and treatment of an emerging fungal pathogen resistant to amphotericin B. *J. Infect. Dis.* **2003,** *188* (2), 305-319.

126. Young, L. Y.; Hull, C. M.; Heitman, J., Disruption of ergosterol biosynthesis confers resistance to amphotericin B in *Candida lusitaniae*. *Antimicrob. Agents Chemother.* **2003,** *47* (9), 2717-2724.

127. Mesa-Arango, A. C.; Rueda, C.; Roman, E.; Quintin, J.; Terron, M. C.; Luque, D.; Netea, M. G.; Pla, J.; Zaragoza, O., Cell wall changes in amphotericin B-resistant strains from *Candida tropicalis* and relationship with the immune responses elicited by the host. *Antimicrob. Agents Chemother.* **2016,** *60* (4), 2326-2335.

128. Dick, J. D.; Rosengard, B. R.; Merz, W. G.; Stuart, R. K.; Hutchins, G. M.; Saral, R., Fatal disseminated candidiasis due to amphotericin-B-resistant *Candida guilliermondii*. *Ann. Intern. Med.* **1985,** *102* (1), 67-68.

129. Sterling, T. R.; Merz, W. G., Resistance to amphotericin B: Emerging clinical and microbiological patterns. *Drug. Resist. Updat.* **1998,** *1* (3), 161-165.

130. Veses, V.; Gow, N. A., Pseudohypha budding patterns of *Candida albicans*. *Med. Mycol.* **2009,** *47* (3), 268-275.

131. Hebeka, E. K.; Solotorovsky, M., Development of resistance to polyene antibiotics in *Candida albicans*. *J. Bacteriol.* **1965,** *89*, 1533-1539.

132. Konuma, T.; Takahashi, S.; Kiyuna, T.; Miharu, Y.; Suzuki, M.; Shibata, H.; Kato, S.; Takahashi, S.; Tojo, A., Breakthrough fungemia due to *Candida fermentati* with *fks1p* mutation under micafungin treatment in a cord blood transplant recipient. *Transpl. Infect. Dis.* **2017,** *19* (1).

133. Perlin, D. S., Mechanisms of echinocandin antifungal drug resistance. *Ann. N. Y. Acad. Sci.* **2015,** *1354*, 1-11.

134. Jensen, R. H.; Johansen, H. K.; Arendrup, M. C., Stepwise development of a homozygous S80P substitution in Fks1p, conferring echinocandin resistance in *Candida tropicalis*. *Antimicrob. Agents Chemother.* **2013,** *57* (1), 614-617.

135. Jensen, R. H.; Justesen, U. S.; Rewes, A.; Perlin, D. S.; Arendrup, M. C., Echinocandin failure case due to a previously unreported FKS1 mutation in *Candida krusei*. *Antimicrob. Agents Chemother.* **2014,** *58* (6), 3550-3552.

136. Zimbeck, A. J.; Iqbal, N.; Ahlquist, A. M.; Farley, M. M.; Harrison, L. H.; Chiller, T.; Lockhart, S. R., FKS mutations and elevated echinocandin MIC values among *Candida glabrata* isolates from U.S. population-based surveillance. *Antimicrob. Agents Chemother.* **2010,** *54* (12), 5042-5047.

137. Hou, X.; Xiao, M.; Chen, S. C.; Kong, F.; Wang, H.; Chu, Y. Z.; Kang, M.; Sun, Z. Y.; Hu, Z. D.; Li, R. Y.; Lu, J.; Liao, K.; Hu, T. S.; Ni, Y. X.; Zou, G. L.; Zhang, G.; Fan, X.; Zhao, Y. P.; Xu, Y. C., Molecular epidemiology and antifungal susceptibility of *Candida glabrata* in China (August 2009 to July 2014): A multi-center study. *Front. Microbiol.* **2017,** *8*, 880.

138. Park, S.; Kelly, R.; Kahn, J. N.; Robles, J.; Hsu, M. J.; Register, E.; Li, W.; Vyas, V.; Fan, H.; Abruzzo, G.; Flattery, A.; Gill, C.; Chrebet, G.; Parent, S. A.; Kurtz, M.; Teppler, H.; Douglas, C. M.; Perlin, D. S., Specific substitutions in the echinocandin target Fks1p account for reduced susceptibility of rare laboratory and clinical *Candida* sp. isolates. *Antimicrob. Agents Chemother.* **2005,** *49* (8), 3264-3273.

139. Suwunnakorn, S.; Wakabayashi, H.; Kordalewska, M.; Perlin, D. S.; Rustchenko, E., *FKS2* and *FKS3* genes of opportunistic human pathogen *Candida albicans*

influence echinocandin susceptibility. *Antimicrob. Agents Chemother.* **2018,** *62* (4), e02299-17.

140. Perlin, D. S., Resistance to echinocandin-class antifungal drugs. *Drug Resist. Updat.* **2007,** *10* (3), 121-130.

141. Johnson, M. E.; Edlind, T. D., Topological and mutational analysis of *Saccharomyces cerevisiae* Fks1. *Eukaryot. Cell* **2012,** *11* (7), 952-960.

142. Xiao, M.; Fan, X.; Hou, X.; Chen, S. C.; Wang, H.; Kong, F.; Sun, Z. Y.; Chu, Y. Z.; Xu, Y. C., Clinical characteristics of the first cases of invasive candidiasis in China due to pan-echinocandin-resistant *Candida tropicalis* and *Candida glabrata* isolates with delineation of their resistance mechanisms. *Infect. Drug Resist.* **2018,** *11*, 155-161.

143. Locke, J. B.; Almaguer, A. L.; Zuill, D. E.; Bartizal, K., Characterization of *in vitro* resistance development to the novel echinocandin CD101 in *Candida* species. *Antimicrob. Agents Chemother.* **2016,** *60* (10), 6100-6107.

144. Garcia-Effron, G.; Lee, S.; Park, S.; Cleary, J. D.; Perlin, D. S., Effect of *Candida glabrata* FKS1 and FKS2 mutations on echinocandin sensitivity and kinetics of 1,3-beta-D-glucan synthase: Implication for the existing susceptibility breakpoint. *Antimicrob. Agents Chemother.* **2009,** *53* (9), 3690-3699.

145. Costa-de-Oliveira, S.; Marcos Miranda, I.; Silva, R. M.; Pinto, E. S. A.; Rocha, R.; Amorim, A.; Goncalves Rodrigues, A.; Pina-Vaz, C., FKS2 mutations associated with decreased echinocandin susceptibility of *Candida glabrata* following anidulafungin therapy. *Antimicrob. Agents Chemother.* **2011,** *55* (3), 1312-1314.

146. Drakulovski, P.; Dunyach, C.; Bertout, S.; Reynes, J.; Mallie, M., A *Candida albicans* strain with high MIC for caspofungin and no FKS1 mutations exhibits a high chitin content and mutations in two chitinase genes. *Med. Mycol.* **2011,** *49* (5), 467-474.

147. Healey, K. R.; Katiyar, S. K.; Castanheira, M.; Pfaller, M. A.; Edlind, T. D., *Candida glabrata* mutants demonstrating paradoxical reduced caspofungin susceptibility but increased micafungin susceptibility. *Antimicrob. Agents Chemother.* **2011,** *55* (8), 3947-3949.

148. Yang, F.; Zhang, L.; Wakabayashi, H.; Myers, J.; Jiang, Y.; Cao, Y.; Jimenez-Ortigosa, C.; Perlin, D. S.; Rustchenko, E., Tolerance to caspofungin in *Candida albicans* is associated with at least three distinctive mechanisms that govern expression of *FKS* genes and cell wall remodeling. *Antimicrob. Agents Chemother.* **2017,** *61* (5), e00071-17.

149. Beyda, N. D.; John, J.; Kilic, A.; Alam, M. J.; Lasco, T. M.; Garey, K. W., FKS mutant *Candida glabrata*: Risk factors and outcomes in patients with candidemia. *Clin. Infect. Dis.* **2014,** *59* (6), 819-825.

150. Katiyar, S.; Pfaller, M.; Edlind, T., *Candida albicans* and *Candida glabrata* clinical isolates exhibiting reduced echinocandin susceptibility. *Antimicrob. Agents Chemother.* **2006,** *50* (8), 2892-2894.

151. Castanheira, M.; Messer, S. A.; Jones, R. N.; Farrell, D. J.; Pfaller, M. A., Activity of echinocandins and triazoles against a contemporary (2012) worldwide collection of yeast and moulds collected from invasive infections. *Int. J. Antimicrob. Agents* **2014,** *44* (4), 320-326.

152. Pfaller, M. A.; Messer, S. A.; Diekema, D. J.; Jones, R. N.; Castanheira, M., Use of micafungin as a surrogate marker to predict susceptibility and resistance to caspofungin among 3,764 clinical isolates of *Candida* by use of CLSI methods and interpretive criteria. *J. Clin. Microbiol.* **2014,** *52* (1), 108-114.

153. Castanheira, M.; Woosley, L. N.; Messer, S. A.; Diekema, D. J.; Jones, R. N.; Pfaller, M. A., Frequency of fks mutations among *Candida glabrata* isolates from a 10-year global collection of bloodstream infection isolates. *Antimicrob. Agents Chemother.* **2014,** *58* (1), 577-580.

154. Alexander, B. D.; Johnson, M. D.; Pfeiffer, C. D.; Jimenez-Ortigosa, C.; Catania, J.; Booker, R.; Castanheira, M.; Messer, S. A.; Perlin, D. S.; Pfaller, M. A., Increasing echinocandin resistance in *Candida glabrata*: Clinical failure correlates with presence of FKS mutations and elevated minimum inhibitory concentrations. *Clin. Infect. Dis.* **2013,** *56* (12), 1724-1732.

155. Castanheira, M.; Deshpande, L. M.; Davis, A. P.; Rhomberg, P. R.; Pfaller, M. A., Monitoring antifungal resistance in a global collection of invasive yeasts and molds: Application of CLSI epidemiological cutoff values and whole-genome sequencing analysis for detection of azole resistance in *Candida albicans*. *Antimicrob. Agents Chemother.* **2017,** *61* (10), e00906-17.

156. Castanheira, M.; Woosley, L. N.; Diekema, D. J.; Messer, S. A.; Jones, R. N.; Pfaller, M. A., Low prevalence of fks1 hot spot 1 mutations in a worldwide collection of *Candida* strains. *Antimicrob. Agents Chemother.* **2010,** *54* (6), 2655-2659.

157. Pfeiffer, C. D.; Garcia-Effron, G.; Zaas, A. K.; Perfect, J. R.; Perlin, D. S.; Alexander, B. D., Breakthrough invasive candidiasis in patients on micafungin. *J. Clin. Microbiol.* **2010,** *48* (7), 2373-2380.

158. Garcia-Effron, G.; Chua, D. J.; Tomada, J. R.; DiPersio, J.; Perlin, D. S.; Ghannoum, M.; Bonilla, H., Novel FKS mutations associated with echinocandin resistance in *Candida* species. *Antimicrob. Agents Chemother.* **2010,** *54* (5), 2225-2227.

159. Shields, R. K.; Nguyen, M. H.; Press, E. G.; Cumbie, R.; Driscoll, E.; Pasculle, A. W.; Clancy, C. J., Rate of FKS mutations among consecutive *Candida* isolates causing bloodstream infection. *Antimicrob. Agents Chemother.* **2015,** *59* (12), 7465-7470.

160. Pham, C. D.; Iqbal, N.; Bolden, C. B.; Kuykendall, R. J.; Harrison, L. H.; Farley, M. M.; Schaffner, W.; Beldavs, Z. G.; Chiller, T. M.; Park, B. J.; Cleveland, A. A.; Lockhart, S. R., Role of FKS mutations in *Candida glabrata*: MIC values, echinocandin resistance, and multidrug resistance. *Antimicrob. Agents Chemother.* **2014,** *58* (8), 4690-4696.

161. Asner, S. A.; Giulieri, S.; Diezi, M.; Marchetti, O.; Sanglard, D., Acquired multidrug antifungal resistance in *Candida lusitaniae* during therapy. *Antimicrob. Agents Chemother.* **2015,** *59* (12), 7715-7722.

162. Sasso, M.; Roger, C.; Lachaud, L., Rapid emergence of FKS mutations in *Candida glabrata* isolates in a peritoneal candidiasis. *Med. Mycol. Case Rep.* **2017,** *16*, 28-30.

163. Prigent, G.; Ait-Ammar, N.; Levesque, E.; Fekkar, A.; Costa, J. M.; El Anbassi, S.; Foulet, F.; Duvoux, C.; Merle, J. C.; Dannaoui, E.; Botterel, F., Echinocandin resistance in *Candida* species isolates from liver transplant recipients. *Antimicrob. Agents Chemother.* **2017,** *61* (2), e01229-16.

164. Naicker, S. D.; Magobo, R. E.; Zulu, T. G.; Maphanga, T. G.; Luthuli, N.; Lowman, W.; Govender, N. P., Two echinocandin-resistant *Candida glabrata* FKS mutants from South Africa. *Med. Mycol. Case Rep.* **2016,** *11*, 24-26.

165. Lackner, M.; Tscherner, M.; Schaller, M.; Kuchler, K.; Mair, C.; Sartori, B.; Istel, F.; Arendrup, M. C.; Lass-Florl, C., Positions and numbers of FKS mutations in *Candida albicans* selectively influence *in vitro* and *in vivo* susceptibilities to echinocandin treatment. *Antimicrob. Agents Chemother.* **2014,** *58* (7), 3626-3635.

166. Johnson, M. E.; Katiyar, S. K.; Edlind, T. D., New Fks hot spot for acquired echinocandin resistance in *Saccharomyces cerevisiae* and its contribution to intrinsic resistance of *Scedosporium* species. *Antimicrob. Agents Chemother.* **2011,** *55* (8), 3774-3781.

167. Shin, J. H.; Kee, S. J.; Shin, M. G.; Kim, S. H.; Shin, D. H.; Lee, S. K.; Suh, S. P.; Ryang, D. W., Biofilm production by isolates of *Candida* species recovered from nonneutropenic patients: Comparison of bloodstream isolates with isolates from other sources. *J. Clin. Microbiol.* **2002,** *40* (4), 1244-1248.

168. Loussert, C.; Schmitt, C.; Prevost, M. C.; Balloy, V.; Fadel, E.; Philippe, B.; Kauffmann-Lacroix, C.; Latge, J. P.; Beauvais, A., *In vivo* biofilm composition of *Aspergillus fumigatus*. *Cell Microbiol.* **2010,** *12* (3), 405-410.

169. Walsh, T. J.; Schlegel, R.; Moody, M. M.; Costerton, J. W.; Salcman, M., Ventriculoatrial shunt infection due to *Cryptococcus neoformans*: An ultrastructural and quantitative microbiological study. *Neurosurgery* **1986,** *18* (3), 373-375.

170. Dyavaiah, M.; Ramani, R.; Chu, D. S.; Ritterband, D. C.; Shah, M. K.; Samsonoff, W. A.; Chaturvedi, S.; Chaturvedi, V., Molecular characterization, biofilm analysis and experimental biofouling study of *Fusarium* isolates from recent cases of fungal keratitis in New York State. *BMC Ophthalmol.* **2007,** *7*, 1.

171. Davis, L. E.; Cook, G.; Costerton, J. W., Biofilm on ventriculo-peritoneal shunt tubing as a cause of treatment failure in coccidioidal meningitis. *Emerg. Infect. Dis.* **2002,** *8* (4), 376-379.

172. Di Bonaventura, G.; Pompilio, A.; Picciani, C.; Iezzi, M.; D'Antonio, D.; Piccolomini, R., Biofilm formation by the emerging fungal pathogen *Trichosporon asahii*: Development, architecture, and antifungal resistance. *Antimicrob. Agents Chemother.* **2006,** *50* (10), 3269-3276.

173. Cannizzo, F. T.; Eraso, E.; Ezkurra, P. A.; Villar-Vidal, M.; Bollo, E.; Castella, G.; Cabanes, F. J.; Vidotto, V.; Quindos, G., Biofilm development by clinical isolates of *Malassezia pachydermatis*. *Med. Mycol.* **2007,** *45* (4), 357-361.

174. D'Antonio, D.; Parruti, G.; Pontieri, E.; Di Bonaventura, G.; Manzoli, L.; Sferra, R.; Vetuschi, A.; Piccolomini, R.; Romano, F.; Staniscia, T., Slime production by clinical isolates of *Blastoschizomyces capitatus* from patients with hematological malignancies and catheter-related fungemia. *Eur. J. Clin. Microbiol. Infect. Dis.* **2004,** *23* (10), 787-789.

175. Singh, R.; Shivaprakash, M. R.; Chakrabarti, A., Biofilm formation by zygomycetes: Quantification, structure and matrix composition. *Microbiology* **2011,** *157* (Pt 9), 2611-2618.

176. Desai, J. V.; Mitchell, A. P.; Andes, D. R., Fungal biofilms, drug resistance, and recurrent infection. *Cold Spring Harb. Perspect. Med.* **2014,** *4* (10), a019729.

177. Ramirez-Villalva, A.; Gonzalez-Calderon, D.; Gonzalez-Romero, C.; Morales-Rodriguez, M.; Jauregui-Rodriguez, B.; Cuevas-Yanez, E.; Fuentes-Benites, A., A facile synthesis of novel miconazole analogues and the evaluation of their antifungal activity. *Eur. J. Med. Chem.* **2015,** *97*, 275-279.

178. Dogan, I. S.; Sarac, S.; Sari, S.; Kart, D.; Essiz Gokhan, S.; Vural, I.; Dalkara, S., New azole derivatives showing antimicrobial effects and their mechanism of antifungal activity by molecular modeling studies. *Eur. J. Med. Chem.* **2017,** *130*, 124-138.

179. Gonzalez-Calderon, D.; Mejia-Dionicio, M. G.; Morales-Reza, M. A.; Ramirez-Villalva, A.; Morales-Rodriguez, M.; Jauregui-Rodriguez, B.; Diaz-Torres, E.; Gonzalez-Romero, C.; Fuentes-Benites, A., Azide-enolate 1,3-dipolar cycloaddition in the synthesis of novel triazole-based miconazole analogues as promising antifungal agents. *Eur. J. Med. Chem.* **2016,** *112*, 60-65.

180. Zhang, Y.; Damu, G. L. V.; Cui, S. F.; Mi, J. L.; Tangadanchu, V. K. R.; Zhou, C. H., Discovery of potential antifungal triazoles: Design, synthesis, biological evaluation, and preliminary antifungal mechanism exploration. *MedChemComm* **2017,** *8* (8), 1631-1639.

181. Corey, E. J.; Chaykovsky, M., Dimethylsulfoxonium. methylide. *J. Am. Chem. Soc.* **1962,** *84* (5), 867-868.

182. Corey, E. J.; Chaykovsky, M., Dimethyloxosulfonium Methylide ((CH3)2SOCH2) and Dimethylsulfonium Methylide ((CH3)2SCH2). Formation and Application to Organic Synthesis. *J. Am. Chem. Soc.* **1965,** *87* (6), 1353-1364.

183. Shrestha, S. K.; Garzan, A.; Garneau-Tsodikova, S., Novel alkylated azoles as potent antifungals. *Eur. J. Med. Chem.* **2017,** *133*, 309-318.

184. Thamban Chandrika, N.; Shrestha, S. K.; Ngo, H. X.; Tsodikov, O. V.; Howard, K. C.; Garneau-Tsodikova, S., Alkylated piperazines and piperazine-azole hybrids as antifungal agents. *J. Med. Chem.* **2018,** *61* (1), 158-173.

185. Xu, K.; Huang, L.; Xu, Z.; Wang, Y.; Bai, G.; Wu, Q.; Wang, X.; Yu, S.; Jiang, Y., Design, synthesis, and antifungal activities of novel triazole derivatives containing the benzyl group. *Drug. Des. Devel. Ther.* **2015,** *9*, 1459-1467.

186. He, X.; Jiang, Y.; Zhang, Y.; Wu, S.; Dong, G.; Liu, N.; LIu, Y.; Yao, J.; Miao, Z.; Wang, Y.; Zhang, W.; Sheng, C., Discovery of highly potent triazole antifungal agents agents with piperidine-oxadiazole side chains. *MedChemComm* **2015,** *6*, 653-664.

187. Hashemi, S. M.; Badali, H.; Irannejad, H.; Shokrzadeh, M.; Emami, S., Synthesis and biological evaluation of fluconazole analogs with triazole-modified scaffold as potent antifungal agents. *Bioorg. Med. Chem.* **2015,** *23* (7), 1481-1491.

188. Cao, X.; Xu, Y.; Cao, Y.; Wang, R.; Zhou, R.; Chu, W.; Yang, Y., Design, synthesis, and structure-activity relationship studies of novel thienopyrrolidone

derivatives with strong antifungal activity against *Aspergillus fumigates*. *Eur. J. Med. Chem.* **2015,** *102*, 471-476.

189. Klimek, K.; Strubinska, J.; Czernel, G.; Ginalska, G.; Gagos, M., *In vitro* evaluation of antifungal and cytotoxic activities as also the therapeutic safety of the oxidized form of amphotericin B. *Chem. Biol. Interact.* **2016,** *256*, 47-54.

190. Zhang, J.; Ma, J.; Dong, Y.; Zhao, W.; Feng, J., Synthesis and characterization of NH2-(AEEA)n-amphotericin B derivatives. *J. Antibiot.* **2019,** *72* (4), 210-217.

191. Antillon, A.; de Vries, A. H.; Espinosa-Caballero, M.; Falcon-Gonzalez, J. M.; Flores Romero, D.; Gonzalez-Damian, J.; Jimenez-Montejo, F. E.; Leon-Buitimea, A.; Lopez-Ortiz, M.; Magana, R.; Marrink, S. J.; Morales-Nava, R.; Periole, X.; Reyes-Esparza, J.; Rodriguez Lozada, J.; Santiago-Angelino, T. M.; Vargas Gonzalez, M. C.; Regla, I.; Carrillo-Tripp, M.; Fernandez-Zertuche, M.; Rodriguez-Fragoso, L.; Ortega-Blake, I., An amphotericin B derivative equally potent to amphotericin B and with increased safety. *PLoS One* **2016,** *11* (9), e0162171.

192. Tevyashova, A. N.; Korolev, A. M.; Trenin, A. S.; Dezhenkova, L. G.; Shtil, A. A.; Polshakov, V. I.; Savelyev, O. Y.; Olsufyeva, E. N., New conjugates of polyene macrolide amphotericin B with benzoxaboroles: Synthesis and properties. *J. Antibiot.* **2016,** *69* (7), 549-560.

193. Won, H. J.; Kim, H. J.; Jang, J. Y.; Kang, S. H.; Choi, S. S.; Kim, E. S., Improved recovery and biological activities of an engineered polyene NPP analogue in *Pseudonocardia autotrophica*. *J. Ind. Microbiol. Biotechnol.* **2017,** *44* (9), 1293-1299.

194. James, K. D.; Laudeman, C. P.; Malkar, N. B.; Krishnan, R.; Polowy, K., Structure-activity relationships of a series of echinocandins and the discovery of CD101, a highly stable and soluble echinocandin with distinctive pharmacokinetic properties. *Antimicrob. Agents Chemother.* **2017,** *61* (2), e01541-16.

195. Teng, X.; Wang, Y.; Gu, J.; Shi, P.; Shen, Z.; Ye, L., Antifungal agents: Design, synthesis, antifungal activity and molecular docking of phloroglucinol derivatives. *Molecules* **2018,** *23* (12), 3116.

196. Wani, M. Y.; Ahmad, A.; Kumar, S.; Sobral, A. J., Flucytosine analogues obtained through Biginelli reaction as efficient combinative antifungal agents. *Microb. Pathog.* **2017,** *105*, 57-62.

197. Fang, X. F.; Li, D.; Tangadanchu, V. K. R.; Gopala, L.; Gao, W. W.; Zhou, C. H., Novel potentially antifungal hybrids of 5-flucytosine and fluconazole: Design, synthesis and bioactive evaluation. *Bioorg. Med. Chem. Lett.* **2017,** *27* (22), 4964-4969.

198. Fang, X. J.; Jeyakkumar, P.; Avula, S. R.; Zhou, Q.; Zhou, C. H., Design, synthesis and biological evaluation of 5-fluorouracil-derived benzimidazoles as novel type of potential antimicrobial agents. *Bioorg. Med. Chem. Lett.* **2016,** *26* (11), 2584-2588.

199. Elgemeie, G. H.; Salah, A. M.; Abbas, N. S.; Hussein, H. A.; Mohamed, R. A., Pyrimidine non-nucleoside analogs: A direct synthesis of a novel class of *N*-substituted amino and *N*-sulfonamide derivatives of pyrimidines. *Nucleosides Nucleotides Nucleic Acids* **2017,** *36* (3), 213-223.

200. Zhao, D.; Zhao, S.; Zhao, L.; Zhang, X.; Wei, P.; Liu, C.; Hao, C.; Sun, B.; Su, X.; Cheng, M., Discovery of biphenyl imidazole derivatives as potent antifungal agents: Design, synthesis, and structure-activity relationship studies. *Bioorg. Med. Chem.* **2017,** *25* (2), 750-758.

201. Wani, M. Y.; Ahmad, A.; Shiekh, R. A.; Al-Ghamdi, K. J.; Sobral, A. J., Imidazole clubbed 1,3,4-oxadiazole derivatives as potential antifungal agents. *Bioorg. Med. Chem.* **2015,** *23* (15), 4172-4180.

202. Khalil, A.; Edwards, J. A.; Rappleye, C. A.; Tjarks, W., Design, synthesis, and biological evaluation of aminothiazole derivatives against the fungal pathogens *Histoplasma capsulatum* and *Cryptococcus neoformans*. *Bioorg. Med. Chem.* **2015,** *23* (3), 532-547.

203. Edwards, J. A.; Kemski, M. M.; Rappleye, C. A., Identification of an aminothiazole with antifungal activity against intracellular *Histoplasma capsulatum*. *Antimicrob. Agents Chemother.* **2013,** *57* (9), 4349-4359.

204. Laczkowski, K. Z.; Konklewska, N.; Biernasiuk, A.; Malm, A.; Salat, K.; Furgala, A.; Dzitko, K.; Bekier, A.; Baranowska-Laczkowska, A.; Paneth, A., Thiazoles with cyclopropyl fragment as antifungal, anticonvulsant, and anti-Toxoplasma gondii agents: Synthesis, toxicity evaluation, and molecular docking study. *Med. Chem. Res.* **2018,** *27* (9), 2125-2140.

205. Thamban Chandrika, N.; Shrestha, S. K.; Ngo, H. X.; Garneau-Tsodikova, S., Synthesis and investigation of novel benzimidazole derivatives as antifungal agents. *Bioorg. Med. Chem.* **2016,** *24* (16), 3680-3686.

206. Zhao, S.; Zhao, L.; Zhang, X.; Liu, C.; Hao, C.; Xie, H.; Sun, B.; Zhao, D.; Cheng, M., Design, synthesis, and structure-activity relationship studies of benzothiazole derivatives as antifungal agents. *Eur. J. Med. Chem.* **2016,** *123*, 514-522.

207. Ramirez-Villalva, A.; Gonzalez-Calderon, D.; Rojas-Garcia, R. I.; Gonzalez-Romero, C.; Tamariz-Mascarua, J.; Morales-Rodriguez, M.; Zavala-Segovia, N.; Fuentes-Benites, A., Synthesis and antifungal activity of novel oxazolidin-2-one-linked 1,2,3-triazole derivatives. *MedChemComm* **2017,** *8* (12), 2258-2262.

208. Treitler, D. S.; Leung, S.; Lindrud, M., Development and demonstration of a safer protocol for the synthesis of 5-aryltetrazoles from aryl nitriles. *Org. Proc. Res. Dev.* **2017,** *21* (3), 460-467.

209. Lukowska-Chojnacka, E.; Mierzejewska, J.; Milner-Krawczyk, M.; Bondaryk, M.; Staniszewska, M., Synthesis of novel tetrazole derivatives and evaluation of their antifungal activity. *Bioorg. Med. Chem.* **2016,** *24* (22), 6058-6065.

210. Backes, G. L.; Jursic, B. S.; Neumann, D. M., Potent antimicrobial agents against azole-resistant fungi based on pyridinohydrazide and hydrazomethylpyridine structural motifs. *Bioorg. Med. Chem.* **2015,** *23* (13), 3397-3407.

211. Shrestha, S. K.; Kril, L. M.; Green, K. D.; Kwiatkowski, S.; Sviripa, V. M.; Nickell, J. R.; Dwoskin, L. P.; Watt, D. S.; Garneau-Tsodikova, S., Bis(*N*-amidinohydrazones) and *N*-(amidino)-*N*'-aryl-bishydrazones: New classes of antibacterial/antifungal agents. *Bioorg. Med. Chem.* **2017,** *25* (1), 58-66.

212. Thamban Chandrika, N.; Dennis, E. K.; Shrestha, S. K.; Ngo, H. X.; Green, K. D.; Kwiatkowski, S.; Deaciuc, A. G.; Dwoskin, L. P.; Watt, D. S.; Garneau-Tsodikova,

S., *N*,*N'*-diaryl-bishydrazones in a biphenyl platform: Broad spectrum antifungal agents. *Eur. J. Med. Chem.* **2019,** *164*, 273-281.

213. Ajdacic, V.; Senerovic, L.; Vranic, M.; Pekmezovic, M.; Arsic-Arsnijevic, V.; Veselinovic, A.; Veselinovic, J.; Solaja, B. A.; Nikodinovic-Runic, J.; Opsenica, I. M., Synthesis and evaluation of thiophene-based guanylhydrazones (iminoguanidines) efficient against panel of voriconazole-resistant fungal isolates. *Bioorg. Med. Chem.* **2016,** *24* (6), 1277-1291.

214. Wei, S.; Li, L.; Shu, Y.; Zhao, K.; Ji, Z., Synthesis, antifungal and antitumor activity of two new types of imidazolin-2-ones. *Bioorg. Med. Chem.* **2017,** *25* (24), 6501-6510.

215. Nguyen, S. T.; Kwasny, S. M.; Ding, X.; Williams, J. D.; Peet, N. P.; Bowlin, T. L.; Opperman, T. J., Synthesis and antifungal evaluation of head-to-head and head-to-tail bisamidine compounds. *Bioorg. Med. Chem.* **2015,** *23* (17), 5789-5798.

216. Kumar, S.; Lim, S. M.; Ramasamy, K.; Vasudevan, M.; Shah, S. A. A.; Narasimhan, B., Bis-pyrimidine acetamides: Design, synthesis and biological evaluation. *Chem. Cent. J.* **2017,** *11* (1), 80.

217. Bardiot, D.; Thevissen, K.; De Brucker, K.; Peeters, A.; Cos, P.; Taborda, C. P.; McNaughton, M.; Maes, L.; Chaltin, P.; Cammue, B. P.; Marchand, A., 2-(2-oxo-morpholin-3-yl)-acetamide derivatives as broad-spectrum antifungal agents. *J. Med. Chem.* **2015,** *58* (3), 1502-1512.

218. Ji, Q.; Ge, Z.; Ge, Z.; Chen, K.; Wu, H.; Liu, X.; Huang, Y.; Yuan, L.; Yang, X.; Liao, F., Synthesis and biological evaluation of novel phosphoramidate derivatives

of coumarin as chitin synthase inhibitors and antifungal agents. *Eur. J. Med. Chem.* **2016,** *108*, 166-176.

219. Mohammad, H.; Kyei-Baffour, K.; Younis, W.; Davis, D. C.; Eldesouky, H.; Seleem, M. N.; Dai, M., Investigation of aryl isonitrile compounds with potent, broad-spectrum antifungal activity. *Bioorg. Med. Chem.* **2017,** *25* (11), 2926-2931.

220. Davis, D. C.; Mohammad, H.; Kyei-Baffour, K.; Younis, W.; Creemer, C. N.; Seleem, M. N.; Dai, M., Discovery and characterization of aryl isonitriles as a new class of compounds versus methicillin- and vancomycin-resistant *Staphylococcus aureus*. *Eur. J. Med. Chem.* **2015,** *101*, 384-390.

221. Shaikh, S. K. J.; Kamble, R. R.; Somagond, S. M.; Devarajegowda, H. C.; Dixit, S. R.; Joshi, S. D., Tetrazolylmethyl quinolines: Design, docking studies, synthesis, anticancer and antifungal analyses. *Eur. J. Med. Chem.* **2017,** *128*, 258-273.

222. Vandekerckhove, S.; Van Herreweghe, S.; Willems, J.; Danneels, B.; Desmet, T.; de Kock, C.; Smith, P. J.; Chibale, K.; D'Hooghe, M., Synthesis of functionalized 3-, 5-, 6- and 8-aminoquinolines via intermediate (3-pyrrolin-1-yl)- and (2-oxopyrrolidin-1-yl)quinolines and evaluation of their antiplasmodial and antifungal activity. *Eur. J. Med. Chem.* **2015,** *92*, 91-102.

223. Ahmad, A.; Wani, M. Y.; Patel, M.; Sobral, A.; Duse, A. G.; Aqlan, F. M.; Al-Bogami, A. S., Synergistic antifungal effect of cyclized chalcone derivatives and fluconazole against *Candida albicans*. *MedChemComm* **2017,** *8* (12), 2195-2207.

224. Friggeri, L.; Hargrove, T. Y.; Wawrzak, Z.; Blobaum, A. L.; Rachakonda, G.; Lindsley, C. W.; Villalta, F.; Nes, W. D.; Botta, M.; Guengerich, F. P.; Lepesheva, G. I., Sterol 14alpha-demethylase structure-based design of VNI ((*R*)-*N*-(1-(2,4-

dichlorophenyl)-2-(1H-imidazol-1-yl)ethyl)-4-(5-phenyl-1,3,4-oxadiazol-2-yl)benzamide)) derivatives to target fungal infections: Synthesis, biological evaluation, and crystallographic analysis. *J. Med. Chem.* **2018,** *61* (13), 5679-5691.

225. Ge, Z.; Ji, Q.; Chen, C.; Liao, Q.; Wu, H.; Liu, X.; Huang, Y.; Yuan, L.; Liao, F., Synthesis and biological evaluation of novel 3-substituted amino-4-hydroxylcoumarin derivatives as chitin synthase inhibitors and antifungal agents. *J. Enzyme Inhib. Med. Chem.* **2016,** *31* (2), 219-228.

226. Alwan, W. S.; Karpoormath, R.; Palkar, M. B.; Patel, H. M.; Rane, R. A.; Shaikh, M. S.; Kajee, A.; Mlisana, K. P., Novel imidazo[2,1-b]-1,3,4-thiadiazoles as promising antifungal agents against clinical isolate of *Cryptococcus neoformans*. *Eur. J. Med. Chem.* **2015,** *95*, 514-525.

227. Carradori, S.; Bizzarri, B.; D'Ascenzio, M.; De Monte, C.; Grande, R.; Rivanera, D.; Zicari, A.; Mari, E.; Sabatino, M.; Patsilinakos, A.; Ragno, R.; Secci, D., Synthesis, biological evaluation and quantitative structure-active relationships of 1,3-thiazolidin-4-one derivatives. A promising chemical scaffold endowed with high antifungal potency and low cytotoxicity. *Eur. J. Med. Chem.* **2017,** *140*, 274-292.

228. Shankar, B.; Jalapathi, P.; Saikrishna, B.; Perugu, S.; Manga, V., Synthesis, anti-microbial activity, cytotoxicity of some novel substituted (5-(3-(1*H*-benzo[d]imidazol-2-yl)-4-hydroxybenzyl)benzofuran-2-yl)(phenyl)methanone analogs. *Chem. Cent. J.* **2018,** *12* (1), 1.

229. Pawar, K.; Yadav, A.; Prasher, P.; Mishra, S.; Singh, B.; Singh, P. K.; Komath, S. S., Identification of an indole–triazole–amino acid conjugate as a highly effective antifungal agent. *MedChemComm* **2015,** *6*, 1352-1359.

230. Wu, J. S.; Zhang, X.; Zhang, Y. L.; Xie, J. W., Synthesis and antifungal activities of novel polyheterocyclic spirooxindole derivatives. *Org. Biomol. Chem.* **2015,** *13* (17), 4967-4975.

231. Altintop, M. D.; Ozdemir, A.; Turan-Zitouni, G.; Ilgin, S.; Atli, O.; Demirel, R.; Kaplancikli, Z. A., A novel series of thiazolyl-pyrazoline derivatives: Synthesis and evaluation of antifungal activity, cytotoxicity and genotoxicity. *Eur. J. Med. Chem.* **2015,** *92*, 342-352.

232. Ramirez, J.; Svetaz, L.; Quiroga, J.; Abonia, R.; Raimondi, M.; Zacchino, S.; Insuasty, B., Synthesis of novel thiazole-based 8,9-dihydro-7*H*-pyrimido[4,5-b][1,4]diazepines as potential antitumor and antifungal agents. *Eur. J. Med. Chem.* **2015,** *92*, 866-875.

233. Altintop, M. D.; Atli, O.; Ilgin, S.; Demirel, R.; Ozdemir, A.; Kaplancikli, Z. A., Synthesis and biological evaluation of new naphthalene substituted thiosemicarbazone derivatives as potent antifungal and anticancer agents. *Eu.r J. Med. Chem.* **2016,** *108*, 406-414.

234. Ramirez-Prada, J.; Robledo, S. M.; Velez, I. D.; Crespo, M. D. P.; Quiroga, J.; Abonia, R.; Montoya, A.; Svetaz, L.; Zacchino, S.; Insuasty, B., Synthesis of novel quinoline-based 4,5-dihydro-1H-pyrazoles as potential anticancer, antifungal, antibacterial and antiprotozoal agents. *Eur. J. Med. Chem.* **2017,** *131*, 237-254.

235. Liberto, N. A.; Simoes, J. B.; de Paiva Silva, S.; da Silva, C. J.; Modolo, L. V.; de Fatima, A.; Silva, L. M.; Derita, M.; Zacchino, S.; Zuniga, O. M. P.; Romanelli, G. P.; Fernandes, S. A., Quinolines: Microwave-assisted synthesis and their antifungal, anticancer and radical scavenger properties. *Bioorg. Med. Chem.* **2017,** *25* (3), 1153-1162.

236. Lynch, E. D.; Kil, J., Development of ebselen, a glutathione peroxidase mimic, for the prevention and treatment of noise-induce hearing loss. *Seminars in Hearing* **2009,** *30* (01), 047-055.

237. Parnham, M. J.; Sies, H., The early research and development of ebselen. *Biochem. Pharmacol.* **2013,** *86* (9), 1248-1253.

238. Benhamou, R. I.; Steinbuch, K. B.; Fridman, M., Antifungal imidazole-decorated cationic amphiphiles with markedly low hemolytic activity. *Chemistry* **2016,** *22* (32), 11148-11151.

239. Shaul, P.; Benhamou, R. I.; Herzog, I. M.; Louzoun Zada, S.; Ebenstein, Y.; Fridman, M., Synthesis and evaluation of membrane permeabilizing properties of cationic amphiphiles derived from the disaccharide trehalose. *Org. Biomol. Chem.* **2016,** *14* (11), 3012-3015.

240. Zhang, Q.; Alfindee, M. N.; Shrestha, J. P.; Nziko, V. P.; Kawasaki, Y.; Peng, X.; Takemoto, J. Y.; Chang, C. T., Divergent synthesis of three classes of antifungal amphiphilic kanamycin derivatives. *J. Org. Chem.* **2016,** *81* (22), 10651-10663.

241. Fosso, M.; AlFindee, M. N.; Zhang, Q.; Nziko Vde, P.; Kawasaki, Y.; Shrestha, S. K.; Bearss, J.; Gregory, R.; Takemoto, J. Y.; Chang, C. W., Structure-activity

relationships for antibacterial to antifungal conversion of kanamycin to amphiphilic analogues. *J. Org. Chem.* **2015,** *80* (9), 4398-4411.

242. Steinbuch, K. B.; Benhamou, R. I.; Levin, L.; Stein, R.; Fridman, M., Increased degree of unsaturation in the lipid of antifungal cationic amphiphiles facilitates selective fungal cell disruption. *ACS Infect. Dis.* **2018,** *4* (5), 825-836.

243. Shrestha, S. K.; Fosso, M. Y.; Green, K. D.; Garneau-Tsodikova, S., Amphiphilic tobramycin analogues as antibacterial and antifungal agents. *Antimicrob. Agents Chemother.* **2015,** *59* (8), 4861-4869.

244. Shrestha, S. K.; Fosso, M. Y.; Garneau-Tsodikova, S., A combination approach to treating fungal infections. *Sci. Rep.* **2015,** *5*, 17070.

245. Fosso, M. Y.; Shrestha, S. K.; Thamban Chandrika, N.; Dennis, E. K.; Green, K. D.; Garneau-Tsodikova, S., Differential effects of linkers on the activity of amphiphilic tobramycin antifungals. *Molecules* **2018,** *23* (4), 899.

246. Subedi, Y. P.; Roberts, P.; Grilley, M.; Takemoto, J. Y.; Chang, C. T., Development of fungal selective amphiphilic kanamycin: Cost-effective synthesis and use of fluorescent analogs for mode of action investigation. *ACS Infect. Dis.* **2019,** *5* (3), 473-483.

247. Thamban Chandrika, N.; Shrestha, S. K.; Ranjan, N.; Sharma, A.; Arya, D. P.; Garneau-Tsodikova, S., New application of neomycin B-bisbenzimidazole hybrids as antifungal agents. *ACS Infect. Dis.* **2018,** *4* (2), 196-207.

248. Nahar, S.; Ranjan, N.; Ray, A.; Arya, D. P.; Maiti, S., Potent inhibition of miR-27a by neomycin-bisbenzimidazole conjugates. *Chem. Sci.* **2015,** *6* (10), 5837-5846.

249. Ranjan, N.; Fulcrand, G.; King, A.; Brown, J.; Jiang, X.; Leng, F.; Arya, D. P., Selective inhibition of bacterial topoisomerase I by alkynyl-bisbenzimidazoles. *MedChemComm* **2014,** *5* (6), 816-825.

250. Jaber, Q. Z.; Benhamou, R. I.; Herzog, I. M.; Ben Baruch, B.; Fridman, M., Cationic amphiphiles induce macromolecule denaturation and organelle decomposition in pathogenic yeast. *Angew. Chem.* **2018,** *57* (50), 16391-16395.

251. Benhamou, R. I.; Bibi, M.; Berman, J.; Fridman, M., Localizing antifungal drugs to the correct organelle can markedly enhance their efficacy. *Angew. Chem.* **2018,** *57* (21), 6230-6235.

252. Shrestha, J. P.; Baker, C.; Kawasaki, Y.; Subedi, Y. P.; Vincent de Paul, N. N.; Takemoto, J. Y.; Chang, C. T., Synthesis and bioactivity investigation of quinone-based dimeric cationic triazolium amphiphiles selective against resistant fungal and bacterial pathogens. *Eur. J. Med. Chem.* **2017,** *126*, 696-704.

253. Ngo, H. X.; Shrestha, S. K.; Garneau-Tsodikova, S., Identification of ebsulfur analogues with broad-spectrum antifungal activity. *ChemMedChem* **2016,** *11* (14), 1507-1516.

254. Pace, J. R.; DeBerardinis, A. M.; Sail, V.; Tacheva-Grigorova, S. K.; Chan, K. A.; Tran, R.; Raccuia, D. S.; Wechsler-Reya, R. J.; Hadden, M. K., Repurposing the clinically efficacious antifungal agent itraconazole as an anticancer chemotherapeutic. *J. Med. Chem.* **2016,** *59* (8), 3635-3649.

255. Rangel-Vega, A.; Bernstein, L. R.; Mandujano-Tinoco, E. A.; Garcia-Contreras, S. J.; Garcia-Contreras, R., Drug repurposing as an alternative for the treatment of recalcitrant bacterial infections. *Front. Microbiol.* **2015,** *6*, 282.

256. Holbrook, S. Y. L.; Garzan, A.; Dennis, E. K.; Shrestha, S. K.; Garneau-Tsodikova, S., Repurposing antipsychotic drugs into antifungal agents: Synergistic combinations of azoles and bromperidol derivatives in the treatment of various fungal infections. *Eur. J. Med. Chem.* **2017,** *139*, 12-21.

257. Dennis, E. K.; Garneau-Tsodikova, S., Synergistic combinations of azoles and antihistamines against *Candida* species *in vitro*. *Med. Mycol.* **2018**, DOI: 10.1093/mmy/myy088.

258. Mood, A. D.; Premachandra, I. D.; Hiew, S.; Wang, F.; Scott, K. A.; Oldenhuis, N. J.; Liu, H.; Van Vranken, D. L., Potent antifungal synergy of phthalazinone and isoquinolones with azoles against *Candida albicans*. *ACS Med. Chem. Lett.* **2017,** *8* (2), 168-173.

259. Li, S.; Shi, H.; Chang, W.; Li, Y.; Zhang, M.; Qiao, Y.; Lou, H., Eudesmane sesquiterpenes from Chinese liverwort are substrates of Cdrs and display antifungal activity by targeting Erg6 and Erg11 of *Candida albicans*. *Bioorg. Med. Chem.* **2017,** *25* (20), 5764-5771.

260. Bhattacharya, A. K.; Chand, H. R.; John, J.; Deshpande, M. V., Clerodane type diterpene as a novel antifungal agent from *Polyalthia longifolia var. pendula*. *Eur. J. Med. Chem.* **2015,** *94*, 1-7.

261. Jiang, Z.; Liu, N.; Hu, D.; Dong, G.; Miao, Z.; Yao, J.; He, H.; Jiang, Y.; Zhang, W.; Wang, Y.; Sheng, C., The discovery of novel antifungal scaffolds by structural simplification of the natural product sampangine. *Chem. Commun.* **2015,** *51* (78), 14648-14651.

262. Liu, N.; Zhong, H.; Tu, J.; Jiang, Z.; Jiang, Y.; Jiang, Y.; Jiang, Y.; Li, J.; Zhang, W.; Wang, Y.; Sheng, C., Discovery of simplified sampangine derivatives as novel fungal biofilm inhibitors. *Eur. J. Med. Chem.* **2018,** *143*, 1510-1523.

263. Lin, S.; Sin, W. L. W.; Koh, J. J.; Lim, F.; Wang, L.; Cao, D.; Beuerman, R. W.; Ren, L.; Liu, S., Semisynthesis and biological evaluation of xanthone amphiphilics as selective, highly potent antifungal agents to combat fungal resistance. *J. Med. Chem.* **2017,** *60* (24), 10135-10150.

264. Wuts, P. G.; Simons, L. J.; Metzger, B. P.; Sterling, R. C.; Slightom, J. L.; Elhammer, A. P., Generation of broad-spectrum antifungal drug candidates from the natural product compound aureobasidin A. *ACS Med. Chem. Lett.* **2015,** *6* (6), 645-649.

265. Al Mubarak, S.; Robert, A. A.; Baskaradoss, J. K.; Al-Zoman, K.; Al Sohail, A.; Alsuwyed, A.; Ciancio, S., The prevalence of oral *Candida infections* in periodontitis patients with type 2 diabetes mellitus. *J. Infect. Public Health* **2013,** *6* (4), 296-301.

266. Atabek, M. E.; Akyurek, N.; Eklioglu, B. S., Frequency of vaginal *Candida* colonization and relationship between metabolic parameters in children with type 1 diabetes mellitus. *J. Pediatr. Adolesc. Gynecol.* **2013,** *26* (5), 257-260.

267. Nyirjesy, P.; Zhao, Y.; Ways, K.; Usiskin, K., Evaluation of vulvovaginal symptoms and *Candida* colonization in women with type 2 diabetes mellitus treated with canagliflozin, a sodium glucose co-transporter 2 inhibitor. *Curr. Med. Res. Opin.* **2012,** *28* (7), 1173-1178.

268. Spampinato, C.; Leonardi, D., *Candida* infections, causes, targets, and resistance mechanisms: Traditional and alternative antifungal agents. *Biomed. Res. Int.* **2013,** *2013*, 204237.

269. Austin, N.; Cleminson, J.; Darlow, B. A.; McGuire, W., Prophylactic oral/topical non-absorbed antifungal agents to prevent invasive fungal infection in very low birth weight infants. *Cochrane Database Syst. Rev.* **2015,** (10), CD003478.

270. Hawkins, D. M.; Smidt, A. C., Superficial fungal infections in children. *Pediatr. Clin. North Am.* **2014,** *61* (2), 443-455.

271. Horvath, E. E.; Murray, C. K.; Vaughan, G. M.; Chung, K. K.; Hospenthal, D. R.; Wade, C. E.; Holcomb, J. B.; Wolf, S. E.; Mason, A. D., Jr.; Cancio, L. C., Fungal wound infection (not colonization) is independently associated with mortality in burn patients. *Ann. Surg.* **2007,** *245* (6), 978-985.

272. Sarabahi, S.; Tiwari, V. K.; Arora, S.; Capoor, M. R.; Pandey, A., Changing pattern of fungal infection in burn patients. *Burns* **2012,** *38* (4), 520-528.

273. Wang, F. J.; Zhang, D.; Liu, Z. H.; Wu, W. X.; Bai, H. H.; Dong, H. Y., Species distribution and *in vitro* antifungal susceptibility of vulvovaginal *Candida* isolates in China. *Chin. Med. J.* **2016,** *129* (10), 1161-1165.

274. Goncalves, B.; Ferreira, C.; Alves, C. T.; Henriques, M.; Azeredo, J.; Silva, S., Vulvovaginal candidiasis: Epidemiology, microbiology and risk factors. *Crit. Rev. Microbiol.* **2016,** *42* (6), 905-927.

275. Sarbu, I.; Pelinescu, D.; Stoica, I.; Marutescu, L.; Vassu, T., Phenotypic profiles of virulence in different *Candida* species isolated from vulvovaginal infections. *Roum. Arch. Microbiol. Immunol.* **2013,** *72* (4), 225-233.

276. Sobel, J. D.; Vazquez, J. A., Symptomatic vulvovaginitis due to fluconazole-resistant *Candida albicans* in a female who was not infected with human immunodeficiency virus. *Clin. Infect. Dis.* **1996,** *22* (4), 726-727.

277. Perlin, D. S.; Rautemaa-Richardson, R.; Alastruey-Izquierdo, A., The global problem of antifungal resistance: Prevalence, mechanisms, and management. *Lancet Infect. Dis.* **2017,** *17* (12), e383-e392.

278. Tobudic, S.; Kratzer, C.; Presterl, E., Azole-resistant *Candida* spp. – emerging pathogens? *Mycoses* **2012,** *55 (Suppl. 1)*, 24-32.

279. Bondaryk, M.; Kurzatkowski, W.; Staniszewska, M., Antifungal agents commonly used in the superficial and mucosal candidiasis treatment: Mode of action and resistance development. *Postepy Dermatol. Alergol.* **2013,** *30* (5), 293-301.

280. Stylianou, M.; Kulesskiy, E.; Lopes, J. P.; Granlund, M.; Wennerberg, K.; Urban, C. F., Antifungal application of nonantifungal drugs. *Antimicrob. Agents Chemother.* **2014,** *58* (2), 1055-1062.

281. Hu, Y.; Sieck, D. E.; Hsu, W. H., Why are second-generation H1-antihistamines minimally sedating? *Eur. J. Pharmacol.* **2015,** *765*, 100-106.

282. Hait, W. N.; Gesmonde, J. F.; Murren, J. R.; Yang, J. M.; Chen, H. X.; Reiss, M., Terfenadine (Seldane): A new drug for restoring sensitivity to multidrug resistant cancer cells. *Biochem. Pharmacol.* **1993,** *45* (2), 401-406.

283. Chen, C.; Li, G.; Liao, W.; Wu, J.; Liu, L.; Ma, D.; Zhou, J.; Elbekai, R. H.; Edin, M. L.; Zeldin, D. C.; Wang, D. W., Selective inhibitors of CYP2J2 related to terfenadine exhibit strong activity against human cancers *in vitro* and *in vivo*. *J. Pharmacol. Exp. Ther.* **2009,** *329* (3), 908-918.

284. Perlmutter, J. I.; Forbes, L. T.; Krysan, D. J.; Ebsworth-Mojica, K.; Colquhoun, J. M.; Wang, J. L.; Dunman, P. M.; Flaherty, D. P., Repurposing the antihistamine terfenadine for antimicrobial activity against *Staphylococcus aureus*. *J. Med. Chem.* **2014,** *57* (20), 8540-8562.

285. Lewis, R. E., Current concepts in antifungal pharmacology. *Mayo Clin. Proc.* **2011,** *86* (8), 805-817.

286. Sobel, J. D., Recurrent vulvovaginal candidiasis. *Am. J. Obstet. Gynecol.* **2016,** *214* (1), 15-21.

287. Fleischer, A. B., Jr.; Feldman, S. R., Prescription of high-potency corticosteroid agents and clotrimazole-betamethasone dipropionate by pediatricians. *Clin. Ther.* **1999,** *21* (10), 1725-1731.

288. Crowley, P. D.; Gallagher, H. C., Clotrimazole as a pharmaceutical: Past, present and future. *J. Appl. Microbiol.* **2014,** *117* (3), 611-617.

289. Greenberg, H. L.; Shwayder, T. A.; Bieszk, N.; Fivenson, D. P., Clotrimazole/betamethasone diproprionate: A review of costs and complications in the treatment of common cutaneous fungal infections. *Pediatr. Dermatol.* **2002,** *19* (1), 78-81.

290. Tang, M. M.; Corti, M. A.; Stirnimann, R.; Pelivani, N.; Yawalkar, N.; Borradori, L.; Simon, D., Severe cutaneous allergic reactions following topical antifungal therapy. *Contact Dermatitis* **2013,** *68* (1), 56-57.

291. Sahni, K.; Singh, S.; Dogra, S., Newer topical treatments in skin and nail dermatophyte infections. *Indian Dermatol. Online J.* **2018,** *9* (3), 149-158.

292. Gupta, A. K.; Cooper, E. A., Update in antifungal therapy of dermatophytosis. *Mycopathologia* **2008,** *166* (5-6), 353-367.

293. Zahran, K. M.; Agban, M. N.; Ahmed, S. H.; Hassan, E. A.; Sabet, M. A., Patterns of *Candida biofilm* on intrauterine devices. *J. Med. Microbiol.* **2015,** *64* (Pt 4), 375-381.

294. Nobile, C. J.; Johnson, A. D., *Candida albicans* biofilms and human disease. *Ann. Rev. Microbiol.* **2015,** *69*, 71-92.

295. Ramage, G.; Saville, S. P.; Thomas, D. P.; Lopez-Ribot, J. L., *Candida* biofilms: An update. *Eukaryot. Cell* **2005,** *4* (4), 633-638.

296. Harriott, M. M.; Lilly, E. A.; Rodriguez, T. E.; Fidel, P. L.; Noverr, M. C., *Candida albicans* forms biofilms on the vaginal mucosa. *Microbiology* **2010,** *156* (Pt 12), 3635-3644.

297. Tsui, C.; Kong, E. F.; Jabra-Rizk, M. A., Pathogenesis of *Candida albicans* biofilm. *Pathog. Dis.* **2016,** *74* (4), ftw018.

298. Hawser, S. P.; Douglas, L. J., Biofilm formation by *Candida* species on the surface of catheter materials i*n vitro*. *Infect. Immun.* **1994,** *62* (3), 915-921.

299. Fonseca, E.; Silva, S.; Rodrigues, C. F.; Alves, C. T.; Azeredo, J.; Henriques, M., Effects of fluconazole on *Candida glabrata* biofilms and its relationship with ABC transporter gene expression. *Biofouling* **2014,** *30* (4), 447-457.

300. Llopis-Torregrosa, V.; Husekova, B.; Sychrova, H., Potassium uptake mediated by Trk1 is Crucial for *Candida glabrata* growth and fitness. *PLoS One* **2016,** *11* (4), e0153374.

301. Liu, J. D.; Wang, Y. J.; Chen, C. H.; Yu, C. F.; Chen, L. C.; Lin, J. K.; Liang, Y. C.; Lin, S. Y.; Ho, Y. S., Molecular mechanisms of G0/G1 cell-cycle arrest and apoptosis induced by terfenadine in human cancer cells. *Mol. Carcinog.* **2003,** *37* (1), 39-50.

302. Nicolau-Galmes, F.; Asumendi, A.; Alonso-Tejerina, E.; Perez-Yarza, G.; Jangi, S. M.; Gardeazabal, J.; Arroyo-Berdugo, Y.; Careaga, J. M.; Diaz-Ramon, J. L.; Apraiz, A.; Boyano, M. D., Terfenadine induces apoptosis and autophagy in melanoma cells through ROS-dependent and -independent mechanisms. *Apoptosis* **2011,** *16* (12), 1253-1267.

303. Wang, W. T.; Chen, Y. H.; Hsu, J. L.; Leu, W. J.; Yu, C. C.; Chan, S. H.; Ho, Y. F.; Hsu, L. C.; Guh, J. H., Terfenadine induces anti-proliferative and apoptotic activities in human hormone-refractory prostate cancer through histamine receptor-independent Mcl-1 cleavage and Bak up-regulation. *Naunyn Schmiedebergs Arch. Pharmacol.* **2014,** *387* (1), 33-45.

304. Segura-Cabrera, A.; Tripathi, R.; Zhang, X.; Gui, L.; Chou, T. F.; Komurov, K., A structure- and chemical genomics-based approach for repositioning of drugs against VCP/p97 ATPase. *Sci. Rep.* **2017,** *7*, 44912.

305. Clinical and Laboratory Standards Institute. *Reference method for broth dilution antifungal susceptibility testing of yeasts - Approved standard. CLSI document M27-A3. Wayne, PA.* 2008.

306. Garcia, L. S., Synergism testing: Broth microdilution checkerboard and broth madrodilution methods. In *Clinical microbiology procedures handbook*, 3rd edition ed.; ASM Press: Washington, DC, 2016; pp 1-23.

307. Meletiadis, J.; Mouton, J. W.; Meis, J. F.; Verweij, P. E., *In vitro* drug interaction modeling of combinations of azoles with terbinafine against clinical *Scedosporium prolificans* isolates. *Antimicrob. Agents Chemother.* **2003,** *47* (1), 106-117.

308. Klepser, M. E.; Malone, D.; Lewis, R. E.; Ernst, E. J.; Pfaller, M. A., Evaluation of voriconazole pharmacodynamics using time-kill methodology. *Antimicrob. Agents Chemother.* **2000,** *44* (7), 1917-1920.

309. Pierce, C. G.; Uppuluri, P.; Tristan, A. R.; Wormley, F. L., Jr.; Mowat, E.; Ramage, G.; Lopez-Ribot, J. L., A simple and reproducible 96-well plate-based method for the formation of fungal biofilms and its application to antifungal susceptibility testing. *Nat. Protoc.* **2008,** *3* (9), 1494-1500.

310. Garzan, A.; Willby, M. J.; Ngo, H. X.; Gajadeera, C. S.; Green, K. D.; Holbrook, S. Y.; Hou, C.; Posey, J. E.; Tsodikov, O. V.; Garneau-Tsodikova, S., Combating enhanced intracellular survival (Eis)-mediated kanamycin resistance of *Mycobacterium tuberculosis* by novel pyrrolo[1,5-a]pyrazine-based Eis inhibitors. *ACS Infect. Dis.* **2017,** *3* (4), 302-309.

311. Quave, C. L.; Estevez-Carmona, M.; Compadre, C. M.; Hobby, G.; Hendrickson, H.; Beenken, K. E.; Smeltzer, M. S., Ellagic acid derivatives from *Rubus ulmifolius* inhibit *Staphylococcus aureus* biofilm formation and improve response to antibiotics. *PLoS One* **2012,** *7* (1), e28737.

312. Hall, B. S.; Bot, C.; Wilkinson, S. R., Nifurtimox activation by trypanosomal type I nitroreductases generates cytotoxic nitrile metabolites. *J. Biol. Chem.* **2011,** *286* (15), 13088-13095.

313. Xu, W.; Zhu, X.; Tan, T.; Li, W.; Shan, A., Design of embedded-hybrid antimicrobial peptides with enhanced cell selectivity and anti-biofilm activity. *PLoS One* **2014,** *9* (6), e98935.

314. Fosso, M. Y.; Shrestha, S. K.; Green, K. D.; Garneau-Tsodikova, S., Synthesis and bioactivities of kanamycin B-derived cationic amphiphiles. *J. Med. Chem.* **2015,** *58* (23), 9124-9132.

315. Bassetti, M.; Bouza, E., Invasive mould infections in the ICU setting: Complexities and solutions. *J. Antimicrob. Chemother.* **2017,** *72* (suppl_1), i39-i47.

316. Arendrup, M. C.; Perlin, D. S., Echinocandin resistance: An emerging clinical problem? *Curr. Opin. Infect. Dis.* **2014,** *27* (6), 484-492.

317. Jeffery-Smith, A.; Taori, S. K.; Schelenz, S.; Jeffery, K.; Johnson, E. M.; Borman, A.; *Candida auris* Incident Management, T.; Manuel, R.; Brown, C. S., *Candida auris*: A review of the literature. *Clin. Microbiol. Rev.* **2018,** *31* (1), e00029-17.

318. Sarma, S.; Upadhyay, S., Current perspective on emergence, diagnosis and drug resistance in *Candida auris*. *Infect. Drug Resist.* **2017,** *10*, 155-165.

319. Yu, Z.; Gunn, L.; Wall, P.; Fanning, S., Antimicrobial resistance and its association with tolerance to heavy metals in agriculture production. *Food Microbiol.* **2017,** *64*, 23-32.

320. Lazarevic, T.; Rilak, A.; Bugarcic, Z. D., Platinum, palladium, gold and ruthenium complexes as anticancer agents: Current clinical uses, cytotoxicity studies and future perspectives. *Eur. J. Med. Chem.* **2017,** *142*, 8-31.

321. Ndagi, U.; Mhlongo, N.; Soliman, M. E., Metal complexes in cancer therapy - an update from drug design perspective. *Drug Des. Devel. Ther.* **2017,** *11*, 599-616.

322. Mjos, K. D.; Orvig, C., Metallodrugs in medicinal inorganic chemistry. *Chem. Rev.* **2014,** *114* (8), 4540-4563.

323. Berners-Price, S. J.; Mirabelli, C. K.; Johnson, R. K.; Mattern, M. R.; McCabe, F. L.; Faucette, L. F.; Sung, C. M.; Mong, S. M.; Sadler, P. J.; Crooke, S. T., *In vivo* antitumor activity and *in vitro* cytotoxic properties of bis[1,2-bis(diphenylphosphino)ethane]gold(I) chloride. *Cancer Res.* **1986,** *46* (11), 5486-5493.

324. Ssemaganda, A.; Low, L. M.; Verhoeft, K. R.; Wambuzi, M.; Kawoozo, B.; Nabasumba, S. B.; Mpendo, J.; Bagaya, B. S.; Kiwanuka, N.; Stanisic, D. I.; Berners-Price, S. J.; Good, M. F., Gold(I) phosphine compounds as parasite attenuating agents for malaria vaccine and drug development. *Metallomics* **2018,** *10* (3), 444-454.

325. Glisic, B. D.; Djuran, M. I., Gold complexes as antimicrobial agents: An overview of different biological activities in relation to the oxidation state of the gold ion and the ligand structure. *Dalton Trans* **2014,** *43* (16), 5950-5969.

326. Madeira, J. M.; Gibson, D. L.; Kean, W. F.; Klegeris, A., The biological activity of auranofin: Implications for novel treatment of diseases. *Inflammopharmacology* **2012,** *20* (6), 297-306.

327. Fuchs, B. B.; RajaMuthiah, R.; Souza, A. C.; Eatemadpour, S.; Rossoni, R. D.; Santos, D. A.; Junqueira, J. C.; Rice, L. B.; Mylonakis, E., Inhibition of bacterial and fungal pathogens by the orphaned drug auranofin. *Future Med. Chem.* **2016,** *8* (2), 117-132.

328. Aguinagalde, L.; Diez-Martinez, R.; Yuste, J.; Royo, I.; Gil, C.; Lasa, I.; Martin-Fontecha, M.; Marin-Ramos, N. I.; Ardanuy, C.; Linares, J.; Garcia, P.; Garcia, E.; Sanchez-Puelles, J. M., Auranofin efficacy against MDR *Streptococcus pneumoniae* and *Staphylococcus aureus* infections. *J. Antimicrob. Chemother.* **2015,** *70* (9), 2608-2617.

329. AbdelKhalek, A.; Abutaleb, N. S.; Elmagarmid, K. A.; Seleem, M. N., Repurposing auranofin as an intestinal decolonizing agent for vancomycin-resistant *enterococci*. *Sci. Rep.* **2018,** *8* (1), 8353.

330. Owings, J. P.; McNair, N. N.; Mui, Y. F.; Gustafsson, T. N.; Holmgren, A.; Contel, M.; Goldberg, J. B.; Mead, J. R., Auranofin and *N*-heterocyclic carbene gold-analogs are potent inhibitors of the bacteria *Helicobacter pylori*. *FEMS Microbiol. Lett.* **2016,** *363* (14), fnw148.

331. Siles, S. A.; Srinivasan, A.; Pierce, C. G.; Lopez-Ribot, J. L.; Ramasubramanian, A. K., High-throughput screening of a collection of known pharmacologically active small compounds for identification of *Candida albicans* biofilm inhibitors. *Antimicrob. Agents Chemother.* **2013,** *57* (8), 3681-3687.

332. Wiederhold, N. P.; Patterson, T. F.; Srinivasan, A.; Chaturvedi, A. K.; Fothergill, A. W.; Wormley, F. L.; Ramasubramanian, A. K.; Lopez-Ribot, J. L., Repurposing auranofin as an antifungal: *In vitro* activity against a variety of medically important fungi. *Virulence* **2017,** *8* (2), 138-142.

333. Thangamani, S.; Maland, M.; Mohammad, H.; Pascuzzi, P. E.; Avramova, L.; Koehler, C. M.; Hazbun, T. R.; Seleem, M. N., Repurposing approach identifies

auranofin with broad spectrum antifungal activity that targets Mia40-Erv1 pathway. *Front. Cell Infect. Microbiol.* **2017,** *7*, 4.

334. Diaz, R. S.; Shytaj, I. L.; Giron, L. B.; Obermaier, B.; Libera, E. D., Jr.; Galinskas, J.; Dias, D.; Hunter, J.; Janini, M.; Gosuen, G.; Ferreira, P. A.; Sucupira, M. C.; Maricato, J.; Fackler, O.; Lusic, M.; Savarino, A.; group, S. w., Potential impact of the antirheumatic agent auranofin on proviral HIV-1 DNA in individuals under intensified antiretroviral therapy: Results from a randomized clinical trial. *Int. J. Antimicrob. Agents* **2019**.

335. Capparelli, E. V.; Bricker-Ford, R.; Rogers, M. J.; McKerrow, J. H.; Reed, S. L., Phase I clinical trial results of auranofin, a novel antiparasitic agent. *Antimicrob. Agents Chemother.* **2017,** *61* (1).

336. Harbut, M. B.; Vilcheze, C.; Luo, X.; Hensler, M. E.; Guo, H.; Yang, B.; Chatterjee, A. K.; Nizet, V.; Jacobs, W. R., Jr.; Schultz, P. G.; Wang, F., Auranofin exerts broad-spectrum bactericidal activities by targeting thiol-redox homeostasis. *Proc. Natl. Acad. Sci., U. S. A.* **2015,** *112* (14), 4453-4458.

337. Gandin, V.; Fernandes, A. P., Metal- and semimetal-containing inhibitors of thioredoxin reductase as anticancer agents. *Molecules* **2015,** *20* (7), 12732-12756.

338. Thamban Chandrika, N.; Shrestha, S. K.; Ngo, H. X.; Howard, K. C.; Garneau-Tsodikova, S., Novel fluconazole derivatives with promising antifungal activity. *Bioorg. Med. Chem.* **2018,** *26* (3), 573-580.

339. Gukathasan, S.; Parkin, S.; Awuah, S. G., Cyclometalated gold(III) complexes bearing DACH ligands. *Inorg. Chem.* **2019,** *58* (14), 9326-9340.

340. Kim, J. H.; Reeder, E.; Parkin, S.; Awuah, S. G., Gold(I/III)-phosphine complexes as potent antiproliferative agents. *Sci. Rep.* **2019,** *9*, 12335.

341. Uson, R.; Laguna, A.; Laguna, M.; Briggs, D. A.; Murray, H. H.; Fackler Jr, J. P., *(Tetrahydrothiophene)gold(I) and gold(III) complexes*. Wiley: 1989; Vol. 26.

342. Mohamed, A. A.; Krause Bauer, J. A.; Bruce, A. E.; Bruce, M. R., [Mu-*o*-phenylenebis(diphenylphosphine)-kappa^{2}P:P']bis[chlorogold(I)], dppbz$(AuCl)_2$. *Acta Crystallogr. C* **2003,** *59* (Pt 3), m84-86.

343. Osawa, M.; Kawata, I.; Igawa, S.; Tsuboyama, A.; Hashizume, D.; Hoshino, M., Phosphorescence color alteration by changing counter anions on tetrahedral gold(I) complexes; intra- and interligand π–π interactions. *Eur. J. Inorg. Chem.* **2009,** (25), 3708-3711.

344. Costerton, J. W.; Stewart, P. S.; Greenberg, E. P., Bacterial biofilms: A common cause of persistent infections. *Science* **1999,** *284* (5418), 1318-1322.

345. Ciofu, O.; Rojo-Molinero, E.; Macia, M. D.; Oliver, A., Antibiotic treatment of biofilm infections. *APMIS* **2017,** *125* (4), 304-319.

346. Percival, S. L.; Suleman, L.; Vuotto, C.; Donelli, G., Healthcare-associated infections, medical devices and biofilms: Risk, tolerance and control. *J. Med. Microbiol.* **2015,** *64* (Pt 4), 323-334.

347. Costa-Orlandi, C. B.; Sardi, J. C. O.; Pitangui, N. S.; de Oliveira, H. C.; Scorzoni, L.; Galeane, M. C.; Medina-Alarcon, K. P.; Melo, W.; Marcelino, M. Y.; Braz, J. D.; Fusco-Almeida, A. M.; Mendes-Giannini, M. J. S., Fungal biofilms and polymicrobial diseases. *J. Fungi (Basel)* **2017,** *3* (2), e22.

348. Turan, H.; Demirbilek, M., Biofilm-forming capacity of blood-borne *Candida albicans* strains and effects of antifungal agents. *Rev. Argent. Microbiol.* **2018,** *50* (1), 62-69.

349. Kojic, E. M.; Darouiche, R. O., *Candida* infections of medical devices. *Clin. Microbiol. Rev.* **2004,** *17* (2), 255-267.

350. Nett, J.; Lincoln, L.; Marchillo, K.; Massey, R.; Holoyda, K.; Hoff, B.; VanHandel, M.; Andes, D., Putative role of beta-1,3 glucans in *Candida albicans* biofilm resistance. *Antimicrob. Agents Chemother.* **2007,** *51* (2), 510-520.

351. Ramage, G.; Bachmann, S.; Patterson, T. F.; Wickes, B. L.; Lopez-Ribot, J. L., Investigation of multidrug efflux pumps in relation to fluconazole resistance in *Candida albicans* biofilms. *J. Antimicrob. Chemother.* **2002,** *49* (6), 973-980.

352. Fiori, B.; Posteraro, B.; Torelli, R.; Tumbarello, M.; Perlin, D. S.; Fadda, G.; Sanguinetti, M., *In vitro* activities of anidulafungin and other antifungal agents against biofilms formed by clinical isolates of different *Candida* and *Aspergillus* species. *Antimicrob. Agents Chemother.* **2011,** *55* (6), 3031-3035.

353. Hasan, F.; Xess, I.; Wang, X.; Jain, N.; Fries, B. C., Biofilm formation in clinical *Candida* isolates and its association with virulence. *Microbes Infect.* **2009,** *11* (8-9), 753-761.

354. Rodriguez-Cerdeira, C.; Gregorio, M. C.; Molares-Vila, A.; Lopez-Barcenas, A.; Fabbrocini, G.; Bardhi, B.; Sinani, A.; Sanchez-Blanco, E.; Arenas-Guzman, R.; Hernandez-Castro, R., Biofilms and vulvovaginal candidiasis. *Colloids Surf. B Biointerfaces* **2019,** *174*, 110-125.

355. Nett, J. E.; D, R. A., Fungal biofilms: *In vivo* models for discovery of anti-biofilm drugs. *Microbiol. Spectr.* **2015,** *3* (3), e30.

356. Pongracz, J.; Benedek, K.; Juhasz, E.; Ivan, M.; Kristof, K., *In vitro* biofilm production of *Candida* bloodstream isolates: Any association with clinical characteristics? *J. Med. Microbiol.* **2016,** *65* (4), 272-277.

357. Tumbarello, M.; Posteraro, B.; Trecarichi, E. M.; Fiori, B.; Rossi, M.; Porta, R.; de Gaetano Donati, K.; La Sorda, M.; Spanu, T.; Fadda, G.; Cauda, R.; Sanguinetti, M., Biofilm production by *Candida* species and inadequate antifungal therapy as predictors of mortality for patients with candidemia. *J. Clin. Microbiol.* **2007,** *45* (6), 1843-1850.

358. Wang, Y.; Liu, M.; Cao, R.; Zhang, W.; Yin, M.; Xiao, X.; Liu, Q.; Huang, N., A soluble bis-chelated gold(I) diphosphine compound with strong anticancer activity and low toxicity. *J. Med. Chem.* **2013,** *56* (4), 1455-1466.

359. Jeswani, G.; Alexander, A.; Saraf, S.; Saraf, S.; Qureshi, A.; Ajazuddin, Recent approaches for reducing hemolytic activity of chemotherapeutic agents. *J. Control. Release* **2015,** *211*, 10-21.

360. Radwan, M. A.; AlQuadeib, B. T.; Siller, L.; Wright, M. C.; Horrocks, B., Oral administration of amphotericin B nanoparticles: Antifungal activity, bioavailability and toxicity in rats. *Drug Deliv.* **2017,** *24* (1), 40-50.

361. Uchida, M.; Sun, Y.; McDermott, G.; Knoechel, C.; Le Gros, M. A.; Parkinson, D.; Drubin, D. G.; Larabell, C. A., Quantitative analysis of yeast internal architecture using soft X-ray tomography. *Yeast* **2011,** *28* (3), 227-236.

362. Fujioka, A.; Terai, K.; Itoh, R. E.; Aoki, K.; Nakamura, T.; Kuroda, S.; Nishida, E.; Matsuda, M., Dynamics of the Ras/ERK MAPK cascade as monitored by fluorescent probes. *J. Biol. Chem.* **2006,** *281* (13), 8917-8926.

363. Gonzalez-Arellano, C.; Corma, A.; Iglesias, M.; Sanchez, F., Enantioselective hydrogenation of alkenes and imines by a gold catalyst. *Chem. Commun.* **2005,** (27), 3451-3453.

364. Krause, L.; Herbst-Irmer, R.; Sheldrick, G. M.; Stalke, D., Comparison of silver and molybdenum microfocus X-ray sources for single-crystal structure determination. *J. Appl. Crystallogr.* **2015,** *48* (Pt 1), 3-10.

365. Bruker-AXS (2016). APEX3 Bruker-AXS Inc., Madison, WI, USA. **2016**.

366. Sheldrick, G. M., Crystal structure refinement with SHELXL. *Acta Crystallogr. C Struct. Chem.* **2015,** *71* (Pt 1), 3-8.

367. Sheldrick, G. M., SHELXT - integrated space-group and crystal-structure determination. *Acta Crystallogr. A Found. Adv.* **2015,** *71* (Pt 1), 3-8.

368. Spek, A. L., Structure validation in chemical crystallography. *Acta Crystallogr. D Biol. Crystallogr.* **2009,** *65* (Pt 2), 148-155.

369. Parkin, S., Expansion of scalar validation criteria to three dimensions: The R tensor. *Acta Crystallogr. A* **2000,** *56* (Pt 3), 157-162.

370. Clinical and Laboratory Standards Institute. *Reference method for broth dilution antifungal susceptibility testing of filamentous fungi - 2nd Edition: CLSI document M38-A2. Wayne, PA.* 2008.

371. Nett, J. E.; Cain, M. T.; Crawford, K.; Andes, D. R., Optimizing a *Candida* biofilm microtiter plate model for measurement of antifungal susceptibility by tetrazolium salt assay. *J. Clin. Microbiol.* **2011,** *49* (4), 1426-1433.

372. Lafleur, M. D.; Sun, L.; Lister, I.; Keating, J.; Nantel, A.; Long, L.; Ghannoum, M.; North, J.; Lee, R. E.; Coleman, K.; Dahl, T.; Lewis, K., Potentiation of azole antifungals by 2-adamantanamine. *Antimicrob. Agents Chemother.* **2013,** *57* (8), 3585-3592.

373. Dartois, V.; Sanchez-Quesada, J.; Cabezas, E.; Chi, E.; Dubbelde, C.; Dunn, C.; Granja, J.; Gritzen, C.; Weinberger, D.; Ghadiri, M. R.; Parr, T. R., Jr., Systemic antibacterial activity of novel synthetic cyclic peptides. *Antimicrob. Agents Chemother.* **2005,** *49* (8), 3302-3310.

374. Evans, B. C.; Nelson, C. E.; Yu, S. S.; Beavers, K. R.; Kim, A. J.; Li, H.; Nelson, H. M.; Giorgio, T. D.; Duvall, C. L., *Ex vivo* red blood cell hemolysis assay for the evaluation of pH-responsive endosomolytic agents for cytosolic delivery of biomacromolecular drugs. *J. Vis. Exp.* **2013,** (73), e50166.

375. Paderu, P.; Park, S.; Perlin, D. S., Caspofungin uptake is mediated by a high-affinity transporter in *Candida albicans*. *Antimicrob. Agents Chemother.* **2004,** *48* (10), 3845-3849.

376. Zhang, W.; Cao, Y.; Gong, J.; Bao, X.; Chen, G.; Liu, W., Identification of residues important for substrate uptake in a glucose transporter from the filamentous fungus *Trichoderma reesei*. *Sci. Rep.* **2015,** *5*, 13829.

377. Alangaden, G. J., Nosocomial fungal infections: Epidemiology, infection control, and prevention. *Infect Dis. Clin. North Am.* **2011,** *25* (1), 201-225.

378. Caston-Osorio, J. J.; Rivero, A.; Torre-Cisneros, J., Epidemiology of invasive fungal infection. *Int. J. Antimicrob. Agents* **2008,** *32 Suppl 2*, S103-109.

379. Perlroth, J.; Choi, B.; Spellberg, B., Nosocomial fungal infections: Epidemiology, diagnosis, and treatment. *Med. Mycol.* **2007,** *45* (4), 321-346.

380. Suleyman, G.; Alangaden, G. J., Nosocomial fungal infections: Epidemiology, infection control, and prevention. *Infect. Dis. Clin. North Am.* **2016,** *30* (4), 1023-1052.

381. Pappas, P. G.; Alexander, B. D.; Andes, D. R.; Hadley, S.; Kauffman, C. A.; Freifeld, A.; Anaissie, E. J.; Brumble, L. M.; Herwaldt, L.; Ito, J.; Kontoyiannis, D. P.; Lyon, G. M.; Marr, K. A.; Morrison, V. A.; Park, B. J.; Patterson, T. F.; Perl, T. M.; Oster, R. A.; Schuster, M. G.; Walker, R.; Walsh, T. J.; Wannemuehler, K. A.; Chiller, T. M., Invasive fungal infections among organ transplant recipients: Results of the Transplant-Associated Infection Surveillance Network (TRANSNET). *Clin. Infect. Dis.* **2010,** *50* (8), 1101-1111.

382. Shoham, S.; Marr, K. A., Invasive fungal infections in solid organ transplant recipients. *Future Microbiol.* **2012,** *7* (5), 639-655.

383. Khan, A.; El-Charabaty, E.; El-Sayegh, S., Fungal infections in renal transplant patients. *J. Clin. Med. Res.* **2015,** *7* (6), 371-378.

384. Silveira, F. P.; Husain, S., Fungal infections in solid organ transplantation. *Med. Mycol.* **2007,** *45* (4), 305-320.

385. Limper, A. H.; Adenis, A.; Le, T.; Harrison, T. S., Fungal infections in HIV/AIDS. *Lancet Infect. Dis.* **2017,** *17* (11), e334-e343.

386. Sipsas, N. V.; Kontoyiannis, D. P., Invasive fungal infections in patients with cancer in the Intensive Care Unit. *Int. J. Antimicrob. Agents* **2012,** *39* (6), 464-471.

387. Mousset, S.; Buchheidt, D.; Heinz, W.; Ruhnke, M.; Cornely, O. A.; Egerer, G.; Kruger, W.; Link, H.; Neumann, S.; Ostermann, H.; Panse, J.; Penack, O.; Rieger, C.; Schmidt-Hieber, M.; Silling, G.; Sudhoff, T.; Ullmann, A. J.; Wolf, H. H.; Maschmeyer, G.; Bohme, A., Treatment of invasive fungal infections in cancer patients-updated recommendations of the Infectious Diseases Working Party (AGIHO) of the German Society of Hematology and Oncology (DGHO). *Ann. Hematol.* **2014,** *93* (1), 13-32.

388. Wiederhold, N. P., Antifungal resistance: Current trends and future strategies to combat. *Infect. Drug Resist.* **2017,** *10*, 249-259.

389. Fisher, M. C.; Hawkins, N. J.; Sanglard, D.; Gurr, S. J., Worldwide emergence of resistance to antifungal drugs challenges human health and food security. *Science* **2018,** *360* (6390), 739-742.

390. Howard, K. C.; Dennis, E. K.; Watt, D. S.; Garneau-Tsodikova, S., A comprehensive overview of the medicinal chemistry of antifungal drugs: Perspectives and promise. *Chem. Soc. Rev.* **2020,** *49* (8), 2426-2480.

391. Parente-Rocha, J. A.; Bailao, A. M.; Amaral, A. C.; Taborda, C. P.; Paccez, J. D.; Borges, C. L.; Pereira, M., Antifungal resistance, metabolic routes as drug targets, and new antifungal agents: An overview about endemic dimorphic fungi. *Mediators Inflamm.* **2017,** *2017*, 9870679.

392. Satoh, K.; Makimura, K.; Hasumi, Y.; Nishiyama, Y.; Uchida, K.; Yamaguchi, H., *Candida auris* sp. *nov*., a novel ascomycetous yeast isolated from the external ear

canal of an inpatient in a Japanese hospital. *Microbiol. Immunol.* **2009,** *53* (1), 41-44.

393. Welsh, R. M.; Bentz, M. L.; Shams, A.; Houston, H.; Lyons, A.; Rose, L. J.; Litvintseva, A. P., Survival, persistence, and isolation of the emerging multidrug-resistant pathogenic yeast *Candida auris* on a plastic health care surface. *J. Clin. Microbiol.* **2017,** *55* (10), 2996-3005.

394. Mizusawa, M.; Miller, H.; Green, R.; Lee, R.; Durante, M.; Perkins, R.; Hewitt, C.; Simner, P. J.; Carroll, K. C.; Hayden, R. T.; Zhang, S. X., Can multidrug-resistant *Candida auris* be reliably identified in clinical microbiology laboratories? *J. Clin. Microbiol.* **2017,** *55* (2), 638-640.

395. Richtel, M.; Jacobs, A., A mysterious infection spanning the globe in a climate of secracy. April 6, 2019. *The New York Times* 2019.

396. Richtel, M.; Jacobs, A., Nursuing homes are a breeding ground for a fatal fungus. *The New York Times* **2019**, September 11, 2019.

397. Richtel, M.; Jacobs, A., New York identifies hospitals and nursing homes with deadly fungus. *The New York Times* **2019**, November 13, 2019.

398. Jacobs, A., Lifelines at risk as bankruptcies stall antibiotics. **2019**, December 26, 2019.

399. Fosso, M. Y.; Li, Y.; Garneau-Tsodikova, S., New trends in aminoglycosides use. *MedChemComm* **2014,** *5* (8), 1075-1091.

400. Keller, P.; Muller, C.; Engelhardt, I.; Hiller, E.; Lemuth, K.; Eickhoff, H.; Wiesmuller, K. H.; Burger-Kentischer, A.; Bracher, F.; Rupp, S., An antifungal

benzimidazole derivative inhibits ergosterol biosynthesis and reveals novel sterols. *Antimicrob. Agents Chemother.* **2015,** *59* (10), 6296-6307.

401. Allen, D.; Wilson, D.; Drew, R.; Perfect, J., Azole antifungals: 35 years of invasive fungal infection management. *Expert Rev. Anti Infect. Ther.* **2015,** *13* (6), 787-798.

402. Bendaha, H.; Yu, L.; Touzani, R.; Souane, R.; Giaever, G.; Nislow, C.; Boone, C.; El Kadiri, S.; Brown, G. W.; Bellaoui, M., New azole antifungal agents with novel modes of action: Synthesis and biological studies of new tridentate ligands based on pyrazole and triazole. *Eur. J. Med. Chem.* **2011,** *46* (9), 4117-4124.

403. Fakhim, H.; Emami, S.; Vaezi, A.; Hashemi, S. M.; Faeli, L.; Diba, K.; Dannaoui, E.; Badali, H., *In vitro* activities of novel azole compounds ATTAF-1 and ATTAF-2 against fluconazole-susceptible and -resistant isolates of *Candida* species. *Antimicrob. Agents Chemother.* **2017,** *61* (1).

404. Ji, C.; Liu, N.; Tu, J.; Li, Z.; Han, G.; Li, J.; Sheng, C., Drug repurposing of haloperidol: Discovery of new benzocyclane derivatives as potent antifungal agents against cryptococcosis and candidiasis. *ACS Infect. Dis.* **2020,** *6* (5), 768-786.

405. Dennis, E. K.; Kim, J. H.; Parkin, S.; Awuah, S. G.; Garneau-Tsodikova, S., Distorted gold(I)-phosphine complexes as antifungal agents. *J. Med. Chem.* **2020,** *63* (5), 2455-2469.

406. Thangamani, S.; Eldesouky, H. E.; Mohammad, H.; Pascuzzi, P. E.; Avramova, L.; Hazbun, T. R.; Seleem, M. N., Ebselen exerts antifungal activity by regulating glutathione (GSH) and reactive oxygen species (ROS) production in fungal cells. *Biochim. Biophys. Acta Gen. Subj.* **2017,** *1861* (1 Pt A), 3002-3010.

407. Venturini, T. P.; Chassot, F.; Loreto, E. S.; Keller, J. T.; Azevedo, M. I.; Zeni, G.; Santurio, J. M.; Alves, S. H., Antifungal activities of diphenyl diselenide and ebselen alone and in combination with antifungal agents against *Fusarium* spp. *Med. Mycol.* **2016,** *54* (5), 550-555.

408. Eggimann, P.; Que, Y. A.; Revelly, J. P.; Pagani, J. L., Preventing invasive *Candida* infections. Where could we do better? *J. Hosp. Infect.* **2015,** *89* (4), 302-308.

409. Mavor, A. L.; Thewes, S.; Hube, B., Systemic fungal infections caused by *Candida* species: Epidemiology, infection process and virulence attributes. *Curr. Drug Targets* **2005,** *6* (8), 863-874.

410. Girishkumar, H.; Yousuf, A. M.; Chivate, J.; Geisler, E., Experience with invasive *Candida* infections. *Postgrad. Med. J.* **1999,** *75* (881), 151-153.

411. Nolla-Salas, J.; Sitges-Serra, A.; Leon-Gil, C.; Martinez-Gonzalez, J.; Leon-Regidor, M. A.; Ibanez-Lucia, P.; Torres-Rodriguez, J. M., Candidemia in non-neutropenic critically ill patients: Analysis of prognostic factors and assessment of systemic antifungal therapy. Study Group of Fungal Infection in the ICU. *Intensive Care Med.* **1997,** *23* (1), 23-30.

412. Leon, C.; Ostrosky-Zeichner, L.; Schuster, M., What's new in the clinical and diagnostic management of invasive candidiasis in critically ill patients. *Intensive Care Med.* **2014,** *40* (6), 808-819.

413. Park, J. Y.; Bradley, N.; Brooks, S.; Burney, S.; Wassner, C., Management of patients with *Candida auris* fungemia at community hospital, Brooklyn, New York, USA, 2016-2018(1). *Emerg. Infect. Dis.* **2019,** *25* (3), 601-602.

414. Adams, E.; Quinn, M.; Tsay, S.; Poirot, E.; Chaturvedi, S.; Southwick, K.; Greenko, J.; Fernandez, R.; Kallen, A.; Vallabhaneni, S.; Haley, V.; Hutton, B.; Blog, D.; Lutterloh, E.; Zucker, H.; Candida auris Investigation, W., *Candida auris* in healthcare facilities, New York, USA, 2013-2017. *Emerg. Infect. Dis.* **2018,** *24* (10), 1816-1824.

415. El-Nakeeb, M. A.; Abou-Shleib, H. M.; Khalil, A. M.; Omar, H. G.; El-Halfawy, O. M., In vitro antibacterial activity of some antihistaminics belonging to different groups against multi-drug resistant clinical isolates. *Braz J Microbiol* **2011,** *42* (3), 980-91.

416. Genaro-Mattos, T. C.; Tallman, K. A.; Allen, L. B.; Anderson, A.; Mirnics, K.; Korade, Z.; Porter, N. A., Dichlorophenyl piperazines, including a recently-approved atypical antipsychotic, are potent inhibitors of DHCR7, the last enzyme in cholesterol biosynthesis. *Toxicol Appl Pharmacol* **2018,** *349*, 21-28.

417. Korade, Z.; Liu, W.; Warren, E. B.; Armstrong, K.; Porter, N. A.; Konradi, C., Effect of psychotropic drug treatment on sterol metabolism. *Schizophr Res* **2017,** *187*, 74-81.

418. Fromtling, R. A., Overview of medically important antifungal azole derivatives. *Clin Microbiol Rev* **1988,** *1* (2), 187-217.

419. Nami, S.; Aghebati-Maleki, A.; Morovati, H.; Aghebati-Maleki, L., Current antifungal drugs and immunotherapeutic approaches as promising strategies to treatment of fungal diseases. *Biomed Pharmacother* **2019,** *110*, 857-868.

420. Martin, H.; Kavanagh, K.; Velasco-Torrijos, T., Targeting adhesion in fungal pathogen Candida albicans. *Future Med Chem* **2020**.

VITA

Emily K. Dennis

EDUCATION

2015 **B.S. in Biochemistry & Molecular Biology**
Centre College, Danville, KY

HONORS AND AWARDS

2020 Peter G. Glavinos, Jr., Ph.D. Travel Award to present my research at a conference. (*Institutional*: $500 to present my research at a conference, 5 awards given).

2019 – 2020 UK CoP Pharmaceutical Sciences Excellence in Graduate Achievement Fellowship. (*Institutional*: $6,000 for stipend and $2,000 increase to stipend, 6 awards given).

2019 Elevator talk winner at the 10th Annual TODD Symposium. ($100 awarded to 12 competitors) Nov. 12, 2019.

2019 UK Graduate Student Congress Summer Travel Award. (*Institutional*: $300 to present my research at a conference, 7 awards given)

2019 Peter G. Glavinos, Jr., Ph.D. Travel Award to present my research at a conference. (*Institutional*: $500 to present my research at a conference, 5 awards given).

2011 – 2015 Colonel Scholarship from Centre College for undergraduate tuition.

PUBLICATIONS

1. Kim, S.K., Ngo, H.X., **Dennis, E.K.**, Chandrika, N.T., DeShong, P., Garneau-Tsodikova, S., & Lee, V.T. (2020). Inhibition of *Pseudomonas aeruginosa* alginate synthesis by ebselen, ebsulfur, and their analogues. Submitted for publication.
2. Thamban Chandrika, N.,† **Dennis, E.K.,**† Brubaker, K.R., Kwiatkowski, K., Watt, D.S.,* & Garneau-Tsodikova, S. (2020). Broad-spectrum antifungal agents: Fluorinated aryl- and heteroaryl-substituted hydrazones. Submitted for publication.
3. **Dennis, E. K.*** & Garneau-Tsodikova, S.* (2020). Substance use disorders: Leading the road to recovery. *RSC Med. Chem.*, *11*, 741-744.
4. Punetha, A., Ngo, H.X., Holbrook, S.Y.L., Green, K.D., Willby, M.J., Bonnett, S.A., Krieger, K., **Dennis, E.K.**, Posey, J.E., Parish, T., Tsodikov, O.V., & Garneau-Tsodikova, S. (2020). Structure-guided optimization of inhibitors of acetyltransferase Eis from *Mycobacterium tuberculosis*. *ACS Chem. Bio.*, *15(6)*, 1581-1594.
5. Howard, K.C.,† **Dennis, E.K.,**† Watt, D.S., & Garneau-Tsodikova, S. (2020). A comprehensive overview of the medicinal chemistry of antifungal drugs: Perspectives and promise. *Chem. Soc. Rev.*, *49*, 2426-2480.

6. **Dennis, E.K.**, Kim, J.H., Parkin, S., Awuah, S.G., & Garneau-Tsodikova, S. (2019). Distorted gold(I)-phosphine complexes as antifungal agents. *J. Med. Chem. (special issue on Women in Medicinal Chemistry), 63(5)*, 2455-2469.
7. **Dennis, E.K.** (2019, Oct. 10) "How going back to elementary school has helped me with my Ph.D." *Public Engagement Reflections*. https://www.aaas.org/programs/center-public-engagement-science-and-technology/reflections/how-going-back-elementary
8. **Dennis, E.K.** & Garneau-Tsodikova, S. (2019). Synergistic combinations of azoles and antihistamines against *Candida* species *in vitro*. *Med. Mycol.*, *57(7)*, 874-884.
9. Thamban Chandrika, N., **Dennis, E.K.**, Shrestha, S.K., Ngo, H.X., Green, K.D., Kwiatkowski, S., Deaciuc, G.A., Dwoskin, L.P., Watt, D.S., & Garneau-Tsodikova, S. (2018). *N-N'*-diaryl-bishydrazones in a biphenyl platform: Broad spectrum antifungal agents. *Eur. J. Med. Chem.*, *164*, 273-281.
10. Fosso, M.Y., Shrestha, S.K., Thamban Chandrika, N., **Dennis, E.K.**, Green, K.D., & Garneau-Tsodikova, S. (2018). Differential effects of linkers on the activity of amphiphilic tobramycin antifungals. *Molecules*, *23(4)*, E899.
11. Holbrook, S.L., Garzan, A., **Dennis, E.K.**, Shrestha, S.K., & Garneau-Tsodikova, S. (2017). Repurposing antipsychotic drugs into antifungal agents: Synergistic combinations of azoles and bromperidol derivatives in the treatment of various fungal infections. *Eur. J. Med. Chem.*, *139*, 12-21.
12. Sledge, S.M., Khimji, H., Borchman, D., Oliver, A.L., Michael, H., **Dennis, E.K.**, Gerlach, D., Bhola, R., Stephen, E. (2016). Evaporation and hydrocarbon chain conformation of surface lipid films. *Ocul Surf.*, *14(4)*, 447-459.